UNIVERSITY OF CALIFORNIA

Santa Barbara

Organic Chemistry in Aqueous Surfactant Media: Batch and Flow Technologies

A dissertation submitted in partial satisfaction of the requirements for the degree Doctor of Philosophy in Chemistry

by

Alex Benjamin Wood

Committee in charge:

Professor Bruce H. Lipshutz, Chair

Professor Javier Read de Alaniz

Professor R. Daniel Little

Professor Todd Squires

June 2022

The dissertation of Alex Benjamin Wood is approved.

_____

Javier Read de Alaniz

_____

R. Daniel Little

_____

Todd Squires

_____

Bruce H. Lipshutz, Committee Chair

June 2022

Organic Chemistry in Aqueous Surfactant Media:

Batch and Flow Technologies

Alex Benjamin Wood

ACKNOWLEDGEMENTS

First and foremost, I must thank my Principal Investigator, mentor, and now dear friend Bruce Howard Lipshutz for his undying support throughout this entire doctoral degree process. Words cannot fully express my gratitude for everything you've done for me. You've cultivated my skills as a scientist, advocated for me on my behalf to key players in the chemical industry and academy, gone out of your way to provide me with the tools to be successful, and guided me as I grew as a person. You watched me succeed, as well as struggle, and you were always there for me in whatever capacity I needed at the time. For that, I know in my heart that I could not have chosen a better professor to have the privilege to work with. Thank you, sincerely.

To my parents, Craig and Ann Wood, I cannot say enough about how you have supported me through this time of my life. Without you this all would not have been possible. You were always there when I needed you the most and you went through great lengths to ensure that I was safe and well. You offered me your home and love when I needed it and made sure to come and see me often in California. I am proud to be your son. I also need to thank my sister Kelly and her partner Elisa; you guys are the best!

To my friends, those who I have been with since we were children. Tony Wloch, David Naylor, Devin Nigh, Samantha Ellis, Tara Malcom, and your respective families have been amazing support and I am grateful to have you in my life. I must also take this space to thank my friend Darren Phillips and his guidance for the past few years, as well as my dear college friend and fraternity brother Alex Chen for always making sure to check in on me!

I would like to acknowledge my committee members: Prof. Javier Read de Alaniz, Prof. R. Daniel Little, and Prof. Todd Squires. Thank you for accepting my invitation to oversee my research and writing efforts alongside Bruce. I've had a wonderful time working with you.

I must take this opportunity to thank all of the Lipshutz group members who helped me grow as a scientist as well as offer support as friends: Dr. Nicholas R. Lee, Dr. Margery Cortes-Clerget, Dr. Roscoe Linstadt, Dr. Dan Lippincott, Dr. Christopher Gabriel, Dr. Evan Landstrom, Dr. Piyatida "Nok" Klumphu, Dr. Sachin Handa, Dr. Ye Wang, Dr. Balaram Takale, Dr. Ruchita Thakore, Dr. David Fialho, Dr. Jade Dussart-Gautheret, Dr. Nico Fleck, Dr. Nnamdi Akporji, Dr. Haobo Pang, Dr. Bo Jin, Dr. Rahul Kavthe, Dr. Yitao Zhang, Daniel Roa, Julie Yu, Joseph Kincaid, Vani Singhania, Yuting Hu, Xiaohan Li, Juan Caravez, Rohan Thomas, Katie Freiberg, Karthik Iyer, Maddy Wong, Chandler Nelson, Erfan Oftadeh, and other visiting students throughout the years. There are other UCSB professors, students, and post docs outside of the Lipshutz group, as well as administrative staff, that deserve recognition as well, but there are far too many to list. I would also like to thank the hundreds of undergraduate students that I taught as well, wherever they all are now. Thank you all for making my time at UCSB memorable and enjoyable. I believe that this place attracts incredibly talented and overall amazing people.

I would also like to thank the wonderful people that I worked with while I was at Novartis. This list especially includes Dr. Scott Plummer, Dr. Richard Robinson, and Dr. Fabrice Gallou, all of whom supported me in fantastic ways both in Boston as well as back in Santa Barbara. It was an incredibly rare opportunity to work with these chemists. I would also like to thank those in Dr. Klavs Jensen's lab at MIT Chemical Engineering for their help

facilitating next generation solutions for surfactant flow chemistry, as well as David Gunn from PHT for helping create and fund the CSTR flow system at UCSB.

To those reading this dissertation: the road to a Ph.D. is an incredibly long and arduous one, and success is not based solely on talent in the art. Accomplishing such a feat is nigh impossible on just one persons will power and intellect alone. There is an old saying that it takes a village to raise a child. This can also be said for developing a Ph.D. organic chemist, who upon completion of a doctoral degree is now given the responsibility to not only further the frontiers of the science, but also to give back and mentor the practitioners coming behind them in various stages of their careers. This honor is not to be taken lightly, and if you are lucky, you will be mentored by those who take that to heart, much like Bruce does. Challenge yourself to be teachable, to be gregarious, and to be a leader.

A colleague I met near the beginning of my journey told me to steel myself against very dark days, which turned out to be true; however, many brilliant moments were also encountered which made the path a unique and worthwhile endeavor… and despite the struggles, stresses, and ever plaguing self-doubt, there was a vast fun about it all.

Alex Benjamin Wood

Curriculum Vitae as of June 2022

Education

Ph. D., Organic Chemistry. University of California, Santa Barbara. *June 2022.* GPA: 3.98

B.Sc., Chemistry. University of California, Davis. *June 2011.* GPA: 3.21

Employment

Graduate Student Researcher – Lipshutz Group / Visiting Scholar – Novartis Pharmaceuticals (2016-2022)

- Developed projects that have a high impact factor for pharmaceutical API development in a non-traditional aqueous medium.

- Led teams of chemists, including those with doctorates, on complicated, multi-faceted chemical programs.

- Gave presentations to teams of professional scientists to sell the Lipshutz Group surfactant technology to the pharmaceutical industry.

    - Multiple research subgroups at Novartis Pharmaceuticals are currently developing their own technology using research from talks I provided from my six-month internship.

- Managed a joint effort between the Lipshutz Lab, Novartis Pharmaceuticals, and MIT Chemical Engineering to develop a continuous flow system for surfactant-based green chemical synthesis.

    - Developed both methodology and engineering in this respect for plug-flow reactor type models.

- Scientific manuscripts are published or are currently being written for projects including chemical synthesis method development, flow engineering, and surfactant development technology.

Origin Materials – Scientist (2013-2016)

- Developed non-obvious and novel chemical processing approaches for the conversion of low value biomass to valuable commodity chemicals and platform chemicals.

- Worked internally and externally with research groups to produce a highly selective route from carbohydrate-derived furans to *para*-xylene.

- Explored lab scale experimentation for industrially feasible purification processes of unstable, large volume product streams currently used in pilot plant operations.

- Performed due-diligence research for the scale-up and long-term feasibility of a highly complex continuous reaction system.

- Collaborated with a design engineering department for the scaling and cost estimation of down-stream processing for a multiphase and multiple product process.

- Applied researched and independently developed analytical techniques to study physical and process characteristics of target compounds such as partition coefficients, solubility, and stability.

- Studied chemical processes for the application and valorization of hydrothermal carbon produced from the furan synthesis.

- Advanced a synthesis program around the furanic platform which aims to develop a chemical product portfolio congruent to public demand for a renewable, bio-based chemical market.

Origin Materials – Assistant Scientist (2011- 2013)

- Performed synthetic organic chemical reactions and purified final products utilizing a variety of applied synthesis techniques.

- Participated in reaction optimization experiments in order to produce high-yielding and economically sound procedures.

- Developed and used analytical methods using UV-Vis absorption, mass spectrum detection, and GC-FID detection to determine the concentration of product in a reaction mixture.

- Used analytical techniques such as EI/ESI-MS and NMR to determine the chemical structure of unknown compounds.

Publications

Wood, A. B.; Kincaid, J. R. A.; Lipshutz, B. H. Dehydration of Primary Amides to Nitriles in Water. Lage-stage Functionalization and 1-Pot Multistep Chemoenzymatic Processes Under Micellar Catalysis Conditions. *Green Chem.* **2022**, *24*, 2853-2858.

Li, X.; **Wood, A. B.;** Lee, N. R.; Gallou, F.; Lipshutz, B. H. Allylations of Aryl/Heteroaryl Ketones : Neat, Clean, and Green. Applications to Targets in the Pharma- and Nutraceutical Industries. *Manuscript submitted.*

Wood, A. B.; Plummer, S.; Robinson, R. I.; Gallou, F.; Lipshutz, B. H. Continuous Slurry Plug Flow of Fe/ppm Pd Nanoparticle-Catalyzed Suzuki-Miyaura Couplings in Water Utilizing Novel Solids-Handling Equipment. *Green Chem.* **2021**, *23*, 7724-7730.

Wood, A. B.; Roa, D. E.; Gallou, F.; Lipshutz, B. H. α-Arylation of (Hetero)aryl Ketones in Aqueous Surfactant Medium. *Green Chem.* **2021**, *23*, 4858-4865.

Wood, A. B.; Cortes-Clerget, M; Kincaid, J. R. A.; Akkachairin, B.; Singhania, V.; Gallou, F.; Lipshutz, B. H. Nickel Nanoparticle-Catalyzed Mono- and Di-Reductions of *gem*-Dibromocyclopropanes Under Mild, Aqueous Micellar Conditions. *Angew. Chem., Int. Ed.* **2020**, *59*, 17587-17593.

Wood, A. B.; Nandiwale, K. T.; Mo, Y.; Jin, B.; Pomberger, A.; Shultz, V. L.; Gallou, F.; Jensen, K. F.; Lipshutz, B. H. Continuous Flow Suzuki-Miyaura Couplings in Water Under Micellar Conditions in a CSTR Cascade Catalyzed by Fe/ppm Pd Nanoparticles. *Green Chem*. **2020**, *22*, 3441-3444.

Lee, N. R.; Cortes-Clerget, M.; **Wood, A. B**.; Lippincott, D. J.; Pang, H.; Moghadam, F.; Gallou, F.; Lipshutz, B.H. Coolade. A Low-Foaming Surfactant for Organic Synthesis in Water. *Chem. Sus. Chem.* **2019**, *12*, 3159-3165.

Knapp, J. M.; **Wood, A. B**.; Phuan, P. W.; Lodewyk, M. W.; Tantillo, D. J.; Verkman, A. S.; Kurth, M. J. Improved Activity of Cyanoquinolines as ΔF508-CFTR Correctors and Potentiators. *J. Med. Chem.* **2012,** *55*, 1242-1251.

Knapp, J. M.; Zhu, J.; **Wood, A. B**.; Kurth, M. J. Expedient Synthesis of a 72-Membered Isoxazolino-β-ketoamide Library by a 2•3-Component Reaction. *ACS Combi. Sci.* **2012,** *14*, 85-88.

Phuan, P. W.; Yang, B.; Knapp, J. M.; **Wood, A. B**.; Lukacs, G. L.; Kurth, M. J.; Verkman, A.S. Cyanoquinolines with Independent Corrector and Potentiator Activities Restore ΔF508-CFTR Chloride Channel Function in Cystic Fibrosis. *Mol. Pharmacol.* **2011,** *80*, 683-693.

Patents

Henton, D. R.; Goralski, C. T. (Michigan Molecular Institute, USA); Masuno, M. N.; Smith, R. L.; **Wood, A. B**.; Hirsch-Weil, D. A.; Araiza, R. J. (Micromidas Inc, USA). Oxidation chemistry on furan aldehydes. PCT Int. Appl. WO 2017049211, March 23, 2017.

Wood, A. B.; Masuno, M. N.; Smith, R.L.; Bissell, J.; Araiza, R. J.; Hirche-Weil, D. A. (Micromidas Inc., USA). Methods for production of aryldiamine compounds, aryldinitro compounds and other compounds. PCT Int. Appl. WO 2016033348, March 3, 2016.

Smith, R. L.; J. A. Bissell; Browning, S.M.; **Wood, A. B.**; Araiza, R. J.; Dornath, P. J.; Joh, A.; Hirsch-Weil, D. A.; Masuno, M. N. (Micromidas, Inc., USA). Gregory, T.D. (Michigan Molecular Institute, USA). Activated Carbon Materials, And Methods of Preparing Thereof and Uses Thereof. PCT. Int. Appl. WO 2016168675, April 15, 2015.

Wood, A. B.; Masuno, M. N.; Smith, R. L.; Bissell, J.; Hirsche-Weil, D. A.; Araiza, R. J. (Micromidas Inc. USA). Henton, D.R.; Plonka, J.H. (Michigan Molecular Institute, USA). Methods for producing 5-halomethyl) furfural from renewable biomass resources. PCT Int. Appl. WO 2015042407, March 26, 2015.

Hirsh-Weil, D. A.; Masuno, M. N.; Bissell, J.; **Wood, A. B.**; Araiza, R. J. (Micromidas Inc. USA). Hucul, D.; Henton, D.R. (Michigan Molecular Institute, USA). Methods of producing alkylfurans. PCT Int. Appl. WO 2015023918, February 19, 2015.

Smith, R. L.; Bissell, J.; Masuno, M. N.; Cannon, D.; **Wood, A. B**.; Foster, M. (Micromidas Inc. USA) Polyhydroxyalkanoate derivatives, preparation and uses thereof. U.S. Pat. Appl. Publ. (2015), US 20150148560.

Wood, A. B.; Browning, S. M.; Masuno, M. N.; Smith, R. L.; Bissell, J.; Hirsch-Weil, D. A. (Micromidas Inc., USA). Methods for purifying 5-(halomethyl)furfural. PCT Int. Appl. WO 2014159741, March 14, 2014.

Browning, S. M.; Bissell, J.; Smith, R. L.; Masuno, M. N.; **Wood, A. B.** (Micromidas Inc., USA). Methods for producing 5-(halomethyl)furfural from feedstock comprising six-carbon sugars. PCT Int. Appl. WO 2014066746, May 1, 2014.

Smith, R. L.; Bissell, J.; Masuno, M. N.; Cannon, D.; **Wood, A. B**.; Foster, M. (Micromidas Inc., USA). Polyhydroxyalkanoate derivaties, preparation and uses thereof. PCT Int. Appl. WO 2013181604, Dec 5, 2013.

Masuno, M. N.; Cannon, D.; Bissell, J.; Smith, R. L.; Foster, M.; **Wood, A. B.** (Micromidas Inc., USA). Smith, P. B.; Hucul, D. A. (Michigan Molecular Institute, USA). Method of producing p-xylene by reacting 2,5-dimethylfuran with ethylene in the presence of Lewis

acid catalyst and oxidation of p-xylene to terephthalic acid. PCT Int. Appl. WO 2013040514, Mar 21, 2013.

Masuno, M. N.; Bissell, J.; Smith, R. L.; Higgins, B.; **Wood, A. B**.; Foster, M. (Micromidas Inc., USA). Utilizing a multiphase reactor for the conversion of biomass to produce substituted furans in the presence of gaseous acid, proton donor, and solvent. PTC Int. Appl. WO 2012170520, Dec 13, 2013.

Reviews / Books

Cortes-Clerget M., Akporji N., Takale B. S., **Wood A**., Landstrom E., Lipshutz B. H. (2020) Earth-Abundant and Precious Metal Nanoparticle Catalysis. In: *Topics in Organometallic Chemistry*. Springer, Berlin, Heidelberg.

Presentations

Wood, A. B. "Synthesis of β-Ketoamide Isoxazolines via a One Pot, Multicomponent Reaction" Presented at the 5th annual Larock Undergraduate Research Conference, Davis, CA, 2011.

Honors and Awards

University of California, Santa Barbara Chemistry and Biochemistry Chair Fellowship (2021).

Best Presenter Award, U.C. Davis Larock Undergraduate Research Conference (2011).

ABSTRACT

Organic Chemistry in Aqueous Surfactant Media:

Batch and Flow Technologies

By: Alex Benjamin Wood

I. Nickel Catalyzed Reductions of *gem*-Dibromocyclopropanes to Cyclopropanes in Water

II. α-Arylations of (Hetero)Aryl Ketones in Aqueous Micellar Media

III. Palladium Catalyzed Dehydration of Primary Amides to Nitriles in Water

IV. Solid Handling Equipment Advancements for Nanoparticle Catalyzed Flow Chemistry in Aqueous Micellar Media

I. New techniques to access cyclopropanes are of great importance to the fine chemical industry. One route to this valuable moiety is through the synthesis of *gem*-dibromocyclopropanes followed by the reduction of the halides to access the saturated cyclopropane. However, contemporary reduction methods are plagued with selectivity and safety issues, as well as environmentally deleterious solvents and reagents. Herein are described both mild mono- and di-hydrodehalogenative reductions of *gem*-dibromocyclopropanes enabled by aqueous micellar media, providing an environmentally responsible alternative. The chemistry is performed using a ligated 0.5-5.0 mol % nickel catalyst activated by sodium borohydride *in situ* and boasts a wide substrate scope including pharmaceutically relevant compounds.

II. α-Arylation chemistry is traditionally limited to organic solvents due to the high pK_a of the ketone alpha proton, especially with respect to the relative acidity of water. However, the introduction of a micellar array to an aqueous media creates a hydrophobic environment suitable to facilitate deprotonation of the ketone followed by coupling with an aryl halide. This is provided that the correct lipophilic base, which can gain access into the micelle inner core, is chosen to effect enolization. Under such conditions, using a Pd(I) bromide dimer pre-catalyst, α-arylation of aryl and heteroaryl ketones can be performed in recyclable water using as low as 2500 ppm of the transition metal under near ambient conditions.

III. Conventional methods to dehydrate primary amides to nitriles require the use of highly toxic, reactive, and moisture sensitive reagents, and are oftentimes performed at high temperatures (*ca*. >80 °C) in rigorously dry organic solvents. Recent mild techniques have been developed using palladium salts and a "sacrificial" nitrile, resulting in a water-shifting reaction to form the desired nitrile and a cheap amide byproduct. However, this chemistry is performed in mixtures of acetonitrile/water, obviating the overall "greenness" of the technology. This chapter discusses the development of ppm Pd-catalyzed dehydration chemistry in aqueous micellar media, removing the need for excess acetonitrile as co-solvent. This method uses highly reactive water-acceptor nitriles, methoxyacetonitrile or fluoroacetonitrile, tuned specifically for their respective amide reagents in aqueous micelles.

IV. Flow chemistry has evolved to be a disruptive technology in the field, resulting in novel techniques which have revolutionized the chemical industry. However, issues with solids, which can result in clogging of lines and equipment, have remained an unsolved problem. Herein, aqueous micellar nanoparticle-catalyzed Suzuki-Miyaura couplings are utilized as a

method to probe novel solids handling equipment for plug flow and continuously-stirred tank reactor systems.

TABLE OF CONTENTS

I. Nickel Catalyzed Reductions of *gem*-Dibromocyclopropanes to Cyclopropanes in Water

Wood, A. B.; Cortes-Clerget, M.; Kincaid, J. R. A.; Akkachairin, B.; Singhania, V.; Gallou, F.; Lipshutz, B. H. Nickel Nanoparticle-Catalyzed Mono- and Di-Reductions of gem-Dibromocyclopropanes Under Mild, Aqueous Micellar Conditions *Angew. Chem., Int. Ed.* **2020**, 59, 17587–17593.

1.1 Personal Account

It was July of the year 2016, and the weight of my decisions up until this point had fully started to settle in on me as I was sitting in Bruce's office, the second time I had ever been there and the first time in my Ph.D. career. I had just moved to graduate student housing in Isla Vista, into what was essentially a dorm room, from a nice one-bedroom apartment in downtown Sacramento. I had also, and more importantly, just exited from a startup company, Micromidas Inc. (now Origin Materials), wherein which I was employed as what was essentially a process engineer, not so much an organic chemist. One reason for leaving was due to my wish to improve my career by pursuing a Ph.D. in my chosen field of organic chemistry; another reason was due to what appeared to be writing on the wall for a company that was massively laying off people because of funding issues and, although I made it through a round of 75% personnel cuts, I did not want to be caught in a fragile state. Believe it or not I bet wrong in one way, because as of the time of writing this dissertation the company is worth 1.8 billion dollars. However, I sat across from Bruce as he started writing on his whiteboard for the project I was going to start and, ostensibly, work on with a postdoc in our lab, ready to put in my best work.

Bruce outlined a project that was initially proposed by Fabrice Gallou at Novartis Pharmaceuticals. They were interested in adding a cyclopropane-containing amino acid derivative, (S)-5-azaspiro[2.4]heptane-6-carboxylic acid (from L-proline), into their building-block repertoire *en route* to ledipasvir and they wanted to use aqueous-based chemistry in order to do so. The overall goal was to convert *geminal*-dibromocyclopropanes to the corresponding saturated ring system, minimizing the use of traditional organic solvents or precious metals. This two-step process is considered to be safer than traditional direct ring installation methods

(*vide infra*), and the second step had promise for a green upgrade compared to the dismal amount of literature available for the hydrodehalogenation step.

I was to work with a postdoc in our group, to apply this hydrodehalogenation chemistry in water to form the saturated cyclopropane. This ended up not completely happening as Ye Wang, who had developed some preliminary data surrounding the project, decided that he wanted to hand it off to me entirely. Therefore, my first project in the group ended up being my initial first authorship paper, albeit years down the road when the data were finally published.

1.2 Introduction and Background

The cyclopropane ring has emerged as a major substructure in the synthetic and chemical biology fields.[1] This can be seen, for example, based on the ubiquity of cyclopropanes in the natural world. The ring is readily observed as a key structural element of natural products, such as in pyrethrum extracts from the *Tanacetum cinerariifolium*, of the genus Chrysanthemum, which yield cyclopropane-bearing molecules that are responsible for the insecticidal activity of the flower.[2] Similar biological activity can also be observed in dihydrosterculic acid, a cyclopropane derivative of oleic acid. This fatty acid is then further dehydrogenated to form sterculic acid, a cyclopropene fatty acid which makes up most of the seed extract from *Sterculia foetida* and acts as an antiparasitic (Figure 1).[3]

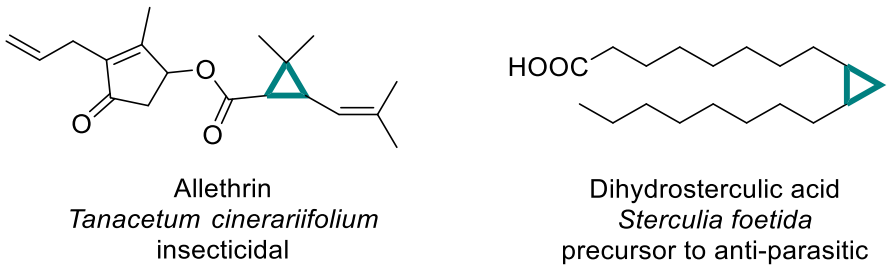

Figure 1: Cyclopropane-containing natural products

With this background in mind, it is not necessarily all too surprising that the cyclopropane moiety has found a home in the pharmaceutical industry as a common structural motif in biologically active, manmade molecules. Indeed, cyclopropane-containing targets represent a massive population in the active pharmaceutical ingredient (API) database, with hundreds of bioactive compounds bearing this substructure in a near limitless array of chemical environments (*i.e.*, near or influencing other functional groups). This also includes eleven out

of the top two-hundred drugs of 2018 based on sales, three of which are illustrated below (Figure 2).[4]

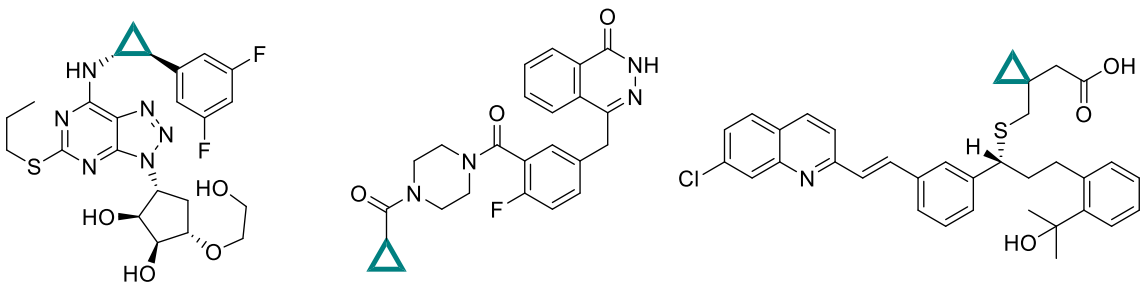

Figure 2: Representative top selling pharmaceuticals bearing a cyclopropane ring

Medicinal interest in cyclopropanes is due to the unique chemical and biological attributes of this scaffold.[5] The strained ring imparts interesting bonding properties, as opposed to ethane, the carbon-carbon bonds are shorter and contain more pronounced π-character. Also, in consideration are the carbon-hydrogen bonds, which gain significantly more σ-character and concomitant strengthening of the bond to an increase of greater than 5 kcal/mol (106 kcal/mol) compared to a purely aliphatic system (101 kcal/mol).[6] This can result in greater metabolic stability at the site of the cyclopropane compared to that of an alkyl group, which may be used as a handle for oxidation. Furthermore, the planar and less lipophilic character of cyclopropanes can be utilized to substitute other functional groups within a molecule as a bioisostere. These include olefins, α,β-unsaturated ketones (which can act as Michael acceptors),[7] and isopropyl groups.[8] It can also act as a surrogate for aromatics, replacing phenyl groups which can significantly lower the log P of a target molecule.[9] These attributes, along with the ability to modify of pK_a values of other functional groups in proximity by the addition

of a cyclopropane, ultimately allow for a greater space of structural activity relationships (SAR) to model binding pockets for influencing, and ultimately controlling, pharmacological activity.

There exists an exigency in the field of synthetic methodology to develop new and better ways to insert this ring system, preferably onto late-stage, pharmaceutically relevant chemical intermediates or final products. This is in response to the state of the literature surrounding the direct installation of the ring and the pitfalls associated with current methods.[10-11] There are a variety of reaction types that can yield substituted and unsubstituted cyclopropane rings (Figure 3).

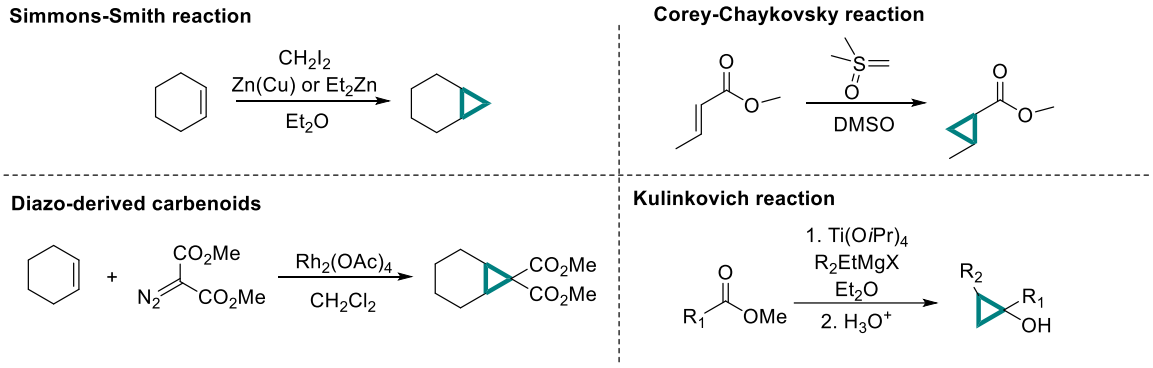

Figure 3: Examples of common cyclopropane synthetic methods in the literature

However, there are very few examples of direct cyclopropane syntheses that take into consideration the impact of the method with respect to its environmental footprint, as well as safety. Reactions such as Simmons-Smith,[12-13] decomposition of diazo compounds to form carbenes,[14] Corey-Chaykovky,[15] and Kulinkovich[16] require, in many instances, stoichiometric amounts of dangerous reagents, as in the case of diethylzinc or titanium(IV) isopropoxide, or starting materials such as diazo compounds which are explosive. Furthermore, as in the case

of diazo-derived carbenoids, the use of expensive and non-renewable precious metal catalysts is required. These drawbacks can become major considerations with respect to route selection towards a target compound bearing a cyclopropane, especially in industrial settings where safety and selectivity take precedence, especially when done at scale. Regardless, except in the case of some methods based on (expensive) rhodium-based diazo-derived carbenoid chemistry,[17-18] the reactions listed above are limited in overall "greenness" due to the overwhelming use of organic solvents as reaction media and the exclusion of advantageous air and moisture.

An often overlooked, alternative route to the preparation of cyclopropanes is through the addition of a *geminal*-dihalocyclopropane, which can then be chemically altered at the site of the halogens to provide a variety of synthetic derivatives. This initial cyclopropanation is achieved via a cycloaddition between a dihalocarbene and an olefin.[19] In 1862, Geuther found that dihalocarbenes could be easily prepared via a highly exothermic alkaline hydrolysis of haloforms, such as chloroform and bromoform.[20] This carbene formation occurs via deprotonation of the haloform hydrogen by the base to form the trihalomethyl anion, followed by α-elimination of a halogen resulting in an open *p*-orbital. In their now seminal work, Doering and Hoffman were able to utilize the dihalocarbene as a carbon source for the formation of a halogenated cyclopropane.[21] Their approach involved dissolution of cyclohexene in a saturated solution of potassium *t*-butoxide in *t*-butanol, followed by dropwise addition of chloroform. The resulting exothermic reaction produced the dihalocarbene, which was then trapped via [2+1] annulation with cyclohexene resulting in 7,7-dichlorobicyclo[4.1.0]heptane, formed in 59% yield (Figure 4).

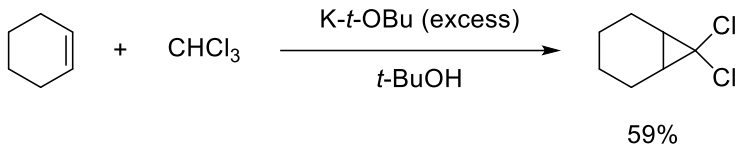

Figure 4: Doering and Hoffman's synthesis of 7,7-dichlorobicyclo[4.1.0]heptane

While incredibly important and influential, this reaction protocol has been shown to have limited applications, only being useful in the situation where simply alkyl olefins are used. The synthetic utility of this dihalocarbene approach, however, was greatly advanced by the work of Mαkosza and Wawrzyniewicz in 1969.[22] In their studies, they found that a biphasic system between chloroform or bromoform and 50 wt % NaOH with a quaternary amine phase transfer catalyst, such as triethylbenzylammonium chloride (TEBA), produces the *gem*-dihalocyclopropane in high yields when an olefin is present in the organic phase. The postulated mechanism that results in the improved yield, even under conditions where the hydrolysis of the carbene is expected, is due to the nature of the phase transfer catalyst and its role in mediating the formation of the carbene in the organic phase. Firstly, anion exchange between the chloride in TEBA and the aqueous hydroxide results in an ammonium hydroxide. This ammonium hydroxide then travels into both the aqueous and organic phases, where the hydroxide deprotonates the haloform and yields the quaternary ammonium of the trihalomethyl anion. The lipophilic derivative then α-eliminates a halogen in the organic phase, regenerating the catalyst and producing the dihalocarbene that reacts with the olefin with limited possibility of hydrolysis (Figure 5).

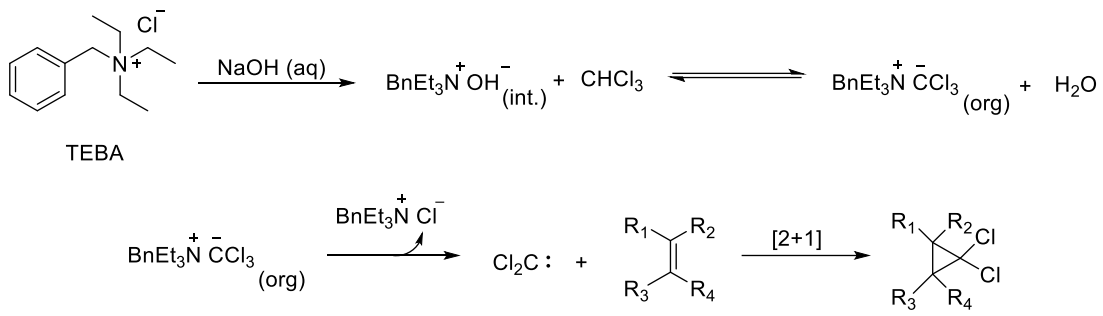

Figure 5: Mαkosza's proposed mechanism for biphasic dihalocarbene cyclopropanation

As previously stated, the resulting halogenated ring opens a variety of possibilities for further derivatization, including the hydrodehalogenation of the halides to result in the corresponding unsubstituted ring, typically in the case of the *gem*-dibromocyclopropanes. Despite being a two-step process, designing a synthetic route through the *gem*-dibromocyclopropane towards the hydrogenated cyclopropane can make sense in the chemical industry, as the actual formation of the cyclopropane using Mαkosza's method requires significantly less solvent (usually only requiring the haloform used for generating the carbene, or a small amount of dichloromethane), no precious metals, catalytic amounts of transfer agent, and is ultimately safer overall compared to contemporary methods. A case study can be seen in a multitude of synthesis routes explored by Novartis for development of a scaleup towards a 4-spirocyclopropane substituted proline scaffold, (*S*)-5-(*tert*-butoxycarbonyl)-5-azasprio-[2.4]heptane-6-carboxylic acid, which is a building block *en route* to ledipasvir (Figure 6).[23]

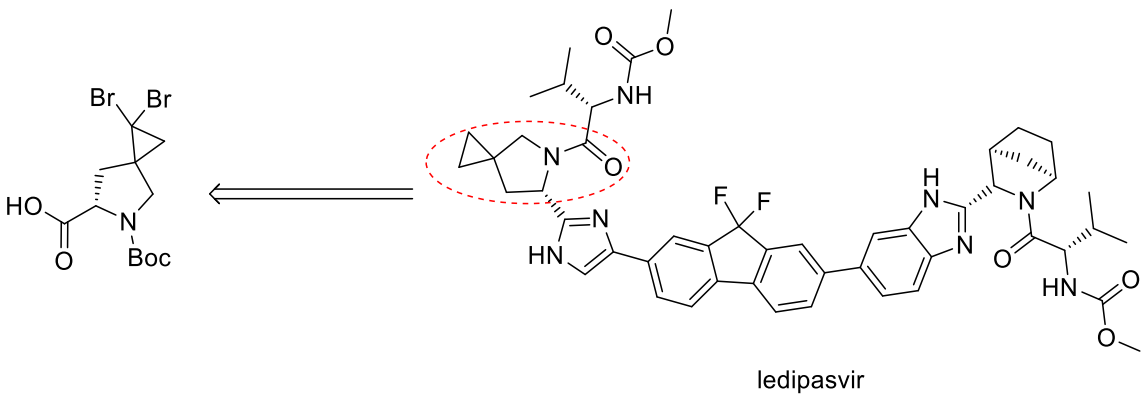

Figure 6: Desired cyclopropyl-substituted proline fragment within ledipasvir

In this case, a variety of traditional cyclopropanation chemistries were attempted on intermediates, such as Simmons-Smith and Corey-Chaykovsky, to produce the desired 4-spiro cyclopropane scaffold directly. Issues were encountered with scalability of the Corey-Chaykovsky method on a protected intermediate, with yields dropping from 70% on lab scale to 20% on a 20 kg scale and necessitated that reactions be run on an order of magnitude smaller batches to achieve only 55% yield. The Simmons-Smith method was run on the exomethylene derivative of the Boc-protected proline resulting in high yield; however, the authors noted that safety issues encountered at scale limited the pursuit of this synthetic strategy. Ultimately, scaleup towards the fully saturated cyclopropyl proline fragment was developed around an initial *gem*-dibromocyclopropanation, due to ease of setup and safety, followed by concomitant hydrodehalogenation with palladium-on-carbon and hydrogen pressure to form the saturated cyclopropane.

Despite the obvious synthetic utility of a dibrominated cyclopropane with respect to access of the fully saturated product, there exists a dearth of methodologies in the literature dedicated towards this transformation that would be applicable to the complexity of molecules encountered in the pharmaceutical industry. Most commonly, dangerous and wasteful hydride

reagents such as tributyltin hydride or lithium aluminum hydride are employed, the former of which produces toxic byproducts that require separation, and the latter is not selective and can reduce other functionality present in a target molecule.[24] Likewise, Birch-type conditions have also been reported, which are greatly limited to mostly alkane-based structures.[25] Other reducing conditions such as palladium-on-carbon or Raney nickel are also represented in the literature; however, the pressurized flammable gas required, the use of precious metals (in the case of Pd), and selectivity issues with respect to ring opening byproducts present in mass balance analysis (in the case of Ra Ni) all have severely stymied applications.[23]

Notwithstanding these methodologies, a running theme associated with this transformation is the requirement of using non-renewable, environmentally deleterious organic solvents as the reaction medium. This feature also plagues the most recent entry into the *gem*-dibromocyclopropane reduction literature by Gütz in 2015, wherein the bromides are removed electrochemically (Figure 7).[26]

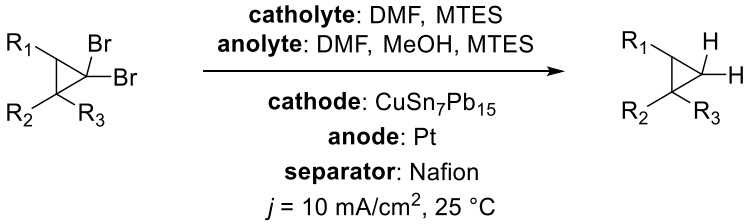

Figure 7: Gütz's electrochemical reduction of *gem*-dibromocyclopropanes

While this synthetic method does offer the most environmentally friendly reducing reagent in the form of electrons, the overall greenness of the method is narrowed with respect to the choice and amounts of solvent involved. The reaction takes place in either DMF or acetonitrile at a very low concentration of 0.065 M, taking only into consideration the catholyte where the

reaction takes place (the anolyte runs using the same amount of solvent, albeit a 1:2 mixture of methanol and DMF). Furthermore, the electrochemistry requires a large quantity of supporting electrolyte, in this case being MTES ($[Et_3NMe]O_3SOMe$), as well as a custom leaded bronze cathode. Clearly, specialized equipment is required. Interestingly, however, the reaction can be tuned to access either the di-debrominated or mono-debrominated product based on the amount of applied current, albeit with no stereocontrol with respect to the mono-debrominated product. Nonetheless, it is applicable to some more complex molecules, including Novartis's 4-spiroproline derivative as well as a derivative of cyclosporine A in high yields.

As of this latest report, there has been no effort to optimize double dehalogenation of *gem*-dibromocyclopropanes in an environmentally responsible manner. This is apparent given the egregious nature of the media required for this overall transformation. In many cases, the solvent of choice for the reduction is bulk THF, acetonitrile, or DMF. Furthermore, the reagent choices in these systems are woefully limited to toxic and non-selective substances used in stoichiometric amounts. Herein, we report a 3,4,7,8-tetramethyl-1,10-phenanothroline ligated nickel species that is activated by sodium borohydride to selectively hydrodehalogenate *gem*-dibromocyclopropanes to the corresponding cyclopropanes. Furthermore, this conversion takes place in an aqueous micellar medium with minimal organic solvent as co-solvent, vastly improving the environmental impact of the chemistry, especially with respect to scale. The chemistry is exemplified by the array of functionalized molecules that participate, that would otherwise not be amenable to use of other reduction methodologies. The utility of this aqueous-based transformation is enhanced due to the selectivity of mono- vs. di-dehalogenation based on the ligand choice and catalyst loading, alongside the amount of reductant required (Figure

8). Also, characteristic of this new technology is its exceptionally low E Factor, opportunities for recycling of the reaction medium, as well as multistep processes that can be affected, all in water.

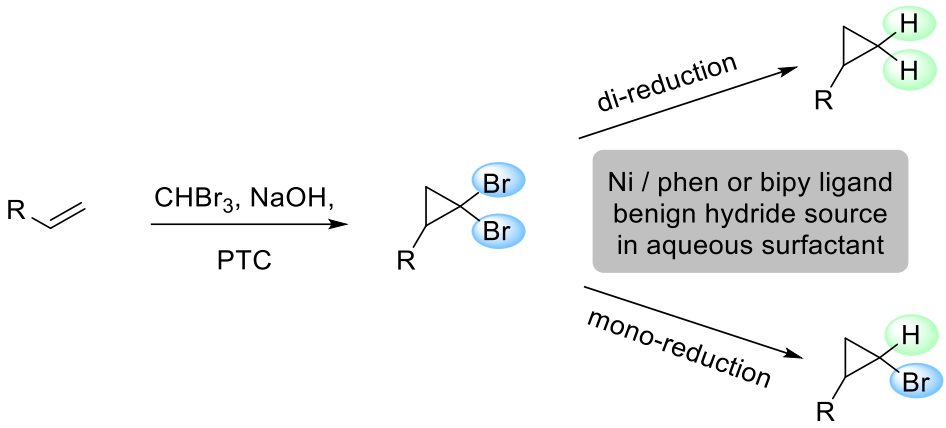

Figure 8: Mono- and di-reduction using a ligated nickel catalyst and hydride source in water

1.3 Results and Discussion

Initial investigation into the double reduction of *geminal*-dibromocyclopropanes began by exploring zinc dehalogenation chemistry using ammonium chloride as a proton source in water. This chemistry was originally put forth from our lab by Nicholas Isley in 2015,[27] where it was found that fine zinc metal particles were incredibly efficient in the dehalogenation of alkyl chlorides and bromides in even highly functionalized molecules. In this disclosure, however, issues were encountered with both conversion and selectivity of (2,2-dibromo-1-methylcyclopropyl)benzene to the corresponding fully reduced cyclopropane (Figure 9).

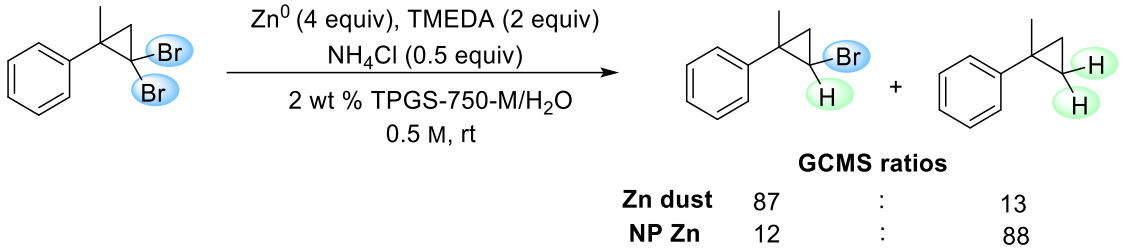

Figure 9: Initial trial for reduction of a *gem*-dibromocyclopropane using two zinc sources

Two zinc types were used with ammonium chloride. Zinc dust (<10 micron) resulted in a much greater majority of the mono-reduced product *vs*. the di-reduced (87:13 respectively) by GCMS analysis. It was found that use of zinc nanoparticles could affect greater conversion to the di-debrominated product (12:88 mono- vs. di-reduction); however, conversion and selectivity remained an issue.

In order to determine if conversion issues with zinc were an artifact of the electronic positioning of the *gem*-dibromocyclopropane (*i.e.*, derived from a styrene), substrate **1** was

prepared and tested against two forms of inexpensive Zn sources of varying size to form di-reduced product **2** (Table 1).

Table 1: Di-reduction of an alkyl *gem*-dibromocyclopropane using zinc metal

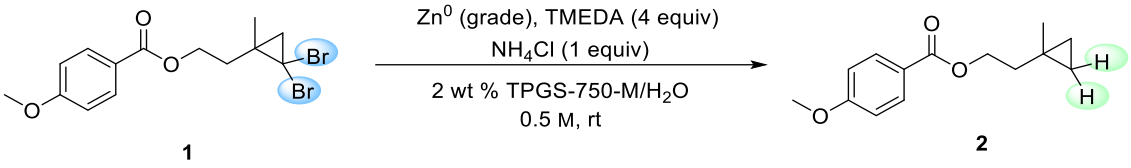

Entry	Metal Size	Equiv	Time	% Yield **2**
1	Zn powder (150 micron)	8	4 d	43
2	Zn dust (<10 micron)	4	24 h	38

The easily isolable di-reduced product was recovered via silica gel column chromatography from the starting material and mono-reduced intermediate to determine absolute yield. Unfortunately, data from this set of experiments validated the selectivity issues encountered with the previous substrate. While conversion to **2** was improved, GCMS analysis indicated that a large amount of the mono-reduced bromocycopropane diastereomers was present. This observation is congruent with Bänziger's attempts from Novartis,[23] with indications from their lab that selectivity issues plagued this methodology specifically in these cyclopropyl cases.

With this result, we decided to switch direction away from a stoichiometric transition metal as the reducing agent, instead opting for a catalytic system. Inspired by the use of Raney nickel in other applications, including the reduction of *gem*-dibromocyclopropanes (*vide supra*), our goal then became to explore the use of nickel boride as a potential catalyst, which had not yet been investigated in the literature for this application. The use of nickel boride in water is attractive from an industrial standpoint due to the ease of preparation of the catalyst, as the

resulting non-pyrophoric nanoparticles are synthesized *in situ* with the simple addition of sodium borohydride to a Ni(II) salt such as $Ni(OAc)_2 \cdot 4H_2O$ dissolved in aqueous media.[28] Furthermore, we also postulated that the use of a ligand could potentially enhance the reactivity of the catalyst. Previous work from our lab found that 1,10-phenanthroline (phen) can be used to improve the reductive capacity of nickel boride in water with respect to 6-chloro and 6-fluoropyridines to form the dehalogenated heterocycle.[29] This could be performed in an aqueous micellar medium using 5 mol % Ni and 10 mol % of the phenanthroline ligand with sodium borohydride as the terminal reductant. The search was further expanded to incorporate a variety of phen derivatives, which have found privileged activity in aqueous micellar media in other applications (Table 2).[30a-b]

Table 2: Ligand screening for nickel boride reduction of *gem*-dibromocyclopropanes

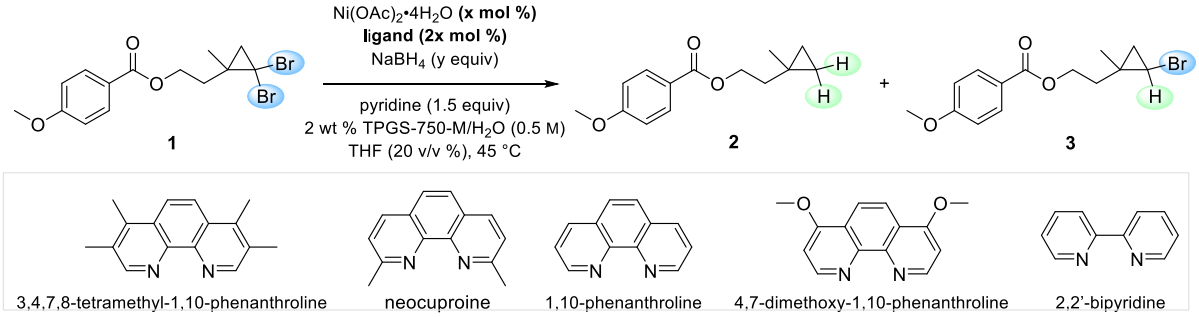

Entry	Catalyst (mol %)	Ligand (mol %)	$NaBH_4$ (equiv)	**1** / **2** / **3**[a]
1	$Ni(OAc)_2•4H_2O$ (5)	/	5	0 / 12 / 88
2	$Ni(OAc)_2•4H_2O$ (5)	3,4,7,8-tetramethyl-1,10-phenanthroline (5)	5	0 / 100 (82)[b] / 0
3	**$Ni(OAc)_2•4H_2O$ (5)**	**3,4,7,8-tetramethyl-1,10-phenanthroline (10)**	**5**	**0 / 100 (91)[b] / 0**
4	$Ni(OAc)_2•4H_2O$ (5)	3,4,7,8-tetramethyl-1,10-phenanthroline (15)	5	0 / 23 / 77
5	/	/	5	100 / 0 / 0
6	$Ni(OAc)_2•4H_2O$ (5)	neocuproine (10)	5	0 / 20 / 80
7	$Ni(OAc)_2•4H_2O$ (5)	1,10-phenanthroline (10)	5	0 / 19 / 81
8	$Ni(OAc)_2•4H_2O$ (5)	4,7-dimethoxy-1,10-phenanthroline (10)	5	0 / 10 / 90
9	$Ni(OAc)_2•4H_2O$ (5)	2,2'-bipyridine (10)	5	0 / 13 / 87
10	**$Ni(OAc)_2•4H_2O$ (0.25)**	**/**	**2.5**	**0 / traces / >99**
11	**$Ni(OAc)_2•4H_2O$ (0.5)**	**2,2'-bipyridine (1)**	**2.5**	**0 / 3 / 97**

[a] Determined by NMR yield. [b] Isolated yield in parentheses.

Data from this set of experiments indicate that catalytic nickel boride, loaded at 5 mol % without ligand (entry 1), was adept at completely consuming the starting *gem*-dibromocyclopropane **1** along with producing a large amount of hydrogen gas, which is a known byproduct.[31] However, NMR analysis of the crude mixture found that the majority of the converted material halted at the monobromocyclopropane **3**, even when using a vast excess of sodium borohydride at five equivalents. Introduction of phen as a ligand (entry 7) saw only minimal, if any, improvement towards the fully reduced cyclopropane. Similar results were obtained when using neocuproine (entry 6), 4,7-dimethoxy-1,10-phenanthroline (entry 8), and 2,2'-bipyridine (entry 9). Interestingly, high selectivity (by NMR analysis) towards the monobromocyclopropane could be obtained when the nickel catalyst loading was dropped by greater than an order of magnitude with no ligand, as well as depletion in the amount of sodium borohydride used (entry 10). Introduction of 2,2'-bipyridine to the reduced catalyst loading system also saw similar selectivity (entry 11) and was instrumental towards a broader scope of mono-debrominations (*vide infra*). To prove the requirement of the transition metal for conversion, a trial using no nickel was conducted (entry 5) resulting in zero conversion of the starting material to **2** or **3**.

Introduction of 3,4,7,8-tetramethyl-1,10-phenanthroline (TMPhen), however, saw vast improvement toward selectivity of the fully reduced cyclopropane **2**. When added at 10 mol %, with 5 mol % nickel (Table 2, entry 3), the cyclopropane was fully dehalogenated with no observed **3** by either GCMS of the reaction or crude NMR analysis of the product mixture and gave a 91% isolated yield of **2**. It should be noted that catalyst loadings as low as 1 % nickel and 2 % TMPhen could also be used for simple substrates, but is not applicable towards more pharmaceutically relevant compounds, and thus 5 mol % metal was chosen as the general

condition. Improved activity of the catalyst when TMPhen is used could potentially be explained based on two points. Firstly, TMPhen is one of the most basic of the phen ligands tried, with a conjugate acid pK_a of 6.31 (compared to phen, which is 4.86) which enhances σ-donation into the nickel. Secondly, analysis of the crude product mixture saw the formation of reduced phen derivatives under the reaction conditions in other phen ligand choices excluding TMPhen.

Observation of the pre-catalyst prior to the addition of sodium borohydride indicates differences that exist between this ligand and other 1,10-phenanthroline- or 2,2'bipyridine-type ligands. Whereas all other metal/ligand mixtures prior to sodium borohydride addition gave a blue liquid (color of nickel(II) acetate tetrahydrate) with undissolved white material (the ligand), the combination of $Ni(OAc)_2 \bullet 4H_2O$ with TMPhen resulted in a bright pink, homogeneous solution. This is then converted into a dark purple slurry upon the addition of $NaBH_4$ (Figure 10).

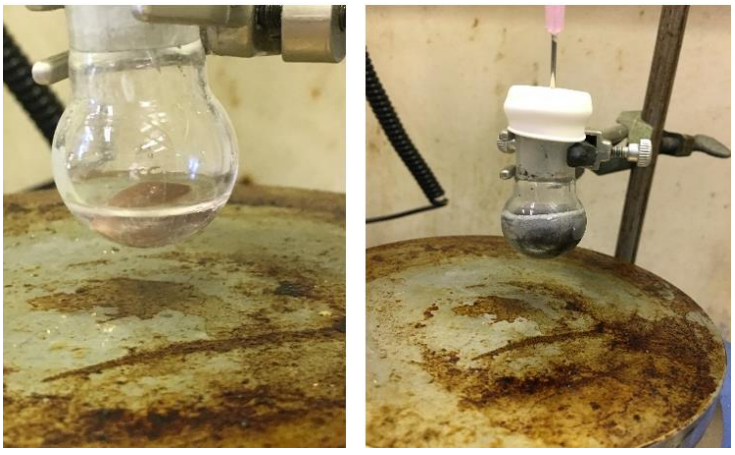

Figure 10: Pink Ni/TMPhen reaction pre-catalyst in water (left) and addition of $NaBH_4$ (right)

The loading of TMPhen with respect to the nickel was also found to be of great importance. Reducing the ligand to nickel ratio from 2:1 to 1:1 (Table 2, entry 2) saw similar conversion of starting material and selectivity for the fully dehalogenated ring but resulted in a loss in yield to 82% upon isolation. Increasing the ratio to 3:1 (entry 4) saw dramatic loss in activity of the catalyst for double dehalogenation, with a crude NMR ratio of 23:77 for **2** and **3**, respectively. Observationally, the increase of ligand results in very sluggish formation of, presumably, the active purple catalyst. With lower ligand ratios, formation of the catalyst is near instantaneous upon the addition of $NaBH_4$, whereas the 3:1 ligand to metal ratio requires minutes to form a significantly less vibrant purple material. This is congruent with a report from Holah *et. al.* which described similar activity when using phen ligated to nickel activated by sodium borohydride.[32] They found that, at high ligand to metal ratios, $Ni(phen)_3$ is prepared prior to addition of the borohydride and inhibits formation of the active hydride catalyst, whereas at lower ligand loadings a strong reducing agent, $Niphen_2BH_4 \cdot 2H_2O$, could be formed quickly.

Excess borohydride was found to be required for this transformation to proceed in high yield of the fully dehalogenated cyclopropane (Table 3). This is due to the known decomposition pathway of borohydrides in the presence of nickel borides, where a large quantity of hydrogen gas is produced quickly. The yield of **2** appears to have a strong relationship with respect to the amount of borohydride salt used. Addition of two equivalences of sodium borohydride (entry 1), already in great excess of available hydride compared to the halogenated starting material, resulted in a very poor yield of 19%. Increasing the sodium borohydride amount to between 3-5 equivalents (entries 2, 3, and 4) saw somewhat similar yields, with an increasing trend with respect to added hydride, with five equivalents reaching

77% yield. Interestingly, while keeping the amount of borohydride at five equivalents, the addition of 20 v/v % THF as co-solvent led to a marked increase in yield to 91% (entry 5). This is a known phenomenon characteristic of micellar catalysis, where the addition of an organic co-solvent has the possibility of greatly influencing the reaction yield, usually based on improved homogeneity of the reaction mixture, and/or "swelling" of the micelles.[33] Previous research from our group found that switching from sodium to potassium as the counterion associated with the borohydride can also have a beneficial effect on the yield of reduced product;[34] however, in the case of this transformation there was no difference between $NaBH_4$ and KBH_4 (entry 6).

Table 3: Effect of $NaBH_4$ on double dehalogenation

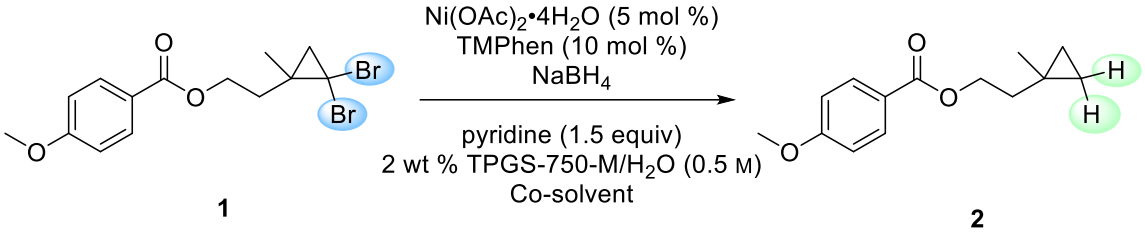

Entry	$NaBH_4$ (equiv)	Yield **2** (%)[a]
1	2	19
2	3	70
3	4	71
4	5	77
5	5	91[b]
6	5	91[b],[c]

[a] Isolated yields; [b] In presence of 20 v/v % THF; [c] KBH_4 instead of $NaBH_4$

The base used for the reaction was also intensively screened with respect to the yield of **2** (Table 4). No base (entry 1) and inorganic base K_3PO_4 (entry 2) resulted in inferior yields compared to organic bases with isolated yields of 78% and 83%, respectively. Triethylamine (entry 6) was also found to produce the dehalogenated product in a similar, lower yield of 82%. Organic bases such as DBU (entry 3), 2,6-lutidine (entry 4), and pyridine (entry 5), which share structural similarities, all gave yields between 88-91% yield. While the need for a base in this transformation is apparent, the disparity between different yields using organic bases, in the case of triethylamine *vs.* the other organic bases screened, can also be explained by the way of co-solvent effects, where DBU, lutidine, and pyridine may act as a better co-solvent and thus results in slightly higher yields.

Table 4: Organic and inorganic base screening

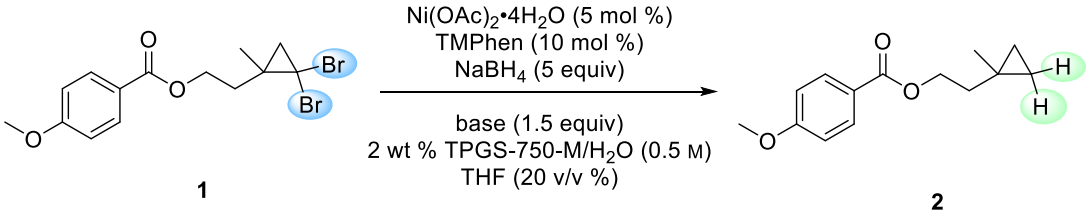

Entry	Base	Yield (%)[a]
1	no base	78
2	K_3PO_4	83
3	DBU	89
4	2,6-lutidine	88
5	pyridine	91
6	TEA	82

[a] Isolated yields

The choice in reaction medium was also determined via not only the conversion of model substrate **1** to **2**, but also from the highly lipophilic *gem*-dibromocyclopropyl fatty ester **4** to the corresponding saturated cyclopropyl ester **5** (Table 5). With respect to the model compound **1**, conversion "on-water"[35] was found to go to completion with an isolated yield of 79%. Addition of 20 v/v% THF to the on-water trial (entry 2) resulted in a boost in yield to 86%, near the optimized yield of a 2 wt % TPGS-750-M/H_2O (with 20 v/v % THF as co-solvent) micellar system (entry 8). Use of another surfactant structurally similar to TPGS-750-M, Triton X-100,[36] produced near identical conversion without co-solvent (entry 5) at 76% yield, whereas beta-sitosterol-based surfactant "Nok"[37] (entry 6) gave a lower yield of only 44%. Interestingly, switching the aqueous to organic ratio, to where THF was most of the solvent and aqueous surfactant was a 20 v/v % co-solvent (entry 10), provided **2** in quantitative yield, surpassing that of a water-based system. This contrasts with a THF only system where no water is present (entry 4), giving zero conversion of the *gem*-dibromocyclopropane. Attempting the reaction in ethanol (entry 11) resulted in a violent, highly exothermic reaction and thus was not pursued further. While conversion of **1** to **2** saw high reactivity just on-water, with and without 20 v/v% THF co-solvent, the exceedingly lipophilic **4** would not convert at all under similar conditions (entry 3). However, addition of 2 wt % TPGS-750-M to the water (entry 9) resulted not only in conversion, but also a good yield of **5** at 72%.

Table 5: Effect of reaction medium on reduction of *gem*-dibromocyclopropane

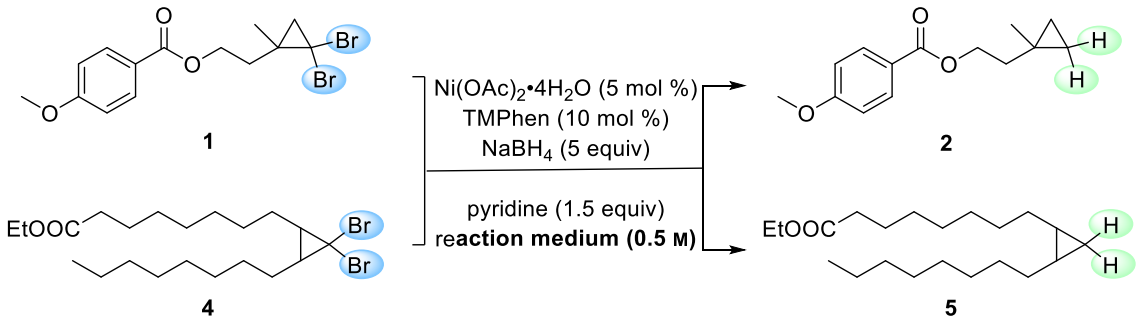

Entry	SM	Medium	Co-solvent	Yield (%)[a]
1	**1**	water	---	79
2	**1**	water	THF (20 v/v %)	86
3	**4**	water	THF (20 v/v %)	0
4	**1**	THF	---	0
5	**1**	2 wt % Tritron X-100/H_2O	---	76
6	**1**	2 wt % Nok/H_2O	---	44
7	**1**	2 wt % TPGS-750-M/H_2O	---	77
8	**1**	**2 wt % TPGS-750-M/H_2O**	**THF (20 v/v %)**	**91**
9	**4**	2 wt % TPGS-750-M/H_2O	THF (20 v/v %)	72
10	**1**	THF	2 wt % TPGS-750-M/H_2O (20 v/v %)	99
11	**1**	EtOH	---	---[b]

[a] Isolated yields of either products **2** or **5**; [b] A violent reaction ensued

We decided to move forward with the best conditions discovered for double reduction of the *gem*-dibromocyclopropane to the fully saturated cyclopropane. These conditions were found to be 5 mol % $Ni(OAc)_2$•$4H_2O$ as the nickel source, 10 mol % TMPhen ligand, 1.5 equivalents of pyridine, and 5 equivalents of $NaBH_4$ as the borohydride source. This was performed at a concentration of 0.5 M in 2 wt % TPGS-750-M/H_2O using 20 v/v % THF as co-solvent. This chemistry was found to perform best at a reaction temperature of 45 °C; however, some improvement was noted when the starting material is first dissolved in the THF

and added dropwise to the cooled, pre-made catalyst mixture in water prior to heating to reaction temperature. The transformation was also observed to be incredibly quick, requiring only 30 minutes for most substrates attempted for full conversion. The reaction can also be run under argon pressure or using the H_2 gas produced as a byproduct in a sealed system. The system can be maintained at one atmosphere by sealing the reaction in a round bottomed flask with a septum and piercing the septum with a syringe, where the hydrogen can move the plunger as more gas is produced. Running the reaction under air, however, results in zero conversion of the starting material, and the reaction can be halted by opening up the flask to the ambient atmosphere. Unfortunately, while these conditions worked very well for the di-dehalogenation of *gem*-dibromocycloproapnes, *gem*-dichlorocyclopropanes resisted reduction or would produce a variety of compounds observed by thin-layer chromatography which ultimately caused us to abandon this potential route.

With these conditions developed from the optimization of **2** in hand, we set forth to apply this methodology to an array of functionalized, pharmaceutically relevant substrates (Figure 11). Ethyl dihydrosterculate **5**, an ester of a precursor to a natural antiparasitic sterculic acid, was prepared in aqueous medium at 72% yield despite its high lipophilicity. This can also be seen in the transformation of a perbenzylated glucal derivative **6**, which could be dehalogenated in a similar yield of 73% with no observed deprotection of the alcohols. The δ-lactam **7**, a fragment of a precursor to an inhibitor of a nitric oxide synthase,[38] was also synthesized in 91% yield; however, due to the delicate nature of the fused ring, the reaction had to be performed at room temperature. Tosylate **8**, which could be considered labile in basic aqueous media in the presence of nickel, was also well tolerated and afforded an 82% yield. Naphthyl ester **9**, which would not survive other reported reduction methods such as $LiAlH_4$

or Birch-type conditions, was dehalogenated in high yield (91%). Compound **10** was found to be especially difficult to convert in a mostly aqueous system due to the size and hydrophobicity of the cholesterol side chain and formed a gum under traditional conditions. However, increasing the aqueous surfactant/THF ratio to 1:1 resulted in a mixable medium that gave the cyclopropyl product in 73% yield with no observed reduction of the olefin. Interestingly, running this same substrate in a bomb reactor allowed for depletion of the amount of THF required, where now 20 v/v % compared to the aqueous medium at a global concentration of 0.5 M was sufficient to produce **10** in 60% yield. Lipophilic furoate ester **11** was converted in a modest yield (60%) with no detection of reduction of the heterocycle to either dihydro- or tetrahydro-furan side products. Tryptophan derivative **12** was also converted in high yield. Surprisingly, protection of the indole nitrogen was not required in this case, which exemplifies the robustness of this method. A derivative of the Novartis Boc-protected spiroproline could be recovered in 86% yield; unfortunately, the dehalogenation could not be performed directly on the acid, and thus had to be used as the benzyl ester which, again, was stable under these conditions. Compound **14**, which originally had a bromide on the 4-position of the aromatic ring, saw dehalogenation not only at the site of the cyclopropane, but also on the aromatic halogen. This was observed to be the case of aromatic chlorides by GMCS analysis, as well. Olaparib[39] precursor **15** was synthesized in 70% yield despite the proximity of the cyclopropane to an electron withdrawing group. Unprotected 2-aminopyrimidine **16** was also well-tolerated giving 71% conversion to the cyclopropane; however, this product, as well as compounds **12** and **19**, needed to be treated post-reaction with dilute HCl in methanol to remove the nitrogen-borane complex formed from the reaction conditions. Styrene derivative **17** gave a very high yield of 96%. This is in stark contrast to other cyclopropyl styrene-related

compounds that are not substituted at the *beta*-position of the originating olefin, which only gave polymer as product from attempts at reduction. Unsurprisingly, **18** resulted in product with a reasonably good yield of 79%. Finally, while electron-rich pyridine **19** could be prepared in a decent yield of 66%, other electron-poor pyridines such as nicotinoyl derivatives resulted not only in dehalogenation, but also in varying degrees of reduction of the heterocycle.

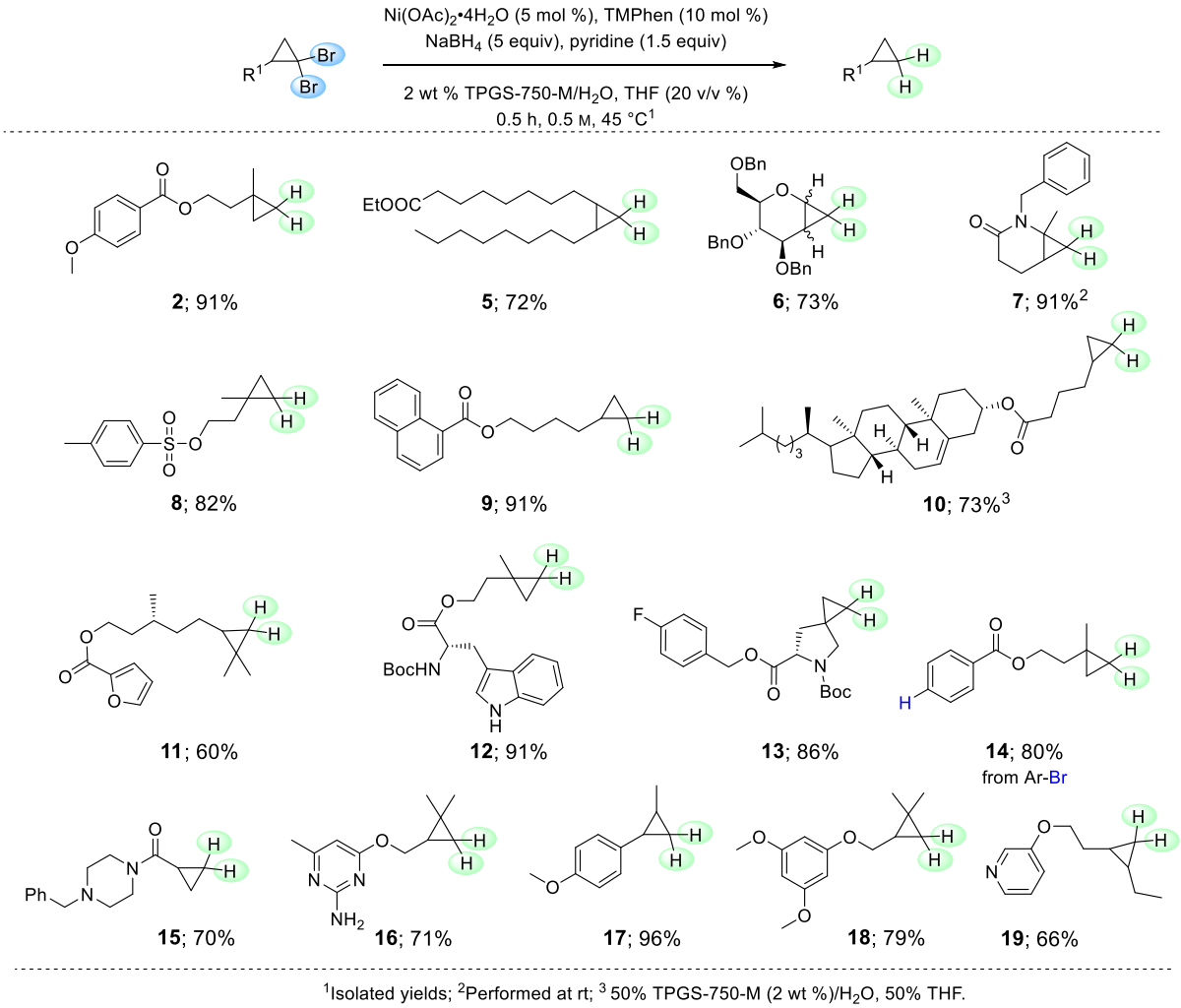

Figure 11: Substrate scope of the di-dehalogenation of *gem*-dibromocyclopropanes

Given the success of this di-dehalogenation chemistry applied to a wide array of functionalized molecules, we found it imperative next to explore the scope of mono-debrominations to form the interesting bromocyclopropyl building block. There exists quite a bit of overlap in the literature between mono-dehalogenation and di-dehalogenation, including the use of $LiAlH_4$,[40] Bu_3SnH,[41], and electrochemistry.[26] Other reports, such as use of methylmagnesium bromide,[42] also exist but still fall prey to the requirement of using non-renewable, environmentally deleterious organic solvents. As a recent alternative to the dehalogenation route, Ideka *et. al.*[43] put forth a chromium-based methodology to directly form the monobromocyclopropane from an olefin; however, the use of the toxic metal obviates a significant amount of the industrial applicability of this approach.

As previously noted, a significantly lower catalyst loading with 2,2'-bypridine as ligand, with less sodium borohydride at 2.5 equivalents, results in a high isolated yield of **3** of 91% with near quantitative selectivity based on an analysis of crude material by NMR. We then attempted these same conditions on a small subset of examples from the di-dehalogenation section (Figure 12). A variety of substrates, including brominated aromatic **20** (98% yield), tryptophan derivative **22** (88% yield), and spiroproline **23** (90% yield) could all be isolated in very high yields.

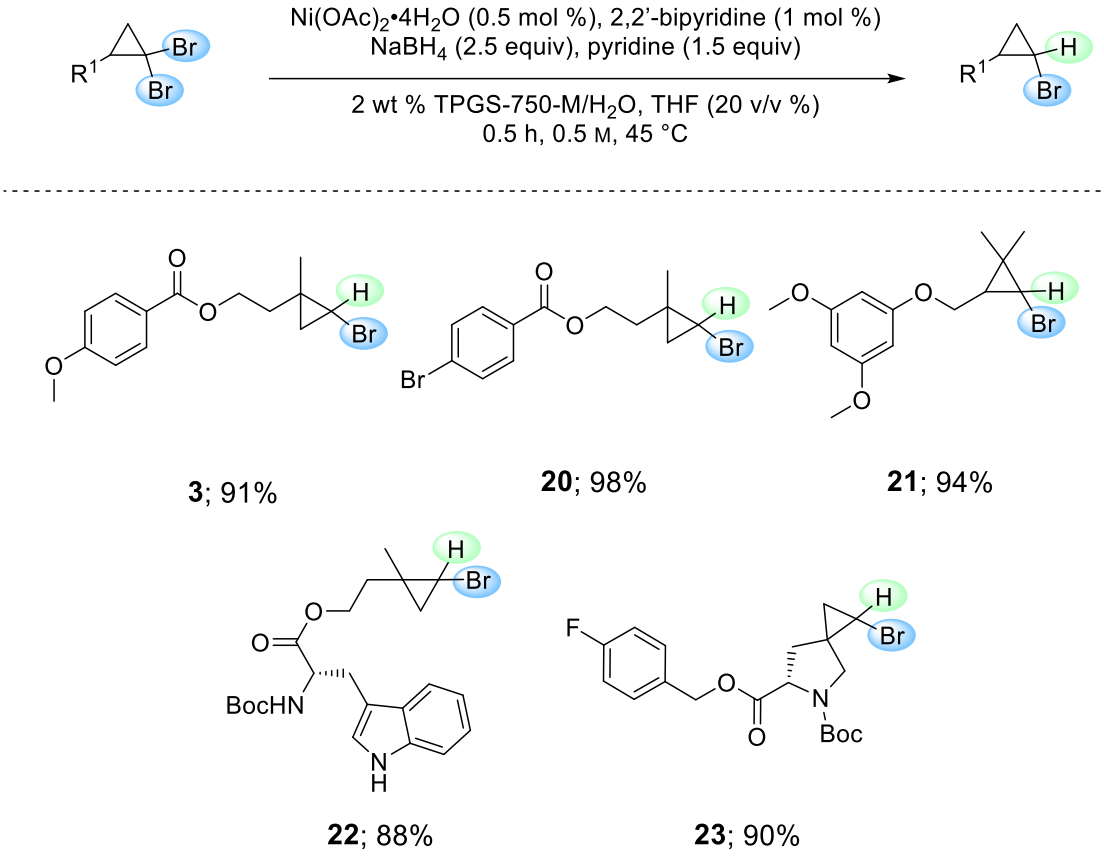

Figure 12: Scope of mono-debromination of *gem*-dibromocyclopropanes

Most interestingly, compound **20** elucidates a powerful aspect of the mono-debromination methodology. Given tribrominated starting material **24**, the *gem*-dibromocyclopropane could be selectively mono-dehalogenated in the presence of an aromatic bromide (Figure 13). This is in contrast to the di-dehalogenation chemistry using TMPhen as the ligand, which is not selective for the cyclopropyl bromides only and dehalogenates the molecule globally.

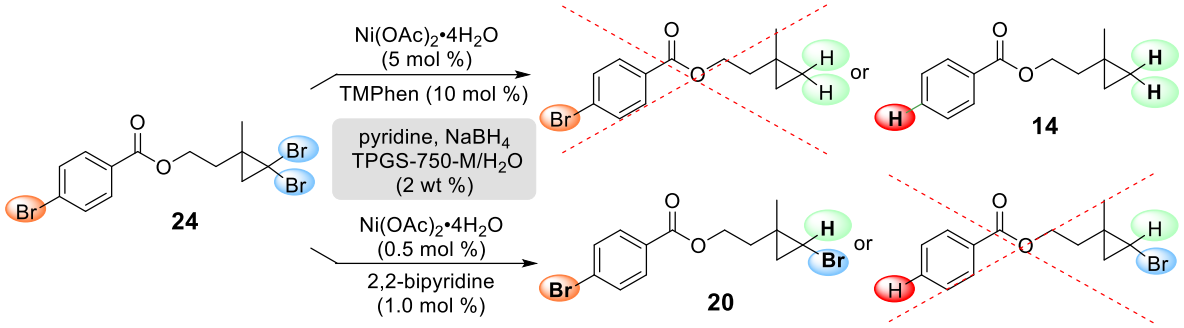

Figure 13: Mono-debromination chemistry vs di-debromination methods for dehalogenation selectivity

Of great importance to the pharmaceutical industry is the issue of residual metals in the organic products post-reaction. Indeed, the FDA maximum allowed concentration limits of nickel for components used in oral drug products is <20 μg/g, or 20 ppm/dose/day.[44] We found that, in the case of workup for **2**, product from this methodology could simply be extracted from the aqueous phase using ethyl acetate. Passing these organics through a plug of silica gel results in a nickel concentration of <2 ppm, well below the FDA allowance with no need of expensive metal scavenging chemistry (Figure 14).

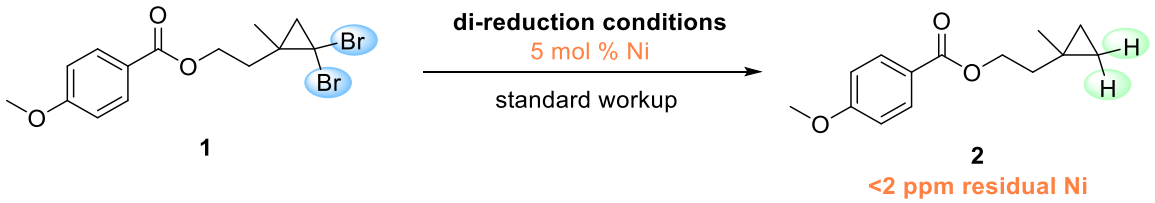

Figure 14: Residual nickel analysis of di-reduction product

A powerful attribute of aqueous based chemistry is the aspect of being a universal reaction medium, *i.e.*, where multiple reactions benefit from, and are amenable to, micellar catalysis.

This can be taken advantage of with respect to route selection, where multiple reactions can be run in tandem in the same medium and in the same reactor. This results in improvements of both "pot"[45] and "time"[46] economy, as well as reducing the amount of waste produced from running multiple reactions in a stepwise sequence where, at minimum, solvent would need to be used for workup and transferring of material.[47] Therefore, we developed a 2-step, 1-pot sequence taking into consideration the robustness of the nickel reduction chemistry (Figure 15). Firstly, tribrominated compound **24** could easily be coupled with 4-methoxy-2-methylphenyl boronic acid involving a new group ligand, N_2Phos,[48] using only 1000 ppm, or 0.1 mol %, palladium. Then, without workup, the *gem*-dibromocyclopropane was cleanly di-dehalogenated in the same reaction vial simply by adding the Ni/TMPhen pre-catalyst with pyridine in water followed by activation with sodium borohydride to result in product **25** in 86% yield over two steps.

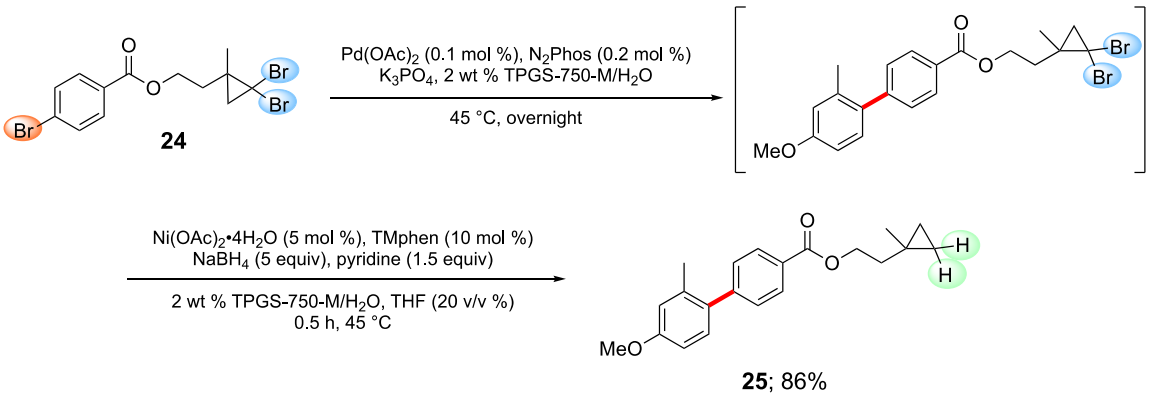

Figure 15: 2-step, 1-pot sequence utilizing *gem*-dibromocyclopropane di-dehalogenation method

A major beneficial facet of aqueous based chemistry is the depletion of wasteful organic solvent used for the reaction. This can be measured in one way by the reaction E Factor as

defined by Sheldon,[49] or the quotient of the mass of waste produced *vs.* the mass of product formed. The "greenness" of micellar chemistry is based in the recyclability of the reaction medium, whereas extraction or filtration of the product opens up the possibility of reusing the water which, hence, is not factored into the E Factor equation. Therefore, the E Factor of the reaction from **1** to **2** can be observed to be impressively low, as only a minimal amount of organic extraction solvent is needed. Thus, only 80 μL of ethyl acetate used three times *vs.* 400 μL of 2 wt % TPGS-750-M/H_2O post-reaction (Figure 16), when taken into consideration with the THF used for the reaction, results in an astoundingly low E Factor of 5. This is in comparison to other pharmaceutical reactions which can be as high as 25-100.

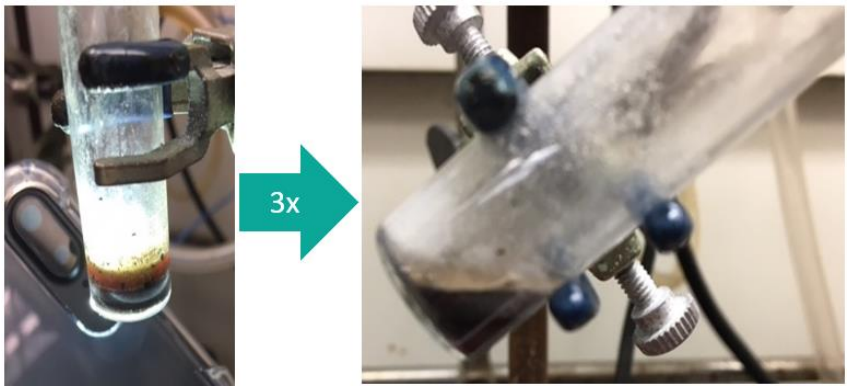

Figure 16: First (left) and third (right) minimal extractions of aqueous phase

Furthermore, we found that the aqueous phase could be recycled a minimum of three times at a 0.75 mmol scale (Table 6). This can be accomplished by extracting product from the aqueous phase, followed by filtration of the water through Celite to remove insoluble material. The reaction can then be set up again using the same aqueous surfactant without consequence by adding fresh metal, ligand, base, and sodium borohydride.

Table 6: Recycling of the aqueous phase used for the reduction method

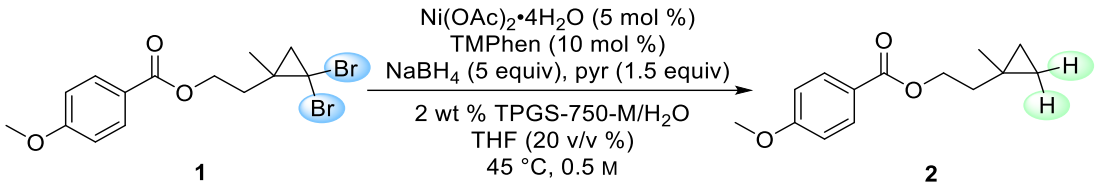

Entry	Reaction	Mass Product (mg)	Yield (%)
1	Initial	171.8	85
2	First recycle	183.1	90
3	Second recycle	169.9	84

The use of hydride reagents to produce a cyclopropyl protium species behooves investigation into an analogous incorporation of deuterium using deuteride reagents. We decided to first explore the mono-deuteration of the cyclopropane using the mono-debromination methodology with 2,2'-bipyridine as ligand (Table 7). Using sodium borodeuteride by itself (entry 1) found minimal deuterium incorporation on the ring of 18% by NMR analysis of the product mixture. In order to determine if other reagents were responsible for the source of the hydride equivalent for the reduction chemistry, a variety of other deuterated reagents were tested in this system in a methodical manner. Using $NaBD_4$, THF-d_8 (entry 2), D_2O (entry 3), and pyridine-d_5 (entry 4) by themselves all gave little to no deuterium incorporation. Increasing the number of deuterated reagents together led to incorporations between 30-84% (entries 5-8), where the greatest deuteration on the bromocyclopropane resulted when all deuterated species were present with 2 wt % TPGS-750-M. A final trial found that removal of TPGS-750-M from the aqueous phase resulted in nearly quantitative mono-deuteration.

Table 7: Mono-deuteration of a *gem*-dibromocyclopropane using mono-reduction chemistry with varying deuterated species

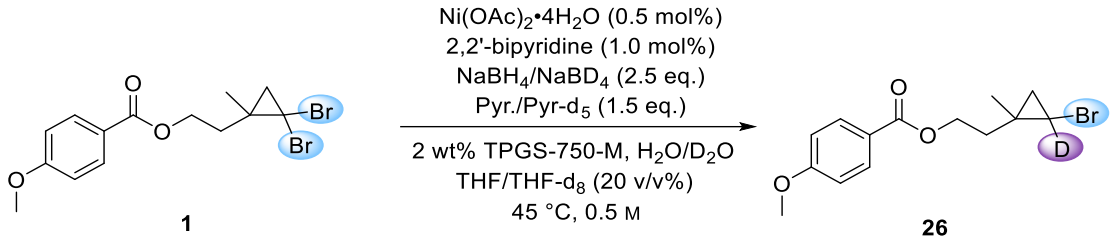

Entry	Reductant	Organic Solvent	Aqueous Solvent	Base	Observations- Crude NMR
1	$NaBD_4$	THF	H_2O	pyridine	18% D incorporation
2	$NaBH_4$	THF-d_8	H_2O	pyridine	6% D incorporation
3	$NaBH_4$	THF	D_2O	pyridine	No D incorporation
4	$NaBH_4$	THF	H_2O	pyridine-d_5	3% D incorporation
5	$NaBD_4$	THF	D_2O	pyridine	30% D incorporation
6	$NaBD_4$	THF- d_8	D_2O	pyridine	68% D incorporation
7	$NaBD_4$	THF- d_8	D_2O	pyridine	71% D incorporation
8	$NaBD_4$	THF- d_8	D_2O	pyridine-d_5	84% D incorporation
9	$NaBD_4$	THF- d_8	D_2O; no TPGS	pyridine-d_5	93% D incorporation

This result is highly interesting, and potentially provides insight towards a mechanistic explanation for this reduction. In this case, TPGS-750-M is acting as a source of protons, pointing towards a radical chain mechanism for this first dehalogenation. As previously stated, Holah *et al*. found that treatment of nickel ligated with either phenanthroline or 2,2'-bipyridine ligands results in a strong reducing agent, $Ni(ligand)_2BH_4 \cdot 2H_2O$.[32] This Ni(I) species, which is most likely the active catalyst could, in turn, prepare a borane radial anion which is responsible for the chemistry. This could open up TPGS-750-M as a potential source of available protons, leading to non-selective isotope incorporation onto the ring.

Experimentation using deuterium chemistry also leads to the possibility that the two bromides are reduced stepwise via distinct mechanisms, where the ligands dictate the selectivity towards mono-dehalogenation *vs*. di-dehalogenation. This can be observed when

monobromocyclopropane **3** is further subjected either to a second trial of mono-dehalogenation chemistry using 2,2'-bipyridine as ligand and sodium borodeuteride as reductant or is followed up with di-dehalogenation conditions under the same stipulations (Figure 17). The reaction does not proceed further when subjected to Condition 1, returning only starting material. However, addition of TMPhen in place of the bipyridine ligand results in complete conversion of the monobromocyclopropane to the saturated mixed isotope cyclopropane, as well as complete deuterium incorporation.

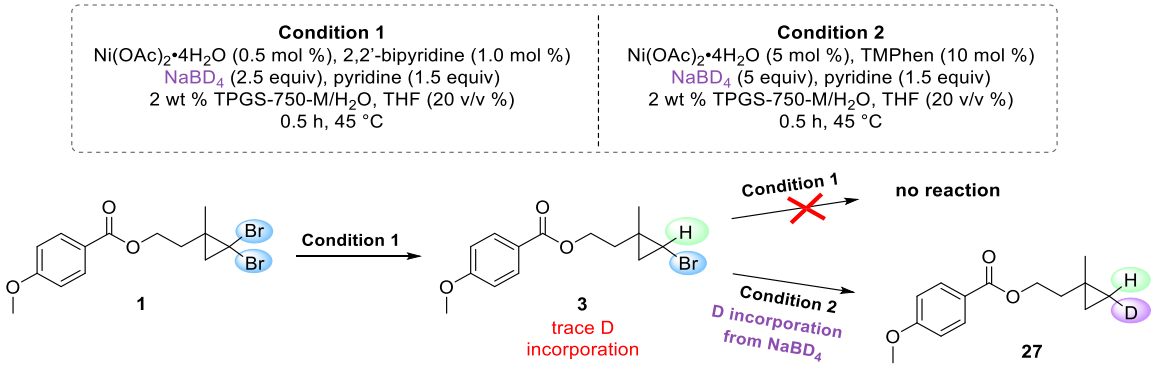

Figure 17: Investigation into the second dehalogenation mechanism using mono- and di-reduction methods

These results lead us to explore dideuteration directly on **1** using the didehalogenation chemistry with TMPhen as ligand (Table 8). Similar to the monodeuteration attempts, trials using only D_2O (entry 1) or THF-d_8 (entry 2) as the deuterium source gave zero deuterium incorporation onto the ring. Interestingly, use of sodium borodeuteride by itself gave predominantly monodeuterium incorporation with full consumption of the starting material to didehalogenated product (entry 3), whereas similar conditions but adding D_2O (entry 5) or

THF-d_8 (entry 6) to the mixture with sodium borodeuteride yielded a mixture of mono- and di-deuterium incorporated product.

Table 8: Deuteration permutations for di-debromination of **1**

Entry	Reductant	Organic Solvent	Aqueous Solvent	Product(s) - Crude NMR
1	$NaBH_4$	THF	D_2O	No D incorporation
2	$NaBH_4$	THF-d_8	H_2O	No D incorporation
3	$NaBD_4$	THF	H_2O	Mono- D incorporation
4	**$NaBD_4$**	**THF-d_8**	**D_2O**	**Di- D incorporation**
5	$NaBD_4$	THF	D_2O	Mono and di- D incorporation
6	$NaBD_4$	THF-d_8	H_2O	Mono and di- D incorporation

As in the monodeuteration chemistry, the method for didehalogenation in the presence of fully deuterated reagents sodium borodeuteride, THF-d_8, and D_2O resulted majorly in dideuterium incorporation based on analysis of the crude material by NMR. Use with and without TPGS-750-M did not apparently give any difference in incorporation in this case. This material could be separated via column chromatography to result in the dideuterated isotope cyclopropane **28** in 53% yield (Figure 18).

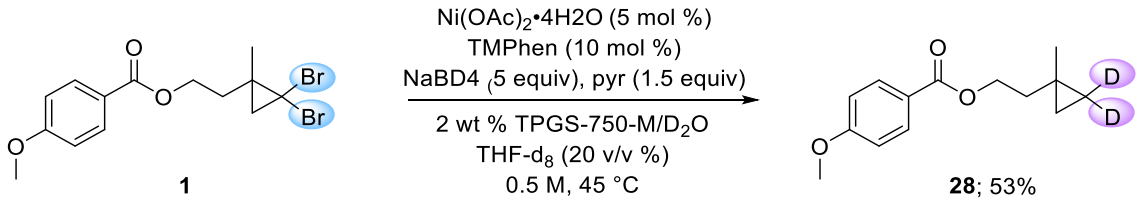

Figure 18: Di-deuteration of a *gem*-dibromocyclopropane

Put together, the combination of different mono- and di-dehalogenation techniques for this system can be employed together to form any desired cyclopropane isotope permutation (Figure 19).

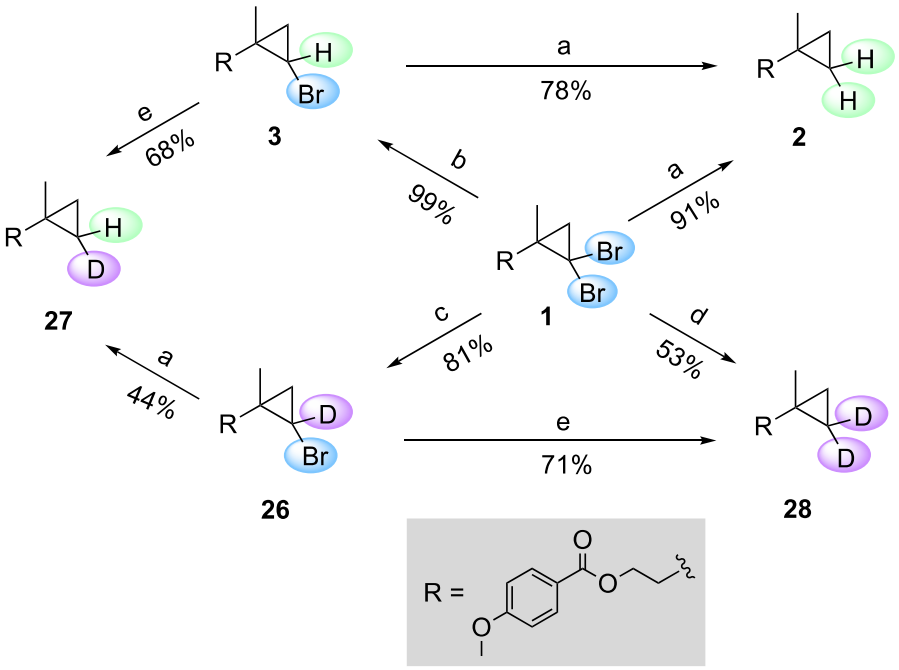

(a) $Ni(OAc)_2•4H_2O$ (5 mol %), TMPhen (10 mol %), pyridine (1.5 equiv), and $NaBH_4$ (5 equiv) in 2 wt % $TPGS/H_2O$ (20 v/v % THF).

(b) $Ni(OAc)_2•4H_2O$ (0.5 mol %), BiPy (1.0 mol %), pyridine (1.5 equiv), and $NaBH_4$ (2.5 equiv) in 2 wt % $TPGS/H_2O$ (20 v/v % THF).

(c) $Ni(OAc)_2•4H_2O$ (0.5 mol %), BiPy (1.0 mol %), pyridine-d_5 (1.5 equiv), and $NaBD_4$ (2.5 equiv) in 2 wt % $TPGS/D_2O$ (20 v/v % THF-d_8).

(d) $Ni(OAc)_2•4H_2O$ (5 mol %), TMPhen (10 mol %), pyridine (1.5 equiv), and $NaBD_4$ (5 equiv) in 2 wt % $TPGS/D_2O$ (20 v/v % THF-d_8).

(e) $Ni(OAc)_2•4H_2O$ (5 mol %), TMPhen (10 mol %), pyridine (1.5 equiv), and $NaBD_4$ (5 equiv) in 2 wt % $TPGS/H_2O$ (20 v/v % THF).

Figure 19: Permutations of mono- and di-dehalogenations to provide protium/deuterium cyclopropanes

1.4 Conclusions

In conclusion, a robust methodology for the mono- and di-reduction of *gem*-dibromocyclopropanes in aqueous micellar media has been developed. This chemistry is safe, while the catalyst is easy to prepare, simply requiring an inexpensive and catalytic nickel(II) salt, TMPhen or 2,2'-bipyridine as ligands, pyridine, and sodium borohydride as an activating agent in 2 wt % TPGS-750-M/H_2O that benefits from a small amount (20 v/v %) of THF as organic co-solvent. The reaction can be run at or near ambient temperatures and atmosphere, requiring no pressurized gas to enact hydrogenation. This transformation boasts a large, diverse substrate scope of pharmaceutically interesting, functionalized molecules for both the mono- and di-reduction conditions, providing good-to-excellent yields of the corresponding cyclopropane product. The overall environmentally friendly aspects of the chemistry are exemplified by low residual metal in the products after a simple workup protocol, low E Factors even when organic solvents are used for extraction, and recycling capabilities of the aqueous phase for multiple reactions without need for replenishing with fresh water between runs. Finally, deuterium incorporation is possible for both methodologies, and offers interesting insight into the potentially radical-based nature of this method of cyclopropane formation.

1.5 References

1. Wu, W.; Lin, Z.; Jiang, H. *Org. Biomol. Chem.* **2018**, *16*, 7315–7329.
2. Matsuo, N. *Proc. Jpn. Acad., Ser. B* **2019**, *95*, 378–400.
3. Nunn, J. R. *J. Org. Chem.* **1952**, 313-318.
4. Njardarson Group, *Top 200 Pharmaceutical Products by Retail Sales in 2018* - https://njardarson.lab.arizona.edu/sites/njardarson.lab.arizona.edu/files/2018Top200PharmaceuticalRetailSalesPosterLowResFinalV2.pdf, **2019**. (Accessed January 3, 2022).
5. Talele, T. T. *J. Med. Chem.* **2016**, *59*, 8712–8756.
6. Blanksby, S. J.; Ellison, G. B. *Acc. Chem. Res.* **2003**, *36*, 255–263.
7. Gentles, R. G.; Ding, M.; Bender, J. A.; Bergstrom, C. P.; Grant-Young, K.; Hewawasam, P.; Hudyma, T.; Martin, S.; Nickel, A.; Regueiro-Ren, A.; Tu, Y.; Yang, Z.; Yeung, K.-S.; Zheng, X.; Chao, S.; Sun, J.-H.; Beno, B. R.; Camac, D. M.; Chang, C.-H.; Gao, M.; Morin, P. E.; Sheriff, S.; Tredup, J.; Wan, J.; Witmer, M. R.; Xie, D.; Hanumegowda, U.; Knipe, J.; Mosure, K.; Santone, K. S.; Parker, D. D.; Zhuo, X.; Lemm, J.; Liu, M.; Pelosi, L.; Rigat, K.; Voss, S.; Wang, Y.; Wang, Y.-K.; Colonno, R. J.; Gao, M.; Roberts, S. B.; Gao, Q.; Ng, A.; Meanwell, N. A.; Kadow, J. F. *J. Med. Chem.* **2014**, *57*, 1855–1879.
8. Yu, K.-L.; Sin, N.; Civiello, R. L.; Wang, X. A.; Combrink, K. D.; Gulgeze, H. B.; Venables, B. L.; Wright, J. J. K.; Dalterio, R. A.; Zadjura, L.; Marino, A.; Dando, S.; D'Arienzo, C.; Kadow, K. F.; Cianci, C. W.; Li, Z.; Clarke, J.; Genovesi, E. V.; Medina, I.; Lamb, L.; Colonno, R. J.; Yang, Z.; Krystal, M.; Meanwell, N. A. *Bioorg. & Med. Chem. Lett.* **2007**, *17*, 895–901.

9. Wityak, J.; Das, J.; Moquin, R. V.; Shen, Z.; Lin, J.; Chen, P.; Doweyko, A. M.; Pitt, S.; Pang, S.; Shen, D. R.; Fang, Q.; de Fex, H. F.; Schieven, G. L.; Kanner, S. B.; Barrish, J. C. *Bioorg. & Med. Chem. Lett.* **2003**, *13*, 4007–4010.
10. Kulinkovich, O. G. *Cyclopropanes in Organic Synthesis: Kulinkovich/Cyclopropanes in Organic Synthesis*; John Wiley & Sons, Inc: Hoboken, NJ, **2015**.
11. Ebner, C.; Carreira, E. M. *Chem. Rev.* **2017**, *117*, 11651–11679.
12. Simmons, H. E.; Smith, R. D. *J. Am. Chem. Soc.* **1958**, *80*, 5323–5324.
13. Simmons, H. E.; Smith, R. D. *J. Am. Chem. Soc.* **1959**, *81*, 4256–4264.
14. Davies, H. M. L.; Beckwith, R. E. J. *Chem. Rev.* **2003**, *103*, 2861–2904.
15. Corey, E. J.; Chaykovsky, M. *J. Am. Chem. Soc.* **1965**, *87*, 1353–1364.
16. Kulinkovich, O. G.; Sviridov, S. V.; Vasilevskii, D. A.; Prityts kaya, T. S. *Zh. Org. Khim.* **1989**, *25*, 2244−2245.
17. Nicolas, I.; Le Maux, P.; Simonneaux, G. *Coordination Chemistry Reviews,* **2008**, *252*, 727–735.
18. Wurz, R. P.; Charette, A. B. *Org. Lett.* **2002**, *4*, 4531–4533.
19. Fedoryński, M. *Chem. Rev.* **2003**, *103*, 1099–1132.
20. Geuther, A. *Ann.*, **1862**, *123*, 121.
21. von E. Doering, W.; Hoffmann, A. K. *J. Am. Chem. Soc.* **1954**, *76*, 6162–6165.
22. Mαkosza, M.; Wawrzyniewicz, M. *Tetrahedron Lett.* **1969,** *53*, 4659-4662.
23. Bänziger, M.; Bucher, C. *Chim. Oggi.* **2015**, *33*, 50-55.
24. For representative examples of hydride reduction of *gem*-dibromocyclopropanes, see: a) Averina, E. B.; Budynina, E. M.; Grishin, Y. K.; Zefirov, A. N.; Kuznetsova, T. S.; Zefirov, N. S. *Russ. J. Org. Chem.* **2001**, *37*, 1409-1413; b) Baldwin, J. E.; Adlington,

R. M.; Marquess, D. G.; Pitt, A. R.; Porter, M. J.; Russell, A. T. *Tetrahedron* **1996**, *52*, 2515–2536; c) Tsue, H.; Imahori, H.; Kaneda, T.; Tanaka, Y.; Okada, T.; Tamaki, K.; Sakata, Y. J. *J. Am. Chem. Soc.* **2000**, *122*, 2279–2288; d) Fernandez-Megia, E.; Gourlaouen, N.; Ley, S. V.; Rowlands, G. J. *Synlett* **1998**, *1998*, 991–994; e) Seyferth, D.; Yamazaki, H.; Alleston, D. L. *J. Org. Chem.* **1963**, *28*, 703–706; f) Mataka, S.; Sawada, T.; Tashiro, M.; Taniguchi, M.; Mitroma, Y. *J. Chem Res.* **1997**,*2*, 48–49; g) Jefford, C. W.; Kirkpatrick, D.; Delay, F. *J. Am. Chem. Soc.* **1972**, *94*, 8905–8907; h) Ramana, C. V.; Murali, R.; Nagarajan, M. *J. Org. Chem.* **1997**, *62*, 7694–7703.

25. For representative examples of Birch-type conditions for reduction of *gem*-dibromocyclopropanes, see: a) von Seebach, M.; Kozhushkov, S. I.; Boese, R.; Benet-Buchholz, J.; Yufit, D. S.; Howard, J. A. K.; de Meijere, A. *Angew. Chem. Int. Ed.* **2000**, *39*, 2495–2498; b) Oku, A.; Tsuji, H.; Yoshida, M.; Yoshiura, N. *J. Am. Chem. Soc.* **1981**, *103*, 1244–1246; c) Martínez-Pérez, J. A.; Sarandeses, L.; Granja, J.; Palenzuela J.; Mouriño, A. *Tettrahedron Lett.* **1998**, *39*, 4725-4728; d) Vogel, E.; Wiedemann, W.; Roth, H. D.; Eimer, J.; Günther, H. *Justus Liebigs Ann. Chem.* **1972**, *759*, 1–36; e) Sugimura, T.; Futagawa, T.; Karagiri, T.; Nishiyama, N.; Tai, A. *Tetrahedron Lett.* **1996**, *37*, 7303–7306; f) Paquette, L. A.; Chamot, E.; Browne, A. R. *J. Am. Chem. Soc.* **1980**, *102*, 637–643; g) Baldwin, J. E.; Shukla, R. *J. Phys. Chem. A.* **1999**, *103*, 7821–7825; h) Kraus, W.; Klein, G.; Sadlo, H.; Rothenwöhrer, W. *Synthesis*, **1972**, 485-487; i) Sheikh, Y. M.; Leclercq, J.; Djerassi, C. *J. Chem. Soc., Perkin Trans.* **1974**, 909-914.
26. Gütz, C.; Selt, M.; Bänziger, M.; Bucher, C.; Römelt, C.; Hecken, N.; Gallou, F.; Galvão, T. R.; Waldvogel, S. R. *Chem. Eur. J.* **2015**, *21*, 13878–13882.

27. Isley, N. A.; Hageman, M. S.; Lipshutz, B. H. *Green Chem.* **2015**, *17*, 893–897.

28. Khurana, J. M.; Gogia, A. *Org. Prep. Proced. Int.* **1997**, *29*, 1–32.

29. Isley, N. A.; Wang, Y.; Gallou, F.; Handa, S.; Aue, D. H.; Lipshutz, B. H. *ACS Catal.* **2017**, *7*, 8331–8337.

30. (a) Pang, H.; Wang, Y.; Gallou, F.; Lipshutz, B. H. *J. Am. Chem. Soc*. **2019**, *141*, 17117–17124. (b) Lippincott, D. J.; Trejo-Soto, P. J.; Gallou, F.; Lipshutz, B. H. *Org. Lett.* **2018**, *20*, 5094–5097.

31. Brown, C. A.; Brown, H. C. *J. Am. Chem. Soc.* **1963**, *85*, 1003–1005.

32. Holah, D. G.; Hughes, A. N.; Hui, B. C. *Can. J. Chem*. **1977**, *55*, 4048–4055.

33. Gabriel, C. M.; Lee, N. R.; Bigorne, F.; Klumphu, P.; Parmentier, M.; Gallou, F.; Lipshutz, B. H. *Org. Lett.* **2017**, *19*, 194–197.

34. Gabriel, C. M.; Parmentier, M.; Riegert, C.; Lanz, M.; Handa, S.; Lipshutz, B. H.; Gallou, F. *Org. Process Res. Dev*. **2017**, *21*, 247–252.

35. Rideout, D. C.; Breslow, R. *J. Am. Chem. Soc.* **1980**, 102, 7816–7817.

36. Koley, D.; Bard, A. J. *PNAS* **2010**, *107*, 16783–16787.

37. Klumphu, P.; Lipshutz, B. H. *J. Org. Chem*. **2014**, *79*, 888–900.

38. Kawanaka, Y.; Kobayashi, K.; Kusuda, S.; Tatsumi, T.; Murota, M.; Nishiyama, T.; Hisaichi, K.; Fujii, A.; Hirai, K.; Naka, M.; Komeno, M.; Nakai, H.; Toda, M. *Eur. J. Med. Chem.* **2003**, *38*, 277–288.

39. *Small Molecules in Oncology*; Martens, U. M., Ed.; Recent Results in Cancer Research; Springer International Publishing: Cham, **2018**; Vol. 211.

40. Masuno, M. N.; Young, D. M.; Hoepker, A. C.; Skepper, C. K.; Molinski, T. F. *J. Org. Chem.* **2005**, *70*, 4162–4165.

41. Seyferth, D.; Yamazaki, H.; Alleston, D. L. *J. Org. Chem*. **1963**, *28*, 703–706.

42. Seyferth, D.; Prokai, B. *J. Org. Chem.* **1966**, *31*, 1702–1704.

43. Ikeda, H.; Nishi, K.; Tsurugi, H.; Mashima, K. *Chem. Sci.* **2020**, *11*, 3604–3609.

44. USP, *Elemental Impurities – Limits* Https://www.usp.org/sites/default/files/usp/document/our-work/chemical-medicines/key-issues/c232-usp-39.pdf (Accessed January 3, 2022).

45. Hayashi, Y. *Chem. Sci*. **2016**, *7*, 866–880.

46. Hayashi, Y. *J. Org. Chem*. **2021**, *86*, 1–23.

47. Cosgrove, S. C.; Thompson, M. P.; Ahmed, S. T.; Parmeggiani, F.; Turner, N. J. *Angew. Chem., Int. Ed.* **2020**, *59*, 18156–18160.

48. Akporji, N.; Thakore, R. R.; Cortes-Clerget, M.; Andersen, J.; Landstrom, E.; Aue, D. H.; Gallou, F.; Lipshutz, B. H. *Chem. Sci.* **2020**, *11*, 5205–5212.

49. Sheldon, R. A. *Green Chem.* **2007**, *12, 1261-1384.*

1.6 Experimental Data

1. General Information

All commercial reagents were used without further purification unless otherwise noted. Organic solvents specified as dry and/or degassed such as THF or toluene were either taken from a solvent purification system (Pure-Solv 400, Innovative Technology, Inc. (now Inert, Inc.)), or degassed using a stream of bubbling argon for a minimum of 1 h and involved less than 25 mL of volume. All other solvents were used as received, such as MeOH, EtOAc, hexanes, and Et_2O, unless otherwise noted, and purchased from Fisher Scientific. Sodium borohydride was purchased from Millipore-Sigma and stored in a dry, argon-filled glove box. The surfactant, TPGS-750-M, was prepared via a standard literature procedure,[1] or can be purchased from Millipore-Sigma (catalog #733857 for a 2 wt % solution of the wax dissolved in water). A standard 2 wt % aqueous solution of TPGS-750-M was typically prepared on a 100 g scale by dissolving 2 g of the wax into 98 g of thoroughly degassed (steady stream of argon, minimum of 1 h bubbling time with stirring) HPLC grade water in a 250 mL round bottomed flask equipped with a stir bar and allowed to dissolve overnight with vigorous stirring under argon pressure (NOTE: Do not attempt to degas the aqueous phase with surfactant wax submerged; vigorous foaming to the point of overflowing may occur). The 2 wt % TPGS-750-M/H2O solution, once prepared, was kept under argon pressure at all times. Thin-layer chromatography (TLC) was performed using Silica Gel 60 F254 plates (Merck, 0.25 mm thick). Flash chromatography is either performed in glass columns or an automated Biotage system using Silica Gel 60 (Silicycle, 40-63 nm). ^{1}H and ^{13}C NMR were recorded at 25 °C on a Varian Unity Inova 400 MHz, a Varian Unity Inova 500 MHz, or on a Varian Unity Inova 600 MHz spectrometer in $CDCl_3$ with residual $CHCl_3$ (^{1}H = 7.26 ppm, ^{13}C =

77.16 ppm) or in DMSO-d_6 with residual $(CH_3)_2SO$ (^1H = 2.50 ppm, ^{13}C = 39.52 ppm) as internal standards. Chemical shifts are reported in parts per million (ppm). NMR Data are reported as follows: chemical shift, multiplicity (s = singlet, d = doublet, dd = doublet of doublets, ddd = doublet of doublet of doublets, t = triplet, td = triplet of doublets, q = quartet, quin = quintet, m = multiplet), coupling constant (if applicable), and integration. High-resolution mass analyses (HRMS) were recorded on a Waters Micromass LCT TOF ES+ Premier mass spectrometer using ESI ionization.

2. General procedure for the synthesis of *gem*-dibromocyclopropanes

The following library of *gem*-dibromocyclopropanes was synthesized according to the literature.[2,3]

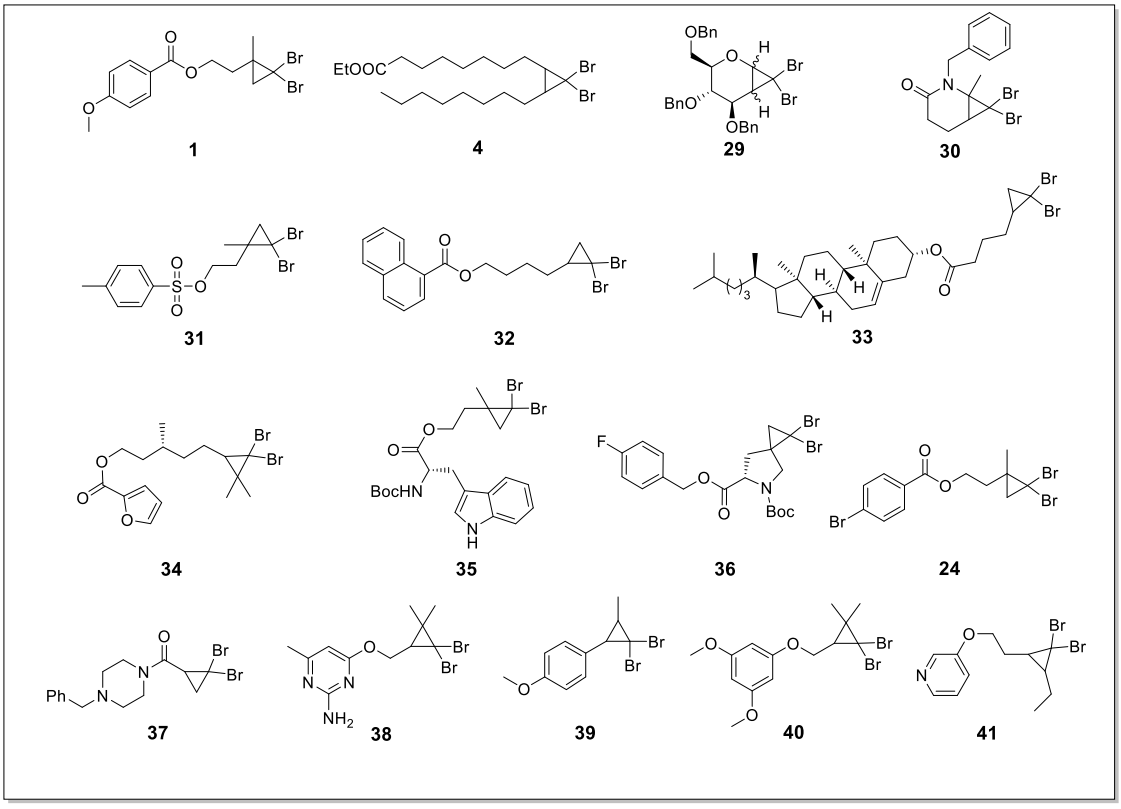

3. General Procedure for the di-reduction of *gem*-dibromocyclopropanes

In a 5 mL round-bottom flask, was added $Ni(OAc)_2 \cdot 4H_2O$ (2.5 mg, 5 mol %) and 3,4,7,8-tetramethyl-1,10-phenanthroline (TMPhen - 4.7 mg, 10 mol %). A septum was adapted, and the flask was purged with argon. A 2 wt % solution of TPGS-750-M/H_2O (0.32 mL, 0.5 M total) was added. Formation of a purple complex was allowed by stirring the solution for 10 min. Pyridine (24 µL, 0.3 mmol, 1.5 equiv) was added. After 5 min, $NaBH_4$ (37.8 mg, 1 mmol, 5 equiv) was added in one portion and the vial was capped again and sealed to prevent any leak. The *gem*-dibromocyclopropane (0.2 mmol, 1 equiv) was dissolved in THF (80 µL, 20 v/v%) and added as a solution to the flask through the septum. A 6 mL syringe (containing 0.1 mL of THF) was added through the septum to accept evolving hydrogen gas. The reaction was stirred for 30 min at 45 °C (Note: in the case of fused cycle **7**, the reaction was performed at rt). If the volume of gas generated exceeds the volume of the syringe, the syringe must be emptied outside of the flask and adapted again. After completion, the reaction was dissolved in EtOAc (3 mL) and filtered through a pad of silica. The pad was rinsed with EtOAc (3 x 3 mL). The organic layer was dried over anhydrous $MgSO_4$, filtered, and concentrated under vacuum. Purification by flash chromatography was then performed.

Note: For compounds that are poorly soluble in THF, the *gem*-dibromocyclopropane (0.2 mmol) and THF (80 uL) were added after the pyridine, separately. The resulting heterogeneous mixture was stirred until adequately combined. The flask was then quickly uncapped and sodium borohydride (4-5 equiv, 98% purity, stored in glovebox) was added in one portion. The flask was then sealed using a septum and the reaction was performed as described above.

4. General procedure for the di-reduction of *gem*-dibromocyclopropanes on > 1 mmol scale

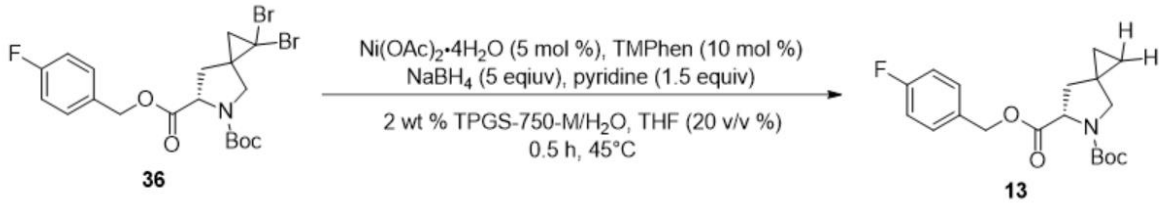

36 **13**

In a 25 mL round-bottom flask was added $Ni(OAc)_2•4H_2O$ (19.0 mg, 5 mol %) and 3,4,7,8-tetramethyl-1,10-phenanthroline (TMPhen – 36.0 mg, 10 mol %). The flask was cooled in an ice-bath. A septum was adapted, and the flask was purged with argon. A 2 wt % solution of TPGS-750-M/H_2O (3.0 mL, 0.5 M) was added. Formation of a purple complex was allowed by stirring the solution for 10 min. Pyridine (184.0 µL, 3.3 mmol, 1.5 equiv) was added. After 5 min, $NaBH_4$ (288.2 mg, 7.6 mmol, 5 equiv) was added in one portion and the vial was capped again and sealed to prevent any leak. Substrate **36** (772.7 mg, 1.52 mmol, 1 equiv) was dissolved in THF (300 µL, 10 v/v %) and added as a solution to the flask through the septum. The vial containing **36** was rinsed with another portion of THF (300 µL, 20 v/v % total). A 12 mL syringe (containing 0.1 mL of THF) was added through the top of the septum to accept evolving hydrogen gas. The reaction was stirred for 30 min at 45 °C. If the volume of gas generated exceeds the volume of the syringe, the syringe must be emptied outside of the flask and adapted again. After completion, the reaction was dissolved in EtOAc (10 mL) and filtered through a pad of silica. The pad was rinsed with EtOAc (3 x 10 mL). The organic layer was dried over anhydrous $MgSO_4$, filtered, and concentrated under vacuum. Purification by flash chromatography was performed (silica, 0 → 20% EtOAc/hexanes) and a colorless oil was obtained (414.4 mg, 78%).

5. General procedure for the mono-reduction of *gem*-dibromocyclopropanes

In a 5 mL round-bottom flask was added $Ni(OAc)_2 \cdot 4H_2O$ (1.2 mg, 0.5 mol %) and bipyridine (1.6 mg, 1 mol %). A septum was adapted, and the flask was purged with argon. A 2 wt % solution of TPGS-750-M/H_2O (2.0 mL, 0.5 M) was added. Formation of a purple complex is allowed by stirring the solution for 10 min. Pyridine (121 µL, 1.5 mmol, 1.5 equiv) was added. After 5 min, $NaBH_4$ (94.6 mg, 5 mmol, 5 equiv) was added in one portion and the vial was capped again and sealed to prevent any leak. The *gem*-dibromocyclopropane (1.0 mmol, 1 equiv) was dissolved in THF (0.4 mL, 20 v/v%) and added as a solution to the flask through the septum. A 6 mL syringe (containing 0.1 mL of THF) was added as through the top of the septum to accept evolving hydrogen gas. The reaction was stirred for 30 min at 45 °C. If the volume of gas generated exceeds the volume of the syringe, the syringe must be emptied outside of the flask and adapted again. After completion, the reaction was dissolved in EtOAc (3 mL) and filtered through a pad of silica. The pad was rinsed with EtOAc (3 x 3 mL). The organic layer was dried over anhydrous $MgSO_4$, filtered, and concentrated under vacuum. Purification by flash chromatography was then performed.

6. Ligand screening procedure

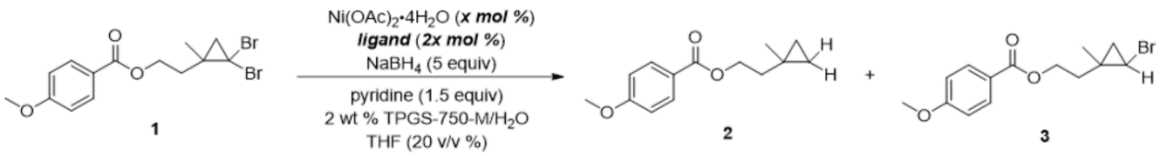

In a 5 mL round-bottom flask, was added $Ni(OAc)_2 \cdot 4H_2O$ (0.25-5 mol %) and the ligand (0-15 mol %). A septum was adapted, and the flask was purged with argon. A 2 wt % solution of TPGS-750-M/H_2O (0.32 mL, 0.5 M total) was added. The formation of a purple complex is

observed upon stirring the solution for 10 min. Pyridine (24 µL, 0.3 mmol, 1.5 equiv) was added. After 5 min, $NaBH_4$ (2.5 or 5 equiv) was added in one portion and the vial was capped again and sealed to prevent any leak. The *gem*-dibromocyclopropane (0.2 mmol, 1 equiv) was dissolved in THF (80 µL, 20 v/v %) and added as a solution to the flask through the septum. A 6 mL syringe (containing 0.1 mL of THF) was added through the top of the septum to accept evolving hydrogen gas. The reaction was stirred for 30 min at 45 °C. If the volume of gas generated exceed the volume of the syringe, the syringe must be emptied outside of the flask and the syringe repositioned. After completion, the reaction was dissolved in EtOAc (3 mL) and filtered through a pad of silica. The pad was rinsed with EtOAc (3 x 3 mL). The organic layer was dried over anhydrous $MgSO_4$, filtered, and concentrated under vacuum. Purification by flash chromatography was performed.

7. Impact of the amount of $NaBH_4$ procedure

In a 5 mL round-bottom flask, was added $Ni(OAc)_2$•$4H_2O$ (2.5 mg, 5 mol %) and 3,4,7,8-tetramethyl-1,10-phenanthroline (TMPhen - 4.7 mg, 10 mol %). A septum was adapted, and the flask was purged with argon. A 2 wt % solution of TPGS-750-M/H_2O (0.4 mL, 0.5 M) was added. The formation of a purple complex is allowed by stirring the solution for 10 min. Pyridine (24 µL, 0.3 mmol, 1.5 equiv) was added. After 5 min, $NaBH_4$ (0.4-1 mmol, 2-5 equiv) was added in one portion, followed by **1** (78.4 mg, 0.2 mmol, 1 equiv) and the vial was capped again and sealed to prevent any leak. A 6 mL syringe (containing 0.1 mL of THF) was added through the septum to accept the evolving hydrogen gas. The reaction was stirred for 30 min at 45 °C. If the volume of gas generated exceed the volume of the syringe, the syringe must be emptied outside of the flask and adapted again. After completion, the reaction was extracted with EtOAc (3 mL) and filtered through a pad of silica. The pad was rinsed with

EtOAc (3 x 3 mL). The organic layer was dried over anhydrous $MgSO_4$, filtered, and concentrated under vacuum. Purification by flash chromatography was then performed.

8. Base screening procedure

In a 5 mL round-bottom flask, was added $Ni(OAc)_2•4H_2O$ (2.5 mg, 5 mol %) and 3,4,7,8-tetramethyl-1,10-phenanthroline (TMPhen - 4.7 mg, 10 mol %). A septum was adapted, and the flask was purged with argon. A 2 wt % solution of TPGS-750-M/H_2O (0.32 mL, 0.5 M) was added. The formation of a purple complex is allowed by stirring the solution for 10 min. The base (0.3 mmol, 1.5 equiv) was added. After 5 min, $NaBH_4$ (37.8 mg, 1 mmol, 5 equiv) was added in one portion and the vial was capped again and sealed to prevent any leak. The *gem*-dibromo- cyclopropane (0.2 mmol, 1 equiv) was dissolved in THF (80 µL, 20 v/v %) and added as a solution to the flask through the septum. A 6 mL syringe (containing 0.1 mL of THF) was added through the top of the septum to accept evolving hydrogen gas. The reaction was stirred for 30 min at 45 °C. If the volume of gas generated exceed the volume of the syringe, the syringe must be emptied outside of the flask and adapted again. After completion, the reaction was dissolved in EtOAc (3 mL) and filtered through a pad of silica. The pad was rinsed with EtOAc (3 x 3 mL). The organic layer was dried over anhydrous $MgSO_4$, filtered, and concentrated under vacuum. Purification by flash chromatography was performed.

9. Screening of the reaction medium procedure

In a 5 mL round-bottom flask, was added $Ni(OAc)_2•4H_2O$ (2.5 mg, 5 mol %) and the ligand (10 mol %). A septum was adapted, and the flask was purged with argon. The solvent (0.4 mL, 0.5 M, or 0.32 mL if co-solvent is added) was added. The formation of a purple complex was observed upon stirring the solution for 10 min. Pyridine (24 µL, 0.3 mmol, 1.5 equiv) was

added. If no co-solvent, or water as a co-solvent, is used, the *gem*-dibromocyclopropane substrate is added as a solid and stirred. After 5 min, $NaBH_4$ (1 mmol, 5 equiv) was added in one portion and the vial was capped again and sealed to prevent any leak. If using organic co-solvent, the *gem*-dibromo substrate **1** (78.4 mg, 0.2 mmol, 1 equiv) was dissolved in THF (80 µL, 20 v/v %) and added as a solution to the flask through the septum. A 6 mL syringe (containing 0.1 mL of THF) was added on through the septum to accept evolving hydrogen gas. The reaction was stirred for 30 min at 45 °C. If the volume of gas generated exceed the volume of the syringe, the syringe must be emptied and repositioned. After completion, the reaction was extracted with EtOAc (3 mL) and filtered through a pad of silica. The pad was rinsed with EtOAc (3 x 3 mL). The organic layer was dried over anhydrous $MgSO_4$, filtered, and concentrated under vacuum. Purification by flash chromatography was then performed.

10. Residual nickel analysis

Robertson Microlit Laboratories

1705 U.S. Highway 46 / Suite 1D / Ledgewood, NJ 07852 / (973) 966-6668 / Fax (973) 966-0136

www.robertson-microlit.com

Min-Kyu Cho

Novartis Institute for Biomedical Research

250 Mass. Ave.

Cambridge, Massachusetts 02139

CIB001

Sample #: REILJO3-001-EXP087 **Test #:** 1 **Received:** 05/30/2017 **Completed:** 06/01/2017

ICP-OES: Nickel = < 2 ppm

Services
ICP-OES

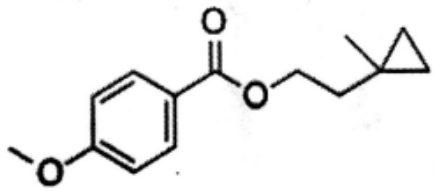

11. **2-step, 1-pot procedure**

A 1-dram vial was charged with 2-(2,2-dibromo-1-methylcyclopropyl)ethyl 4-bromobenzoate (**24**; 88.2 mg, 0.2 mmol, 1.0 equiv), 4-methoxy-2-methylphenylboronic acid (49.8 mg, 0.3 mmol, 1.5 equiv) and K_3PO_4 (63.7 mg, 0.3 mmol, 1.5 equiv). The vial was capped with a septum and purged with argon. A 2 wt % solution of TPGS-750-M/H_2O (0.5 mL) was added, followed by adding the catalyst stock solution* (100 µL, 0.1 mol %). The reaction was stirred for overnight at 45 °C, and completion of the reaction was determined by thin-layer chromatography. After completion of the Suzuki-Miyaura cross-coupling, $Ni(OAc)_2$•$4H_2O$ (2.5 mg, 5 mol %) and 3,4,7,8-tetramethyl-1,10-phenanthroline (TMPhen; 4.7 mg, 10 mol %) were added to a separate 1-dram vial. A septum was adapted and the vial was purged with argon. A 2 wt % solution of TPGS-750-M/H_2O (0.3 mL) was added. The formation of a purple complex was observed upon stirring the solution for 10 min. Pyridine (24 µL, 0.3 mmol, 1.5 equiv) was added. After 5 min, the complex solution was transferred to the reaction vial via syringe. THF (160 µL, 20 v/v % of total solvent) was added to reaction mixture. $NaBH_4$ (37.8 mg, 1 mmol, 5 equiv) was then added in one portion and the vial was capped and sealed to prevent any leak. A 6 mL syringe (containing 0.1 mL of THF) was added through the top of the septum to accept the evolving hydrogen gas. The reaction was stirred for 30 min at 45 °C. If the volume of gas generated exceed the volume of the syringe, the syringe must be emptied outside of the flask and repositioned. After completion, as determined by TLC (1:9 EtOAc/hexane), the reaction was dissolved in EtOAc (3 mL) and filtered through a pad of silica. The pad was rinsed with EtOAc (3 x 3 mL). The organic layer was dried over anhydrous $MgSO_4$, filtered, and concentrated under vacuum.The crude

product was then purified by flash chromatography to afford 56.0 mg (86%) of the product biaryl **25**.

* Catalyst stock solution contains $Pd(OAc)_2$ (1.1 mg) and N_2Phos (7.6 mg) in toluene (1 mL).

12. General procedure for E Factor determination

The E Factor was calculated for the synthesis of **2**, on a 0.4 mmol scale. The calculation includes the organic layer (THF as co-solvent and EtOAc as extraction solvent). After completion of the reduction of **1**, 80 µL of EtOAc was added to the flask. The mixture was centrifuged, and the top organic layer was collected. This step was repeated 2 more times.

A synthesis of **2** from **1** was performed as outlined in the general procedure above on a 0.4 mmol scale. After the reaction, the aqueous phase was extracted with a minimal amount of EtOAc (3 x 80 µL). In order to do this, the extraction solvent was added to the product mixture and allowed to stir *gently* for 5 min. The resulting bi-phase was then centrifuged, and the less dense phase was carefully removed using a 100 µL syringe. This process was repeated twice until a minimally detectable amount of product was observed via TLC. The E Factor mass balance is as follows:

Mass of THF for reaction
δ THF: 0.89 mg/mL
0.16 mL x 0.89 mg/mL = 142.4 mg of THF
Mass of EtOAc for extraction
δ EtOAc: 0.9 mg/mL
(0.08 mL x 0.9 mg/mL) x 3 extractions = 216 mg EtOAc
Mass of Product
m = 72 mg
Yield = 80%

$$\textbf{E Factor} = \frac{142.4\ \text{mg (THF)} + 216\ \text{mg (EtOAc)}}{72\ \text{mg (product)}} = \mathbf{5}$$

13. Recycling studies procedure

In a 25 mL round-bottom flask was added $Ni(OAc)_2•4H_2O$ (9.3 mg, 5 mol %) and 3,4,7,8-tetramethyl-1,10-phenanthroline (TMPhen – 17.7 mg, 10 mol %). A septum was adapted, and the flask was purged with argon. A 2 wt % solution of TPGS-750-M/H_2O (1.5 mL, 0.5 M) was added. The formation of a purple complex was observed upon stirring the solution for 10 min. Pyridine (91 µL, 1.1 mmol, 1.5 equiv) was added. After 5 min, $NaBH_4$ (89.0 mg, 1.1 mmol, 5 equiv) was added in one portion and the vial was capped again and sealed to prevent any leak. Substrate **1** (0.75 mmol, 1 equiv) was dissolved in THF (300 µL, 20 v/v %) and added as a solution to the flask through the septum. A 6 mL syringe (containing 0.1 mL of THF) was added through the top of the septum to accept evolving gas. The reaction was stirred for 30 min at 45 °C. After completion, the reaction was dissolved in EtOAc (2 mL) and filtered through a pad of Celite. The pad was rinsed with EtOAc (3 x 2 mL). The organic layer was collected with a pipette, dried over anhydrous $MgSO_4$, filtered, and concentrated under vacuum. A purification by flash chromatography was performed.

The synthesis of **2** has been performed three times on a 0.86 mmol scale, reusing the same aqueous phase and using the same general procedure. Post reaction, the aqueous layer was extracted with EtOAc and passed through a plug of Celite. Fresh nickel(II) acetate tetrahydrate and TMPhen were then added and the reaction repeated. This overall procedure was repeated twice, resulting in two recycles of the aqueous phase.

14. Deuterium studies procedure

In a 5 mL round-bottom flask, was added the catalyst (5 mol %) and 3,4,7,8-tetramethyl-1,10-phenanthroline (TMPhen - 4.7 mg, 10 mol %). A septum was adapted, and the flask was

purged with argon. TPGS-750-M/2 wt % in H_2O or D_2O (0.32 mL, 0.5 M total) was added. The formation of a purple complex was observed upon stirring the solution for 10 min. Pyridine or pyridine-d_5 (24 µL, 0.3 mmol, 1.5 equiv) was added. After 5 min, the $NaBH_4$ or $NaBD_4$ (1 mmol, 5 equiv) was added in one portion and the vial was capped again and sealed to prevent any leak. The *gem*-dibromocyclopropane (0.2 mmol, 1 equiv) was dissolved in THF or THF-d_8 (80 µL, 20 v/v %) and added as a solution to the flask through the septum. A 6 mL syringe (containing 0.1 mL of THF) was added through the septum to accept evolving gas. The reaction was stirred for 30 min at 45 °C. If the volume of gas generated exceed the volume of the syringe, the syringe must be emptied outside of the flask and the syringe adapted again. After completion, the reaction was dissolved in EtOAc (3 mL), filtered through a pad of silica and the crude was analyzed by ^{1}H NMR to determine the extent of deuterium incorporation.

15. Analytical data

2-(2,2-Dibromo-1-methylcyclopropyl)ethyl 4-methoxybenzoate (1)

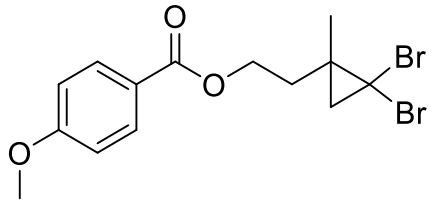

Brown solid

R_f = 0.26 (90:10 hexanes/EtOAc); **mp** 39-41 °C; **^{1}H NMR** (400 MHz, $CDCl_3$) δ 8.16 – 7.88 (m, 2H, Ar-*H*), 7.04 – 6.84 (m, 2H, Ar-*H*), 4.51 (td, *J* = 6.8, 2.2, 2H, O-C*H*$_2$), 3.87 (s, 3H, O-C*H*$_3$), 2.16 (hept, *J* = 7.6, 7.2, 2H, C*H*$_2$), 1.57 (d, *J* = 7.5, 1H, C*H*$_2$), 1.49 (d, *J* = 2.4, 1H, C*H*$_2$), 1.48 (s, 3H, C*H*$_3$); **^{13}C NMR** (101 MHz, $CDCl_3$) δ 166.4, 163.5, 131.8, 122.6, 113.8, 62.2,

55.6, 38.4, 37.1, 34.6, 27.8, 22.8; **HRMS (ESI)**: *m/z* calcd for $C_{14}H_{16}Br_2O_3Na^+$: 412.9364 $[M+Na]^+$; found: 412.9367.

2-(1-Methylcyclopropyl)ethyl 4-methoxybenzoate (2)

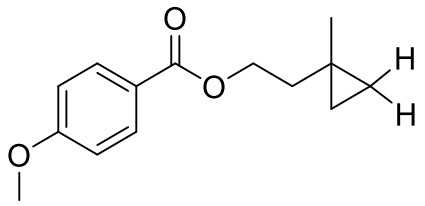

Colorless oil; isolated 42.5 mg; 91%

R_f = 0.40 (95:5 hexanes/EtOAc); **^{1}H NMR** (400 MHz, $CDCl_3$) δ 7.99 (d, 2H, Ar-*H*), 6.91 (d, 2H, Ar-*H*), 4.40 (t, *J* = 6.9, 2H, O-CH_2), 3.85 (s, 3H, O-CH_3), 1.69 (t, *J* = 6.9, 2H, CH_2), 1.11 (s, 3H, CH_3), 0.38 – 0.25 (m, 4H, 2 x CH_2); **^{13}C NMR** (101 MHz, $CDCl_3$) δ 166.6, 163.3, 131.7, 123.1, 113.7, 63.5, 55.5, 38.2, 23.0, 13.2, 12.9; **HRMS (ESI):** *m/z* calcd for $C_{14}H_{18}O_3$+Na^+: 257.1154 [*M*+Na]$^+$; found: 257.1148.

2-(2-Bromo-1-methylcyclopropyl)ethyl 4-methoxybenzoate (3)

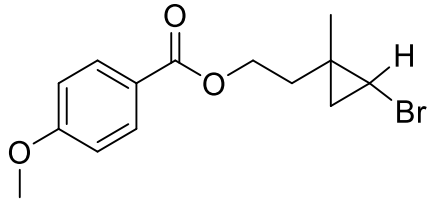

Colorless oil; 1 mmol scale; isolated 285.7 mg; 91%

R_f = 0.74 (80:20 hexanes/EtOAc); **^{1}H NMR** (500 MHz, $CDCl_3$) *major diastereoisomers* δ 8.01 (tt, *J* = 8.5, 1.6, 2H, Ar-*H*), 6.99 – 6.87 (m, 2H, Ar-*H*), 4.45 – 4.34 (m, 2H, CH_2), 3.96 – 3.78 (s, 3H, CH_3), 2.95 (ddd, *J* = 6.2, 4.5, 1.6, 1H, C*H*-Br), 2.03 (td, *J* =7.0, 1.9, 1H, CH_2), 1.76 – 1.66 (m, 1H, CH_2), 1.35 (s, 3H, CH_3), 1.14 – 1.07 (m, 1H, CH_2), 0.71 (ddd, *J* = 6.4, 4.4, 1.8,

1H, CH_2); *minor diastereoisomers* δ 8.01 (tt, *J* = 8.5, 1.6, 2H, Ar-*H*), 6.99 – 6.86 (m, 2H, Ar-*H*), 4.48 (tdd, *J* = 7.3, 4.3, 2.9, 2H, CH_2), 3.96 – 3.78 (s, 3H, CH_3), 2.88 (ddd, *J* = 7.7, 4.4, 1.7, 1H, C*H*-Br), 2.03 (td, *J* = 7.0, 1.9, 1H, CH_2), 1.80 (dtd, *J* = 12.5, 6.2, 1.7, 1H, CH_2), 1.24 – 1.17 (s, 3H, CH_3), 1.05 (ddd, *J* = 8.1, 6.3, 1.8, 1H, CH_2), 0.80 (ddd, *J* = 6.5, 4.6, 1.9, 1H, CH_2); **^{13}C NMR** (126 MHz, $CDCl_3$) *major diastereoisomers* δ 166.4, 163.5, 131.8, 122.8, 113.8, 62.4, 55.6, 37.7, 35.3, 29.4, 22.3, 20.3, 19.1; *minor diastereoisomers* δ = 166.5, 163.5, 131.8, 122.9, 113.8, 62.8, 55.6, 37.7, 35.3, 29.5, 22.8, 22.6, 20.3, 19.2; **HRMS (ESI):** *m/z* calcd for $C_{14}H_{17}BrO_3$+Na^+: 335.0259 [*M*+Na]$^+$; found: 335.0268.

Ethyl 8-(2,2-dibromo-3-octylcyclopropyl)octanoate (4)

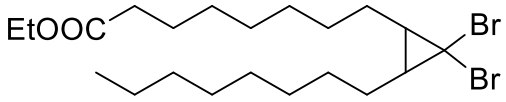

Light yellow oil

R_f = 0.43 (90:10 hexanes/EtOAc); **^{1}H NMR** (500 MHz, $CDCl_3$) δ 4.14 (qd, *J* = 7.1, 3.1, 2H), 2.30 (t, *J* = 7.5, 2H), 1.71 – 1.17 (m, 32H), 0.89 (dq, *J* = 7.0, 4.1, 2.8, 3H); **^{13}C NMR** (126 MHz, $CDCl_3$) δ 174.0, 60.3, 38.5, 34.5, 34.0, 33.9, 32.0, 29.7, 29.6, 29.4, 29.3, 29.2, 28.6, 28.5, 27.2, 27.1, 25.1, 22.8, 14.4, 14.4, 14.3; **HRMS (ESI):** *m/z* calcd for $C_{21}H_{38}Br_2O_2$+Na^+: 503.1136 [*M*+Na]$^+$; found: 503.1143.

Ethyl 8-(2-octylcyclopropyl)octanoate (5)

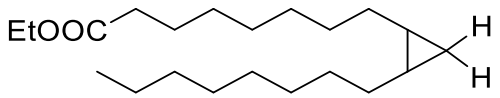

Yellow oil; 0.2 mmol scale; isolated 48.0 mg; 72%

R_f = 0.48 (90:10 hexanes/EtOAc); **^{1}H NMR** (400 MHz, $CDCl_3$) δ 4.13 (q, *J* = 7.1 Hz, 2H, O-C*H*$_2$), 2.29 (t, *J* = 7.5 Hz, 2H, C(O)-C*H*$_2$), 1.62 (q, *J* = 7.0 Hz, 2H, C(O)-CH$_2$-C*H*$_2$), 1.50 – 1.08 (m, 28H, C*H*$_2$), 0.89 (t, *J* = 6.8 Hz, 3H, C*H*$_3$), 0.65 (ddd, *J* = 10.7, 6.7, 3.9 Hz, 2H, C*H*), 0.56 (td, *J* = 8.1, 3.9 Hz, 1H, C*H*$_2$), -0.33 (q, *J* = 5.0 Hz, 1H, C*H*$_2$); **^{13}C NMR** (101 MHz, $CDCl_3$) δ 174.1 (*C*(O)), 60.3 (*C*H$_2$-C(O)), 34.6 (*C*H$_2$), 32.1 (*C*H$_2$), 30.4 (*C*H$_2$), 30.3 (*C*H$_2$), 29.8 (*C*H$_2$), 29.6 (*C*H$_2$), 29.5 (*C*H$_2$), 29.5 (*C*H$_2$), 29.3 (*C*H$_2$), 28.9 (*C*H$_2$), 28.8 (*C*H$_2$), 25.1 (*C*H$_2$), 22.9 (*C*H$_2$), 15.9 (*C*H), 15.9 (*C*H), 14.4 (*C*H$_3$), 14.3 (*C*H$_3$), 11.1 (*C*H$_2$); **HRMS (ESI):** *m/z* calcd for $C_{21}H_{40}O_2$: 324.3028 $[M]^+$; found: 324.3041.

(1*R*,3*R*,4*S*,5*R*,6*S*)-4,5-bis(Benzyloxy)-3-((benzyloxy)methyl)-2-oxabicyclo[4.1.0]heptane (6)[4]

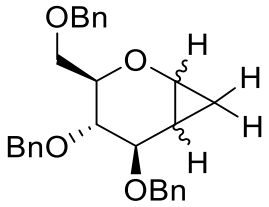

Light yellow oil; 0.15 mmol scale; isolated 42.8 mg; 73%

R_f = 0.38 (80:20 hexanes/EtOAc); **^{1}H NMR** (500 MHz, $CDCl_3$) δ 7.38 – 7.15 (m, 15H, Ar-*H*), 4.74 (dd, *J* = 11.6, 1.9 Hz, 2H, C*H*$_2$-benzyl), 4.55 (dd, *J* = 30.1, 11.7 Hz, 2H, C*H*$_2$-benzyl), 4.49 (q, *J* = 12.2 Hz, 2H, C*H*$_2$-benzyl), 3.73 (td, *J* = 6.1, 3.6 Hz, 1H, C*H*-O), 3.63 (dd, *J* = 10.4, 6.2 Hz, 1H, C*H*-O), 3.58 (dd, *J* = 7.6, 3.7 Hz, 1H, C*H*-O), 3.54 (td, *J* = 6.3, 2.9 Hz, 1H, C*H*-O), 3.52 – 3.46 (m, 2H, C*H*$_2$), 0.89 (dtd, *J* = 10.1, 6.6, 3.7 Hz, 1H, C*H*), 0.73 – 0.58 (m, 2H, C*H*$_2$); **^{13}C NMR** (126 MHz, $CDCl_3$) δ 138.7 (Ar), 138.5 (Ar), 138.4 (Ar), 128.5 (Ar), 128.5 (Ar), 128.4 (Ar), 128.1 (Ar), 127.8 (Ar), 127.8 (Ar), 127.7 (Ar), 127.7 (Ar), 80.2 (*C*H-O), 77.1

(*C*H-O), 76.9 (*C*H_2-benzyl), 73.6 (*C*H_2-benzyl), 73.4 (*C*H_2-benzyl), 71.2 (*C*H_2-O), 70.1 (*C*H-O), 49.8 (*C*H-O), 14.9 (*C*H), 11.6 (*C*H_2).

2-Benzyl-1-methyl-2-azabicyclo[4.1.0]heptan-3-one (7)[5]

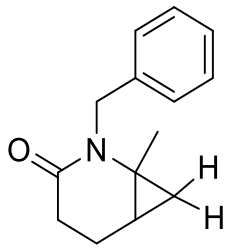

Colorless oil; 0.2 mmol scale; isolated 39.2 mg; 91%

R_f = 0.28 (70:30 hexanes/EtOAc); **^{1}H NMR** (500 MHz, $CDCl_3$) δ 7.33 – 7.19 (m, 5H, Ar-*H*), 4.79 (d, *J* = 14.9 Hz, 1H, C*H*$_2$-benzyl), 4.56 (d, *J* = 14.9 Hz, 1H, C*H*$_2$-benzyl), 2.52 – 2.24 (m, 3H, C*H*$_2$, C*H*), 1.47 – 1.33 (m, 1H, C*H*$_2$), 1.26 (s, 3H, C*H*$_3$), 1.20 – 1.10 (m, 1H, C*H*$_2$), 0.74 (dd, *J* = 8.7, 5.1 Hz, 1H, C*H*$_2$), 0.36 (t, *J* = 5.5 Hz, 1H, C*H*$_2$); **^{13}C NMR (101 MHz, $CDCl_3$)**: δ 173.1, 138.7, 128.3, 128.2, 126.9, 47.0, 38.0, 32.7, 25.4, 25.2, 23.8, 20.8.

2-(1-Methylcyclopropyl)ethyl 4-methylbenzenesulfonate (8)[6]

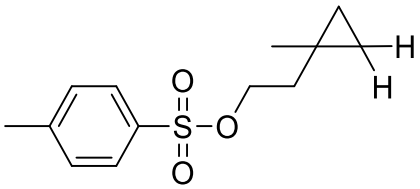

Colorless oil; 0.2 mmol scale; isolated 41.6 mg; 82%

R_f = 0.44 (85:15 hexanes/EtOAc); **^{1}H NMR** (600 MHz, $CDCl_3$) δ 7.83 – 7.77 (m, 2H, Ar-*H*), 7.35 (d, *J* = 8.0 Hz, 2H, Ar-*H*), 4.13 (t, *J* = 7.0 Hz, 2H, O-C*H*$_2$), 2.45 (s, 3H, Ar-C*H*$_3$), 1.58 (t, *J* = 7.0 Hz, 2H, O-CH$_2$-C*H*$_2$), 0.95 (s, 3H, C*H*$_3$), 0.32 – 0.16 (m, 4H, 2 x C*H*$_2$); **^{13}C NMR** (151 MHz, $CDCl_3$) δ 144.8 (Ar), 133.3 (Ar), 129.9 (Ar), 128.0 (Ar), 69.4 (*C*H_2), 38.2 (*C*H_3), 22.6 (*C*H_3), 21.7 (*C*H_2), 12.8 (*C*H_2), 12.6 (*C*H_2).

4-Cyclopropylbutyl 1-naphthoate (9)

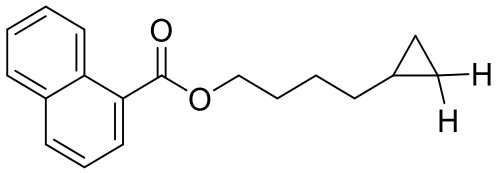

Pale yellow oil; 0.2 mmol scale; isolated 48.8 mg; 91%

R_f = 0.65 (90:10 hexanes/EtOAc); **^{1}H NMR** (400 MHz, $CDCl_3$) δ 8.93 (d, *J* = 8.6 Hz, 1H, Ar-*H*), 8.20 (d, *J* = 7.2 Hz, 1H, Ar-*H*), 8.03 (d, *J* = 8.2 Hz, 1H, Ar-*H*), 7.90 (d, *J* = 8.1 Hz, 1H, Ar-*H*), 7.63 (td, *J* = 7.3, 6.8, 1.4 Hz, 1H, Ar-*H*), 7.53 (dt, *J* = 12.1, 7.7 Hz, 2H, Ar-*H*), 4.44 (t, *J* = 6.7 Hz, 2H, O-CH_2), 1.88 (p, *J* = 6.9 Hz, 2H, CH_2), 1.62 (p, *J* = 7.4 Hz, 2H, CH_2), 1.30 (dt, *J* = 13.7, 6.8 Hz, 2H, CH_2), 0.71 (ddt, *J* = 10.1, 7.4, 3.6 Hz, 1H), 0.50 – 0.28 (m, 2H, CH_2), 0.05 (t, *J* = 4.9 Hz, 2H, CH_2); **^{13}C NMR** (101 MHz, $CDCl_3$) δ 167.9 (*C*(O)), 134.0 (Ar), 133.3 (Ar), 131.5 (Ar), 130.2 (Ar), 128.7 (Ar), 127.8 (Ar), 127.7 (Ar), 126.3 (Ar), 126.0 (Ar), 124.7 (Ar), 65.4 (O-*C*H_2), 34.5 (CH_2), 28.8 (CH_2), 26.3 (CH_2), 10.9 (*C*H), 4.6 (CH_2); **HRMS (ESI):** *m/z* calcd for $C_{10}H_{17}NO_2$+Na^+: 291.1361 [*M*+Na]$^+$; found: 291.1361.

(3*S*,8*S*,9*S*,10*R*,13*R*,14*S*)-10,13-Dimethyl-17-((*R*)-6-methylheptan-2-yl)-2,3,4,7,8,9,10,11,12,13,14,15,16,17-tetradecahydro-1*H*-cyclopenta[*a*]phenanthren-3-yl 4-cyclopropylbutanoate (10)

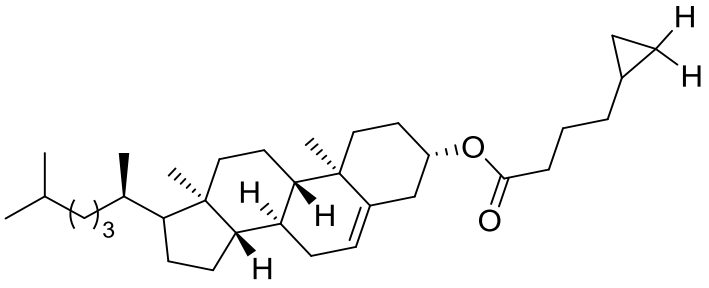

White solid; 0.2 mmol scale; isolated 72 mg; 73%

R_f = 0.63 (98:2 hexanes/EtOAc); **mp** = 95-98 °C; **^{1}H NMR** (400 MHz, $CDCl_3$) δ 5.38 (d, *J* = 5.1 Hz, 1H), 4.62 (qd, *J* = 10.0, 8.3, 4.5 Hz, 2H), 2.32 (dd, *J* = 8.8, 5.7 Hz, 4H), 2.10 – 0.76 (m, 41H), 0.68 (s, 4H), 0.42 (d, *J* = 7.5 Hz, 2H), 0.02 (d, *J* = 4.9 Hz, 2H); **^{13}C NMR** (101 MHz, $CDCl_3$) δ 173.4, 139.9, 122.7, 73.8, 56.8, 56.3, 50.2, 42.5, 39.9, 39.7, 38.3, 37.2, 36.7, 36.3, 35.9, 34.6, 34.2, 32.1, 32.0, 28.4, 28.2, 28.0, 25.3, 24.4, 24.0, 23.0, 22.7, 21.2, 19.5, 18.9, 12.0, 10.6, 4.5, **HRMS (ESI):** *m/z* calcd for $C_{34}H_{56}O_2$+Na^++CH_3OH: 551.4432 [*M*+Na+CH_3OH]$^+$; found: 551.4440.

(3*R*)-5-(2,2-Dimethylcyclopropyl)-3-methylpentyl furan-2-carboxylate (11)

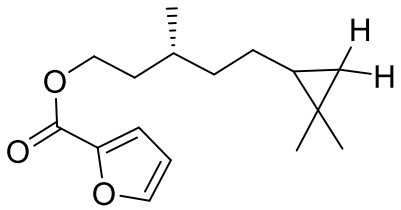

Colorless oil; 0.2 mmol scale; isolated 31.7 mg; 60%

R_f = 0.63 (80:20 hexanes/EtOAc); **^{1}H NMR (400 MHz, $CDCl_3$):** δ 7.57 (d, *J* = 2.2 Hz, 1H), 7.16 (d, *J* = 3.5 Hz, 1H), 6.50 (dd, *J* = 3.5, 1.8 Hz, 1H), 4.34 (dtt, *J* = 7.0, 4.5, 2.1 Hz, 2H), 1.88 – 1.72 (m, 1H), 1.69 – 1.51 (m, 2H), 1.48 – 1.15 (m, 5H), 1.04 – 0.99 (m, 6H), 0.94 (d, *J* = 6.5 Hz, 3H), 0.49 – 0.37 (m, 1H), 0.34 (ddd, *J* = 8.6, 4.1, 2.0 Hz, 1H), -0.10 – -0.22 (m, 1H); **^{13}C NMR (101 MHz, $CDCl_3$):** δ 158.8, 146.1, 144.8, 117.6, 111.7, 63.6, 63.6, 37.4, 37.4, 35.6, 35.4, 29.7, 29.7, 27.6, 27.6, 27.1, 27.0, 24.8, 24.7, 19.9, 19.9, 19.7, 19.6, 19.6, 19.5, 15.3, 15.2; **HRMS (ESI):** *m/z* calcd for $C_{16}H_{24}O_3$+Na^+: 287.1623 [*M*+Na]$^+$; found: 287.1620.

2-(1-Methylcyclopropyl)ethyl (*t*-butoxycarbonyl)-*L*-tryptophanate (12)

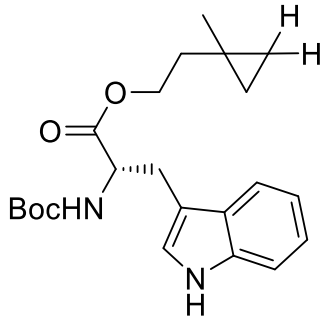

White solid; 0.2 mmol scale; isolated 70.3 mg; 91%

R_f = 0.60 (60:40 hexanes/EtOAc); **mp** 86-90 °C; **^{1}H NMR** (500 MHz, $CDCl_3$) δ 8.20 (bs, 1H, N*H*), 7.57 (d, *J*=7.9, 1H, Ar-*H*), 7.35 (d, *J* = 8.1, 1H, Ar-*H*), 7.20 (t, *J* = 7.5, 1H, Ar-*H*), 7.12 (t, *J* = 7.5, 1H, Ar-*H*), 7.01 (bs, 1H, N*H*), 5.10 (d, *J*=8.3, 1H, C*H*=), 4.64 (d, *J* = 6.9, 1H, C*H*□), 4.16 (tq, *J* = 11.1, 5.6, 3.9, 2H, O-C*H*$_2$), 3.38 – 3.21 (m, 1H, C□-C*H*$_2$), 1.44 (s, 9H, C(C*H*$_3$)$_3$), 1.40 – 1.23 (m, 2H, C*H*$_2$), 1.00 (s, 3H, C*H*$_3$), 0.24 (d, *J* = 9.8, 4H, C*H*$_2$); **^{13}C NMR** (126 MHz, $CDCl_3$) δ 172.5 (*C*=O), 155.4 (*C*=O Boc), 136.3 (Ar), 127.8 (Ar), 122.9 (Ar), 122.2 (Ar), 119.6 (Ar), 118.9 (Ar), 111.3 (Ar), 110.3 (Ar), 79.9 (*C*-(CH$_3$)$_3$), 64.2 (O-*C*H2), 54.4 (*C*□), 37.7 (*C*H$_2$), 28.5 (*C*H$_2$), 28.2 (*C*H$_2$), 22.8 (*C*H$_2$), 12.9 (*C*H$_2$), 12.8 (*C*H$_3$). **HRMS (ESI):** *m/z* calcd for $C_{22}H_{30}N_2O_4$+Na^+: 409.2103 [*M*+Na]$^+$; found: 409.2091.

5-(*t*-Butyl) 6-(4-fluorobenzyl) (*S*)-5-azaspiro[2.4]heptane-5,6-dicarboxylate (13)

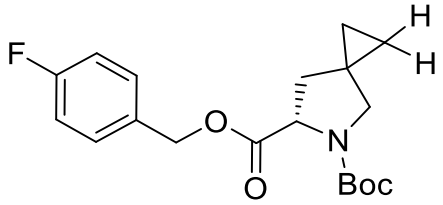

Colorless oil; 0.2 mmol scale; isolated 60.1 mg; 86%

R_f = 0.41 (80:20 hexanes/EtOAc); **^{1}H NMR** (400 MHz, $CDCl_3$) *mixture of rotamers* δ 7.35 (td, *J* = 8.5, 5.5, 2H, Ar-*H*), 7.04 (q, *J* = 8.6, 2H, Ar-*H*), 5.28 – 5.02 (m, 2H, *CH*$_2$-O), 4.52 (dd, *J* = 8.5, 3.6, 0.5H, C*H*□), 4.40 (dd, *J* = 8.5, 4.1, 0.5H, C*H*□), 3.45 – 3.20 (m, 2H, N-C*H*$_2$), 2.29 (d, *J* = 8.5, 1H, C*H*$_2$), 2.26 (d, *J* = 8.5, 1H, C*H*$_2$), 1.78 (dd, *J* = 12.7, 4.1, 1H, C*H*$_2$), 1.72 (dd, *J* = 12.7, 3.6, 1H, C*H*$_2$), 1.45 (s, 4H, 3C*H*$_3$), 1.36 (s, 5H, 3C*H*$_3$), 0.69 – 0.48 (m, 3H, C*H*$_2$), 0.43 – 0.31 (m, 1H, C*H*$_2$); **^{13}C NMR** (126 MHz, $CDCl_3$) δ 172.8, 172.5, 163.9, 163.7, 161.9, 154.4, 153.8, 131.9, 131.7, 130.7, 130.6, 130.4, 130.3, 115.7, 115.6, 115.5, 115.4, 80.1, 80.0, 66.1, 66.0, 59.8, 59.5, 54.2, 53.8, 39.2, 38.3, 28.6, 28.4, 20.8, 20.1, 12.9, 12.4, 9.1, 8.5; **HRMS (ESI):** *m/z* calcd for $C_{19}H_{24}FNO_4$+Na^+: 372.1587 [*M*+Na]$^+$; found: 372.1593.

2-(1-methylcyclopropyl)ethyl benzoate (14)[7]

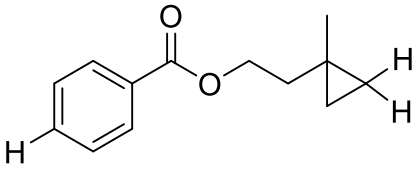

colorless oil; 0.2 mmol scale; isolated 32.7 mg; 80%

R_f = 0.77 (80:20 hexanes/EtOAc); **^{1}H NMR** (600 MHz, $CDCl_3$) δ 8.07 – 8.03 (m, 2H, Ar-*H*), 7.58 – 7.54 (m, 1H, Ar-*H*), 7.48 – 7.42 (m, 2H, Ar-*H*), 4.44 (t, *J* = 6.9 Hz, 2H, O-C*H*$_2$), 1.72 (t, J = 6.9 Hz, 2H, O-CH$_2$-C*H*$_2$), 1.13 (s, 3H, C*H*$_3$), 0.41 – 0.27 (m, 4H, 2 x C*H*$_2$); **^{13}C NMR** (151 MHz, $CDCl_3$) δ 166.8 (*C*=O), 132.9 (Ar), 130.7 (Ar), 129.7 (Ar), 128.5 (Ar), 63.9 (O-*C*H$_2$), 38.2 (O-*C*H$_2$-CH$_2$), 23.0, 13.2, 13.0.

(4-Benzylpiperazin-1-yl)(cyclopropyl)methanone (15)

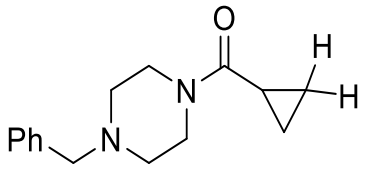

Yellow oil; 0.2 mmol scale; isolated 35.3 mg; 70%

R_f = 0.44 (EtOAc); **^{1}H NMR (400 MHz, $CDCl_3$):** δ 7.37 – 7.22 (m, 5H), 3.74 – 3.59 (m, 4H), 3.52 (s, 2H), 2.51 – 2.39 (m, 4H), 1.78 – 1.64 (m, 1H), 0.97 (dd, *J* = 4.7, 2.9 Hz, 2H), 0.74 (dd, *J* = 8.0, 2.9 Hz, 2H). **^{13}C NMR (101 MHz, $CDCl_3$):** δ 171.9, 137.7, 129.1, 128.3, 127.2, 62.91, 53.3, 52.8, 45.5, 42.1, 10.9, 7.3. **HRMS (ESI):** *m/z* calcd for $C_{15}H_{20}N_2O+Na^+$: 267.1473 [*M*+Na]$^+$; found: 267.1479.

4-((2,2-Dimethylcyclopropyl)methoxy)-6-methylpyrimidin-2-amine (16)

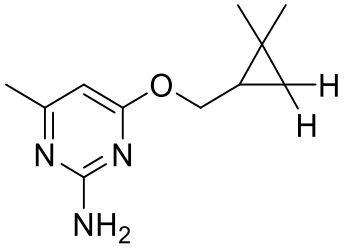

Colorless oil; 0.2 mmol scale; isolated 52 mg; 71%

R_f = 0.43 (1:1 hexanes/EtOAc); **^{1}H NMR** (400 MHz, $CDCl_3$) δ 5.98 – 5.93 (m, 1H, Ar-*H*), 4.98 (s, 2H, N*H*$_2$), 4.35 (dd, *J* = 11.4, 6.7 Hz, 1H, O-C*H*$_2$), 4.07 (dd, *J* = 11.4, 8.7 Hz, 1H, O-C*H*$_2$), 2.25 (s, 3H, Ar-C*H*$_3$), 1.11 (s, 3H, C*H*$_3$), 1.09 (s, 3H, C*H*$_3$), 1.04 (tdd, *J* = 8.7, 6.7, 5.2 Hz, 1H, C*H*), 0.55 (dd, *J* = 8.6, 4.5 Hz, 1H, C*H*$_2$), 0.23 (t, *J* = 4.9 Hz, 1H, C*H*$_2$); **^{13}C NMR (101 MHz, $CDCl_3$)** δ 170.8, 167.9, 162.6, 97.0, 67.5, 27.1, 23.6, 22.7, 19.9, 18.5, 16.2.; **HRMS (ESI):** *m/z* calcd for $C_{11}H_{17}N_3ONa$: 230.1269 [*M*]$^+$; found: 230.1267.

1-Methoxy-4-(2-methylcyclopropyl)benzene (17)[8]

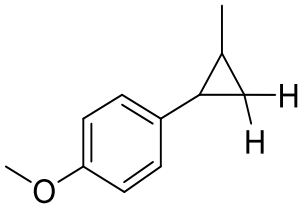

Colorless oil; 0.2 mmol scale; isolated 31.1 mg; 96%

R_f = 0.43 (95:5 hexanes/EtOAc); **^{1}H NMR** (400 MHz, $CDCl_3$) δ 7.04 – 6.96 (m, 2H, Ar-*H*), 6.86 – 6.79 (m, 2H, Ar-*H*), 3.80 (s, 3H, O-C*H*$_3$), 1.56 (dt, *J* = 9.1, 5.0 Hz, 1H, C*H*), 1.20 (d, *J* = 5.9 Hz, 3H, C*H*$_3$), 1.05 – 0.94 (m, 1H, C*H*), 0.89 – 0.78 (m, 1H, C*H*$_2$), 0.70 (dt, *J* = 8.3, 5.0 Hz, 1H, C*H*$_2$); **^{13}C NMR** (101 MHz, $CDCl_3$) δ 157.6 (Ar), 136.2 (Ar), 127.1 (Ar), 126.7 (Ar), 113.9 (Ar), 55.5 (*C*H_3-O), 23.7 (*C*H_3), 19.2 (*C*H), 17.4 (*C*H_2), 17.1 (*C*H-CH_3).

1-((2,2-Dimethylcyclopropyl)methoxy)-3,5-dimethoxybenzene (18)

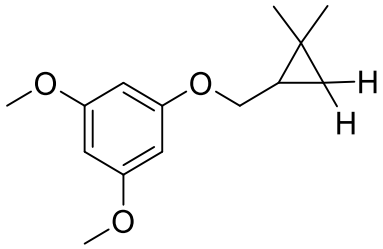

Light yellow oil; 0.2 mmol scale; isolated 37.2 mg; 79%

R_f = 0.51 (90:10 hexanes/EtOAc); **^{1}H NMR** (600 MHz, $CDCl_3$) δ 6.08 (d, *J* = 2.2 Hz, 2H, Ar-*H*), 6.05 (t, *J* = 2.2 Hz, 1H, Ar-*H*), 3.99 (dd, *J* = 10.1, 6.5 Hz, 1H, O-C*H*$_2$), 3.78 (dd, *J* = 10.1, 8.3 Hz, 1H, O-C*H*$_2$), 3.75 (s, 6H, 2 x O-C*H*$_3$), 1.10 (s, 6H, 2 x C*H*$_3$), 1.04 (tdd, *J* = 8.4, 6.5, 5.2 Hz, 1H, C*H*), 0.57 (dd, *J* = 8.6, 4.6 Hz, 1H, C*H*$_2$), 0.22 (t, *J* = 4.9 Hz, 1H, C*H*$_2$); **^{13}C NMR** (126 MHz, $CDCl_3$) δ 161.4 (Ar), 161.1 (Ar), 93.5 (Ar), 92.8 (Ar), 69.4 (*C*H_2-O), 55.3 (*C*H_2-

O), 27.1 (*C*H), 23.0 (*C*H), 19.9 (*C*), 18.5 (*C*H_2), 16.2 (*C*H_2); **HRMS (ESI):** *m/z* calcd for $C_{14}H_{20}O_3$: 236.1413 $[M]^+$; found: 236.1405.

3-(2-(2-Ethylcyclopropyl)ethoxy)pyridine (19)

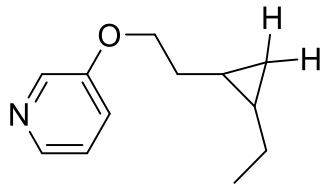

Colorless oil; 0.2 mmol scale; isolated 25.2 mg isolated; 66%

R_f = 0.32 (75:25 hexanes/EtOAc); **^{1}H NMR** (400 MHz $CDCl_3$) δ 8.31 (d, *J* = 2.7 Hz, 1H, Ar-*H*), 8.19 (q, *J* = 2.8 Hz, 1H, Ar-*H*), 7.23 – 7.14 (m, 2H, Ar-*H*), 4.04 (td, *J* = 6.6, 2.5 Hz, 2H, O-C*H*$_2$), 1.80 – 1.57 (m, 2H, C*H*$_2$), 1.36 – 1.09 (m, 2H, C*H*$_2$), 0.93 (td, *J* = 7.4, 2.6 Hz, 3H, C*H*$_3$), 0.52 (dddt, *J* = 27.2, 9.4, 6.9, 2.7 Hz, 2H, 2 x C*H*), 0.26 (td, *J* = 6.7, 2.5 Hz, 2H, C*H*$_2$); **^{13}C NMR** (101 MHz, $CDCl_3$) δ 155.4 (Ar), 142.0 (Ar), 138.2 (Ar), 123.9 (Ar), 121.1 (Ar), 68.5 (O-*C*H_2), 33.9 (*C*H_2), 27.2 (*C*H_2), 20.7 (*C*H), 15.1 (*C*H_3), 13.8 (*C*H), 11.5 (*C*H); **HRMS (ESI):** *m/z* calcd for $C_{12}H_{17}NO+H^+$: 192.1388 $[M+H]^+$; found: 192.1381.

2-(2-Bromo-1-methylcyclopropyl)ethyl 4-bromobenzoate (20)

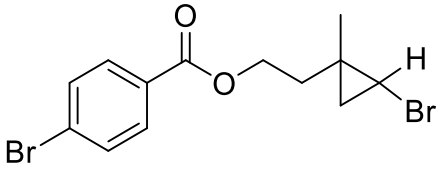

Colorless oil; 0.64 mmol scale; isolated 70.8 mg; 98%

R_f = 0.69 (80:20 hexanes/EtOAc); **^{1}H NMR** (500 MHz, $CDCl_3$) δ 7.95 – 7.88 (m, 2H), 7.62 – 7.57 (m, 2H), 4.51 (t, *J* = 6.9 Hz, 2H), 2.88 (dd, *J* = 7.7, 4.4 Hz, 1H), 2.04 (td, *J* = 7.0, 1.3 Hz, 2H), 1.19 (s, 3H), 1.05 (dd, *J* = 7.7, 6.3 Hz, 1H), 0.78 (dd, *J* = 6.3, 4.4 Hz, 1H); **^{13}C NMR** (126

MHz, $CDCl_3$) δ 166.0, 131.9, 131.3, 129.4, 128.2, 63.4, 35.2, 29.4, 22.8, 22.5, 19.1; **HRMS (ESI):** *m/z* calcd for $C_{13}H_{14}Br_2O_3+H^+$ ($^{79}Br+^{81}Br$): 362.9419 $[M+H]^+$; found: 362.9416.

1-((3-Bromo-2,2-dimethylcyclopropyl)methoxy)-3,5-dimethoxybenzene (21)

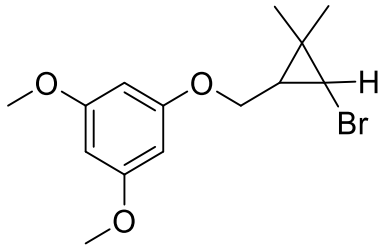

Light yellow oil; 0.7 mmol scale; isolated 206.5 mg; 94%

R_f = 0.44 (90:10 hexanes/EtOAc); **^{1}H NMR** (600 MHz, $CDCl_3$) *mix of diastereoisomers* δ 6.11 – 6.04 (m, 3H, Ar-*H*), 4.06 (ddd, *J* = 24.7, 10.3, 6.5 Hz, 1H, O-C*H*$_2$), 3.96 (dd, *J* = 10.2, 7.0 Hz, 0.5H, O-C*H*$_2$), 3.79 (dd, *J* = 10.4, 8.3 Hz, 0.5H, O-C*H*$_2$), 3.75 (s, 3H, O-C*H*$_3$), 3.75 (s, 3H, O-C*H*$_3$), 3.04 (d, *J* = 7.7 Hz, 0.4H, C*H*Br), 2.79 (d, *J* = 4.2 Hz, 0.6H, C*H*Br), 1.38 (ddd, *J* = 8.3, 6.1, 4.2 Hz, 0.5H, C*H*), 1.31 (s, 2H, C*H*$_3$), 1.23 (dt, *J* = 7.8, 7.0 Hz, 0.5H, C*H*), 1.19 (s, 1H, C*H*$_3$), 1.18 (s, 1H, C*H*$_3$), 1.16 (s, 2H, C*H*$_3$); **^{13}C NMR** (126 MHz, $CDCl_3$) *mix of diastereoisomers* δ 161.5 (Ar), 160.8 (Ar), 160.6 (Ar), 93.6 (Ar), 93.2 (Ar), 93.1 (Ar), 66.9 (O-*C*H$_2$), 66.8 (O-*C*H$_2$), 55.3 (O-*C*H$_3$), 34.6 (*C*HBr), 33.4 (*C*H), 32.5 (*C*H), 26.9 (*C*HBr), 25.4 (CH_3), 24.4 (CH_3), 22.2 (*C*), 19.9 (*C*), 19.6 (CH_3), 17.2 (CH_3); **HRMS (ESI):** *m/z* calcd for $C_{14}H_{19}BrO_3$: 314.0518 $[M]^+$; found: 314.0524.

2-(2-Bromo-1-methylcyclopropyl)ethyl (*t*-butoxycarbonyl)-*L*-tryptophanate (22)

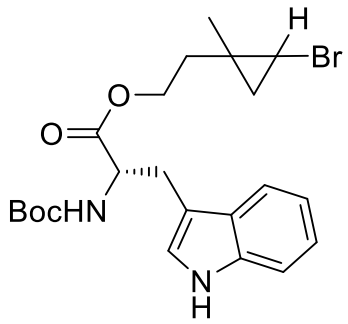

Colorless oil; 0.68 mmol scale; isolated 277.4 mg; 88%

R_f = 0.53 (70:30 hexanes/EtOAc); **^{1}H NMR** (600 MHz, $CDCl_3$) δ 8.42 (t, *J* = 8.8 Hz, 1H, N*H*), 7.57 (td, *J* = 9.8, 8.9, 2.6 Hz, 1H, Ar-*H*), 7.35 (dd, *J* = 8.3, 2.5 Hz, 1H, Ar-*H*), 7.19 (t, *J* = 7.6 Hz, 1H, Ar-*H*), 7.12 (td, *J* = 7.5, 4.1 Hz, 1H, Ar-*H*), 7.00 (t, *J* = 2.9 Hz, 1H, Ar-*H*), 5.15 (d, *J* = 8.6 Hz, 1H, N*H*), 4.72 – 4.58 (m, 1H, *H*□), 4.32 – 3.97 (m, 2H, O-C*H*$_2$), 3.30 (q, *J* = 8.7, 7.5 Hz, 2H, C*H*$_{2\text{-ind}}$), 2.78 – 2.65 (3 x m, 1H, C*H*Br), 1.87 (t, *J* = 7.1 Hz, 1H, C*H*$_2$-CH$_2$-O), 1.78 (t, *J* = 7.1 Hz, 1H, C*H*$_2$-CH$_2$-O), 1.45 (s, 9H, C(C*H*$_3$)$_3$), 1.42 – 1.30 (m, 0.5H, C*H*$_2$-CHBr), 1.29 (s, 1H, C*H*$_3$), 1.26 (s, 0.5H, C*H*$_3$), 1.19 (s, 0.5H, C*H*$_3$), 1.14 (s, 0.5H, C*H*$_3$), 1.01 (d, *J* = 4.0 Hz, 1H, C*H*$_3$), 0.90 (dt, *J* = 11.8, 5.7 Hz, 0.5H, C*H*$_2$-CHBr), 0.65 (p, *J* = 5.8 Hz, 0.5H, C*H*$_2$-CHBr), 0.57 (dt, *J* = 6.8, 3.4 Hz, 0.5H, C*H*$_2$-CHBr); **^{13}C NMR** (151 MHz, $CDCl_3$) δ 172.5 (C=O$_{ester}$), 172.4 (C=O$_{ester}$), 172.4 (C=O$_{ester}$), 155.4 (C=O$_{Boc}$), 136.2 (Ar), 127.7 (Ar), 122.9 (Ar), 122.2 (Ar), 122.2 (Ar), 119.7 (Ar), 119.6 (Ar), 118.7 (Ar), 111.4 (Ar), 111.3 (Ar), 110.1 (Ar), 108.8 (Ar), 80.0 (*C*(CH$_3$)$_3$), 63.4 (*C*), 63.4 (*C*), 63.1 (*C*), 62.9 (*C*), 62.8 (*C*), 54.4 (*C*H$_2$-O), 37.0 (*C*HBr), 36.7 (*C*HBr), 34.8 (*C*HBr), 34.3 (*C*HBr), 29.3 (*C*H$_2$-CH$_2$-O), 29.2 (*C*H$_2$-CH$_2$-O), 28.4 (C(CH$_3$)$_3$), 27.4 (*C*H$_{2\text{-ind}}$), 27.3 (*C*H$_{2\text{-ind}}$), 22.4 (*C*H$_3$), 22.2 (*C*H$_3$), 22.0 (*C*H$_3$), 21.9 (*C*H$_3$), 20.1 (*C*H$_2$-CHBr), 20.0 (*C*H$_2$-CHBr), 18.8 (C$_{\text{-quat}}$), 18.8 (C$_{\text{-quat}}$), 18.6 (C$_{\text{-quat}}$); **HRMS (ESI):** *m/z* calcd for $C_{22}H_{29}BrN_2O_4$+Na^+: 487.1201 [*M*+Na]$^+$; found: 487.1209.

5-(*t*-Butyl) 6-(4-fluorobenzyl) 1-bromo-5-azaspiro[2.4]heptane-5,6-dicarboxylate (23)

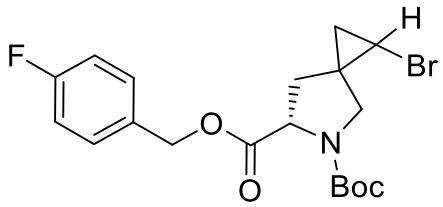

Colorless oil; 0.58 mmol scale; isolated 226.3 mg; 90%

R_f = 0.48 (50:50 hexanes/EtOAc); **^{1}H NMR** (600 MHz, $CDCl_3$) *mix of diastereoisomers* δ = 7.33 (dtdd, *J*=11.9, 8.7, 5.4, 2.6, 2H), 7.02 (dtt, *J* = 13.3, 8.4, 2.7, 2H), 5.25 – 4.97 (m, 2H), 4.53 (ddd, *J* = 24.4, 8.7, 3.9, 0.5H), 4.40 (ddd, *J* = 32.0, 8.6, 4.3, 0.5H), 3.72 (dd, *J* = 34.1, 10.9, 0.5H), 3.52 – 3.41 (m, 0.5H), 3.36 (dd, *J* = 54.2, 9.7, 1H), 3.06 – 2.88 (m, 1H), 2.60 – 2.29 (m, 1H), 1.92 (ddd, *J* = 40.5, 13.3, 4.5, 1H), 1.72 (td, *J* = 13.3, 3.7, 1H), 1.50 – 1.32 (m, 9H), 1.28 – 1.06 (m, 1H), 0.88 (dddd, *J* = 76.7, 22.2, 6.9, 4.5, 1H); **^{13}C NMR** (151 MHz, $CDCl_3$) *mix of diastereoisomers* δ = 172.4, 172.3, 172.1, 172.0, 163.6, 162.0, 154.2, 153.5, 131.6, 131.4, 130.7, 130.7, 130.7, 130.6, 130.3, 130.3, 130.3, 130.3, 115.7, 115.5, 115.4, 80.4, 80.3, 80.3, 66.1, 66.1, 59.9, 59.5, 59.1, 58.8, 53.1, 52.9, 52.8, 52.6, 38.0, 37.2, 37.1, 36.5, 28.4, 28.4, 28.2, 28.2, 26.5, 26.5, 25.8, 25.8, 25.1, 24.4, 23.7, 23.5, 22.3, 22.2, 21.9, 21.1; **HRMS (ESI):** *m/z* calcd for $C_{19}H_{23}BrFNO_4$+Na^+: 450.0692 [*M*+Na]$^+$; found: 450.0675.

2-(2,2-dibromo-1-methylcyclopropyl)ethyl 4-bromobenzoate (24)

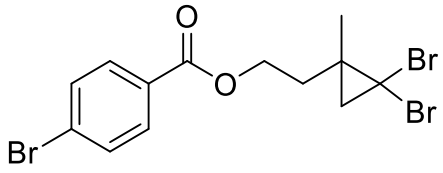

White solid

R_f = 0.62 (80:20 hexanes/EtOAc); **mp** 37-38 °C; **^{1}H NMR** (500 MHz, $CDCl_3$) δ 7.96 – 7.91 (m, 2H, Ar-*H*), 7.63 – 7.57 (m, 2H, Ar-*H*), 4.59 – 4.48 (m, 2H, C*H*$_2$-O), 2.23 – 2.10 (m, 2H, C*H*$_2$), 1.55 (d, *J* = 7.4 Hz, 1H, C*H*$_2$), 1.50 (d, *J* = 7.3 Hz, 1H, C*H*$_2$), 1.48 (s, 3H, C*H*$_3$); **^{13}C NMR** (126 MHz, $CDCl_3$) δ 166.0 (*C*=O), 131.9 (Ar), 131.3 (Ar), 129.1 (Ar), 128.3 (Ar), 62.7 (*C*H_2-O), 38.2 (O-CH_2-*C*H_2), 37.1 (CH_2), 34.6(*C*-Br_2), 27.7 (C_{IV}), 22.8 (*C*H_3); **HRMS (ESI):** *m/z* calcd for $C_{13}H_{13}Br_3O_3+H^+$: 438.8544 $[M+H]^+$; found: 438.8542.

2-(1-Methylcyclopropyl)ethyl 4'-methoxy-2'-methyl-[1,1'-biphenyl]-4-carboxylate (25)

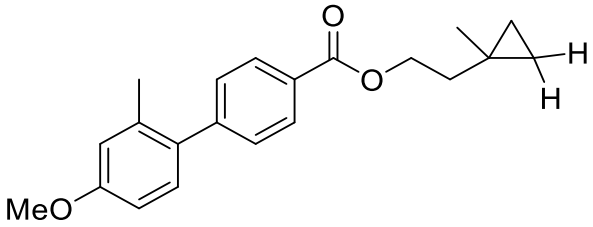

Colorless oil; 0.2 mmol scale; isolated 56.0 mg; 86%

R_f = 0.52 (90:10 hexanes/EtOAc); **^{1}H NMR** (500 MHz, $CDCl_3$) δ 8.11 – 8.05 (m, 2H), 7.41 – 7.36 (m, 2H), 7.17 (d, *J* = 8.3 Hz, 1H), 6.86 – 6.79 (m, 2H), 4.47 (t, *J* = 6.9 Hz, 2H), 3.85 (s, 3H), 2.28 (s, 3H), 1.74 (t, *J* = 6.9 Hz, 2H), 1.15 (s, 3H), 0.43 – 0.30 (m, 4H); **^{13}C NMR** (126 MHz, $CDCl_3$) δ 166.8, 159.3, 146.5, 136.8, 133.7, 130.8, 129.6, 129.5, 128.8, 116.0, 111.4, 63.8, 55.4, 38.2, 23.0, 20.8, 13.2, 13.0; **HRMS (CI)**: *m/z* calcd for $C_{21}H_{24}O_3+H^+$: 325.1804 $[M+H]^+$; found: 325.1802.

2-(2-Bromo-1-methylcyclopropyl-2-*d*)ethyl 4-methoxybenzoate (26)

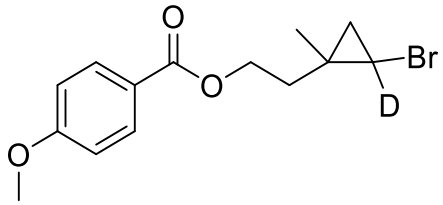

Colorless oil; 0.5 mmol scale; isolated 127.2 mg; 81%

R_f = 0.45 (90:10 hexane/EtOAc); **^{1}H NMR** (400 MHz, $CDCl_3$) *major diastereomers* δ 8.05 – 7.96 (m, 2H), 6.96 – 6.90 (m, 2H, Ar-*H*), 4.52 – 4.33 (m, 2H), 3.86 (s, 3H), 2.02 (t, *J* = 6.9 Hz, 1H), 1.70 (dt, *J* = 14.2, 7.0 Hz, 1H), 1.34 (s, 3H), 1.09 (d, *J* = 6.3 Hz, 1H), 0.69 (d, *J* = 6.3 Hz, 1H); *minor diastereomers* δ 8.05 – 7.96 (m, 2H), 6.96 – 6.90 (m, 2H), 4.52 – 4.33 (m, 2H), 3.86 (s, 3H), 2.02 (t, *J* = 6.9 Hz, 1H), 1.79 (dt, *J* = 14.2, 6.2 Hz, 1H), 1.19 (s, 3H), 1.03 (d, *J* = 6.3 Hz, 1H), 0.78 (d, *J* = 6.3 Hz, 1H); **^{13}C NMR** (101 MHz, cdcl$_3$) *major diastereomers* δ 166.25 (s), 163.34 (s), 131.57 (s), 122.53 (s), 113.60 (s), 62.23 (s), 55.41 (s), 37.43 (s), 35.07 (s), 22.41 (s), 20.14 (s), 18.86 (s); *minor diastereomers* δ 166.33 (s), 163.34 (s), 131.57 (s), 122.70 (s), 113.57 (s), 62.67 (s), 55.41 (s), 37.43 (s), 35.07 (s), 22.33 (s), 21.95 (s), 18.90 (s); **HRMS ESI:** *m/z* calcd for $C_{14}H_{16}Br\ DO_3$+Na^+: 336.0322 [*M*+Na]$^+$; found: 336.0325.

2-(1-Methylcyclopropyl-2-*d*)ethyl 4-methoxybenzoate (27)

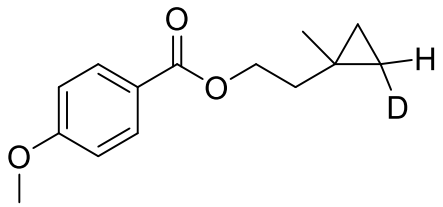

Colorless oil; 0.2 mmol scale; isolated 20.6 mg; 44%

R_f = 0.43 (90:10 hexane/EtOAc); **^{1}H NMR** (400 MHz, $CDCl_3$) *mixture of diastereomers* δ 7.99 (d, *J* = 8.9 Hz, 2H), 6.92 (d, *J* = 8.9 Hz, 2H), 4.40 (t, *J* = 6.9 Hz, 2H), 3.86 (s, 3H), 1.69

(t, *J* = 6.9 Hz, 2H), 1.11 (s, 3H), 0.37 – 0.25 (m, 3H); **^{13}C NMR** (101 MHz, $CDCl_3$) δ 166.41 (s), 163.19 (s), 131.49 (s), 122.92 (s), 113.53 (s), 63.37 (s), 55.38 (s), 37.99 (s), 22.79 (s), 12.97 (s), 12.66 (s), 12.81 – 12.41 (m); **HRMS ESI:** *m/z* calcd for $C_{14}H_{17}DO_3$+Na^++CH_3OH: 290.1479 [*M*+Na+CH_3OH]$^+$; found: 290.1471.

2-(1-Methylcyclopropyl-2,2-*d*$_2$)ethyl 4-methoxybenzoate (28)

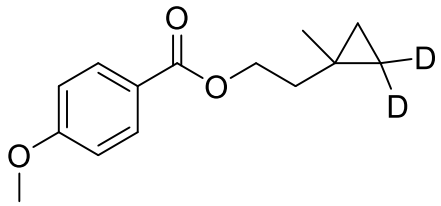

Colorless oil; 0.2 mmol scale; isolated 24.9 mg; 53%

R$_f$ = 0.53 (90:10 hexane/EtOAc); **^{1}H NMR** (400 MHz, $CDCl_3$) δ 7.99z (d, 2H), 6.92 (d, 2H), 4.40 (t, *J* = 6.9 Hz, 2H), 3.86 (s, 3H), 1.69 (t, *J* = 6.9 Hz, 2H), 1.11 (s, 3H), 0.31 (dd, *J* = 26.0, 4.6 Hz, 2H); **^{13}C NMR** (101 MHz, $CDCl_3$) δ 166.40 (s), 163.19 (s), 131.49 (s), 122.92 (s), 113.53 (s), 63.37 (s), 55.38 (s), 37.95 (s), 22.75 (s), 12.87 (s), 12.66 (s), 12.54 (s); **HRMS ESI:** *m/z* calcd for $C_{14}H_{16}D_2O_3$+Na^++CH_3OH: 291.1541 [*M*+Na+CH_3OH]$^+$; found: 291.1541.

(3*R*,4*S*,5*R*)-4,5-*bis*(Benzyloxy)-3-((benzyloxy)methyl)-7,7-dibromo-2-oxabicyclo[4.1.0]heptane (29)[4]

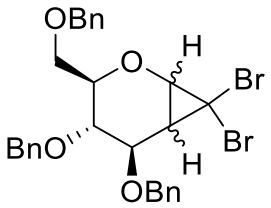

White solid

R_f = 0.55 (80:20 hexanes/EtOAc); **^{1}H NMR** (600 MHz, $CDCl_3$) δ 7.45 – 7.14 (m, 15H, Ar-*H*), 4.89 (d, *J* = 11.2 Hz, 1H, C*H*$_2$-benzyl), 4.80 (d, *J* = 11.7 Hz, 1H, C*H*$_2$-benzyl), 4.69 (d, *J* = 11.7 Hz, 1H, C*H*$_2$-benzyl), 4.52 (dd, *J* = 11.7, 6.3 Hz, 2H, C*H*$_2$-benzyl), 4.43 (d, *J* = 12.2 Hz, 1H, C*H*$_2$-benzyl), 3.93 (d, *J* = 7.7 Hz, 1H, C*H*-O), 3.86 (ddd, *J* = 7.7, 3.8, 2.7 Hz, 1H, C*H*-O), 3.78 (dd, *J* = 9.5, 7.6 Hz, 1H, C*H*-O), 3.67 (dd, *J* = 9.6, 4.8 Hz, 1H, C*H*-O), 3.56 – 3.47 (m, 2H, 2 x C*H*); **^{13}C NMR** (126 MHz, cdcl$_3$) δ 138.2 (Ar), 138.0 (Ar), 137.7 (Ar), 128.5 (Ar), 128.4 (Ar), 128.3 (Ar), 128.2 (Ar), 127.9 (Ar), 127.8 (Ar), 127.8 (Ar), 127.7 (Ar), 127.6 (Ar), 80.3 (*C*H-O), 79.9 (*C*H-O), 75.0 (*C*H$_2$-benzyl), 74.6 (*C*H$_2$-benzyl), 73.3 (*C*H$_2$-benzyl), 71.8 (*C*H$_2$-O), 70.2 (*C*H$_2$-O), 59.3 (*C*H$_2$-O), 35.2 (*C*H), 33.9 (*C*H).

2-Benzyl-7,7-dibromo-1-methyl-2-azabicyclo[4.1.0]heptan-3-one (30)

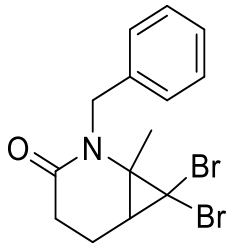

White solid

R_f = 0.55 (50:50 hexanes/EtOAc); **mp** 129-130 °C; **^{1}H NMR** (600 MHz, $CDCl_3$) δ = 7.34 – 7.28 (m, 4H, Ar-*H*), 7.26 – 7.22 (m, 1H, Ar-*H*), 5.48 (d, *J*=15.8, 1H, Ar-C*H*$_2$), 3.88 (d, *J*=15.8, 1H, Ar-C*H*$_2$), 2.61 (dddd, *J*=14.3, 10.0, 6.9, 4.5, 1H, C*H*), 2.46 – 2.34 (m, 2H, C*H*$_2$), 2.07 – 1.90 (m, 2H, C*H*$_2$), 1.51 (s, 3H, *CH*$_3$); **^{13}C NMR** (151 MHz, $CDCl_3$) δ = 171.6 (*C*=O), 138.5 (Ar), 128.6 (Ar), 127.4 (Ar), 127.1 (Ar), 49.7 (*C*-CH$_3$), 48.6 (*C*Br$_2$), 45.4 (*C*H$_2$-Ph), 36.9 (*C*H$_2$-Ph), 30.8 (CO-*C*H$_2$), 23.7 (*C*H$_2$), 23.1 (*C*H$_3$); **HRMS (ESI):** *m/z* calcd for $C_{14}H_{15}Br_2NO_3$+Na^+: 393.9418 [*M*+Na]$^+$; found: 393.9432.

2-(2,2-Dibromo-1-methylcyclopropyl)ethyl 4-methylbenzenesulfonate (31)

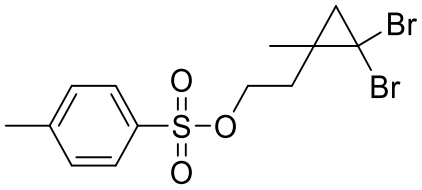

White solid

R_f = 0.45 (75:25 hexanes/EtOAc); **mp** 31-32 °C; **^{1}H NMR** (600 MHz, $CDCl_3$) δ 7.84 – 7.77 (m, 2H, Ar-*H*), 7.36 (d, *J* = 8.1 Hz, 2H, Ar-*H*), 4.23 (ddt, *J* = 10.0, 6.3, 2.8 Hz, 2H, O-CH_2), 2.46 (s, 3H, Ar-CH_3), 2.10 (dt, *J* = 14.6, 7.3 Hz, 1H, CH_2), 1.97 (dt, *J* = 14.5, 6.4 Hz, 1H, CH_2), 1.48 (d, *J* = 7.6 Hz, 1H, CH_2), 1.41 (d, *J* = 7.7 Hz, 1H, CH_2), 1.32 (s, 3H, CH_3); **^{13}C NMR** (151 MHz, $CDCl_3$) δ 145.1, 133.0, 130.0, 128.0, 67.8, 37.4, 37.3, 34.6, 27.1, 22.6, 21.8; **HRMS (ESI):** *m/z* calcd for $C_{13}H_{16}Br_2O_3SNa^+$: 432.9084 [*M*+Na]$^+$; found: 432.9091.

4-(2,2-Dibromocyclopropyl)butyl 1-naphthoate (32)

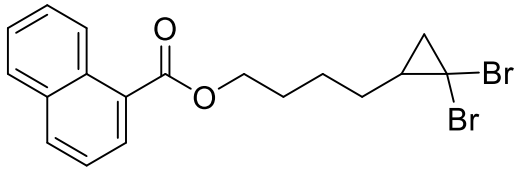

Yellow oil

R_f = 0.54 (90:10 hexanes/EtOAc); **^{1}H NMR** (400 MHz, $CDCl_3$) δ = 8.93 (d, *J*=8.6, 1H, Ar-*H*), 8.21 (dd, *J*=7.3, 1.3, 1H, Ar-*H*), 8.04 (d, *J*=8.2, 1H, Ar-*H*), 7.90 (dd, *J*=8.2, 1.4, 1H, Ar-*H*), 7.63 (ddd, *J*=8.6, 6.8, 1.5, 1H, Ar-*H*), 7.59 – 7.46 (m, 2H, Ar-*H*), 4.47 (t, *J*=6.5, 2H, O-CH_2), 2.10 – 1.49 (m, 8H, CH_2), 1.25 (t, *J*=7.2, 1H, CH_2); **^{13}C NMR** (101 MHz, $CDCl_3$) δ = 167.8 (*C*=O), 134.0 (Ar), 133.4 (Ar), 131.5 (Ar), 130.2 (Ar), 128.7 (Ar), 127.9 (Ar), 127.5 (Ar), 126.3 (Ar), 125.9 (Ar), 124.6 (Ar), 65.0 (O-*C*H_2), 32.4 (*C*H_2), 31.4 (*C*Br_2), 29.3 (*C*H), 28.7

(CH_2), 28.6 (CH_2), 25.2 (CH_2); **HRMS (ESI):** *m/z* calcd for $C_{18}H_{18}Br_2O_2$+Na^+: 446.9571 [*M*+Na]$^+$; found: 446.9586.

(3*S*,8*S*,9*S*,10*R*,13*R*,14*S*)-10,13-Dimethyl-17-((*R*)-6-methylheptan-2-yl)-2,3,4,7,8,9,10,11,12,13,14,15,16,17-tetradecahydro-1*H*-cyclopenta[*a*]phenanthren-3-yl 4-(2,2-dibromocyclopropyl)butanoate (33)

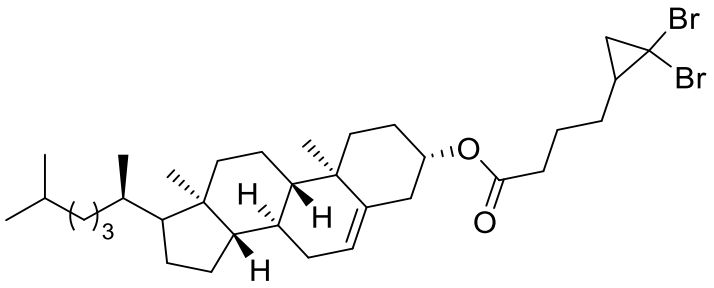

White solid

R_f = 0.62 (90:10 hexanes/EtOAc); **mp** = 61-64 °C; **^{1}H NMR** (400 MHz, $CDCl_3$) δ 5.38 (dd, *J* = 5.1, 2.0 Hz, 1H), 4.63 (dtd, *J* = 13.7, 8.1, 7.5, 4.1 Hz, 2H), 2.43 – 2.27 (m, 3H), 2.08 – 0.81 (m, 40H), 0.68 (s, 3H); **^{13}C NMR** (101 MHz, $CDCl_3$) δ 172.8, 139.7, 122.8, 74.1, 56.8, 56.2, 50.1, 42.4, 39.8, 39.6, 38.3, 37.1, 36.7, 36.3, 35.9, 34.2, 32.0, 32.0, 32.0, 31.1, 29.1, 28.6, 28.4, 28.2, 27.9, 24.4, 24.0, 23.9, 23.0, 22.7, 21.2, 19.5, 18.8, 12.0; **HRMS (ESI):** *m/z* calcd for $C_{34}H_{54}Br_2O_2$+Na^+: 675.2388 [*M*+Na]$^+$; found: 675.2396.

(3*R*)-5-(2.2-Dibromo-3,3-dimethylcyclopropyl)-3-methylpentyl furan-2-carboxylate (34)

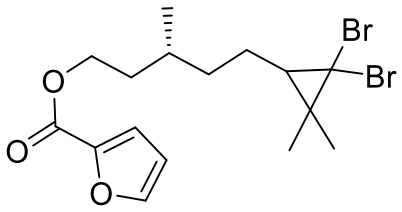

colorless oil

R_f = 0.28 (hexanes/EtOAc 80:20); **^{1}H NMR (400 MHz, $CDCl_3$):** δ 7.57 (dd, *J* = 1.8, 0.9 Hz, 2H), 7.17 (dd, *J* = 3.5, 1.0 Hz, 2H), 6.50 (dd, *J* = 3.5, 1.8 Hz, 2H), 4.42 – 4.30 (m, 2H), 1.88 – 1.75 (m, 1H), 1.73 – 1.53 (m, 3H), 1.53 – 1.40 (m, 3H), 1.37 (s, 3H), 1.18 (d, *J* = 0.9 Hz, 4H), 0.98 (dd, *J* = 6.5, 0.8 Hz, 3H). **^{13}C NMR (101 MHz, $CDCl_3$)**: δ 158.8, 146.2, 144.8, 117.8, 111., 63.32, 48.2, 48.2, 40.0, 35.4, 35.4, 35.3, 35.3, 29.8, 28.0, 28.0, 27.5, 25.4, 19.5, 19.5, 19.3, 19.3. **HRMS (ESI)**: *m/z* calcd for $C_{16}H_{22}Br_2O_3$+Na^+: 444.9814 $[M+Na]^+$; found: 444.9806.

2-(2,2-Dibromo-1-methylcyclopropyl)ethyl (*t*-butoxycarbonyl)-*L*-tryptophanate (35)

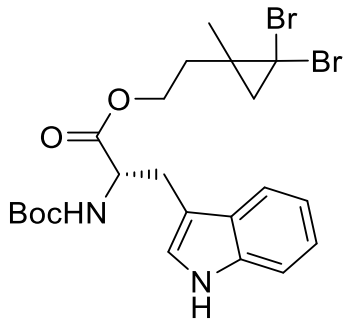

Pale yellow oil

R_f = 0.70 (50:50 hexanes/EtOAc); **^{1}H NMR** (500 MHz, $CDCl_3$) δ 8.11 (s, 1H, N*H*), 7.58 (d, *J* = 7.9, 1H, Ar-*H*), 7.36 (d, *J* = 8.1, 1H, Ar-*H*), 7.20 (t, *J* = 7.6, 1H, Ar-*H*), 7.13 (t, *J* = 7.5, 1H, Ar-*H*), 7.03 (d, *J* = 2.7, 1H, Ar-*H*), 5.10 (d, *J* = 8.3, 1H, C*H*), 4.65 (q, *J* = 6.7, 1H, C*H*), 4.35 – 4.07 (m, 2H, C(O)-CH_2), 3.39 – 3.21 (m, 2H, C$H_{2(Trp)}$), 1.88 (td, *J* = 7.0, 2.4, 2H, CH_2), 1.44 (s, 9H, CH_3), 1.42 – 1.31 (m, 2H, CH_2), 1.29 (s x 2, 3H, CH_3); **^{13}C NMR** (126 MHz, $CDCl_3$) δ 172.4, 155.4, 136.2, 127.6, 123.0, 122.1, 119.5, 118.6, 111.4, 109.8, 80.0, 62.8, 62.7, 54.4, 38.1, 36.6, 36.6, 34.2, 28.4, 28.2, 28.1, 28.0, 27.3, 27.3, 22.4; **HRMS (ESI):** *m/z* calcd for $C_{22}H_{28}Br_2N_2O_4$+Na^+: 565.0314 [*M*+Na]$^+$; found: 565.0309.

5-(*t*-Butyl) 6-(4-fluorobenzyl) (6*S*)-1,1-dibromo-5-azaspiro[2.4]heptane-5,6-dicarboxylate (36)

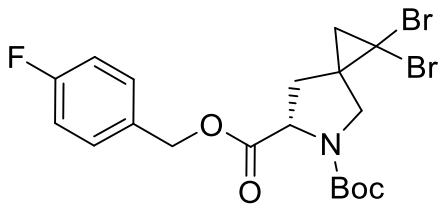

White solid

R_f = 0.43 (80:20 hexanes/EtOAc); **mp** 89-90 °C; **^{1}H NMR** (400 MHz, $CDCl_3$) δ 7.35 (m, 2H, Ar-*H*), 7.06 (m, 2H, Ar-*H*), 5.19 (dd, *J* = 12.1, 4.2, 1H, O-C*H*$_2$), 5.08 (d, *J* = 12.0, 1H, O-C*H*$_2$), 4.60 (ddd, *J* = 54.7, 9.0, 2.2, 1H, C*H*□), 3.88 (dd, *J* = 20.2, 11.2, 1H, N-C*H*$_2$), 3.43 (dd, *J* = 37.6, 11.2, 1H, N-C*H*$_2$), 2.78 (ddd, *J* = 21.8, 13.5, 8.9, 1H, C*H*$_2$), 1.81 (ddd, *J* = 12.2, 9.8, 2.2, 1H, C*H*$_2$), 1.70 (t, *J* = 7.8, 1H, C*H*$_2$), 1.42 (2 x s, 9H, 3 x C*H*$_3$); **^{13}C NMR** (101 MHz, $CDCl_3$) δ 172.1, 154.1, 153.5, 130.9, 130.8, 130.5, 130.4, 115.9, 115.8, 115.7, 115.5, 80.7, 66.4, 60.1, 59.7, 54.2, 39.4, 38.6, 35.6, 35.6, 34.9, 34.1, 29.3, 28.5, 28.3; **HRMS (ESI):** *m/z* calcd for $C_{19}H_{22}Br_2FNO_4$+Na^+: 527.9797 [*M*+Na]$^+$; found: 527.9800.

(4-Benzylpiperazin-1-yl)(2,2-dibromocyclopropyl)methanone (37)

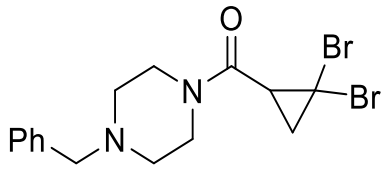

Brown solid

R_f = 0.59 (EtOAc); **mp** 45-47 °C; NMR, **^{1}H NMR** (500 MHz, $CDCl_3$) δ 7.40 – 7.28 (m, 5H, Ar-*H*), 3.96 – 3.77 (m, 2H, N-C*H*$_2$), 3.77 – 3.65 (m, 1H, N-C*H*$_2$), 3.58 (s, 2H, C*H*$_2$-Ar), 3.57 – 3.48 (m, 1H, N-C*H*$_2$), 2.72 – 2.60 (m, 2H, N-C*H*$_2$), 2.56 (dd, *J* = 10.1, 7.7 Hz, 2H, N-C*H*$_2$), 2.45 (ddd, *J* = 11.5, 7.8, 3.3 Hz, 1H, C*H*), 2.26 (t, *J* = 7.7 Hz, 1H, C*H*$_2$), 1.99 (dd, *J* = 10.1, 7.7

Hz, 1H, C*H*$_2$); **^{13}C NMR** (126 MHz, $CDCl_3$) δ 164.5 (*C*=O), 129.3 (Ar), 128.5 (Ar), 127.5 (Ar), 63.0 (*C*H$_2$-N), 53.2 (*C*H$_2$-N), 52.9 (*C*H$_2$-N), 45.8 (*C*H$_2$-N), 42.6 (*C*H$_2$-N), 34.8 (*C*-Br$_2$), 26.6 (*C*H), 21.4 (*C*H); **HRMS (ESI):** *m/z* calcd for $C_{15}H_{18}Br_2N_2O+H^+$: 400.9864 [*M*]$^+$; found: 400.9875.

4-((2,2-Dibromo-3,3-dimethylcyclopropyl)methoxy)-6-methylpyrimidin-2-amine (38)

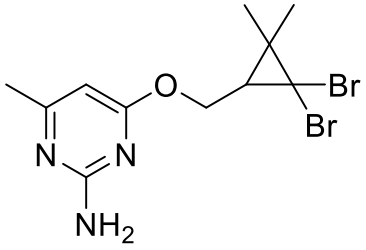

White solid

R$_f$ = (50:50 hexanes/EtOAc); **mp** 61-63 °C; **^{1}H NMR** (500 MHz, $CDCl_3$) δ 6.01 (s, 1H, Ar-*H*), 4.87 (s, 2H, N*H*$_2$), 4.45 (dd, *J* = 11.7, 7.0 Hz, 1H O-C*H*$_2$), 4.27 (dd, *J* = 11.7, 7.2 Hz, 1H O-C*H*$_2$), 2.28 (s, 3H, Ar-C*H*$_3$), 1.77 (t, *J* = 7.1 Hz, 1H, O-CH$_2$-C*H*), 1.46 (s, 3H, C*H*$_3$), 1.32 (s, 3H, C*H*$_3$).; **^{13}C NMR (126 MHz, $CDCl_3$)**: δ 170.3, 168.4, 162.5, 97.1, 64.9, 43.9, 37.3, 28.8, 27.1, 23.7, 19.7.; **HRMS (ESI):** *m/z* calcd for $C_{11}H_{15}Br_2N_3O+H^+$: 363.9660 [*M*+H]$^+$; found: 363.9660.

1-(2,2-Dibromo-3-methylcyclopropyl)-4-methoxybenzene (39)[9]

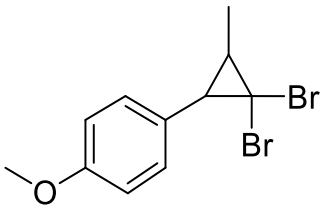

Pale yellow oil

R_f = 0.44 (90:10 hexanes/EtOAc); **^{1}H NMR** (400 MHz, $CDCl_3$) δ 7.20 – 7.13 (m, 2H, Ar-*H*), 6.92 – 6.85 (m, 2H, Ar-*H*), 3.82 (s, 3H, O-C*H*$_3$), 2.40 (d, *J* = 8.3 Hz, 1H, C*H*), 1.90 (dq, *J* = 8.3, 6.2 Hz, 1H, CH_3-C*H*), 1.46 (d, *J* = 6.2 Hz, 3H, C*H*$_3$); **^{13}C NMR** (101 MHz, $CDCl_3$) δ 159.1, 129.9, 128.8, 113.8, 55.4, 41.8, 39.8, 30.5, 17.5.

1-((2,2-Dimethylcyclopropyl)methoxy)-3,5-dimethoxybenzene (40)

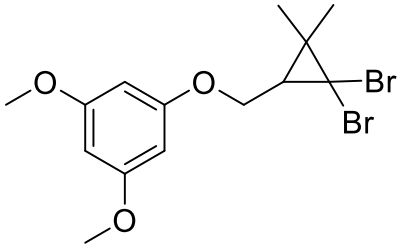

White crystal

R_f = 0.62 (70:30 hexanes/EtOAc); **mp** 68-70 °C; **^{1}H NMR** (600 MHz, $CDCl_3$) δ 6.09 (s, 3H, Ar-*H*), 4.13 (dd, *J* = 10.5, 6.5 Hz, 1H, O-C*H*$_2$), 3.90 (dd, *J* = 10.5, 7.1 Hz, 1H, O-C*H*$_2$), 3.76 (s, 6H, O-C*H*$_3$), 1.74 (t, *J* = 6.8 Hz, 1H, C*H*), 1.45 (s, 3H, C*H*$_3$), 1.28 (s, 3H, C*H*$_3$);**^{13}C NMR** (126 MHz, $CDCl_3$) δ 161.5 (Ar), 160.5 (Ar), 93.7 (Ar), 93.4 (Ar), 67.0 (*C*H_2-O), 55.4 (*C*H_3-O), 43.8 (*C*H), 37.5 (*C*Br2), 28.8 (*C*H), 27.2 (C), 19.6 (*C*H_3); **HRMS (ESI):** *m/z* calcd for $C_{14}H_{17}BrO_3$: 312.0361 [*M*+H]$^+$; found: 312.0350. (*Note: this molecule appears to be decomposing on heating in the GC and only the mono-brominated compound has been observed.)*

3-(2-(2,2-Dibromo-3-ethylcyclopropyl)ethoxy)pyridine (41)

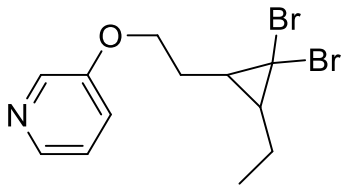

yellow oil

R_f = 0.24 (75:25 hexanes/EtOAc); ^{1}H NMR (500 MHz, $CDCl_3$): δ 8.34 (dd, *J* = 2.2, 1.4 Hz, 1H), 8.23 (dd, *J* = 3.6, 2.4 Hz, 1H), 7.24 – 7.21 (m, 2H), 4.19 – 4.10 (m, 2H), 2.16 (dt, *J* = 20.6, 6.2 Hz, 1H), 1.95 (ddd, *J* = 14.1, 12.9, 6.9 Hz, 1H), 1.68 (dt, *J* = 21.5, 7.3 Hz, 1H), 1.49 (tt, *J* = 14.5, 7.3 Hz, 1H), 1.34 (dd, *J* = 15.0, 7.2 Hz, 1H), 1.20 (dd, *J* = 15.0, 7.3 Hz, 1H), 1.06 (t, *J* = 7.4 Hz, 3H). **^{13}C NMR (126 MHz, $CDCl_3$):** δ 154.9, 142.3, 138.0, 123.8, 121.1, 66.5, 38.4, 37.5, 33.9, 32.3, 26.0, 12.6.; **HRMS (ESI):** *m/z* calcd for $C_{12}H_{15}Br_2NO+H^+$: 347.9599 $[M+H]^+$; found: 347.9603.

16. Experimental references

1. Lipshutz, B. H.; Ghorai, S.; Abela, A. R.; Moser, R.; Nishikata, T.; Duplais, C.; Krasovskiy, A.; Gaston, R. D.; Gadwood, R. C. *J. Org. Chem.* **2011**, *76*, 4379–4391.
2. Brochetta, M.; Borsari, T.; Gandini, A.; Porey, S.; Deb, A.; Casali, E.; Chakraborty, A.; Zanoni, G.; Maiti, D. *Chem. – Eur. J.* **2019**, *25*, 750–753.
3. Moore, P. W.; Schuster, J. K.; Hewitt, R. J.; Stone, M. R. L.; Teesdale-Spittle, P. H.; Harvey, J. E. *Tetrahedron* **2014**, *70*, 7032–7043.
4. Ramana, C. V.; Murali, R.; Nagarajan, M. *J. Org. Chem.* **1997**, *62*, 7694–7703.
5. Wolan, A.; Soueidan, M.; Chiaroni, A.; Retailleau, P.; Py, S.; Six, Y. *Tetrahedron Lett.* **2011**, *52*, 2501–2504.

6. Rhodes, Y. E.; Takakis, I. M.; Scheuler, P. E.; Weiss, R. A. *Tetrahedron Lett.*, **1978**, *28*, 2479-2482.
7. https://pubchem.ncbi.nlm.nih.gov/compound/86775512#section=Chemical-and-Physical-Properties
8. Simmons, H. E.; Smith, R. D. *J. Am. Chem. Soc.* **1959**, *81*, 4256–4264.
9. Ikeda, H.; Akiyama, K.; Takahashi, Y.; Nakamura, T.; Ishizaki, S.; Shiratori, Y.; Ohaku, H.; Goodman, J. L.; Houmam, A.; Wayner, D. D. M.; Tero-Kubota, S.; Miyashi, T. *J. Am. Chem. Soc.* **2003**, *125*, 9147–9157.

1.7 Spectral Data

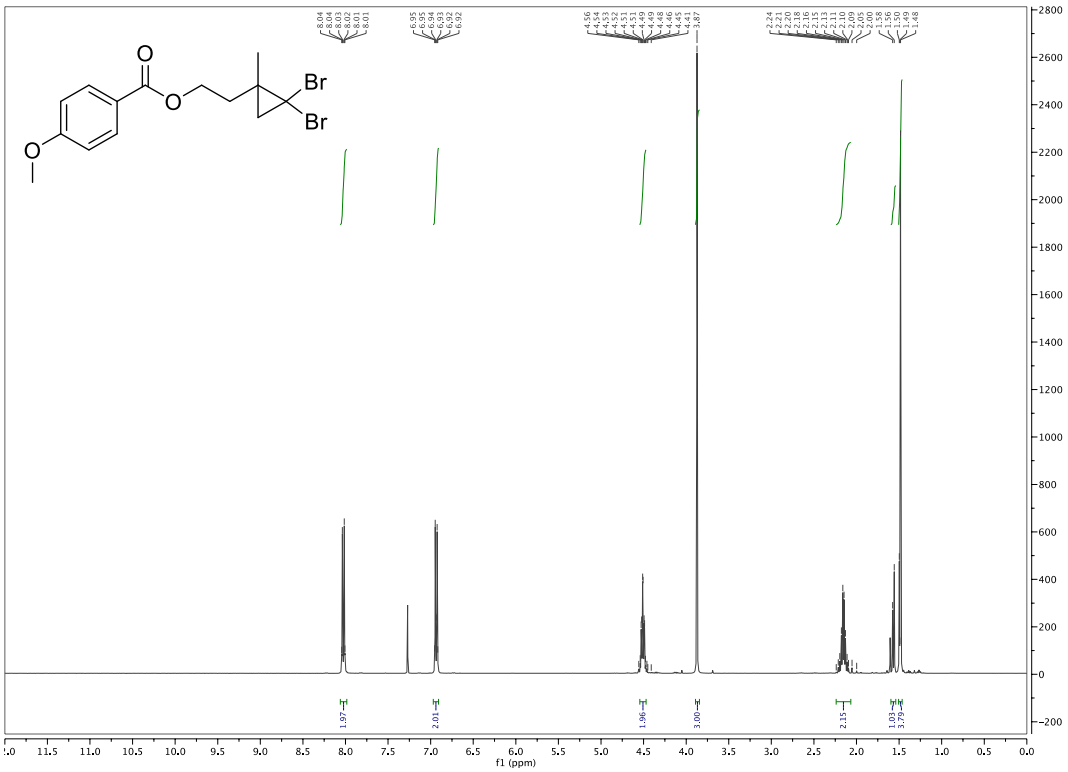

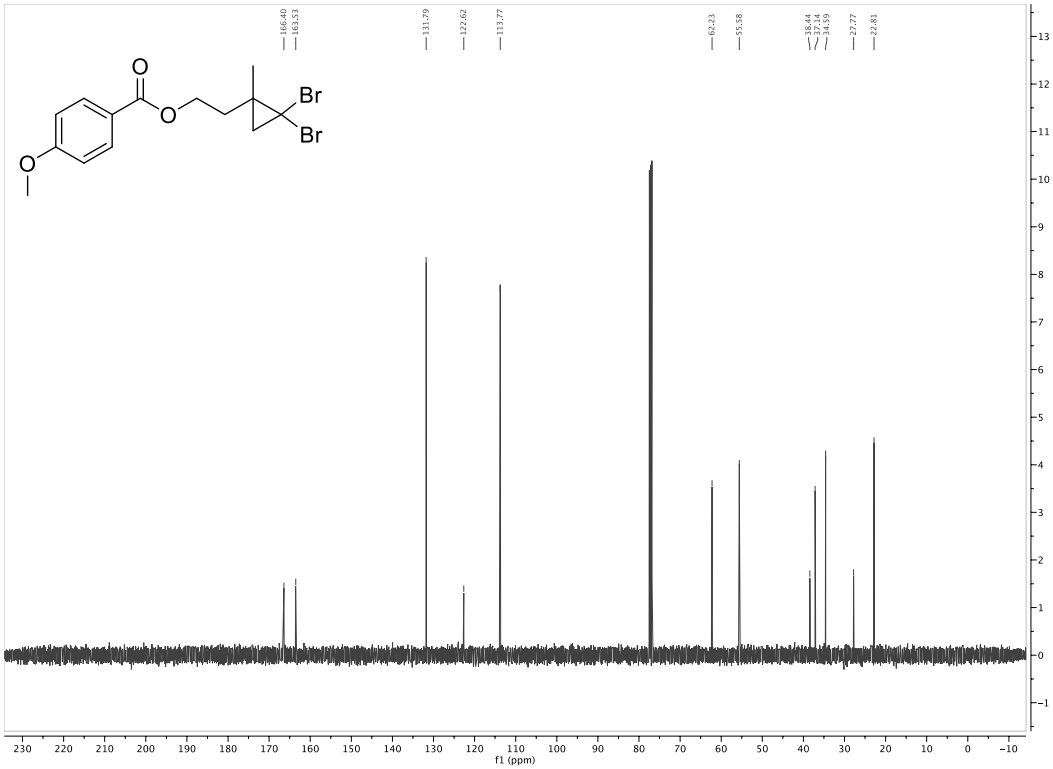

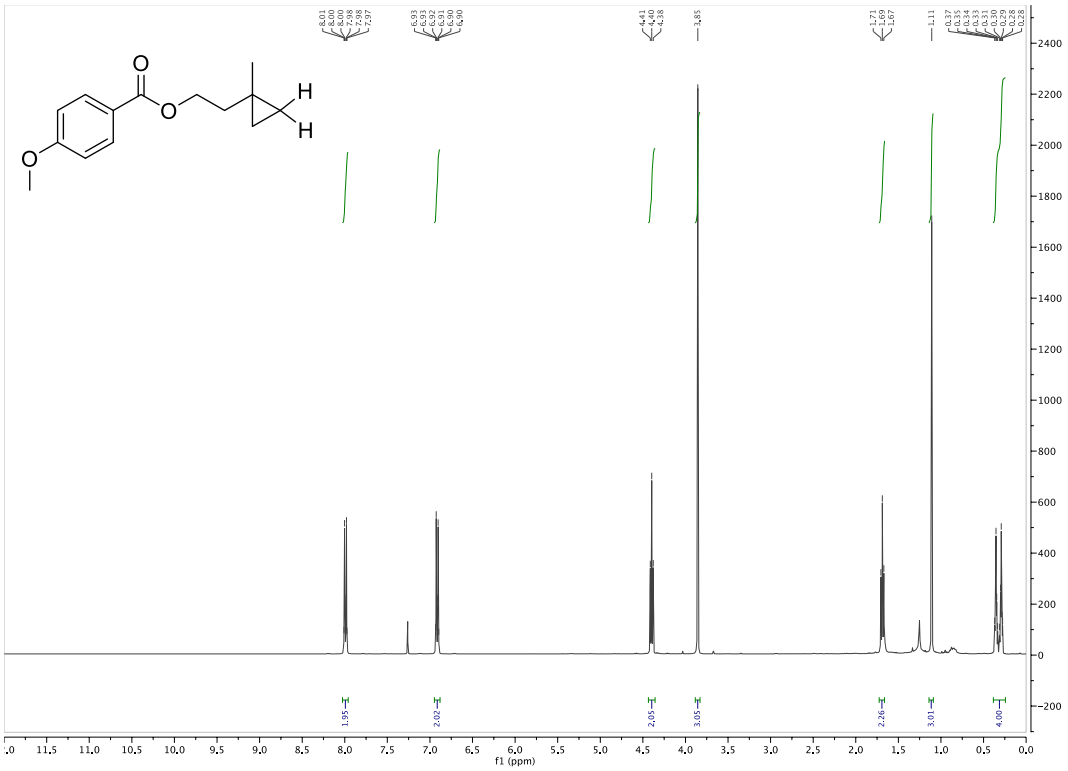
f1 (ppm)

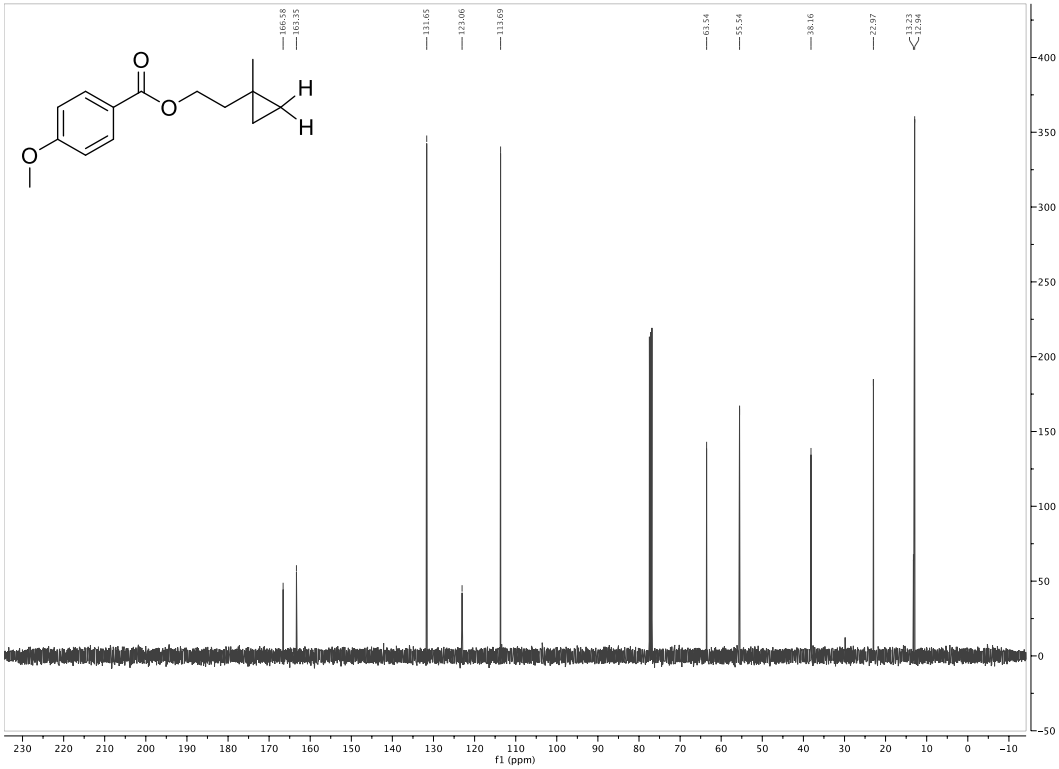
f1 (ppm)

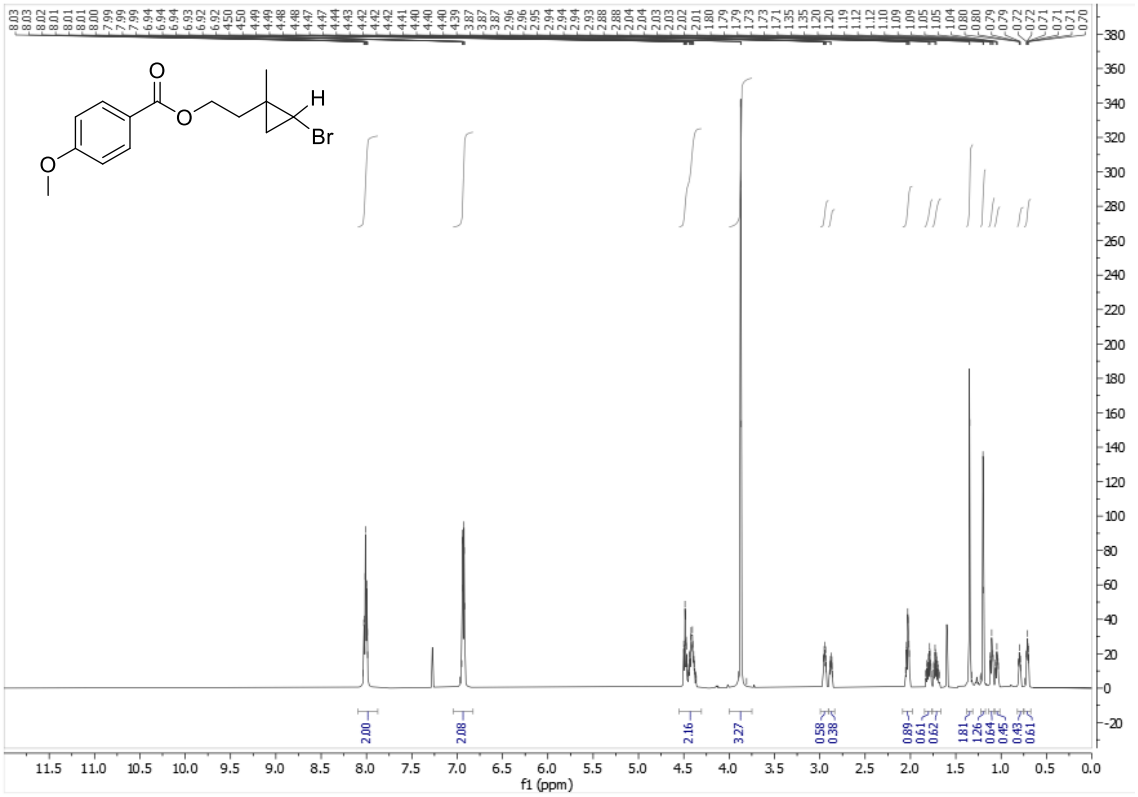
O
O
H
Br
O
f1 (ppm)

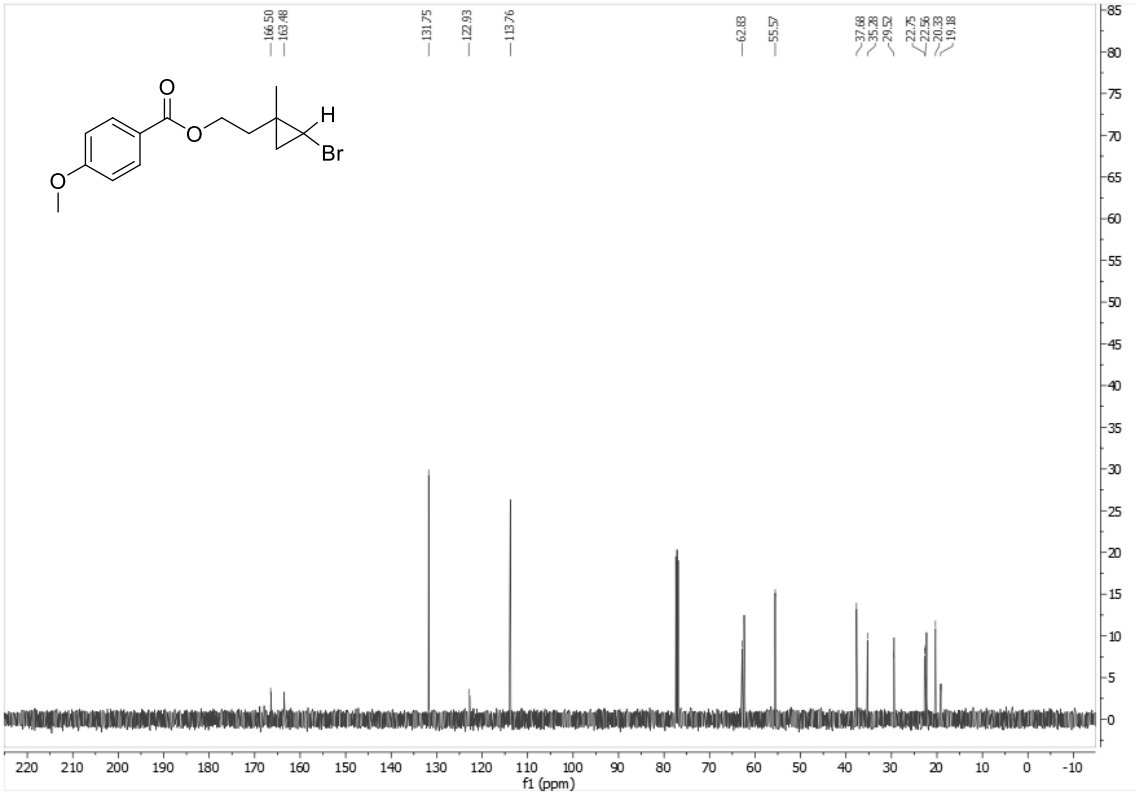
166.50
163.48
131.75
122.93
113.76
62.83
55.57
37.68
35.28
29.52
22.75
22.56
20.33
19.18
O
O
H
Br
O
f1 (ppm)

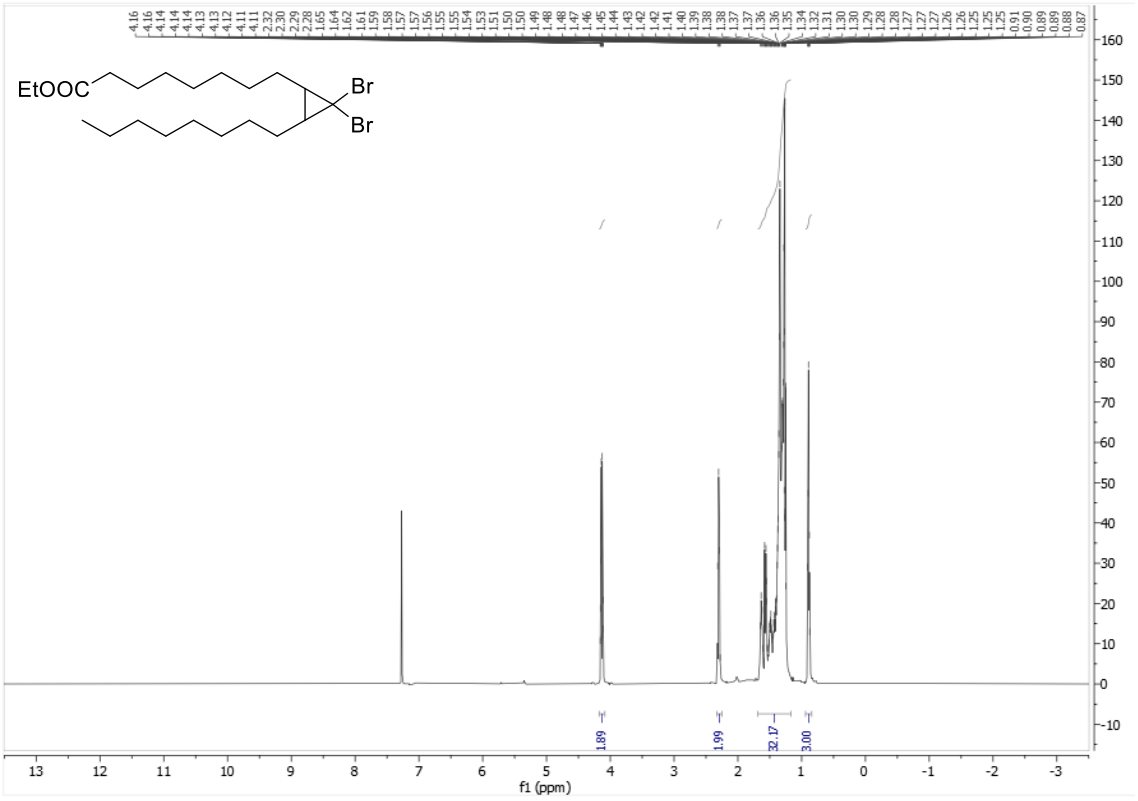
EtOOC
Br
Br
1.89
1.99
32.17
3.00
f1 (ppm)

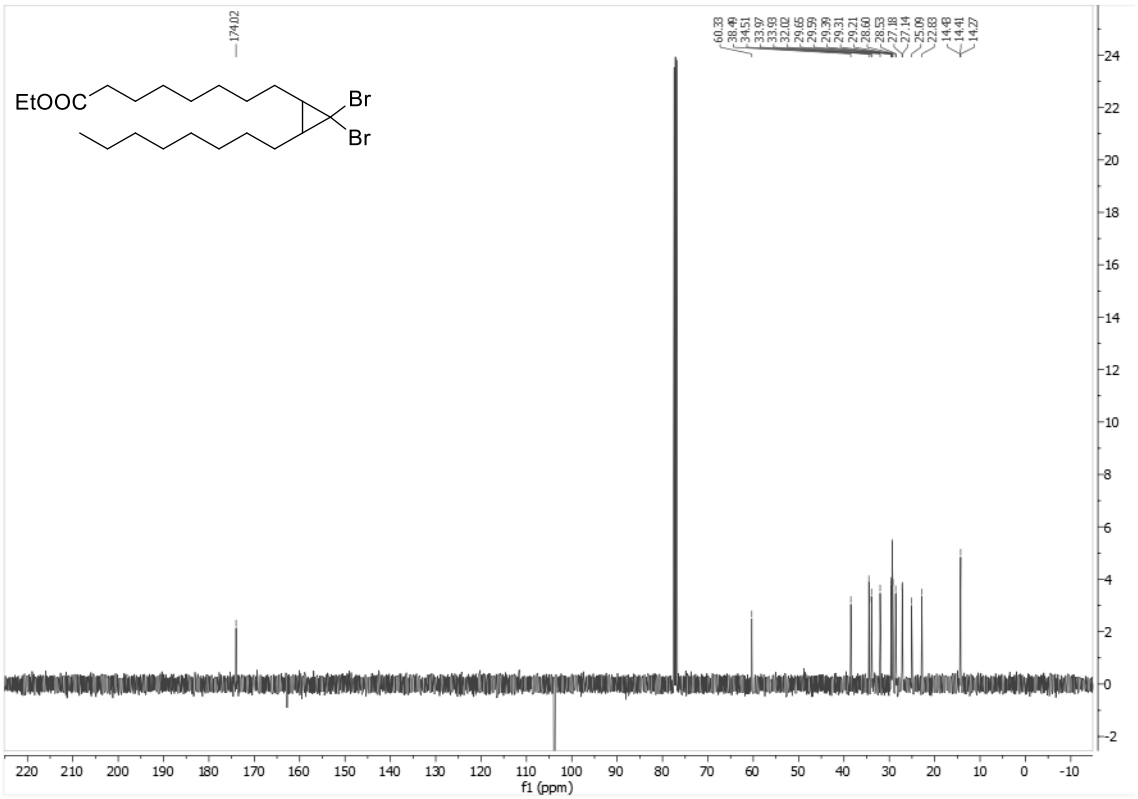
174.02
EtOOC
Br
Br
f1 (ppm)

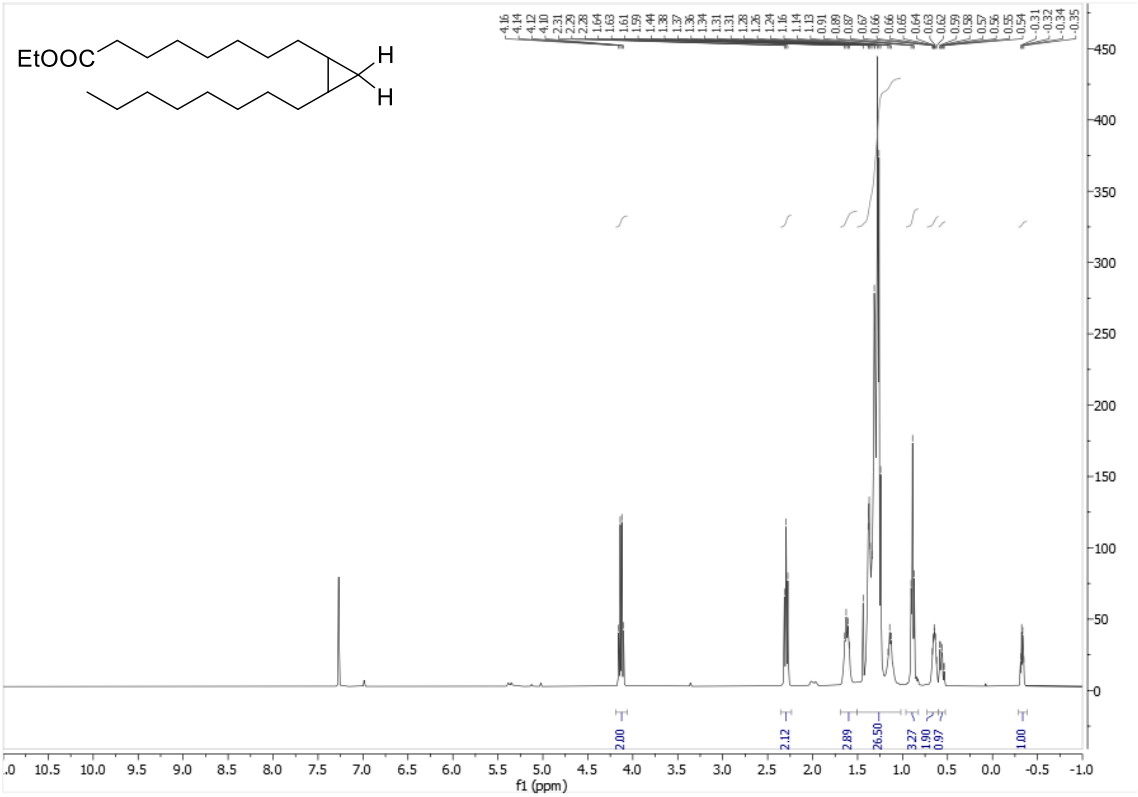
EtOOC
H
H
f1 (ppm)

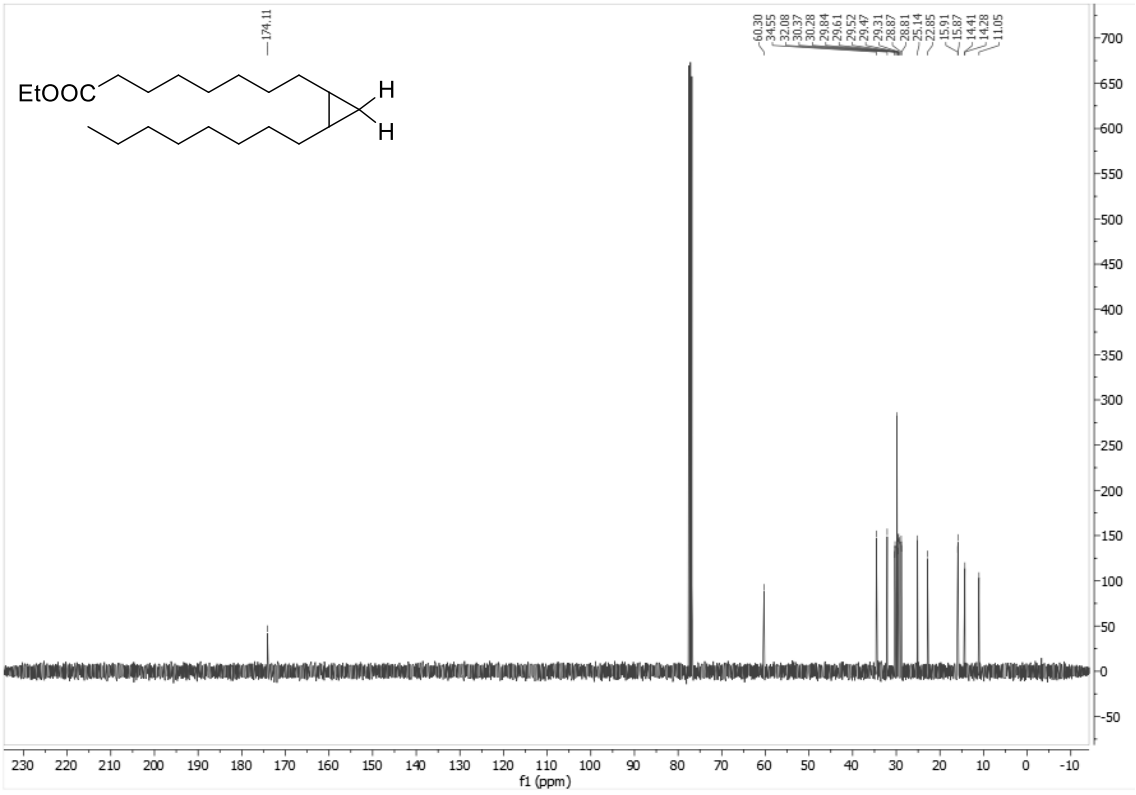
EtOOC
H
H
f1 (ppm)

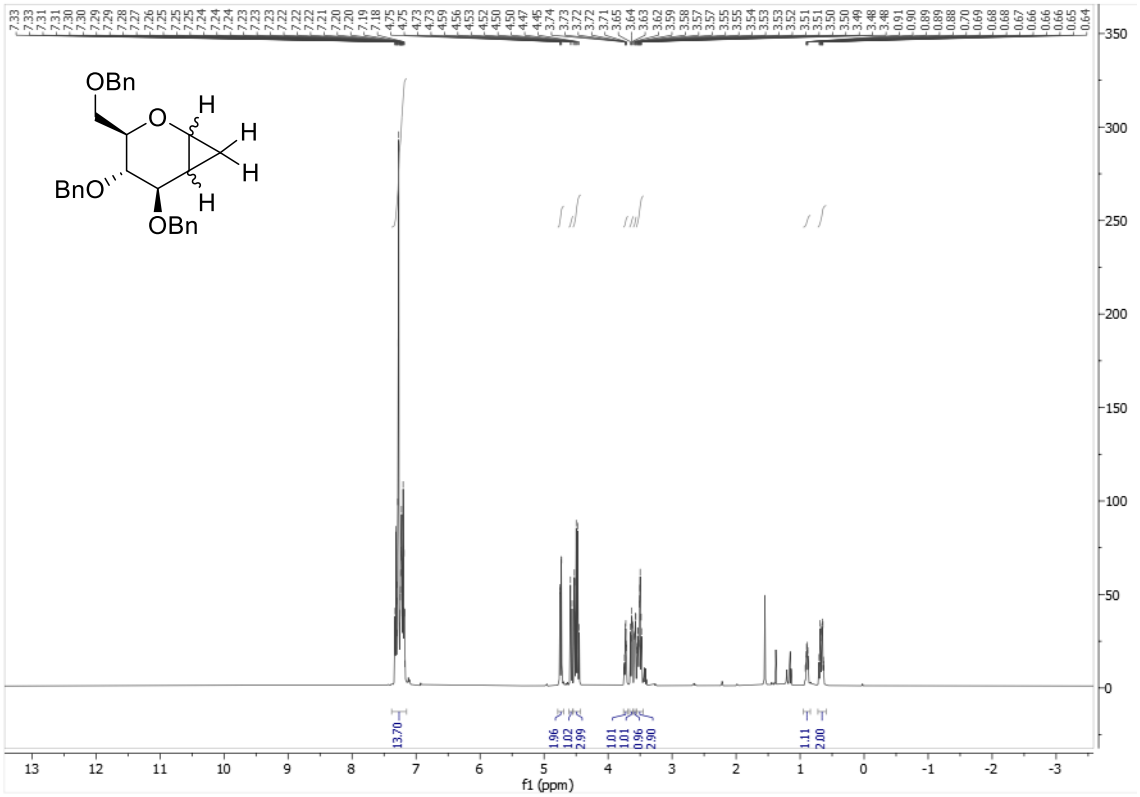
OBn
O
H
H
H
BnO
H
OBn
f1 (ppm)

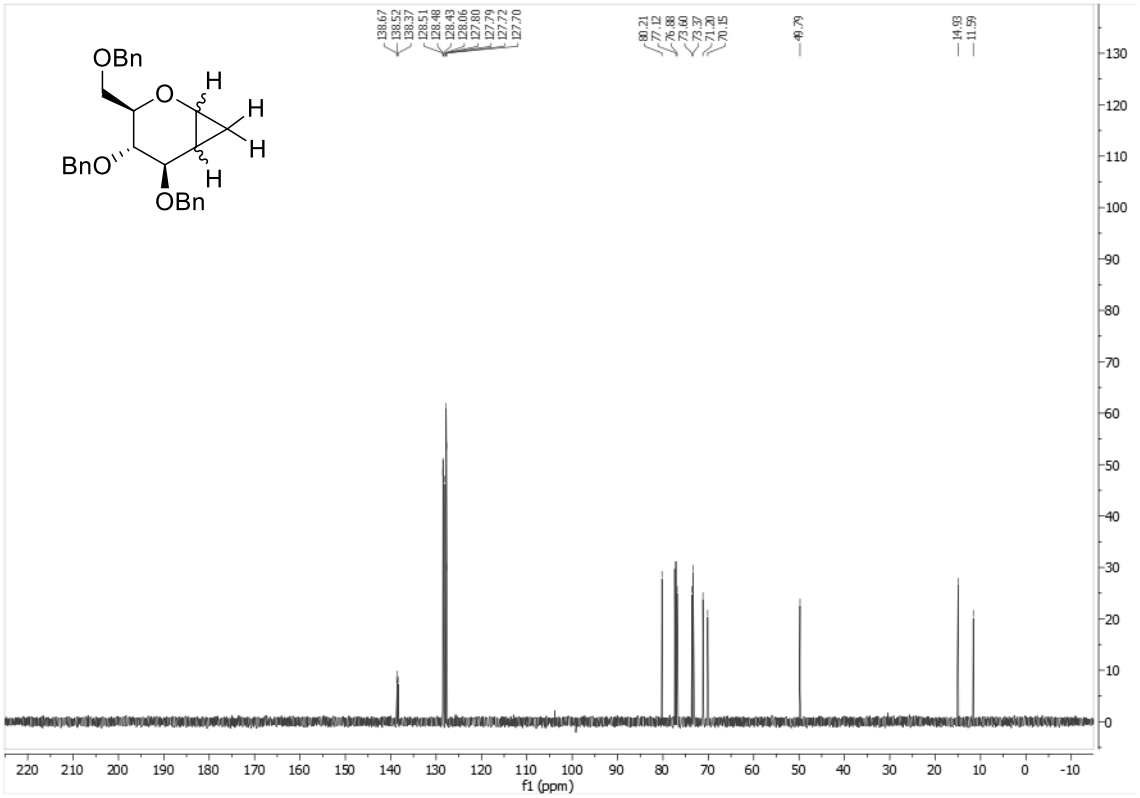
OBn
O
H
H
H
BnO
H
OBn
f1 (ppm)

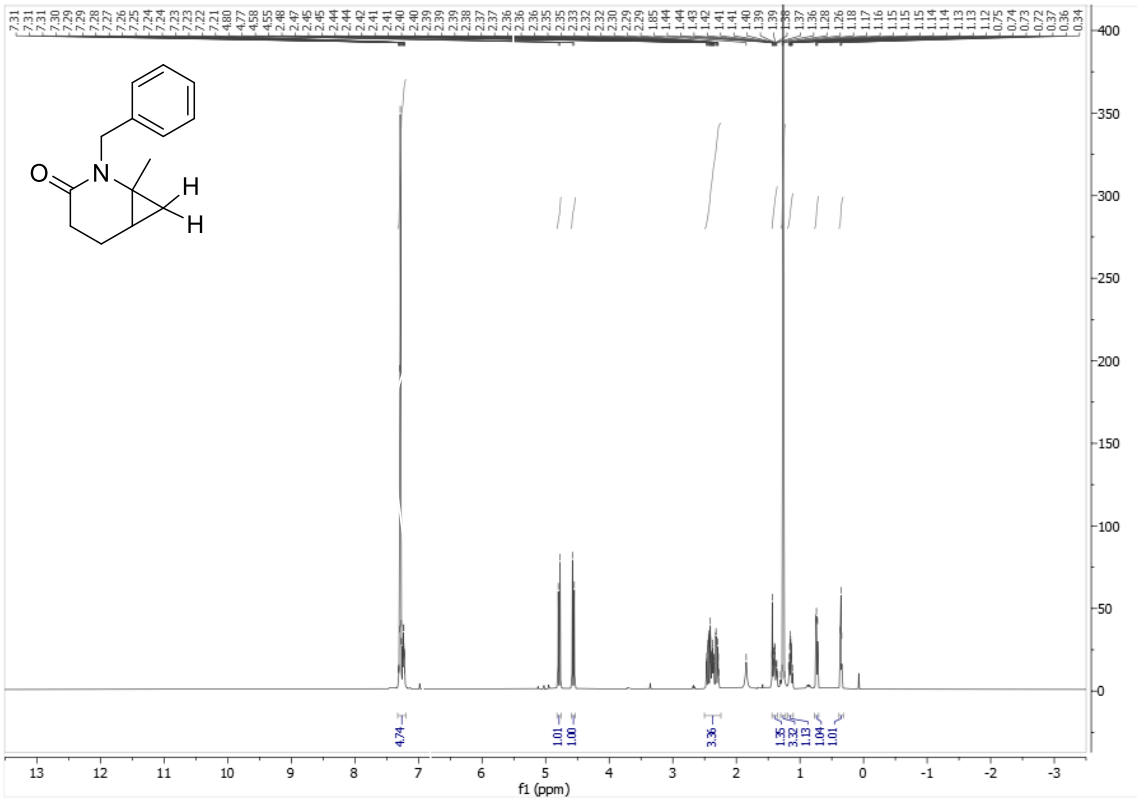
O
N
H
H
f1 (ppm)

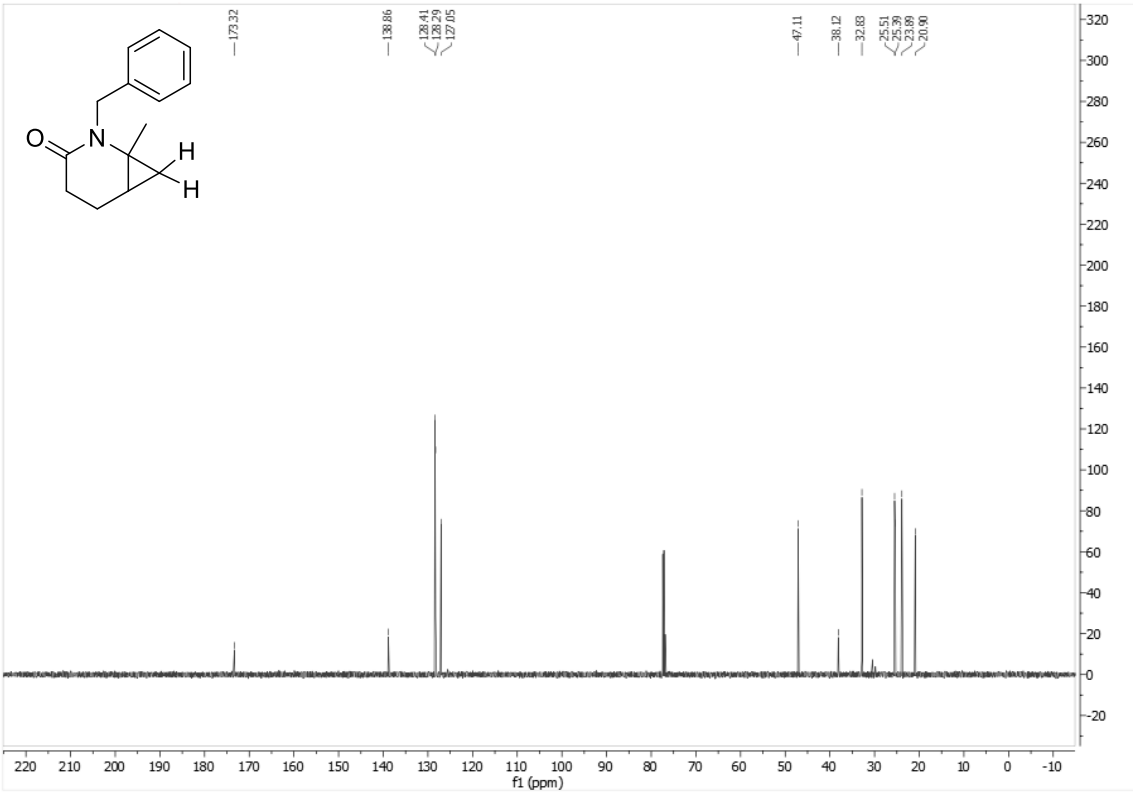
O
N
H
H
173.32
138.86
128.41
128.29
127.05
47.11
38.12
32.83
25.51
25.39
23.89
20.90
f1 (ppm)

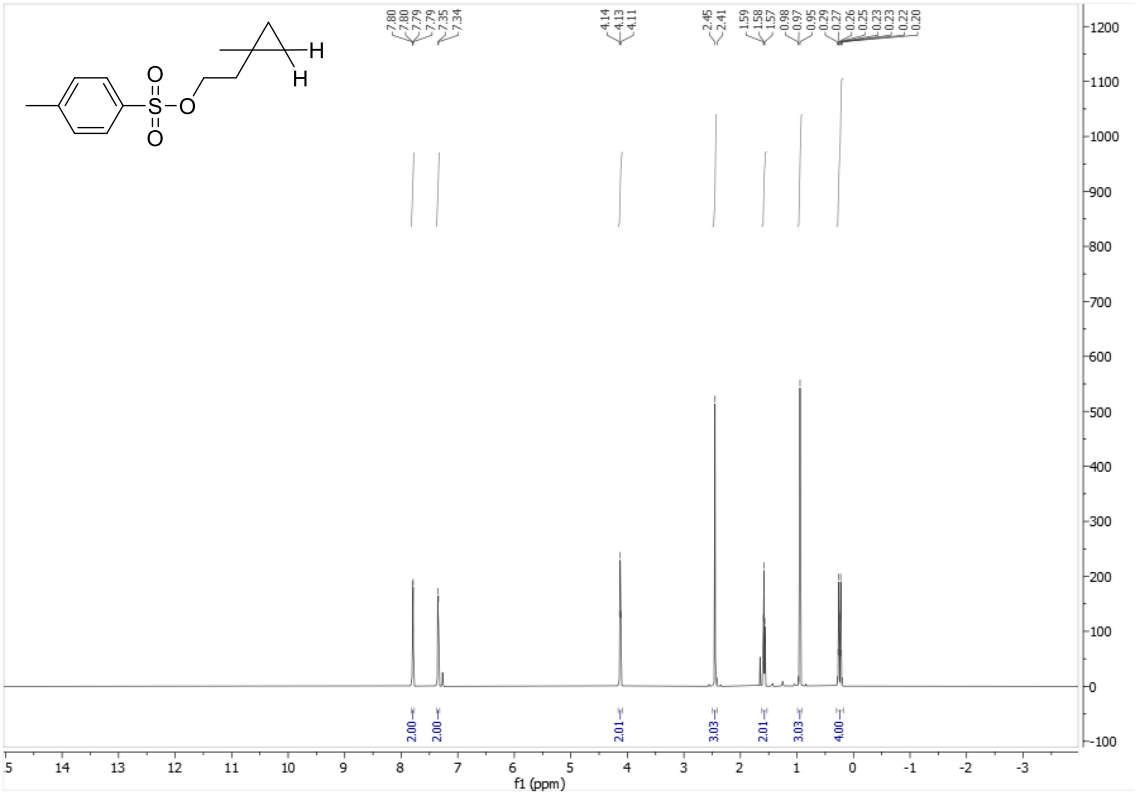
7.80
7.80
7.79
7.79
7.35
7.34
4.14
4.13
4.11
2.45
2.41
1.59
1.58
1.57
0.98
0.97
0.95
0.29
0.27
0.26
0.25
0.23
0.23
0.22
0.20
2.00
2.00
2.01
3.03
2.01
3.03
4.00
f1 (ppm)

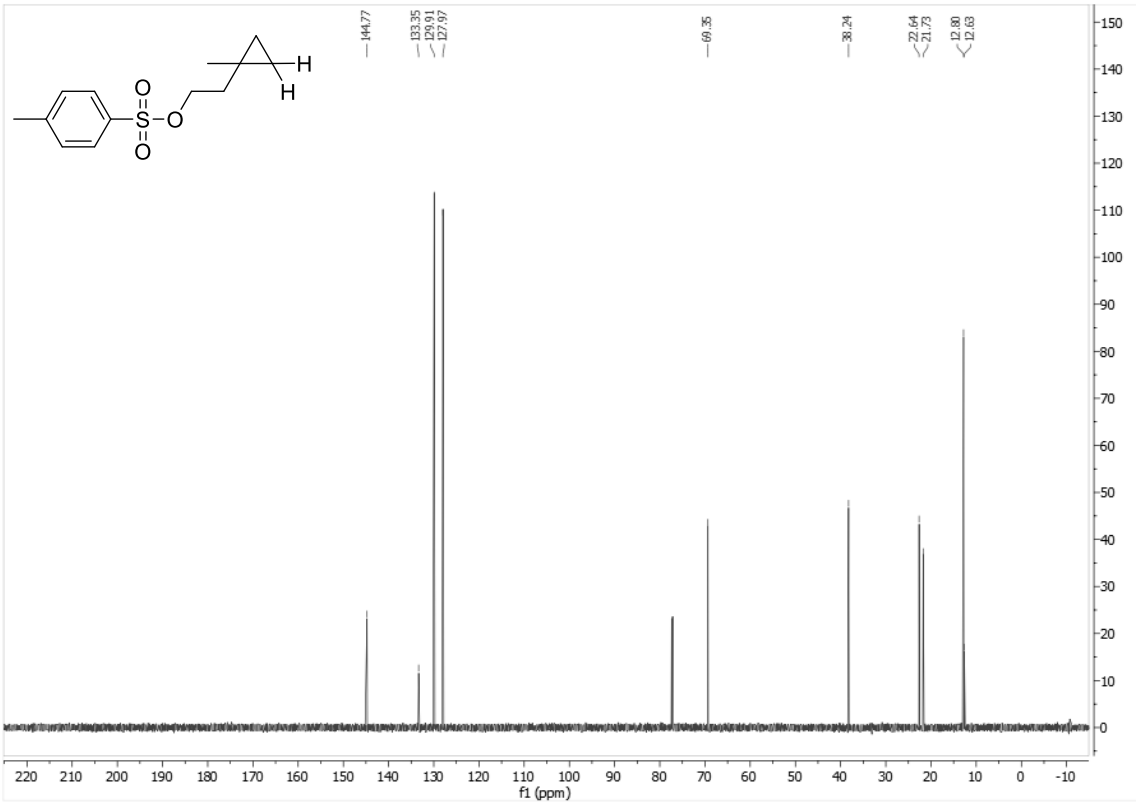
144.77
133.35
129.91
127.97
69.35
38.24
22.64
21.73
12.80
12.63
f1 (ppm)

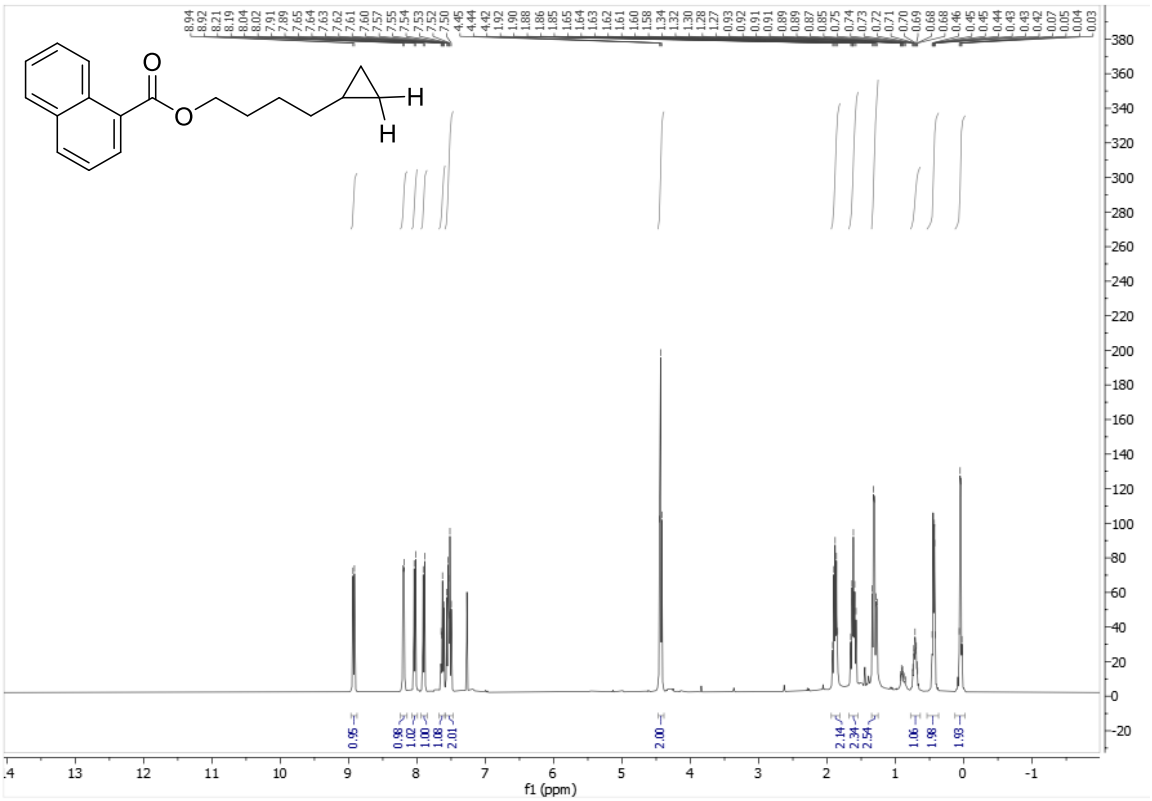
O
O
H
H
f1 (ppm)

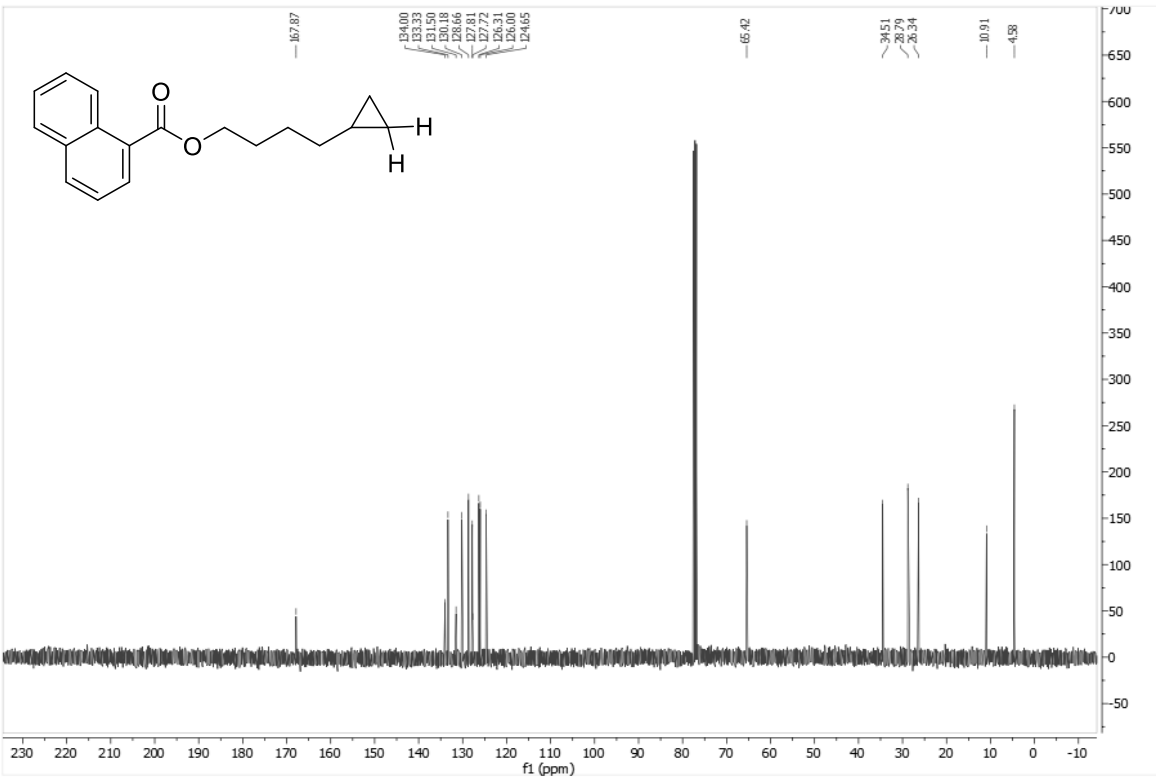
167.87
134.00
133.33
131.50
130.18
128.66
127.81
127.72
126.31
126.00
124.65
65.42
34.51
28.79
26.34
10.91
4.58
O
O
H
H
f1 (ppm)

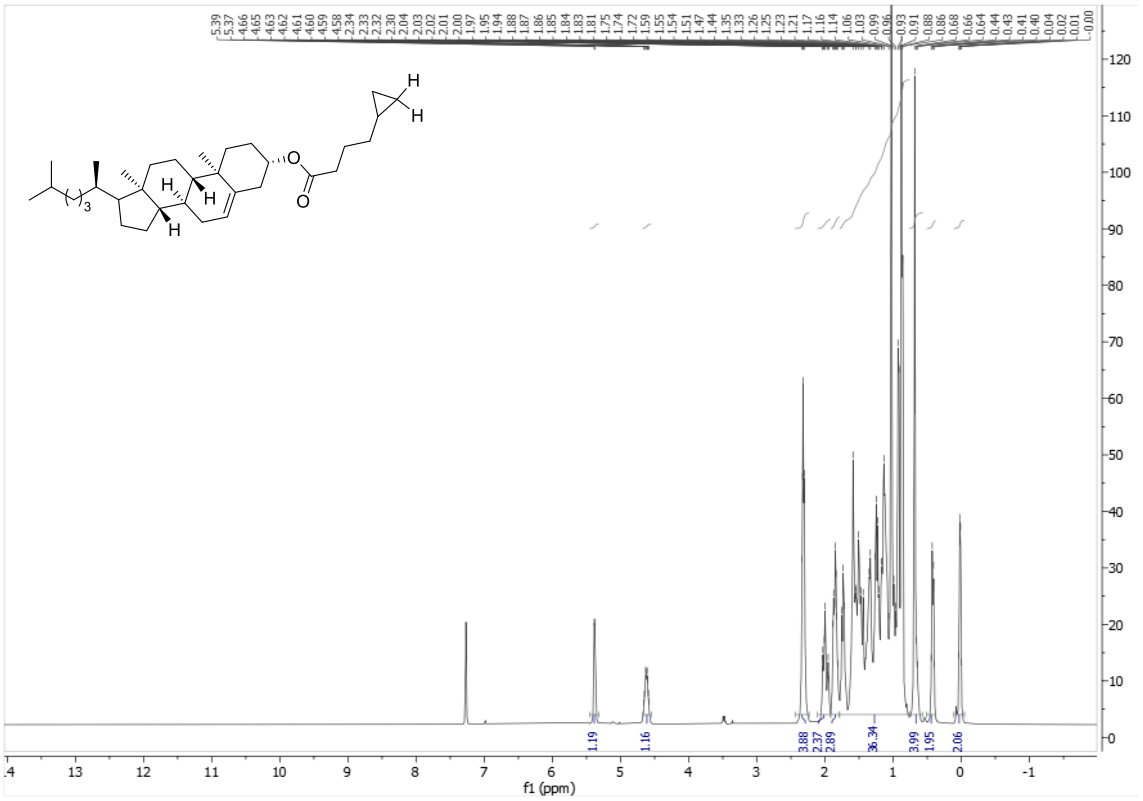
f1 (ppm)

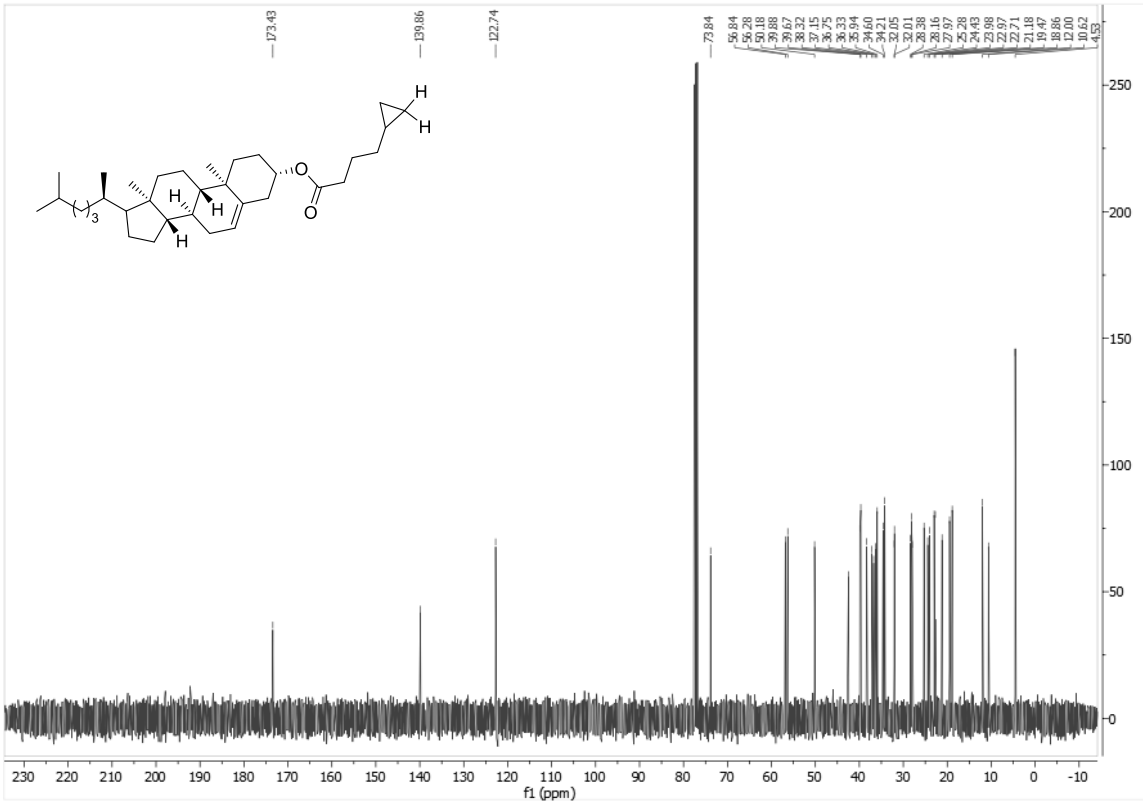
f1 (ppm)

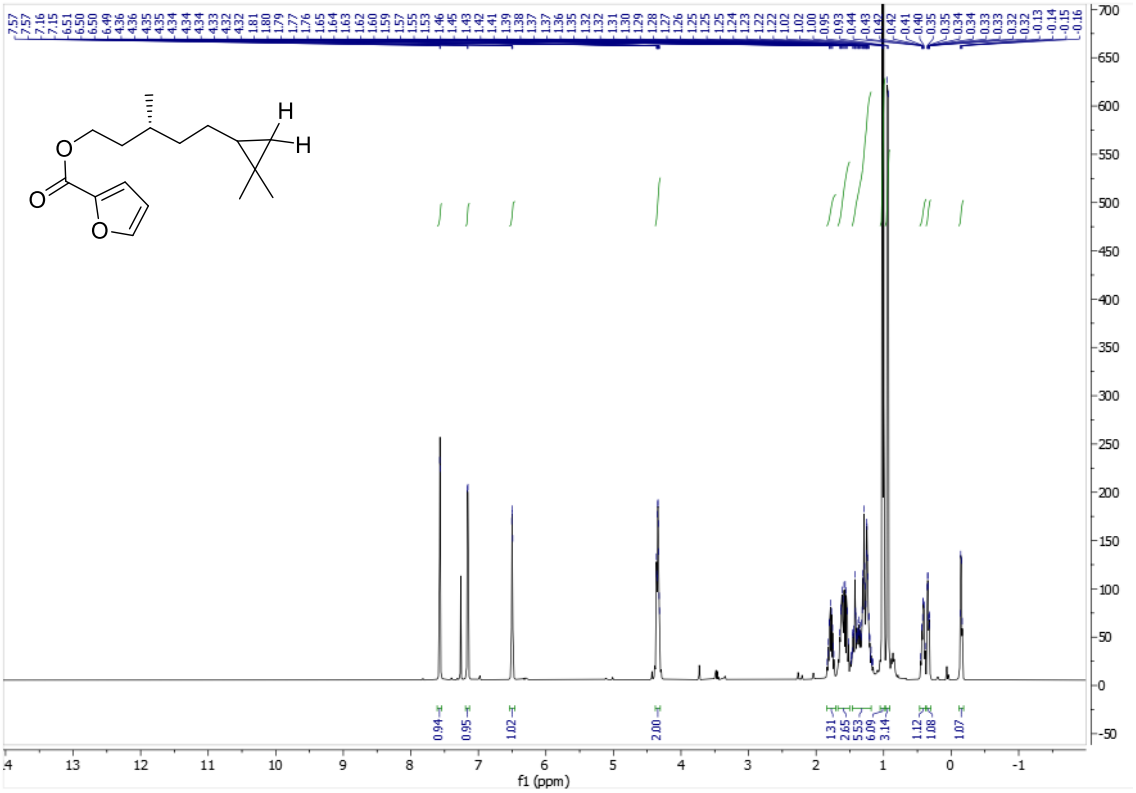
H
H
O
O
O
f1 (ppm)

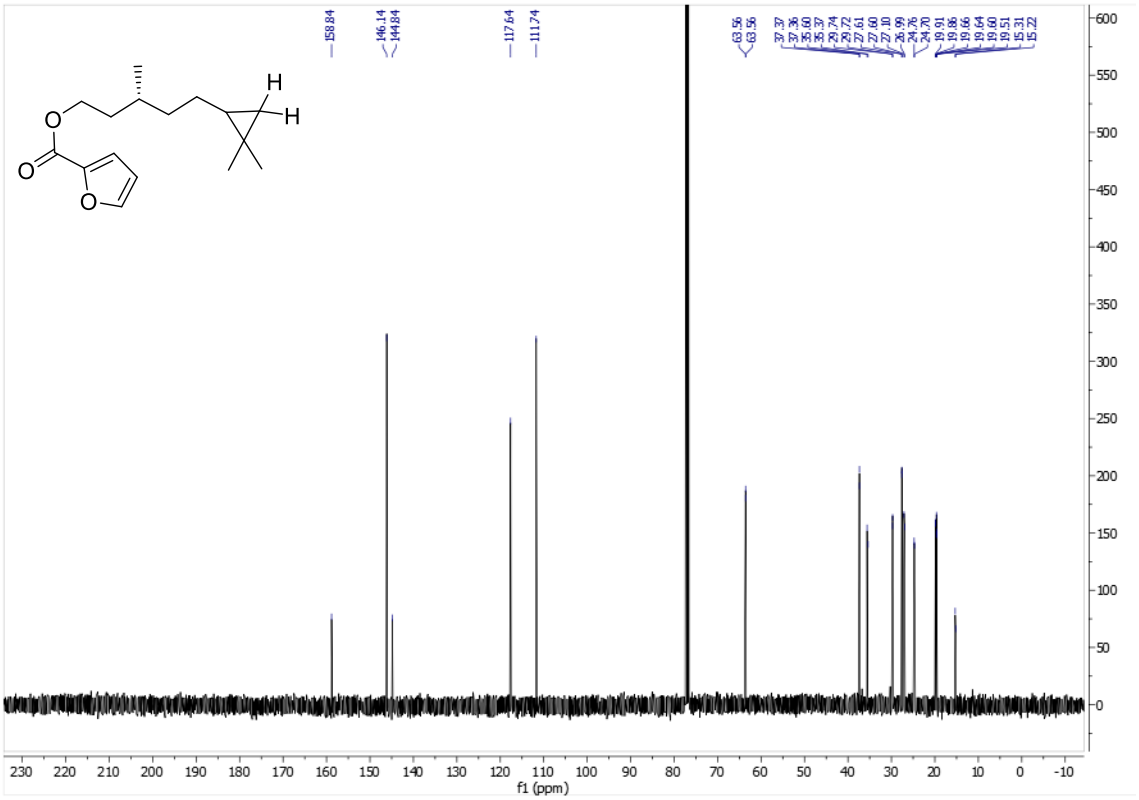
158.84
146.14
144.84
117.64
111.74
63.56
63.36
H
H
O
O
O
f1 (ppm)

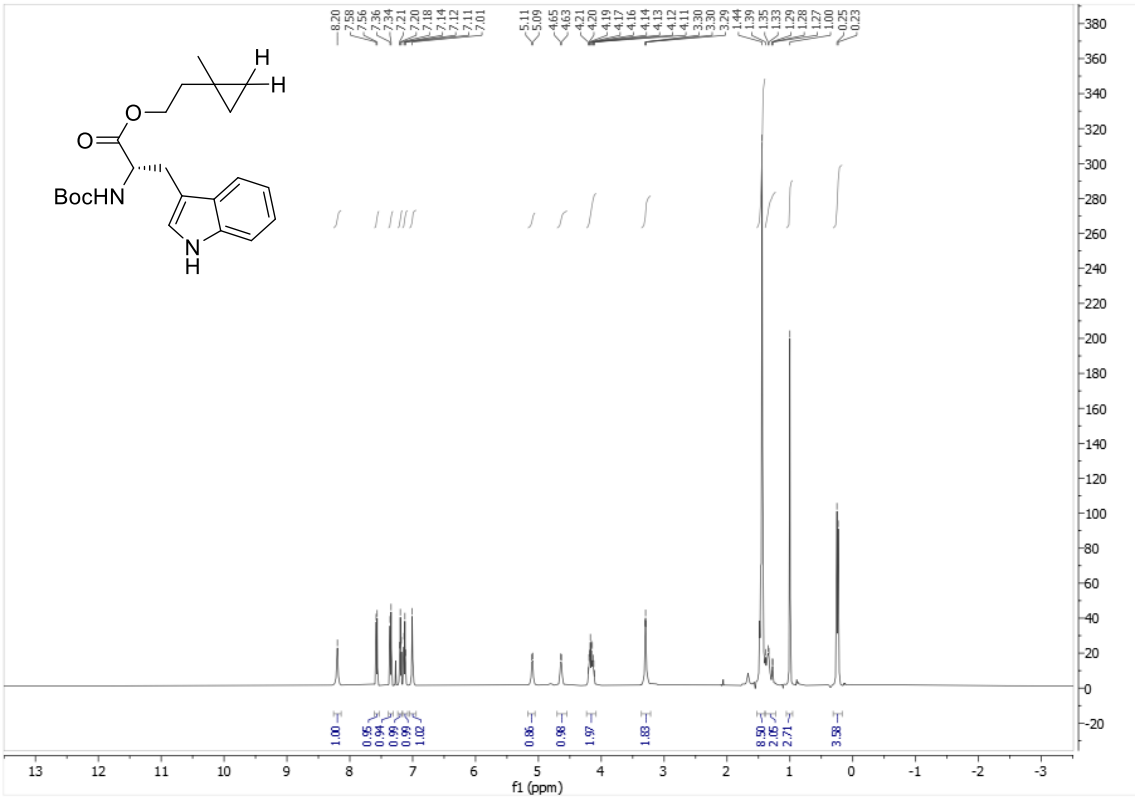
H
H
O
O
BocHN
N
H
8.20
7.58
7.56
7.36
7.34
7.21
7.20
7.18
7.14
7.12
7.11
7.01
5.11
5.09
4.65
4.63
4.21
4.20
4.19
4.17
4.16
4.14
4.13
4.12
4.11
3.30
3.30
3.29
1.44
1.39
1.35
1.33
1.29
1.28
1.27
1.00
0.25
0.23
1.00
0.95
0.94
0.99
0.99
1.02
0.86
0.98
1.97
1.83
8.50
2.05
2.71
3.58
f1 (ppm)

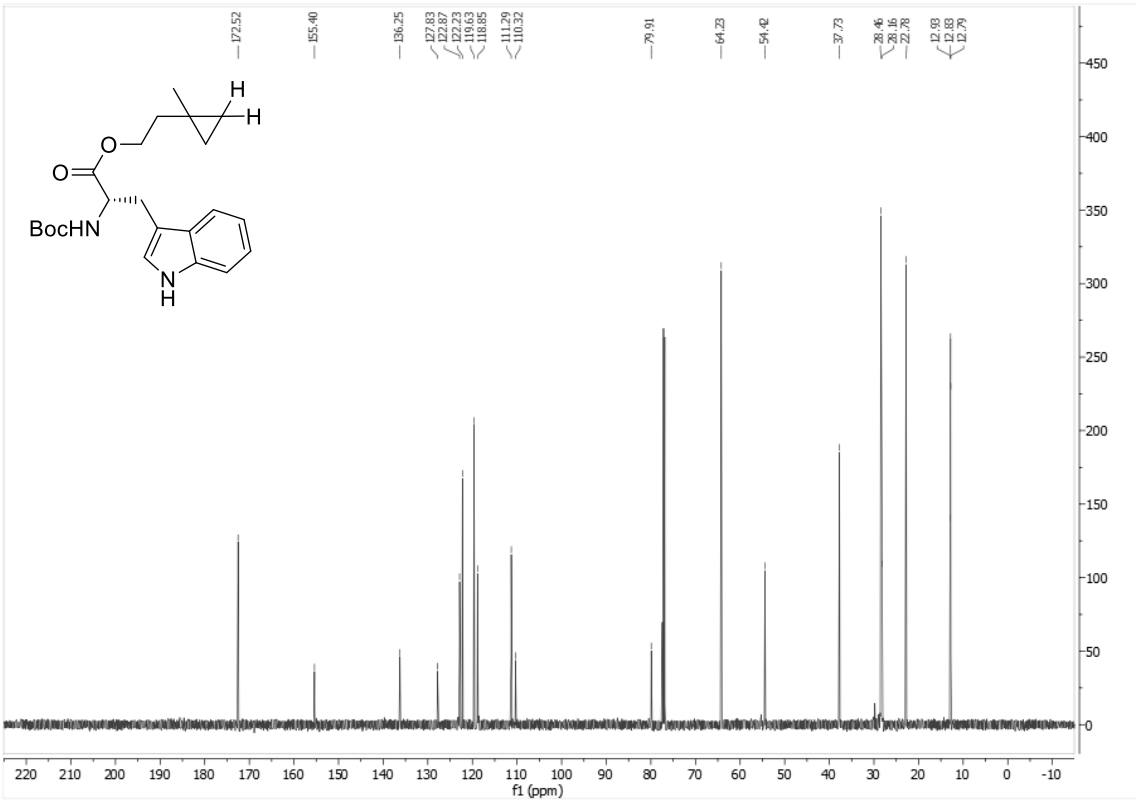
H
H
O
O
BocHN
N
H
172.52
155.40
136.25
127.83
127.27
123.23
119.63
118.85
111.29
110.32
79.91
64.23
54.42
37.73
28.46
28.16
22.78
12.93
12.83
12.79
f1 (ppm)

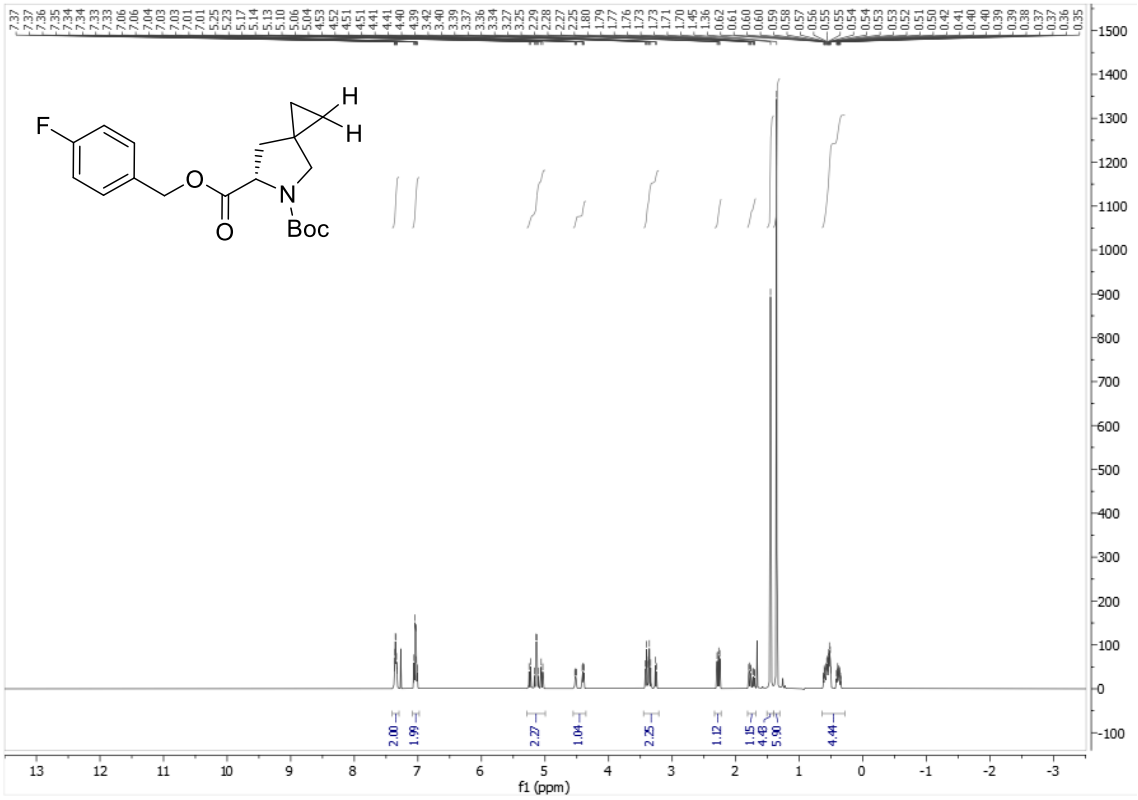
F
O
O
N
Boc
H
H
f1 (ppm)

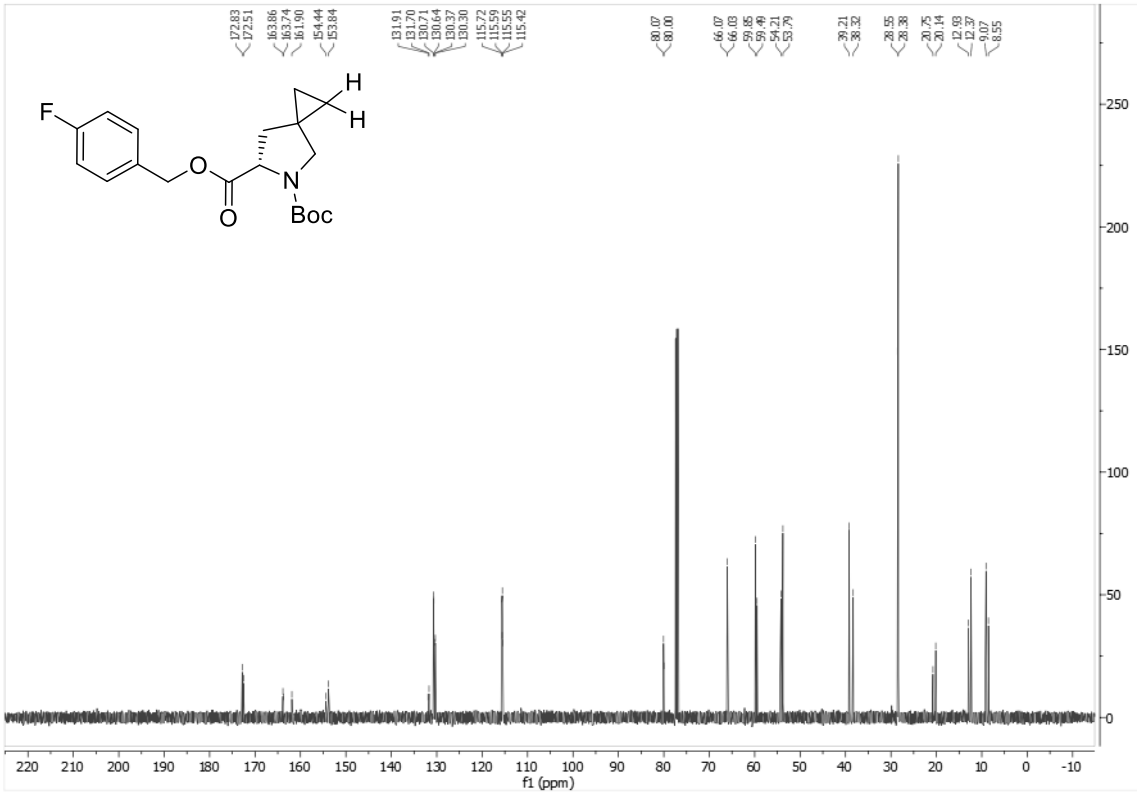
F
O
O
N
Boc
H
H
f1 (ppm)

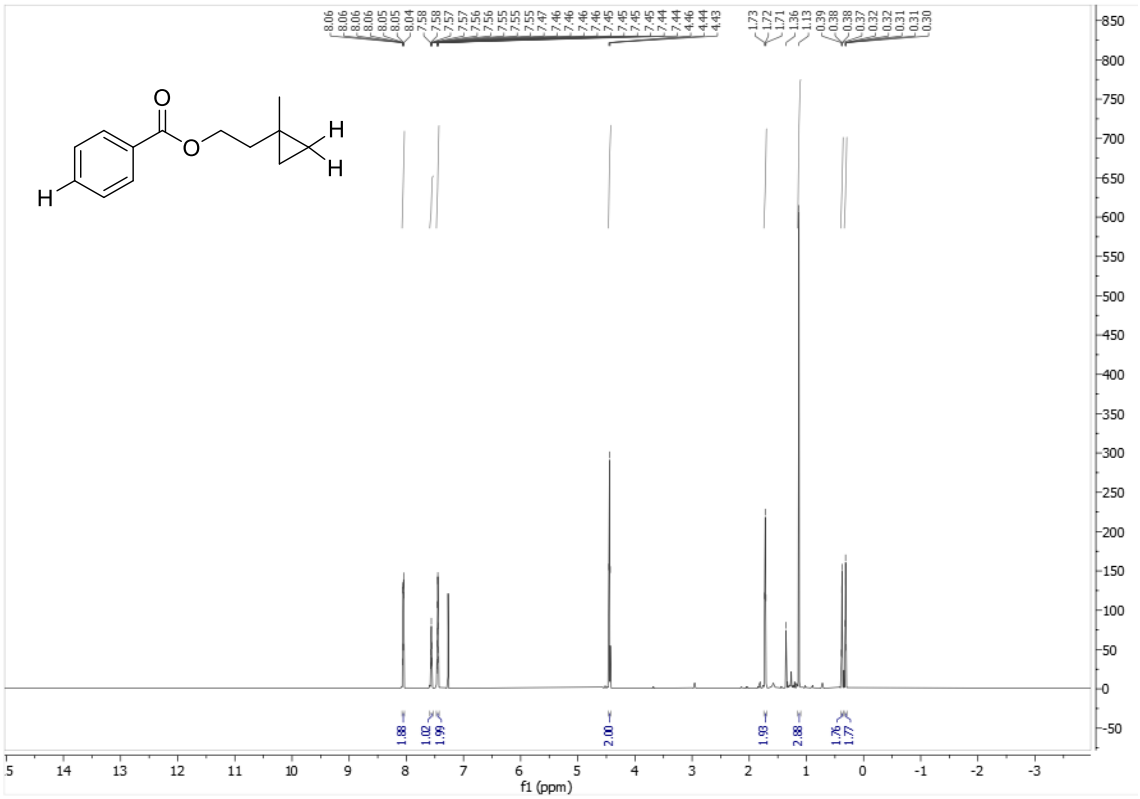
f1 (ppm)

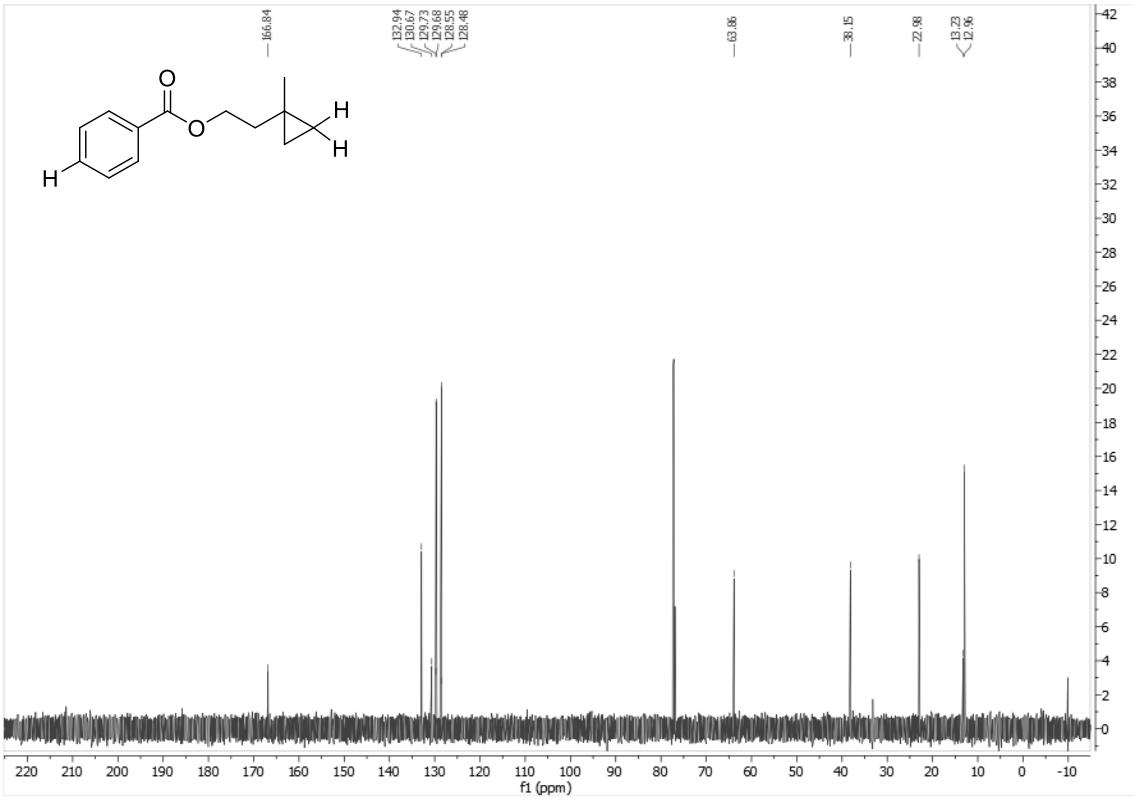
f1 (ppm)

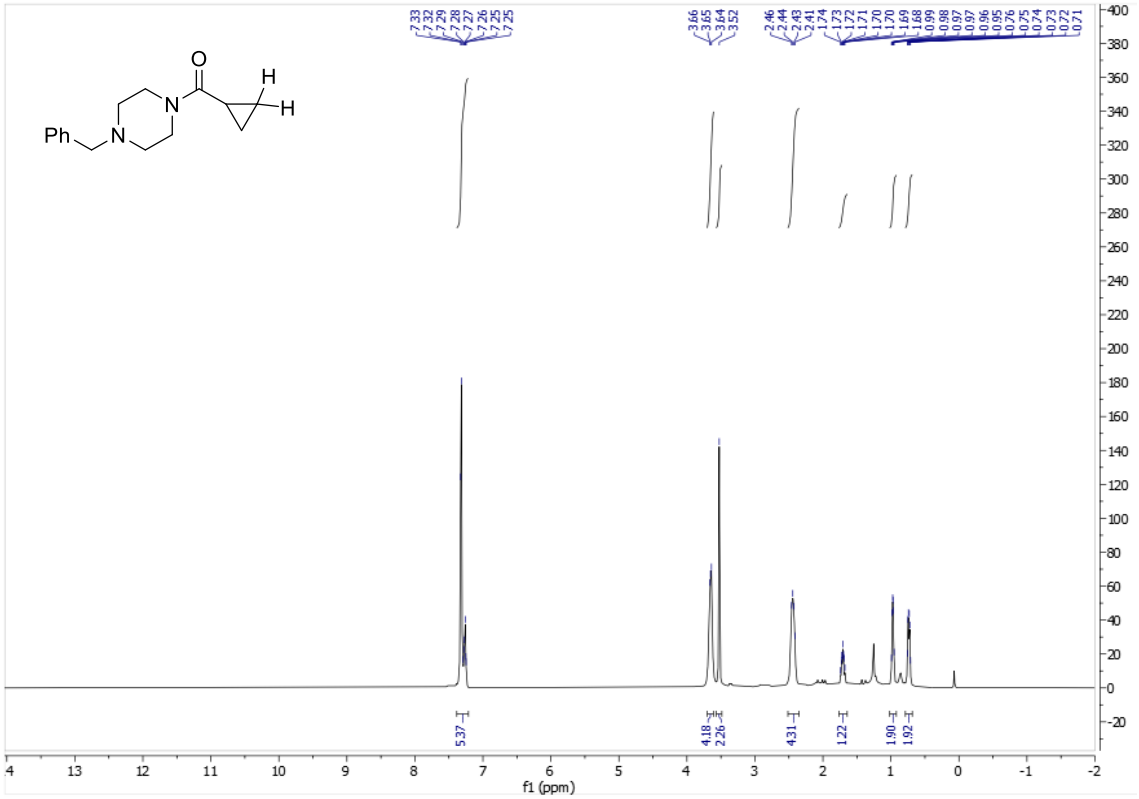
Ph
N
N
O
H
H
f1 (ppm)

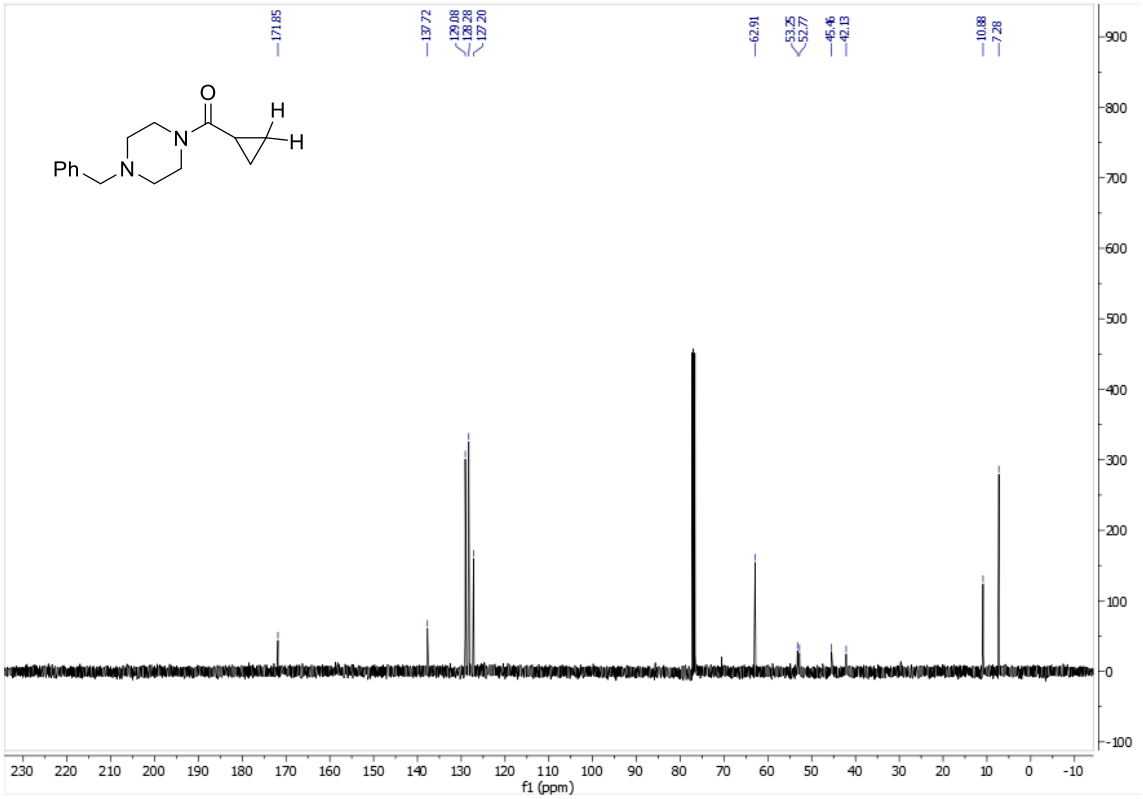
Ph
N
N
O
H
H
f1 (ppm)

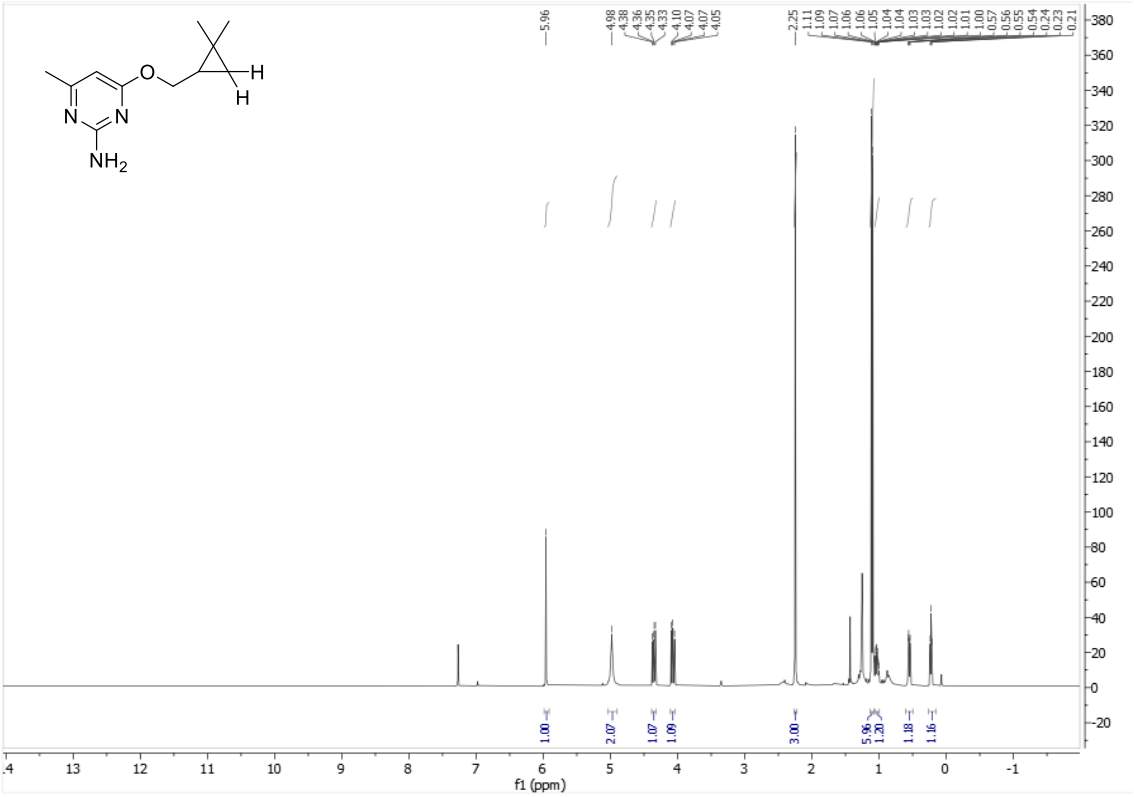
5.96
4.98
4.38
4.36
4.35
4.33
4.10
4.07
4.07
4.05
2.25
1.11
1.09
1.07
1.06
1.06
1.05
1.04
1.04
1.03
1.03
1.02
1.02
1.01
1.00
0.57
0.56
0.55
0.54
0.24
0.23
0.21
1.00
2.07
1.07
1.09
3.00
5.96
1.20
1.18
1.16
f1 (ppm)

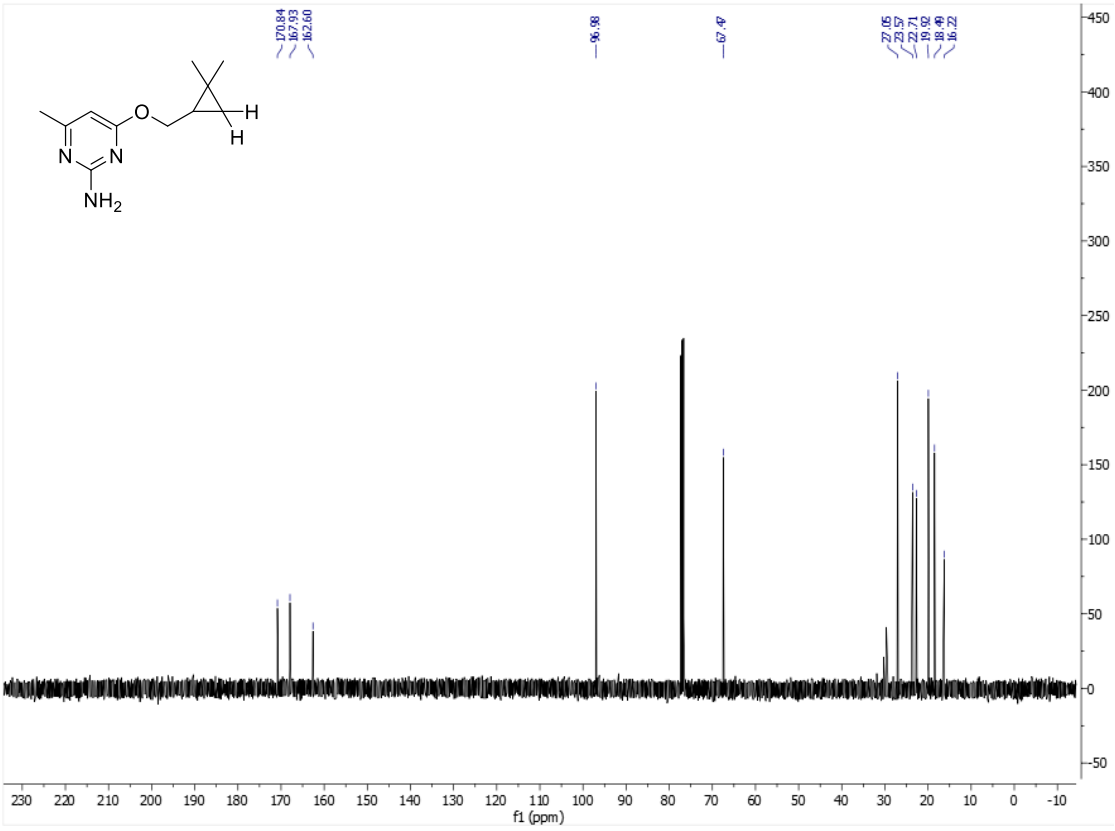
170.84
167.93
162.60
96.98
67.49
27.05
23.57
23.71
19.08
18.49
16.22
f1 (ppm)

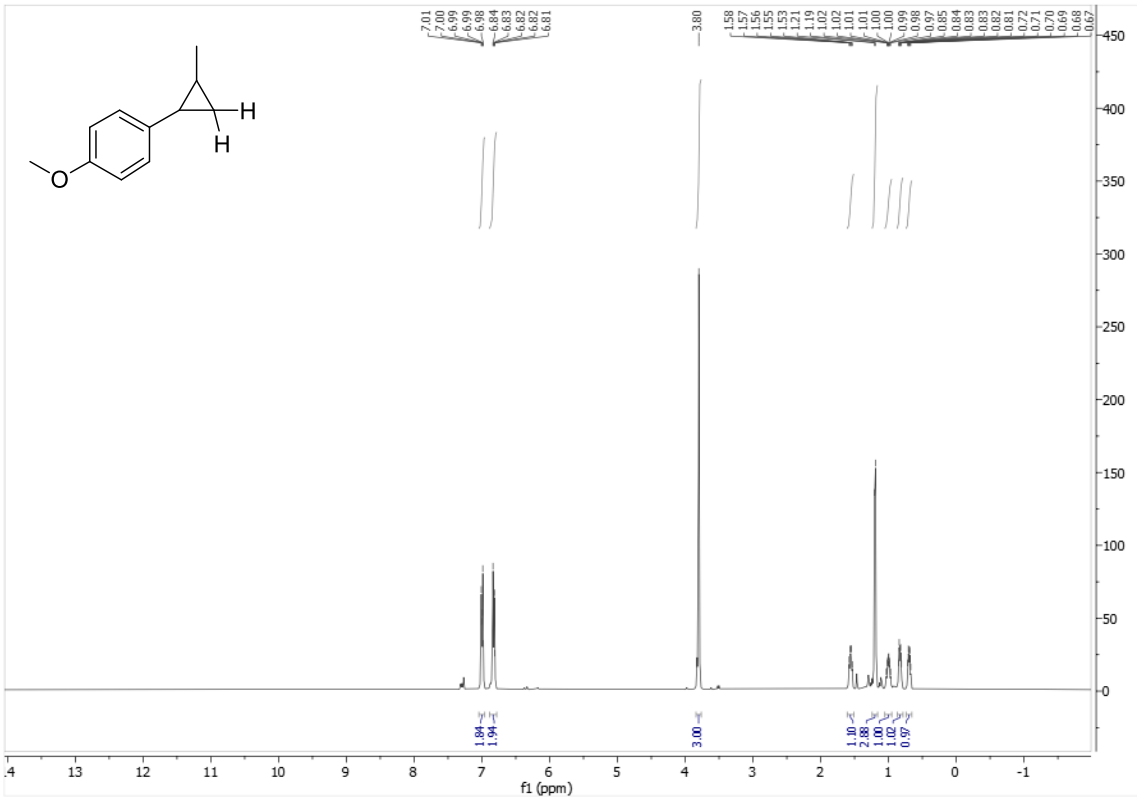
H
H
O
f1 (ppm)

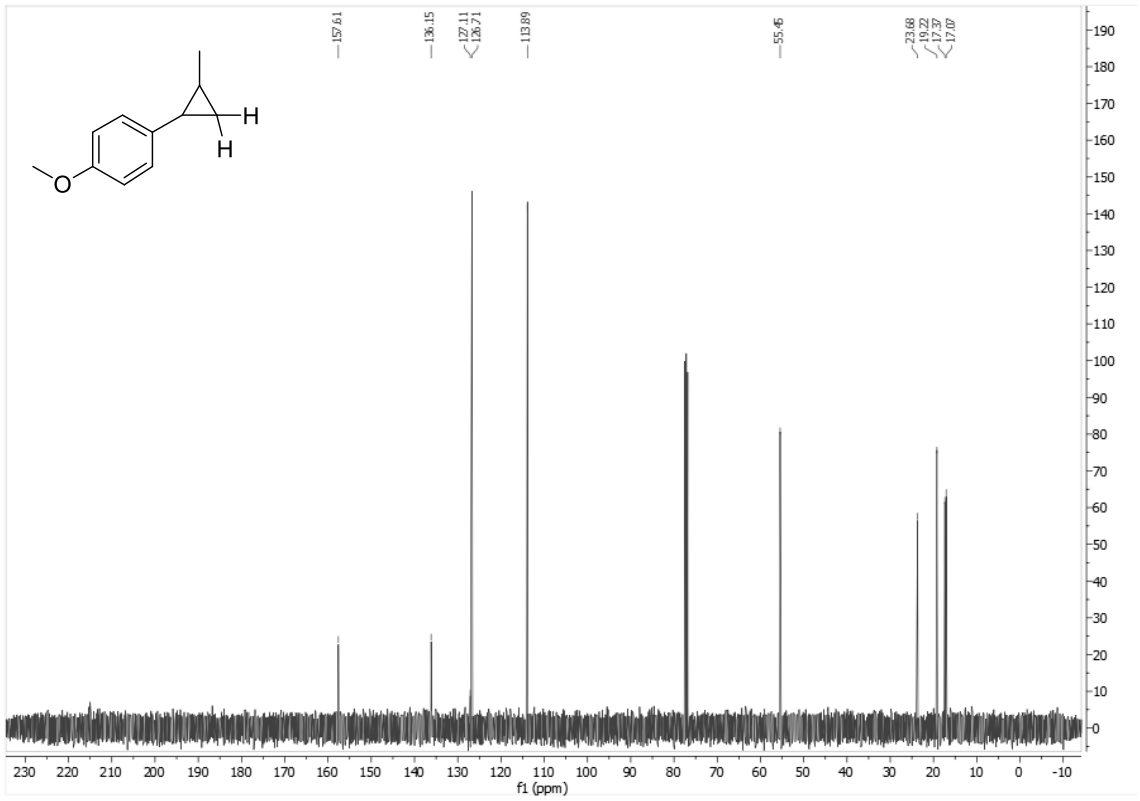
H
H
O
f1 (ppm)

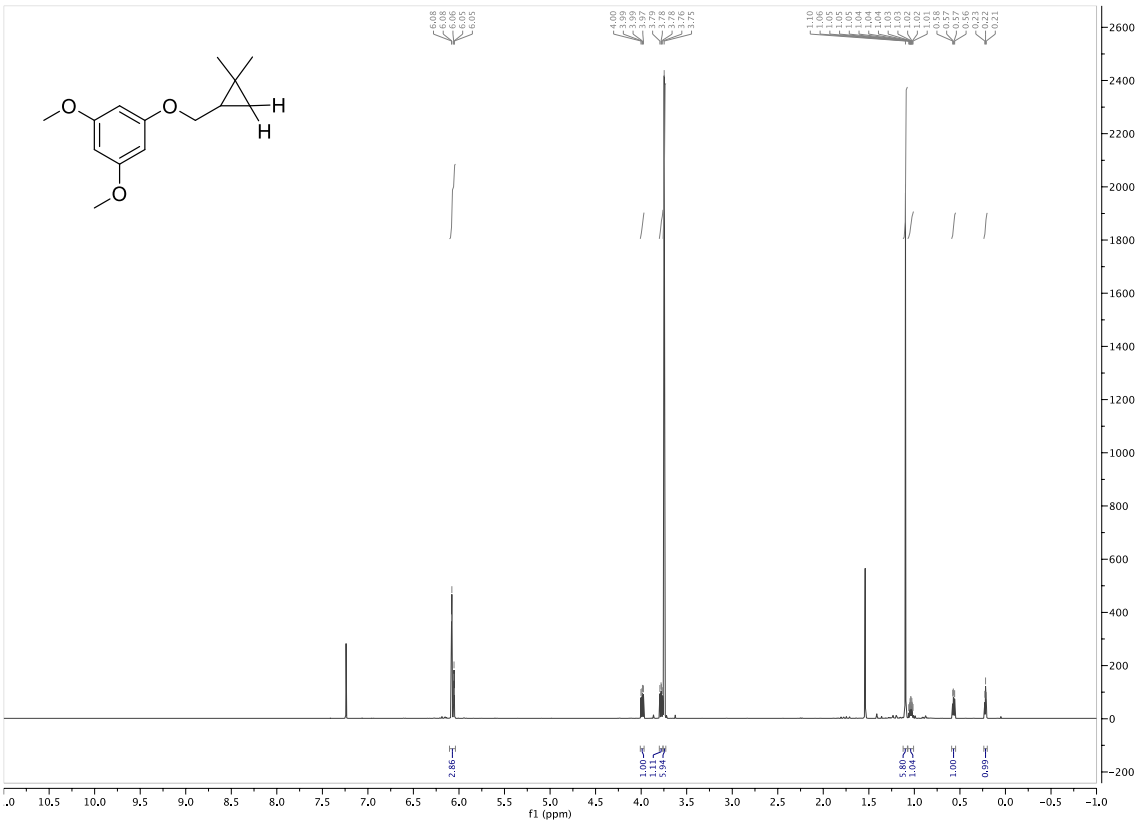
6.08
6.08
6.06
6.05
6.05
4.00
3.99
3.99
3.97
3.79
3.78
3.78
3.76
3.75
1.10
1.06
1.05
1.05
1.05
1.04
1.04
1.04
1.03
1.03
1.02
1.02
1.01
0.58
0.57
0.57
0.56
0.23
0.22
0.21
2.86
1.00
1.11
5.84
5.80
1.04
1.00
0.69
f1 (ppm)

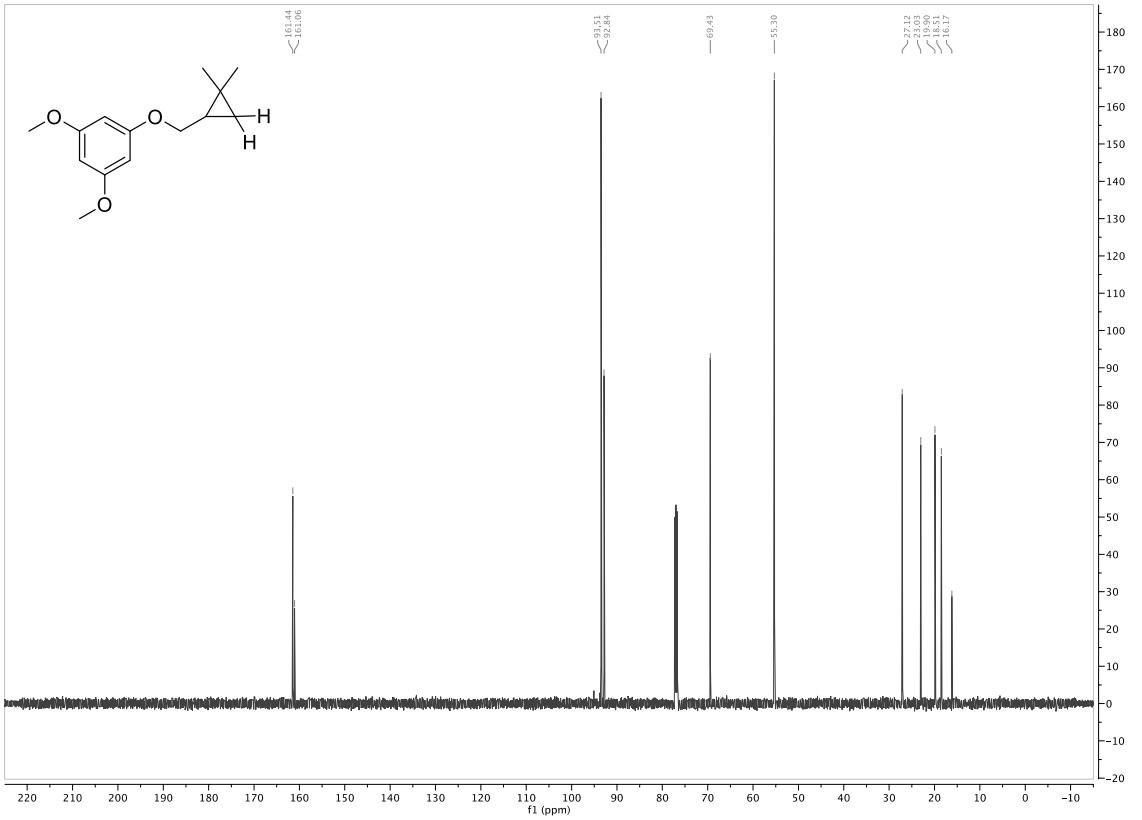
161.44
161.06
93.51
92.84
69.43
55.30
27.12
23.03
19.90
18.51
16.17
f1 (ppm)

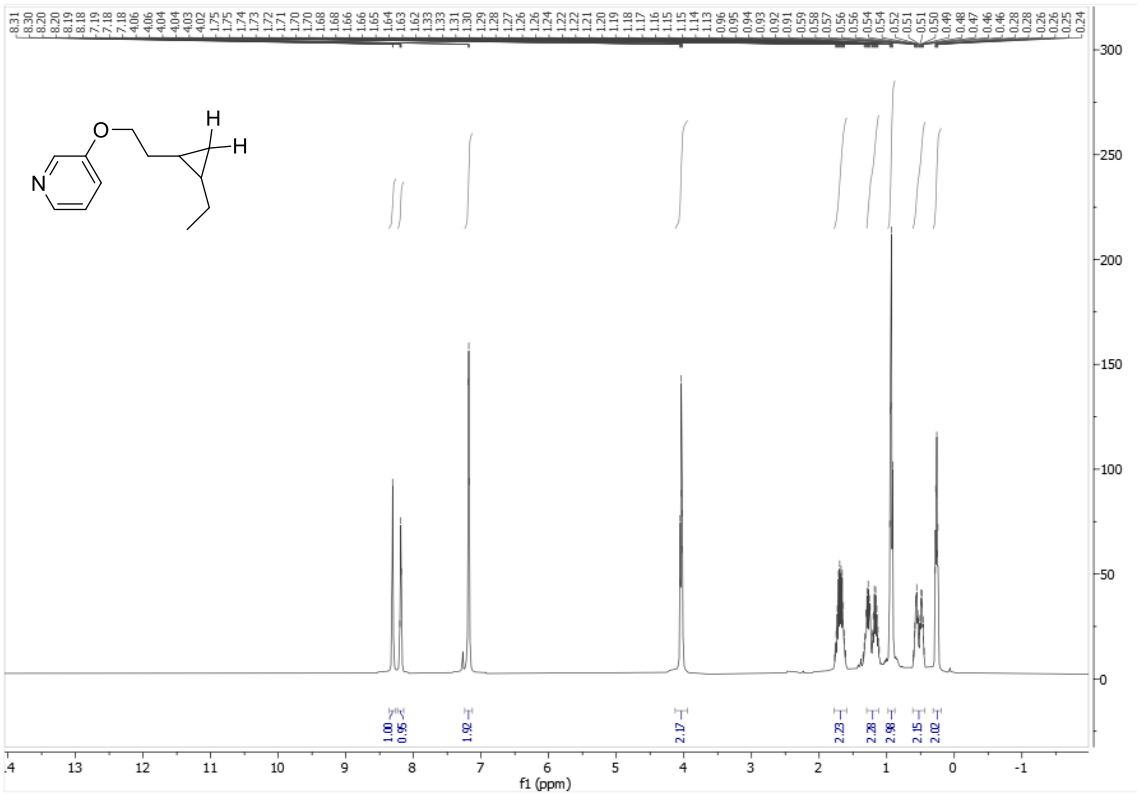
O
N
H
H
f1 (ppm)

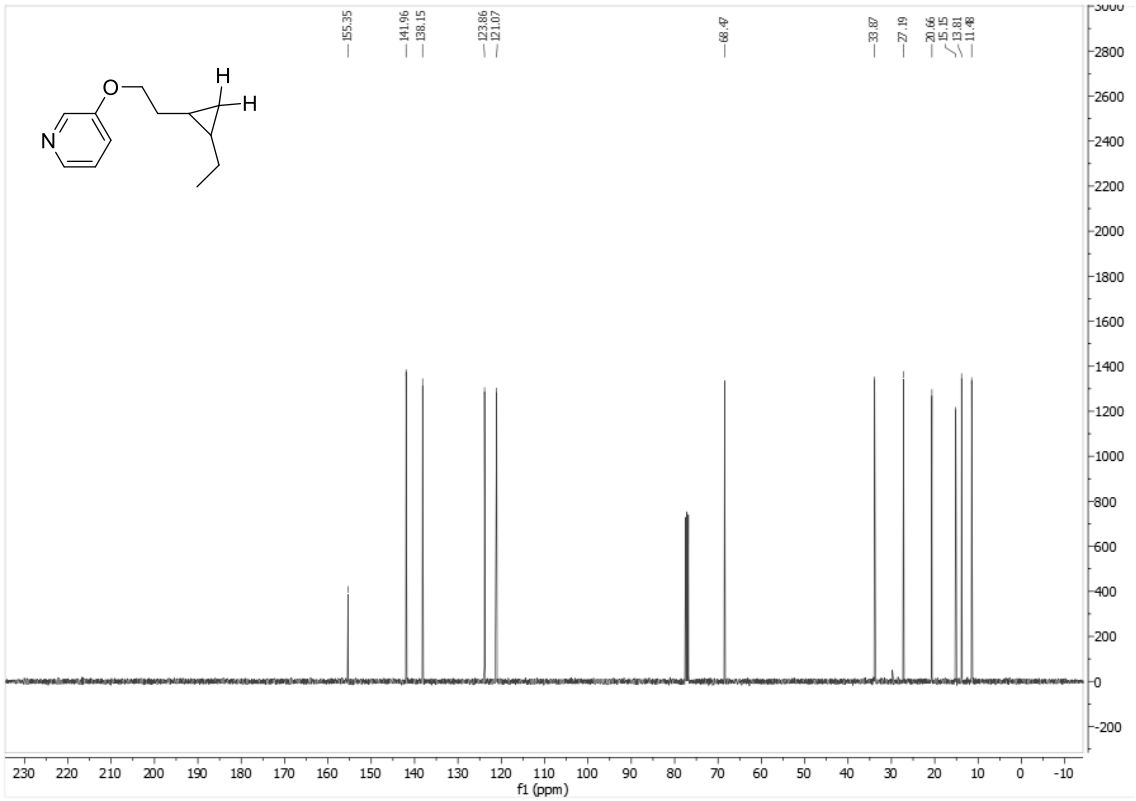
155.35
141.96
138.15
123.86
121.07
68.47
33.87
27.19
20.66
15.15
13.81
11.48
O
N
H
H
f1 (ppm)

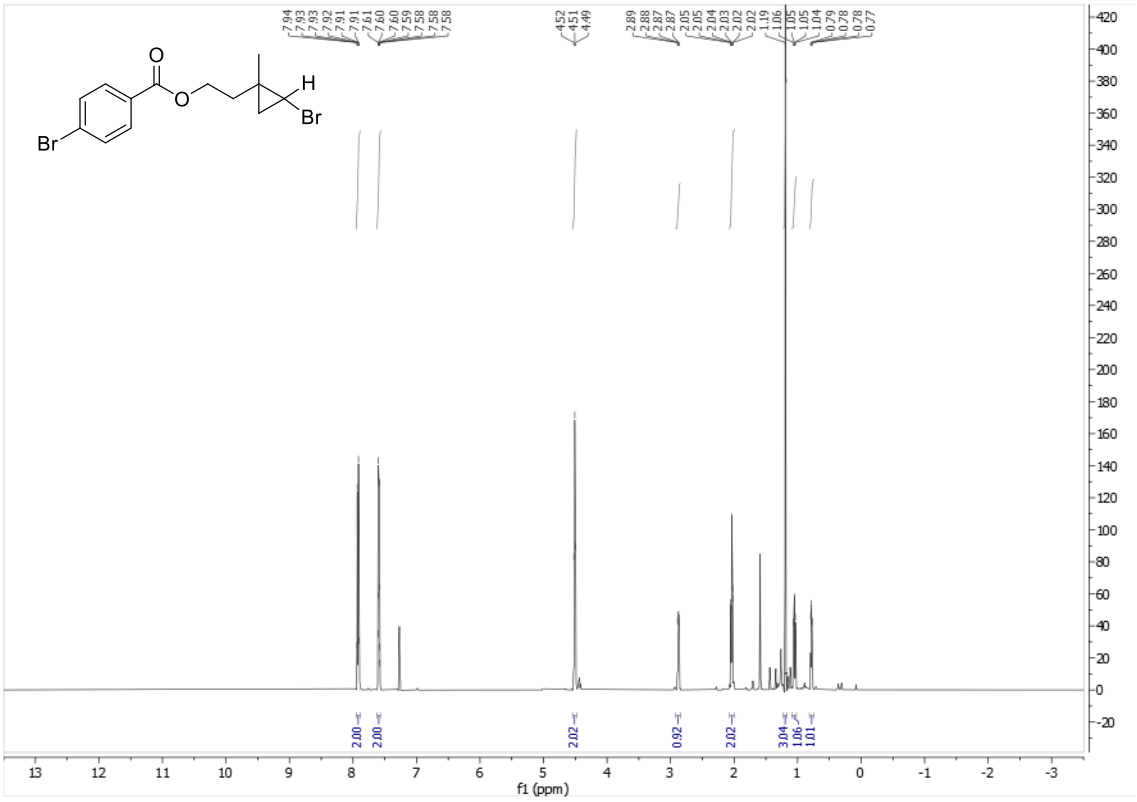
7.94
7.93
7.93
7.92
7.91
7.91
7.61
7.60
7.60
7.59
7.58
7.58
7.58
4.52
4.51
4.49
2.89
2.88
2.87
2.87
2.05
2.05
2.04
2.03
2.02
2.02
1.19
1.06
1.05
1.05
1.04
0.79
0.78
0.78
0.77
O
O
H
Br
Br
2.00
2.00
2.02
0.92
2.02
3.04
1.06
1.01
f1 (ppm)

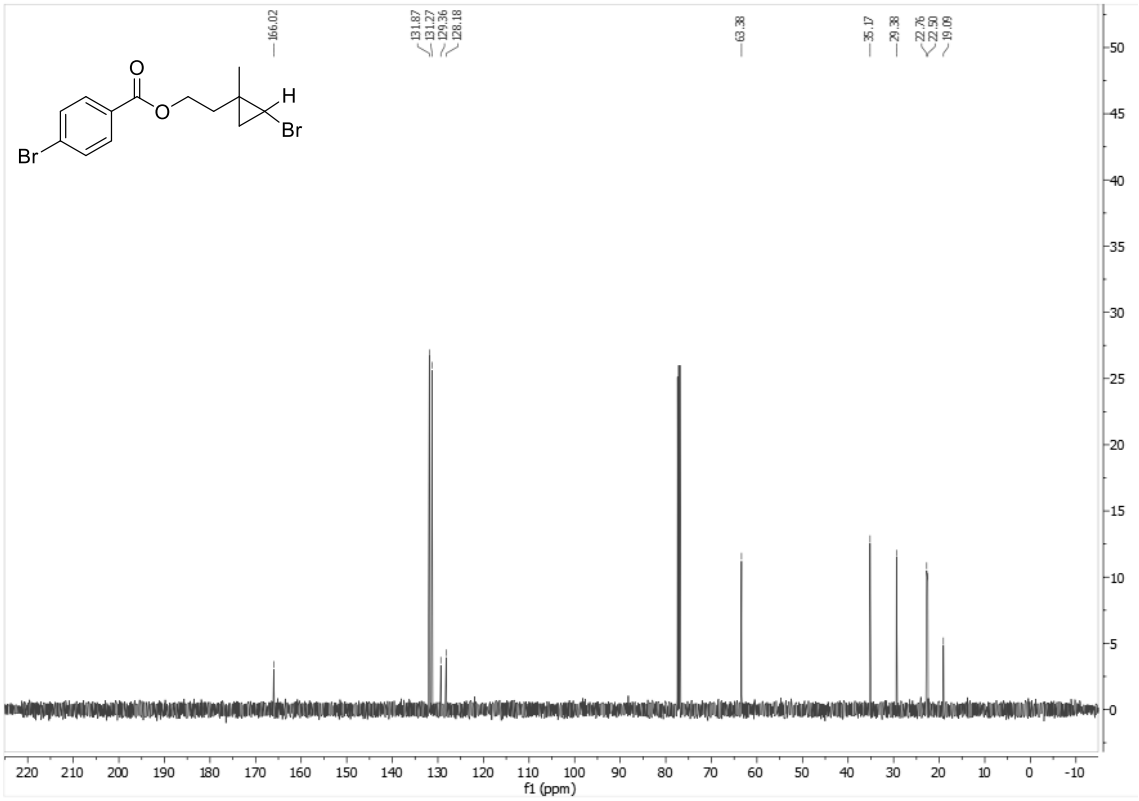
166.02
131.87
131.27
129.36
126.18
63.38
35.17
29.38
22.76
22.50
19.09
O
O
H
Br
Br
f1 (ppm)

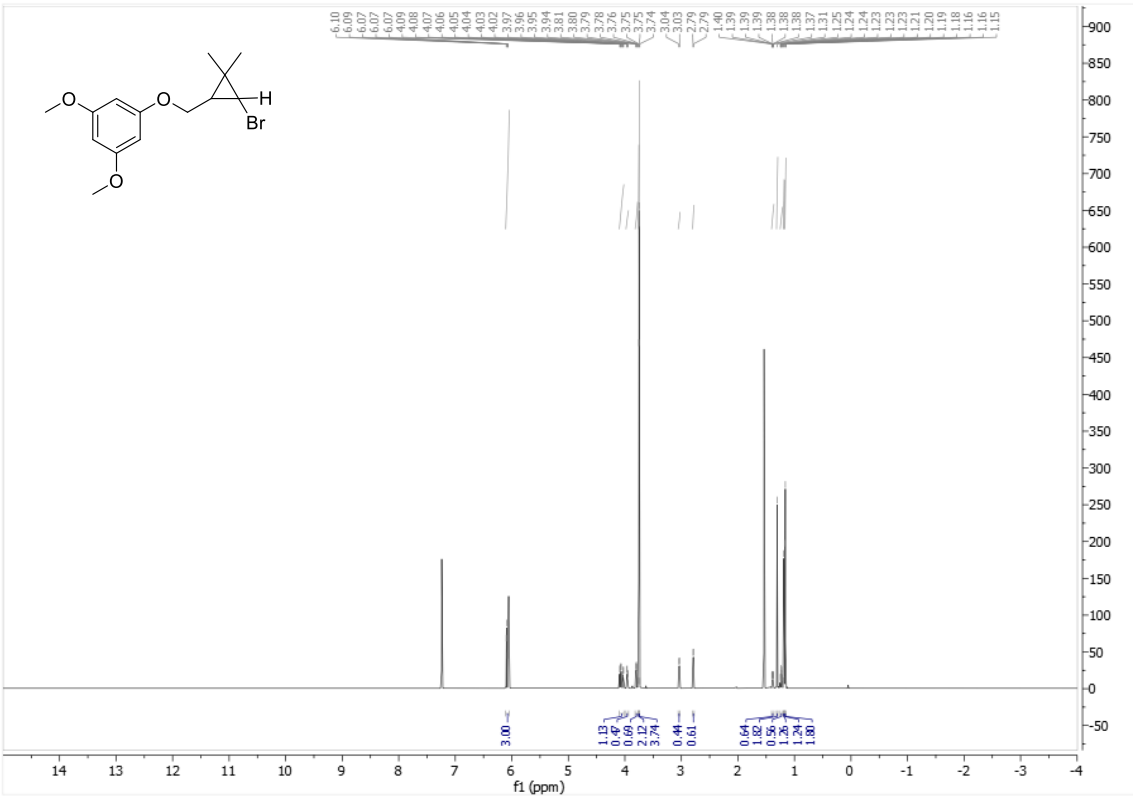
O
O
H
Br
O
f1 (ppm)

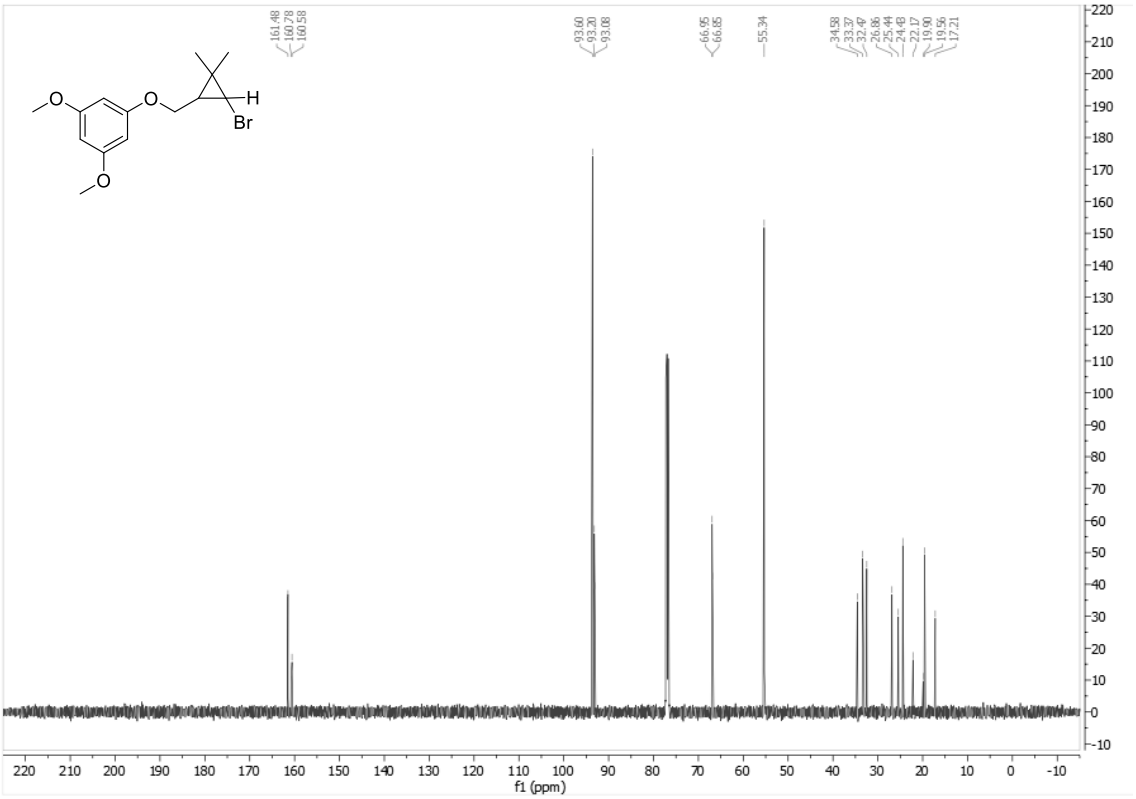
O
O
H
Br
O
f1 (ppm)

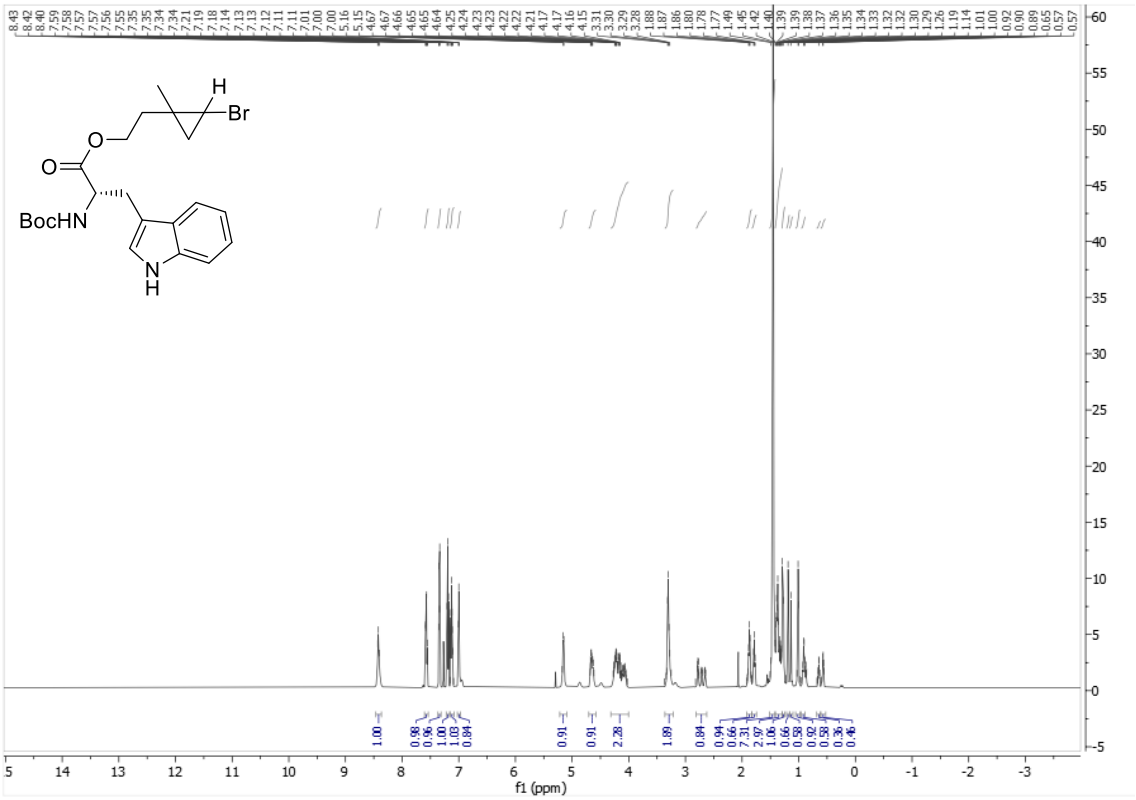
H
Br
O
O
BocHN
N
H
f1 (ppm)

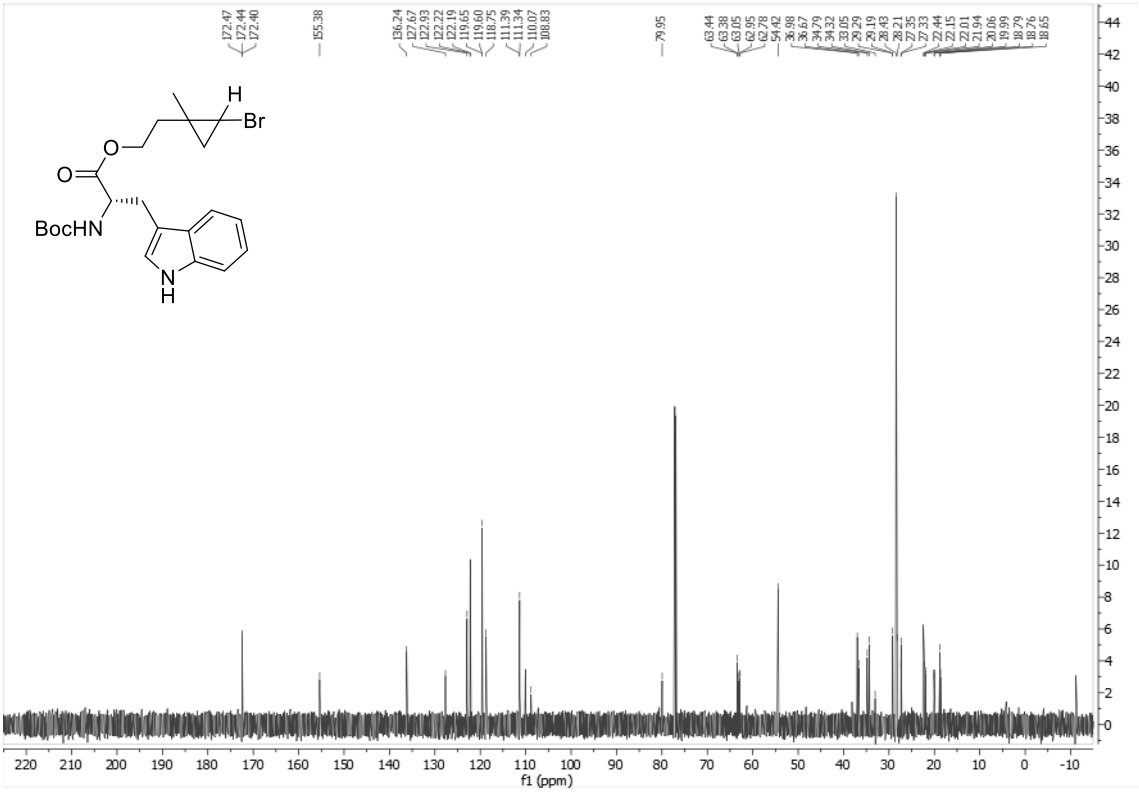
H
Br
O
O
BocHN
N
H
f1 (ppm)

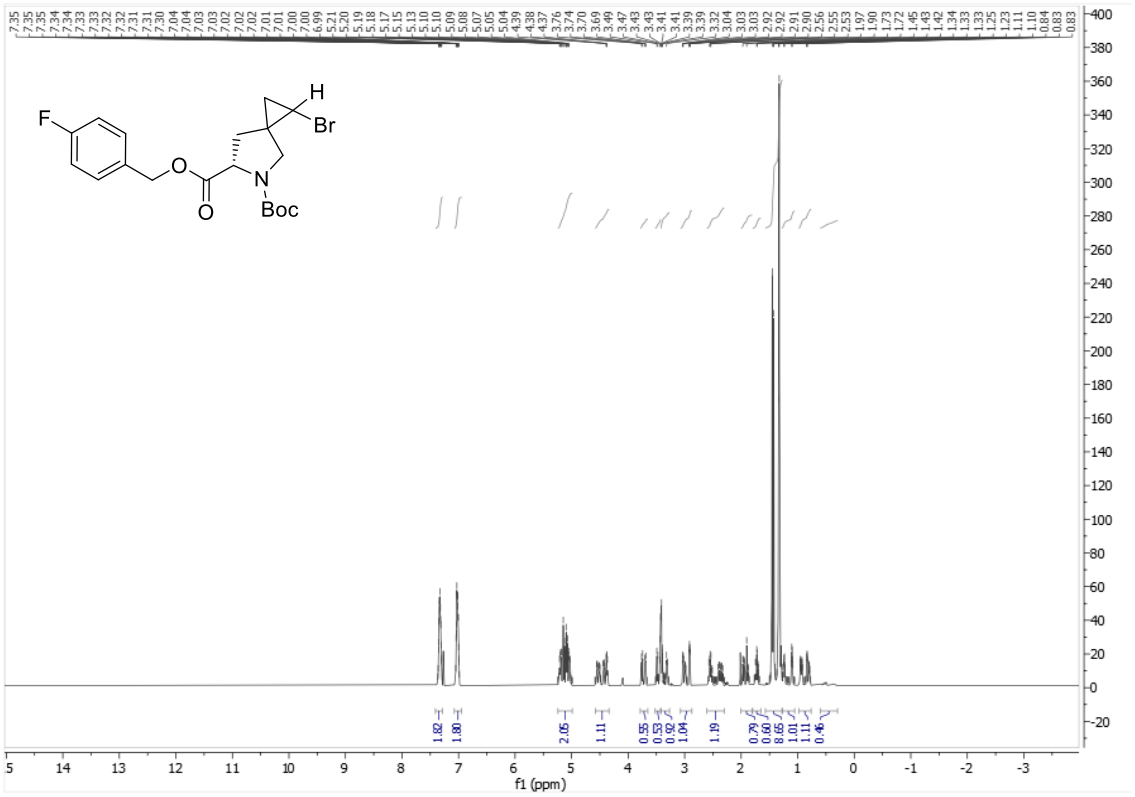
F
O
O
N
Boc
H
Br
f1 (ppm)

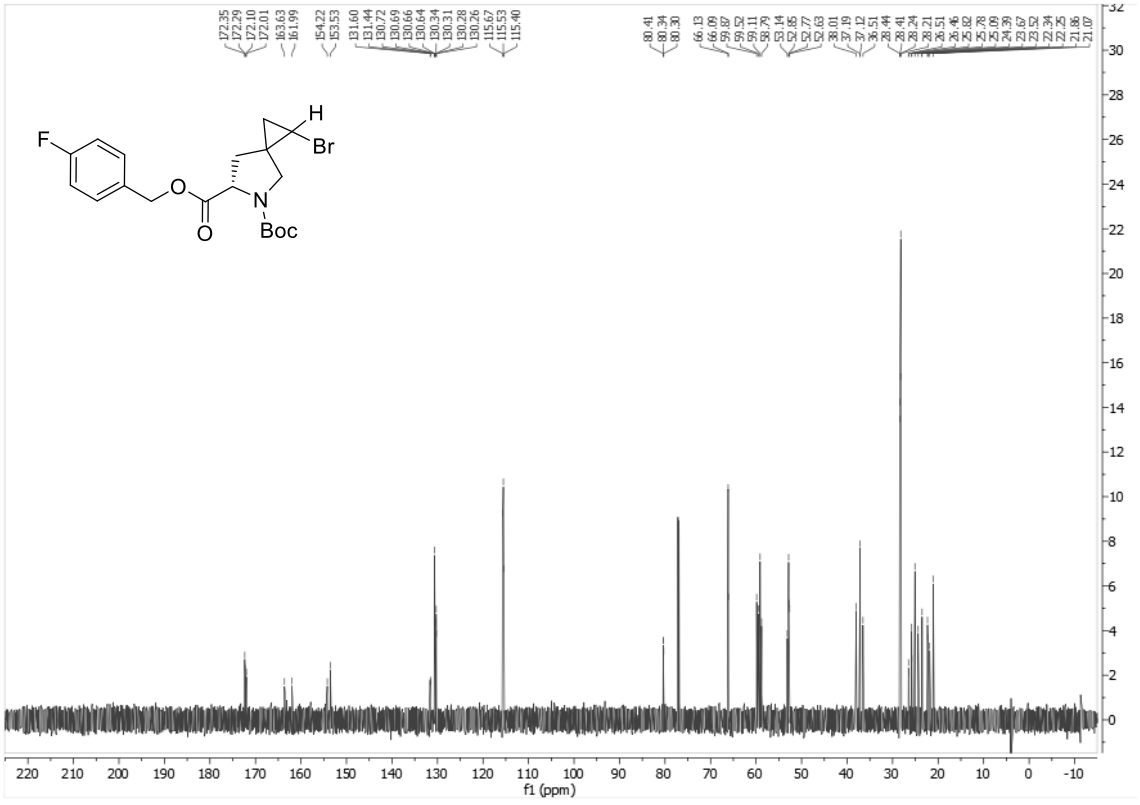
F
O
O
N
Boc
H
Br
f1 (ppm)

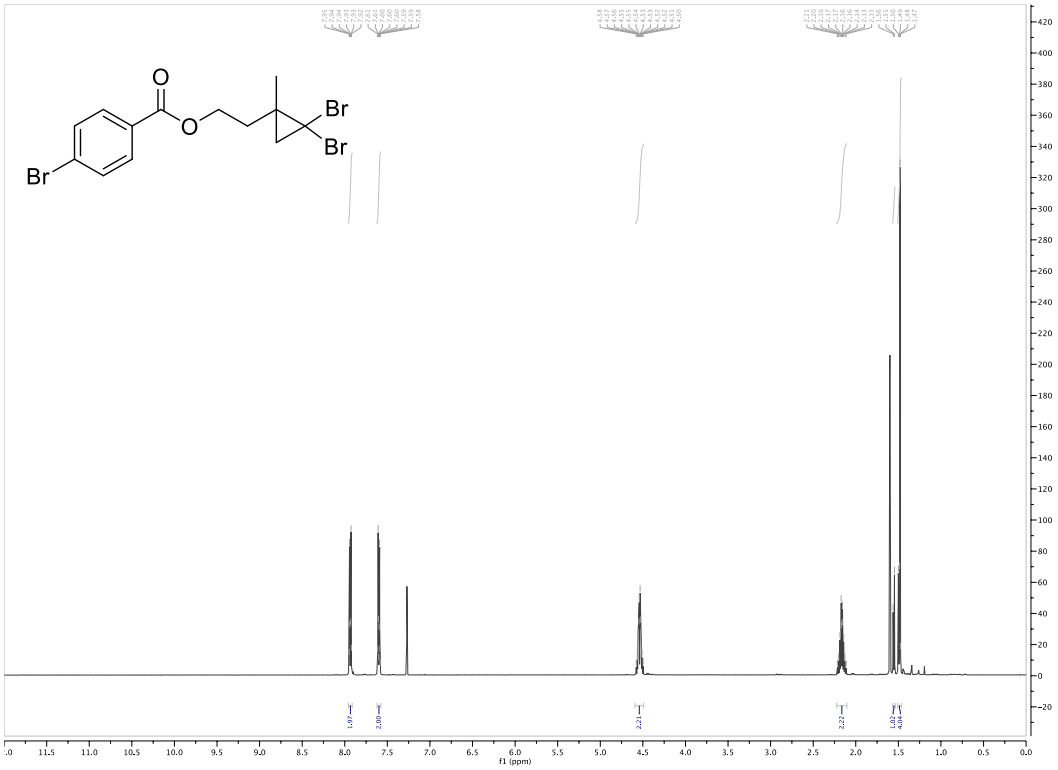
O
O
Br
Br
Br
f1 (ppm)

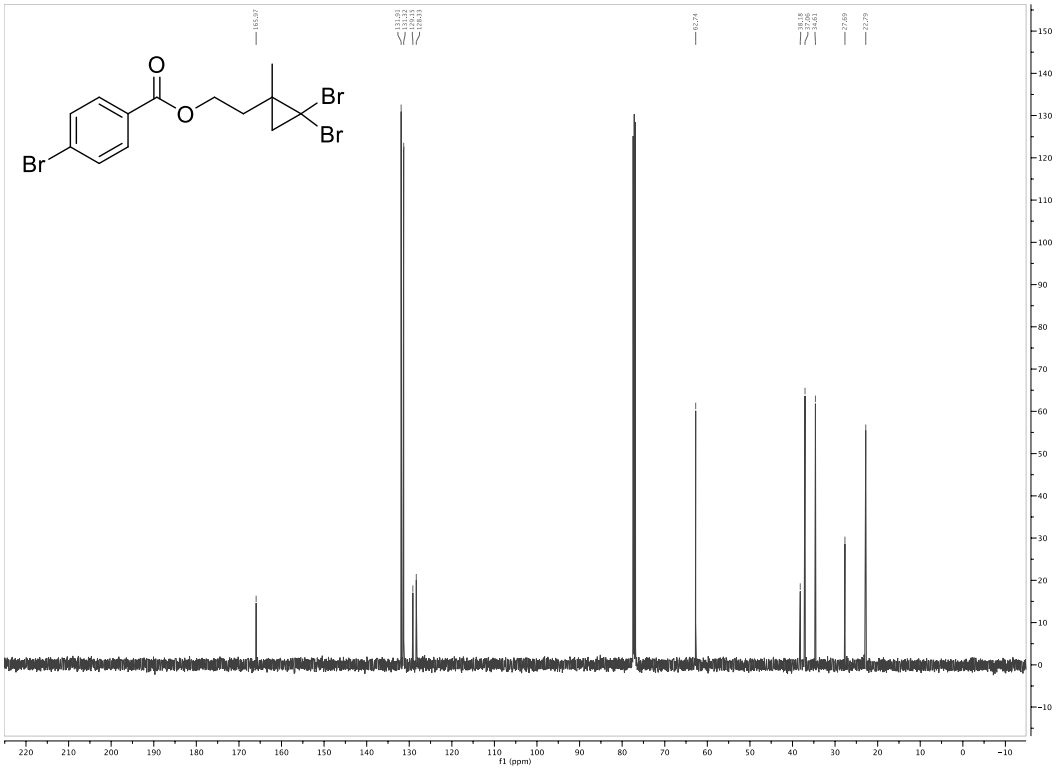
O
O
Br
Br
Br
f1 (ppm)

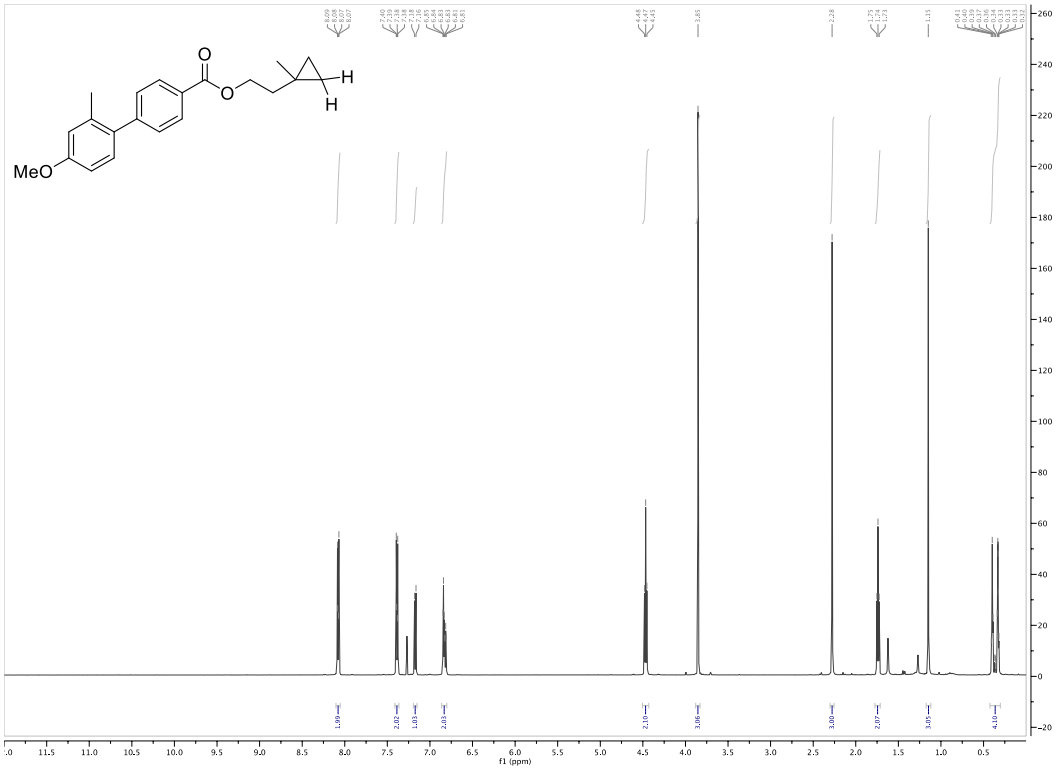
MeO
O
O
H
H
f1 (ppm)

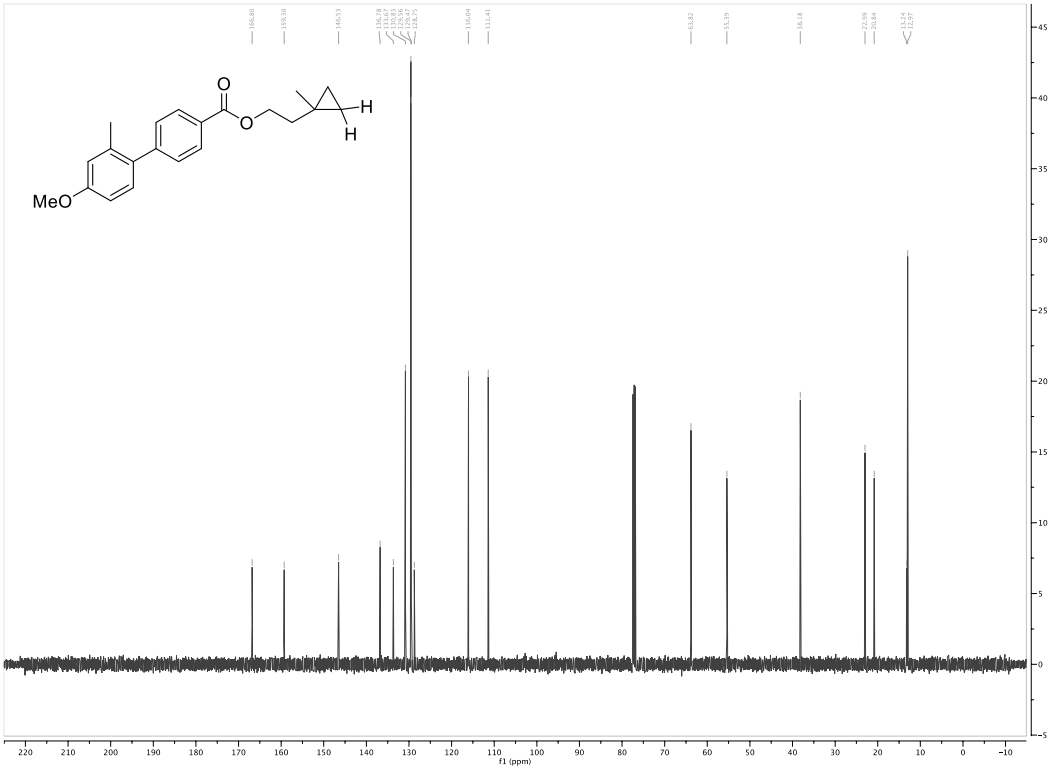
MeO
O
O
H
H
f1 (ppm)

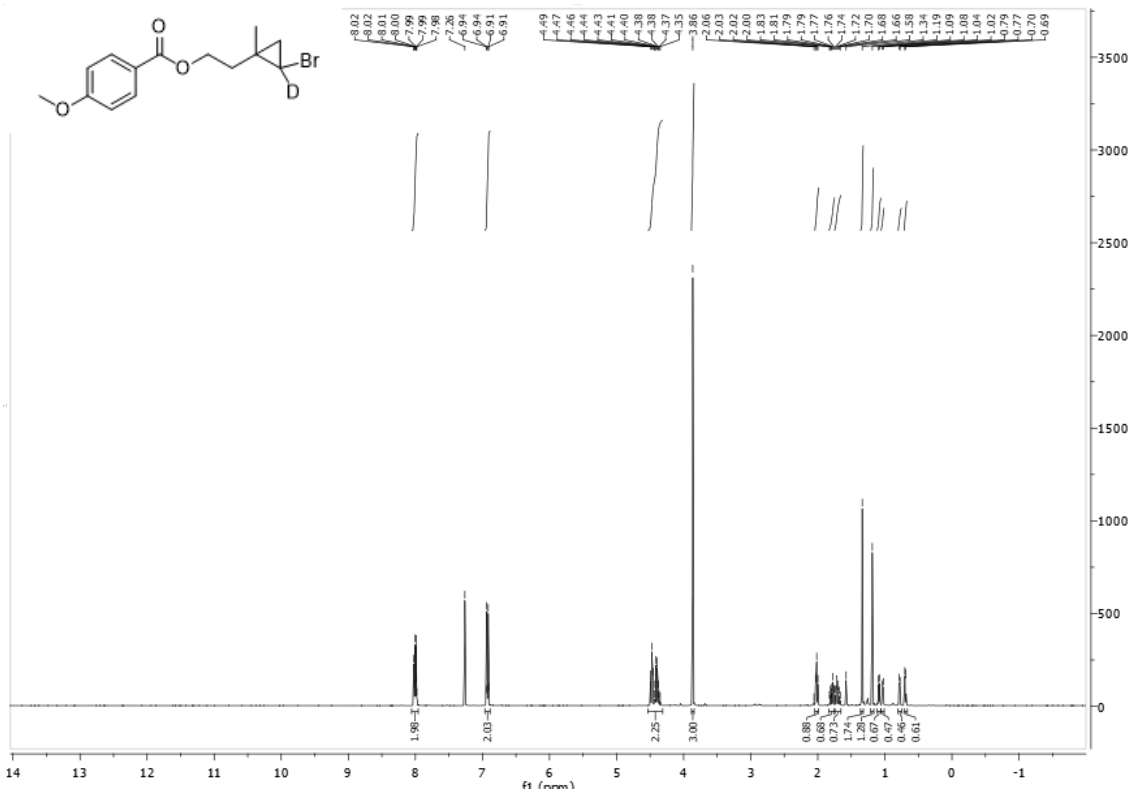
O
O
Br
D
O
f1 (ppm)

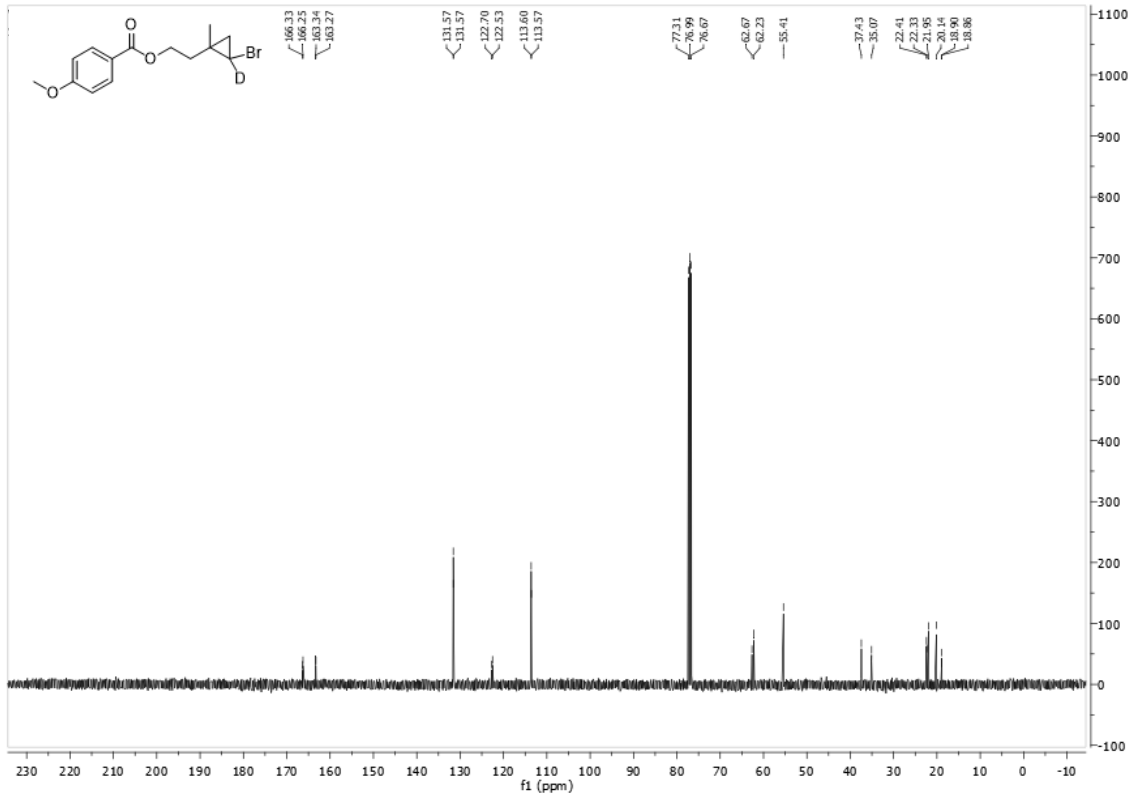
O
O
Br
D
O
f1 (ppm)

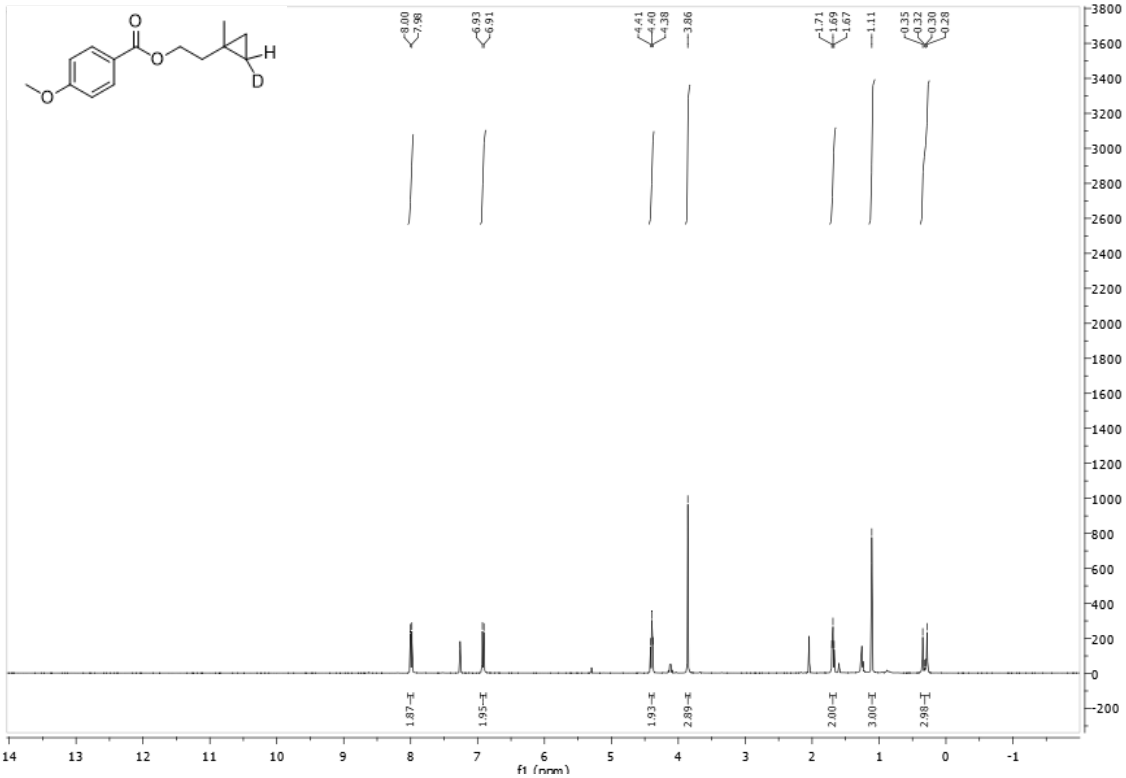
8.00
7.98
6.93
6.91
4.41
4.40
4.38
3.86
1.71
1.69
1.67
1.11
0.35
0.32
0.30
0.28
1.87
1.95
1.93
2.89
2.00
3.00
2.98
ft (ppm)

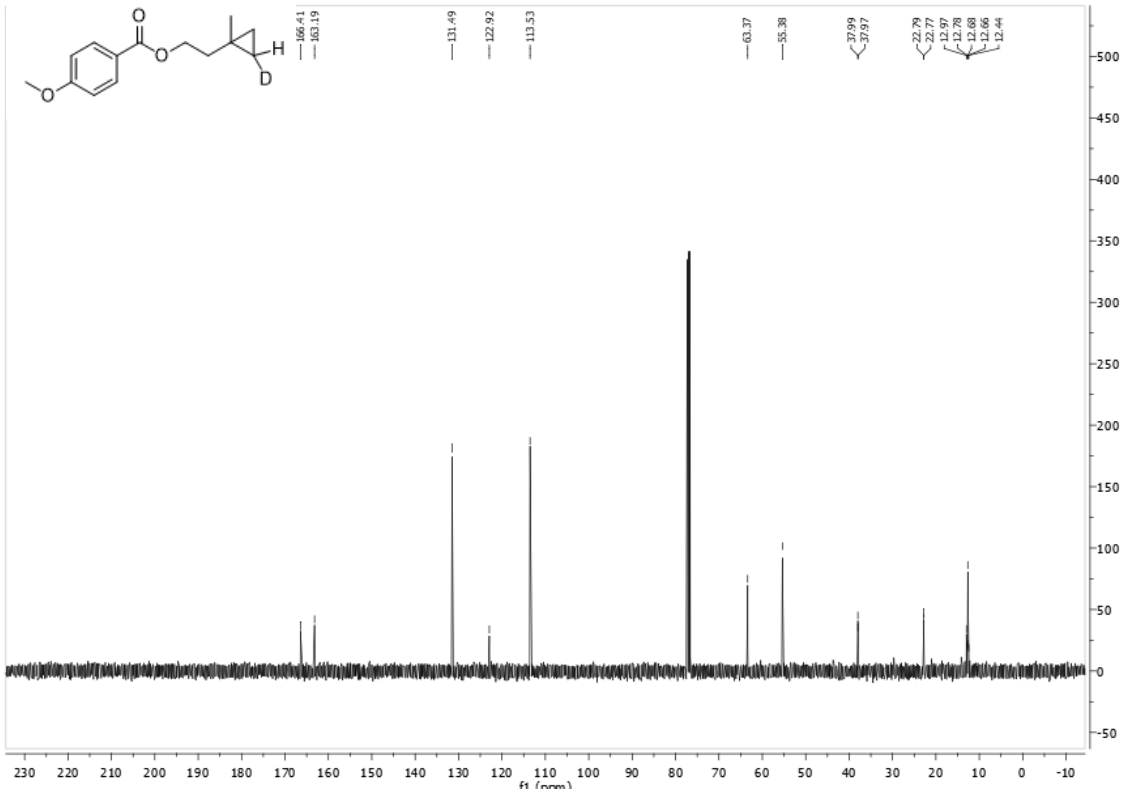
166.41
163.19
131.49
122.92
113.53
63.37
55.38
37.99
37.97
22.79
22.77
12.97
12.78
12.68
12.66
12.44
ft (ppm)

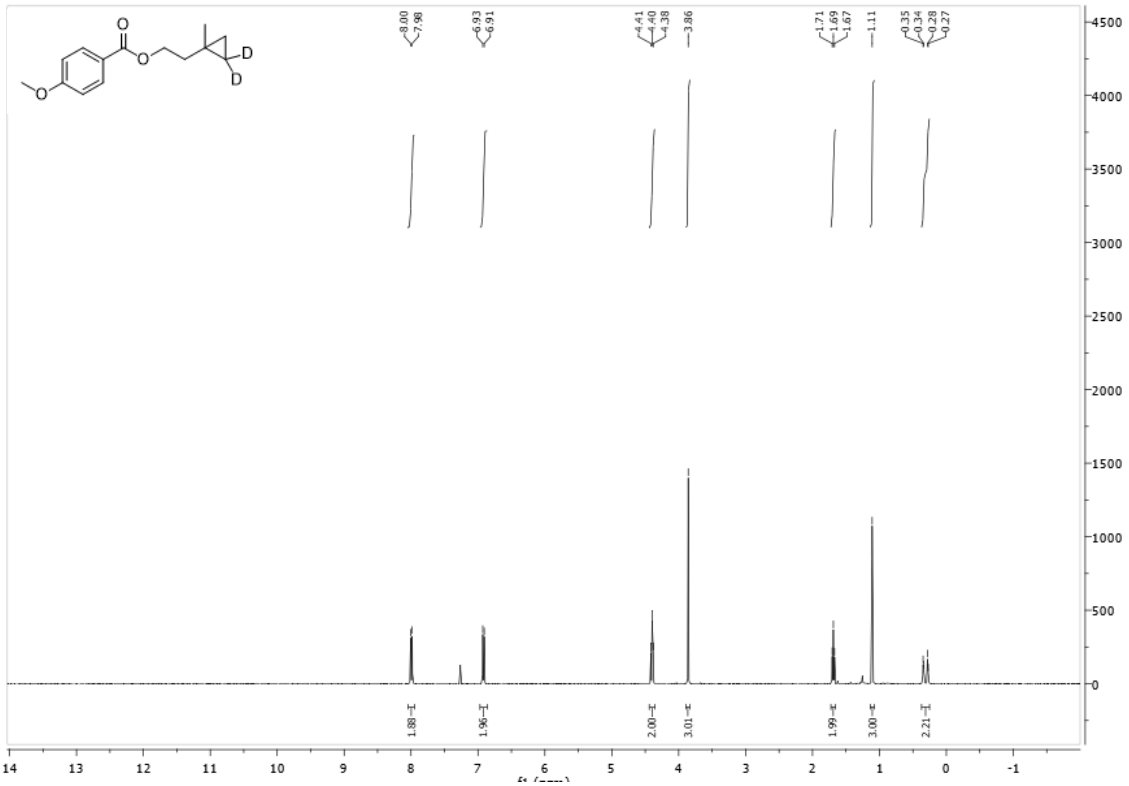
8.00
7.98
6.93
6.91
4.41
4.40
4.38
3.86
1.71
1.69
1.67
1.11
0.35
0.34
0.28
0.27
1.88
1.96
2.00
3.01
1.99
3.00
2.21
D
D
O
O
O

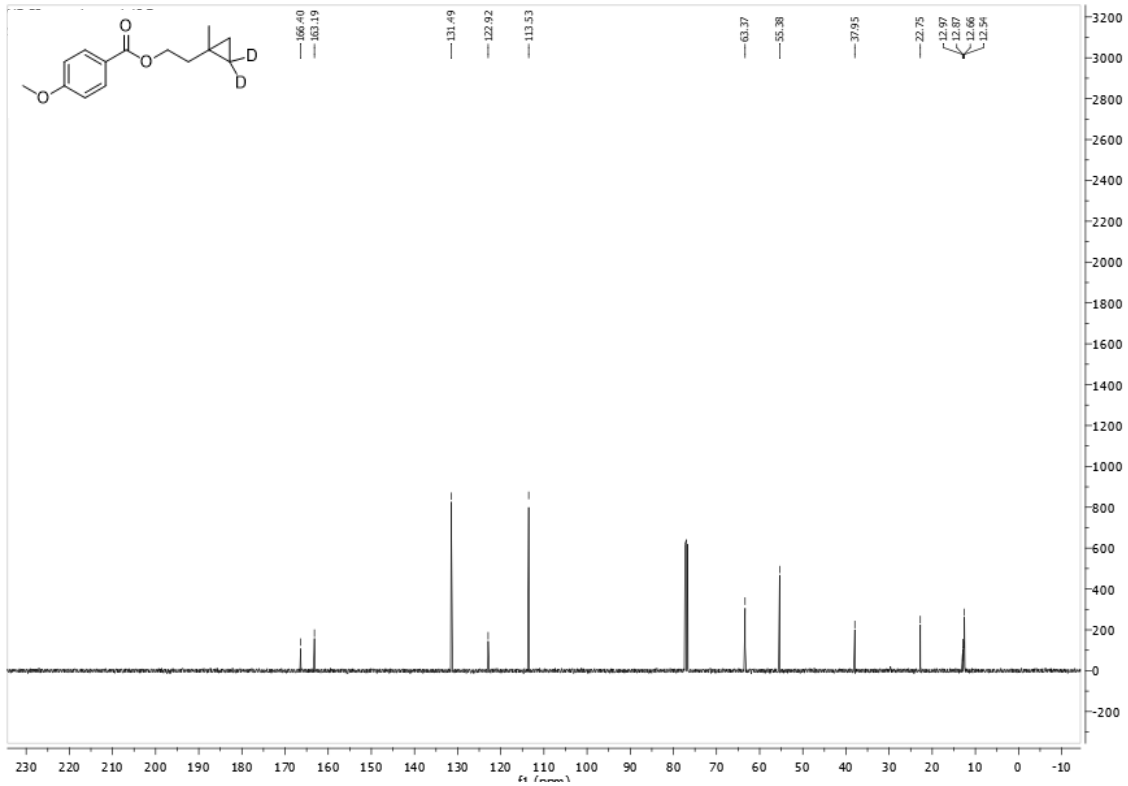
166.40
163.19
131.49
122.92
113.53
63.37
55.38
37.95
22.75
12.97
12.87
12.66
12.54
D
D
O
O
O

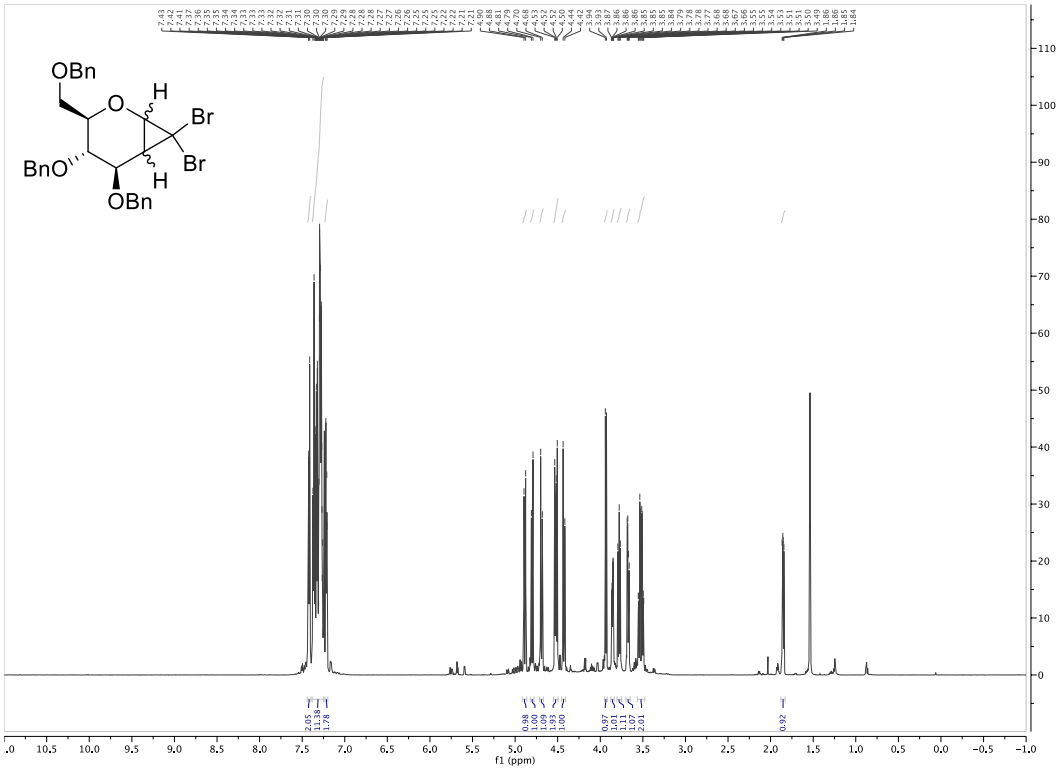
OBn
O
H
Br
Br
BnO
H
OBn
f1 (ppm)

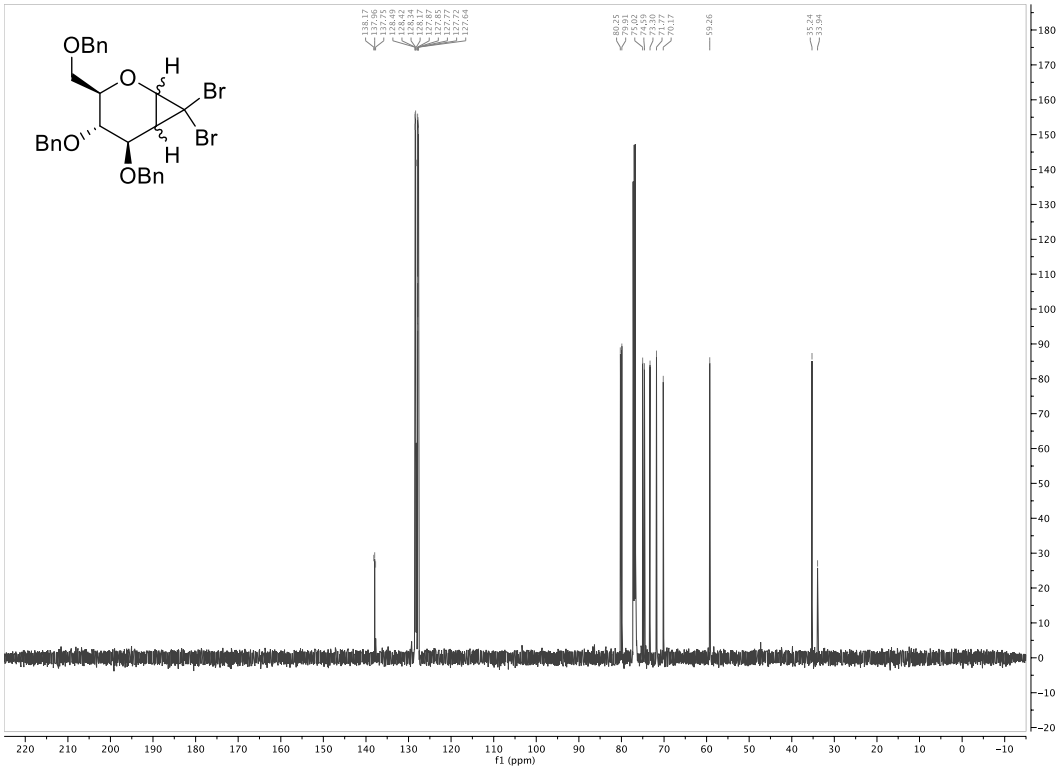
OBn
O
H
Br
Br
BnO
H
OBn
f1 (ppm)

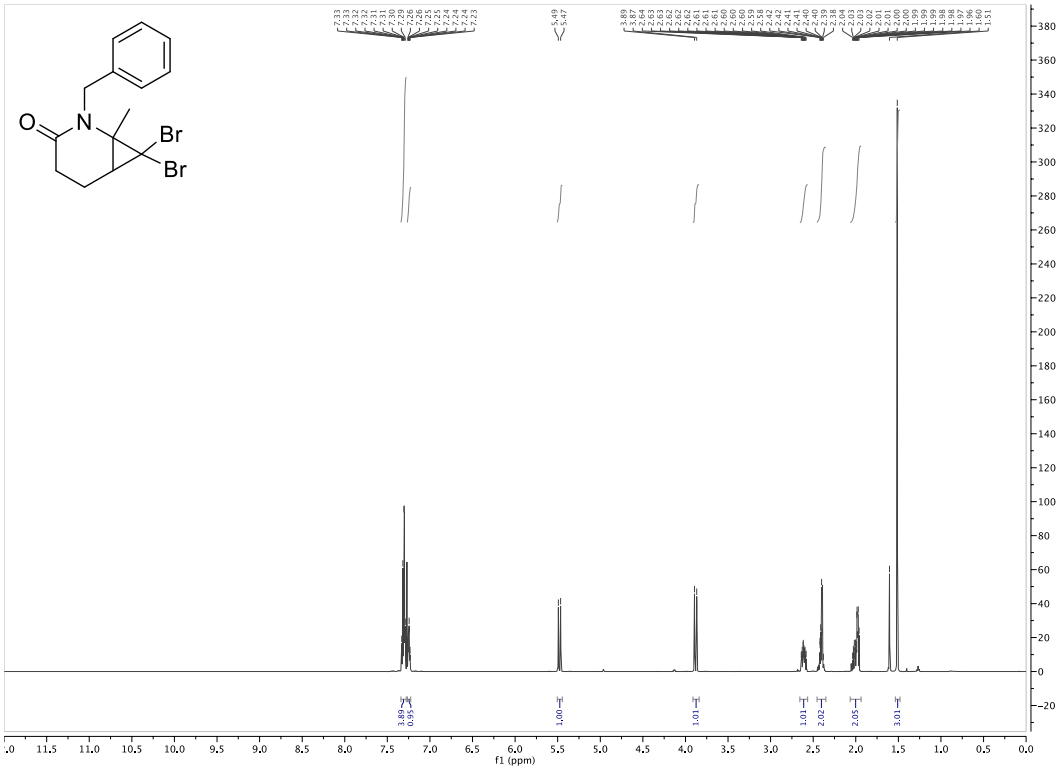
O
N
Br
Br
f1 (ppm)

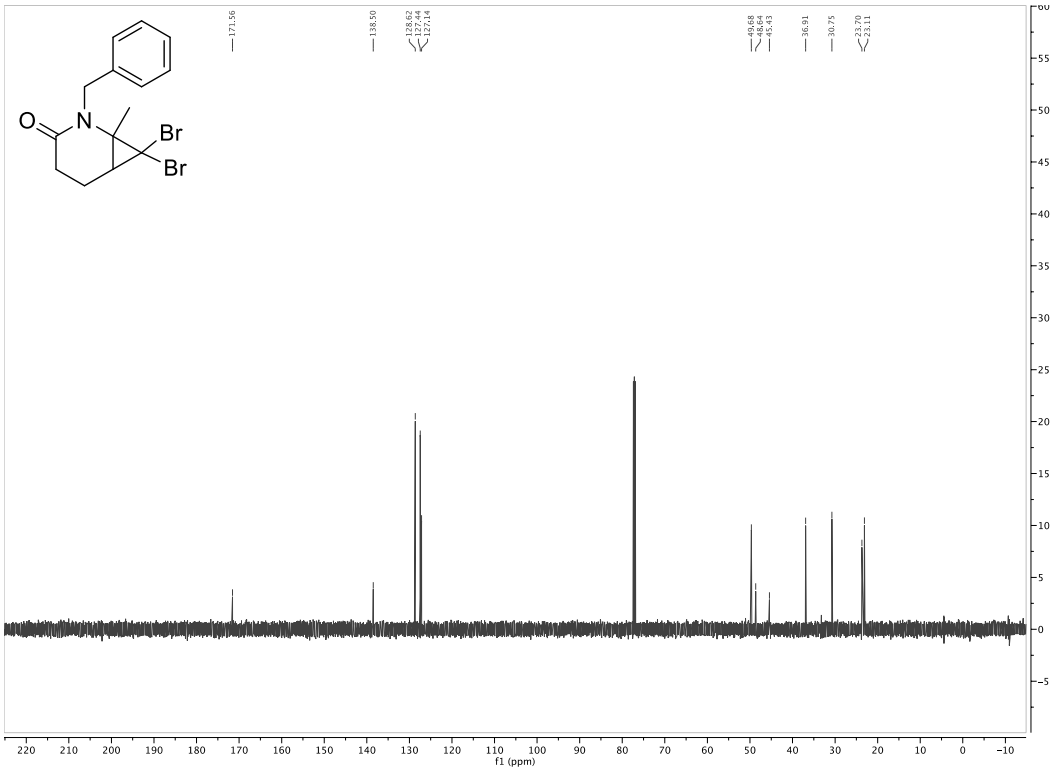
O
N
Br
Br
f1 (ppm)

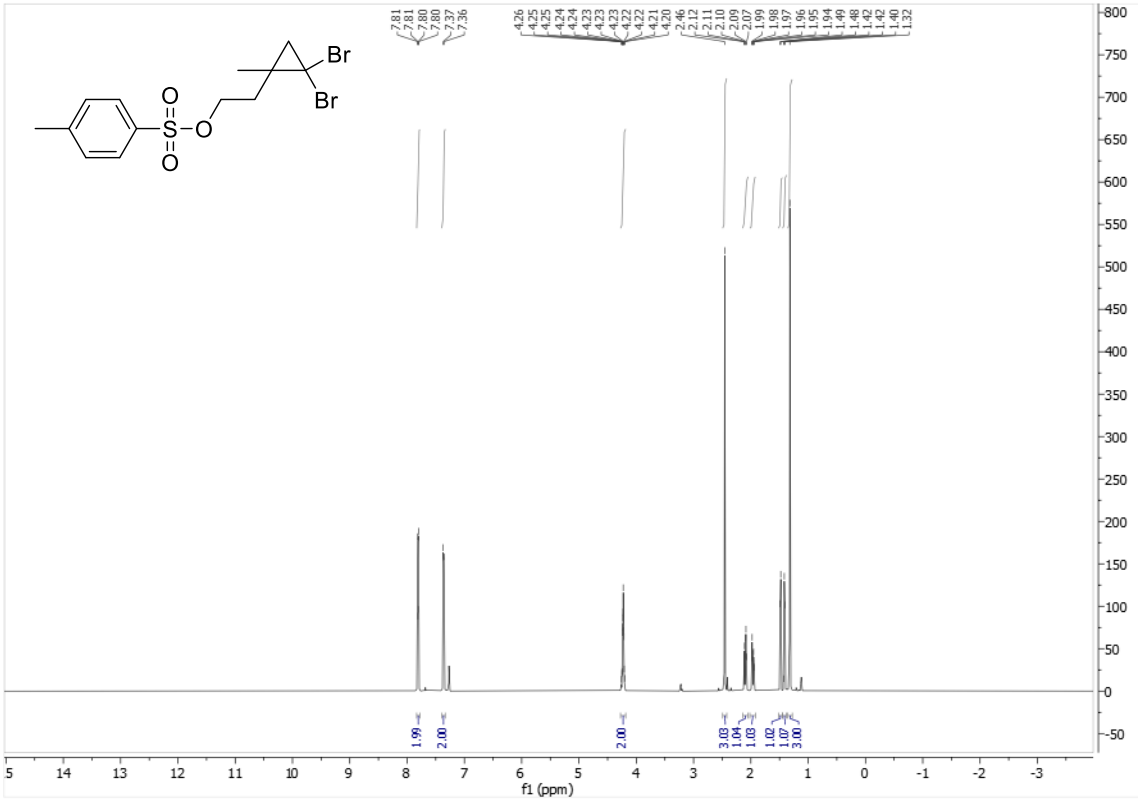
Br
Br
O
S
O
O
f1 (ppm)

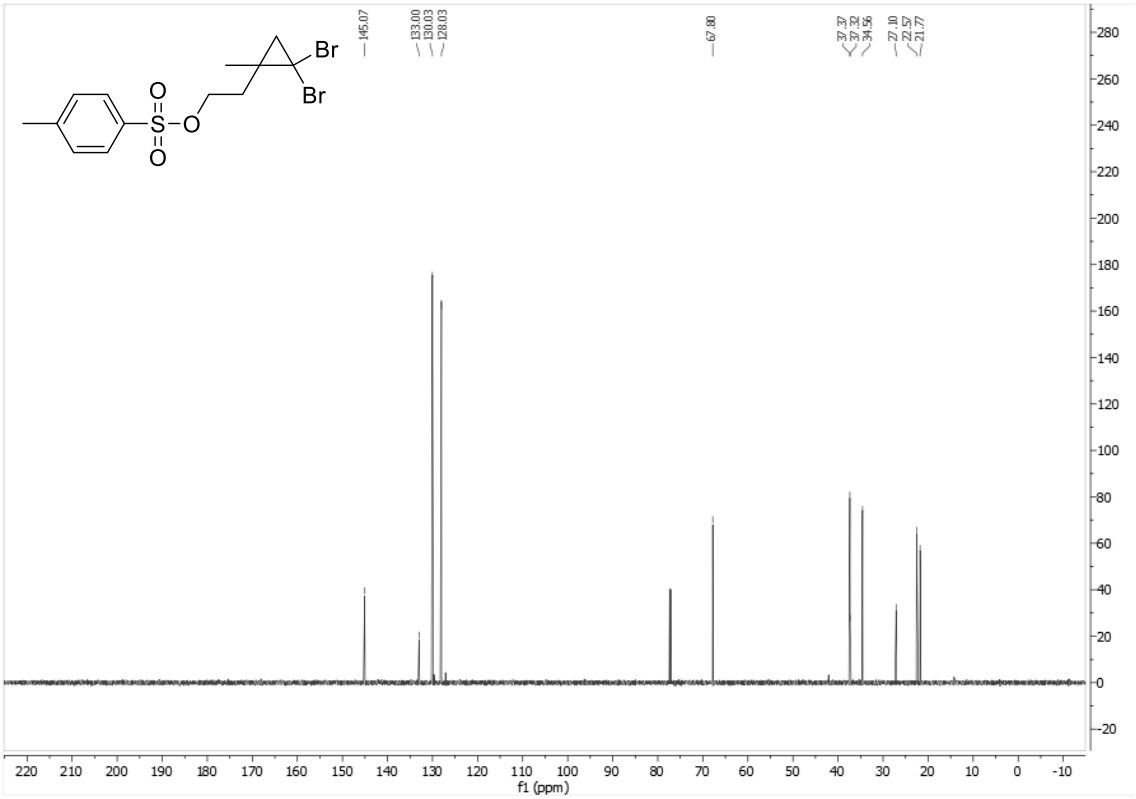
Br
Br
O
S
O
O
f1 (ppm)

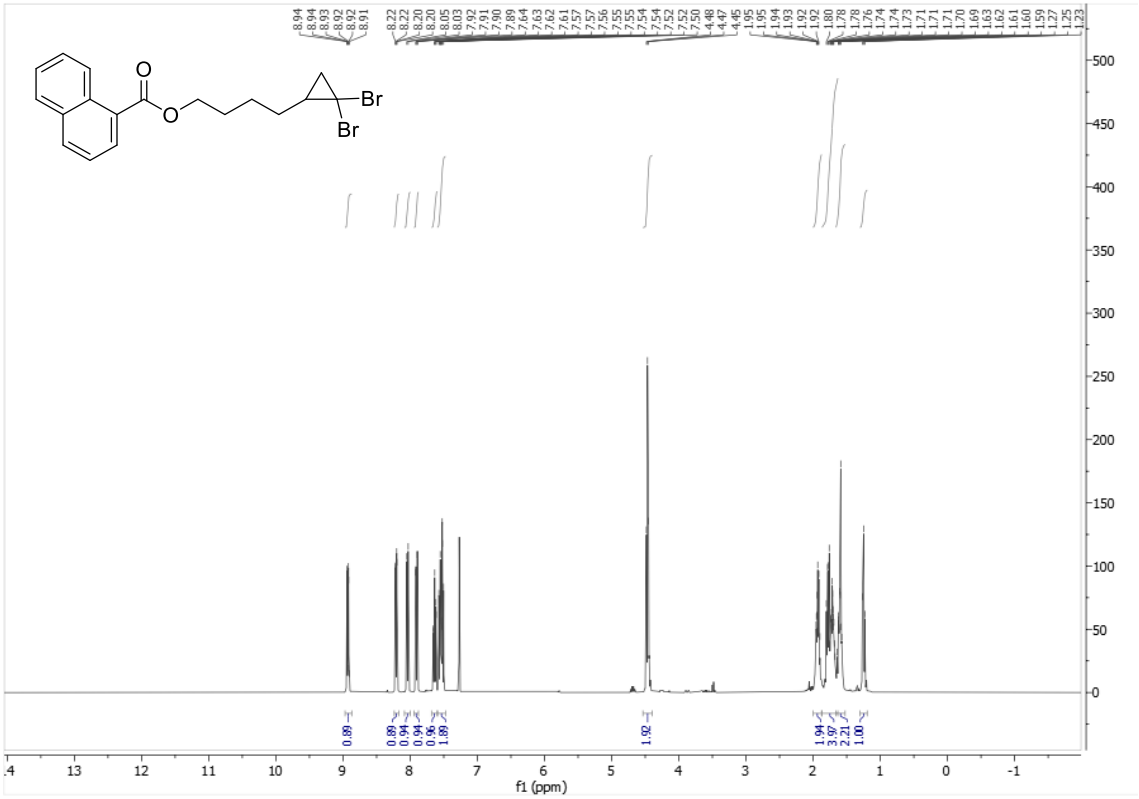
O
O
Br
Br
f1 (ppm)

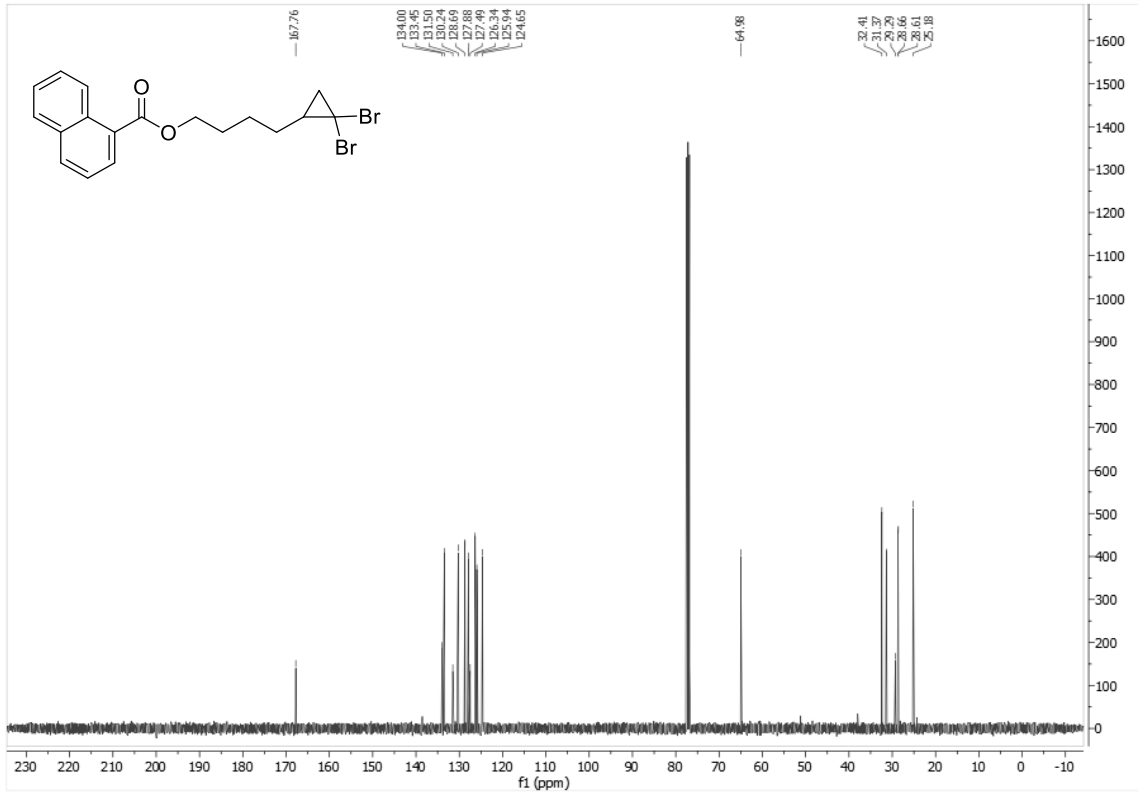
O
O
Br
Br
f1 (ppm)

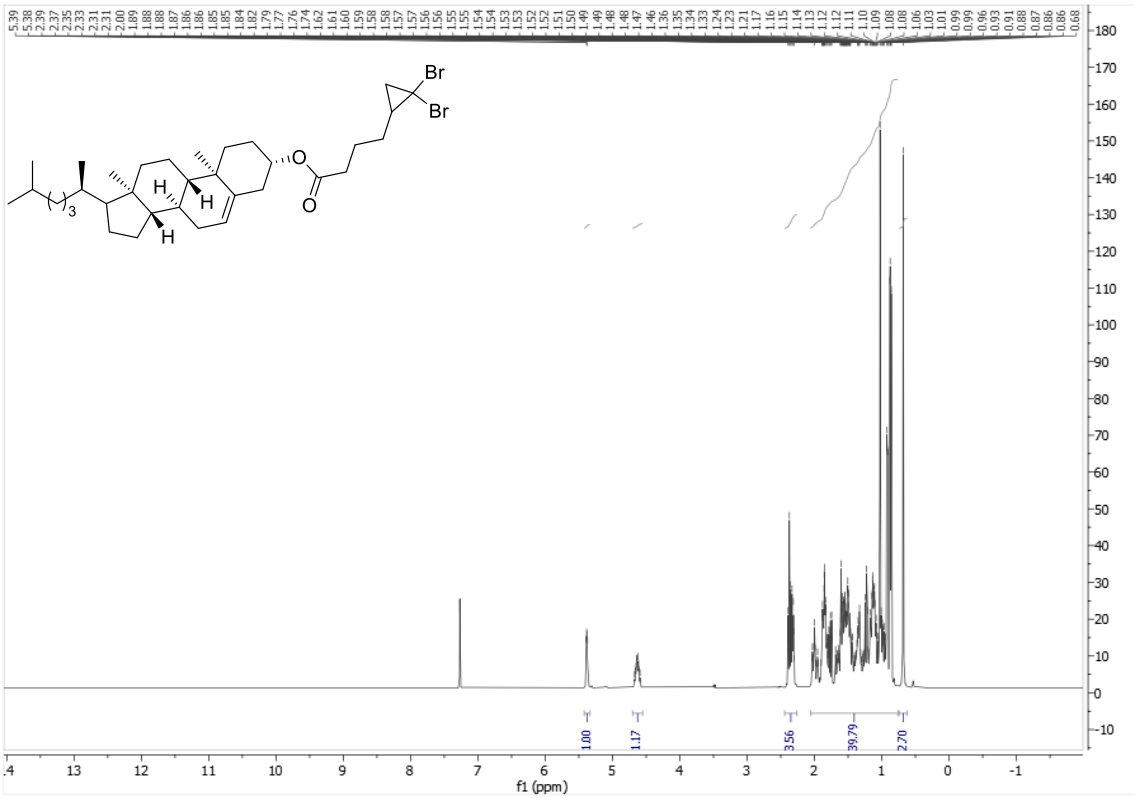
Br
Br
O
O
H
H
H
1.00
1.17
3.56
39.79
2.70
f1 (ppm)

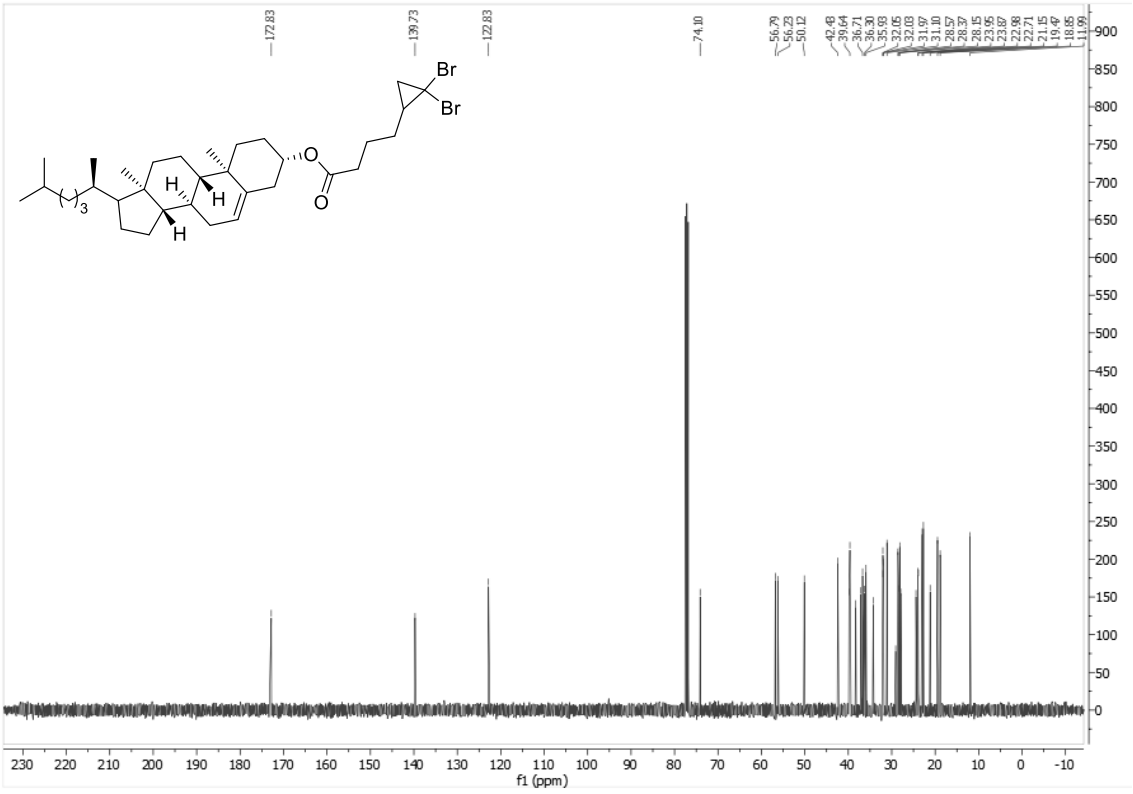
172.83
139.73
122.83
74.10
56.79
56.23
50.12
42.49
39.64
36.71
36.30
35.93
32.05
32.03
31.97
31.10
28.57
28.37
28.15
23.95
23.87
22.98
22.71
21.15
19.49
18.85
11.99
Br
Br
O
O
H
H
H
f1 (ppm)

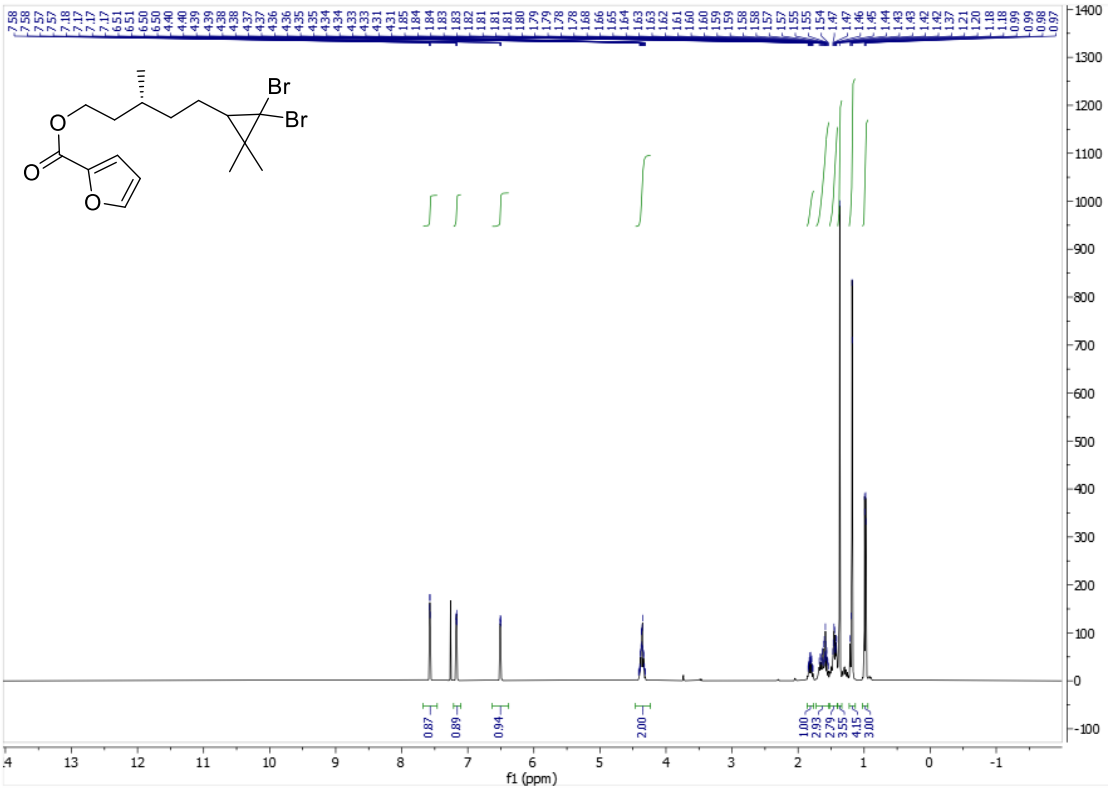
Br
Br
O
O
O
f1 (ppm)

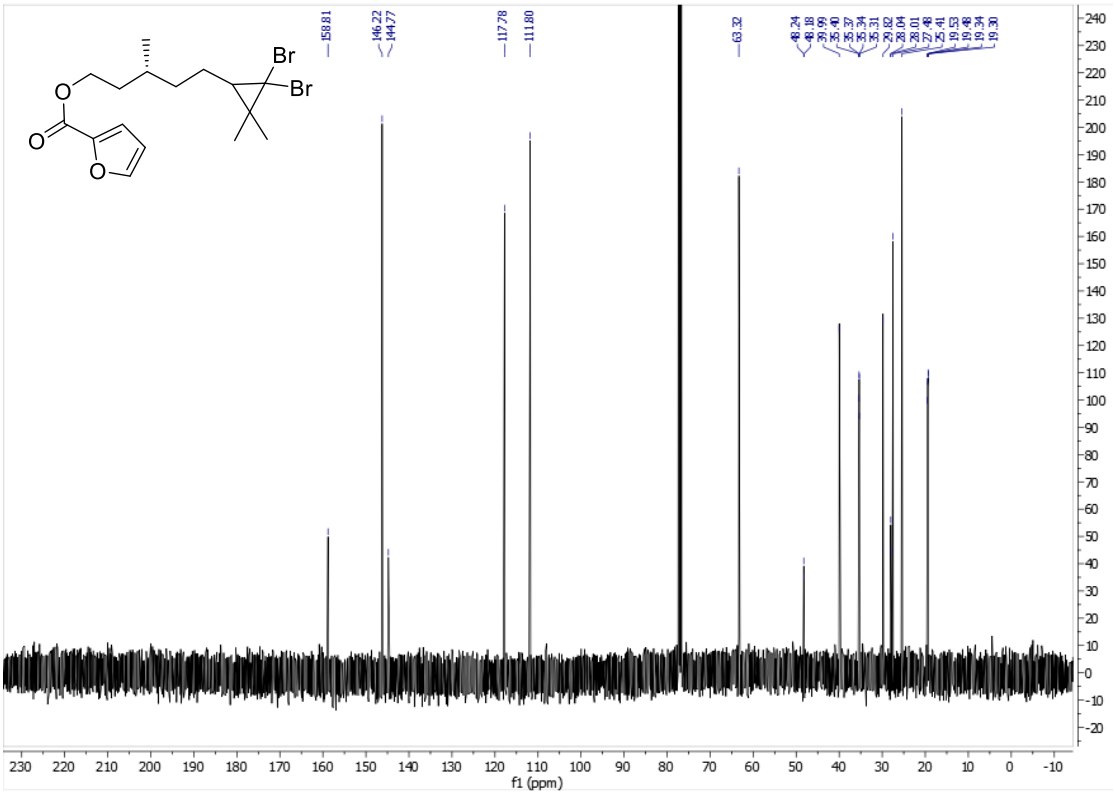
Br
Br
O
O
O
f1 (ppm)

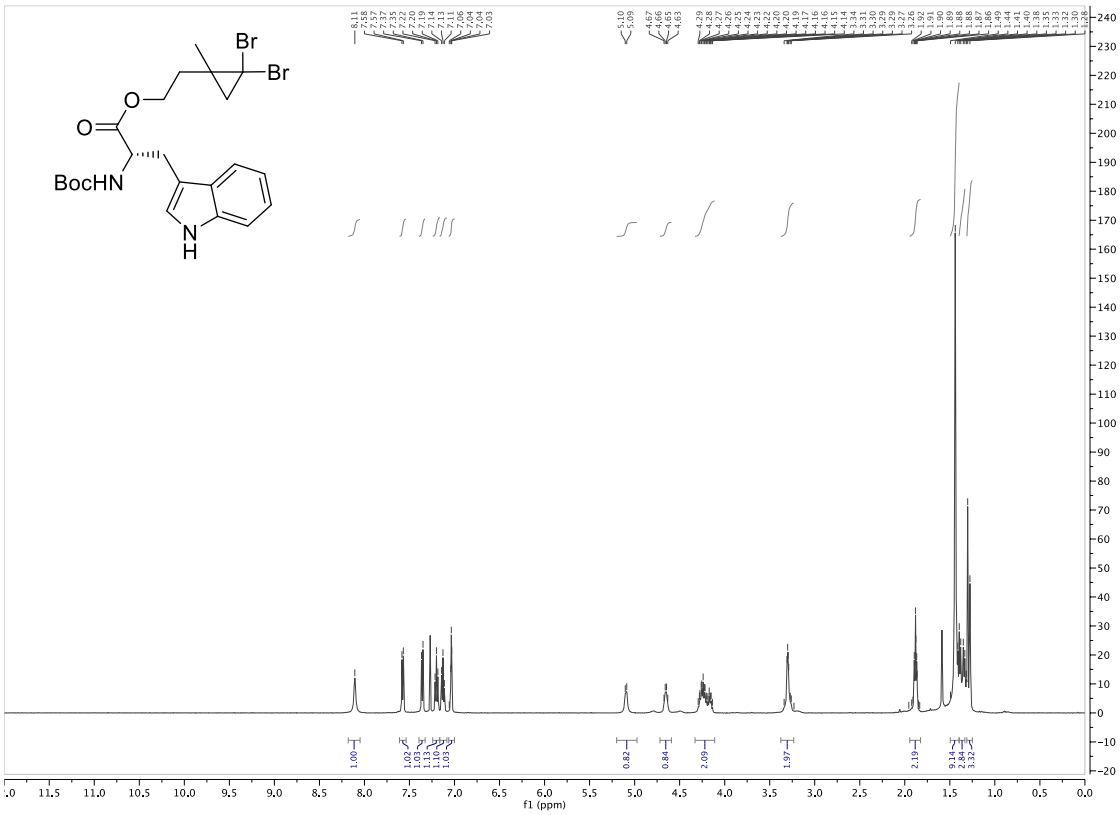
Br
Br
O
O
BocHN
N
H
f1 (ppm)

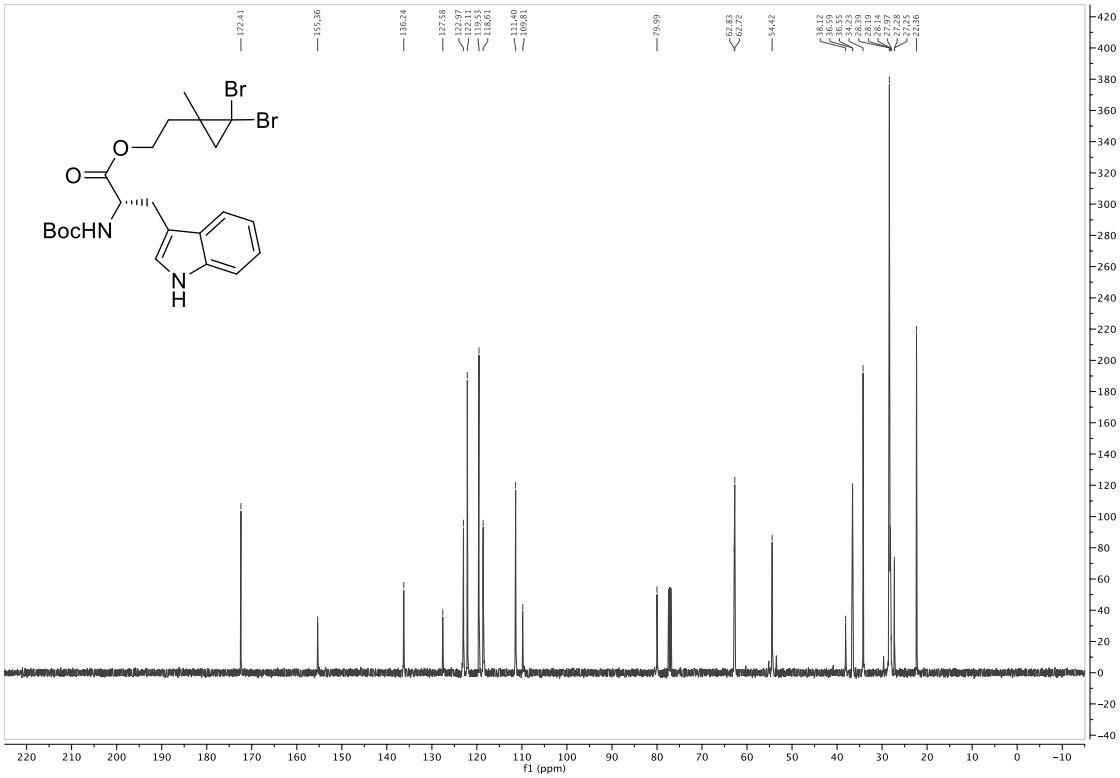
Br
Br
O
O
BocHN
N
H
f1 (ppm)

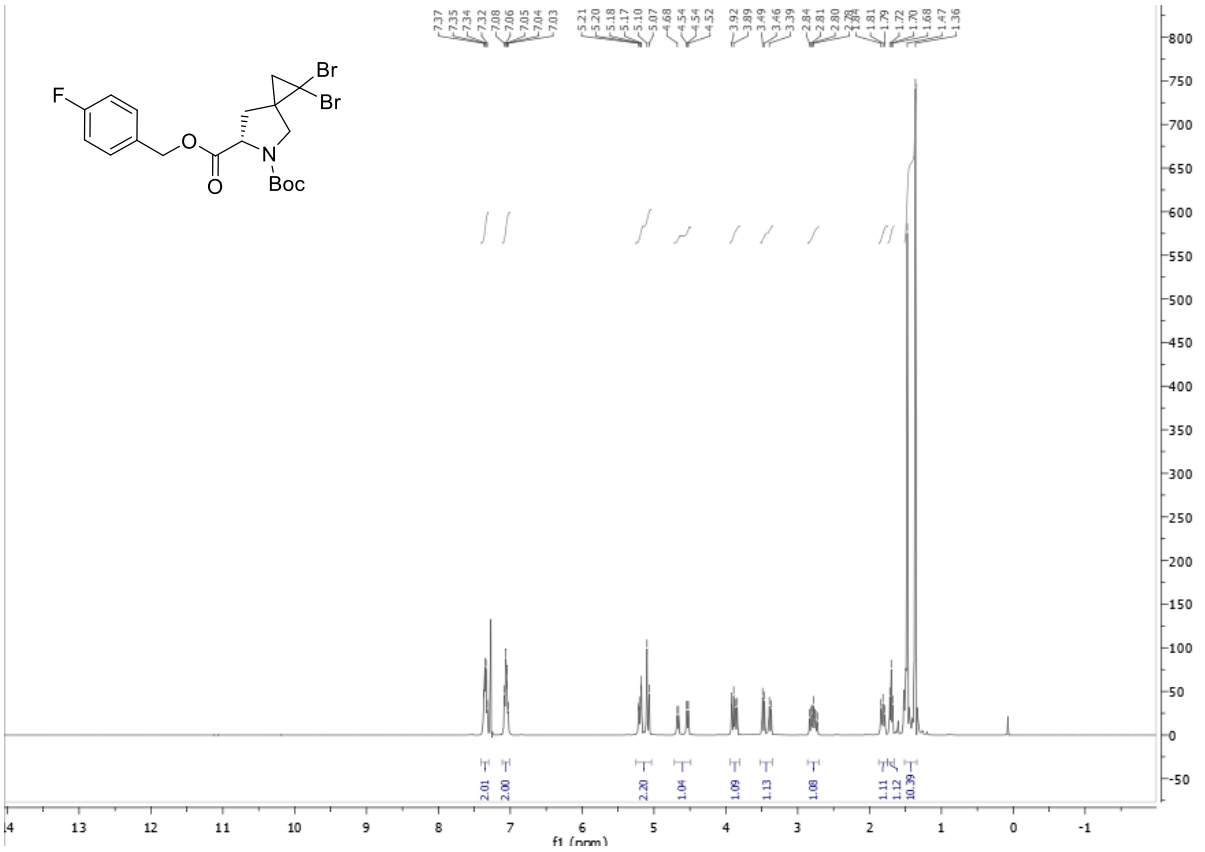
F
Br
Br
O
O
N
Boc
f1 (ppm)

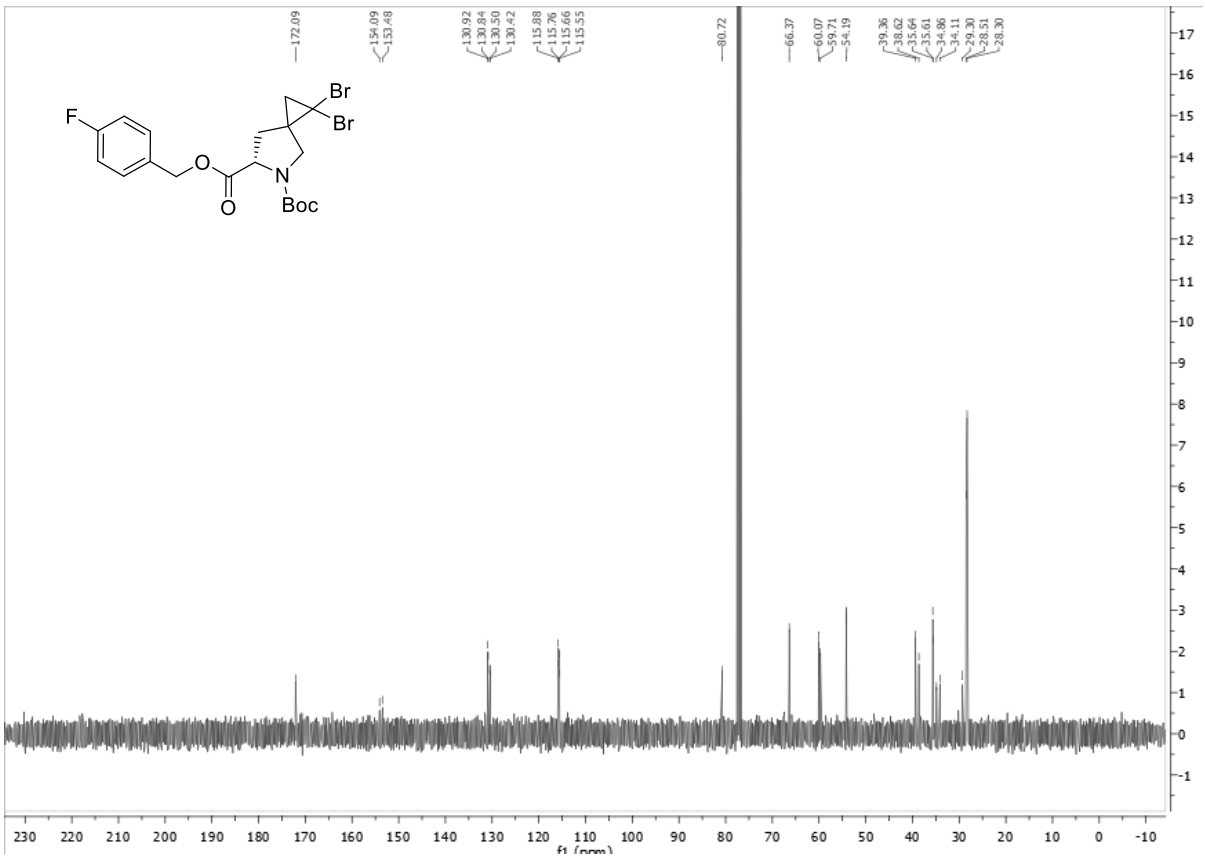
F
Br
Br
O
O
N
Boc
f1 (ppm)

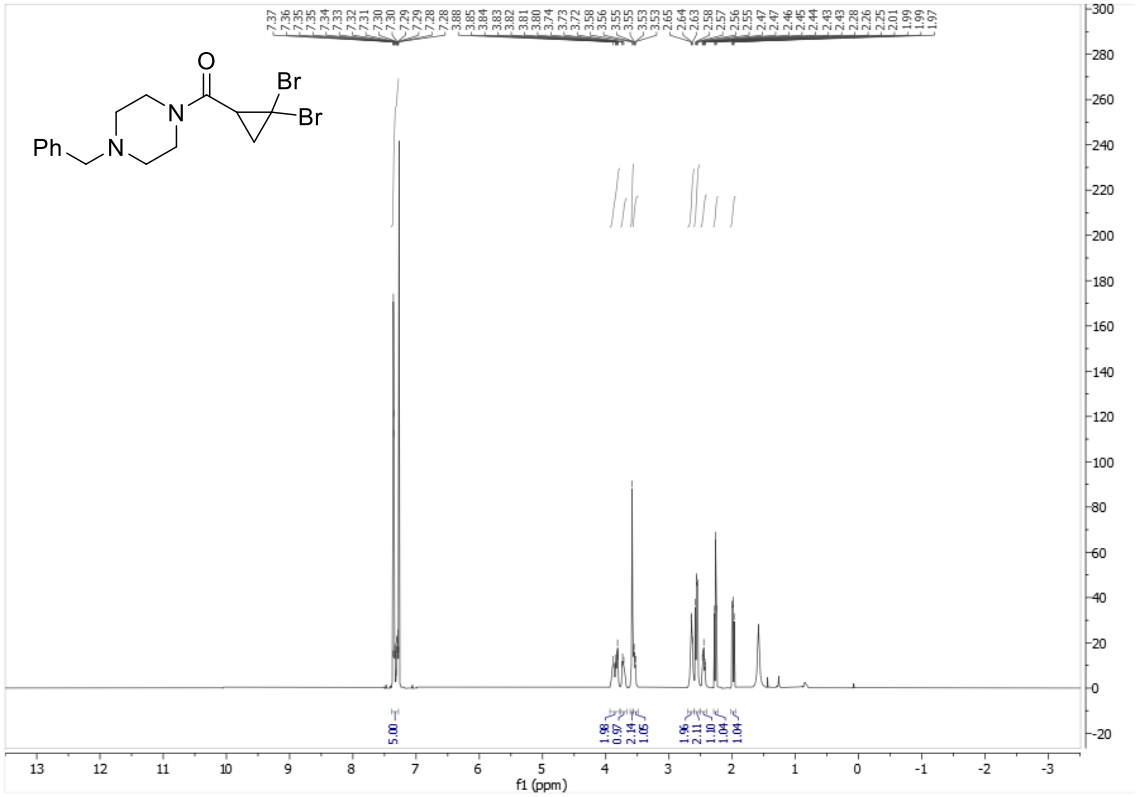
O
Br
Br
N
N
Ph
f1 (ppm)

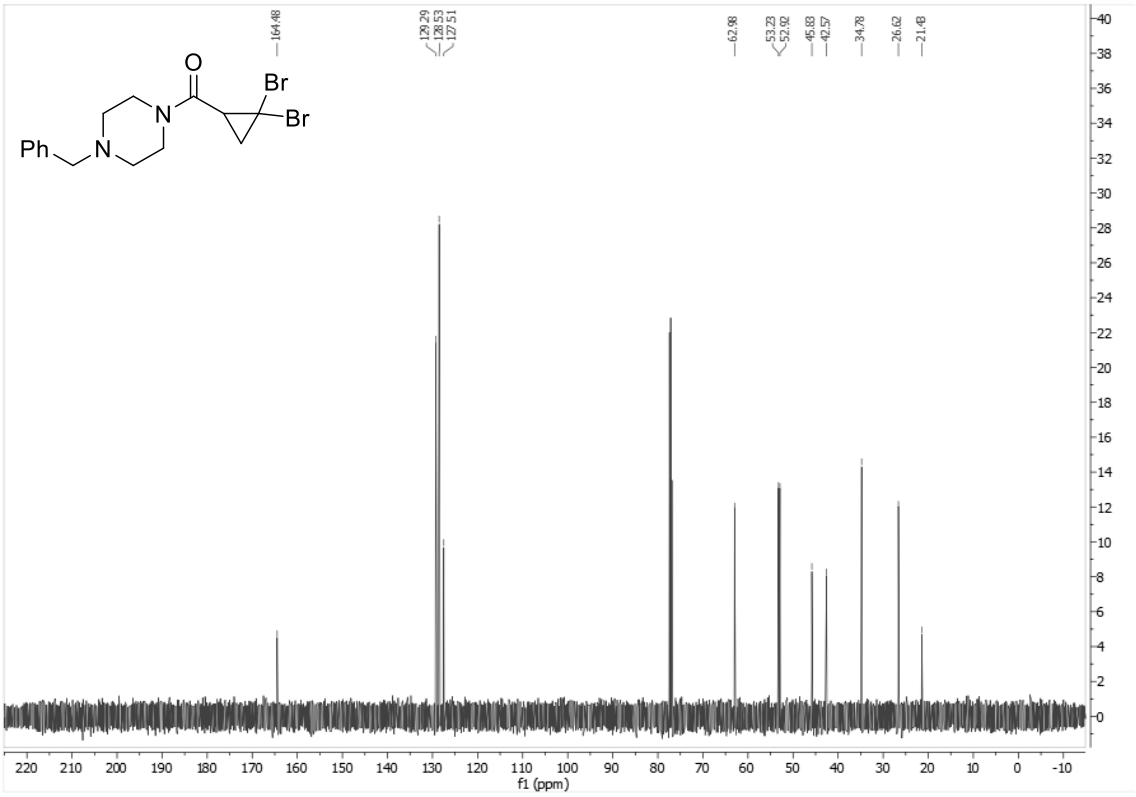
O
Br
Br
N
N
Ph
164.48
129.29
128.53
127.51
62.98
53.23
52.92
45.83
42.57
34.78
26.62
21.48
f1 (ppm)

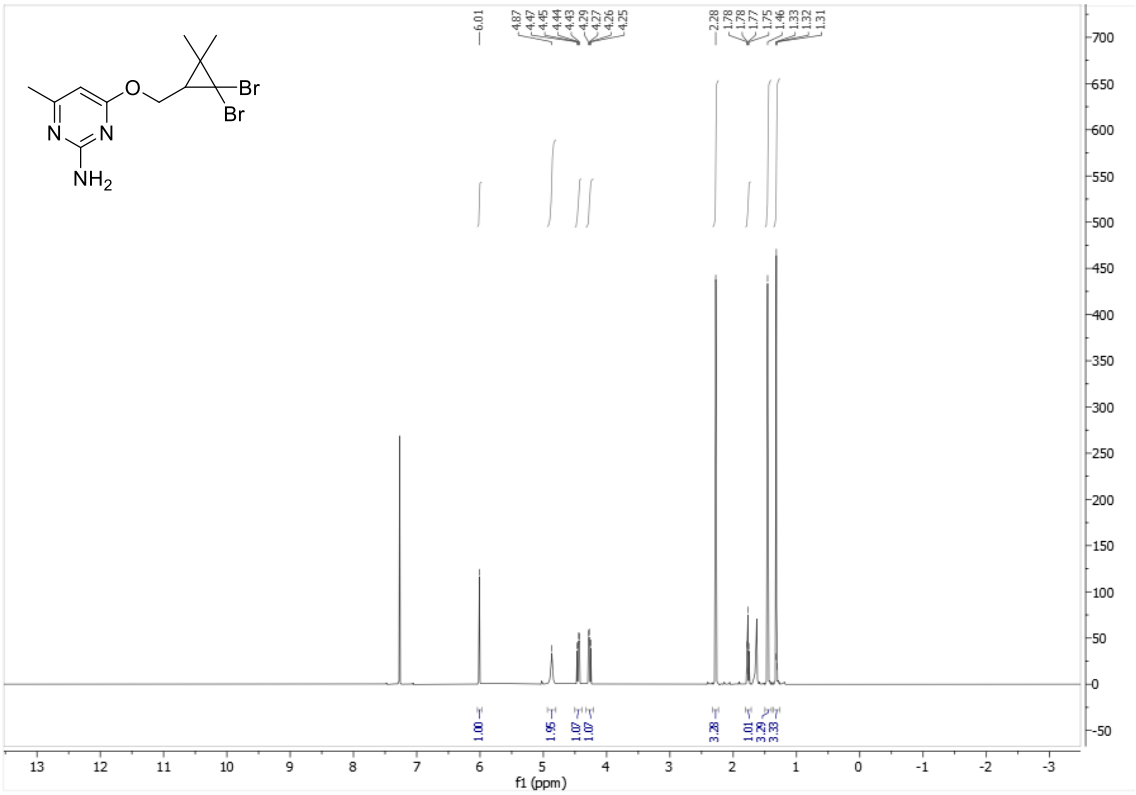
Br
Br
O
N
N
NH2
6.01
4.87
4.47
4.45
4.44
4.43
4.29
4.27
4.26
4.25
2.28
1.78
1.78
1.77
1.75
1.46
1.33
1.32
1.31
1.00
1.95
1.07
1.07
3.28
1.01
3.29
3.33
f1 (ppm)

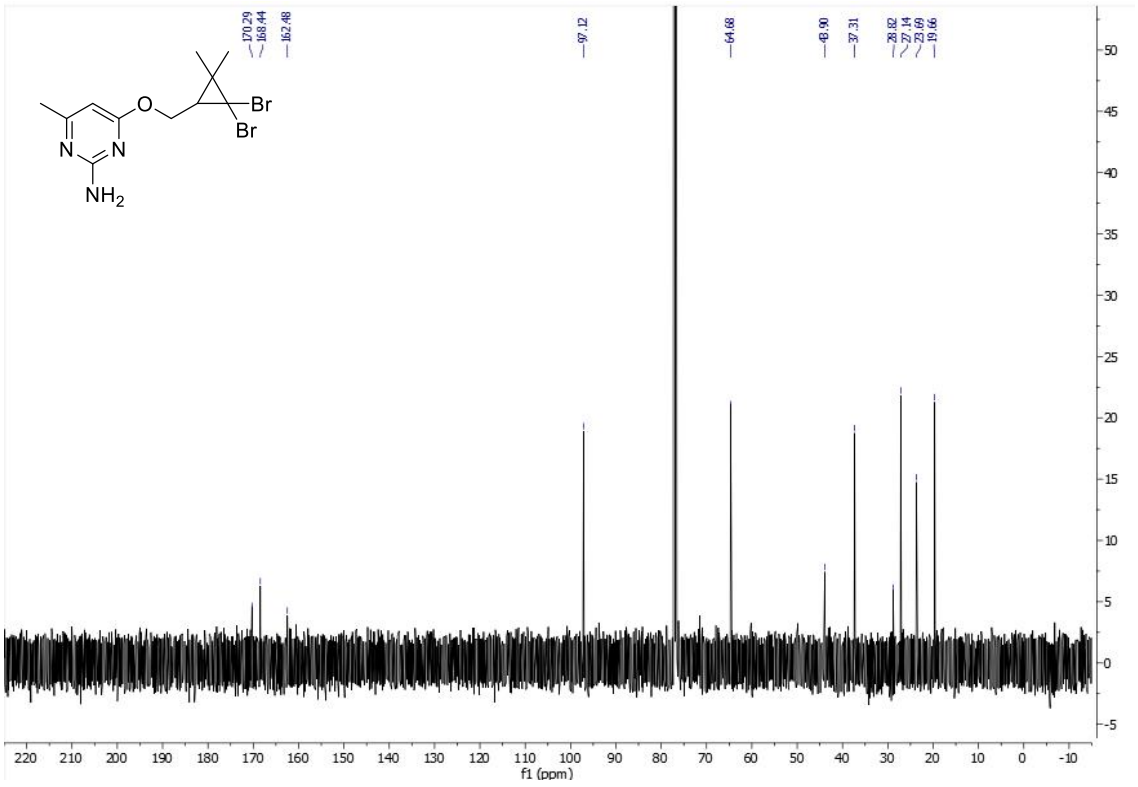
Br
Br
O
N
N
NH2
170.29
168.44
162.48
97.12
64.68
40.90
37.31
28.82
27.14
23.69
19.66
f1 (ppm)

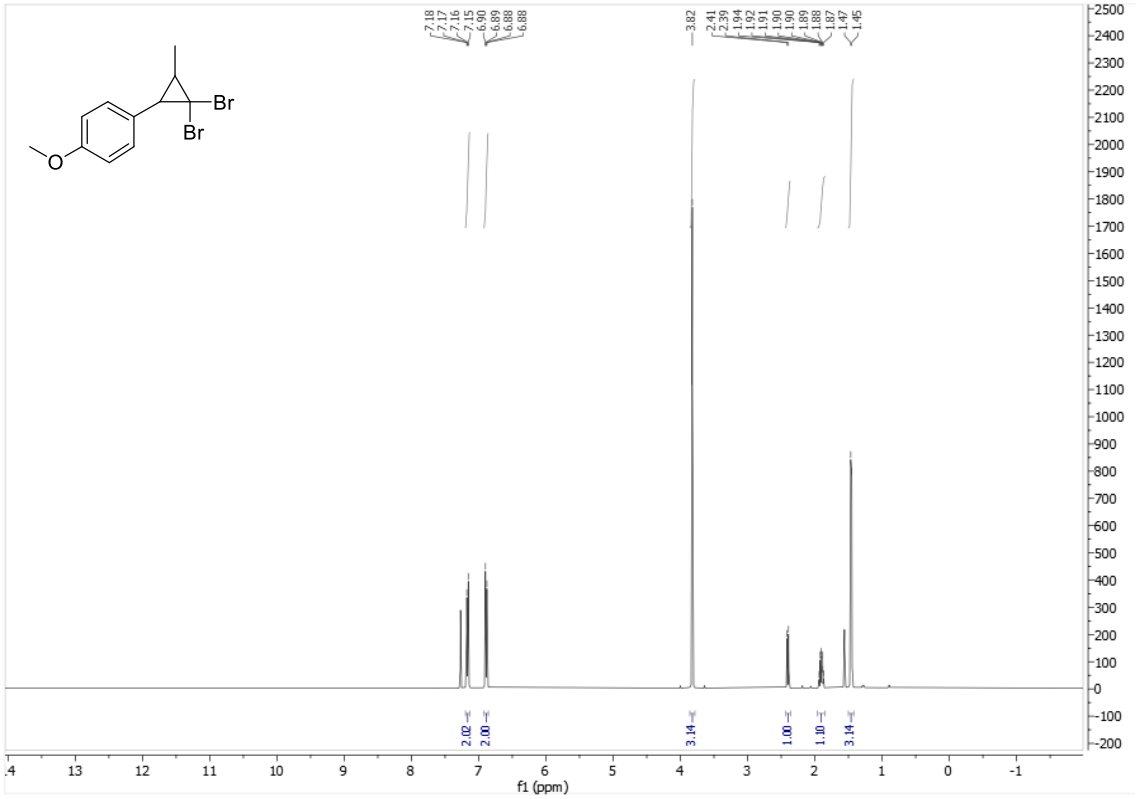
Br
Br
O
f1 (ppm)

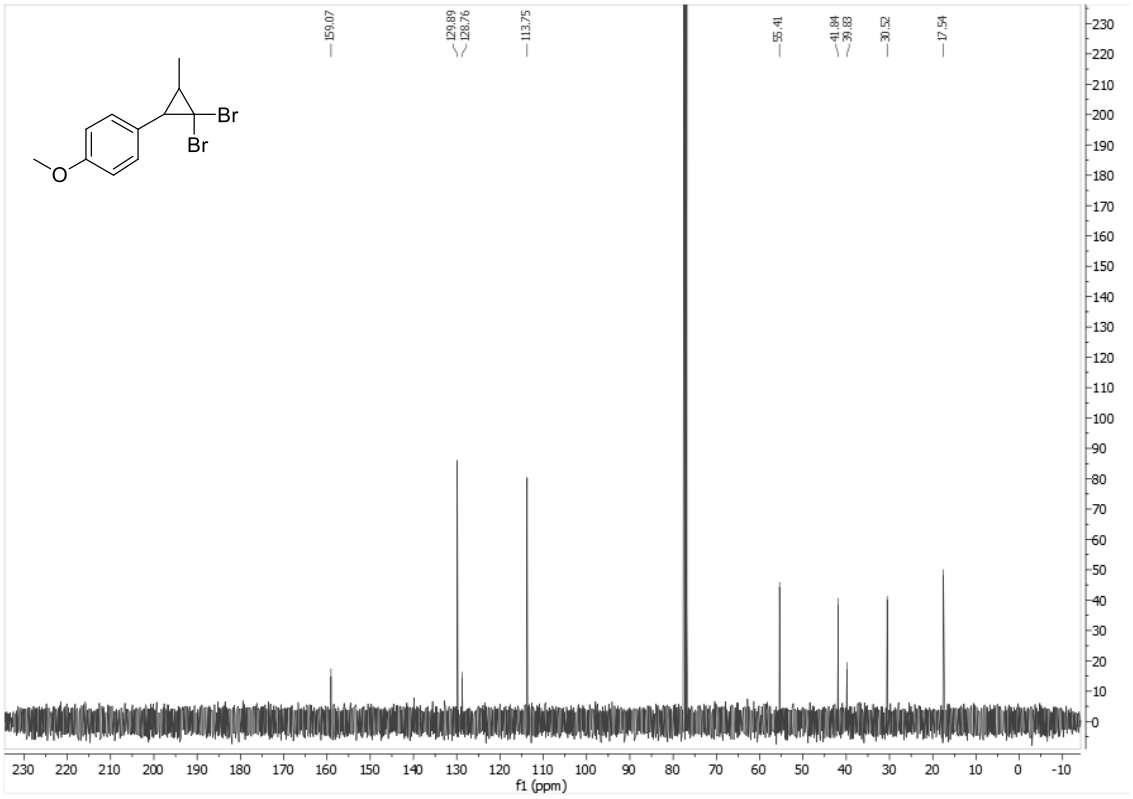
Br
Br
O
f1 (ppm)

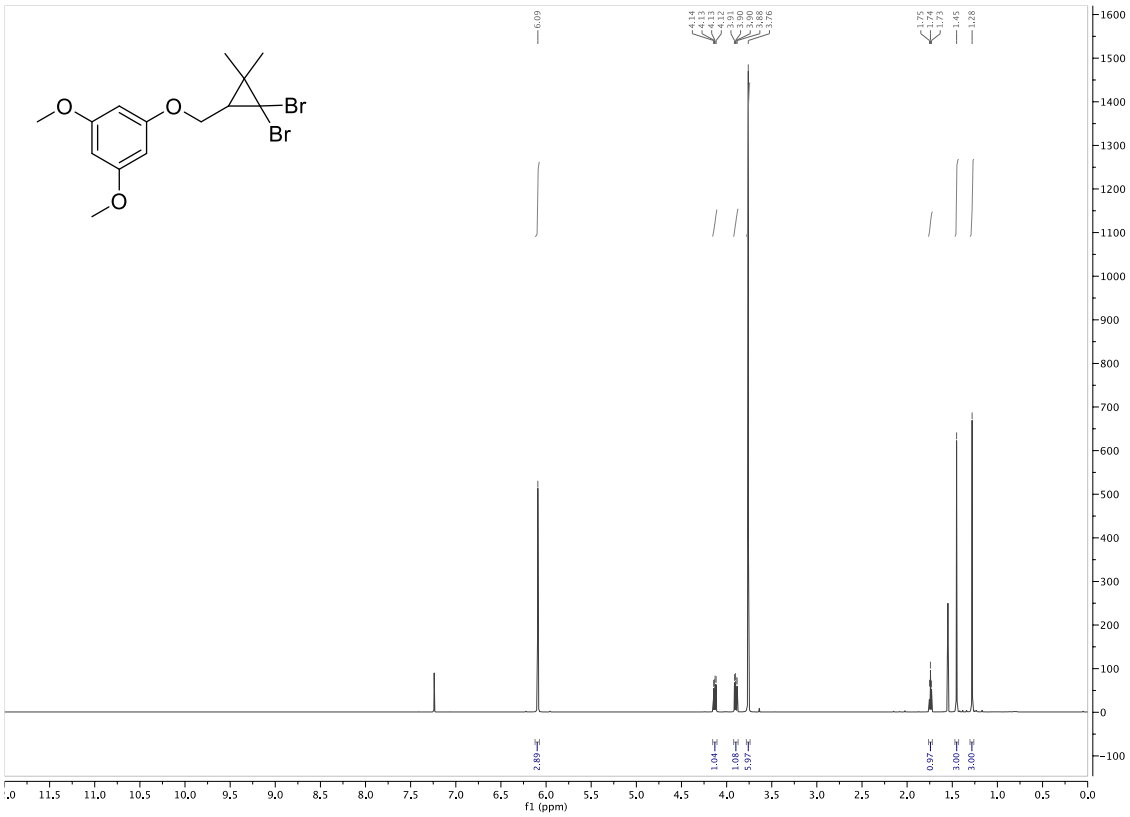
O
O
O
Br
Br
6.09
4.14
4.13
4.13
4.12
3.91
3.90
3.90
3.88
3.76
1.75
1.74
1.73
1.45
1.28
2.89
1.04
1.08
5.97
0.97
3.00
3.00
f1 (ppm)

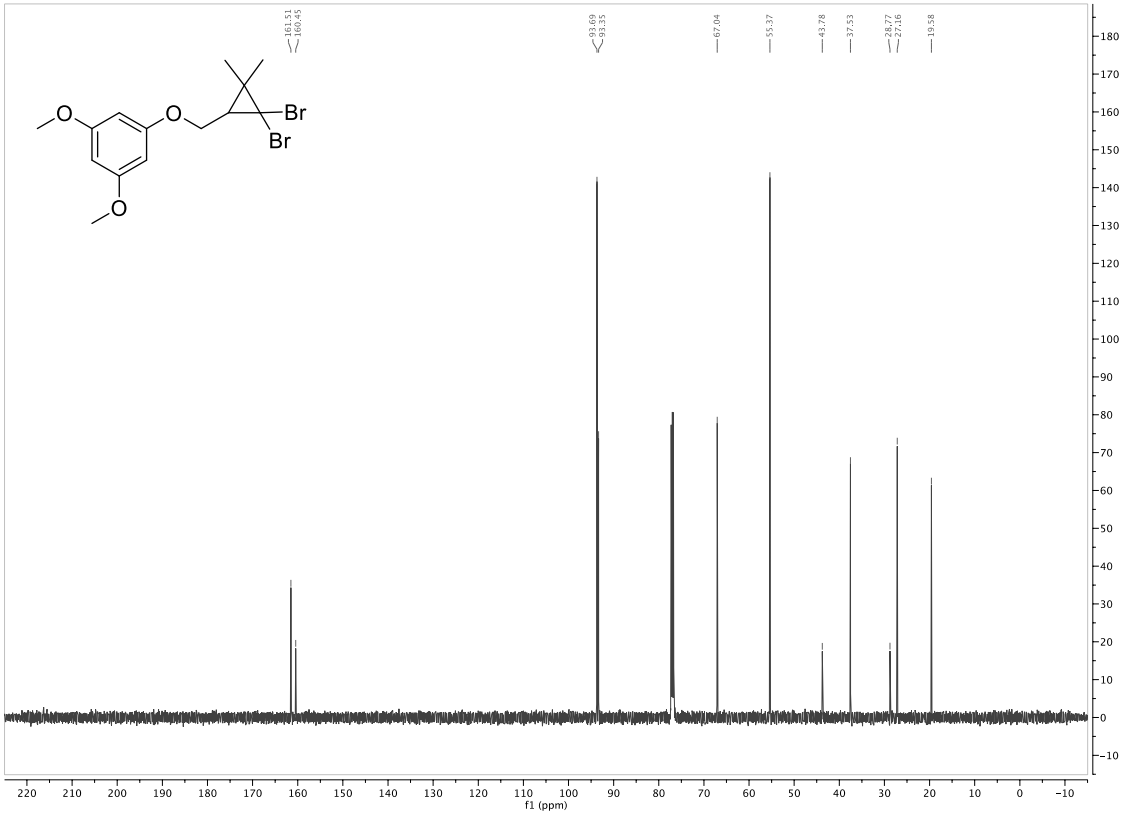
O
O
O
Br
Br
161.51
160.45
93.69
93.35
67.04
55.37
43.78
37.53
28.77
27.16
19.58
f1 (ppm)

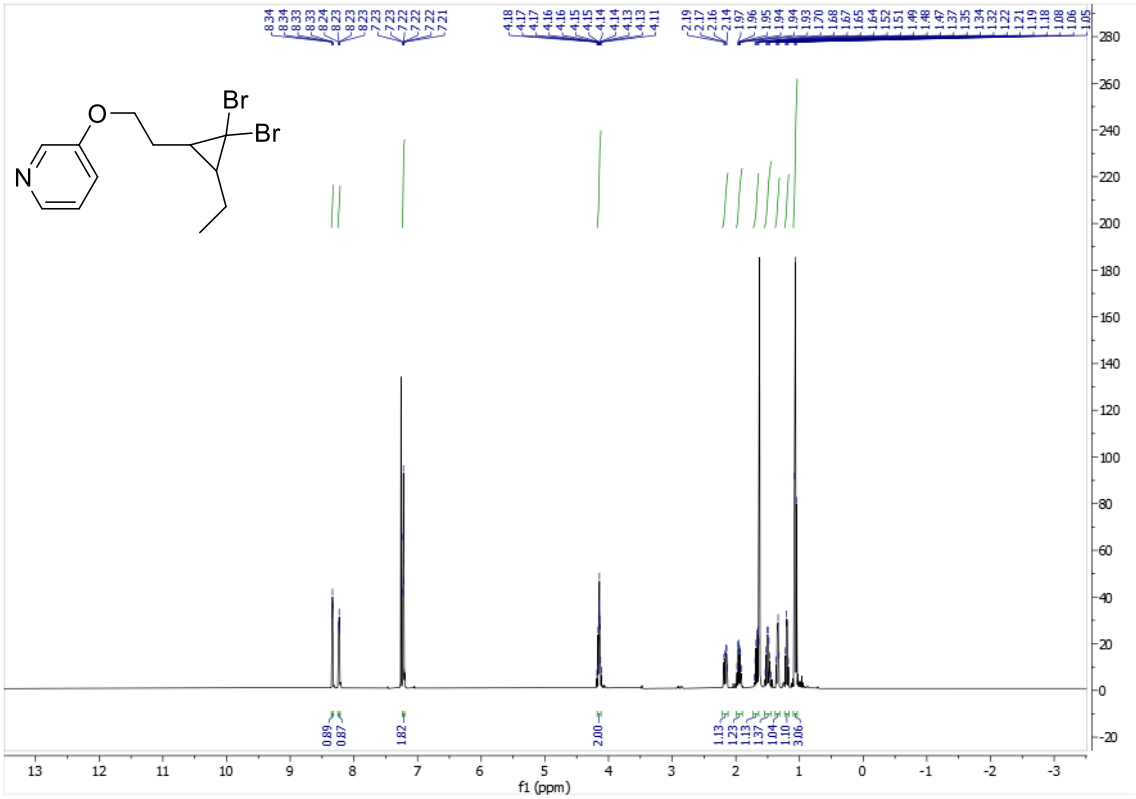
Br
Br
O
N
f1 (ppm)

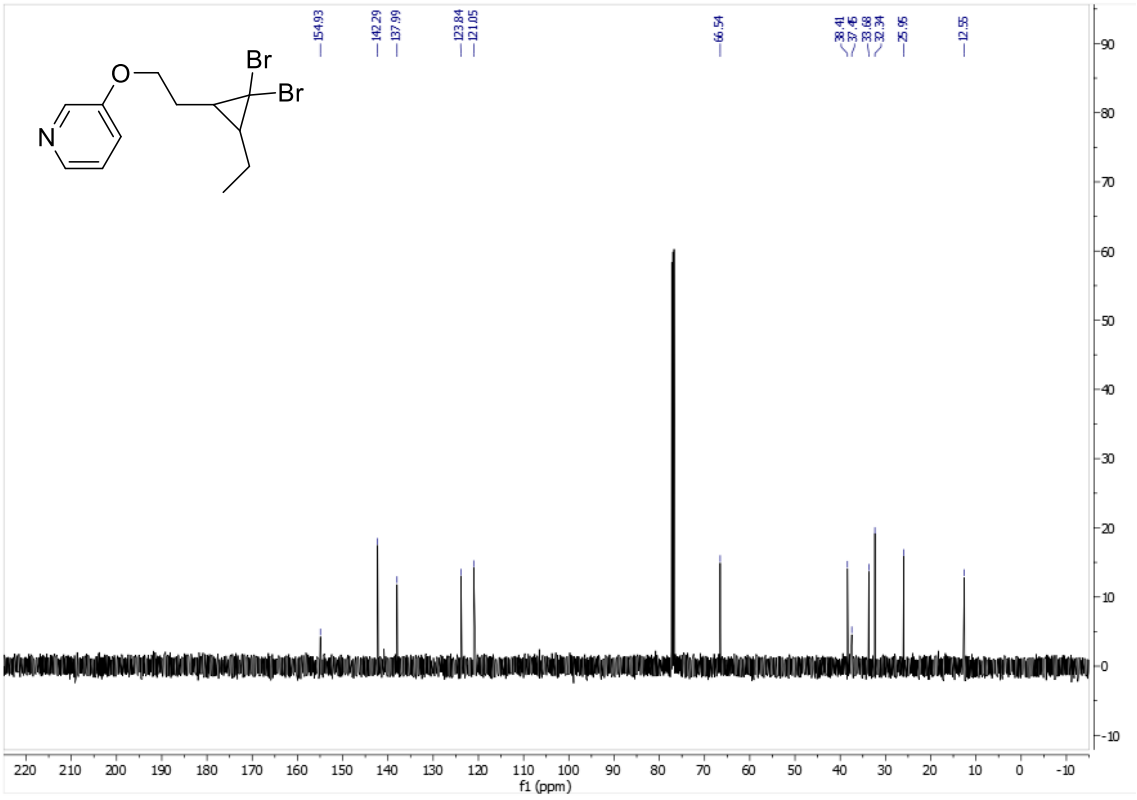
Br
Br
O
N
f1 (ppm)

II. α-Arylations of (Hetero)Aryl Ketones in Aqueous Micellar Media

Reproduced from

Wood, A. B.; Roa, D. E.; Gallou, F.; Lipshutz, B. H. *Green Chem.* **2021**, *23*, 4858–4865.

With permission from The Royal Society of Chemistry

And

Reproduced from

Li, X.; Wood, A. B.; Lee, N. R.; Gallou, F.; Lipshutz, B. H. *Green Chem.* **2022**,

10.1039.D2GC00776B.

With permission from The Royal Society of Chemistry

2.1 Personal Account

I had just gotten back from Boston after completing the research portion of the aqueous slurry plug flow project at Novartis (see Chapter 4), and I went to go see Bruce about adding another project to my workload. The *gem*-dibromocyclopropane manuscript had yet to be written at this point, but I needed something else on my plate to occupy my interests. Again, Fabrice Gallou from Novartis came through with a solid idea for a project in the form of α-arylation of ketones in aqueous micellar medium. This was exciting from the inception because, at face value, the idea of being able to perform enolate cross-coupling chemistry in water seemed crazy based on the orders of magnitude in difference between the acidity of water *vs.* the α-proton of a ketone. However, we postulated that the lipophilic nature of the micellar core would prevail once again (*vide supra*) in defying the impossible.

I immediately set forth to explore the literature surrounding the transformation, as well as set up some trials of the classical model reaction between propiophenone and 4-bromoanisole using strong base and a palladium catalyst inspired by Hartwig's group. Amazingly, the very second reaction that I set up worked in a relatively decent yield of 65%, albeit at 2 mol % palladium loading after running for four days. This prompted Dr. Daniel Lippincott to express his amused surprise; he hoped it was going to at least be harder than just a few trials to get this chemistry to go. That's the power of the micellar system, however, and this success became the impetus for a very enjoyable cross-coupling project that was vastly different from both the cyclopropane dehalogenation and flow projects.

With respect to the allylation chemistry, the origination of this project came after the completion of the arylation project. Bruce called me into his office (as the current group expert in enolate chemistry in water, as he put it) to help advise a then second year graduate student,

Ms. Xiaohan Li, to explore this transformation. The reason why we began this program was that Xiaohan didn't feel that she had enough to do (she was already working on two projects) and wanted something challenging. It turns out that she took the allylation work to a completely different level away from aqueous micellar catalysis and towards neat methodology, which was new territory for our group and very cool to work on. I was given the privilege to apply her method to the total synthesis of CoQ_9 and a variety of vitamin K derivatives, which was ultimately a very fun experience. What's greener than running chemistry without any solvent?

2.2 Introduction and Background

Notwithstanding the incredible advancements in carbon-carbon and carbon-heteroatom coupling techniques developed within the past four decades, improved methods for transition metal catalyzed bond formations remain in high demand in both academia and industry alike.[1] Of these transformations, the ability to construct $C(sp^2)$-$C(sp^3)$ bonds (typically in the form of aryl-alkyl bond formation) is of major importance. However, many methods available in the literature involve preformation of alkylmetallic intermediates derived from alkyl halides (*i.e.*, as seen in organomagnesium halide or organozinc halide reagents) to be transmetalated *in situ* to another transition metal, which is then coupled with the corresponding aryl halide.[2] A powerful alternative to these techniques for forming sp^2-sp^3 carbon bonds is through coupling of an activated carbon adjacent to an electron withdrawing group, and using a Group 1 element as the transmetalating agent.[3] In the case of ketones, this active intermediate is in the form of the enolate which is formed simply by the addition of base, which can then be coordinated directly to a palladium (or, in some cases, nickel, *vide infra*) center which can then be coupled with an aryl ring (Figure 1).

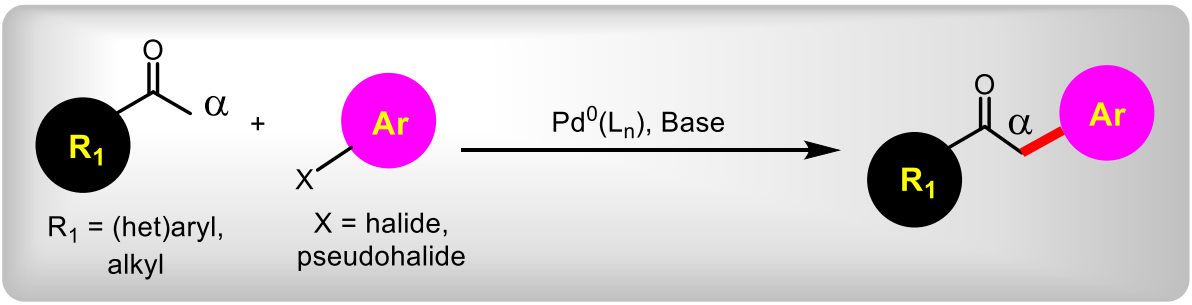

Figure 1: General reaction scheme for arylation at the α-position of a ketone

The α-arylation of ketones has gained modest traction in the field of chemical synthesis. This is due to the prevalence of this connection as a key step towards natural products, active pharmaceutical ingredients (APIs), and agrochemicals. Indeed, pathways *en route* to a variety of high value compounds have been accomplished using this transformation, e.g., Trileptal, which is an anticonvulsant (Figure 2).[4]

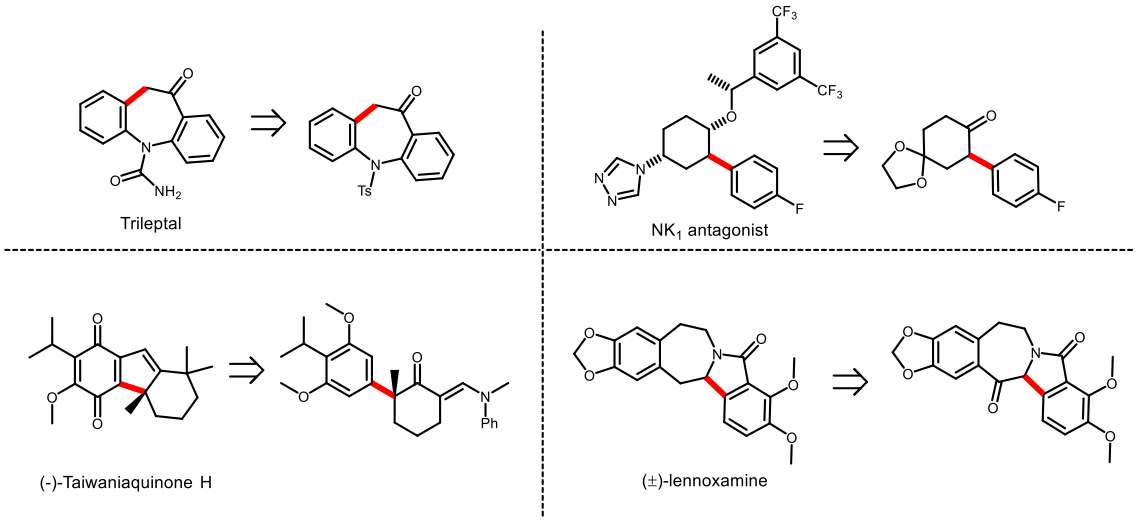

Figure 2: Examples of key α-arylations of ketones towards natural products and APIs

The attractiveness of this technology is due to the commonness of both the ketone and halide coupling partners, which are either easily purchased from chemical vendors or can be synthesized via a variety of known methods. Nonetheless, such α-arylations have been woefully under-evaluated in the literature, certainly relative to most other Pd-catalyzed couplings (i.e., compared to Suzuki-Miyaura, Mizoroki-Heck, etc.), as noted by Colacot and Snieckus in their review on transition metal catalysis.[5]

Historically, the first reported α-arylation of a ketone was by Semmelhack *et al.* in 1975 towards the synthesis of cephalotaxus alkaloids.[6] One methodology explored in their work for

a critical transformation was the Ni^0-catalyzed intramolecular ring closing of an aryl iodide with the α-position of a ketone, utilizing strong base in THF (Figure 3). The authors rationalized the reaction mechanism as a "reverse S_NAr" pathway, given the nature of aryl iodides as unreactive in traditional S_NAr chemistry, where Ni^0 first oxidatively inserts between the aryl ring and the iodide forming a σ-aryl nickel species, which is then attacked by the enolate formed from the abstraction of the α-proton of the ketone via the strong base, resulting in the fused ring in 41% yield.

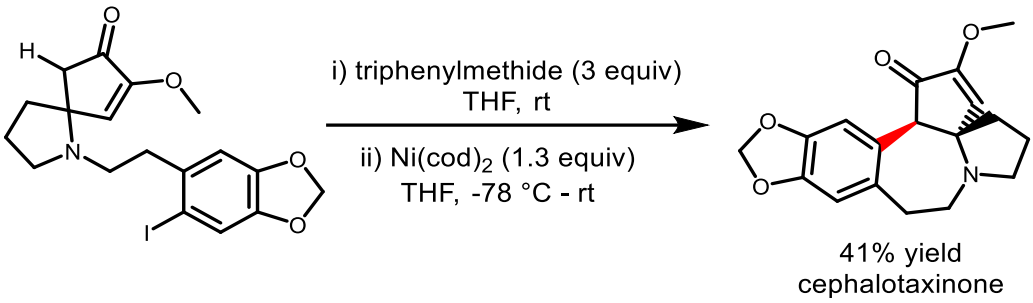

Figure 3: Synthesis of cephalotaxinone using Ni^0-catalyzed α-arylation of an enolate

Prior to reports focusing solely on α-arylation methodology, Muratake *et al.* in 1997 also explored this chemistry, in this case using catalytic palladium for the first time, in the formation of the pharmacophore towards the duocarmycin family.[7] In this report, the authors generated a tricyclic aromatic system arrived at via α-arylation of a heteroaromatic ketone resulting in a novel phenol-forming reaction. This required a large amount of catalyst (10 mol % Pd), but they were ultimately able to use an aryl triflate to affect ring closing followed by trapping a phenoxide with methyl chloroformate in a subsequent step (Figure 4).

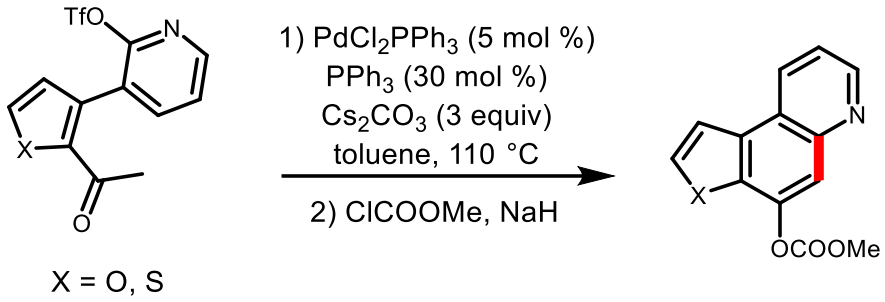

Figure 4: Muratake's α-arylation towards the duocarmycin structural motif

Key advancements into the general applicability of α-arylation of ketones were developed in 1997 by multiple laboratories simultaneously. Initially, Buchwald's group found, in two reports from 1996-1997, that in the effort to form aryl ethers using alkoxides and aryl halides a very small amount of an arylated ketone was formed.[8] This side product was specifically found in the case where electron-neutral and electron-rich aryl bromides were used, where hydrodehalogenation of the aryl bromide was observed with oxidation of the alcohol to a corresponding ketone, which could then couple with a second equivalent of the aryl bromide using the Pd catalyst (Figure 5).

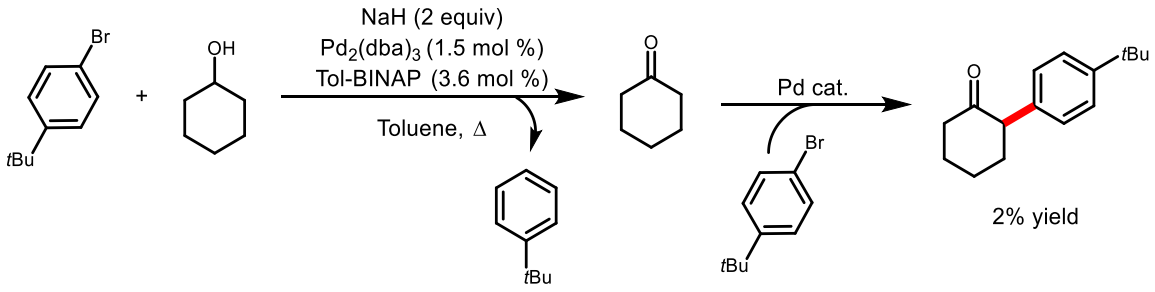

Figure 5: Buchwald's initial discovery of Pd-catalyzed ketone α-arylation

This result precipitated further investigation into this cross-coupling reaction by Buchwald's group, which published a methodological study in 1997.[9] This communication was reported nearly simultaneously with related work from the Hartwig[10] and Miura[11] labs which disclosed similar observations. Miura was able to arylate a ketone, activated at the α-position with an already installed phenyl group, using simply $PdCl_2$ in DMF and Cs_2CO_3 as base, stopping at the diarylated product. However, Buchwald and Hartwig found far superior activity for aryl, heteroaryl, and alkyl ketones when using bulky chelating phosphine ligands, either BINAP or Tol-BINAP in the case of Buchwald and DTPF being used by Hartwig (Figure 6).

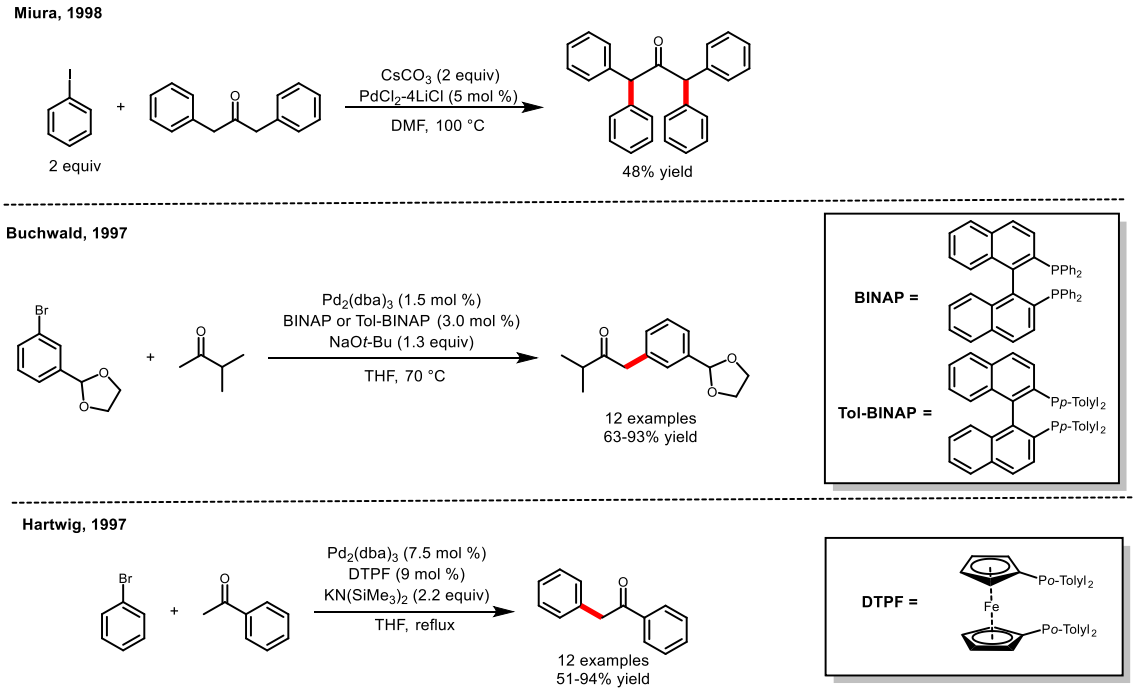

Figure 6: Concurrent reports concerning α-arylation of ketones methodology

Insight into the activity of these bulky phosphines as Pd ligands can be gleaned by taking into consideration the proposed mechanism for this reaction, which generally follows a similar

pathway with consideration to other Pd catalyzed cross-coupling reactions (Figure 7). Firstly, Pd^0 is either added directly into the reaction, or is reduced from Pd^{II} *in situ* to the active metal. As in all palladium catalyzed chemistry, the reduction mechanism is highly dependent upon not only the Pd source (*i.e.*, palladium(II) salts, palladium(I) dimers, etc.), but also the reagents being added or by direct pre-treatment of the metal. For example, Pd(II) salts can be pre-activated either using dioxane/water mixtures[12] or treatment with DIBAL-H in organic solvent,[13] whereas Pd(I) dimer species are typically activated via nucleophile-assisted fragmentation.[14] Regardless, Pd^{II} salt activation to Pd^0 is typically found to be facile in aqueous systems, most of the time not requiring pre-reduction to form the active metal.

Following formation of the active metal catalyst, oxidative addition of the $Pd^0(L_n)$ into an aryl halide or aryl pseudohalide occurs resulting in an organopalladium(II) complex, seen similarly in other cross-couplings such as the mechanism proposed for the Suzuki-Miyaura reaction.[15] The reactivity towards oxidative addition of the aryl halide follows a trend where I > Br = OTf > Cl in terms of rate. Separately, the (typically) Group 1 metal enolate of the ketone is formed following deprotonation using base, and concomitant transmetalation from the alkali element results in an enolate-bound palladium complex. Specific for this reaction, the newly formed palladium(II) enolate can exist between the oxygen- or carbon-bound σ-complexes, or as the η^3 π-complex. The C-bound σ-complex is the reactive penultimate species prior to completion of the catalytic cycle, where larger transition metals such as palladium prefer this carbon-bound complex. Reductive elimination results in the formation of the α-arylated ketone product along with reformation of the active Pd^0 species.

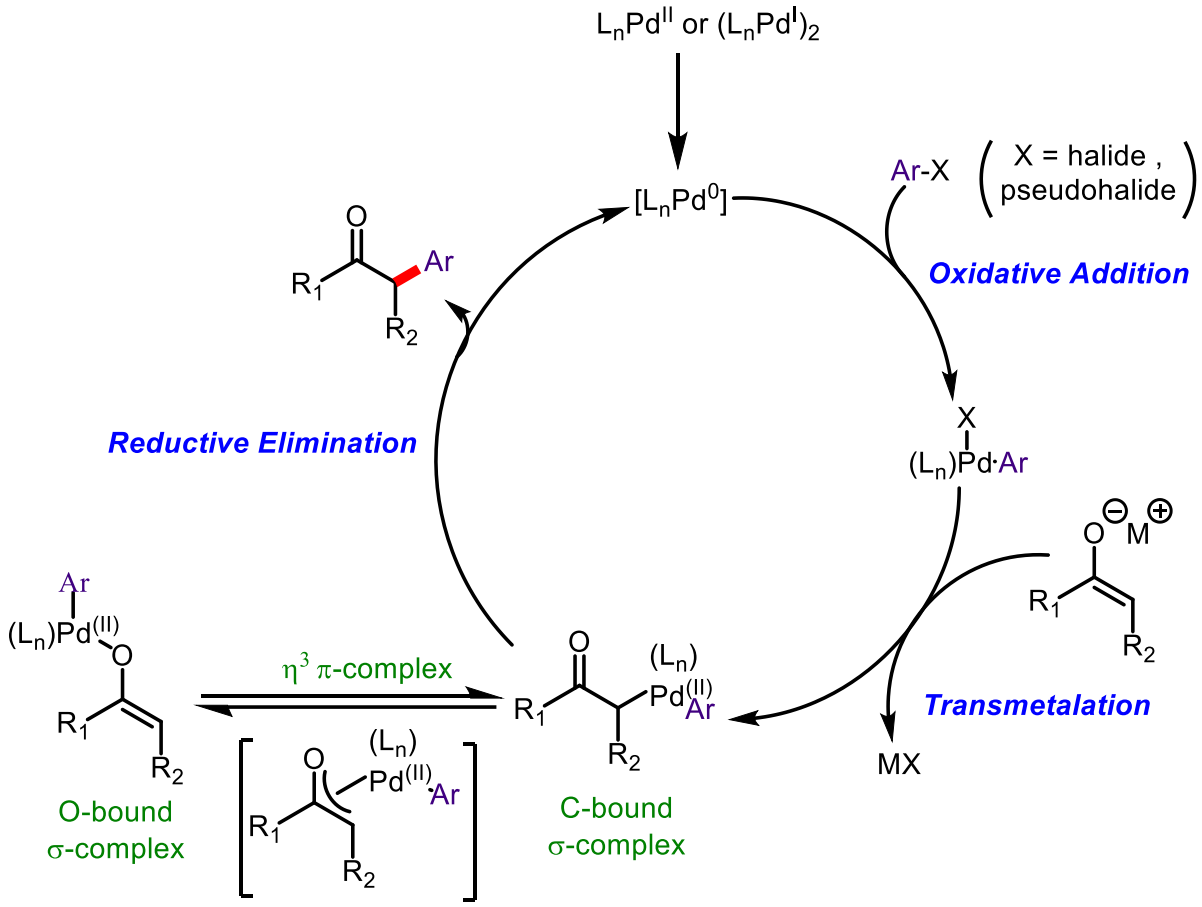

Figure 7: Palladium catalyzed ketone α-arylation mechanism

Based on these initial findings, bulky chelating phosphines were found to be competent first-generation ligands for Pd catalyzed α-arylation cross-couplings reactions. This can be rationalized based on the electron donating attributes of phosphines, which improve the rate of the oxidative addition step. Furthermore, the steric congestion of large ligands not only facilitates the reductive elimination step by forcing the enolate and aryl group into closer proximity around the metal center, but also reduces palladium-catalyzed β-hydride elimination of the ketone to the α,β-unsaturated byproduct.[9-10]

These results led Kawatsura and Hartwig in 1999 to explore alkylphosphine ligands as potential next generation arylation ligands, as opposed to the aryl ligands employed previously.[16] They postulated that even more sterically demanding alkylphosphines would increase the energy of a stable highly coordinated Pd intermediate, which would therefore decrease the relative energy of the low coordinate active Pd^0 intermediate species responsible for the oxidative addition and reductive elimination and hence, increase the overall rate of the reaction. Furthermore, the increased electron donating capabilities of alkyl groups would reduce cleavage of the P-C bonds in the ligand during reaction, improving stability and increasing turnover numbers (TON). Therefore, they hypothesized that the *tert*-butylphosphine ligand 1,1'-bis(di-*tert*-butylphosphino)ferrocene (dtbpf) would be superior to previous arylphosphines used, which turned out to be correct, and resulted in high activity at considerably lower temperatures. Interestingly, ^{31}P NMR analysis found that bulky dtbpf prefers to pass through a 3-coordinate monodentate species based on the two phosphorous resonances found in the spectrum rather than a 4-coordinate species as observed in DPPF, which gave only one resonance (Figure 8). Hence, the 12 e^- Pd species is the considerably more reactive catalyst-derived intermediate. In addition, Colacot in 2007 improved this catalytic system by proposing the preformed $Pd[dtbpf]Cl_2$ as superior compared to mixing the Pd and ligand together *in situ* as a 1:1 mixture, the latter method of which can unintentionally form the stable 18 e^- species ($Pd[dtbpf]_2$) that is far less reactive.[17]

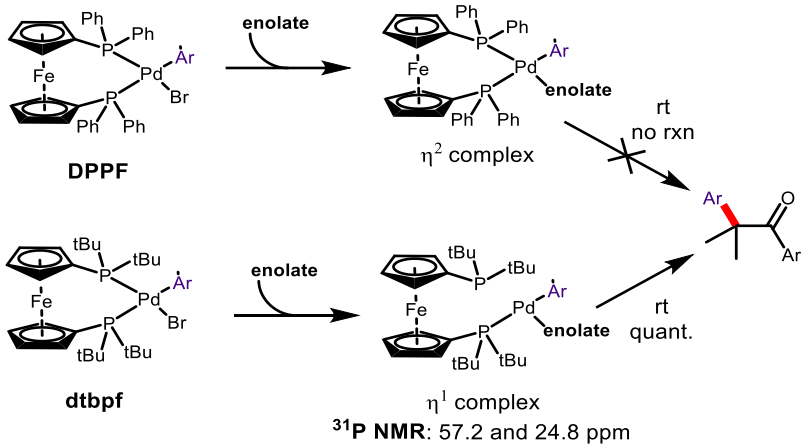

Figure 8: Bidentate 4-coordinate DPPF ligand *vs.* monodentate 3-coordinate dtbpf ligand

Ultimately, this discovery resulted in the exploration of other monodentate, electron-rich alkylphosphine ligands for this chemistry (Figure 9). This ligand class includes *n*-BuPAd$_2$,[18] P(*t*-Bu)$_3$ and P(Cy)$_3$,[16] phosphadamantane,[19] XPhos,[20] MorDalPhos,[21] and DTBNpP.[22] Nolan also described N-heterocyclic carbenes (e.g., [Pd(acac)Cl(IHept)]) as viable monodentate ligands for Pd catalyzed α-arylations at low loadings of Pd.[23]

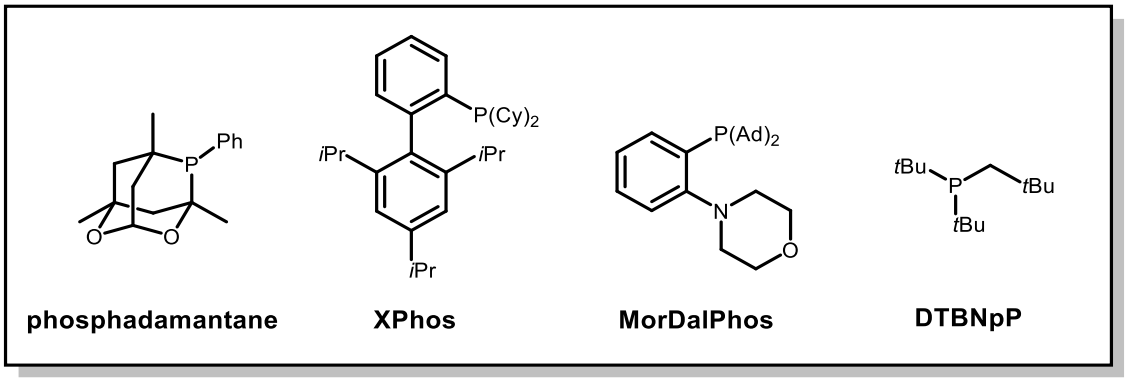

Figure 9: Examples of monodentate alkylphosphine ligands

Given the wide applicability of this reaction, and the ability to access high value targets in multiple disciplines of organic synthesis, it behooves the community to improve this technology with respect to its environmental impact. In nearly all reports, α-arylation of ketones is performed in hot (>80 °C), rigorously dry organic solvents with Pd loadings of 1-5 mol %, if not higher. This is due to the very nature of organic solvents, which dilutes coupling partners and, thus, needs to be driven to completion thermally and with high concentrations of catalyst. Moisture is also traditionally considered forbidden in this reaction, given the relative acidity of water (pK_a 15.7) compared to that of a ketone (pK_a *ca.* 20).[24] However, we postulate that this enolate chemistry can be amenable to aqueous systems if in the presence of a surfactant which provides a lipophilic and hydrophobic pocket to "house" and protect the reactive intermediate and allow for coupling to take place. There has been one report of aqueous-based α-arylations of ketones in the literature prior to this work; however, the optimized conditions in this case required egregious loadings of surfactant (PTS, 15 wt % in water) and palladium catalyst (5 mol %) and was run at refluxing conditions to affect cross-coupling.[25] Furthermore, the scope of this reaction was severely limited to only a small subsection of ketones. In this chapter, we disclose aqueous micellar Pd-catalyzed α-arylations of aryl and heteroaryl ketones under near ambient conditions with, in many cases, parts-per-million Pd loadings in only 2 wt % TPGS-750-M. This chemistry can be applied to late-stage functionalization of pharmaceutical compounds, including the synthesis of a precursor to an API. Furthermore, this methodological advancement boasts a very low environmental impact as evidenced by the associated E Factors, recycling of the aqueous medium, and amenability towards multistep syntheses in 1-pot.

In the spirit of α-functionalization of ketones, and novel methods that take environmental responsibility into consideration, a short section in this chapter will also cover neat α-allylations, which up until this dissertation is an unexplored area of green chemistry for our group. This chemistry was ultimately applied to the total synthesis of a selection of natural products in the form of nutraceuticals, which exemplifies its versatile capabilities.

2.3 Results and Discussion

Micelle catalyzed α-Arylation of Ketones in Water

Initial exploration into aqueous micellar Pd-catalyzed α-arylations of ketones was attempted using a classical cross-coupling model system of propiophenone (**1**) and 4-bromoanisole (**2**) to form the arylated ketone **3** (Table 1). Three general catalyst types were screened, running the reaction at 0.5 M and 45 °C using 2 wt % TPGS-750-M/H_2O, two equivalents of KOH as base, and 2 mol % catalyst. For these initial trials, the stoichiometry between the ketone and aryl bromide was kept at a 1:1 molar ratio.

Table 1: Initial screening of catalysts using hydrophilic base

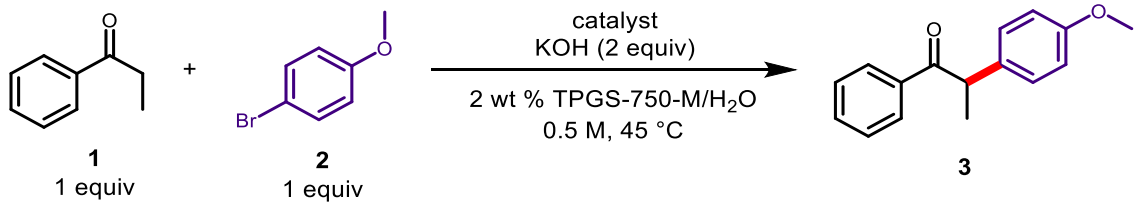

1
1 equiv

2
1 equiv

3

Entry	Catalyst	Yield **3** (%)
1	Pd[dtbpf]Cl_2 (2 mol %)	65
2	Pd[P(*o*-Tol)$_3$]$_2$$Cl_2$ (2 mol %)	0
3	Fe/ppm Pd-SPhos NPs (800 ppm)	0

Results from this set of experiments indicate that triarylphosphine palladium(II) chloride pre-catalyst (entry 2) was inactive under these aqueous base conditions. This is congruent with work by Hartwig,[16] where it was found that aryl phosphines are considerably less reactive under near ambient conditions, and thus higher temperatures may be required for this Pd catalyst to form the arylated ketone. A quick screening of Fe/ppm Pd-SPhos nanoparticles (entry 3) yielded no conversion to product, most likely due to the exceptionally low loading of

Pd (at only 800 ppm Pd with respect to the substrate under published conditions) on the surface of the iron particle which is amenable for other Pd catalyzed reactions such as Suzuki and Sonogashira cross-couplings in water.[26] Luckily, under these unoptimized conditions, the Pd(dtbpf)Cl_2 pre-catalyst (entry 1) exhibited moderate coupling activity, producing **3** in 65% isolated yield, albeit after 56 hours of reaction time. Increasing the equivalents of KOH did not improve conversion using this system based on GCMS analyses. Furthermore, GCMS and TLC indicated high selectivity for the mono-arylated product, in addition to unreacted starting material.

Based on these findings, some initial screening of conditions was performed prior to a full investigation into the optimal ligand for water-based α-arylations using 2 mol % Pd(dtbpf)Cl_2 as catalyst on a 0.5 mmol scale. Based on the potential transient nature of an enolate in aqueous media, even in the presence of lipophilic micelles that could protect the nucleophile, it was postulated that increased reaction concentration could improve reaction conversion (Table 2). Indeed, trials run from 0.5 M (entry 1) to 1.0 M (entry 2) exhibited improved yields of **3** from 85% to 90% yield, respectively, when using K*t*-OBu as base and 2 wt % TPGS-750-M as surfactant. A global concentration of 1.0 M was considered to be optimal for further studies, as increasing the concentration further would render solid substrates and/or products difficult to stir and may unintendedly inhibit reaction conversion. The stoichiometry of the enolate was also increased to 1.2 equivalents to facilitate greater conversion, thereby using the aryl bromide as the limiting reagent for evaluating this methodology.

Table 2: Global concentration screening of aqueous α-arylations

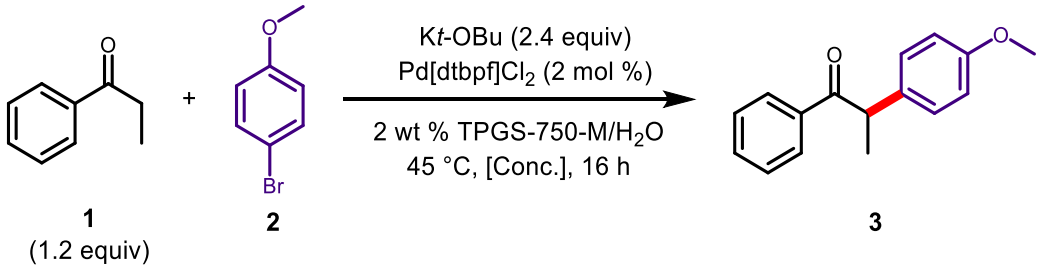

Entry	Concentration (M)	Yield **3** (%)[a]
1	0.5	85
2	**1.0**	**90**

[a] Isolated yields

Moving forward with initial screening protocols, the cation of the lipophilic *tert*-butoxide base was found to be a key factor for conversion in the case where 2 mol % Pd(dtbpf)Cl_2 was used as catalyst (Table 3). In the formation of **3**, a general trend was observed where increasing the size of the Group 1 cation improves yield, even under conditions where the reaction was allowed to run for 16 hours a 1.0 M. This is most likely due to the larger size, and therefore, ease of dissociation of the sodium (entry 2) and potassium (entry 3) ions compared to lithium (entry 1), which would facilitate transmetalation to form the organopalladium enolate intermediate.

Table 3: Cation study using *tert*-butoxide as base

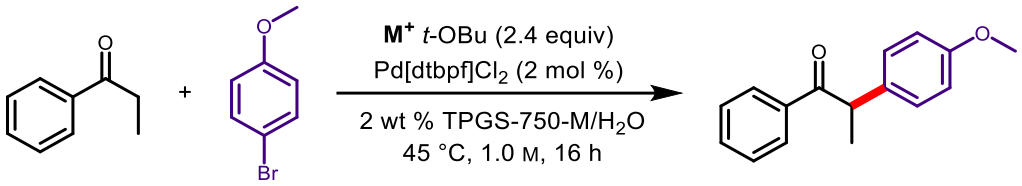

1 (1.2 equiv) **2** **3**

Entry	Cation	Yield **3** (%)[a]
1	Li^+	66
2	Na^+	80
3	**K^+**	**90**

[a] Isolated yields

Taking these early discoveries into consideration, we undertook a more in-depth investigation into the optimal Pd catalyst for this reaction. A variety of Pd catalyst sources were screened at 2 mol %. In some cases, the ligand was combined with $Pd(OAc)_2$ to form the active species directly in water (or, in organic solvent prior to adding to an aqueous system, there was no observed difference in premixing protocols), whereas in other cases the Pd was added as a pre-catalyst salt (Figure 10). *tert*-Butoxide as base was held constant in this study; however, the cation was altered between lithium and potassium, the latter of which was determined to be the optimal counterion. Regardless of this inconsistency, general trends in activity could still be determined based on isolated yields of **3**.

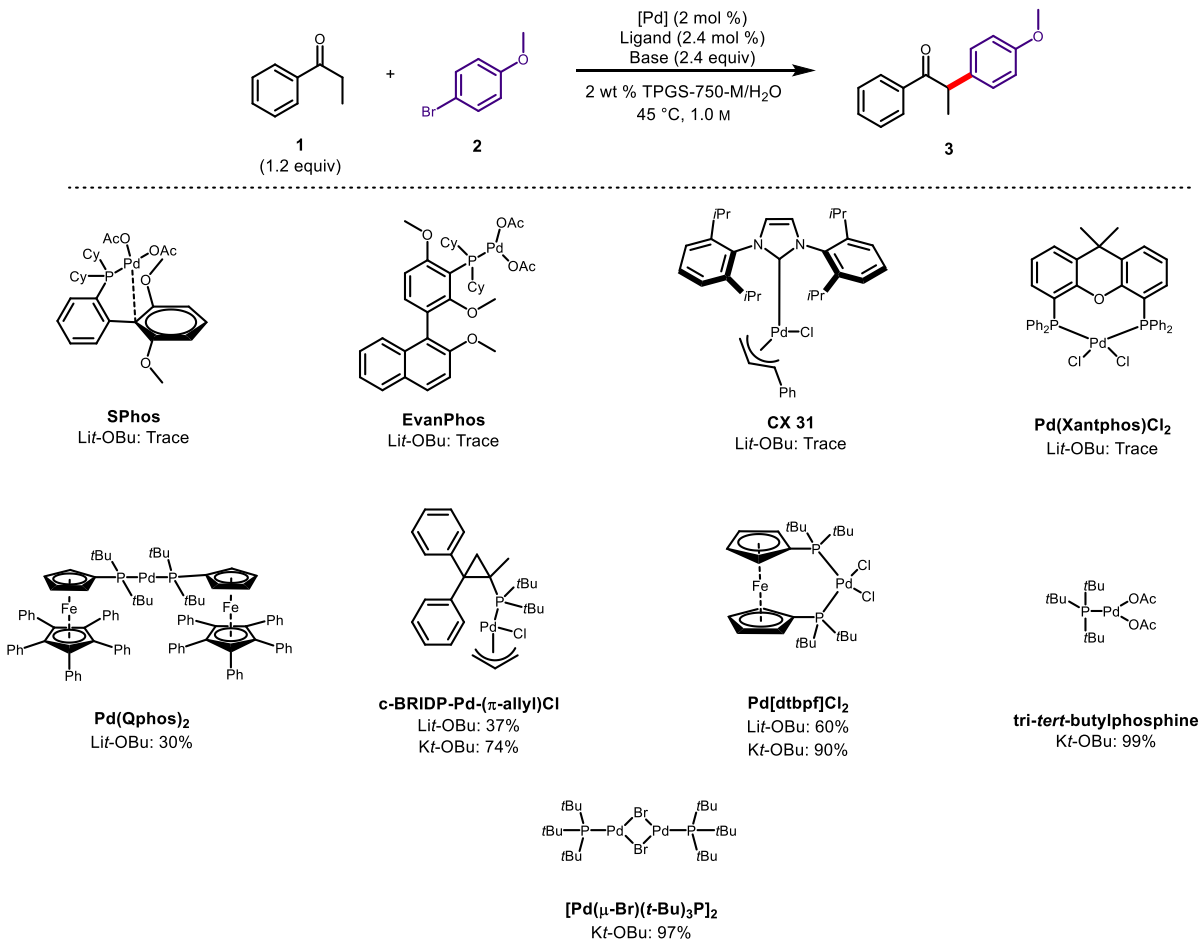

Figure 10: Screening of ligands for α-arylations of ketones in water

Interestingly, the biaryl SPhos ligand was found to be completely inactive for α-arylation cross-couplings with ketones in aqueous micellar media, despite seeing high activity in organic solvents.[27] This was also the case for *N*-heterocyclic carbene ligand CX 31[28] and bidentate phosphine ligand Xantphos,[29] both of which are reported to successfully facilitate this transformation, in some cases even at room temperature. A ligand developed by the Lipshutz lab, EvanPhos,[12] which is known to catalyze Suzuki-Miyaura couplings in high yield even at ppm levels of Pd in water, was also ineffective in the arylation chemistry. The $(Qphos)_2Pd$ catalyst precursor, which Hartwig's group found to be highly active for arylating malonates in

organic solvent,[30] saw only modest conversion when using lithium *tert*-butoxide as base; we postulate that higher yield would be observed if run using the potassium counterion. This effect can be seen in the similar activity of c-BRIDP-Pd-(π-allyl)Cl pre-catalyst, providing **3** in 37% yield using lithium and 74% yield using potassium *tert*-butoxide. $Pd(dtbpf)Cl_2$, known to work well with initial trials in aqueous conditions, gave product in very high yield of 90% when used at 2 mol %.

In searching for an improved catalyst, we hypothesized that Pd(I) dimer species, which have found a variety of applications as pioneered by the Schoenebeck group,[31] would be a highly active pre-catalyst for α-arylations in water. Indeed, the supported single-atom bridged $[Pd(\mu\text{-}Br)(t\text{-}Bu)_3P]_2$ dimer complex[32] saw marked improvement over the previous best result from $Pd(dtbpf)Cl_2$, affording a 97% isolated yield of **3** with 2 mol % Pd (*i.e.*, 1 mol % dimer complex). To determine if the very bulky $(t\text{-}Bu)_3P$ ligand is responsible for this high yield, we tested this same model compound against the mixture of $Pd(OAc)_2$ and the phosphine ligand prepared *in situ* and saw the same excellent conversion giving a 99% isolated yield. Despite the similarity in activity, we felt that the Pd(I)Br dimer was the best catalyst source to pursue this chemistry, especially when taking industrial applications into consideration due to the ease of handling of the complex compared to pyrophoric $(t\text{-}Bu)_3P$, which needs to be set up in an air-free environment. However, reports in the literature of this dimer have indicated moderate air instability and near instantaneous decomposition when oxygen is present in solution; therefore, all reactions moving forward were run in rigorously degassed TPGS-750-M aqueous solution.

With respect to catalyst, we observed a general tendency of *tert*-butylphosphines to be the best ligands for this transformation, compared to cyclohexyl- or phenyl-phosphine ligands.

This is most likely due to two ligand effects: (1) the large Tolman "cone" angle of the *tert*-butyl group forces the enolate and the aryl groups together, which facilitates reductive elimination and to form the desired α-aryl ketone;[33] and (2) the size of the *tert*-butyl groups also provides enough steric congestion to maintain the mono-ligated 12 e^- Pd species, which is highly active for the oxidative addition step.[34]

There exists an exigency in the field of synthetic organic chemistry to optimize low loadings of Pd catalysis, considering the endangered status of this precious transition metal.[35] Therefore, given the success of both Pd(dtbpf)Cl_2 and the $[Pd(\mu\text{-}Br)(t\text{-}Bu)_3P]_2$ at 2 mol % for α-arylations of ketones in aqueous micellar media, we found it important to test the limits of low Pd catalyst loadings for this transformation with respect to the conversion of the model substrate **3** (Table 4). Expectedly, there was a dramatic decrease in conversion when reducing the loading of Pd[dtbpf]Cl_2 from 2 mol % to 0.5 mol %, resulting in a drop from 90% yield (entry 1) to 38% yield (entry 2), respectively, and to zero conversion with further reduction of catalyst. However, we observed a striking difference in performance of the Pd(I) dimer complex, which gave nearly quantitative yield of **3** at loadings as low as 2500 ppm Pd (0.125 mol % dimer complex). This result was highly encouraging for further studies using only parts-per-million levels of Pd in surfactant media, and completely outcompeted the current state of the α-arylation art using this catalyst in organic solvent.[36]

Table 4: Catalyst loading screening for α-arylation chemistry in water

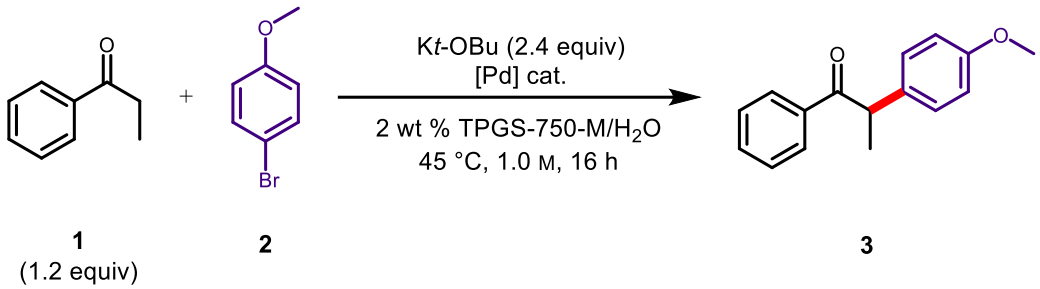

1 (1.2 equiv) **2** **3**

Entry	Pd (mol %)	Yield **3** (%)[a] $Pd[dtbpf]Cl_2$	Yield **3** (%)[a] $[Pd(\mu\text{-}Br)(t\text{-}Bu)_3P]_2$
1	2	90	97
2	0.5	38	91
3	**0.25**	trace	**97**
4	0.125	N/A	incomplete

[a] Isolated yields

Considering the protic nature of the aqueous reaction medium, and the relatively high pK_a of the α-proton of a ketone compared to that of water, we suspected that the choice in base would be paramount for cross-coupling (Table 5). The hypothesis for successful conversion was based not only on the pK_a of the conjugate acid of the base, where increased strength of the base would result in a higher concentration of the enolate, but also its lipophilicity. Therefore, it was not entirely surprising that KOH in surfactant media (entry 1) was inferior compared to the reactivity of the lipophilic and more basic K-O-*t*-Bu (entry 4), which could much more easily gain access into the inner "greasy" organic pocket of the micelle containing the ketone. Interestingly, running the reaction "on-water" (*i.e.*, without surfactant) with KOH (entry 2) saw further reduction in yield compared to the trial in the micellar medium with the same base, most likely providing some insight to the mechanism of even inorganic bases interacting with, what might be, the "surface membrane" of the micelle nanoparticle in the

form of the PEG chain. To test the lipophilicity *vs.* pKa of the conjugate acid of the base as key contributors to reactivity, a trial was performed using a KOH/TIPS-OH mixture (entry 3). The highly lipophilic silanol base, which saw success in previous studies in surfactant media,[37] resulted in very poor yield of **3** (35%). This is most likely due to the low pK_a of the silanol, which is greater than two orders of magnitude more acidic than *t*-BuOH. This trend did not apply to K_3PO_4 (entry 5), however, which gave yields like that of KOH in surfactant media despite having a very low conjugate acid pK_a of 12.3. The organic soluble amine base, triethylamine (entry 6), gave zero conversion, most likely elucidating the importance of a Group 1 cation for the transmetalation event to form the organopalladium enolate intermediate. One hidden aspect of this base study also lays in observation that, when using K-O-*t*-Bu as base, there is a considerable amount of organic co-solvent produced due to the formation of *t*-BuOH. Dr. Nico Fleck found later that, for this same model reaction, similar conversion to using a stoichiometric amount of K-O-*t*-Bu can be achieved when using a mixture of KOH and catalytic *t*-BuOH. However, we believe that the *t*-BuOH co-solvent formation may be critical for emulsifying poorly soluble starting materials, a detail described by other group members for their aqueous based chemistry both in our academic lab as well as in industrial applications.

Table 5: Base screening for α-arylations in water

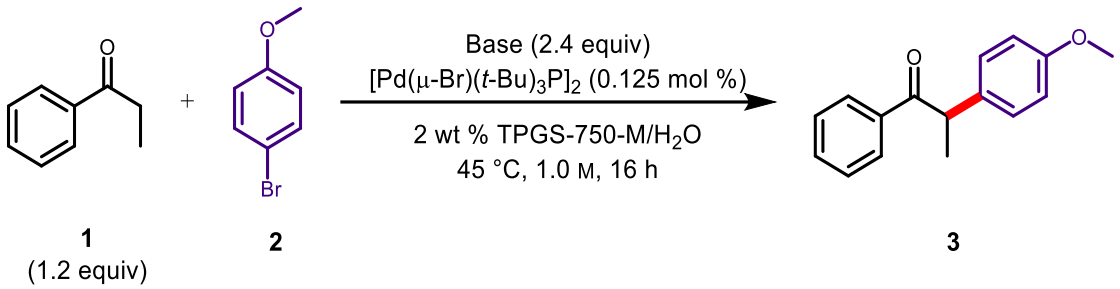

Entry	Base	pK_a conjugate acid	Yield **3** (%)[a]
1	KOH	15.7	63
2	KOH (on water)	15.7	40
3	KOH / TIPS-OH	14.9	35
4	**K-O-*t*-Bu**	**17**	**97**
5	$K_3PO_4 \cdot H_2O$	12.3	57
6	Et_3N	10.8	trace

[a] Isolated yields

Interestingly, there were major differences in the conversion of the model α-arylation reaction with respect to the reaction medium used. One surprising result was the relative success of the "on-water"[38] trial, which gave 76% yield of **3** when allowed to react overnight (entry 1). This is most likely because both substrates **1** and **2** are liquids under the reaction conditions, and therefore benefit from the "on-water" effect that more solid substrates may not be able to exploit. Regardless, addition of 2 wt % TPGS-750-M (entry 2) to the water saw considerable improvement in conversion (97%). Another group surfactant "Coolade"[39] (entry 3) also performed well compared to just water, whereas "Nok"[40] (entry 4) gave nearly identical yield to that of a purely aqueous system. Another PEGylated amphiphile Triton X-100, which bears an alkylaromatic hydrophobic chain akin to α-tocopherol,[41] gave similar yields to that of just water at 82% (entry 5), whereas Brij-35,[42] a PEGylated lauryl alcohol (entry 6), resulted in the poorest conversion of all media tried at 39% yield, most likely due to the very small

aggregates formed in aqueous solution compared to other surfactants. In an odd turn, another α-tocopherol based surfactant, 5 wt % PTS-1000 (entry 7),[43] provided product in no better yields than just water (74% yield), which may be due to the higher concentration of the surfactant in the aqueous solution which could be diluting the coupling partners and lowering the possibility of collision. Ionic surfactant sodium dodecyl sulfate (entry 8), containing an analogous alkyl chain to that of Brij-35, gave similar yield (45%). Gratifyingly, the optimized yields for this aqueous micellar catalyzed α-arylation performed poorly in toluene, a traditional solvent used for this transformation, in both concentrations of 1.0 M (48%) as well as more dilute 0.2 M (60%).

Table 6: Aqueous and organic reaction medium screening

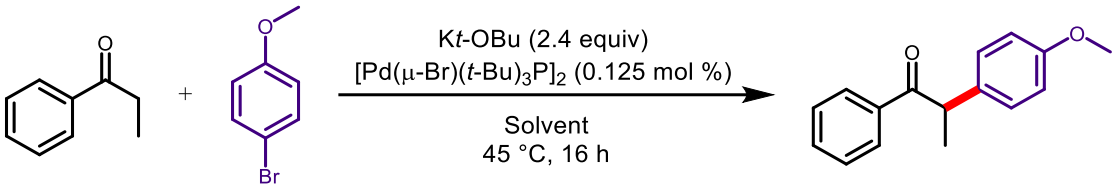

1 (1.2 equiv) **2** **3**

Entry	Medium	Yield **3** (%)[a]
1	water	76
2	**2 wt % TPGS-750-M/H_2O**	**97**
3	2 wt % Nok/H_2O	80
4	2 wt % Coolade/H_2O	89
5	2 wt % Triton X-100/H_2O	82
6	2 wt % Brij-35/H_2O	39
7	5 wt % PTS-1000/H_2O	74
8	2 wt % SDS/H_2O	45
9	toluene (1.0 M)	48
10	toluene (0.2 M)	60

[a] Isolated yields

Efforts to further optimize this reaction led to the finding that arylations perform best at temperatures slightly higher than that of room temperature (Table 7). Lowering the temperature from 45 °C (entry 2) to 30 °C (entry 1) saw a remarkable drop in conversion to **3** under standard conditions.

Table 7: Effect of temperature on conversion

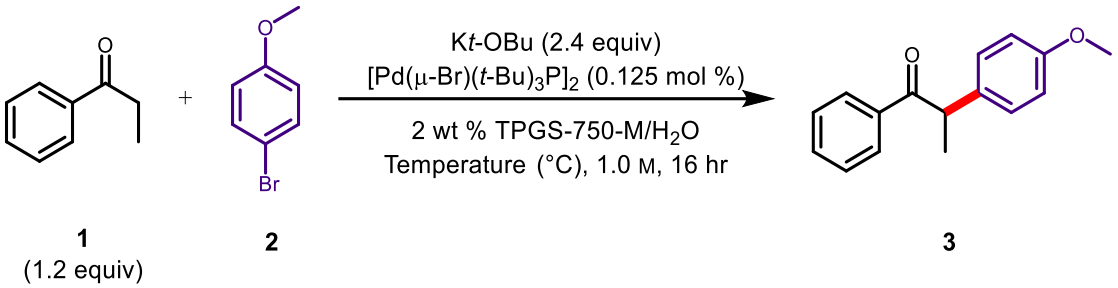

1 (1.2 equiv) **2** **3**

Entry	Temperature (°C)	Yield **3** (%)[a]
1	30	38
2	**45**	**97**

[a] Isolated yields

Using these optimized parameters, we then explored a second set of ligands (Figure 11), some of which have been reported to yield α-arylation of ketones in organic media (*vide supra*). These trials were run at 1 mol % Pd, which is a very high catalyst loading compared to the Pd(I) bromide dimer complex under the best conditions. Not surprisingly, arylphosphine **L1**, which has a considerably smaller Tolman cone angle and electron-donating capabilities compared to (*t*-Bu)$_3$P, gave zero conversion. Similar lack of activity was also observed for MorDalphos (**L4**) and associated ligands from the Stradiotto group (**L2**, **L3**, and palladacycle

L5). Further screening of Buchwald diaryl- and dialkylbiaryl phosphine ligands **L6**, **L7**, and **L8** also provided no product.

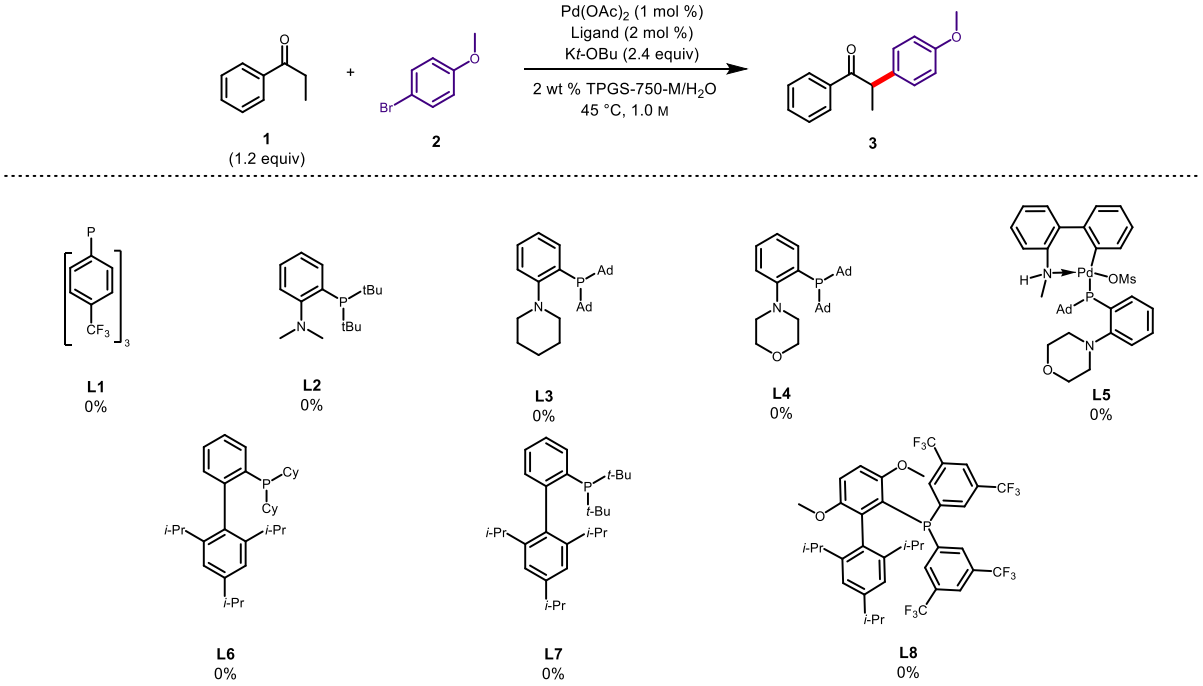

Figure 11: Secondary ligand screen for aqueous α-arylation methodology using 1 mol % Pd

We determined that the optimal conditions for α-arylation of ketones in aqueous media included reaction at 45 °C in 2 wt % TPGS-750-M/H_2O at 1.0 M global concentration with 2.4 equivalents of KO-*t*-Bu as base (which provides *t*-BuOH as co-solvent *in situ*), and [Pd(μ-Br)(*t*-Bu)$_3$]$_2$ as pre-catalyst. Pd loadings between 0.25-2.0 mol % were tested on substrates based on need, where difficulty in cross-coupling required greater amounts of catalyst (Figure 12). Initial inquiry into the scope of the reaction was determined based on the reactivity of propiophenone (**1**) with a variety of electronically diverse aromatics and heterocycles. Electron-rich aryl halides, known to better facilitate the reductive elimination step of the catalytic cycle, produced compounds **3** (97%), **6** (94%), and **8** (91%) in high yields with Pd

loadings between 0.25-0.5 mol %. Substrate **6** was recovered in higher yield under the aqueous micellar conditions using nearly an order of magnitude less Pd than in comparison to the literature run in organic solvent, which also required significantly greater equivalents of propiophenone, base, and higher temperature for conversion (Figure 13).[44] Electron-neutral biphenyl substrate **4** was also prepared in quantitative yield, despite the very low solubility of the product in the aqueous reaction media. Electron-poor heterocycle substrate **5** required 2 mol % Pd to reach completion, but ultimately produced the desired compound in very high yield (97%). Even more electron-deficient substrate **7** was tested with both the chloro- and bromo-arene starting material, the latter of which was found to require a quarter of the required Pd to reach roughly the same yield (54-60%). The nucleophile *p*-tolyl-1-propanone, which is structurally similar to propiophenone, was also found to react with the *N*-benzyl protected 7-azaindole in high yield to form substrate **9** (88%) using only 0.5 mol % Pd. Thiophene precursors to **10** and **16** were able to react with the very electron-rich 4-bromo-*N,N*-dimethylaniline coupling partner in high yields (73% and quant., respectively) using only 0.5 mol % Pd despite the inclusion of the sulfur-containing heterocycle. Aryl methyl ketone products **11** and **12** could be coupled in high yield, albeit requiring an increase of the ketone to 1.7 equivalents. It should be noted that successful mono-arylation is supposed to occur selectively due to the *o,o'*-substitution on the naphthyl and mesitylene bromides, which should sterically prevent a second arylation on the considerably more acidic α-aryl substituted aryl ketone (*vide infra* for cases where double-arylation was selected over mono-arylation). A quaternary carbon center could be made using α-methyl tetralone as the nucleophile and 4-bromo-*N,N*-dimethylaniline as the electrophile, producing compound **13** in 90% yield. Due to the protic nature of the media, we found that the 2-azaindole, as the THP-protected heterocycle,

could first be coupled using a tetralone derivative and 5000 ppm Pd followed by deprotection in 1-pot simply by adding HCl to pH <1 to form the unprotected heteroaromatic **14** in moderate yield (66%) over two steps. The bulky deoxybenzoin, which contains a very acidic α-proton, was coupled in quantitative yield with the aryl morpholine bromide to form substrate **15**. Coupling site selectivity for more acidic protons was achieved over lack of steric hinderance for compound **17**, producing the diarylated carbon using a pyrimidinyl bromide in 60% yield with 2 mol % Pd under standard conditions, but the catalyst loading could be reduced to 5000 ppm Pd when increasing the temperature to 70 °C. Compound **18**, produced in quantitative yield with 0.5 mol % Pd at 0.5 mmol, was scaled to 1.0 mmol with no impact on conversion, and was found to stir just as effectively even with larger reaction volumes producing a homogeneous emulsion. Compounds **19** and **20** were both effectively synthesized using the Boc-protected indole bromide with 2 mol % Pd loading at 87% and 61% yield respectively even, as for the case of **20**, in the presence of a potentially competitive aryl chloride as electrophile. Interestingly, the thiazole ketone was fairly unreactive under these conditions, where the most reactive aryl bromide produced **21** in only 29% yield even with a large amount of the catalyst dimer.

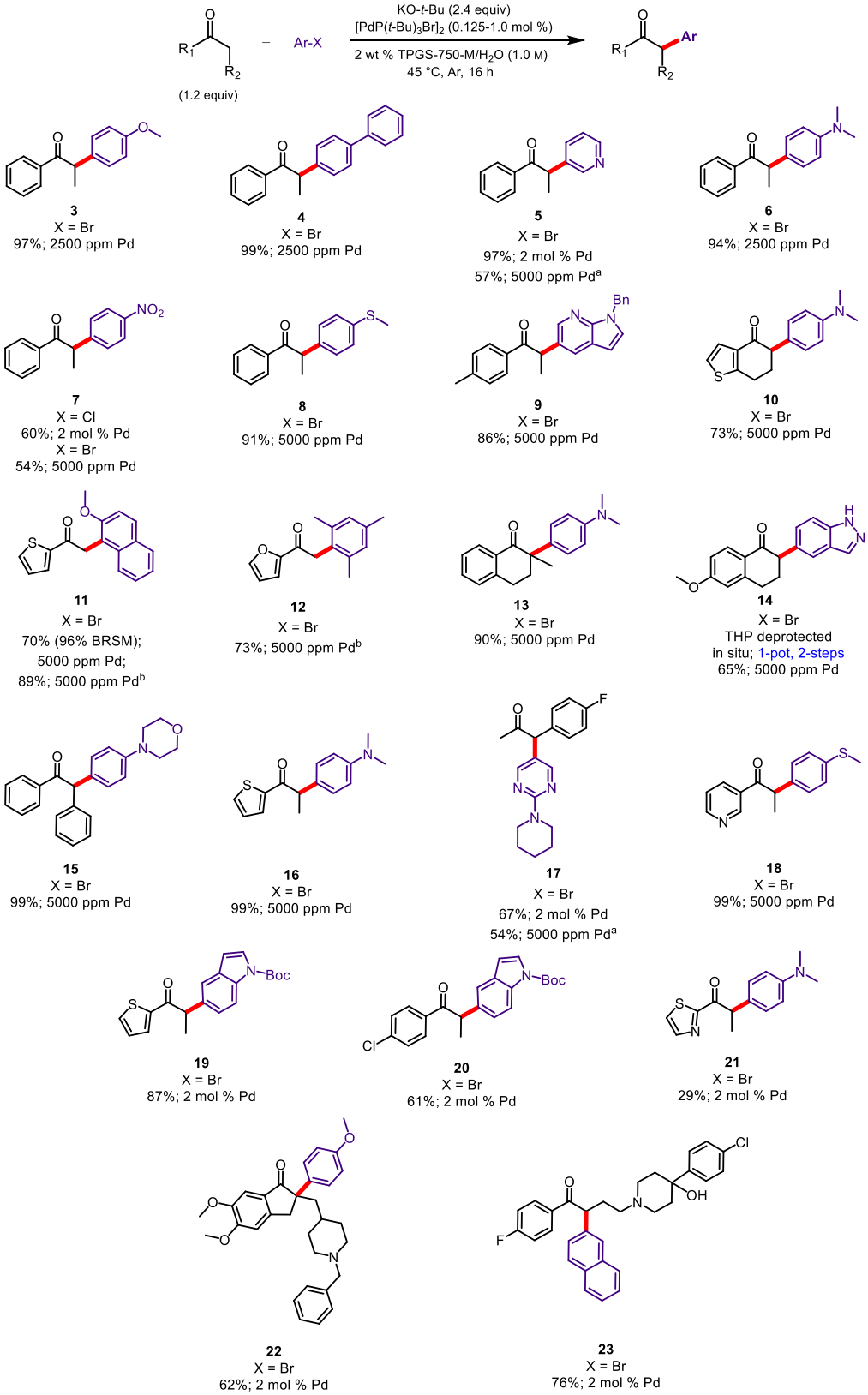

Figure 12: Substrate scope of mono-arylation of ketones in aqueous micellar media

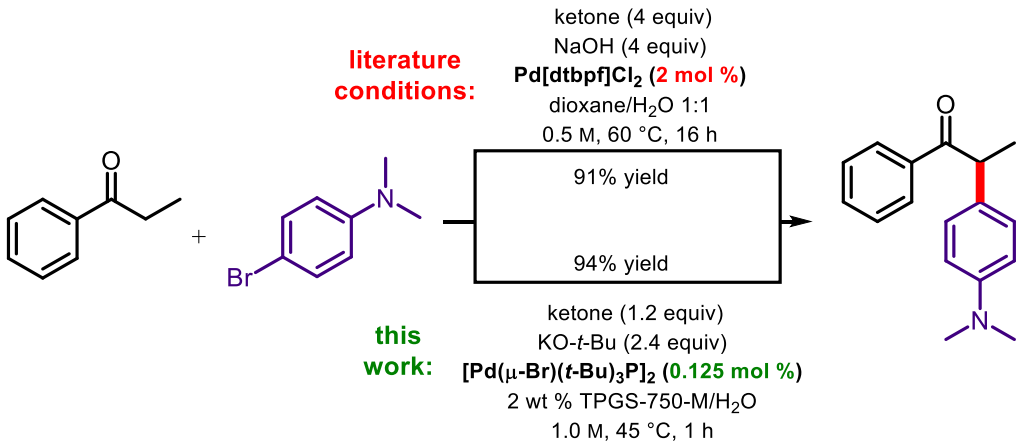

Figure 13: Direct comparison of the aqueous micellar-catalyzed arylation chemistry with respect to the literature using organic solvent

Late-stage functionalization of pharmaceutically relevant molecules has become a very hot topic, especially in the field of medicinal chemistry.[45] This is due to the inherent value in compounds with high complexity and the ability to alter their structure without modifying other functionalities present therein. Therefore, we explored the α-arylation of APIs already on the market, taking advantage of their very nature as "drug-like" molecules, which contain aryl ketones (Figure 12). We found that donepezil, a drug that treats Alzheimer's disease,[46] and haloperidol, a drug that treats schizophrenia,[47] could both be successfully derivatized in good yield (62% for donepezil and 76% for haloperidol) with 2 mol % Pd in the aqueous micellar medium under standard conditions.

Selectivity for mono-arylation was generally unachievable for aryl methyl ketones using most electrophiles. As previously stated, compounds **11** and **12** were thought to be only monoarylated due to the 2,6-substitution of the aryl bromide added to the ketone, resulting in steric congestion at the site of the acidic proton and shielding this position from diarylation. In

other cases, such as for substrates **24**-**27**, diarylation was preferred under standard conditions (Figure 14). This was found to be the result even for **26,** with 2-substitution on the aryl bromide, as well as **27**, with substitution on the aryl methyl ketone near the ketone. All diarylated substrates attempted for this study were found to reach completion in high yield, in most cases only requiring 5000 ppm Pd. Diarylation is most likely selected due to the considerably higher acidity of the resulting α-proton after monoarylation, which has been shown in water to be highly selected even in the presence of a bulky aryl ring.

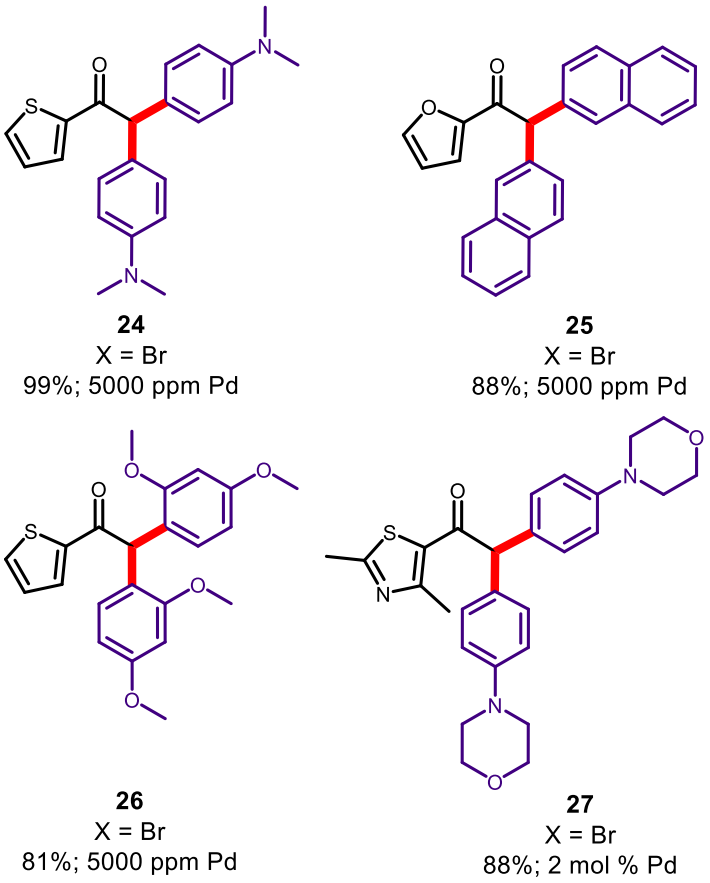

Figure 14: Diarylation of aryl methyl ketones

Unfortunately, not all ketones were amenable to cross-coupling in water, and a selection of these is presented in Figure 15. The aryl methyl ketone derived from *N*-methylpyrrole was found to be completely inactive in this system using a variety of aryl bromide coupling partners. This is unexpected given the success of analogous thiophene and furan-based ketones under similar conditions, as well as other *N*-heterocycles. This may be due to a difference in pK_a of the α-proton, where the pyrrole may decrease the acidity enough to stymie deprotonation; another explanation may be due to water solubility issues. Alkyl ketones, as exemplified by methylpiperidin-4-one and tetrahydropyran-4-one, were not only unreactive under standard conditions in water, but also unexpectedly resulted in dehalogenation of the aryl bromide coupling partner. It was suspected that β-hydride elimination on the ketone was the culprit for this byproduct; however, no α,β-unsaturated ketone was observed by GCMS analysis of the crude product mixture, and this result remains a mystery. Lack of conversion for the β-tetralone and pyridazine ketone was highly surprising given the success of analogous ketones in the substrate scope, and may be due to poor coupling partner compatibility, although other bromides tried for this ketone also did not lead to coupling. The TIPS-protected azaindole ultimately resulted in zero activity due to deprotection of the silyl group under the basic conditions.

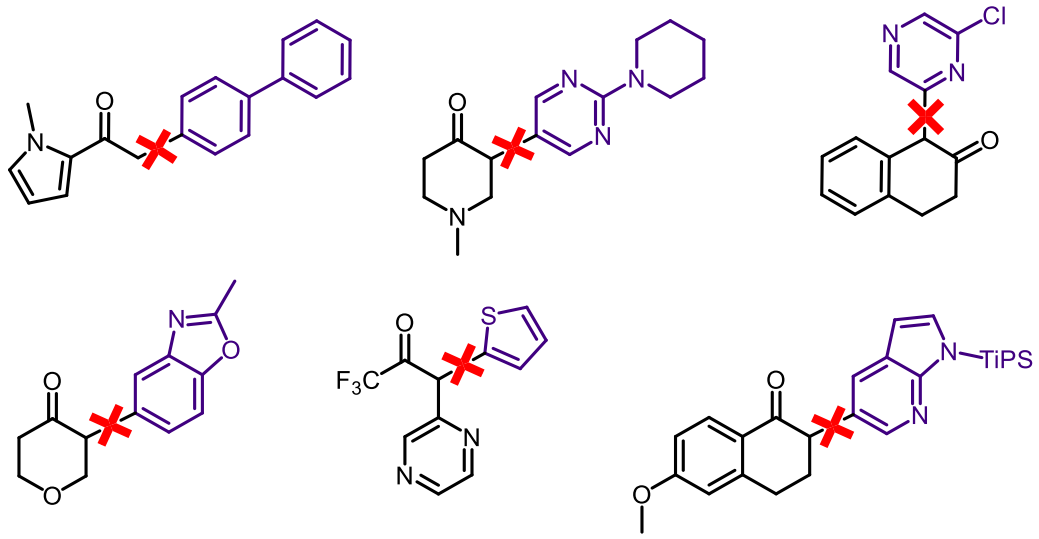

Figure 15: Unsuccessful α-arylations in water under standard coupling conditions

An illustrative application of this chemistry is the synthesis of an intermediate towards the pharmaceutical tamoxifen, which is used to treat breast cancer as an estrogen receptor modulator (Figure 16).[48] Indeed, an intermediate **29** could be synthesized *en route* to tamoxifen utilizing a previously successful enolate derived from deoxybenzoin and the commercially accessible aryl bromide **28**. This cross-coupling went to completion in 98% yield using only 0.5 mol % Pd in aqueous surfactant media. A further 1-pot synthesis towards a more advanced intermediate was attempted by trapping the resulting **29** enolate as a nonaflate, followed by coupling with diethylzinc to form the desired API. However, the initial nonaflation was unsuccessful using perfluorobutanesulfonyl fluoride in water. Previous group members have observed that analogous triflates are hydrolyzed quickly in water, even when ostensibly encapsulated by the micelles present, and this observation may explain the return of only the ketone starting material.

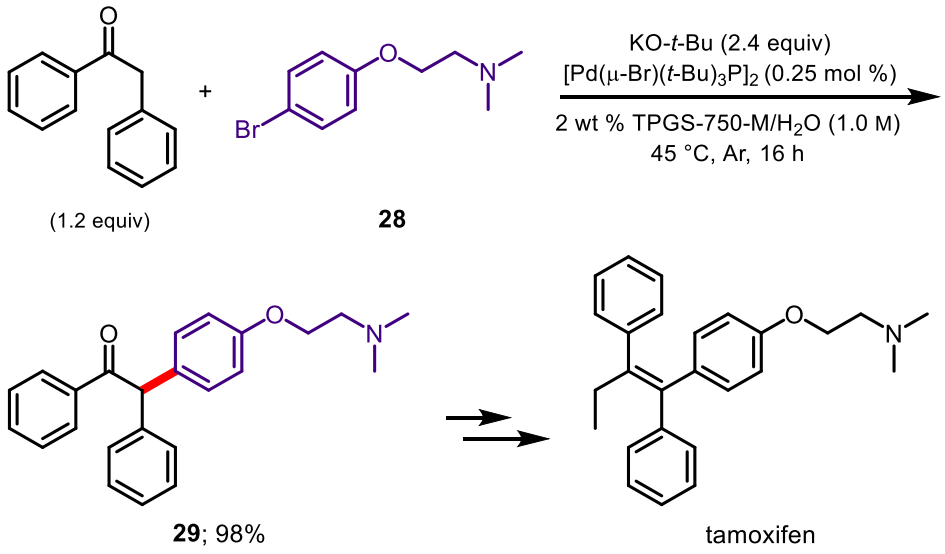

Figure 16: α-Arylation in water *en route* to tamoxifen

The environmental impact of this process was measured by the E Factor of two potential workup outcomes (Figure 17).[49] Firstly, in the case where the product is highly insoluble in the micellar array, the isolation procedure for product required only filtration followed by washing the precipitate with water. This calculation only includes the *t*-BuOH formed in the reaction as well as the unreacted 20 mol % excess propiophenone to be taken into consideration for the organic impact metric. This results in an exceptionally low E Factor of 0.79, thereby producing more product in the form of **4** than all the waste generated (not including the water). In another situation, emulsified product **3** can be extracted using a minimal amount of organic solvent, methyl *tert*-butyl ether, that is also now factored into the equation. The inclusion of this extraction solvent, even considering the low molecular weight of the product, still only results in an E Factor of 3.6.

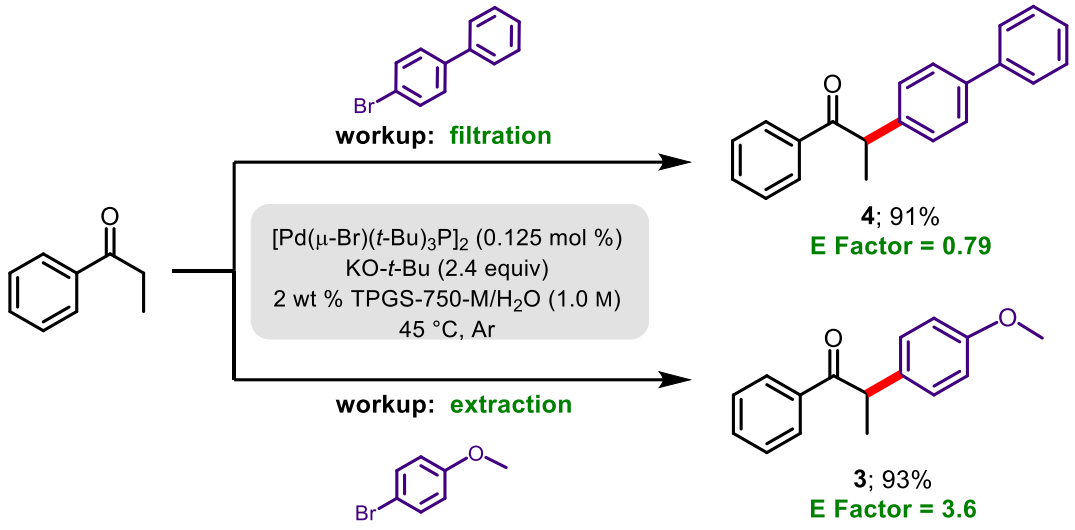

Figure 17: E Factor determination for two process workup options

Further exemplification of the environmental responsibility of this method can also be observed from the recyclability of the aqueous phase between sequential α-arylations (Figure 18). Based on the reaction between propiophenone and 4-bromoanisole to form **3**, the 2 wt % TPGS-750-M/H_2O phase was able to be reused twice after an initial reaction with no loss in yield from subsequent trials. The key to this feature is the extraction protocol after each reaction, which was maintained under strictly air-free conditions (including degassed organic extraction solvent) to avoid decomposition of the oxygen-labile Pd(I) Br pre-catalyst added for the next reaction. Therefore, addition of fresh reagents and base were all that was needed for the next reaction; no additional water was added and therefore the concentration of each sequential reaction was increased slightly due to some water extraction at such a small (1.0 mmol) scale. Hypothetically, this recycling sequence could be increased with the inclusion of fresh water, as after two trials without replenishment the salt buildup results in nearly no available aqueous medium. We also found considerably low residual Pd remaining in the

product at 6.6 ppm after the first recycle, less than the FDA allowance at 10 ppm/dose/day,[50] simply by filtering the extracted organics through silica gel.

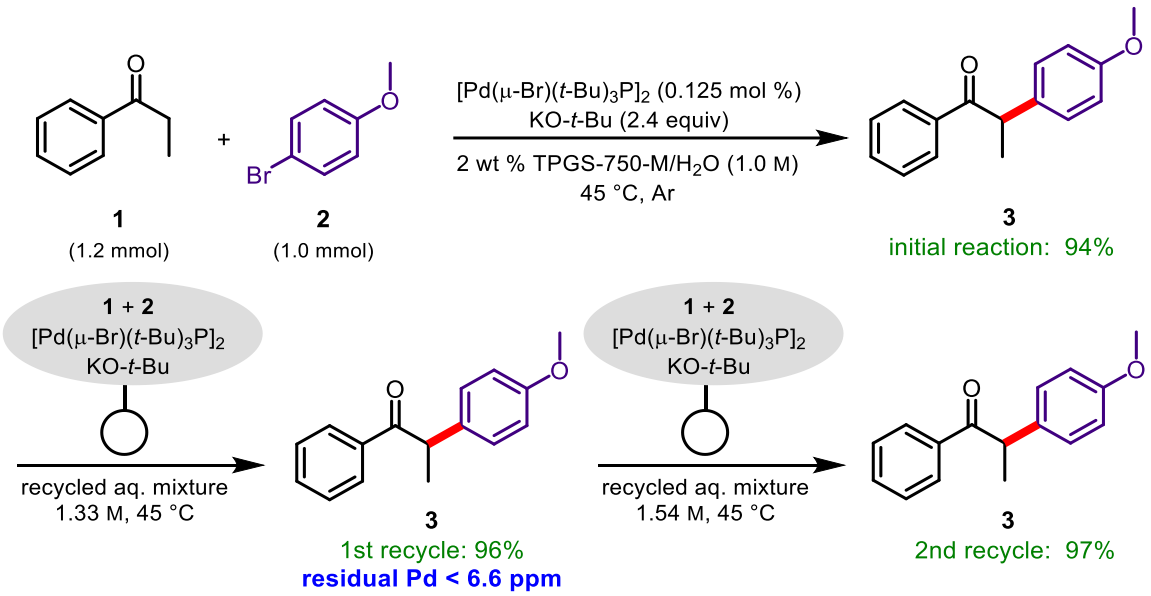

Figure 18: Aqueous recycling studies for α-arylations

As mentioned in Chapter 1, the importance of running multiple reactions in tandem using the same aqueous phase cannot be understated based on the "pot"[51] and "time"[52] economy aspects associated with running a synthetic sequence. Therefore, we set out to develop a challenging multistep, 1-pot series of reactions in water using α-arylation as a key feature (Figure 19). Firstly, we found that standard arylation conditions were amenable for coupling 4'-chloropropiophenone **30** and aryl bromide **31** using only 0.5 mol % Pd in water, resulting in arylated ketone **32**. We theorized that the concomitant Suzuki-Miyaura coupling could then be catalyzed using the same Pd added for the initial step. This was achieved by adding N_2Phos[53] ligand to the aqueous phase containing **32**, thereby performing a "ligand switch" *in situ*, presumably forming the highly active N_2Phos/palladium complex responsible for aryl chloride

couplings with arylboronic acids in water. Addition of 2,4-dimethylphenylboronic acid to this new catalyst system easily formed the intended biaryl compound which, following simple acid-catalyzed hydrolysis of the 1,3-dioxolane in water by adding concentrated HCl until pH <1, resulted in compound **33**. We then used 50 wt % NaOH to adjust the reaction pH back to 7-8, creating a suitable environment for $NaBH_4$ reduction of the aldehyde to form the corresponding benzylic alcohol. Trapping the alcohol with 2-chloronicotinyl chloride was also found to be facile, leading to an unprecedented 5-step, 1-pot sequence to form **34** in 66% overall isolated yield.

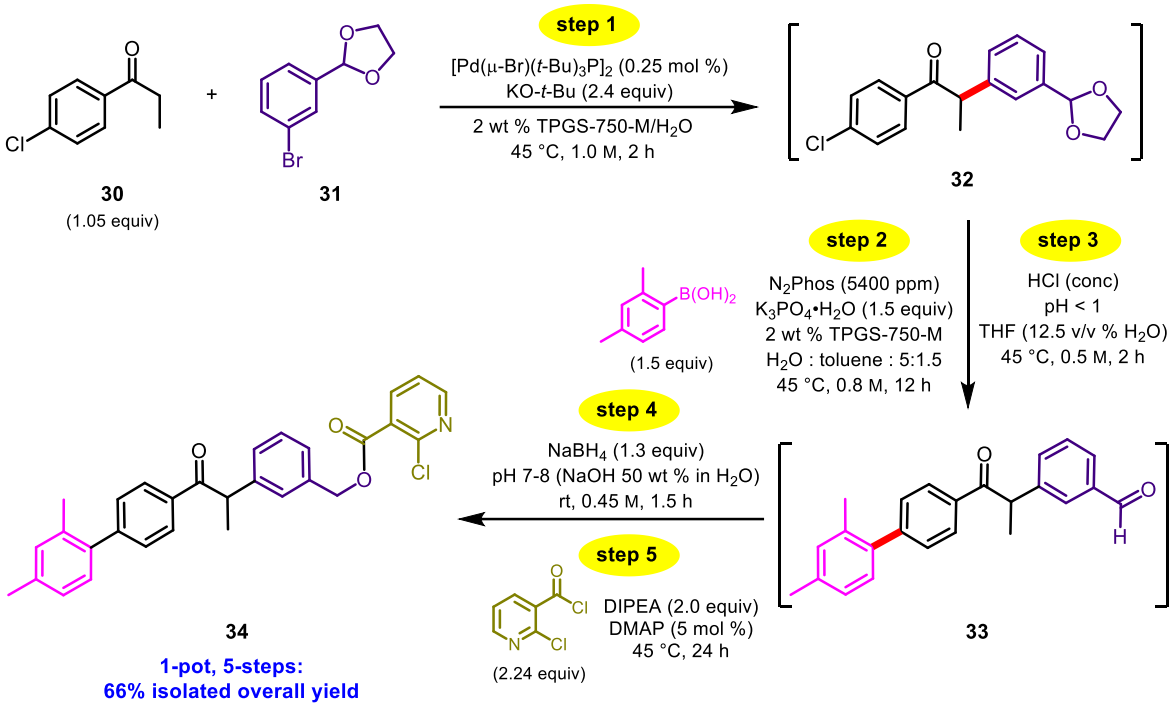

Figure 19: 5-step, 1-pot sequence in water utilizing α-arylation as key step

Finally, based on the protic nature of the reaction media and the acidity of the resulting α-proton of the arylated ketone product, we believed that it would be easy to incorporate deuterium into the product simply by running a reaction in TPGS-750-M/D_2O. Indeed, this

deuteration was trivial and yielded the α-deuterated ketone **35** quantitatively with 100% isotope incorporation based on isolated ^{1}H and ^{13}C NMR (Figure 20).

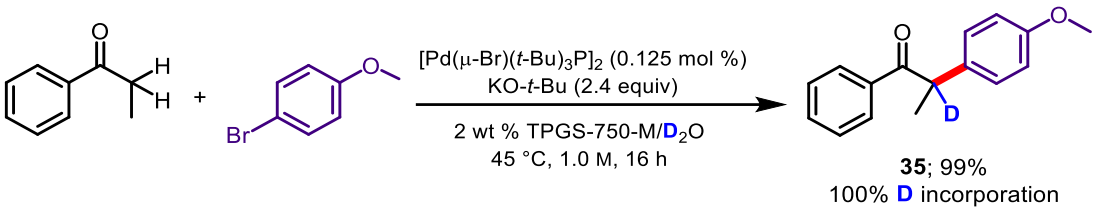

Figure 20: Deuterium incorporation at α-position using D_2O as aqueous media

Neat α-Allylations of Ketones Towards Nutraceuticals

Given the success of the α-arylation of ketones in water using Pd chemistry, we next turned our sights towards the analogous α-allylation reaction. This transformation, in organic solvent, typically does not require a transition metal. Only a base, to deprotonate and form the enolate, is needed followed by nucleophilic substitution on the activated allyl halide. Hence, this methodology is considered "fundamental", typically found in traditional first year organic chemistry classrooms as pedagogy for exemplifying enolate chemistry. However, traditional thinking begets traditional problem solving, and thus most reported literature focuses on running such reactions under strictly anhydrous conditions in dry organic solvents to avoid enolate quenching.

Initial efforts by Ms. Xiaohan Li to allylate the tertiary α-carbon of isobutyrophenone with a relatively simple halide, farnesyl bromide, in water yielded no conversion (entry 1, Table 8). This result held true even upon the addition of either tetrabutylammonium iodide (entry 2), to affect an *in situ* Finkelstein reaction, or the active Pd(I) Br dimer complex known to work for the α-arylation chemistry.

Table 8: Initial attempts to allylate isobutyrophenone in water

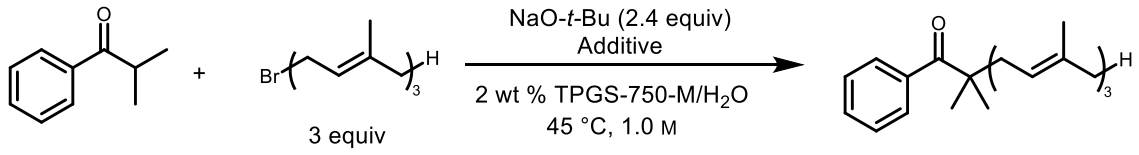

Entry	Additive	Conversion (%)
1	N/A	0
2	TBAI (10 mol %)	0
3	$[Pd(\mu\text{-}Br)(t\text{-}Bu)_3P]_2$	0

Despite these initial reaction failures, Xiaohan attempted to solve this issue by exploring "neat" methodology, or chemistry run without any solvent, to circumvent the presence of water. Indeed, this is a new area of green chemistry for our group and was only recently applied via the mechanochemical synthesis of an intermediate towards the N_2Phos ligand.[53] To our delight, we found that allylation was not only amenable to these conditions, but also resulted in product in high yield with very fast conversion. For this substrate, only a 50% excess of the bromide and base were required for full conversion at room temperature with no additive needed (entry 8).

Table 9: Xiaohan's initial discovery of neat α-allylations of ketones

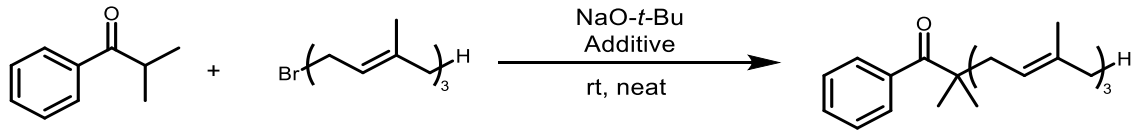

Entry	Bromide (equiv)	NaO-*t*-Bu (equiv)	Additive/Change	Conversion (%)[a]
1	1.5	1	NA	70
2	1.5	1.2	NA	80
3	1.5	1.5	NA	99
4	1.2	1.5	NA	68
5	1.2	1.5	10 mol % TBAI	65
6	1.2	1..5	45 °C	68
7	1.2	2.4	45 °C	83
8	**1.5**	**1.5**	**20 min**	**98**

[a] Yields based on ^{1}H NMR analysis of the crude

Using these neat conditions, Xiaohan set forth to evaluate the scope of both ketone and allyl halide coupling partners. We felt, however, that the robustness of this method made this chemistry applicable towards more synthetically challenging products. The initial inspiration for this project derived from the potential of allylation chemistry to prepare natural products

in the form of valuable nutraceuticals (Figure 21). Our first target molecules came from the menaquinone family, which is a methylnaphthoquinone unit derivatized by varying lengths of isoprene side chains, designated as MK-#, or vitamin K_2 (where # = the number of repeating isoprene units).[54] The goal was to synthesize not only the most biologically pervasive form for humans, MK-7, but also a potentially medically active MK-9 analogue, both of which promote bone and cardiovascular health.[55] Taking advantage of a related quinone substructure, we believed this approach could be applied to the synthesis of the coenzyme Q_n (CoQ) family of compounds. Our focus in this case was also to append a nonaisoprenyl group, derived from solanesol, to the quinone unit resulting in CoQ_9. This analogue was especially interesting given the ubiquity of solanesol on the one hand, as it is recovered from tobacco waste (*ca.* $10-100/kg for 90% pure material),[56] while on the other hand, the staggeringly high price of CoQ_9 ($267/mg).[57]

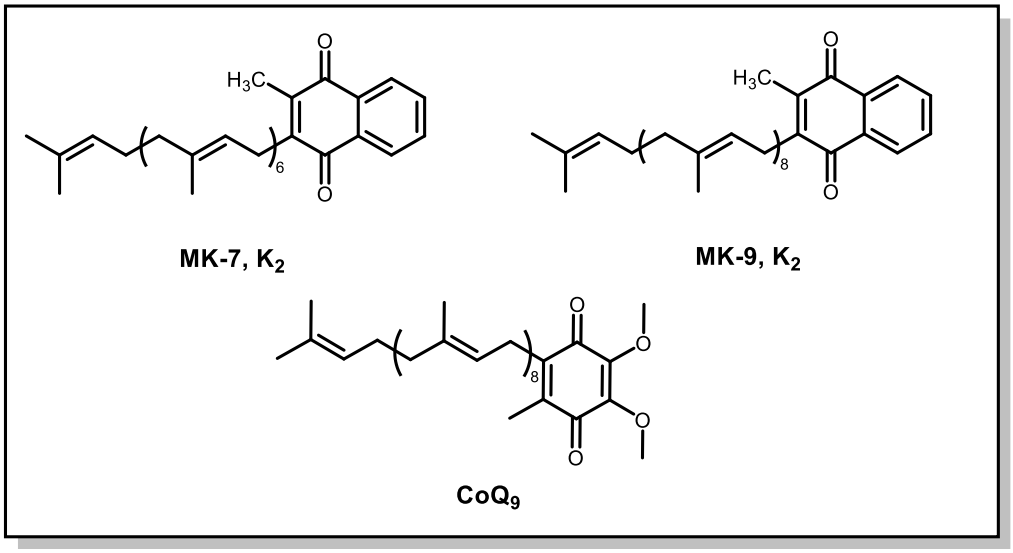

Figure 21: Nutraceutical compounds as targets for neat α-allylations

At first glance, an organic chemist would quickly discover that there is no readily available synthetic handle to directly allylate the quinone unit. This is obvious based on the nature of the quinone ring which provides no acidic α-proton to form a nucleophilic enolate. However, an elegant workaround for this problem was proposed long ago by Rüttimann, where he developed a route first by derivatizing the quinone as the Diels-Alder adduct with cyclopentadiene (Cp), followed by deprotonation of the now sp^3 hybridized α-proton to form the enolate which can perform the substitution reaction. Once complete, the Diels-Alder adduct can be cleanly converted back to the quinone via a retro-Diels-Alder at moderate temperature and reduced pressure without solvent.

MK-9, K_2 was chosen as the first target compound due to the abundance of solanesol as starting material (Table 10). In the case of the MK series, we were also thankfully gifted a large amount of the Diels-Alder adduct of the methylnapthoquinone by Anthem Biosciences. Initial studies for this transformation focused on using solanesyl chloride as the allylic halide, utilizing catalytic sodium iodide to affect an *in situ* Finkelstein reaction. Due to the cost of other isoprenyl compounds, such as the heptaprenyl alcohol used for MK-7, using excess of the Diels-Alder adduct was first attempted. Using two equivalents of the adduct with only 1.5 equivalents of base and 5 mol % NaI resulted in the synthesis of **36** in 43% isolated yield (entry 1). Increasing the amount of base and adduct saw a drop in yield to 33% (entry 2). Continuing to use the allylic chloride, switching the stoichiometry to use excess halide resulted in a boost in yield to 71% (entry 3). Finally switching the halide from chloride to bromide (entry 4) gave nearly quantitative yield after only one hour of reaction time. In the case of the allylic bromide example, the product can be easily recovered by loading the reaction mixture onto Celite

followed by filtering the unreacted allyl bromide through silica using hexanes, followed by diethyl ether/hexane mixture to elute the desired allylated compound.

Table 10: Synthesis methods for preparing MK-9 Diels-Alder adduct

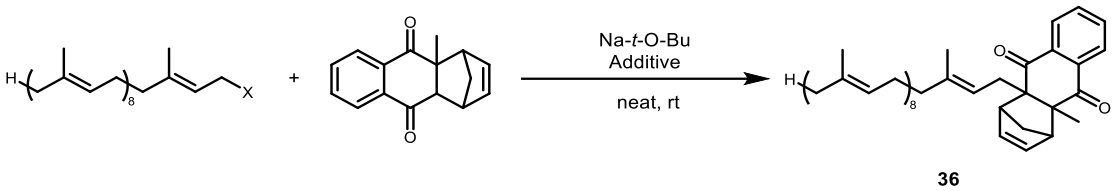

36

Entry	Halide X (equiv)	Diels-Alder adduct (equiv)	NaO-*t*-Bu (equiv)	Additive	Yield **36** (%)[a]
1	Cl (1)	2	1.5	NaI (5 mol %)	43
2	Cl (1)	3	3	NaI (5 mol %)	33
3	Cl (3)	1	3	NaI (5 mol %)	71
4	**Br (3)**	**1**	**3**	**NA**	**94**

[a] Isolated yields

We subsequently found that scaleup of this process worked very well at 3.0 mmol scale producing **36** in quantitative yield upon isolation (Figure 22). It should be noted that a slight exotherm was felt physically upon addition of strong base to the mixture of the allylic bromide and Diels-Alder adduct, which may be a concern upon scaleup. Satisfyingly, the adduct **36** can be reverted to the benzoquinone following retro-Diels-Alder when heated neat to 85 °C at pressures less than 15 torr to provide MK-9 in 77% yield as a yellow solid after isolation (this step was not optimized).

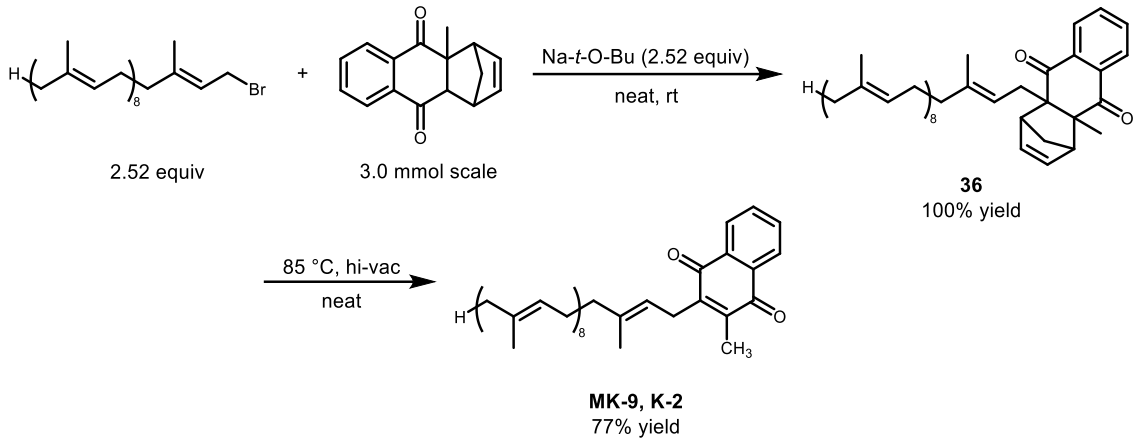

Figure 22: Total synthesis of MK-9, K_2 using neat allylation

After accomplishing the synthesis of MK-9, this same set of conditions was applied to the synthesis of MK-7. The heptaisoprenyl alcohol for this analogue is considerably more expensive than solanesol because it must be synthesized, and therefore the heptaisoprenyl bromide was prepared on smaller scale and used in slightly less excess compared to use of solanesyl bromide. The conditions were essentially identical, exemplifying the robustness of this allylation chemistry leading to **37**, followed by retro-Diels-Alder to form MK-7 (Figure 23).

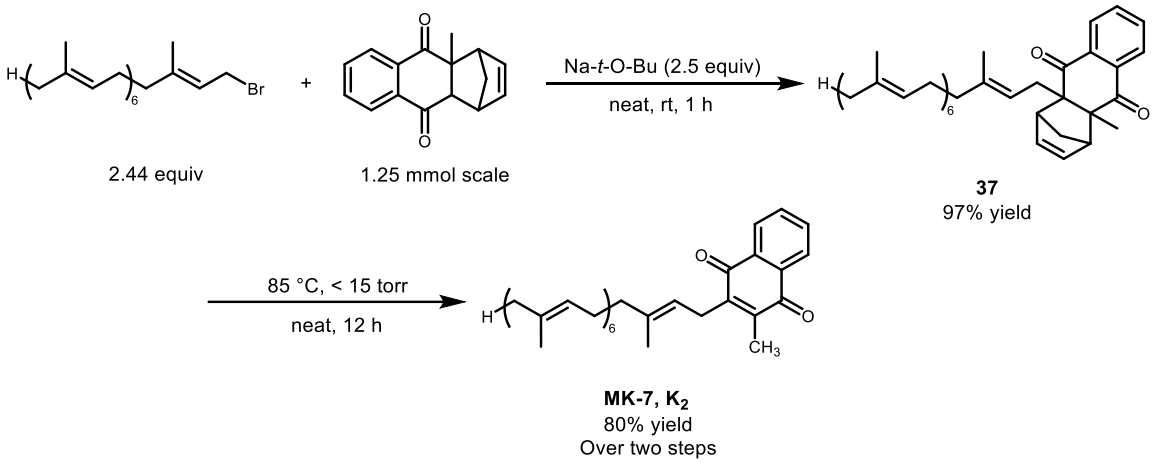

Figure 23: Total synthesis of MK-7, K_2 using neat allylation

This same synthetic approach was applied to the total synthesis of CoQ_9 on a half-gram scale. To synthesize the Diels-Alder adduct of the 2,3-dimethoxy-5-methylquinone, cyclopentadiene was freshly distilled from dicyclopentadiene. Subsequent Diels-Alder reaction then took place in acidic medium at room temperature, yielding adduct **38** (Figure 24).

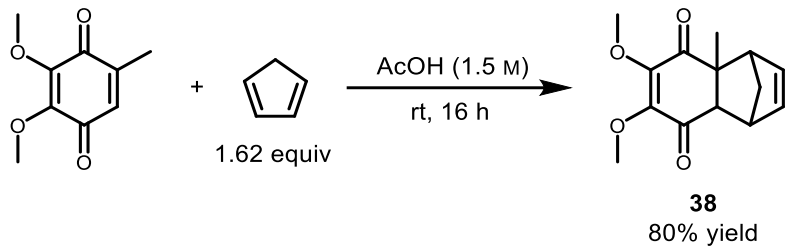

Figure 24: Formation of the Diels-Alder adduct *en route* to CoQ_9

The neat allylation was then run identically as applied to the 2-step process to form the menaquinone derivatives (Figure 25). The formation of allylated Diels-Alder adduct **39** resulted in lower yield compared to the analogous menaquinone reaction, resulting in product in only 70% yield upon isolation. However, retro-Diels-Alder to form CoQ_9 went to completion in very high yield (93%) to result in the desired product as an orange solid at 65% overall yield for two steps.

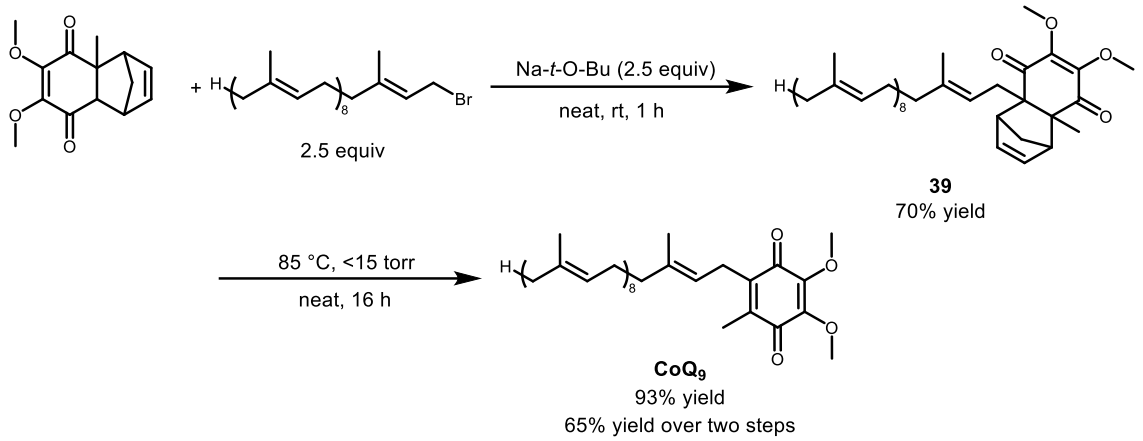

Figure 25: Total synthesis of CoQ_9 using neat allylation

A variety of potential improvements of these reaction conditions for synthesizing CoQ_9 were attempted. First, trying to run this chemistry as a 2-step, 1-pot sequence resulted in similar yield to when the intermediate is isolated (59% over two steps). However, vigorous foaming is encountered if the first reaction is placed under hi-vacuum to run the retro-Diels-Alder (Figure 26).

Figure 26: Intense foaming encountered when first reaction is put under hi-vacuum

Second, another trial involved using mineral oil as a “solvent” to maximize the yield of the allylation step, potentially mitigating some decomposition side reaction. However, isolation of the CoQ_9 from this sequence resulted in poorer yield compared to that of the isolated and 1-pot sequences (55% yield).

2.4 Conclusions

In conclusion, α-arylation of ketones has been achieved in an aqueous micellar system at near ambient conditions. The reaction requires, in many cases, only parts-per-million levels of palladium in the form of a $[Pd(\mu\text{-}Br)(t\text{-}Bu)_3P]_2$ complex to affect cross-couplings of aryl enolates and aryl halides at 45 °C with K-O-*t*-Bu as base. The chemistry is amenable to a variety of aromatic and heteroaromatic couplings partners, including late-stage functionalized molecules in the form of APIs, which can be further derivatized, and intermediates towards a target drug tamoxifen. The robustness of this this method is exemplified by exceptionally low E Factors, aqueous phase recyclability, and an aggressive 5-step, 1-pot sequence that utilizes α-arylation as a key step, including an unprecedented "ligand switch" reaction. The success of α-arylations also sparked inception of a green upgrade to α-allylations. While aqueous-based chemistry was not successful in this regard, the transition to neat-phase chemistry resulted in high yields of allylated ketones. This breakthrough in allylation chemistry was applied directly to the interesting development of syntheses for highly valuable nutraceuticals, such as MK-7, MK-9, and CoQ_9 through a Diels-Alder/retro-Diels Alder route.

2.5 References

1) H. C. Shen in *Applications of Transition Metal Catalysis in Drug Discovery and Development: An Industrial Perspective* (Eds.: M. J. Crawley, B. M. Trost), Wiley, Hoboken, **2012**, Chapter 2, pp 25-95.

2) (a) Haas, D.; Hammann, J. M.; Greiner, R.; Knochel, P. *ACS Catal.* **2016**, *6*, 1540–1552. (b) Yousaf, M.; Zahoor, A. F.; Akhtar, R.; Ahmad, M.; Naheed, S. *Mol Divers* **2020**, *24*, 821–839. (c) Juhász, K.; Magyar, Á.; Hell, Z. *Synthesis* **2020**, *52*, A-T. (d) Sherwood, J.; Clark, J. H.; Fairlamb, I. J. S.; Slattery, J. M. *Green Chem*. **2019**, *21*, 2164–2213.

3) For reviews, please see: (a) Culkin, D. A.; Hartwig, J. F. *Acc. Chem. Res.* **2003**, *36*, 234–245. (b) Bellina, F.; Rossi, R. *Chem. Rev*. **2010**, *110*, 1082–1146. (c) Johansson, C. C. C.; Colacot, T. J. *Angew. Chem. Int. Ed*. **2010**, *49*, 676–707. (d) Lloyd-Jones, G. C. *Angew. Chem., Int. Ed.* **2002**, *41*, 953-956. (e) Hao, Y.-J.; Hu, X.-S.; Zhou, Y.; Zhou, J.; Yu, J.-S. *ACS Catal.* **2020**, *10*, 955–993.

4) (a) Sivanandan, S. T.; Shaji, A.; Ibnusaud, I.; Seechurn, C. C. C. J.; Colacot, T. J. *Eur. J. Org. Chem.* **2015**, *1*, 38–49. (b) Devendar, P.; Qu, R.-Y.; Kang, W.-M.; He, B.; Yang, G.-F. *J. Agric. Food Chem*. **2018**, *66*, 8914–8934. (c) Borths, C. J.; Walker, S. D. *Isr. J. Chem*. **2020**, *60*, 340–350. (d) Dirat, O.; Elliott, J. M.; Jelley, R. A.; Jones, A. B.; Reader, M. *Tetrahedron Letters* **2006**, *47*, 1295–1298. (e) Carril, M.; SanMartin, R.; Domínguez, E.; Tellitu, I. *Tetrahedron* **2007**, *63*, 690–702. (f) Guastavino, J. F.; Rossi, R. A. *J. Org. Chem*. **2012**, *77*, 460–472. (g) Hellal, M.; Singh, S.; Cuny, G. D. *J. Org. Chem*. **2012**, *77*, 4123–4130.

5) Johansson Seechurn, C. C. C.; Kitching, M. O.; Colacot, T. J.; Snieckus, V. *Angew. Chem., Int. Ed.* **2012**, *51*, 5062–5085.

6) Semmelhack, M. F.; Chong, B. P.; Stauffer, R. D.; Rogerson, T. D.; Chong, A.; Jones, L. D. *J. Am. Chem. Soc.* **1975**, *97*, 2507–2516.

7) Muratake, H.; Hayakawa, A.; Natsume, M. *Tet. Lett.* **1997**, *38*, 7577–7580.

8) (a) Palucki, M.; Wolfe, J. P.; Buchwald, S. L. *J. Am. Chem. Soc*. **1996**, *118*, 10333–10334. (b) Palucki, M.; Wolfe, J. P.; Buchwald, S. L. *J. Am. Chem. Soc*. **1997**, *119*, 3395–3396.

9) Palucki, M.; Buchwald, S. L. *J. Am. Chem. Soc.* **1997**, *119*, 11108–11109.

10) Hamann, B. C.; Hartwig, J. F. *J. Am. Chem. Soc.* **1997**, *119*, 12382–12383.

11) Terao, Y.; Fukuoka, Y.; Satoh, T.; Miura, M.; Nomura, M. *Bull. Chem. Soc. Jpn.* **1998**, 71, 2239-2246.

12) Landstrom, E. B.; Handa, S.; Aue, D. H.; Gallou, F.; Lipshutz, B. H. *Green Chem.* **2018**, *20*, 3436–3443.

13) Fors, B. P.; Krattiger, P.; Strieter, E.; Buchwald, S. L. *Org. Lett.* **2008**, *10*, 3505–3508.

14) Aufiero, M.; Scattolin, T.; Proutière, F.; Schoenebeck, F. *Organometallics* **2015**, *34*, 5191–5195.

15) Miyaura, N.; Yamada, K.; Suzuki, A. *Tet. Lett.* **1979**, *20*, 3437-3440.

16) Kawatsura, M.; Hartwig, J. F. *J. Am. Chem. Soc.* **1999**, *121*, 1473–1478.

17) Grasa, G. A.; Colacot, T. J. *Org. Lett.* **2007**, *9*, 5489–5492.

18) Ehrentraut, A.; Zapf, A.; Beller, M., *Adv. Synth. Catal*. **2002**, *344*, 209–217.

19) Adjabeng, G.; Brenstrum, T.; Frampton, C. S.; Robertson, A. J.; Hillhouse, J.; McNulty, J.; Capretta, A. *J. Org. Chem.* **2004**, *69*, 5082–5086.

20) Old, D. W.; Wolfe, J. P.; Buchwald, S. L., *J. Am. Chem. Soc*. **1998**, *120*, 9722 -9723.

21) Hesp, K. D.; Lundgren, R. J.; Stradiotto, M., *J. Am. Chem. Soc*. **2011**, *133*, 5194–5197.

22) Raders, S. M.; Jones, J. M.; Shaughnessy, K. H. et al., *Eur. J. Org. Chem*. **2014**, *2014*, 7395–7404.

23) Marelli, E.; Corpet, M.; Davies, S. R.; Nolan, S. P. Palladium-Catalyzed α-Arylation of Arylketones at Low Catalyst Loadings. *Chem. Eur. J.* **2014**, *20*, 17272–17276.

24) Riprin, D. H.; Evans, D. A. *pKa of Inorganic and Oxo-Acids*. http://ccc.chem.pitt.edu/wipf/MechOMs/evans_pKa_table.pdf (Accessed January 14, 2022).

25) Lessi, M.; Masini, T.; Nucara, L.; Bellina, F.; Rossi, R. *Adv. Synth. Catal.* **2011**, *353*, 501–507.

26) Handa, S.; Wang, Y.; Gallou, F.; Lipshutz, B. H. *Science* **2015**, *349*, 1087–1091.

27) Desai, L. V.; Hay, M. B.; Leahy, D. K.; Wei, C.; Fanfair, D.; Rosner, T.; Hsiao, Y. *Tetrahedron* **2013**, *69*, 5677–5684.

28) Navarro, O.; Marion, N.; Oonishi, Y.; Kelly, R. A.; Nolan, S. P. *J. Org. Chem.* **2006**, *71*, 685–692.

29) Desai, L. V.; Ren, D. T.; Rosner, T. *Org. Lett*. **2010**, *12*, 1032–1035.

30) Beare, N. A.; Hartwig, J. F. *J. Org. Chem.* **2002**, *67*, 541–555.

31) Sperger, T.; Schoenebeck, F. *Synthesis* **2018**, *50*, 4471–4475.

32) Fricke, C.; Sperger, T.; Mendel, M.; Schoenebeck, F. *Angew. Chem., Int. Ed*. **2021**, *60*, 3355–3366.

33) Tolman, C. A. *J. Am. Chem. Soc.* **1974**, *92*, 2956-2965.

34) Christmann, U.; Vilar, R. *Angew. Chem., Int. Ed*. **2005**, *44*, 366-374.

35) Bihani, M.; Ansari, T. N.; Smith, J. D.; Handa, S. *Curr. Opin. Green Sustain. Chem.* **2018**, *11*, 45–53.

36) Hill, L. L.; Crowell, J. L.; Tutwiler, S. L.; Massie, N. L.; Hines, C. C.; Griffin, S. T.; Rogers, R. D.; Shaughnessy, K. H.; Grasa, G. A.; Johansson Seechurn, C. C. C.; Li, H.; Colacot, T. J.; Chou, J.; Woltermann, C. J. *J. Org. Chem.* **2010**, *75*, 6477–6488.

37) Isley, N. A.; Dobarco, S.; Lipshutz, B. H. *Green Chem.* **2014**, *16*, 1480–1488.

38) Rideout, D. C.; Breslow, R. *J. Am. Chem. Soc.* **1980**, *102*, 7816–7817.

39) Lee, N. R.; Cortes-Clerget, M.; Wood, A. B.; Lippincott, D. J.; Pang, H.; Moghadam, F. A.; Gallou, F.; Lipshutz, B. H. *ChemSusChem* **2019**, *12*, 3159–3165.

40) Klumphu, P.; Lipshutz, B. H. *J. Org. Chem.* **2014**, *79*, 888–900.

41) Koley, D.; Bard, A. J. *Proceedings of the National Academy of Sciences* **2010**, *107*, 16783–16787.

42) https://pubchem.ncbi.nlm.nih.gov/compound/Polyoxyethylene-_23_-lauryl-ether. (Accessed January 14, 2022).

43) Lipshutz, B. H.; Aguinaldo, G. T.; Ghorai, S.; Voigtritter, K. *Org. Lett.* **2008**, *10*, 1325–1328.

44) Marelli, E.; Renault, Y.; Sharma, S. V.; Nolan, S. P.; Goss, R. J. M. *Chem. Eur. J.* **2017**, *23*, 3832–3836.

45) Cernak, T.; Dykstra, K. D.; Tyagarajan, S.; Vachal, P.; Krska, S. W. *Chem. Soc. Rev.* **2016**, *45*, 546–576.

46) Dooley, M.; Lamb, H. M. Donepezil: A Review of Its Use in Alzheimer's Disease. Drugs & Aging **2000**, *16*, 199–226.

47) McGrath, J. Review: Haloperidol Is Effective for Schizophrenia but Increases Parkinsonism, Dystonia, and Akathisia. Evidence-Based Mental Health **2001**, *4*, 112–112.

48) (a) Churruca, F.; SanMartin, R.; Tellitu, I.; Domínguez, E. *Org. Lett.* **2002**, *4*, 1591–1594. (b) Churruca, F.; SanMartin, R.; Carril, M.; Tellitu, I.; Domínguez, E. *Tetrahedron* **2004**, *60*, 2393–2408. (c) Danoun, G.; Tlili, A.; Monnier, F.; Taillefer, M. *Angew. Chem., Int. Ed.* **2012**, *51*, 12815–12819.

49) Sheldon, R. A. *Green Chem.* **2007**, *12*, *1261-1384.*

50) Phillips, S.; Holdsworth, D.; Kauppinen, P.; Mac Namara, C. *Johnson Matthey Technol. Rev.* **2016**, *60*, 277–286.

51) Hayashi, Y. *Chem. Sci.* **2016**, *7*, 866–880.

52) Hayashi, Y. *J. Org. Chem*. **2021**, *86*, 1–23.

53) Akporji, N.; Thakore, R. R.; Cortes-Clerget, M.; Andersen, J.; Landstrom, E.; Aue, D. H.; Gallou, F.; Lipshutz, B. H. *Chem. Sci.* **2020**, *11*, 5205–5212.

54) Braasch-Turi, M.; Crans, D. C. *Molecules* **2020**, *25*, 4477-4514.

55) van Ballegooijen, A. J.; Pilz, S.; Tomaschitz, A.; Grübler, M. R.; Verheyen, N. The Synergistic Interplay between Vitamins D and K for Bone and Cardiovascular Health: A Narrative Review. *In. J. Endocrinol.* **2017**, *2017*, 1–12.

56) (a) https://www.made-in-china.com/price/solanesol-price.html. (Accessed January 14, 2022); (b) https://www.alibaba.com/showroom/solanesol-price.html (Accessed January 14, 2022).

57) At the time of this dissertation, the listed price on Millipore-Sigma for CoQ_9 was $1050.00/5 mg. See:

https://www.sigmaaldrich.com/US/en/product/sigma/27597?gclid=CjwKCAiArOqOBhBmEiwAsgeLmbYzc4dEOdaBTZePt9rqlXCDt23JFrZudUjjKeYQMYNEMw5EBUvVHhoCgF4QAvD_BwE (Accessed January 14, 2022).

58) Rüttimann, A; Büchi, G. H. (Hoffman-La Roche Inc., USA). Process for the manufacture of quinone derivatives. PCT Int. 4,603,223, July 29, 1986.

2.6 Experimental Data

1. General Information

All commercial reagents were used without further purification unless otherwise noted. Organic solvents specified as dry and/or degassed such as THF, toluene, and DCM were either taken from a solvent purification system (Pure-Solv 400, Innovative Technology, Inc. (now Inert, Inc.)), or degassed using a stream of bubbling argon for a minimum of 1 h and involved less than 25 mL of volume. All other solvents were used as received, such as MeOH, EtOAc, hexanes, and Et_2O, unless otherwise noted, and purchased from Fisher Scientific. Potassium *t*-butoxide was purchased from Millipore-Sigma (catalog #156671) and stored in an argon purged glove box. All palladium catalysts and ligands were stored in an argon purged glove box. Specifically, di-μ-bromobis(tri-*t*-butylphosphine)dipalladium(I) ($[Pd(\mu\text{-}Br)(t\text{-}Bu)_3P]_2$) was purchased from Strem (catalog #46-0355) and kept rigorously oxygen-free in its solid state within a glove box. Starting ketones and halides were purchased either from Millipore-Sigma or Combi-Blocks. The surfactant, TPGS-750-M, was prepared via a standard literature procedure,[1] or can be purchased from Millipore-Sigma (catalog #733857 for a 2 wt % solution of the wax dissolved in water). A standard 2 wt % aqueous solution of TPGS-750-M was typically prepared on a 100 g scale by dissolving 2 g of the wax into 98 g of thoroughly degassed (steady stream of argon, minimum of 1 h bubbling time with stirring) HPLC grade water in a 250 mL round bottomed flask equipped with a stir bar and allowed to dissolve overnight with vigorous stirring under argon pressure (**NOTE**: Do not attempt to degas the aqueous phase with surfactant wax submerged; vigorous foaming will occur). The 2 wt % TPGS-750-M/H_2O solution, once prepared, was kept under argon pressure at all times. Thin-layer chromatography (TLC) was performed using Silica Gel 60 F_{254} plates (Merck, 0.25 mm

thick). Flash chromatography is either performed in glass columns or an automated Biotage system using Silica Gel 60 (Silicycle, 40-63 nm). ^{1}H and ^{13}C NMR were recorded at 25 °C on a Varian Unity Inova 400 MHz, a Varian Unity Inova 500 MHz, or on a Varian Unity Inova 600 MHz spectrometer in $CDCl_3$ with residual $CHCl_3$ (^{1}H = 7.26 ppm, ^{13}C = 77.16 ppm) or in DMSO-d_6 with residual $(CH_3)_2SO$ (^{1}H = 2.50 ppm, ^{13}C = 39.52 ppm) as internal standards. Chemical shifts are reported in parts per million (ppm). NMR Data are reported as follows: chemical shift, multiplicity (s = singlet, d = doublet, dd = doublet of doublets, ddd = doublet of doublet of doublets, t = triplet, td = triplet of doublets, q = quartet, quin = quintet, m = multiplet), coupling constant (if applicable), and integration. High-resolution mass analyses (HRMS) were recorded on a Waters Micromass LCT TOF ES+ Premier mass spectrometer using ESI ionization.

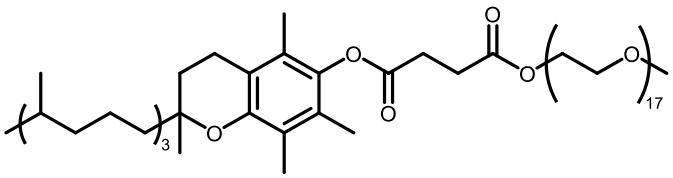

TPGS-750-M

2. General Procedures for α-Arylations of Ketones in Water

2a. General Procedure A: 0.5 mmol scale α-arylation of ketones using 0.125 mol % [Pd(μ-Br)(*t*-Bu)$_3$P]$_2$

To a flame dried 1-dram vial inside of an argon purged glove box was added [Pd(μ-Br)(*t*-Bu)$_3$P]$_2$ (5 mg) and the vial was sealed using a rubber septum and maintained under a steady pressure of argon. Rigorously degassed DCM (500 μL) was then added through the septum and the vial was stirred at ambient temperature until the solids had dissolved to prepare a very

dark green catalyst stock solution. To another flame dried 1-dram vial equipped with an oven dried stir bar inside of a glove box was added K-O-*t*-Bu (135 mg, 1.2 mmol, 2.4 equiv), followed by any solid ketone (0.6 mmol, 1.2 equiv) and solid aryl halide (0.5 mmol, 1.0 equiv) (or oils thereof) used for the reaction, and the vial was sealed using a rubber septum. This vial was then placed under argon pressure on a manifold and a 48 µL aliquot of the catalyst solution was added through the septum (0.48 mg, 6.25×10^{-4} mmol, 0.125 mol %). A vacuum was then pulled on the reaction vial for 2 min to remove all DCM and the vial was backfilled with argon. TPGS-750-M/H_2O (2 wt %) was then added (0.5 mL, 1.0 M) via syringe through the rubber septum followed by any neat liquid reagents via syringe. The contents of the vial were then allowed to stir vigorously (~1500 RPM) under constant argon pressure in a 1-dram vial aluminum block reactor at 45 °C internal temperature (aluminum block set to heat to 50 °C). The reaction was then monitored by thin-layer chromatography and gas chromatography until deemed complete. The contents of the vial were then extracted using EtOAc (3 x 1 mL) and dried directly onto SiO_2 to be purified via column chromatography.

2b. General Procedure B: 0.5 mmol scale α-arylation of ketones using 0.25 mol % [Pd(µ-Br)(*t*-Bu)$_3$P]$_2$

To a flame dried 1-dram vial equipped with an oven dried stir bar inside of a glove box was added [Pd(µ-Br)(*t*-Bu)$_3$P]$_2$ (1 mg, 1.25×10^{-3} mmol, 0.25 mol %), K-O-*t*-Bu (135 mg, 1.2 mmol, 2.4 equiv), followed by any solid ketone (0.6 mmol, 1.2 equiv), and solid aryl halide (0.5 mmol, 1.0 equiv) (or any oils) used for the reaction. The vial was then sealed using a rubber septum inside of the glovebox and then transferred to a manifold under argon pressure. TPGS-750-M/H_2O (2 wt %) was then added (0.5 mL, 1.0 M) via syringe through the rubber septum followed by any neat liquid reagents via syringe. The contents of the vial were then

allowed to stir vigorously (~1500 RPM) under constant argon pressure in a 1-dram vial aluminum block reactor at 45 °C internal temperature (aluminum block set to heat to 50 °C). The reaction was then monitored by thin-layer chromatography and gas chromatography until deemed complete. The contents of the vial were then extracted using EtOAc (3 x 1 mL) and dried directly onto SiO_2 to be purified via column chromatography.

2c. General Procedure C: 0.5 mmol scale α-arylation of ketones using 1.0 mol % [Pd(μ-Br)(*t*-Bu)$_3$P]$_2$

To a flame dried 1-dram vial equipped with an oven dried stir bar inside of a glove box was added [Pd(μ-Br)(*t*-Bu)$_3$P]$_2$ (4 mg, 0.005 mmol, 1.0 mol %). The remainder of the experimental then follows General Procedure B.

3. Scaleup of an α-arylation to 1.0 mmol

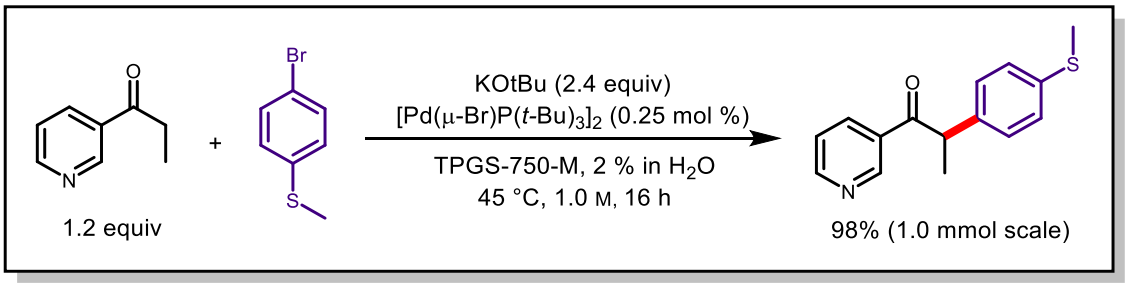

To a flame dried 1-dram vial equipped with an oven dried stir bar was added [Pd(μ-Br)(*t*-Bu)$_3$P]$_2$ (2 mg, 2.50 x 10^{-3} mmol, 0.25 mol %) and K-O-*t*-Bu (270 mg, 2.4 mmol, 2.4 equiv) inside of a glove box. The vial was then sealed using a rubber septum and removed from the glove box. 1-(Pyridin-3-yl)propan-1-one (162 mg, 1.2 mmol, 1.2 equiv) and 4-bromothioanisole (203 mg, 1.0 mmol, 1.0 equiv) were then added very quickly to the uncapped

vial and the vial was resealed. The vial was then adapted to an argon/vacuum manifold and the headspace was evacuated and backfilled with argon three times. TPGS-750-M/H_2O (2 wt %, 1.0 mL, 1.0 M) was then added through the septum and the contents of the vial were then allowed to stir vigorously (~1500 RPM) under constant argon pressure in a 1-dram vial aluminum block reactor at 45 °C internal temperature (aluminum block set to heat to 50 °C) for 16 h. After completion, the contents of the vial were then extracted with EtOAc (3 x 1.0 mL) and dried directly onto SiO_2 to be purified via flash chromatography (50% EtOAc/hexanes). The resulting product was then dried under high vacuum to afford a yellow-orange oil which solidifies slowly over time (252.7 mg, 98% yield).

4. Synthesis of a tamoxifen intermediate

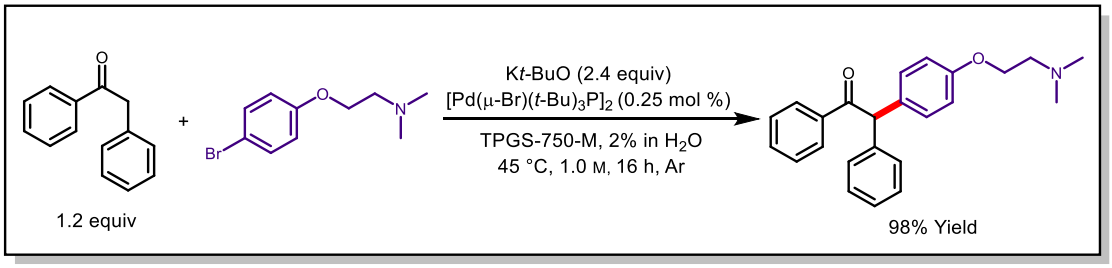

To a flame dried 1-dram vial equipped with an oven dried stir bar was added [Pd(μ-Br)(*t*-Bu)$_3$P]$_2$ (1 mg, 1.25 x 10^{-3} mmol, 0.25 mol %), K-O-*t*-Bu (135 mg, 1.2 mmol, 2.4 equiv), and deoxybenzoin (118 mg, 0.6 mmol, 1.2 equiv). The vial was then sealed using a rubber septum inside of the glovebox and then transferred to a manifold under argon pressure. TPGS-750-M/H_2O (2 wt %) was then added (0.5 mL, 1.0 M) via syringe through the rubber septum followed by 2-(4-bromophenoxy)-*N*,*N*-dimethylethan-1-amine (122 mg, 0.5 mmol, 1.0 equiv) as a liquid through the septum. The contents of the vial were then allowed to stir vigorously (~1500 RPM) under constant argon pressure in a 1-dram vial aluminum block reactor at 45 °C

internal temperature (aluminum block set to heat to 50 °C). The reaction was then monitored by thin-layer chromatography until deemed complete. The contents of the vial were then extracted using EtOAc (3 x 1 mL). The combined organics were then dried onto SiO_2 and purified via flash chromatography (MeOH/DCM/Et_3N 10:90:1). The product was then dried under high vacuum to result in an amber oil (177.1 mg, 98% yield).

5. Aqueous recycling studies

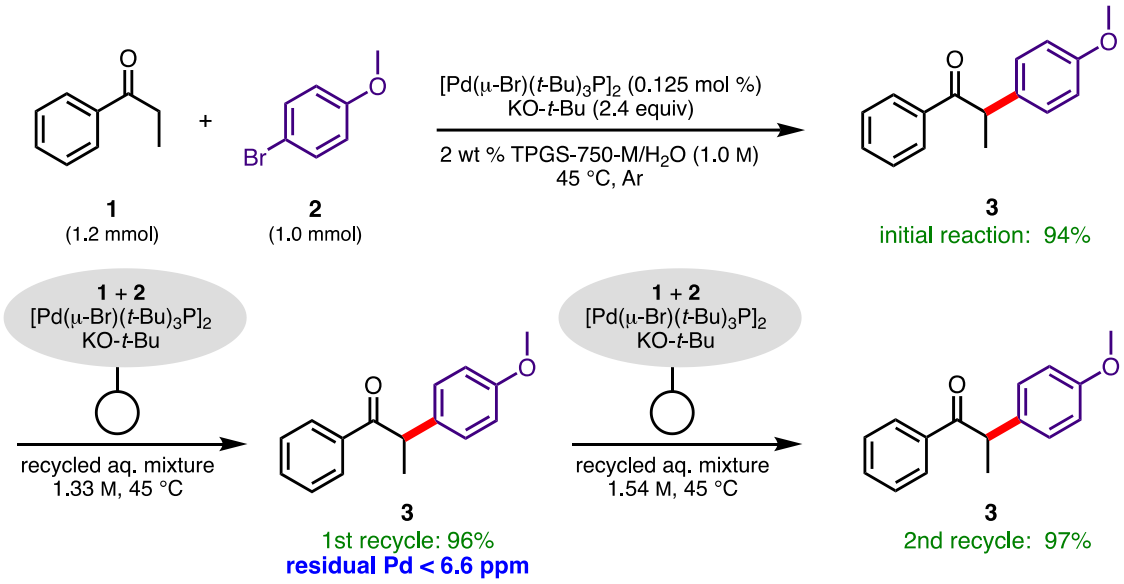

Initial Reaction: To a flame dried 1-dram vial equipped with an oven dried magnetic stir bar was added $[Pd(\mu\text{-}Br)(t\text{-}Bu)_3P]_2$ (1 mg, 1.25 x 10^{-3} mmol, 0.125 mol %) and K-O-*t*-Bu (270 mg, 2.4 mmol, 2.4 equiv) inside of an argon purged glove box. The vial was then sealed using a rubber septum, removed from the glove box, and connected via syringe needle to a manifold under argon pressure. TPGS-750-M/H_2O (2 wt %, 1.0 mL, 1.0 M) followed by 160 µL of **1** (160 mg, 1.2 mmol, 1.2 equiv) and 125 µL of **2** (187 mg, 1.0 mmol, 1.0 equiv) were then added to the vial via syringe through the septum, and the contents of the vial were then allowed to stir vigorously (~1500 RPM) under constant argon pressure in a 1-dram vial aluminum block

reactor at 45 °C internal temperature (aluminum block set to heat to 50 °C). After 2 h, the contents of the vial were then extracted using methyl *t*-butyl ether (MTBE; 1.0 mL x 3) which had been thoroughly degassed with argon. **Note:** The extraction is performed while the vial is still maintained under strict air-free conditions. The extraction solvent is added through the septum to the reaction mixture under argon pressure, allowed to extract via stirring, and then removed under argon pressure using a syringe using a long needle.

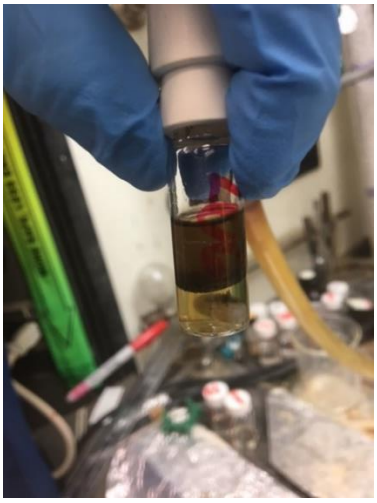

Figure 27: Initial reaction post extraction and settling with degassed MTBE, kept under argon

The combined organics were then dried directly onto SiO_2 and purified via flash chromatography (8% EtOAc/hexanes) and dried under vacuum to afford product as a white solid (226 mg, 94% yield). The remaining volume of aqueous phase was then determined to be 750 µL.

First Recycle: To a separate flamed dried 1-dram vial equipped with an oven dried stir bar was added $[Pd(\mu\text{-}Br)(t\text{-}Bu)_3P]_2$ (1 mg, 1.25 x 10^{-3} mmol, 0.125 mol %) and K-O-*t*-Bu (270 mg, 2.4 mmol, 2.4 equiv) inside of an argon purged glove box. The vial was then sealed using

a rubber septum, removed from the glove box, and connected via syringe needle to a manifold under argon pressure. The remaining TPGS-750-M aqueous phase from the initial reaction was then added (0.75 mL, 1.33 M), followed by 160 µL of 1 (160 mg, 1.2 mmol, 1.2 equiv) and 125 µL of 2 (187 mg, 1.0 mmol, 1.0 equiv) via syringe through the septum, and the contents of the vial were then allowed to stir vigorously (~1500 RPM) under constant argon pressure in a 1-dram vial aluminum block reactor at 45 °C internal temperature (aluminum block set to heat to 50 °C). After 2 h, the contents of the vial were then extracted under argon using MTBE (1.0 mL x 3) which had been thoroughly degassed with argon as previously mentioned. The combined organics were then dried directly onto SiO_2 and purified via flash chromatography (8% EtOAc/hexanes) and dried under vacuum to afford product as a white solid (230 mg, 96% yield). The remaining volume of aqueous phase was determined to be 650 µL.

Second Recycle: To a separate flamed dried 1-dram vial equipped with an oven dried stir bar was added $[Pd(\mu\text{-}Br)(t\text{-}Bu)_3P]_2$ (1 mg, 1.25 x 10^{-3} mmol, 0.125 mol %) and K-O-*t*-Bu (270 mg, 2.4 mmol, 2.4 equiv) inside of an argon purged glove box. The vial was then sealed using a rubber septum, removed from the glove box, and connected via syringe needle to a manifold under argon pressure. The remaining TPGS-750-M aqueous phase from the first recycle was then added (0.65 mL, 1.54 M), followed by 160 µL of 1 (160 mg, 1.2 mmol, 1.2 equiv) and 125 µL of 2 (187 mg, 1.0 mmol, 1.0 equiv) via syringe through the septum, and the contents of the vial were then allowed to stir vigorously (~1500 RPM) under constant argon pressure in a 1-dram vial aluminum block reactor at 45 °C internal temperature (aluminum block set to heat to 50 °C). After 16 h, the contents of the vial were then extracted using MTBE (1.0 mL x 3) which had been thoroughly degassed with argon as previously mentioned. The combined organics were then dried directly onto SiO_2 and purified via flash chromatography (8%

EtOAc/hexanes) and dried under vacuum to afford product as a white solid (232.1 mg, 97% yield). After the second recycle, the aqueous phase had accumulated too much salt for a third viable recycle study to be performed without adding fresh water or surfactant.

Figure 28: Aqueous phase post recycling two times

6. E Factor evaluation

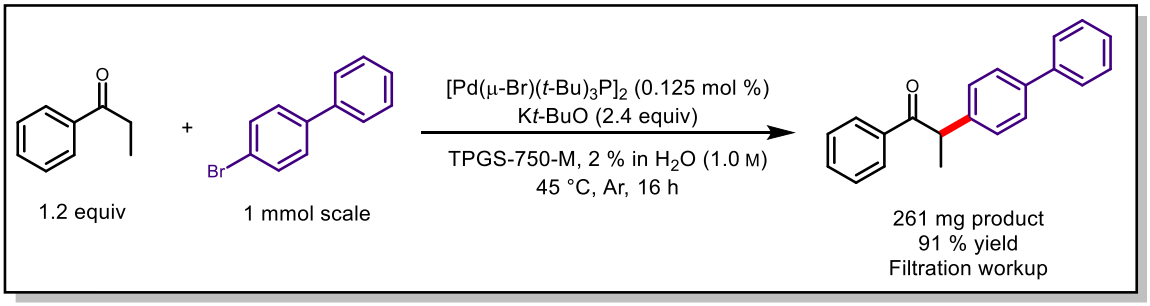

E Factor for filtered product: To a flame dried 1-dram vial equipped with an oven dried stir bar was added $[Pd(\mu\text{-}Br)(t\text{-}Bu)_3P]_2$ (1 mg, 1.25 x 10^{-3} mmol, 0.125 mol %), K-O-*t*-Bu (270 mg, 2.4 mmol, 2.4 equiv), and 4-bromo-1,1'-biphenyl (233 mg, 1.0 mmol, 1.0 equiv) inside of an argon purged glove box. The vial was then sealed using a rubber septum, removed from the

glove box, and connected via syringe needle to a manifold under argon pressure. TPGS-750-M/H_2O (2 wt %, 1.0 mL, 1.0 M) and propiophenone (160 mg, 1.2 mmol, 1.2 equiv) were then added to the vial via syringe through the septum, and the contents of the vial were then allowed to stir vigorously (~1500 RPM) under constant argon pressure in a 1-dram vial aluminum block reactor at 45 °C internal temperature (aluminum block set to heat to 50 °C). After 16 h, a grey solid mass had formed and was suspended in 1.0 mL of deionized water. The solids were then filtered and washed with water (2 x 1.0 mL) and dried over vacuum suction to afford product as an off-white solid (261 mg, 91% yield).

The E Factor was calculated using the mass of excess organics, in this case *t*-BuOH and propiophenone, over the mass of the desired product:

E Factor = (mass waste organics) / (mass product)

$= (mass_{t\text{-}BuOH} + mass_{propiophenone}) / (mass_{product})$

= (179 mg + 27 mg) / 261 mg = ***0.79***

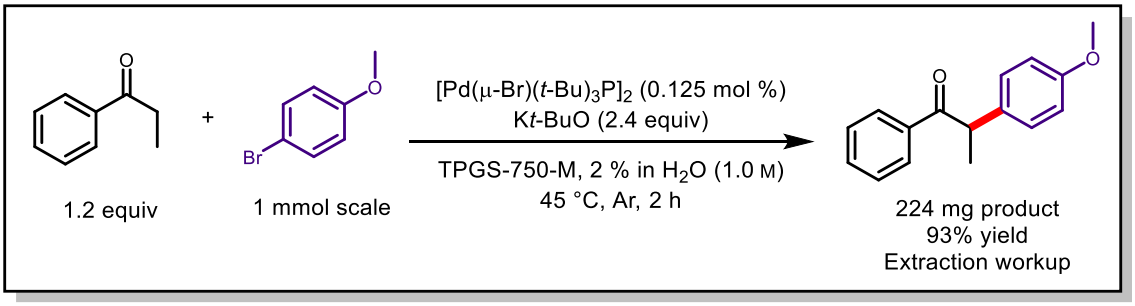

E Factor for extracted product: To a flame dried 1-dram vial equipped with an oven dried stir bar was added [Pd(μ-Br)(*t*-Bu)$_3$P]$_2$ (1 mg, 1.25 x 10^{-3} mmol, 0.125 mol %) and K-O-*t*-Bu (270 mg, 2.4 mmol, 2.4 equiv) inside of an argon purged glove box. The vial was then sealed using a rubber septum, removed from the glove box, and connected via syringe needle

to a manifold under argon pressure. TPGS-750-M/H_2O (2 wt %, 1.0 mL, 1.0 M) followed by 160 µL of propiophenone (160 mg, 1.2 mmol, 1.2 equiv) and 125 µL of 4-bromoanisole (187 mg, 1.0 mmol, 1.0 equiv) were then added to the vial via syringe through the septum, and the contents of the vial were then allowed to stir vigorously (~1500 RPM) under constant argon pressure in a 1-dram vial aluminum block reactor at 45 °C internal temperature (aluminum block set to heat to 50 °C) for 2 h. The contents of the vial were then carefully extracted with MTBE (3 x 270 µL), and the combined organics were dried directly onto SiO_2 and purified via flash chromatography (8% EtOAc/hexanes) to afford the product as a white solid after drying on high vac (224 mg, 93% yield).

The E Factor was calculated using the mass of excess organics, in this case *t*-BuOH, propiophenone, and MTBE used for the extraction (density of MTBE = 0.74 g/mL; therefore 270 µL = 200 mg).

E Factor = (mass waste organics) / (mass product)

$= (mass_{t\text{-}BuOH} + mass_{propiophenone} + mass_{MTBE}) / (mass_{product})$

= (179 mg + 27 mg + 3(200 mg)) / 224 mg =* ***3.6***

7. Tandem reaction procedures

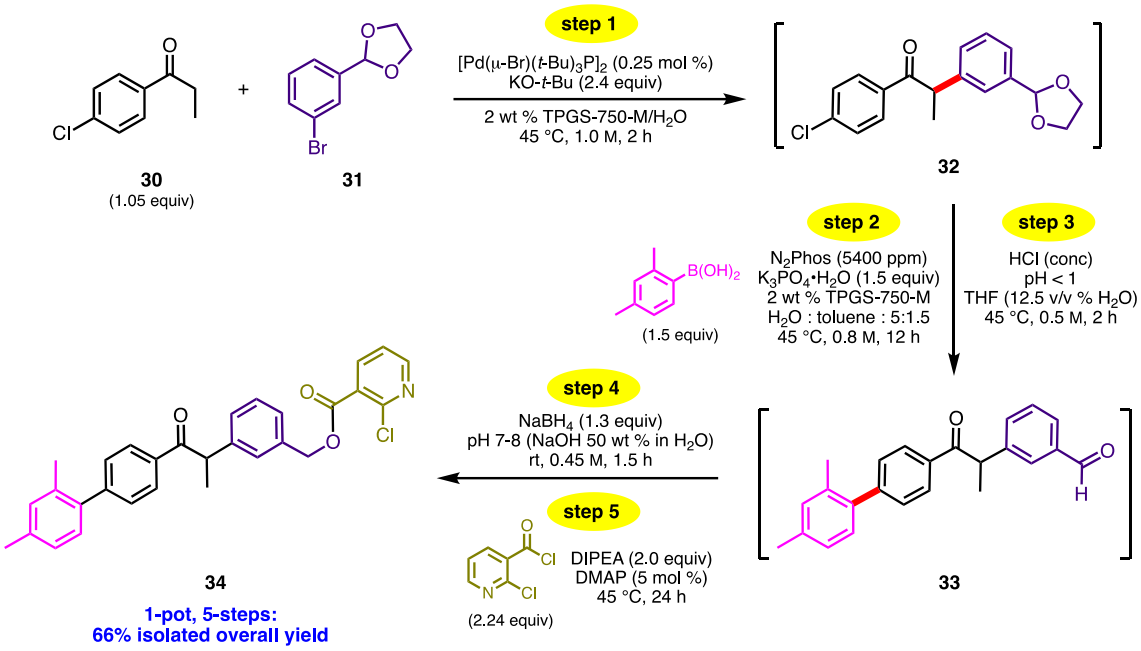

Step 1: To a flame dried 1-dram vial equipped with an oven-dried stir bar was added [Pd(μ-Br)(*t*-Bu)$_3$P]$_2$ (1 mg, 1.25 x 10^{-3} mmol, 0.25 mol %) and K-O-*t*-Bu (135 mg, 1.2 mmol, 2.4 equiv) inside of an argon purged glove box and sealed with a rubber septum. Very quickly outside of the glove box, 4'-chloropropiophenone (90 mg, 0.525 mmol, 1.05 equiv) and 2-(3-bromophenyl)-1,3-dioxolane (114 mg, 0.5 mmol, 1 equiv) were then added and the vial was resealed. The vial was then connected to a manifold and the headspace was evacuated and backfilled with argon three times. TPGS-750-M/H_2O (2 wt %, 0.5 mL, 1.0 M) was then added via syringe through the septum and the contents of the vial were then allowed to stir vigorously (~1500 RPM) under constant argon pressure in a 1-dram vial aluminum block reactor at 45 °C internal temperature (aluminum block set to heat to 50 °C) for 2 h where the reaction was deemed complete by TLC. In one iteration of this multistep study, this reaction was worked up via extraction using EtOAc (3 x 1.0 mL). The combined organics were then dried onto SiO_2

and purified by flash chromatography (20% EtOAc/hexanes) to afford product as a clear oil (128.1 mg, 81% yield).

Steps 2-3: In the situation where the reaction from Step 1 continues as part of the 1-pot series, to the unsealed reaction vial was added (2,4-dimethylphenyl)boronic acid (113 mg, 0.75 mmol, 1.5 equiv) and $K_3PO_4 \cdot H_2O$ (173 mg, 0.75 mmol, 1.5 equiv). The vial was then sealed with a new rubber septum and the headspace was purged using argon and a vent needle for 5 min. Following this, a sample of N_2Phos/toluene stock solution* (150 µL) was added to the vial through the septum and the reaction was allowed to stir vigorously (~1500 RPM) under constant argon pressure in a 1-dram vial aluminum block reactor at 45 °C internal temperature (aluminum block set to heat to 50 °C) for 12 h until deemed complete by TLC. The pH of this mixture was then adjusted to pH <1 using conc. HCl (300 µL) and THF (100 µL) was added to help disperse the solids. The hydrolysis reaction was allowed to stir at 45 °C internal temperature for 3 h until deemed complete by TLC. In one iteration of this multistep study, this reaction series (Steps 1-3) was worked up via extraction using EtOAc (3 x 1.0 mL). The combined organics were dried onto SiO_2 and purified by flash chromatography (15% EtOAc/hexanes) to afford product as an opaque white oil (137.7 mg, 80% yield).

*N_2Phos stock solution was prepared by dissolving 7.5 mg of N_2Phos into rigorously degassed toluene (0.5 mL).

Steps 4-5: In the situation where the reaction from Step 3 continues as part of the 1-pot series, the pH of the reaction was adjusted to pH 7-8 using 50 wt % NaOH aqueous solution (100 µL, followed by dropwise addition to the desired pH). To the resulting stirring mixture at rt was added $NaBH_4$ (10 mg, 0.26 mmol) and the vial was sealed and allowed to react with noticeable bubbling for 30 min. A second portion of $NaBH_4$ (15 mg, 0.40 mmol) was then

added and the reaction was allowed to continue to stir to rt for 1 h until deemed complete by TLC. 2-Chloronicotinoyl chloride (100 mg, 0.56 mmol, 1.12 equiv), DIPEA (175 µL, 2.0 equiv), and DMAP (3 mg, 0.025 mmol, 5 mol %) were added and allowed to stir vigorously for 12 h at 45 °C internal temperature. A second portion of the acid chloride was then added (50 mg, 0.28 mmol, 0.56 equiv) and allowed to react further for 6 h, followed by a third portion (50 mg, 0.28 mmol, 0.56 equiv) for another 6 h until the benzyl alcohol was consumed by TLC. The 5-step, 1-pot reaction was then extracted using EtOAc (3 x 1.0 mL). The combined organics were then dried onto SiO_2 and purified by flash chromatography (25% EtOAc/hexanes). The organics were then isolated via solvent evaporation and dried under high vac to result in product as a clear oil (161.6 mg, 66% yield).

8. Procedure for deuterated analogue

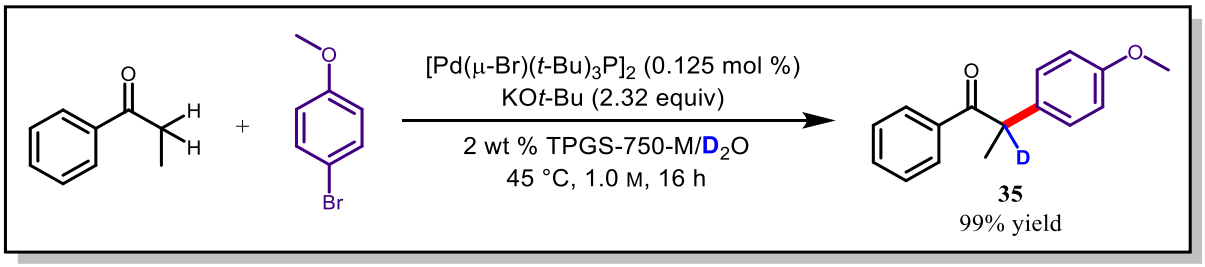

A solution of 2 wt % TPGS-750-M in D_2O was prepared first by degassing 14.7 mL of D_2O (Cambridge Isotope) with argon in a flamed dried 25 mL flask for 1 h followed by addition of 300 mg of fresh TPGS-750-M. This mixture was allowed to stir vigorously overnight under argon pressure resulting in a homogeneous solution, which was kept under an argon atmosphere at all times.

To a flame dried 1-dram vial equipped with an oven dried stir bar was added [Pd(µ-Br)(*t*-Bu)$_3$P]$_2$ (1 mg, 1.25 x 10^{-3} mmol, 0.125 mol %) and K-O-*t*-Bu (270 mg, 2.4 mmol, 2.32 equiv) inside of a glove box. The vial was then sealed using a rubber septum and transferred to an

argon-purged manifold and kept under constant argon pressure. TPGS-750-M/D_2O (2 wt %, 1.0 mL, 1.0 M) was then added followed by propiophenone (160 µL, 160 mg, 1.2 mmol, 1.16 equiv) and 4-bromoanisole (130 µL, 194 mg, 1.035 mmol, 1.0 equiv) via syringe through the septum. The resulting mixture was then allowed to stir vigorously (~1500 RPM) under constant argon pressure in a 1-dram vial aluminum block reactor at 45 °C internal temperature (aluminum block set to heat to 50 °C) for 16 h until deemed complete by TLC. The product mixture was then extracted with EtOAc (3 x 1.0 mL), dried onto SiO_2, and purified via flash chromatography (8% EtOAc/hexanes). The combined organics were then dried to constant mass on high vacuum resulting in deuterated product **35** as an off-white solid (248.1 mg, 99% yield).

9. Residual Pd analysis

Residual palladium analysis was performed using ICP-MS at UCLA Core Facility.

		Palladium		Source
		[µg/g]		
Sample #	Sample weight in analysis [mg]	Average*	stdev	
ABW.03.209	15.50	6.487	0.049	First recycle

**Each sample was done in triplicated measurements with background correction.*
n/a represents below detection limit.

10. Synthesis of allylated intermediate 36 and MK-9

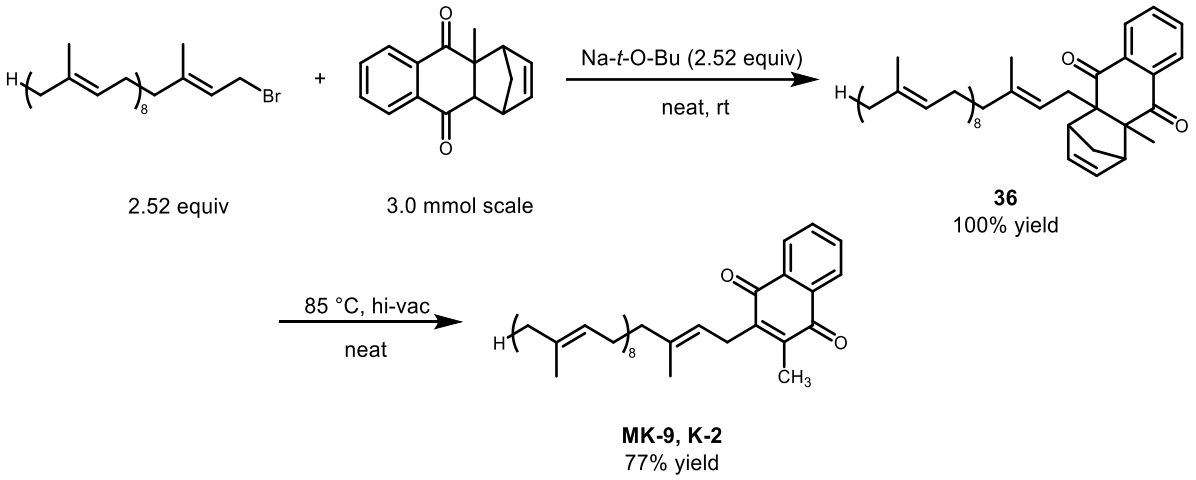

α-Allylation to 36. To a 20 mL oven-dried scintillation vial was added freshly prepared solanesyl bromide (5.3 g, 7.65 mmol, 2.52 equiv) and a stir bar. 4a-Methyl-1,4,4a,9a-tetrahydro-1,4-methanoanthracene-9,10-dione (722 mg, 3.03 mmol, 1.00 equiv) was then added and allowed to disperse with gentle stirring. NaO-*t*-Bu (735 mg, 7.65 mmol, 2.52 equiv) was removed from a glove box in a 1-dram vial and added in one addition to the stirring reaction mixture at rt resulting in a red reaction mixture which warms slightly. The vial was then sealed and stirred rapidly (900 RPM) at rt. After 1 h, the reaction was deemed complete by TLC. The entire reaction mixture was then taken up in Et_2O and dried onto Celite. The crude reaction was then loaded onto a packed silica column (25 mm x 152 mm) and filtered through silica using two column volumes of hexanes, one column volume of 3.5% Et_2O/hexanes, and six column volumes of 7% Et_2O/hexanes, the latter of which was collected. The organics were then evaporated into a 20 mL scintillation vial resulting in a golden yellow oil (2560 mg, quant) which was carried over to the next reaction as is; R_f = 0.38 (8% Et_2O/92% hexanes).

Retro Diels-Alder reaction to MK-9. The vial containing the Diels-Alder adduct was then placed under high vacuum (<15 torr pressure) and heated in a 20 mL scintillation vial aluminum heating block to 85 °C internal temperature neat with no stirring. The reaction was allowed to heat until constant mass was observed from loss of cyclopentadiene as well as completion by TLC. The resulting golden oil was then purified by flash chromatography (eluent: 4% Et_2O/96% hexanes) and dried under high vacuum resulting in a yellow solid (1840.0 mg, 77% yield). R_f = 0.50 (1:9 Et_2O/hexanes).

11. Synthesis of intermediate 37 and MK-7

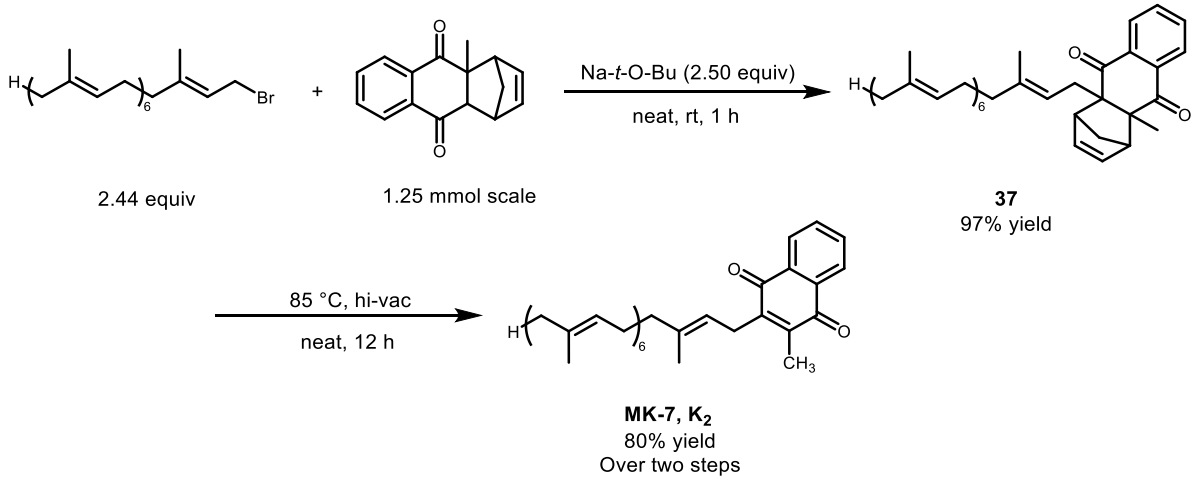

α-Allylation to 37. To a 20 mL oven-dried scintillation vial was added freshly prepared heptaprenyl bromide (1.7 g, 3.05 mmol, 2.44 equiv) and a stir bar. 4a-Methyl-1,4,4a,9a-tetrahydro-1,4-methanoanthracene-9,10-dione (297.5 mg, 1.25 mmol, 1.00 equiv) was then added and allowed to disperse with gentle stirring. NaO-*t*-Bu (300 mg, 3.125 mmol, 2.50 equiv) was removed from a glove box in a 1-dram vial and added in one addition to the stirring reaction mixture at rt resulting in a red reaction mixture. The vial was then sealed and stirred rapidly (900 RPM) at rt. After 1 h, the reaction was deemed complete by TLC. The entire reaction mixture was then taken up in Et_2O and dried onto Celite. The crude reaction was then

loaded onto a packed silica column (25 mm x 152 mm) and filtered through the silica using two column volumes of hexanes, one column volume of 3.5% Et_2O/hexanes, and four column volumes of 7% Et_2O/hexanes, the latter of which was collected. The organics were then evaporated into a 20 mL scintillation vial resulting in 869.4 mg of a golden yellow oil which was carried over directly to the next reaction.

Retro Diels-Alder reaction to MK-7. The vial containing the Diels-Alder adduct was then placed under high vacuum (<15 torr pressure) and heated in a 20 mL scintillation aluminum heating block to 85 °C internal temperature neat with no stirring. The reaction was allowed to heat until constant mass was observed from loss of cyclopentadiene, as well as completion by TLC. The resulting golden oil was then purified by flash chromatography (4% Et_2O/hexanes) and dried under high vacuum resulting in a yellow solid (648.1 mg, 80% yield over two steps). R_f = 0.60 (1:9 Et_2O/hexanes).

12. Synthesis of Diels-Alder adduct 38

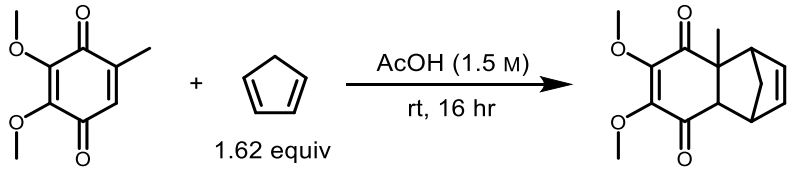

38
80% yield

Cyclopentadiene was freshly distilled from dicyclopentadiene. The dimer was heated in an oven dried round bottom flask with a stir bar in a 180 °C oil bath. The resulting vapors were collected in a water cooled short-path distillation head at 38-40 °C, and the condensed liquid was maintained at below freezing temperature (sodium chloride / ice bath).

To a 50 mL round bottomed flask was added the quinone (5 g, 27.45 mmol, 1 equiv) and acetic acid (18 ml, 1.5 M). Freshly distilled cyclopentadiene (2.95 g, 3.8 mL, 1.62 equiv) was then added to the reaction mixture through a septum at rt. The reaction was then allowed to stir

overnight at rt and was deemed complete by thin-layer chromatography. The pH of the reaction mixture was then adjusted to 9 (satd. bicarbonate solution, 150 mL) and extracted with Et_2O (3 x 100 mL). The combined organics were treated with brine, dried over sodium sulfate, filtered, and dried under reduced pressure followed by high vacuum resulting in an opaque oil that yellowed over time (5.39 g, 80% yield).

13. Synthesis of intermediate 39 and CoQ_9

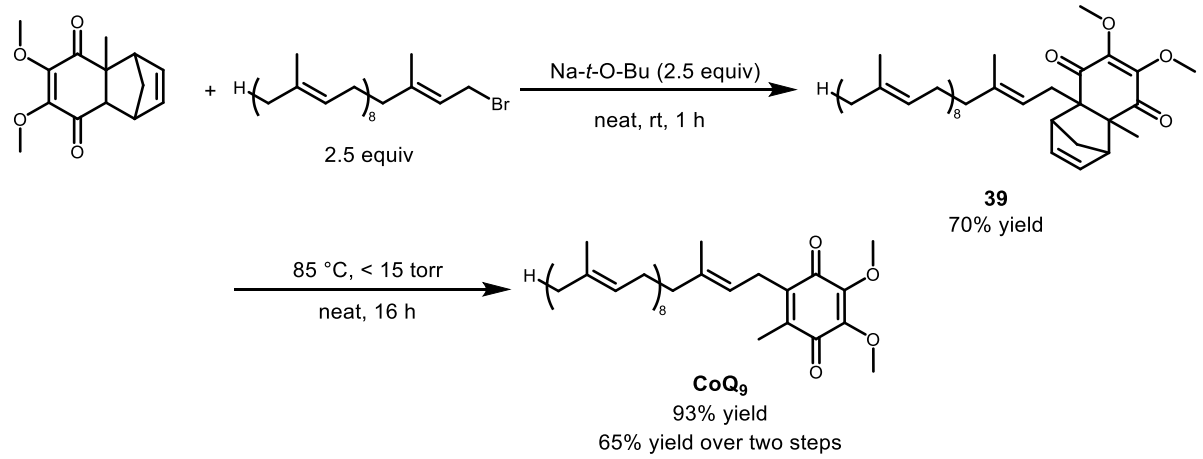

α-Allylation to 39. To a 20 mL scintillation vial was added the Diels-Alder adduct (310 mg, 1.25 mmol, 1 equiv) and freshly prepared solanesyl bromide (2.17 g, 3.125 mmol, 2.5 equiv.) along with a stir bar and the slurry was combined at rt with gentle stirring. NaO^tBu (300 mg, 3.125 mmol, 2.5 equiv) was then added in one portion and the stirring speed was increased to 900 RPM, resulting in a bright red slurry. The reaction was allowed to stir at rt for 1 h. The product mixture was then taken up into DCM, dried onto Celite, and purified via a 6 inch silica gel chromatographic column using two column volumes of hexanes, one of 10% Et_2O/hexanes, and four 20% Et_2O/hexanes, giving the product as a yellowish oil (757.4 mg, 70%).

Retro Diels-Alder reaction to CoQ_9. The oil from the allylation reaction was dried into a 20 mL scintillation vial, which was then evacuated to <15 torr and heated in an 85 °C aluminum

block. After 16 h, the reaction had turned into a dark red oil and the reaction was complete by thin-layer chromatography. The oil was dried onto Celite and purified using 20% Et_2O/hexanes on a silica gel column. The combined organics were then dried to a red oil which solidified under high vacuum to give CoQ_9 (651.5 mg, 93% yield).

14. Analytical data

Synthesis of 2-(4-methoxyphenyl)-1-phenylpropan-1-one (3)

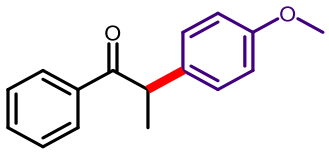

Compound **3** was obtained using the General Procedure A on a 0.5 mmol scale. The crude product was purified by silica gel column chromatography (eluent: 7% EtOAc/93% hexanes) to provide the desired compound as a clear oil that slowly solidifies to a white solid over time (115.9 mg, 97% yield). R_f = 0.38 (1:9 EtOAc/hexanes).

^{1}H NMR (400 MHz, $CDCl_3$): δ 7.95 (d, *J* = 7.3 Hz, 2H), 7.47 (t, *J* = 7.3 Hz, 1H), 7.38 (t, *J* = 7.6 Hz, 2H), 7.20 (d, *J* = 8.7 Hz, 2H), 6.83 (d, *J* = 8.7 Hz, 2H), 4.64 (q, *J* = 6.8 Hz, 1H), 3.75 (s, 3H), 1.51 (d, *J* = 6.8 Hz, 3H).

^{13}C NMR (101 MHz, $CDCl_3$): δ 200.5, 158.4, 136.5, 133.4, 132.7, 128.8, 128.7, 128.4, 114.3, 55.2, 46.9, 19.5.

Spectral data matched those previously reported.[2]

Synthesis of 2-([1,1'-biphenyl]-4-yl)-1-phenylpropan-1-one (4)

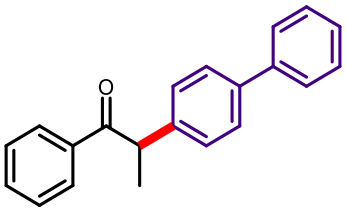

Compound **4** was obtained using the General Procedure A on a 0.5 mmol scale. The crude product was purified by silica gel chromatography (eluent: 5% EtOAc/95% hexanes) to provide the desired compound as a white solid (143.1 mg, 99% yield). R_f = 0.35 (0.5:9.5 EtOAc/hexanes).

^{1}H NMR (400 MHz, $CDCl_3$): δ 8.04 – 7.95 (m, 2H), 7.60 – 7.45 (m, 5H), 7.45 – 7.28 (m, 7H), 4.75 (q, *J* = 6.9 Hz, 1H), 1.58 (d, *J* = 6.9 Hz, 3H).

^{13}C NMR (101 MHz, $CDCl_3$): δ 200.3, 140.6, 140.4, 139.8, 136.4, 132.8, 128.8, 128.7, 128.5, 128.2, 127.7, 127.2, 127.0, 47.4, 19.5.

Spectral data matched those previously reported.[3]

Synthesis of 1-phenyl-2-(pyridin-3-yl)propan-1-one (5)

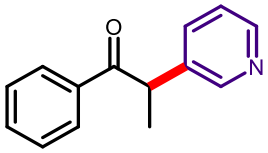

Compound **5** was obtained using the General Procedure C on a 0.5 mmol scale. The crude product was purified by silica gel chromatography (eluent: 0% to 50% EtOAc gradient/hexanes) to provide the desired compound as a white solid (102.1 mg, 97% yield). R_f = 0.32 (1:1 EtOAc/hexanes).

^{1}H NMR (400 MHz, $CDCl_3$): δ 8.59 (s, 1H), 8.44 (d, *J* = 4.0 Hz, 1H), 7.93 (d, *J* = 7.8 Hz, 2H), 7.59 (d, *J* = 7.8 Hz, 1H), 7.49 (t, *J* = 7.2 Hz, 1H), 7.38 (t, *J* = 7.5 Hz, 2H), 7.22 – 7.15 (m, 1H), 4.73 (q, *J* = 6.8 Hz, 1H), 1.54 (d, *J* = 6.9 Hz, 3H).

^{13}C NMR (101 MHz, $CDCl_3$): δ 199.5, 149.5, 148.4, 136.9, 135.9, 135.0, 133.2, 128.7, 128.6, 123.8, 44.9, 19.4.

Spectral data matched those previously reported.[4]

Synthesis of 2-(4-(dimethylamino)phenyl)-1-phenylpropan-1-one (6)

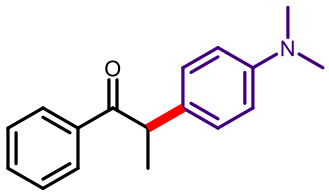

Compound **6** was obtained using the General Procedure A on a 0.5 mmol scale. The crude product was purified by silica gel chromatography (eluent: 0% to 8% EtOAc gradient/hexanes) to provide the desired compound as a yellow solid (119.2 mg, 94% yield). R_f = 0.52 (1:4 EtOAc/hexanes).

^{1}H NMR (400 MHz, $CDCl_3$): δ 7.99 (d, *J* = 7.9 Hz, 2H), 7.47 (t, *J* = 7.3 Hz, 1H), 7.38 (t, *J* = 7.5 Hz, 2H), 7.18 (d, *J* = 8.7 Hz, 2H), 6.68 (d, *J* = 8.7 Hz, 2H), 4.63 (q, *J* = 6.8 Hz, 1H), 2.91 (s, 6H), 1.53 (d, *J* = 6.8 Hz, 3H).

^{13}C NMR (101 MHz, $CDCl_3$): δ 200.7, 149.4, 136.7, 132.5, 129.0, 128.8, 128.4, 128.4, 113.0, 46.9, 40.5, 19.5.

Spectral data matched those previously reported.[5]

Synthesis of 2-(4-nitrophenyl)-1-phenylpropan-1-one (7)

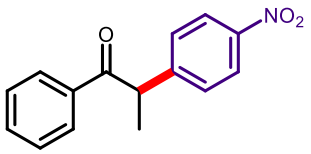

Compound **7** was obtained using the General Procedure B (aryl bromide) or General Procedure C (aryl chloride) on a 0.5 mmol scale. The crude product was purified by silica gel chromatography (eluent: 0% to 10% EtOAc gradient/hexanes) to provide the product as an orange oil (bromide: 68.9 mg, 54% yield; chloride: 76.7 mg, 60% yield). R_f = 0.47 (1:4 EtOAc/hexanes).

^{1}H NMR (600 MHz, $CDCl_3$): δ 8.15 (d, *J* = 8.7 Hz, 2H), 7.93 (d, *J* = 7.4 Hz, 2H), 7.52 (t, *J* = 7.4 Hz, 1H), 7.47 (d, *J* = 8.7 Hz, 2H), 7.42 (t, *J* = 7.8 Hz, 2H), 4.83 (q, *J* = 6.9 Hz, 1H), 1.58 (d, *J* = 6.9 Hz, 3H).

^{13}C NMR (101 MHz, $CDCl_3$): δ 199.2, 148.8, 147.0, 136.0, 133.5, 128.9, 128.8, 124.3, 47.5, 19.5.

HRMS (ESI): *m/z* calcd for $C_{15}H_{12}NO_3$-H^+: 254.0817 [*M*-H]$^-$; found: 254.0808.

Synthesis of 2-(4-(methylthio)phenyl)-1-phenylpropan-1-one (8)

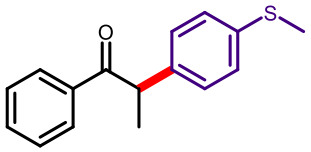

Compound **8** was obtained using the General Procedure B on a 0.5 mmol scale. The crude product was purified by silica gel chromatography (eluent: 5% EtOAc/95% hexanes) to provide the product as a yellow crystalline solid (116.6 mg, 91% yield). R_f = 0.39 (1:9 EtOAc/hexanes).

^{1}H NMR (500 MHz, $CDCl_3$): δ 7.97 – 7.92 (m, 2H), 7.51 – 7.45 (m, 1H), 7.41 – 7.35 (m, 2H), 7.23 – 7.16 (m, 4H), 4.65 (q, *J* = 6.9 Hz, 1H), 2.43 (s, 3H), 1.52 (d, *J* = 6.9 Hz, 3H).

^{13}C NMR (126 MHz, $CDCl_3$): δ 200.2, 138.3, 137.0, 136.4, 132.8, 128.8, 128.5, 128.3, 127.2, 47.3, 19.4, 15.8.

Spectral data matched those previously reported.[6]

Synthesis of 2-(1-benzyl-1H-pyrrolo[2,3-b]pyridin-5-yl)-1-(p-tolyl)propan-1-one (9)

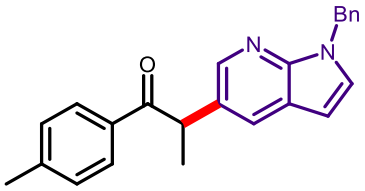

Compound **9** was obtained using the General Procedure B on a 0.5 mmol scale. The crude product was purified by silica gel chromatography (eluent: 10% EtOAc/90% hexanes) to provide the product as an off-white solid (152.4 mg, 86%). R_f = 0.23 (1:9 EtOAc/hexanes).

^{1}H NMR (500 MHz, $CDCl_3$): δ 8.37 (d, *J* = 2.2 Hz, 1H), 7.92 (d, *J* = 8.0 Hz, 2H), 7.84 (d, *J* = 2.2 Hz, 1H), 7.31 – 7.22 (m, 3H), 7.21 – 7.16 (m, 4H), 7.13 (d, *J* = 3.6 Hz, 1H), 6.40 (d, *J* = 3.5 Hz, 1H), 5.50 – 5.39 (m, 2H), 4.84 (q, *J* = 6.8 Hz, 1H), 2.33 (s, 3H), 1.61 (d, *J* = 6.9 Hz, 3H).

^{13}C NMR (126 MHz, $CDCl_3$): δ 199.8, 146.9, 143.5, 143.1, 137.5, 133.7, 129.1, 128.8, 128.6, 128.4, 127.5, 127.4, 127.4, 120.5, 99.9, 47.7, 44.8, 21.4, 19.9.

HRMS (ESI): *m/z* calcd for $C_{24}H_{22}N_2O+H^+$: 355.1810 $[M+H]^+$; found 355.1806.

Synthesis of 5-(4-(dimethylamino)phenyl)-6,7-dihydrobenzo[b]thiophen-4(5H)-one (10)

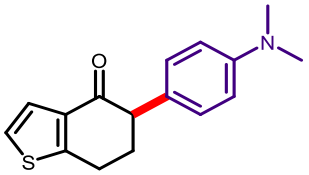

Compound **10** was obtained using the General Procedure B on a 0.5 mmol scale. The crude product was purified by silica gel chromatography (eluent: 8% EtOAc/92% hexanes) to provide the product as a grey solid (99.1 mg, 73% yield). R_f = 0.80 (1:9 EtOAc/hexanes).

^{1}H NMR (500 MHz, $CDCl_3$): δ 7.46 (d, *J* = 5.3 Hz, 1H), 7.10 – 7.04 (m, 3H), 6.75 – 6.70 (m, 2H), 3.69 (t, *J* = 7.2 Hz, 1H), 3.11 (q, *J* = 6.1 Hz, 2H), 2.94 (s, 6H), 2.46 (td, *J* = 6.8, 5.3 Hz, 2H).

^{13}C NMR (126 MHz, $CDCl_3$): δ 193.7, 155.2, 149.7, 137.6, 129.0, 126.9, 125.4, 123.3, 112.9, 52.2, 40.7, 32.7, 24.5.

HRMS (ESI): *m/z* calcd for $C_{16}H_{17}NOS+H^+$: 272.1109 $[M+H]^+$; found 272.1111.

Synthesis of 2-(2-methoxynaphthalen-1-yl)-1-(thiophen-2-yl)ethan-1-one (11)

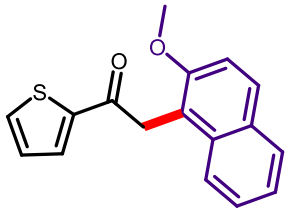

Compound **11** was obtained using the General Procedure B on a 0.5 mmol scale, in this case increasing the aryl ketone to 0.85 mmol (1.7 equiv). The crude product was purified by silica gel chromatography (eluent: 0% to 10% EtOAc gradient/hexanes) to provide the product as a white solid (125.2 mg, 89%). R_f = 0.44 (1:4 EtOAc/hexanes).

^{1}H NMR (500 MHz, $CDCl_3$): δ 7.94 (d, *J* = 3.7 Hz, 1H), 7.90 (d, *J* = 8.6 Hz, 1H), 7.87 – 7.79 (m, 2H), 7.61 (d, *J* = 4.9 Hz, 1H), 7.48 (t, *J* = 7.6 Hz, 1H), 7.36 (t, *J* = 7.5 Hz, 1H), 7.31 (d, *J* = 9.0 Hz, 1H), 7.13 (t, *J* = 4.4 Hz, 1H), 4.73 (s, 2H), 3.94 (s, 3H).

^{13}C NMR (126 MHz, $CDCl_3$): δ 190.9, 154.8, 144.1, 133.6, 133.5, 132.1, 129.3, 129.2, 128.5, 128.0, 126.9, 123.5, 123.3, 116.4, 113.2, 56.6, 36.7.

HRMS (ESI): *m/z* calcd for $C_{17}H_{14}O_2S+Na^+$: 305.0612 $[M+Na]^+$; found 305.0618.

Synthesis of 1-(furan-2-yl)-2-mesitylethan-1-one (12)

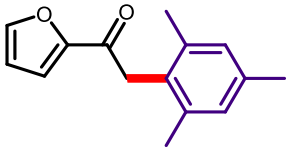

Compound **12** was obtained using the General Procedure B on a 0.5 mmol scale, in this case increasing the aryl ketone to 0.85 mmol (1.7 equiv.). The crude product was purified by silica gel chromatography (eluent: 0% to 10% EtOAc gradient/hexanes) to provide the product as a white solid (83.1 mg, 73% yield). R_f = 0.41 (1:4 EtOAc/hexanes).

^{1}H NMR (500 MHz, $CDCl_3$): δ 7.62 (s, 1H), 7.20 (d, *J* = 2.9 Hz, 1H), 6.90 (s, 2H), 6.59 – 6.53 (m, 1H), 4.22 (s, 2H), 2.29 (s, 3H), 2.24 (s, 6H).

^{13}C NMR (126 MHz, $CDCl_3$): δ 186.5, 152.7, 146.1, 137.0, 136.4, 128.8, 128.5, 116.8, 112.2, 39.2, 20.9, 20.3

HRMS (ESI): *m/z* calcd for $C_{15}H_{16}O_2+Na^+$: 251.1048 $[M+Na]^+$; found: 251.1057.

Synthesis of 2-(4-(dimethylamino)phenyl)-2-methyl-3,4-dihydronaphthalen-1(2H)-one (13)

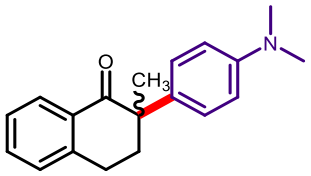

Compound **13** was obtained using the General Procedure B on a 0.5 mmol scale. The crude product was purified by silica gel chromatography (eluent: 0% to 10% EtOAc gradient/hexanes) to provide the product as a white powder (125.0 mg, 90%). R_f = 0.63 (1:4 EtOAc/hexanes).

^{1}H NMR (400 MHz, $CDCl_3$): δ 8.16 (dd, *J* = 7.8, 1.6 Hz, 1H), 7.40 (td, *J* = 7.4, 1.6 Hz, 1H), 7.29 (t, *J* = 7.5 Hz, 1H), 7.16 – 7.05 (m, 3H), 6.70 – 6.61 (m, 2H), 2.89 (s, 7H), 2.79 (dt, *J* = 17.0, 4.1 Hz, 1H), 2.59 (dt, *J* = 13.9, 4.0 Hz, 1H), 2.24 (ddd, *J* = 14.1, 11.9, 4.6 Hz, 1H), 1.50 (s, 3H).

^{13}C NMR (101 MHz, $CDCl_3$): δ 201.6, 149.2, 143.7, 132.8, 132.8, 129.2, 128.6, 127.9, 127.0, 126.4, 112.6, 49.5, 40.5, 36.0, 27.4, 26.2.

HRMS (ESI): *m/z* calcd for $C_{19}H_{21}NO+Na^+$: 302.1521 $[M+Na]^+$; found: 302.1525.

Synthesis of 2-(1H-indazol-5-yl)-6-methoxy-3,4-dihydronaphthalen-1(2H)-one (14)

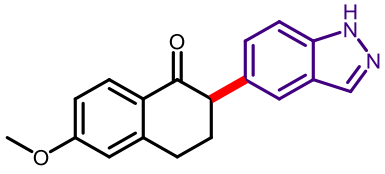

Compound **14** was obtained using the General Procedure B on a 0.5 mmol scale using the THP protected bromide. After completing the coupling reaction by TLC, the aqueous phase was acidified using conc. HCl to pH< 1 and allowed to stir at 45 °C until complete deprotection

to form product **14**. The aqueous phase was neutralized using satd. $NaHCO_3$ and extracted with EtOAc (3 x 1 mL). The crude product was purified by silica gel chromatography (eluent: 60% EtOAc/30% hexanes) to provide the product as a white solid (95.0 mg, 65% yield over two steps). R_f = 0.33 (3:2 EtOAc/hexanes).

^{1}H NMR (500 MHz, DMSO): δ 12.98 (s, 1H), 8.00 (s, 1H), 7.89 (d, *J* = 8.3 Hz, 1H), 7.52 (s, 1H), 7.48 (d, *J* = 8.7 Hz, 1H), 7.17 (d, *J* = 8.7 Hz, 1H), 6.99 – 6.87 (m, 2H), 3.96 (dd, *J* = 11.5, 4.6 Hz, 1H), 3.85 (s, 3H), 3.11 (td, *J* = 11.4, 5.5 Hz, 1H), 2.96 (dt, *J* = 17.1, 4.8 Hz, 1H), 2.39 (tt, *J* = 10.9, 5.7 Hz, 1H), 2.29 (dq, *J* = 9.0, 4.5 Hz, 1H).

^{13}C NMR (126 MHz, DMSO): δ 196.7, 163.2, 146.9, 138.9, 133.2, 132.5, 129.2, 127.3, 126.0, 122.9, 119.5, 113.5, 112.6, 109.7, 55.5, 53.2, 31.2, 28.6.

HRMS (ESI): *m/z* calcd for $C_{18}H_{16}N_2O_2$+Na^+: 315.1110 $[M+Na]^+$; found 315.1111.

Synthesis of 2-(4-morpholinophenyl)-1,2-diphenylethan-1-one (15)

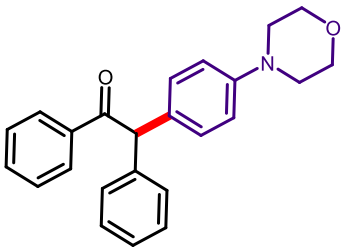

Compound **15** was obtained using the General Procedure B on a 0.5 mmol scale. The crude product was purified by silica gel chromatography (eluent: 30% EtOAc/70% hexanes) to provide the product as a white powder (178.0 mg, 99% yield). R_f = 0.33 (3:7 EtOAc/hexanes).

^{1}H NMR (500 MHz, $CDCl_3$): δ 8.03 (d, *J* = 7.7 Hz, 2H), 7.51 (t, *J* = 7.4 Hz, 1H), 7.41 (t, *J* = 7.7 Hz, 2H), 7.36 – 7.30 (m, 2H), 7.30 – 7.25 (m, 3H), 7.21 (d, *J* = 8.6 Hz, 2H), 6.88 (d, *J* = 8.7 Hz, 2H), 5.99 (s, 1H), 3.91 – 3.78 (m, 4H), 3.19 – 3.09 (m, 4H).

^{13}C NMR (126 MHz, $CDCl_3$): δ 198.4, 150.1, 139.5, 136.9, 132.8, 130.1, 129.8, 129.0, 128.9, 128.5, 128.5, 126.9, 115.7, 66.8, 58.5, 49.0.

HRMS (ESI): *m/z* calcd for $C_{24}H_{23}NO_2$+Na^+: 380.1627 [*M*+Na]$^+$; found: 380.1630.

Synthesis of 2-(4-(dimethylamino)phenyl)-1-(thiophen-2-yl)propan-1-one (16)

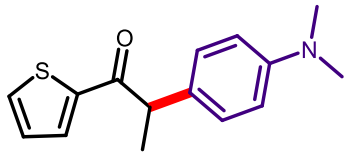

Compound **16** was obtained using the General Procedure B on a 0.5 mmol scale. The crude product was purified by silica gel chromatography (eluent: 0% to 10% EtOAc gradient/hexanes) to provide the product as a yellow solid (129.9 mg, 99% yield). R_f = 0.45 (1:4 EtOAc/hexanes).

^{1}H NMR (400 MHz, $CDCl_3$): δ 7.70 (d, *J* = 4.1 Hz, 1H), 7.52 (d, *J* = 4.9 Hz, 1H), 7.21 (d, *J* = 8.8 Hz, 2H), 7.03 (t, *J* = 4.3 Hz, 1H), 6.69 (d, *J* = 8.8 Hz, 2H), 4.43 (q, *J* = 6.8 Hz, 1H), 2.91 (s, 6H), 1.52 (d, *J* = 6.8 Hz, 3H).

^{13}C NMR (101 MHz, $CDCl_3$): δ 193.8, 149.6, 143.9, 133.2, 132.3, 128.9, 128.4, 128.0, 112.9, 48.4, 40.5, 19.1

HRMS (ESI): *m/z* calcd for $C_{15}H_{17}NOS$+Na^+: 282.0929 [*M*+Na]$^+$; found: 282.0933.

Synthesis of 1-(4-fluorophenyl)-1-(2-(piperidin-1-yl)pyrimidin-5-yl)propan-2-one (17)

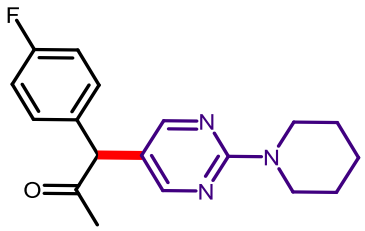

Compound **17** was obtained using the General Procedure B, modified to run at an internal temperature of 70 °C, and, as a separate trial, General Procedure C, both on a 0.5 mmol scale. The crude product was purified by silica gel chromatography (eluent: 25% EtOAc/75% hexanes) to provide the product as a yellow oil (Procedure B: 83.0 mg, 53% yield; Procedure C: 105.1 mg, 67% yield). R_f = 0.28 (1:3 EtOAc/hexanes).

^{1}H NMR (400 MHz, $CDCl_3$): δ 8.12 (s, 2H), 7.23 – 7.13 (m, 2H), 7.09 – 6.97 (m, 2H), 4.82 (s, 1H), 3.78 – 3.66 (m, 4H), 2.22 (s, 3H), 1.68 – 1.52 (m, 6H).

^{13}C NMR (101 MHz, $CDCl_3$): δ 205.4, 162.1 (d, *J* = 246.9 Hz), 160.8, 157.7, 133.3 (d, *J* = 3.4 Hz), 130.1 (d, *J* = 8.1 Hz), 118.5, 115.9 (d, *J* = 21.6 Hz), 58.8, 44.7, 29.5, 25.6, 24.7.

HRMS (ESI): *m/z* calcd for $C_{18}H_{20}FN_3O+H^+$: 314.1669 $[M+H]^+$; found: 314.1674.

Synthesis of 2-(4-(methylthio)phenyl)-1-(pyridin-3-yl)propan-1-one (18)

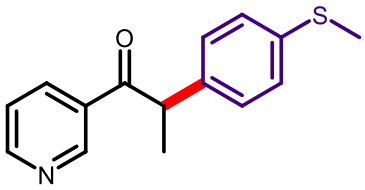

Compound **18** was obtained using the General Procedure B on a 0.5 mmol scale. The crude product was purified by silica gel chromatography (eluent: 35% EtOAc/65% hexanes) to provide the product as a yellow solid (125.6, 98% yield). R_f = 0.36 (2:3 EtOAc/hexanes).

^{1}H NMR (500 MHz, $CDCl_3$): δ 9.12 (d, *J* = 2.6 Hz, 1H), 8.65 (dd, *J* = 4.9, 1.8 Hz, 1H), 8.16 (dt, *J* = 7.9, 1.9 Hz, 1H), 7.31 (ddd, *J* = 8.0, 4.8, 0.8 Hz, 1H), 7.16 (s, 4H), 4.57 (q, *J* = 6.9 Hz, 1H), 2.41 (s, 3H), 1.51 (d, *J* = 6.7 Hz, 3H).

^{13}C NMR (126 MHz, $CDCl_3$): δ 198.9, 153.1, 150.1, 137.6, 137.2, 136.1, 131.6, 128.2, 127.3, 123.6, 48.0, 19.0, 15.7.

HRMS (ESI): *m/z* calcd for $C_{15}H_{15}NOS+H^+$: 258.0953 $[M+H]^+$; found: 258.0955.

Synthesis of *t*-butyl 5-(1-oxo-1-(thiophen-2-yl)propan-2-yl)-1H-indole-1-carboxylate (19)

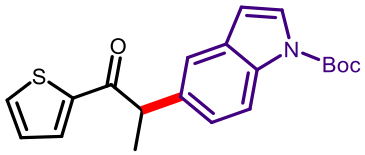

Compound **19** was obtained using the General Procedure C on a 0.5 mmol scale. The crude product was purified by silica gel chromatography (eluent: 10% EtOAc/90% hexanes) to provide the product as a yellow oil (152.1 mg, 87% yield). R_f = 0.33 (1:9 EtOAc/hexanes).

^{1}H NMR (400 MHz, $CDCl_3$): δ 8.07 (d, *J* = 8.7 Hz, 1H), 7.68 (dd, *J* = 3.8, 1.2 Hz, 1H), 7.57 (d, *J* = 3.8 Hz, 1H), 7.54 – 7.47 (m, 2H), 7.28 (dd, *J* = 8.5, 2.0 Hz, 1H), 7.00 (dd, *J* = 5.0, 3.8 Hz, 1H), 6.52 (d, *J* = 3.7 Hz, 1H), 4.60 (q, *J* = 6.9 Hz, 1H), 1.65 (s, 9H), 1.58 (d, *J* = 6.8 Hz, 3H).

^{13}C NMR (101 MHz, $CDCl_3$): δ 193.5, 149.7, 143.7, 135.8, 133.4, 132.5, 131.1, 128.0, 126.4, 124.1, 119.9, 115.6, 107.2, 83.7, 49.3, 28.1, 19.5

HRMS (ESI): *m/z* calcd for $C_{20}H_{21}NO_3S+Na^+$: 378.1140 $[M+Na]^+$; found: 378.1131.

Synthesis of *t*-butyl 5-(1-(4-chlorophenyl)-1-oxopropan-2-yl)-1H-indole-1-carboxylate (20)

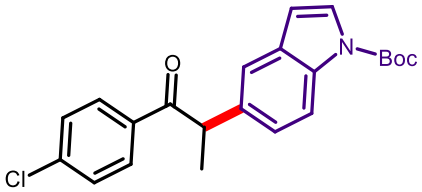

Compound **20** was obtained using the General Procedure C on a 0.5 mmol scale. The crude product was purified by silica gel chromatography (eluent: 5% EtOAc/95% hexanes) to provide the product as a white oil (116.3 mg, 61% yield). R_f = 0.30 (0.5:9.5 EtOAc/hexanes).

^{1}H NMR (400 MHz, $CDCl_3$): δ 8.07 (d, *J* = 8.6 Hz, 1H), 7.89 (d, *J* = 8.6 Hz, 2H), 7.57 (d, *J* = 3.9 Hz, 1H), 7.42 (d, *J* = 2.0 Hz, 1H), 7.31 (d, *J* = 8.6 Hz, 2H), 7.21 (dd, *J* = 8.4, 2.0 Hz, 1H), 6.50 (d, *J* = 3.7 Hz, 1H), 4.69 (q, *J* = 6.8 Hz, 1H), 1.64 (s, 9H), 1.56 (d, *J* = 6.8 Hz, 3H).

^{13}C NMR (101 MHz, $CDCl_3$): δ 199.2, 149.6, 139.0, 135.6, 134.8, 131.2, 130.2, 128.7, 126.5, 123.9, 120.0, 115.8, 107.1, 83.8, 48.0, 28.1, 19.7.

HRMS (ESI): *m/z* calcd for $C_{22}H_{22}ClNO_3$+Na^++CH_3OH: 438.1448 [*M*+Na+CH_3OH]$^+$; found 438.1451.

Synthesis of 2-(4-(dimethylamino)phenyl)-1-(thiazol-2-yl)propan-1-one (21)

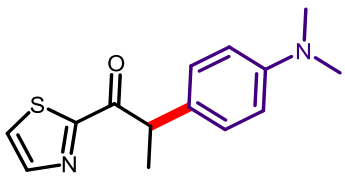

Compound **21** was obtained using the General Procedure C on a 0.5 mmol scale. The crude product was purified by silica gel chromatography (eluent: 7% EtoAC/93% hexanes) to provide the product as a yellow solid (37.9 mg, 29% yield. R_f = 0.20 (1:9 EtOAc/hexanes).

^{1}H NMR (500 MHz, $CDCl_3$): δ 7.97 (d, *J* = 3.0 Hz, 1H), 7.58 (d, *J* = 3.0 Hz, 1H), 7.28 (d, *J* = 8.8 Hz, 2H), 6.67 (d, *J* = 8.8 Hz, 2H), 5.05 (q, *J* = 7.1 Hz, 1H), 2.90 (s, 6H), 1.55 (d, *J* = 7.1 Hz, 3H).

^{13}C NMR (126 MHz, CDC_3): δ 194.0, 167.1, 149.7, 144.6, 129.1, 127.4, 126.1, 112.8, 46.0, 40.5, 18.0.

HRMS (ESI): *m/z* calcd for $C_{14}H_{16}N_2OS+Na^+$: 283.0881 $[M+Na]^+$; found 283.0887.

Synthesis of 2-((1-benzylpiperidin-4-yl)methyl)-5,6-dimethoxy-2-(4-methoxyphenyl)-2,3-dihydro-1H-inden-1-one (22)

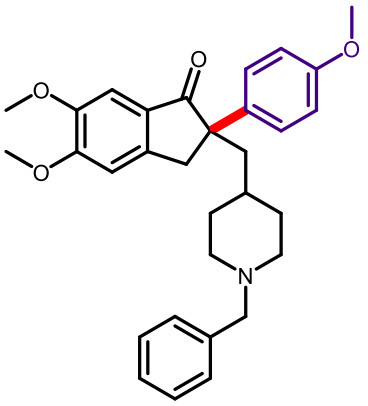

Compound **22** was obtained using General Procedure C on a 0.5 mmol scale, in this case using 0.5 mmol of the aryl ketone and 0.6 mmol of the aryl bromide. The crude product was purified by silica gel chromatography (eluent: 5% MeOH/95% DCM) to provide the product as a white solid (151.2 mg, 62% yield). R_f = 0.28 (0.5:9.5 MeOH/DCM).

^{1}H NMR (400 MHz, $CDCl_3$): δ 7.36 – 7.20 (m, 7H), 7.15 (s, 1H), 6.89 (s, 1H), 6.84 – 6.76 (m, 2H), 3.98 (s, 3H), 3.89 (s, 3H), 3.75 (s, 3H), 3.59 – 3.45 (m, 3H), 3.28 (d, *J* = 17.1 Hz, 1H), 2.89 – 2.74 (m, 2H), 2.20 (d, *J* = 12.1 Hz, 1H), 2.00 – 1.81 (m, 3H), 1.54 – 1.34 (m, 5H).

^{13}C NMR (101 MHz, $CDCl_3$): δ 206.3, 158.1, 155.6, 149.6, 147.5, 134.2, 129.6, 128.3, 128.2, 127.6, 127.4, 113.8, 107.0, 105.1, 62.9, 56.5, 56.2, 56.0, 55.2, 53.4, 51.1, 44.5, 41.0, 33.3, 32.5.

HRMS (ESI): *m/z* calcd for $C_{31}H_{35}NO_4+H^+$: 486.2644 $[M+H]^+$; found 486.2647.

Synthesis of 4-(4-(4-chlorophenyl)-4-hydroxypiperidin-1-yl)-1-(4-fluorophenyl)-2-(naphthalen-2-yl)butan-1-one (23)

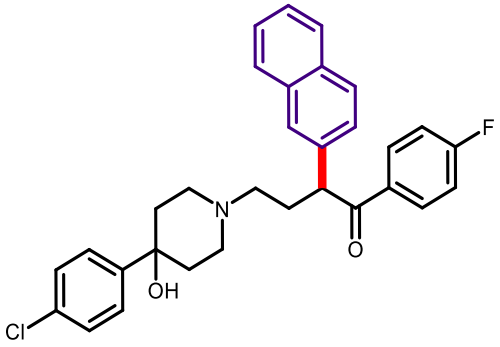

Compound **23** was obtained using General Procedure C on a 0.5 mmol scale, in this case using 0.5 mmol of the aryl ketone and 0.6 mmol of the aryl bromide. The crude product was purified by silica gel chromatography (eluent: 5% MeOH/95% DCM) to provide the product as a white solid (190.2 mg, 76% yield). R_f = 0.27 (0.5:9.5 MeOH/DCM).

^{1}H NMR (400 MHz, $CDCl_3$): δ 8.14 – 7.99 (m, 2H), 7.84 – 7.69 (m, 4H), 7.52 – 7.39 (m, 3H), 7.36 – 7.23 (m, 4H), 7.06 (t, *J* = 8.6 Hz, 2H), 5.29 (s, 1H), 4.84 (t, *J* = 6.9 Hz, 1H), 2.89 – 2.71 (m, 2H), 2.65 (dq, *J* = 15.2, 7.6 Hz, 1H), 2.58 – 2.33 (m, 4H), 2.16 – 1.79 (m, 4H), 1.64 (d, *J* = 13.9 Hz, 2H).

^{13}C NMR (101 MHz, $CDCl_3$): δ 197.7, 165.6 (d, *J* = 254.8 Hz), 146.8, 136.9, 133.7, 133.5 (d, *J* = 3.0 Hz), 132.9, 132.6, 131.5 (d, *J* = 9.3 Hz), 129.0, 128.5, 127.8, 127.8, 127.1, 126.4, 126.2, 126.2, 126.1, 115.7 (d, *J* = 21.8 Hz), 71.0, 56.6, 51.8, 49.9, 48.8, 38.2, 38.1, 31.4.

HRMS (ESI): *m/z* calcd for $C_{31}H_{29}ClFNO_2+H^+$: 502.1949 $[M+H]^+$; found: 502.1949.

Synthesis of 2,2-*bis*(4-(dimethylamino)phenyl)-1-(thiophen-2-yl)ethan-1-one (24)

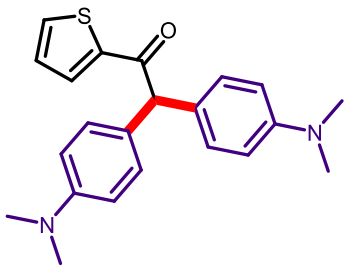

Compound **24** was obtained using the General Procedure B on a 0.5 mmol scale. The crude product was purified by silica gel chromatography (eluent: 0% to 20% EtOAc gradient/hexanes) to provide the product as a yellow solid (90.2 mg, 99% yield). R_f = 0.27 (1:4 EtOAc/hexanes).

^{1}H NMR (400 MHz, $CDCl_3$): δ 7.76 (d, *J* = 3.3 Hz, 1H), 7.55 (d, *J* = 4.7 Hz, 1H), 7.19 (d, *J* = 8.5 Hz, 4H), 7.10 – 7.01 (m, 1H), 6.70 (d, *J* = 8.5 Hz, 4H), 5.71 (s, 1H), 2.92 (s, 12H).

^{13}C NMR (101 MHz, $CDCl_3$): δ 192.3, 149.6, 144.6, 133.4, 132.5, 129.6, 128.0, 127.4, 112.7, 58.9, 40.6.

HRMS (ESI): *m/z* calcd for $C_{22}H_{24}N_2OS+Na^+$: 387.1507 $[M+Na]^+$; found: 387.1507.

Synthesis of 1-(furan-2-yl)-2,2-di(naphthalen-2-yl)ethan-1-one (25)

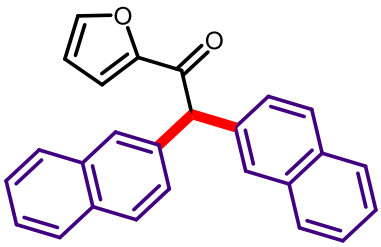

Compound **25** was obtained using the General Procedure B on a 0.5 mmol scale. The crude product was purified by silica gel chromatography (eluent: 0% to 15% EtOAc

gradient/hexanes) to provide the product as a tan solid (83.3 mg, 92% yield). R_f = 0.27 (1:4 EtOAc/hexanes).

^{1}H NMR (500 MHz, $CDCl_3$): δ 7.89 – 7.76 (m, 8H), 7.58 – 7.55 (m, 1H), 7.55 – 7.51 (m, 2H), 7.47 (dd, *J* = 6.2, 3.3 Hz, 4H), 7.33 (d, *J* = 3.5 Hz, 1H), 6.50 (dd, *J* = 3.5, 1.5 Hz, 1H), 6.24 (s, 1H).

^{13}C NMR (126 MHz, $CDCl_3$): δ 187.3, 152.7, 146.8, 136.0, 133.5, 132.6, 128.4, 128.0, 127.9, 127.6, 127.4, 126.2, 126.1, 118.5, 112.6, 59.0.

HRMS (ESI): *m/z* calcd for $C_{26}H_{18}O_2$+Na^+: 385.1205 $[M+Na]^+$; found: 385.1204.

Synthesis of 2,2-*bis*(2,4-dimethoxyphenyl)-1-(thiophen-2-yl)ethan-1-one (26)

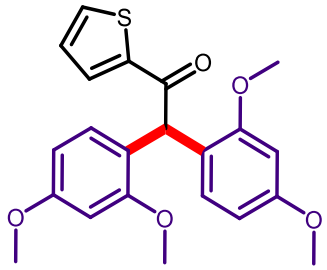

Compound **26** was obtained using the General Procedure B on a 0.5 mmol scale. The crude product was purified by silica gel chromatography (eluent: 0% to 20% EtOAc gradient/hexanes) to provide the product as a white solid (80.2 mg, 81% yield). R_f = 0.18 (1:4 EtOAc/hexanes).

^{1}H NMR (400 MHz, $CDCl_3$): δ 7.81 – 7.70 (m, 1H), 7.58 – 7.49 (m, 1H), 7.07 – 7.00 (m, 1H), 6.95 (d, *J* = 8.4 Hz, 2H), 6.49 (d, *J* = 2.3 Hz, 2H), 6.42 (dd, *J* = 8.5, 2.4 Hz, 2H), 6.36 (s, 1H), 3.78 (s, 6H), 3.77 (s, 6H).

^{13}C NMR (101 MHz, $CDCl_3$): δ 192.5, 160.0, 157.8, 144.3, 132.6, 131.7, 130.3, 127.8, 119.4, 104.0, 98.8, 55.6, 55.3, 46.2.

HRMS (ESI): *m/z* calcd for $C_{22}H_{22}O_5S+Na^+$: 421.1086 $[M+Na]^+$; found: 421.1079.

Synthesis of 1-(2,4-dimethylthiazol-5-yl)-2,2-*bis*(4-morpholinophenyl)ethan-1-one (27)

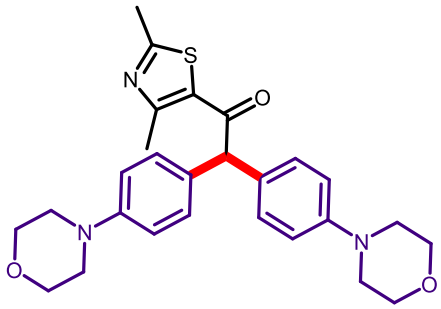

Compound **27** was obtained using the General Procedure C on a 0.5 mmol scale. The crude product was purified by silica gel chromatography (eluent: 0% to 75% EtOAc gradient/hexanes) to afford the product as a light-yellow solid (105.7 mg, 88% yield). R_f = 0.18 (1:1 EtOAc/hexanes).

^{1}H NMR (500 MHz, $CDCl_3$): δ 7.14 (d, *J* = 8.6 Hz, 4H), 6.85 (d, *J* = 8.6 Hz, 4H), 5.38 (s, 1H), 3.87 – 3.79 (m, 8H), 3.17 – 3.07 (m, 8H), 2.70 (s, 3H), 2.62 (s, 3H).

^{13}C NMR (126 MHz, $CDCl_3$): δ 191.9, 168.3, 160.5, 150.3, 129.9, 129.8, 129.6, 115.6, 66.9, 62.9, 49.1, 19.4, 18.3.

HRMS (ESI): *m/z* calcd for $C_{27}H_{31}N_3O_3S+Na^+$: 500.1984 $[M+Na]^+$; found: 500.1984.

Synthesis of 2-(4-(2-(dimethylamino)ethoxy)phenyl)-1,2-diphenylethan-1-one (29)

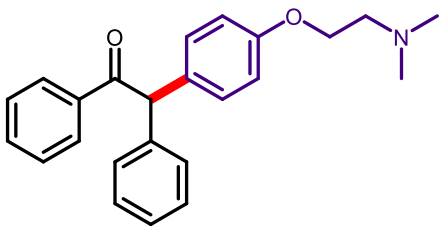

Compound **29** was obtained using the procedure outlined in the tamoxifen synthesis section. The crude product was purified by silica gel chromatography (eluent: 1:9:0.1 MeOH/DCM/Et_3N) to provide the product as a viscous yellow oil (177.1 mg, 98% yield). R_f = 0.30 (1:9:0.1 MeOH/DCM/Et_3N).

^{1}H NMR (400 MHz, $CDCl_3$): δ 8.02 – 7.97 (m, 2H), 7.54 – 7.47 (m, 1H), 7.44 – 7.37 (m, 2H), 7.35 – 7.28 (m, 2H), 7.26 – 7.23 (m, 3H), 7.22 – 7.15 (m, 2H), 6.90 – 6.85 (m, 2H), 5.98 (s, 1H), 4.06 (t, *J* = 5.7 Hz, 2H), 2.77 (t, *J* = 5.7 Hz, 2H), 2.36 (s, 6H).

^{13}C NMR (101 MHz, $CDCl_3$): δ 198.4, 157.8, 139.4, 136.8, 133.0, 131.3, 130.1, 129.0, 128.9, 128.7, 128.6, 127.0, 114.8, 65.6, 58.6, 58.0, 45.6.

HRMS (ESI): *m/z* calcd for $C_{24}H_{25}NO_2+H^+$: 360.1964 $[M+H]^+$; found: 360.1962.

Synthesis of 2-(3-(1,3-dioxolan-2-yl)phenyl)-1-(4-chlorophenyl)propan-1-one (32)

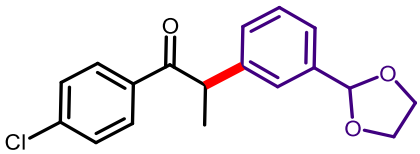

Compound **32** was obtained using the procedure outlined in the tandem procedure. The crude product was purified by silica gel chromatography (eluent: 20% EtOAc/80% hexanes) to provide the product as a clear oil (128.1 mg, 81% yield). R_f = 0.39 (3:7 EtOAc/hexanes).

^{1}H NMR (500 MHz, $CDCl_3$): δ 7.89 – 7.83 (m, 2H), 7.38 (t, *J* = 1.9 Hz, 1H), 7.35 – 7.28 (m, 4H), 7.24 (dt, *J* = 7.3, 1.8 Hz, 1H), 5.75 (s, 1H), 4.63 (q, *J* = 6.9 Hz, 1H), 4.16 – 3.94 (m, 4H), 1.52 (d, *J* = 6.7 Hz, 3H).

^{13}C NMR (126 MHz, $CDCl_3$): δ 199.0, 141.4, 139.3, 138.9, 134.8, 130.3, 129.3, 128.9, 128.6, 126.0, 125.4, 103.6, 65.4, 65.4, 48.1, 19.6.

HRMS (ESI): *m/z* calcd for $C_{18}H_{17}ClO_3$+Na^+: 339.0764 [*M*+Na]$^+$; found: 339.0774.

Synthesis of 3-(1-(2',4'-dimethyl-[1,1'-biphenyl]-4-yl)-1-oxopropan-2-yl)benzaldehyde (33)

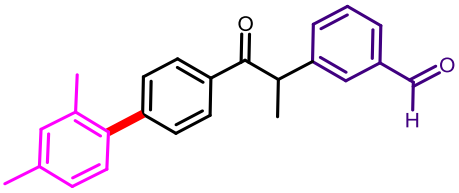

Compound **33** was obtained using the procedure outlined in the tandem procedure. The crude product was purified by silica gel chromatography (eluent: 15% EtOAc/85% hexanes) to provide the product as an opaque clear oil (115.2 mg, 67% yield over three steps). R_f = 0.61 (3:7 EtOAc/hexanes).

^{1}H NMR (500 MHz, $CDCl_3$): δ 10.01 (s, 1H), 8.01 (d, *J* = 8.6 Hz, 2H), 7.89 (s, 1H), 7.79 – 7.74 (m, 1H), 7.65 – 7.61 (m, 1H), 7.50 (t, *J* = 7.7 Hz, 1H), 7.37 (d, *J* = 8.6 Hz, 2H), 7.12 – 7.03 (m, 3H), 4.86 (q, *J* = 6.9 Hz, 1H), 2.36 (s, 3H), 2.22 (s, 3H), 1.61 (d, *J* = 7.0 Hz, 3H).

^{13}C NMR (126 MHz, $CDCl_3$): δ 199.5, 192.1, 147.1, 142.6, 137.7, 137.7, 137.1, 134.9, 134.4, 133.9, 131.3, 129.7, 129.7, 129.5, 129.0, 128.6, 128.6, 126.7, 47.3, 21.1, 20.3, 19.6.

HRMS (ESI): *m/z* calcd for $C_{24}H_{22}O_2$+Na^+: 365.1518 [*M*+Na]$^+$; found 363.1995.

Synthesis of 3-(1-(2',4'-dimethyl-[1,1'-biphenyl]-4-yl)-1-oxopropan-2-yl)benzyl 2-chloronicotinate (34)

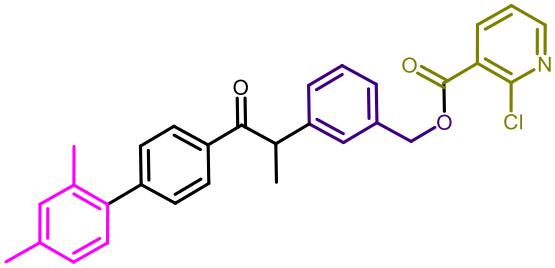

Compound **34** was obtained using the procedure outlined in the tandem procedure. The crude product was purified by silica gel chromatography (eluent: 25% EtOAc/75% hexanes) to provide the product as a clear oil (161.6 mg, 66% yield over five steps). R_f = 0.35 (3:7 EtOAc/hexanes).

^{1}H NMR (400 MHz, $CDCl_3$): δ 8.49 (dd, *J* = 4.9, 1.8 Hz, 1H), 8.20 – 8.11 (m, 1H), 8.01 (d, *J* = 8.2 Hz, 2H), 7.45 (s, 1H), 7.41 – 7.24 (m, 6H), 7.07 (d, *J* = 11.9 Hz, 3H), 5.37 (s, 2H), 4.79 (q, *J* = 6.9 Hz, 1H), 2.36 (s, 3H), 2.21 (s, 3H), 1.58 (d, *J* = 6.8 Hz, 3H).

^{13}C NMR (101 MHz, $CDCl_3$): δ 199.8, 164.3, 152.0, 150.1, 146.8, 142.0, 140.4, 137.7, 137.7, 135.8, 134.9, 134.5, 131.3, 129.5, 129.5, 129.4, 128.6, 128.1, 127.8, 127.0, 126.8, 126.6, 122.1, 67.6, 47.5, 21.1, 20.3, 19.6.

HRMS (ESI): *m/z* calcd for $C_{30}H_{26}ClNO_3$+Na^+: 506.1499 [*M*+Na]$^+$; found: 506.1492.

Synthesis of 2-(4-methoxyphenyl)-1-phenylpropan-1-one-2-d (35)

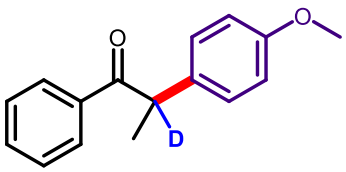

Compound **35** was obtained using the procedure outlined above. The crude product was purified by silica gel chromatography (eluent: 8% EtOAc/92% hexanes) to provide the product as an off-white solid (248.1 mg, 99% yield). R_f = 0.31 (8% EtOAc/92% hexanes).

^{1}H NMR (500 MHz, $CDCl_3$): δ 7.97 (d, *J* = 7.1 Hz, 2H), 7.50 – 7.43 (m, 1H), 7.41 – 7.35 (m, 2H), 7.23 (d, *J* = 8.7 Hz, 2H), 6.84 (d, *J* = 8.8 Hz, 2H), 3.73 (s, 3H), 1.52 (s, 3H).

^{13}C NMR (126 MHz, $CDCl_3$): δ 200.6, 158.5, 128.8, 128.8, 128.5, 114.4, 55.2, 46.5 (t, J = 19.5 Hz), 19.4.

HRMS (EI): *m/z* calcd for $C_{16}H_{15}O_2D^+$: 241.1213 $[M]^+$; found: 241.1217.

Synthesis of 4a-methyl-9a-((2E,6E,10E,14E,18E,22E,26E,30E)-3,7,11,15,19,23,27,31,35-nonamethylhexatriaconta-2,6,10,14,18,22,26,30,34-nonaen-1-yl)-1,4,4a,9a-tetrahydro-1,4-methanoanthracene-9,10-dione (36)

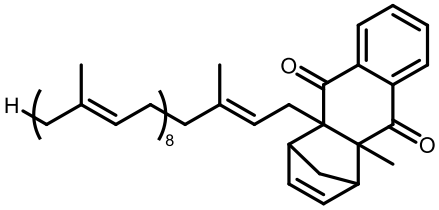

Compound **36** was prepared using the procedure outlined in section 10. Product was recovered as a golden yellow oil (2560 mg, quant.). R_f = 0.38 (8% Et_2O/92% hexanes).

^{1}H NMR (400 MHz, $CDCl_3$): δ 7.98 – 7.92 (m, 1H), 7.92 – 7.85 (m, 1H), 7.69 – 7.61 (m, 2H), 6.09 – 6.00 (m, 2H), 5.18 – 5.02 (m, 7H), 4.96 – 4.88 (m, 2H), 3.25 – 3.18 (m, 1H), 3.18 – 3.10

(m, 1H), 2.86 (dd, *J* = 15.0, 7.1 Hz, 1H), 2.48 (dd, *J* = 15.0, 6.8 Hz, 1H), 2.13 – 1.93 (m, 26H), 1.92 – 1.71 (m, 8H), 1.68 (d, *J* = 1.4 Hz, 3H), 1.63 – 1.55 (m, 26H), 1.51 – 1.43 (m, 4H).

^{13}C NMR (101 MHz, $CDCl_3$): δ 202.4, 201.8, 138.5, 137.9, 137.6, 137.0, 135.2, 135.1, 135.1, 135.1, 135.0, 135.0, 135.0, 134.0, 133.7, 131.4, 127.1, 126.3, 124.5, 124.4, 124.4, 124.3, 124.0, 120.0, 60.7, 57.3, 55.6, 54.3, 43.9, 39.9, 39.9, 39.8, 39.8, 36.6, 29.8, 26.9, 26.8, 26.8, 26.8, 26.5, 25.8, 23.8, 17.8, 16.5, 16.2, 16.1, 16.1, 16.1.

This compound matched spectra data from the literature.[7]

Synthesis of 4a-((2E,6E,10E,14E,18E,22E)-3,7,11,15,19,23,27-heptamethyloctacosa-2,6,10,14,18,22,26-heptaen-1-yl)-9a-methyl-1,4,4a,9a-tetrahydro-1,4-methanoanthracene-9,10-dione (37)

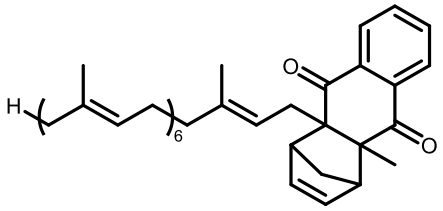

Product **37** was prepared using the procedure outlined in section 11. Product was recovered as a golden oil (869.4 mg, 97% yield). R_f = 0.4 (1:9 Et_2O/hexanes)

^{1}H NMR (500 MHz, $CDCl_3$): δ 7.98 – 7.92 (m, 1H), 7.92 – 7.87 (m, 1H), 7.71 – 7.61 (m, 2H), 6.09 – 6.00 (m, 2H), 5.15 – 5.04 (m, 5H), 4.98 – 4.87 (m, 2H), 3.24 – 3.19 (m, 1H), 3.14 (dd, *J* = 3.1, 1.4 Hz, 1H), 2.86 (dd, *J* = 15.1, 7.1 Hz, 1H), 2.48 (dd, *J* = 15.1, 6.9 Hz, 1H), 2.18 – 1.91 (m, 19H), 1.93 – 1.71 (m, 7H), 1.68 (d, *J* = 1.3 Hz, 3H), 1.65 – 1.50 (m, 20H), 1.52 – 1.43 (m, 4H).

^{13}C NMR (126 MHz, $CDCl_3$): δ 202.3, 201.7, 138.4, 137.7, 137.5, 136.9, 135.1, 135.0, 135.0, 134.9, 134.9, 134.9, 133.9, 133.5, 131.2, 126.9, 126.2, 124.4, 124.3, 124.3, 124.2, 123.9, 119.9,

60.6, 57.2, 55.5, 54.1, 43.7, 39.7, 39.7, 39.7, 39.7, 36.5, 26.8, 26.7, 26.7, 26.7, 26.7, 26.3, 25.7, 23.7, 17.7, 16.3, 16.0, 16.0, 16.0.

This compound matched spectra data from the literature.[8]

Synthesis of 6,7-dimethoxy-4a-methyl-1,4,4a,8a-tetrahydro-1,4-methanonaphthalene-5,8-dione (38)

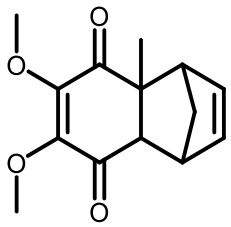

Product **38** was prepared using the procedure outlined in section 12. Product was recovered as an opaque oil that yellowed over time (5.39 g, 80% yield). R_f = 0.25 (1:1 Et_2O/hexanes).

^{1}H NMR (500 MHz, $CDCl_3$): δ 6.12 (dd, *J* = 5.7, 3.0 Hz, 1H), 5.98 (dd, *J* = 5.7, 2.9 Hz, 1H), 3.91 (s, 3H), 3.89 (s, 3H), 3.39 (ddt, *J* = 3.9, 2.7, 1.4 Hz, 1H), 3.05 (ddd, *J* = 2.7, 1.6, 0.9 Hz, 1H), 2.80 (d, *J* = 3.9 Hz, 1H), 1.63 (ddt, *J* = 9.2, 1.6, 0.8 Hz, 1H), 1.52 (dt, *J* = 9.2, 1.8 Hz, 1H), 1.45 (s, 3H).

^{13}C NMR (126 MHz, $CDCl_3$): δ 198.4, 194.8, 150.6, 150.5, 138.1, 134.5, 60.6, 60.6, 57.1, 53.4, 52.5, 48.8, 46.3, 26.5.

This compound matched spectral data from the literature.[9]

Synthesis of 6,7-dimethoxy-4a-methyl-8a-((2E,6E,10E,14E,18E,22E,26E,30E)-3,7,11,15,19,23,27,31,35-nonamethylhexatriaconta-2,6,10,14,18,22,26,30,34-nonaen-1-yl)-1,4,4a,8a-tetrahydro-1,4-methanonaphthalene-5,8-dione (39)

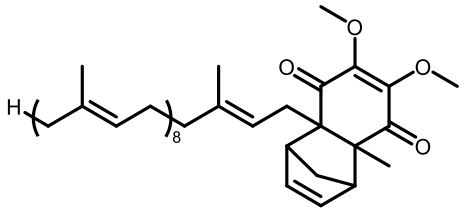

Compound **39** was prepared using the procedure outlined in section 13. Product was recovered as a yellowish oil (757.4 mg, 70%). R_f = 0.45 (1:3 EtOAc/hexanes).

^{1}H NMR (500 MHz, $CDCl_3$): δ 6.09 – 6.02 (m, 2H), 5.16 – 5.00 (m, 9H), 3.90 (s, 2H), 3.88 (s, 2H), 3.09 (q, *J* = 1.8 Hz, 1H), 3.01 (q, *J* = 1.8 Hz, 1H), 2.75 (dd, *J* = 15.2, 7.7 Hz, 1H), 2.47 – 2.37 (m, 1H), 2.05 (q, *J* = 6.7 Hz, 16H), 2.01 – 1.91 (m, 16H), 1.81 – 1.71 (m, 2H), 1.68 (q, *J* = 1.4 Hz, 3H), 1.59 (dd, *J* = 9.3, 1.2 Hz, 26H), 1.51 – 1.44 (m, 4H).

^{13}C NMR (126 MHz, $CDCl_3$): δ 198.8, 198.2, 150.8, 149.1, 138.1, 138.0, 137.2, 135.4, 135.0, 135.0, 134.9, 134.9, 134.9, 134.9, 131.2, 12.4, 124.3, 124.3, 124.3, 124.3, 124.2, 124.1, 123.8, 119.6, 60.3, 60.0, 59.3, 56.1, 54.5, 53.2, 43.5, 40.0, 39.8, 39.7, 36.1, 26.8, 26.7, 26.7, 26.7, 26.7, 26.5, 25.7, 23.4, 17.7, 16.4, 16.0, 16.0.

HRMS (ESI): *m/z* calcd for $C_{59}H_{88}O_4$+Na^+: 883.6572 [*M*+Na]$^+$; found: 883.6580.

Synthesis of 2-methyl-3-((2E,6E,10E,14E,18E,22E,26E,30E)-3,7,11,15,19,23,27,31,35-nonamethylhexatriaconta-2,6,10,14,18,22,26,30,34-nonaen-1-yl)naphthalene-1,4-dione (MK-9, K_2)

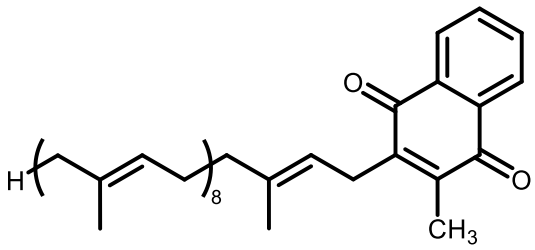

MK-9, K_2 was synthesized using the procedure outlined in section 10. Product was recovered as a yellow solid (1840.0 mg, 77 % yield). R_f = 0.50 (1:9 Et_2O/hexanes).

^{1}H NMR (400 MHz, $CDCl_3$): δ 8.08 (ddt, *J* = 4.8, 3.2, 2.0 Hz, 2H), 7.73 – 7.63 (m, 2H), 5.17 – 4.98 (m, 9H), 3.37 (d, *J* = 6.9 Hz, 2H), 2.19 (s, 3H), 2.12 – 1.91 (m, 32H), 1.80 (d, *J* = 1.3 Hz, 3H), 1.68 (d, *J* = 1.4 Hz, 3H), 1.63 – 1.54 (m, 24H).

^{13}C NMR (101 MHz, $CDCl_3$): δ 185.4, 184.5, 146.1, 143.3, 137.5, 135.2, 134.9, 134.9, 134.9, 133.3, 133.2, 132.2, 132.1, 131.2, 126.3, 126.2, 124.4, 124.3, 124.2, 124.2, 124.1, 123.8, 119.1, 39.7, 39.7, 39.7, 29.7, 26.7, 26.7, 26.7, 26.6, 26.5, 26.0, 25.7, 17.7, 16.4, 16.0, 16.0, 16.0, 12.7. This compound matched spectral data from the literature.[10]

Synthesis of 2-((2E,6E,10E,14E,18E,22E)-3,7,11,15,19,23,27-heptamethyloctacosa-2,6,10,14,18,22,26-heptaen-1-yl)-3-methylnaphthalene-1,4-dione (MK-7, K_2)

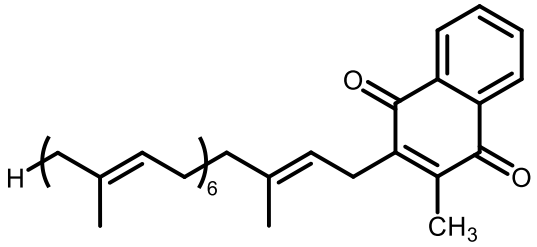

MK-7 was synthesized using the procedure outlined in section 11. Product was recovered as a yellow solid (648.1 mg, 80% yield over two steps). R_f = 0.60 (1:9 Et_2O/hexanes).

^{1}H NMR (400 MHz, $CDCl_3$): δ 8.08 (ddt, *J* = 4.7, 3.1, 2.0 Hz, 2H), 7.68 (dd, *J* = 5.8, 3.3 Hz, 2H), 5.15 – 4.98 (m, 7H), 3.37 (d, *J* = 7.0 Hz, 2H), 2.19 (s, 3H), 2.11 – 1.89 (m, 24H), 1.79 (s, 3H), 1.68 (s, 3H), 1.59 (s, 12H), 1.56 (s, 6H).

^{13}C NMR (101 MHz, $CDCl_3$): δ 185.4, 184.5, 146.1, 143.3, 137.5, 135.2, 134.9, 134.9, 134.9, 133.3, 133.3, 132.2, 132.1, 131.2, 126.3, 126.2, 124.4, 124.2, 124.1, 123.8, 119.0, 39.7, 39.7, 26.7, 26.7, 26.6, 26.5, 26.0, 25.7, 17.7, 16.4, 16.0, 16.0, 16.0, 12.7.

This compound matched spectral data from the literature.[11]

Synthesis of 2,3-dimethoxy-5-methyl-6-((2E,6E,10E,14E,18E,22E,26E,30E)-3,7,11,15,19,23,27,31,35-nonamethylhexatriaconta-2,6,10,14,18,22,26,30,34-nonaen-1-yl)cyclohexa-2,5-diene-1,4-dione (CoQ_9)

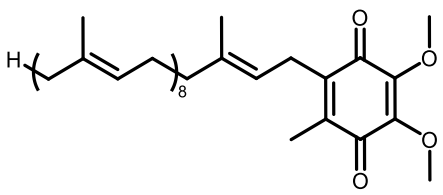

CoQ_9 was synthesized using the procedure outlined in section 13. Product was recovered as an organge solid (651.5 mg, 93% yield). R_f = 0.44 (1:4 Et_2O/hexanes).

^{1}H NMR (500 MHz, $CDCl_3$): δ 5.15 – 5.03 (m, 9H), 4.93 (tq, *J* = 7.1, 1.4 Hz, 1H), 3.99 (s, 3H), 3.97 (s, 3H), 3.18 (d, *J* = 7.1 Hz, 2H), 2.05 (q, *J* = 6.2 Hz, 18H), 2.01 (s, 3H), 2.00 – 1.91 (m, 17H), 1.73 (d, *J* = 1.3 Hz, 3H), 1.67 (d, *J* = 1.4 Hz, 3H), 1.62 – 1.55 (m, 26H).

^{13}C NMR (126 MHz, $CDCl_3$): δ 184.8, 183.9, 144.4, 144.3, 141.7, 138.9, 137.6, 135.2, 135.0, 134.9, 134.9, 134.9, 134.9, 134.9, 131.2, 124.4, 124.3, 124.3, 124.3, 124.3, 124.2, 123.9, 118.9, 61.1, 61.1, 39.8, 39.7, 39.7, 26.8, 26.7, 26.7, 26.7, 26.7, 26.5, 25.7, 25.3, 17.7, 16.3, 16.0, 16.0, 16.0, 11.9.

HRMS (ESI): *m/z* calcd for $C_{54}H_{82}O_4$+Na^+: 817.6114 [*M*+Na]$^+$; found: 817.6111.

15. Experimental references

1. Lipshutz, B. H.; Ghorai, S.; Abela, A. R.; Moster, R.; Nishikata, T. Duplais, C.; Krasovskiy, A. *J. Org. Chem.,* **2011**, *76,* 4379–4391.
2. Pichette Drapeau, M.; Fabre, I.; Grimaud, L.; Ciofini, I.; Ollevier, T.; Taillefer, M. *Angew. Chem., Int. Ed.* **2015**, *54*, 10587–10591.
3. Matsubara, K.; Ueno, K.; Koga, Y.; Hara, K. *J. Org. Chem.* **2007**, *72*, 5069–5076.
4. Marelli, E.; Corpet, M.; Davies, S. R.; Nolan, S. P. *Chem. Eur. J.* **2014**, *20*, 17272–17276.
5. Marelli, E.; Renault, Y.; Sharma, S. V.; Nolan, S. P.; Goss, R. J. M. *Chem. Eur. J.* **2017**, *23*, 3832–3836.
6. Lundin, P. M.; Esquivias, J.; Fu, G. C. *Angew. Chem., Int. Ed.* **2009**, *48*, 154–156.
7. Renzhong, M. Q. CN101029003A, September 5, 2009

8. Sidoryk, K.; Jatczak, K.; Burzynska-Prajzner, A.; Cybulski, M.; Napiorkowski, M.; Pietrzkowska, D.; Jedynak, L.; Kubiszewski, M. WO 2021071372, April 15, 2021.
9. Uno, S.; Masuya, T.; Shinzawa-Itoh, K.; Lasham, J.; Haapanen, O.; Shiba, T.; Inaoka, D. K.; Sharma, V.; Murai, M.; Miyoshi, H. *J. Biol. Chem.* **2020**, *295*, 2449–2463.
10. Yerramsetti, N.; Dampanaboina, L.; Mendu, V.; Battula, S. *Tetrahedron* **2020**, *76*, 131696.
11. Baj, A.; Wałejko, P.; Kutner, A.; Kaczmarek, Ł.; Morzycki, J. W.; Witkowski, S. *Org. Process Res. Dev.* **2016**, *20*, 1026–1033.

2.7 Spectral Data

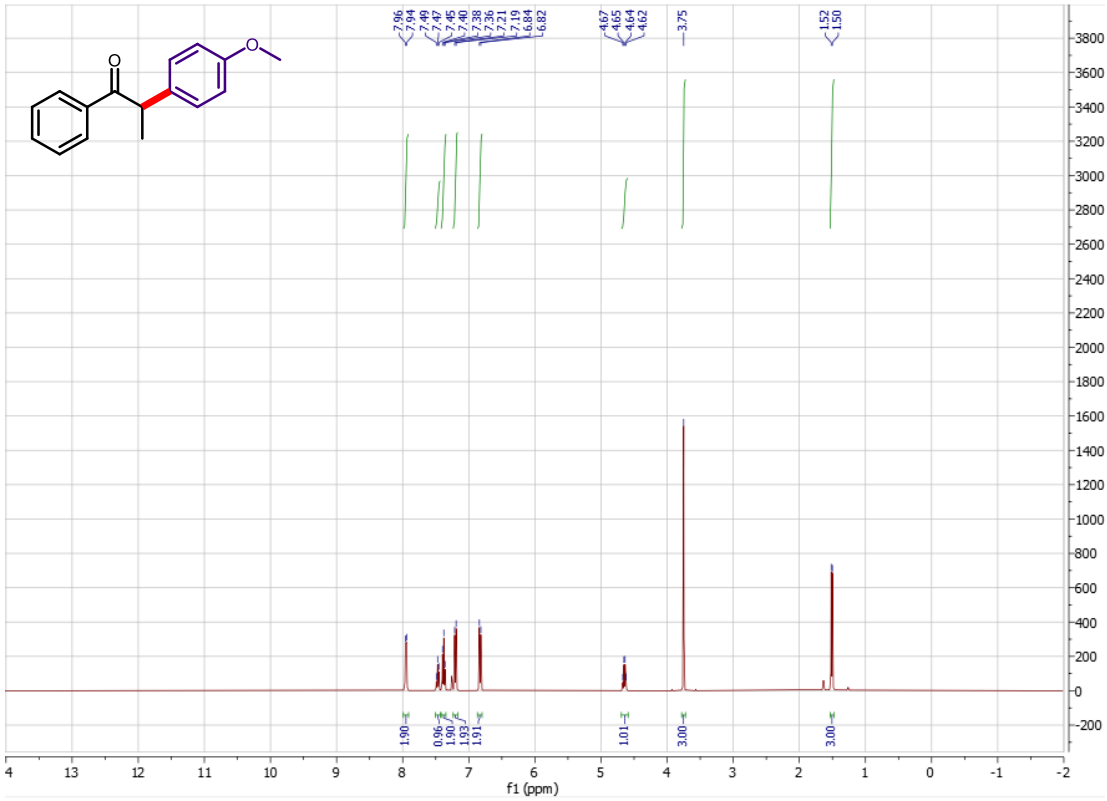

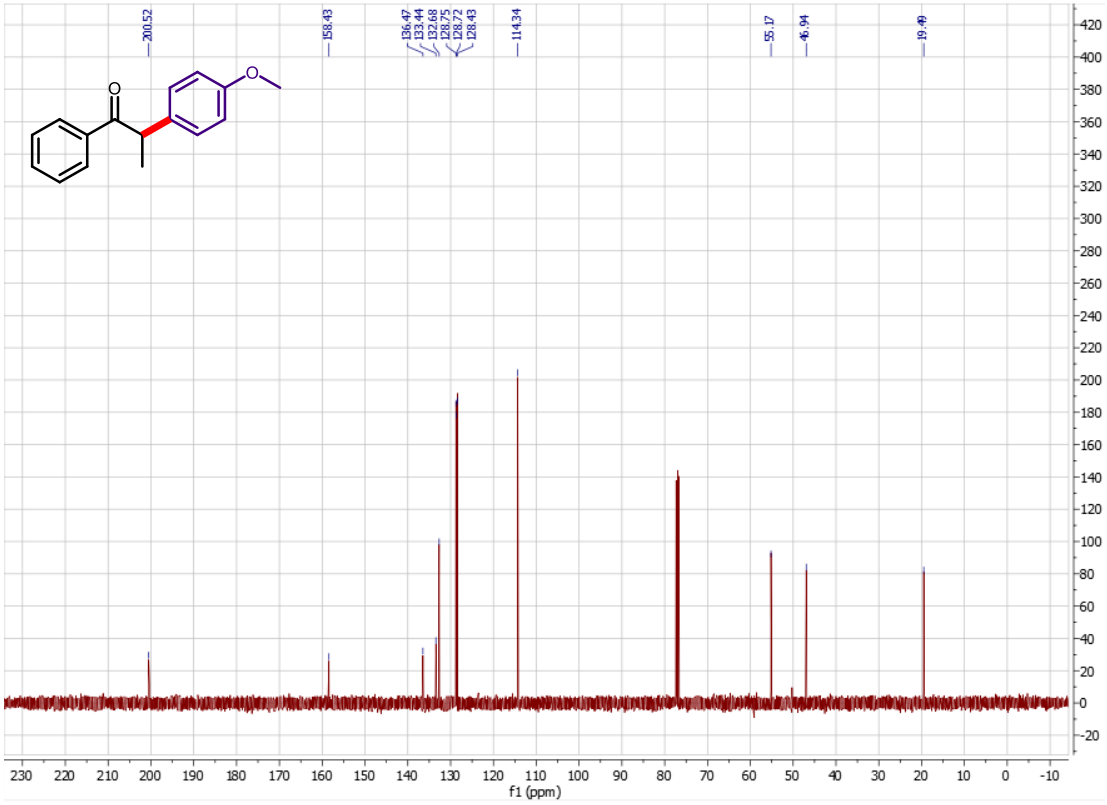

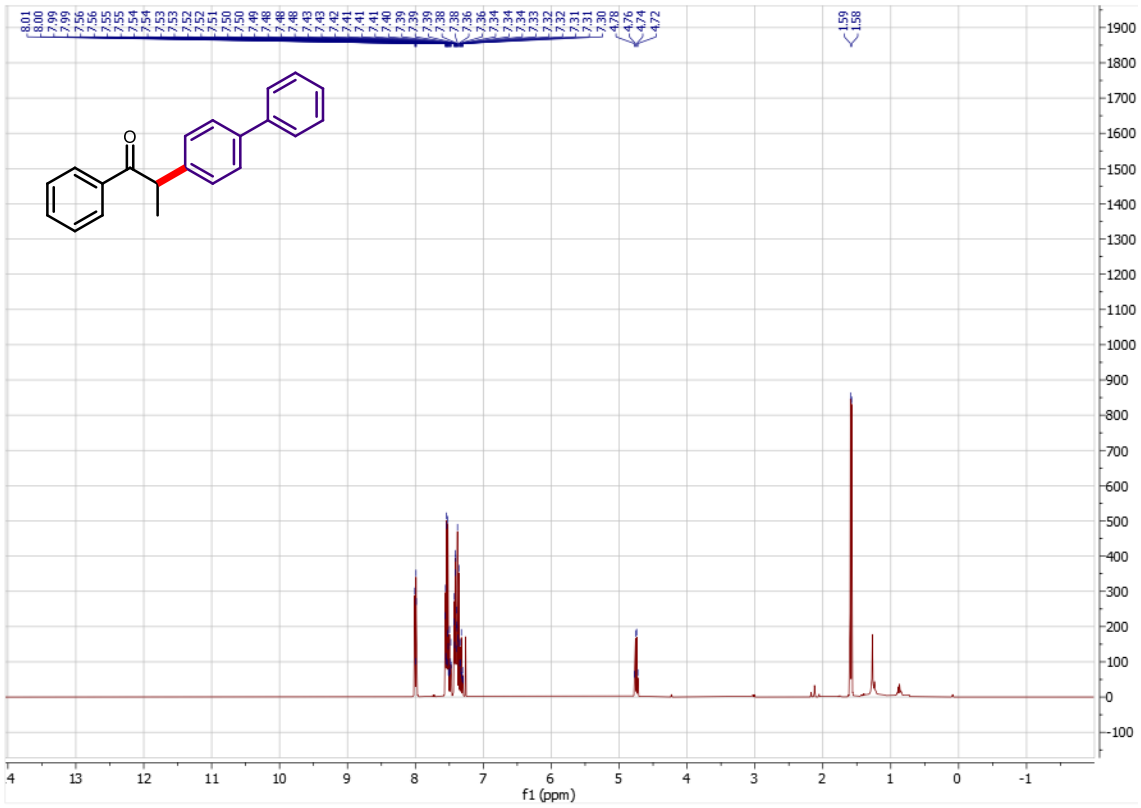
f1 (ppm)

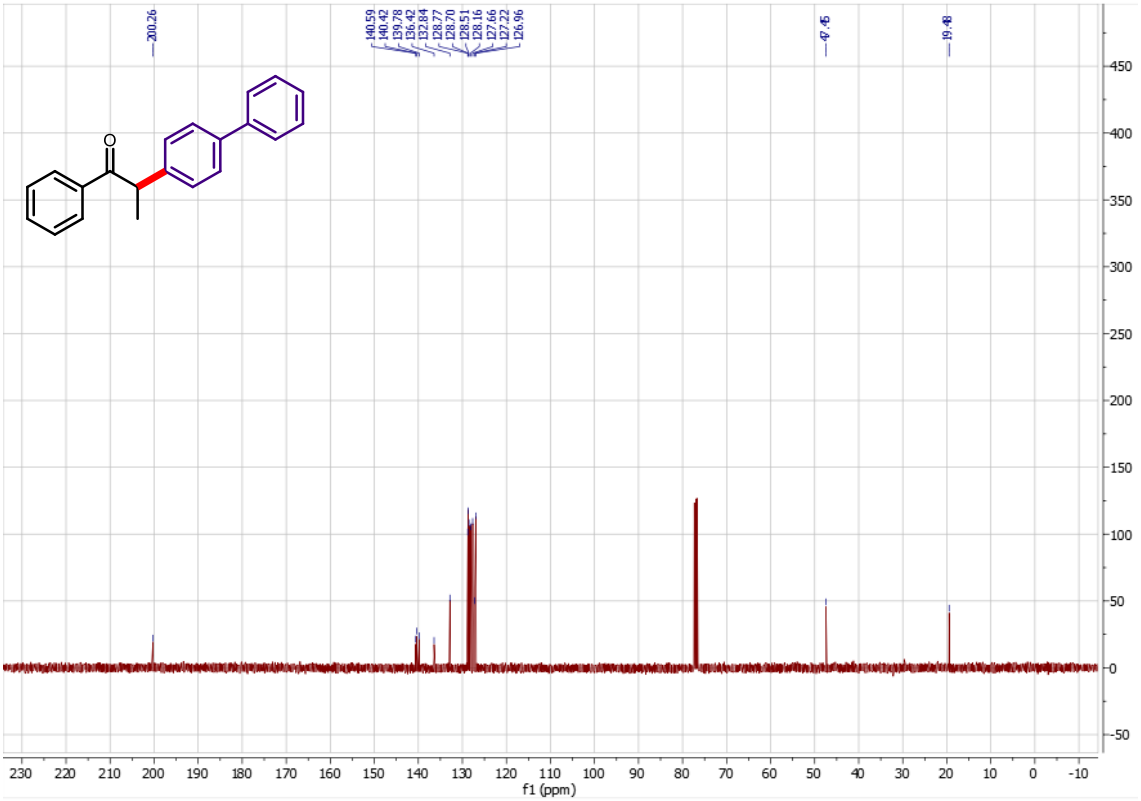
f1 (ppm)

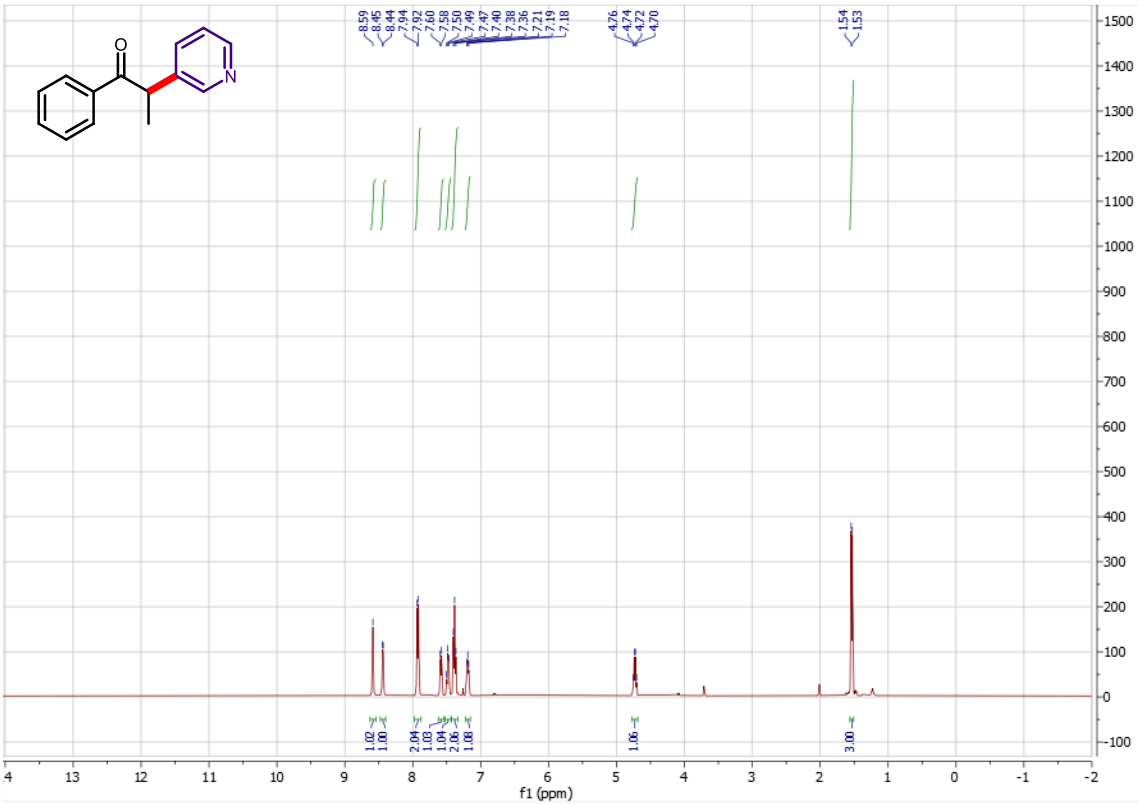
8.59
8.45
8.44
7.94
7.92
7.60
7.58
7.50
7.49
7.47
7.40
7.38
7.36
7.21
7.19
7.18
4.76
4.74
4.72
4.70
1.54
1.53
1.02
1.00
2.04
1.03
1.04
2.06
1.00
1.06
3.00
f1 (ppm)

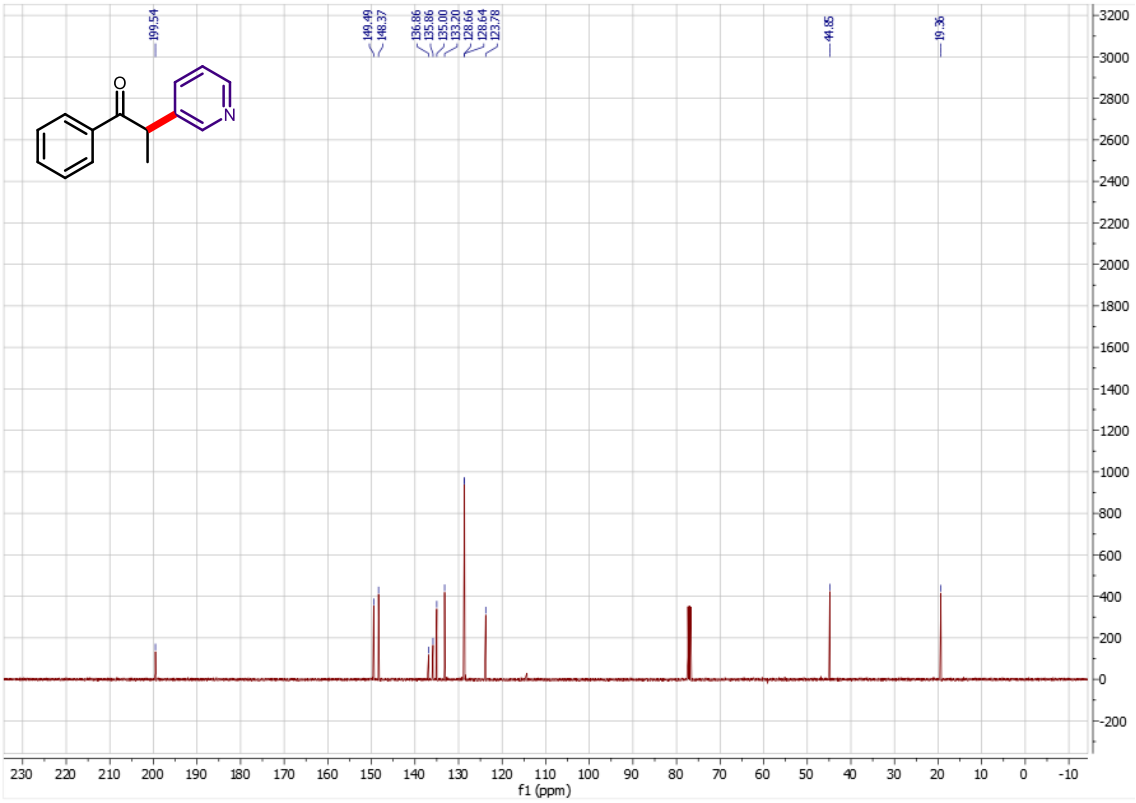
199.54
149.49
148.37
136.86
135.86
135.00
133.20
128.66
128.64
123.78
44.85
19.36
f1 (ppm)

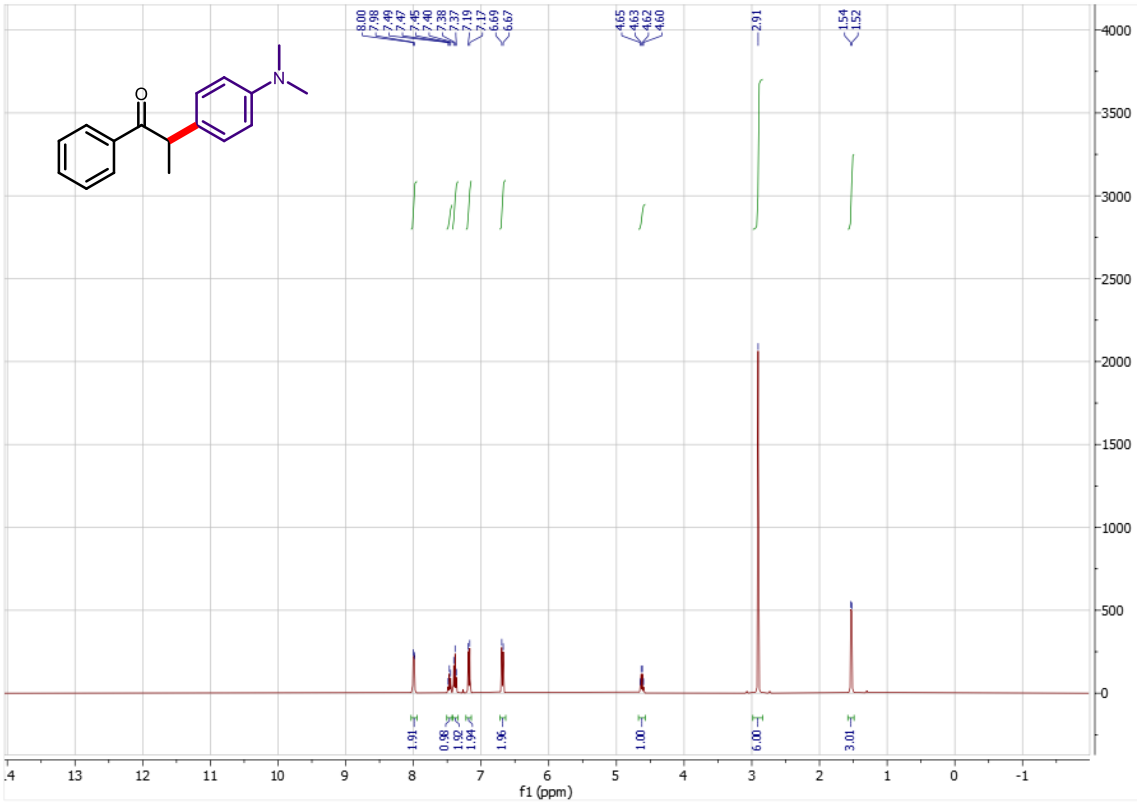
8.00
7.98
7.49
7.47
7.46
7.40
7.38
7.37
7.19
7.17
6.69
6.67
4.65
4.63
4.62
4.60
2.91
1.54
1.52
1.91
0.98
1.02
1.94
1.96
1.00
6.00
3.01
f1 (ppm)

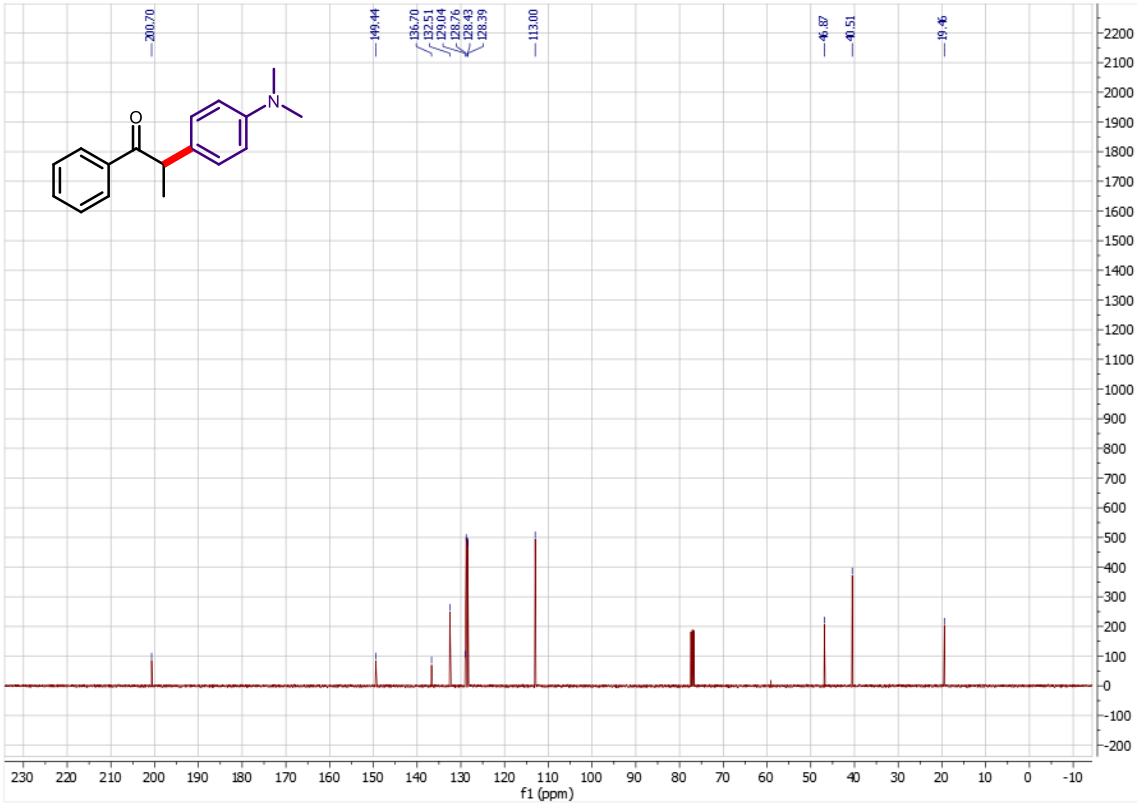
200.70
149.44
136.70
132.51
129.04
128.76
128.43
128.39
113.00
46.87
40.51
19.46
f1 (ppm)

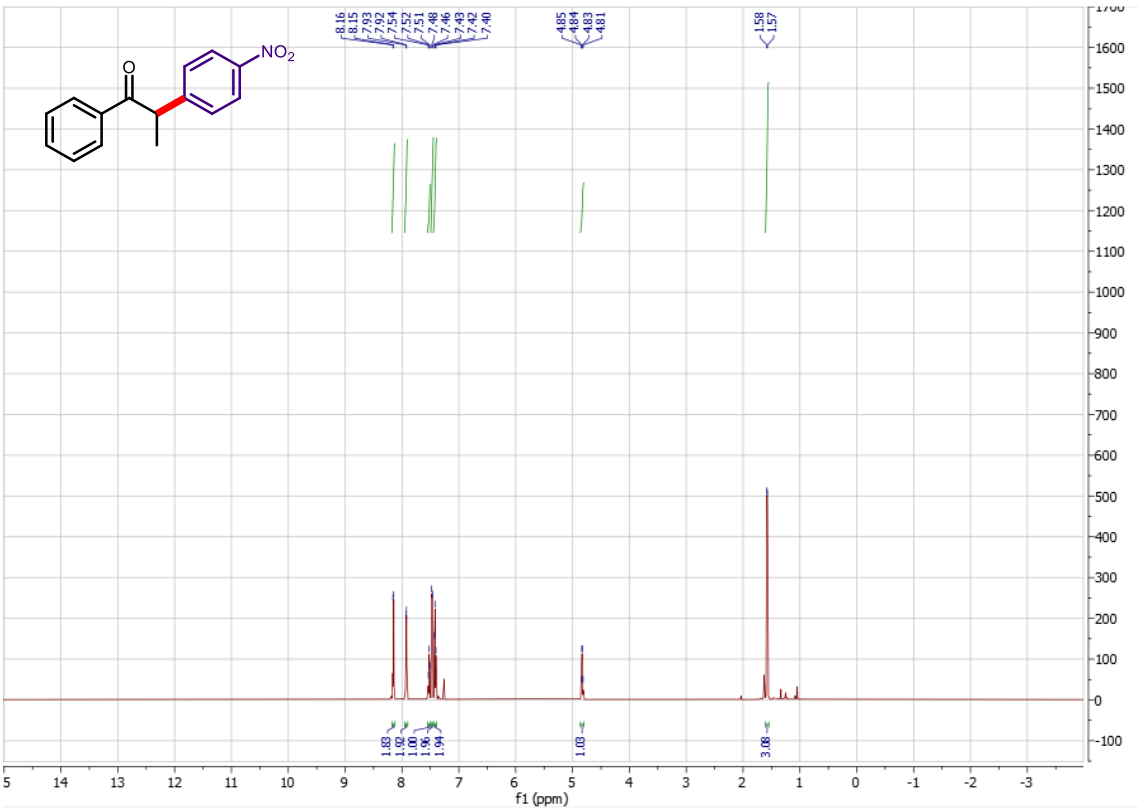
O
NO2
8.16
8.15
7.93
7.92
7.54
7.52
7.51
7.48
7.46
7.43
7.42
7.40
4.85
4.84
4.83
4.81
1.58
1.57
1.83
1.92
1.00
1.96
1.94
1.03
3.08
f1 (ppm)

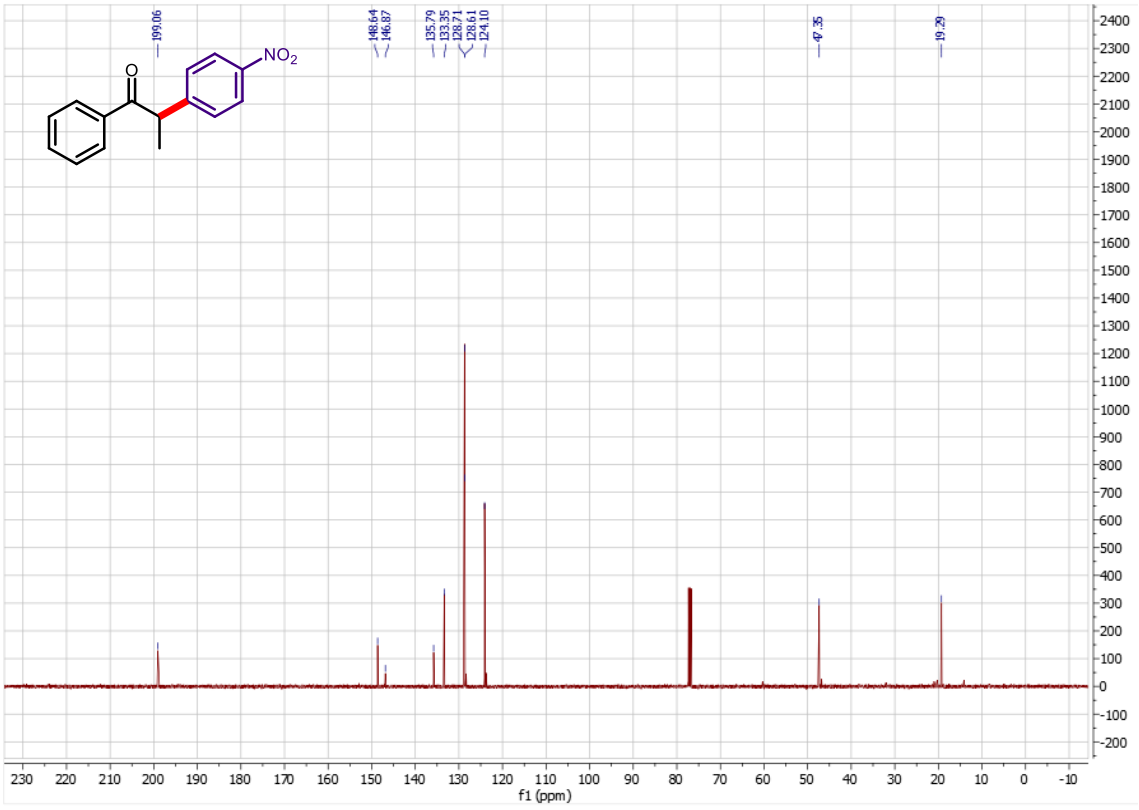
O
NO2
199.06
148.64
146.87
135.79
133.35
129.71
128.61
124.10
47.35
19.29
f1 (ppm)

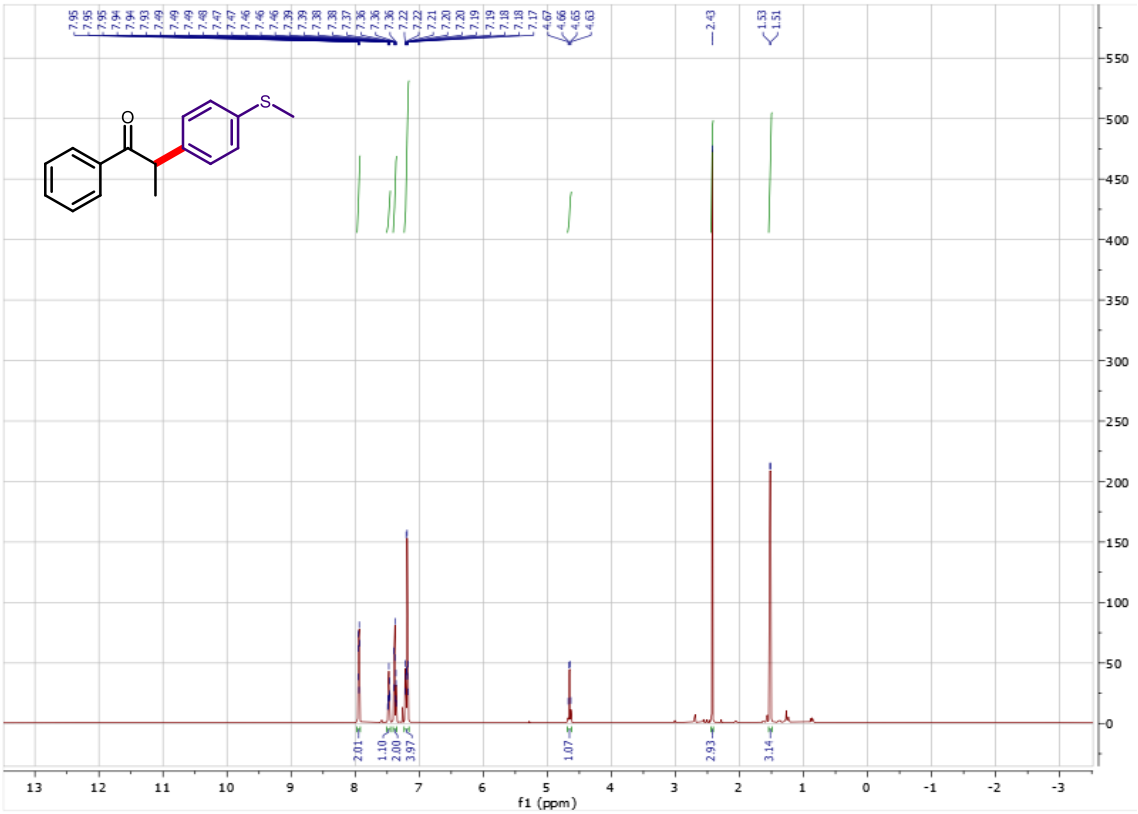
O
S
f1 (ppm)

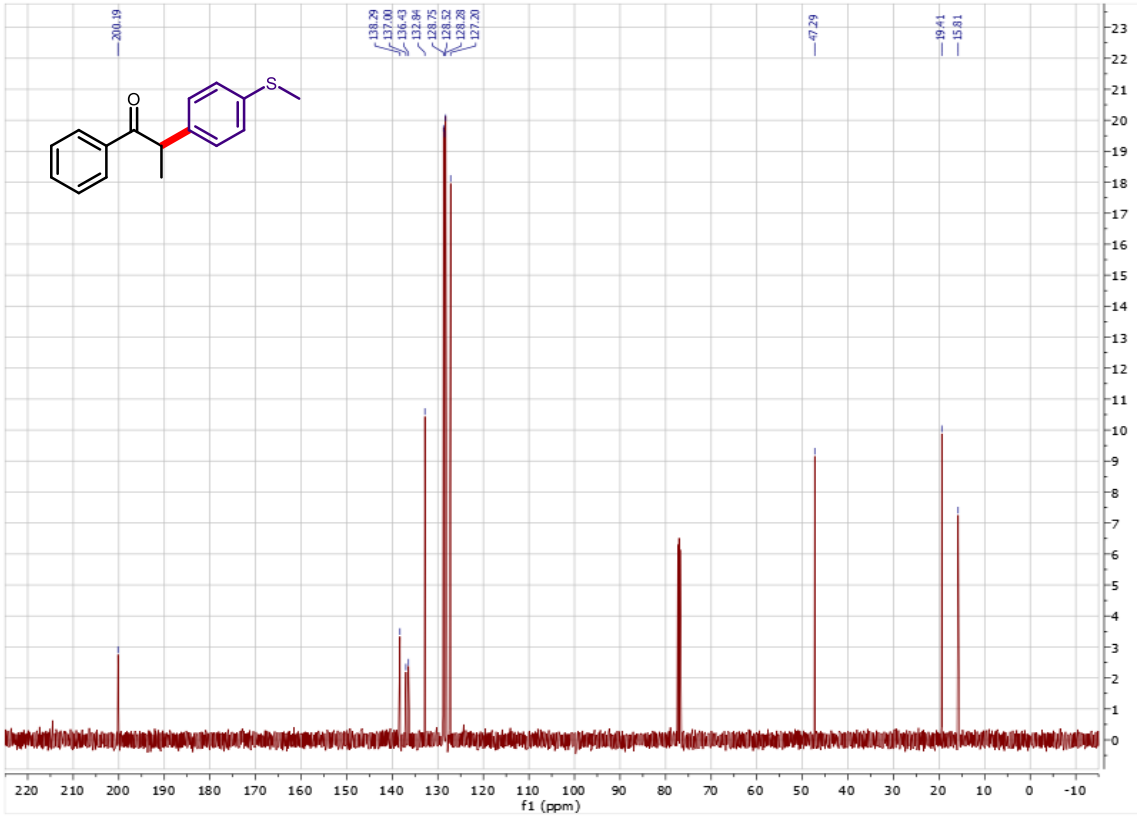
O
S
f1 (ppm)

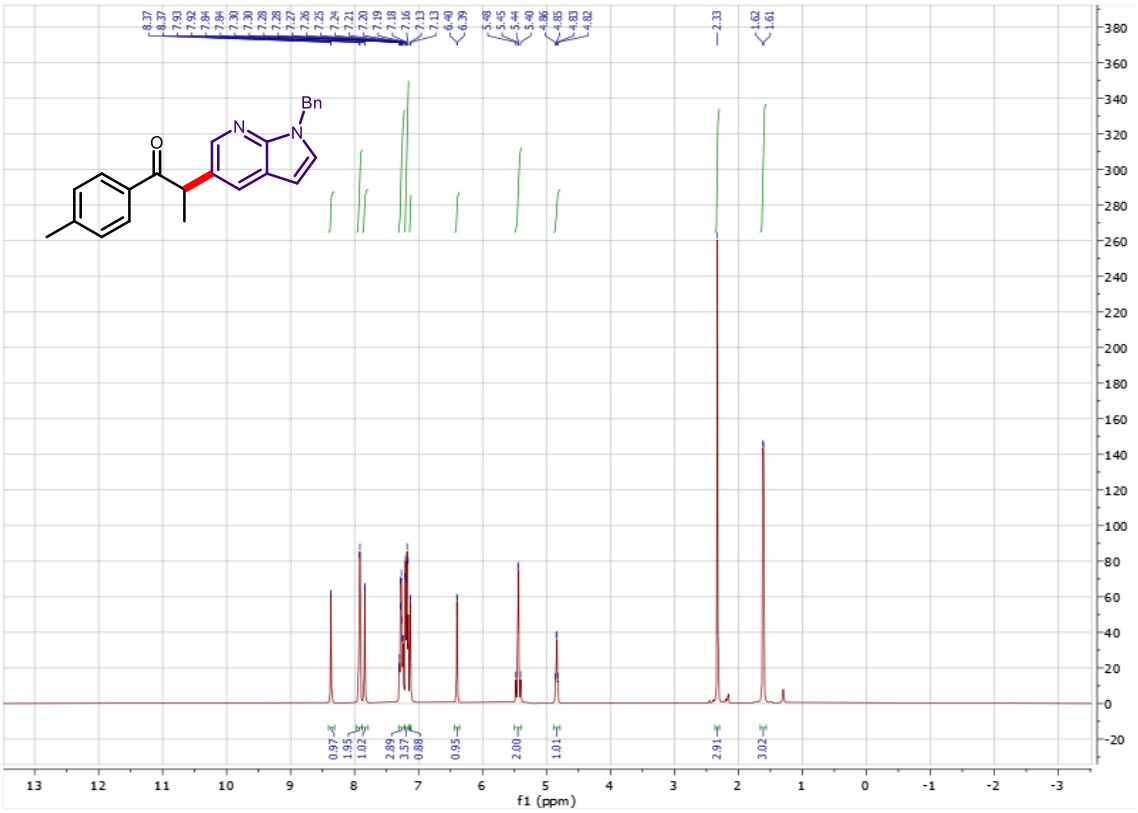
Bn
N
N
O
f1 (ppm)

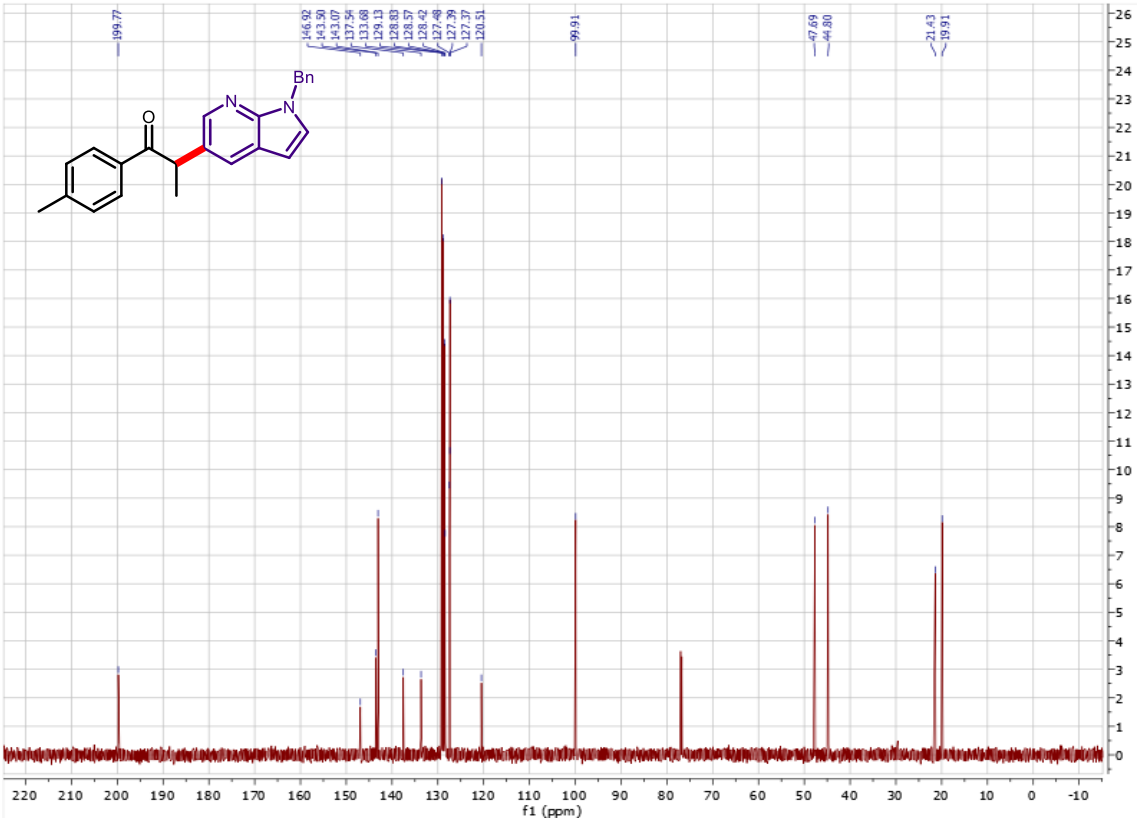
Bn
N
N
O
f1 (ppm)

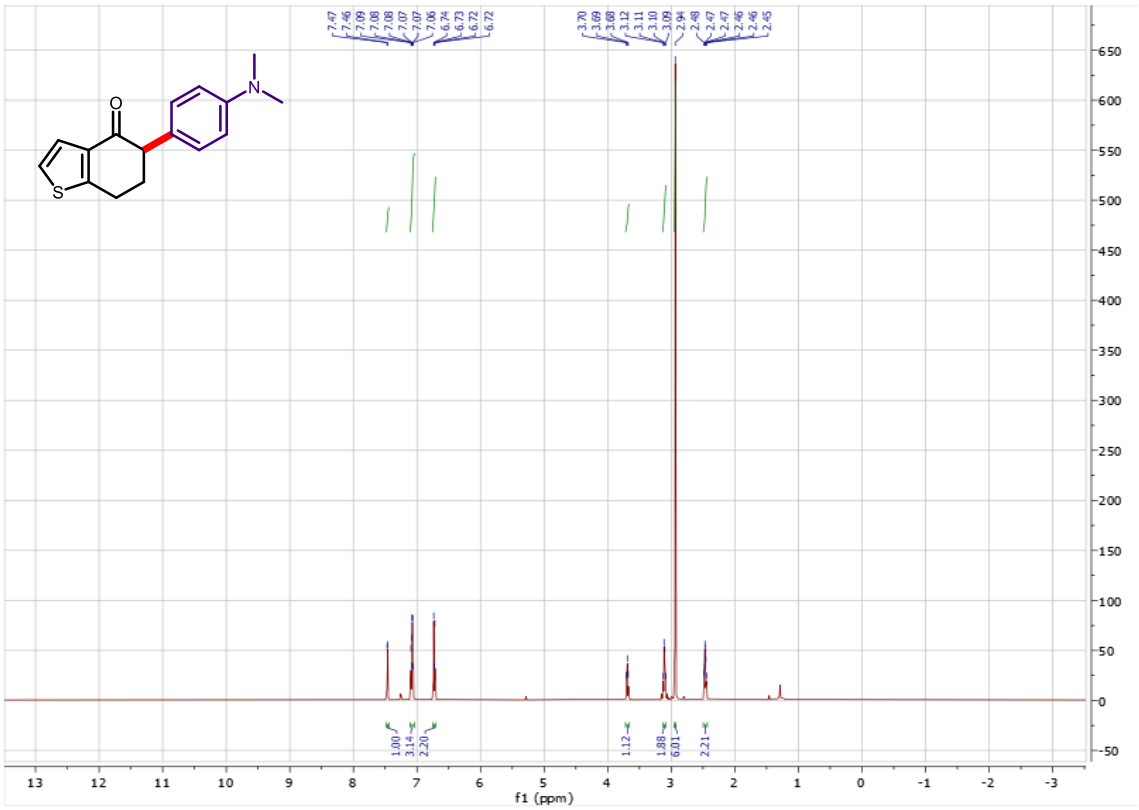
7.47
7.46
7.09
7.08
7.08
7.08
7.07
7.07
7.06
6.74
6.73
6.72
6.72
3.70
3.69
3.68
3.12
3.11
3.10
3.09
2.94
2.48
2.47
2.47
2.46
2.46
2.45
1.00
3.14
2.20
1.12
1.88
6.01
2.21
f1 (ppm)

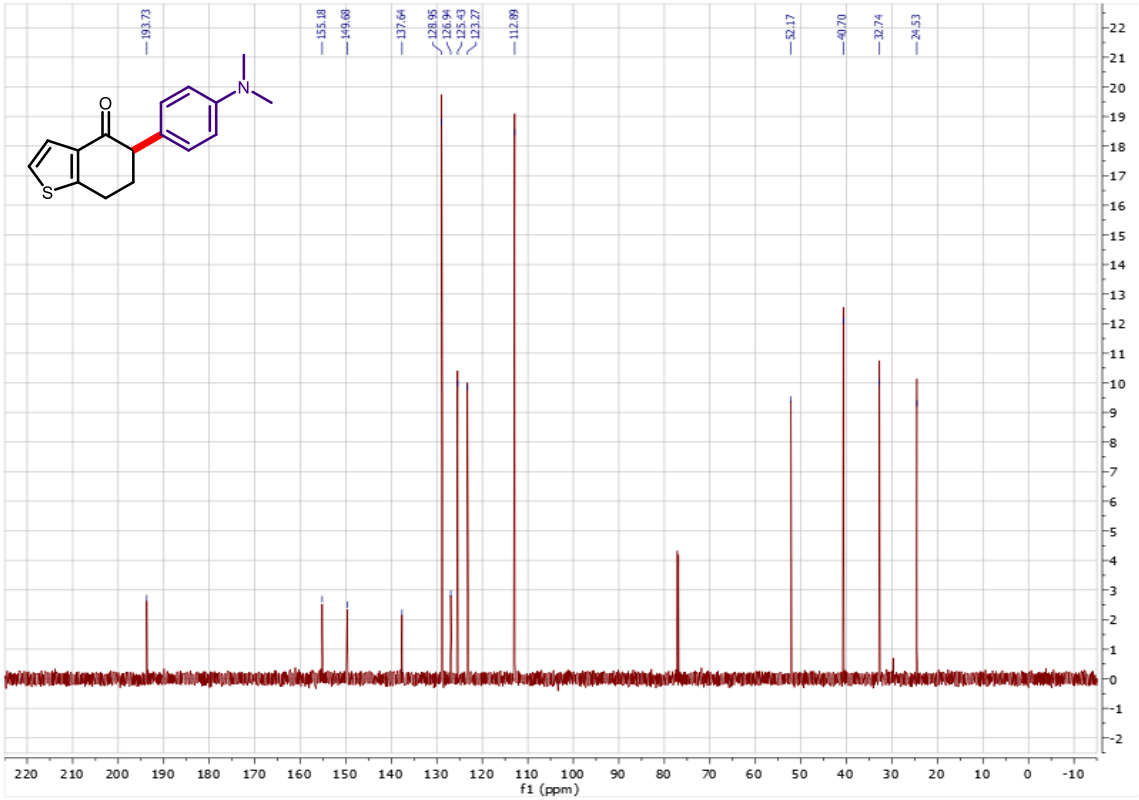
193.73
155.18
149.68
137.64
128.95
126.94
125.43
123.27
112.89
52.17
40.70
32.74
24.53
f1 (ppm)

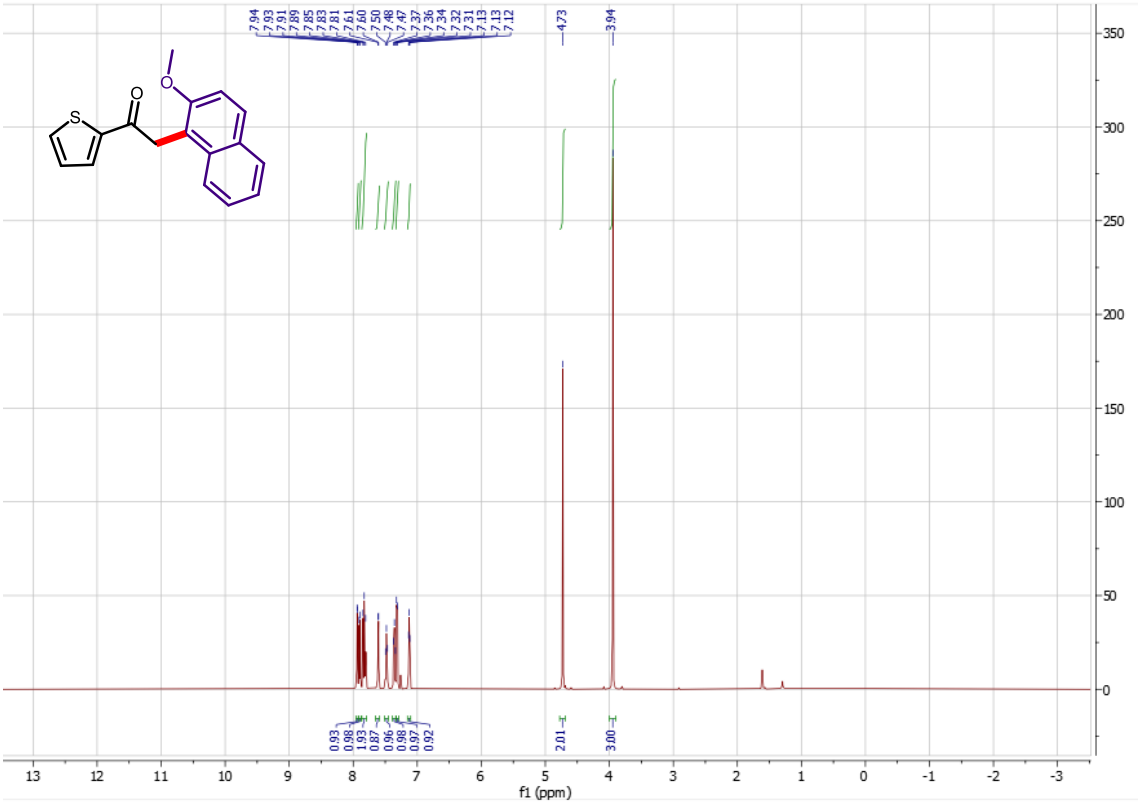
7.94
7.93
7.91
7.89
7.85
7.83
7.81
7.61
7.60
7.50
7.48
7.47
7.37
7.36
7.34
7.32
7.31
7.13
7.13
7.12
4.73
3.94
0.93
0.98
1.93
1.97
0.96
0.98
0.97
0.92
2.01
3.00
f1 (ppm)

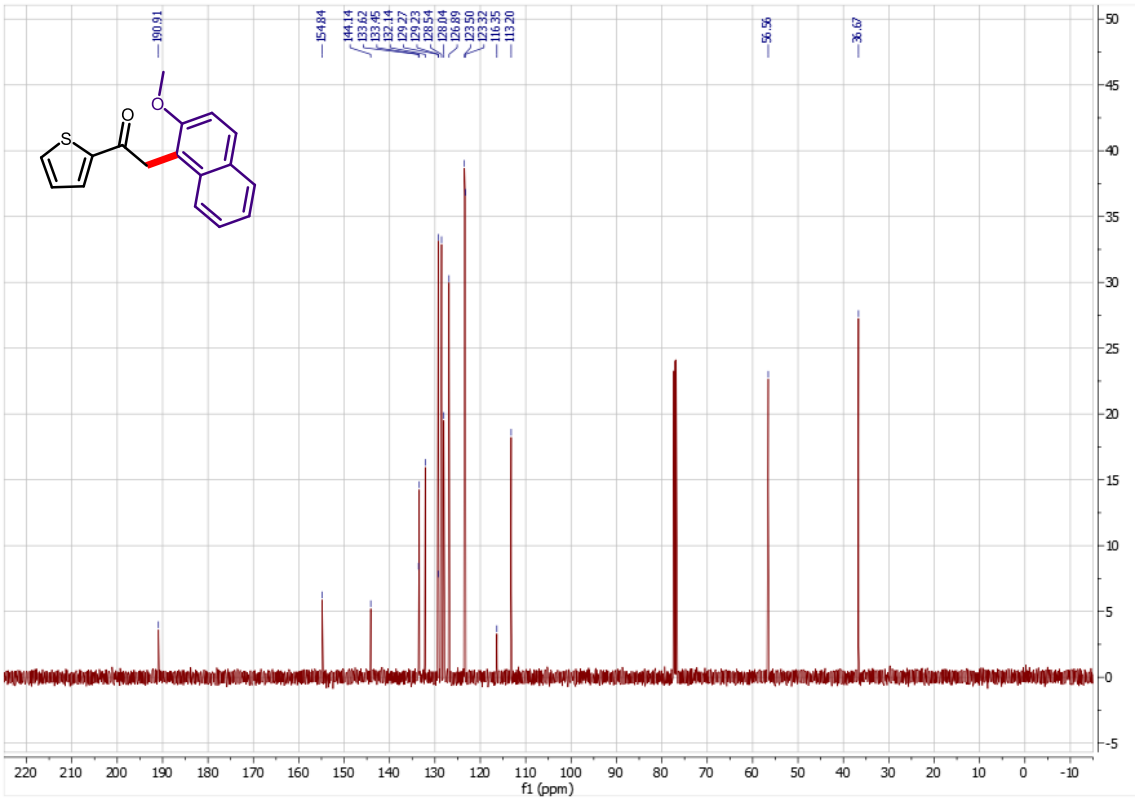
190.91
154.84
144.14
133.62
133.45
132.14
129.27
129.23
128.54
128.04
126.89
125.50
123.32
116.35
113.20
56.56
36.67
f1 (ppm)

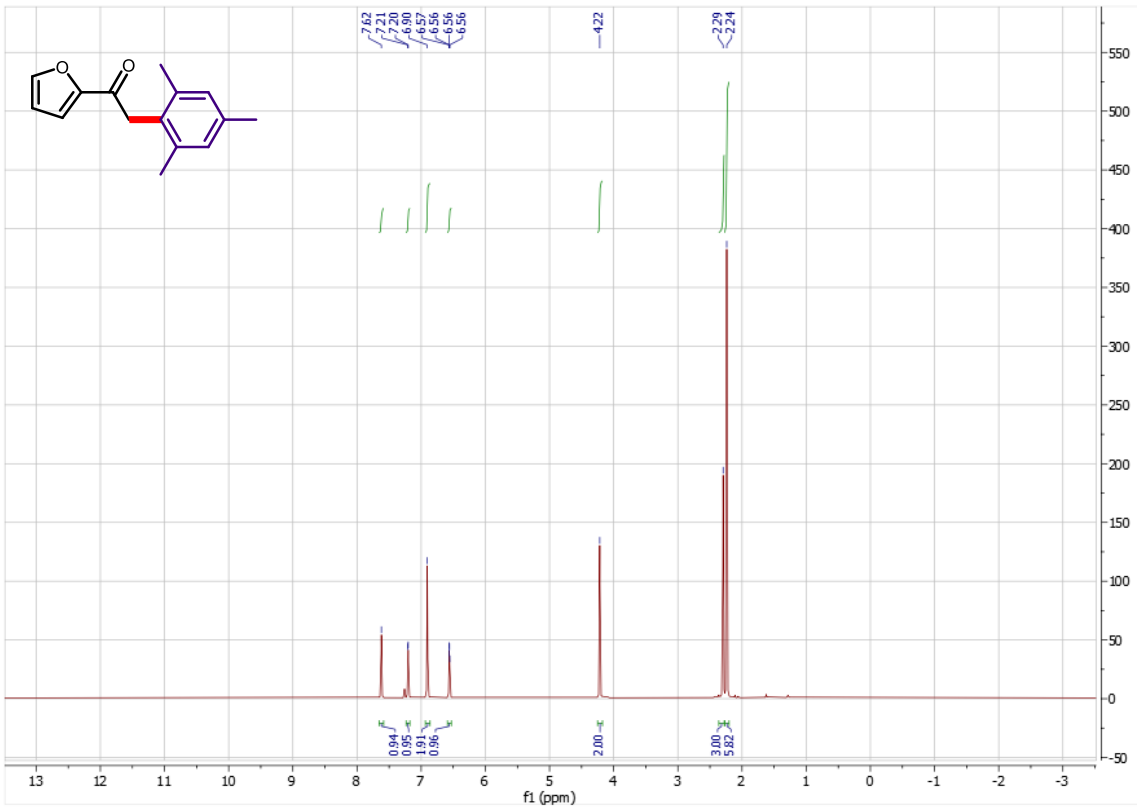
7.62
7.21
7.20
6.90
6.57
6.56
6.56
6.56
6.56
4.22
2.29
2.24
0.94
0.95
1.91
0.96
2.00
3.00
5.82
f1 (ppm)

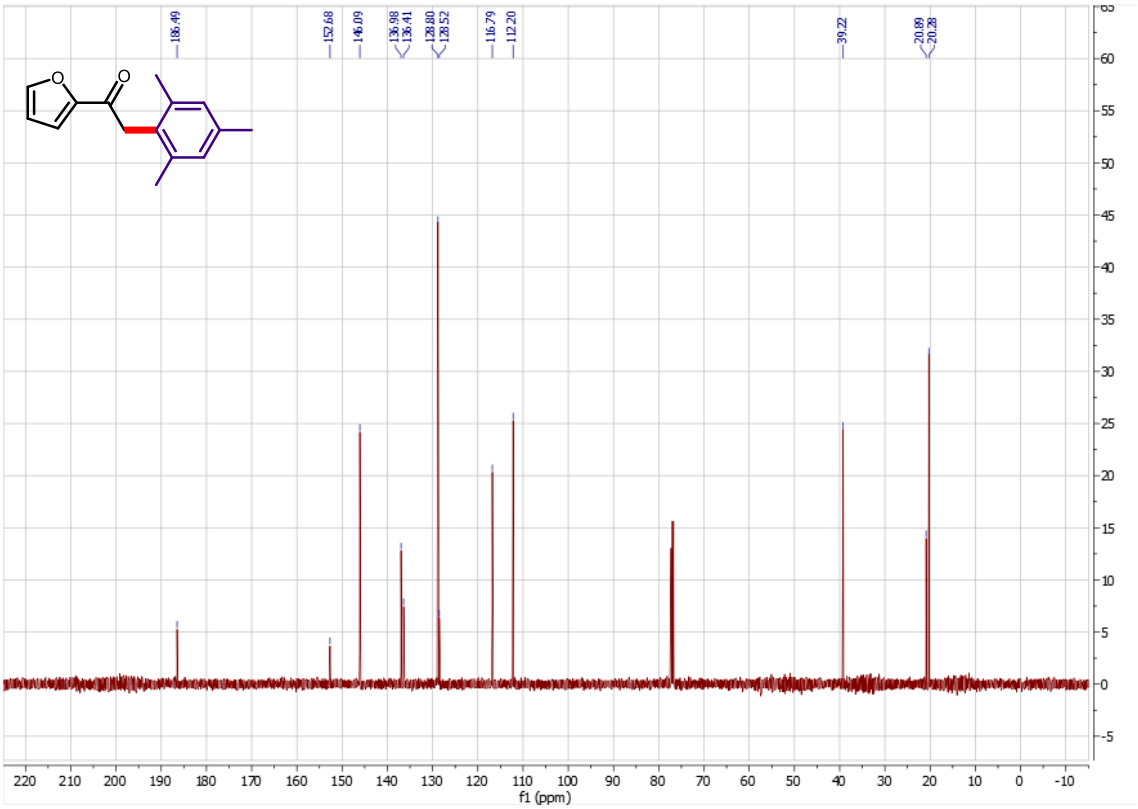
186.49
152.68
146.09
136.98
136.41
128.80
128.52
116.79
112.20
39.22
20.89
20.28
f1 (ppm)

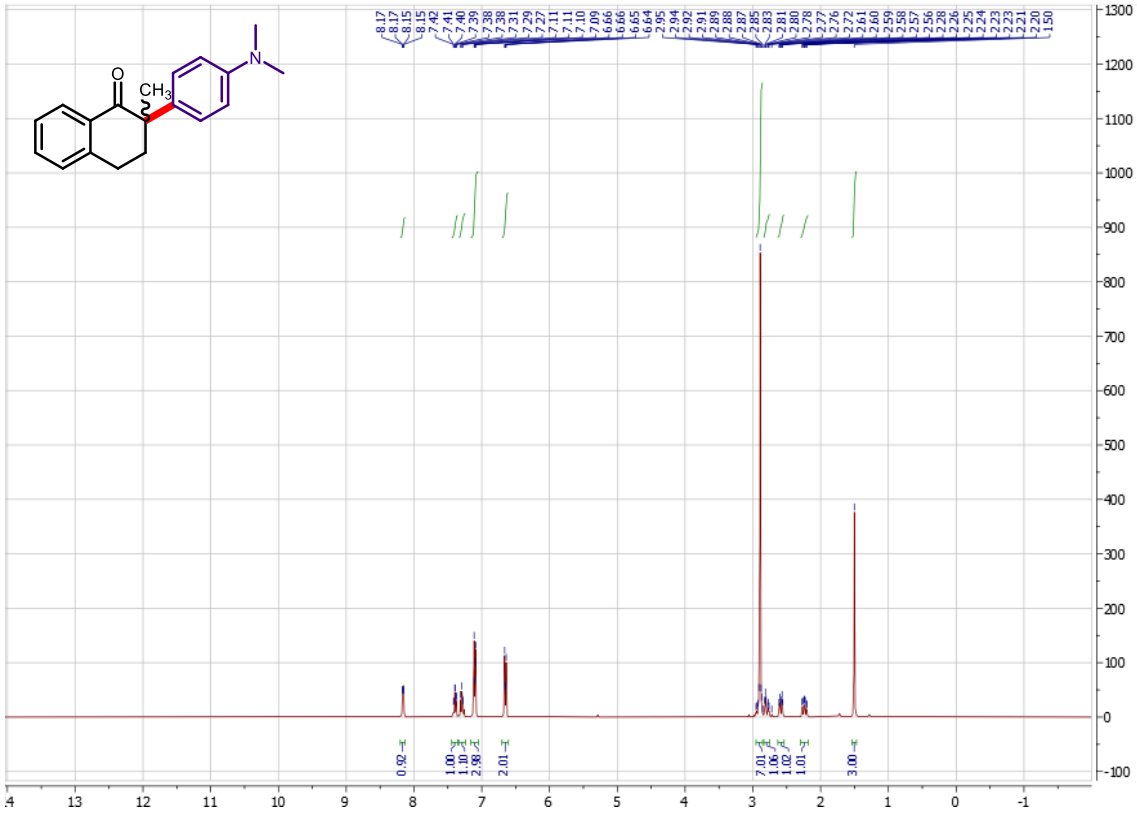
O
CH3
N

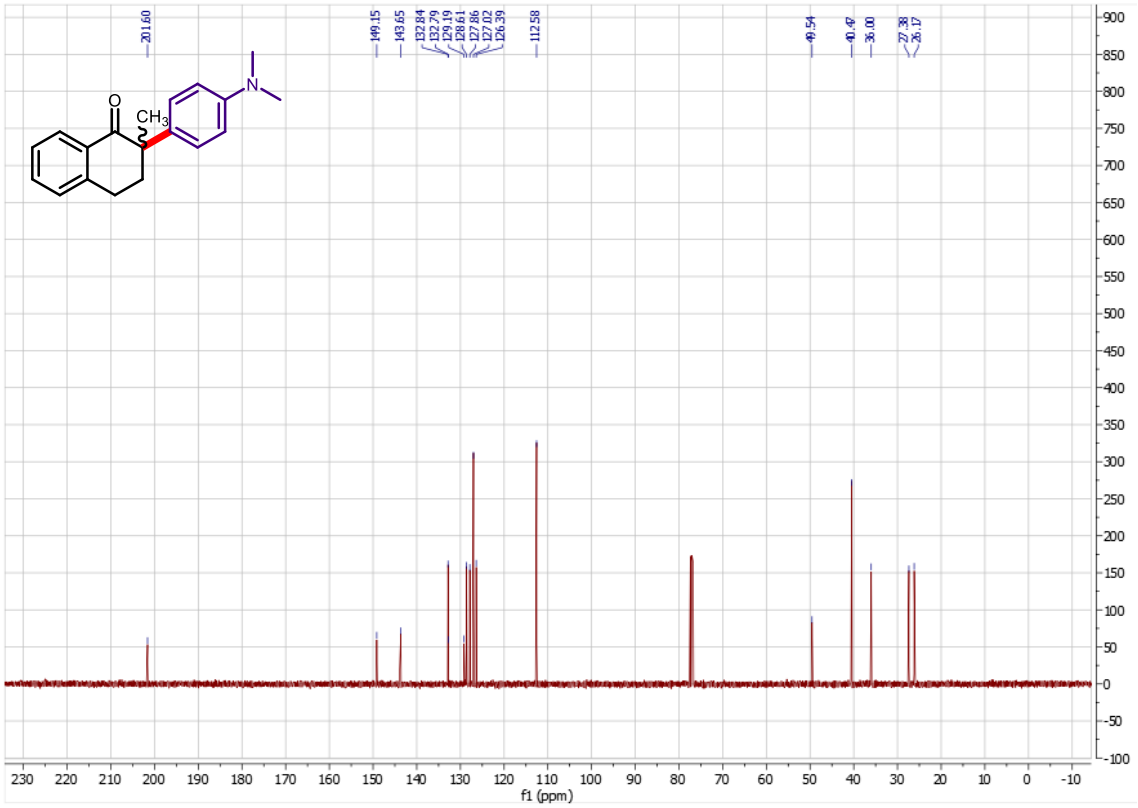
O
CH3
N
f1 (ppm)

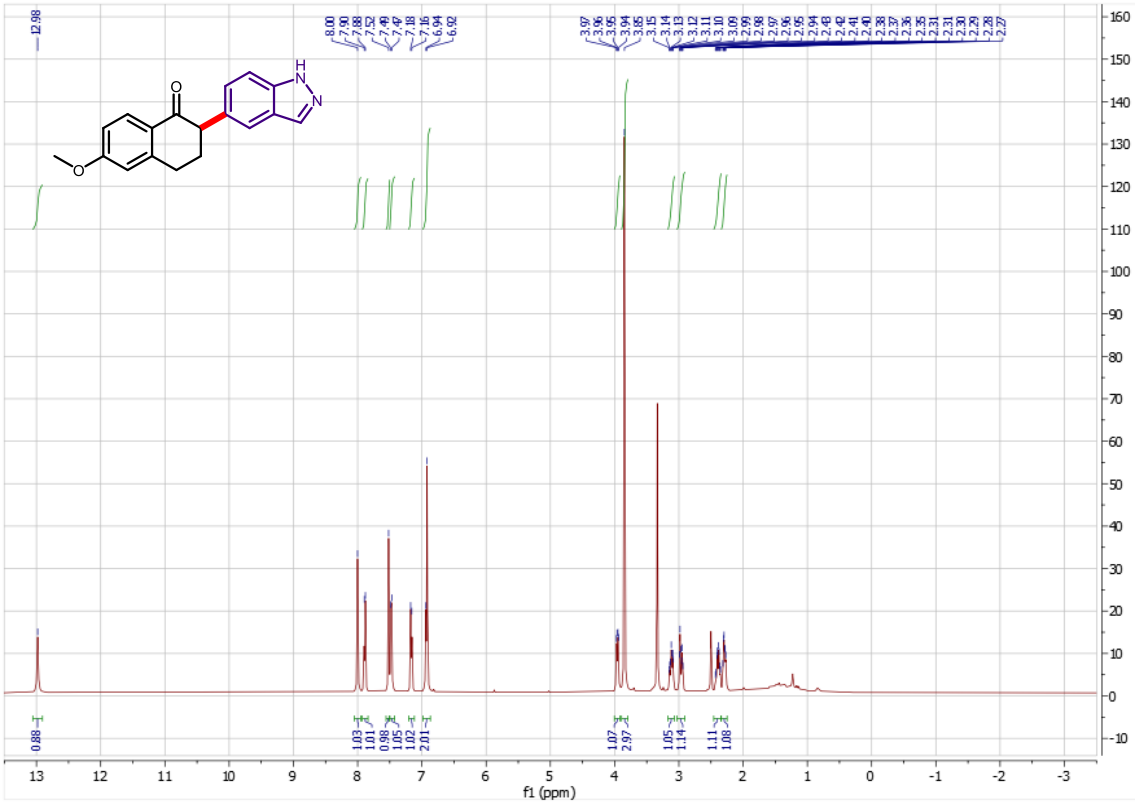
f1 (ppm)

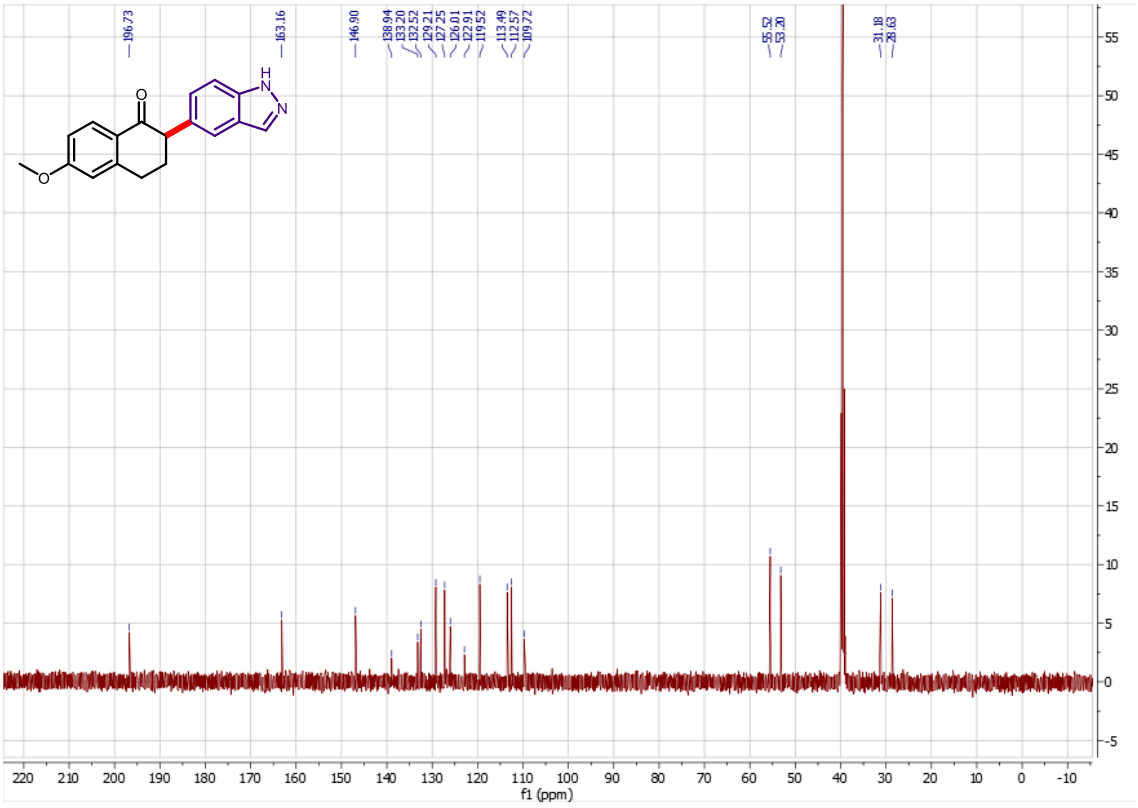
f1 (ppm)

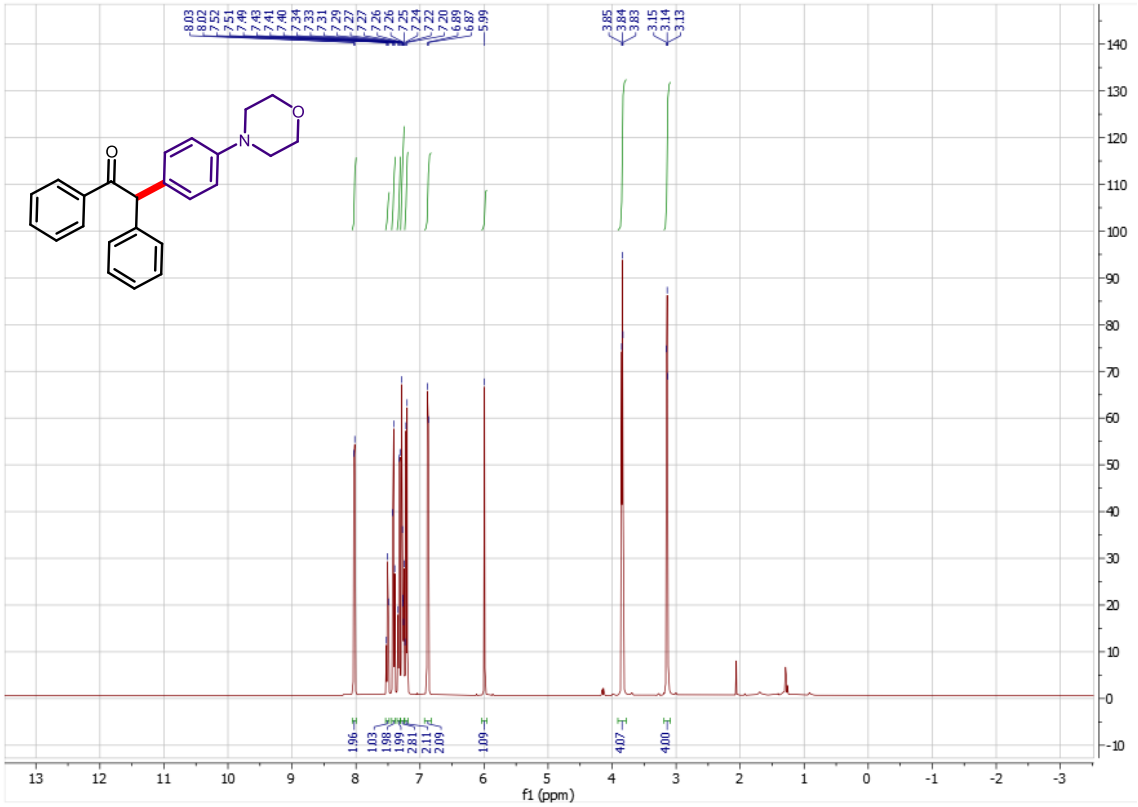
8.03
8.02
7.52
7.51
7.49
7.43
7.41
7.40
7.34
7.33
7.31
7.29
7.27
7.27
7.26
7.26
7.25
7.24
7.22
7.20
6.89
6.87
5.99
3.85
3.84
3.83
3.15
3.14
3.13
O
N
O
1.96
1.03
1.98
1.99
2.81
2.11
2.09
1.09
4.07
4.00
f1 (ppm)

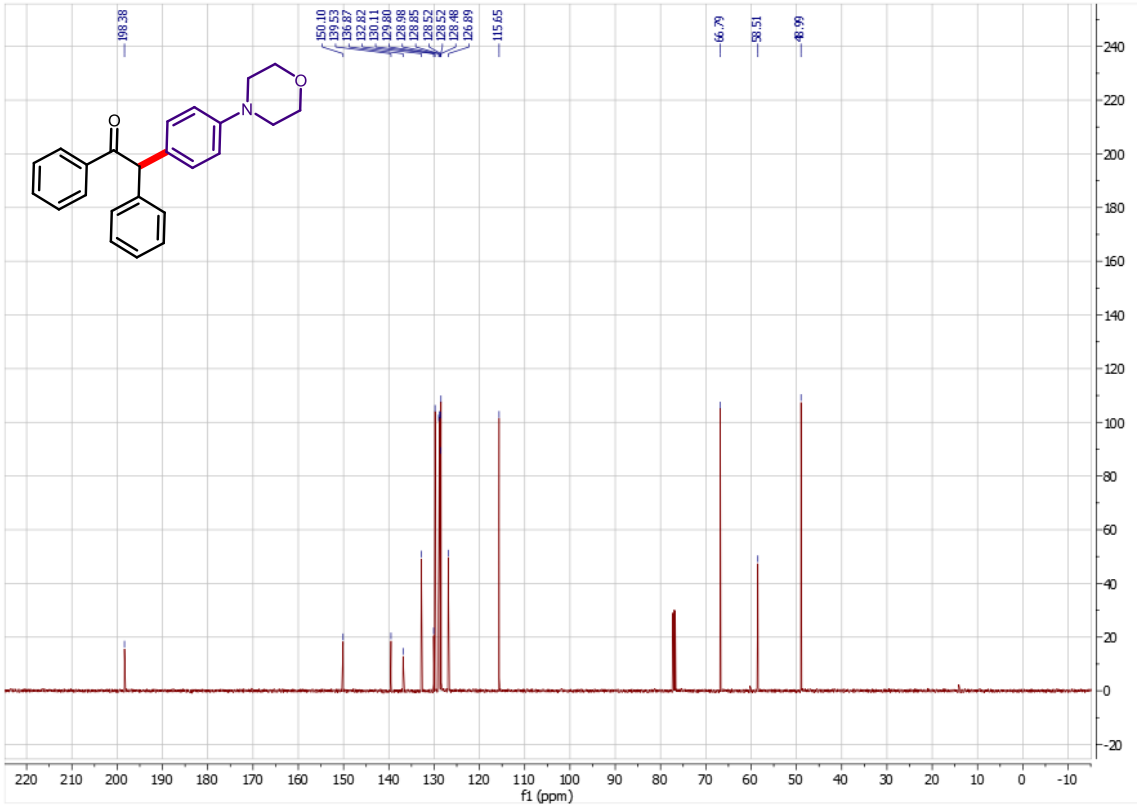
198.38
150.10
139.53
136.87
132.82
130.11
129.90
128.98
128.85
128.52
128.52
128.48
126.89
115.65
66.79
58.51
48.99
O
N
O
f1 (ppm)

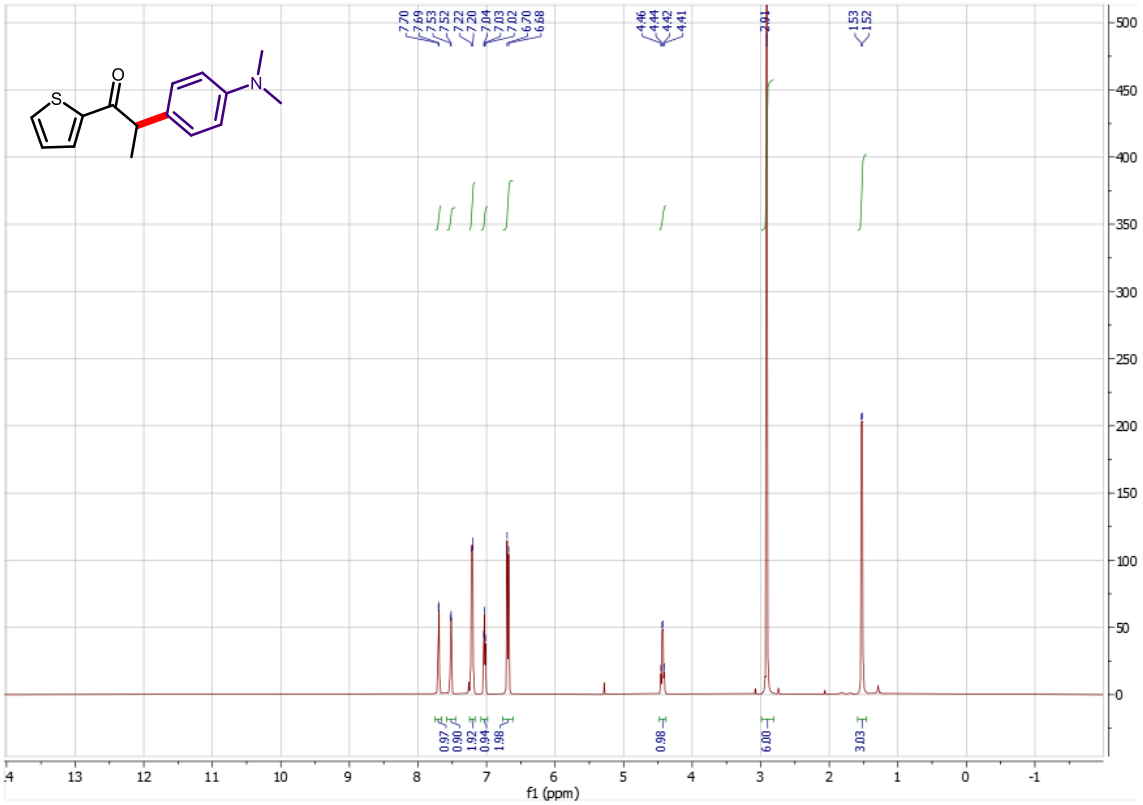
7.70
7.69
7.53
7.52
7.22
7.20
7.04
7.03
7.02
6.70
6.68
4.46
4.44
4.42
4.41
2.91
1.53
1.52
0.97
0.90
1.92
0.94
1.98
0.98
6.00
3.03
f1 (ppm)

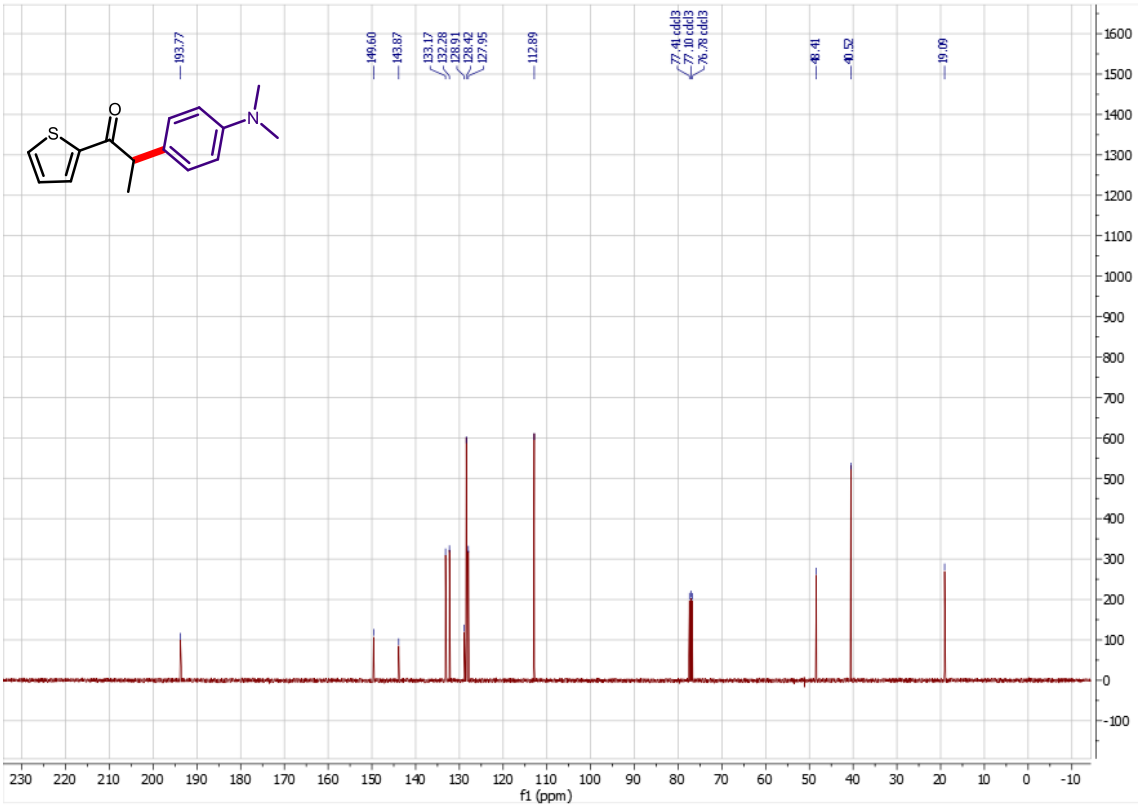
193.77
149.60
143.87
133.17
132.28
128.91
128.42
127.95
112.89
77.41 cdcl3
77.10 cdcl3
76.78 cdcl3
48.41
40.52
19.09
f1 (ppm)

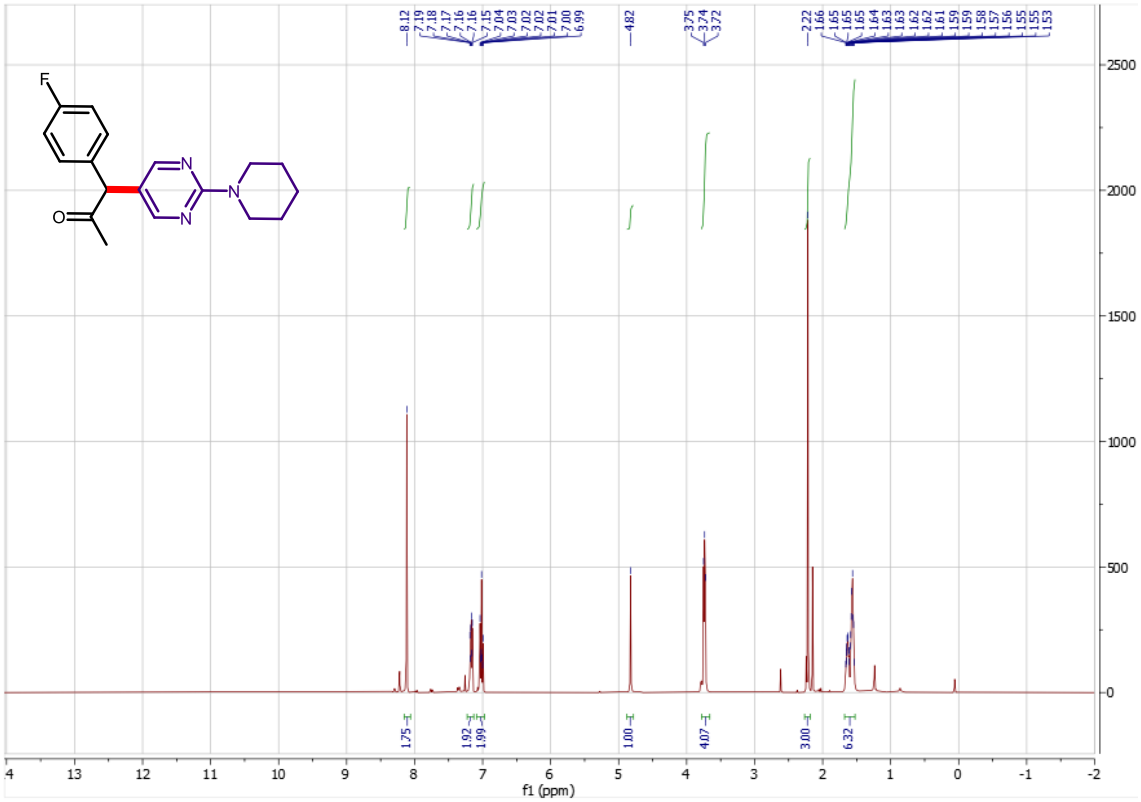
F
O
N
N
N
8.12
7.19
7.18
7.17
7.16
7.16
7.15
7.04
7.03
7.02
7.02
7.01
7.00
6.99
4.82
3.75
3.74
3.72
2.22
1.66
1.65
1.65
1.65
1.64
1.63
1.63
1.62
1.62
1.61
1.59
1.59
1.58
1.57
1.56
1.55
1.55
1.53
1.75
1.92
1.99
1.00
4.07
3.00
6.32
f1 (ppm)

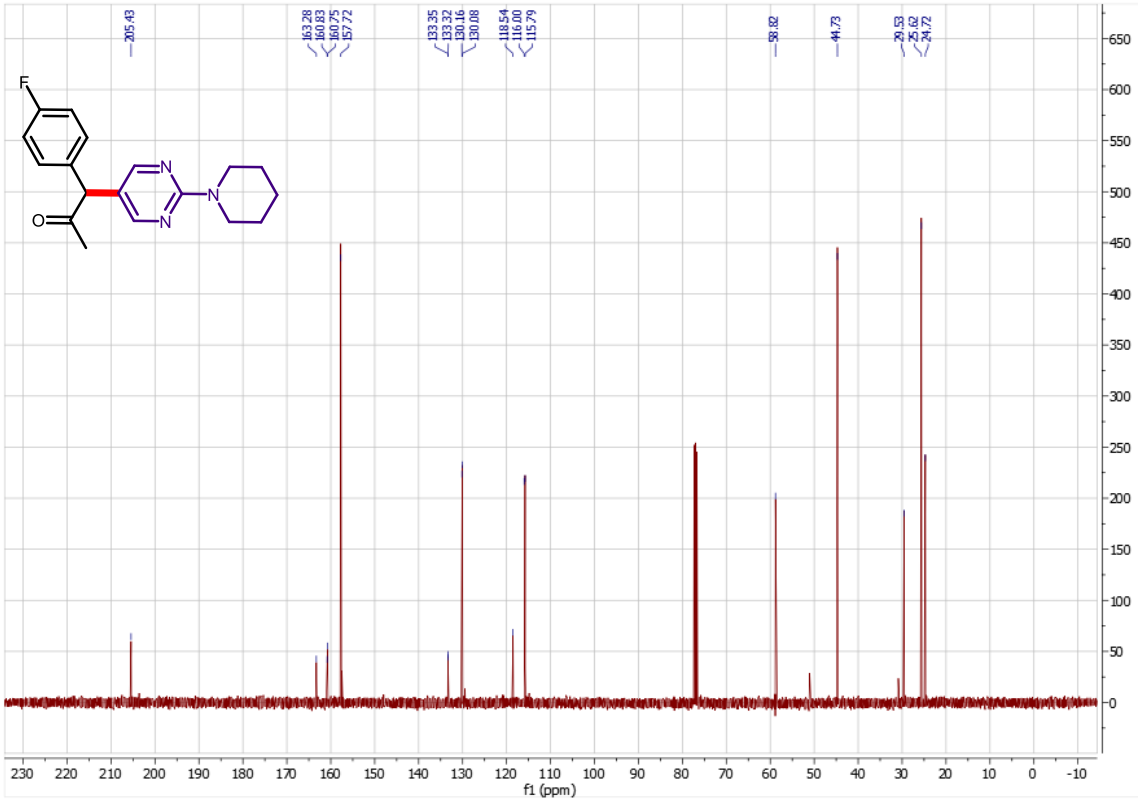
F
O
N
N
N
205.43
163.28
160.83
160.75
157.72
133.35
133.32
130.16
130.08
118.54
116.00
115.79
58.82
44.73
29.53
25.62
24.72
f1 (ppm)

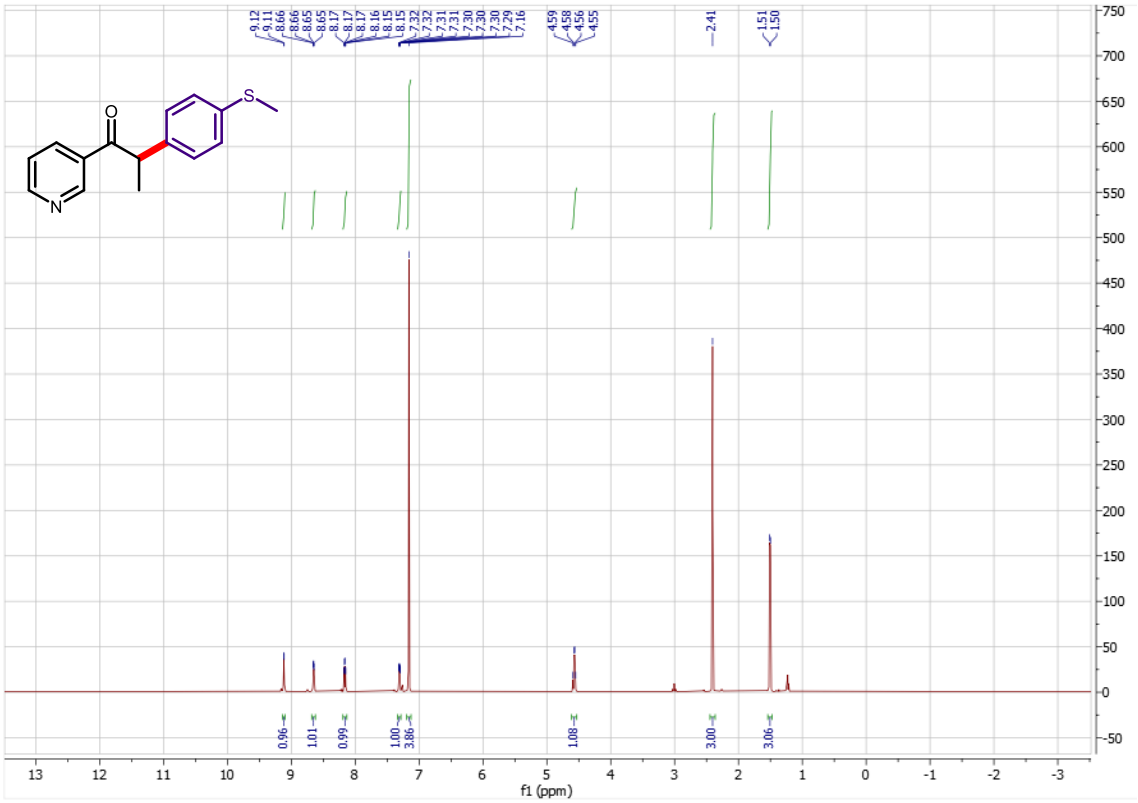
9.12
9.11
8.66
8.66
8.65
8.65
8.17
8.17
8.17
8.17
8.16
8.16
8.15
8.15
7.32
7.32
7.31
7.31
7.30
7.30
7.30
7.29
7.16
4.59
4.58
4.56
4.55
2.41
1.51
1.50
0.96
1.01
0.99
1.00
3.86
1.08
3.00
3.06
f1 (ppm)

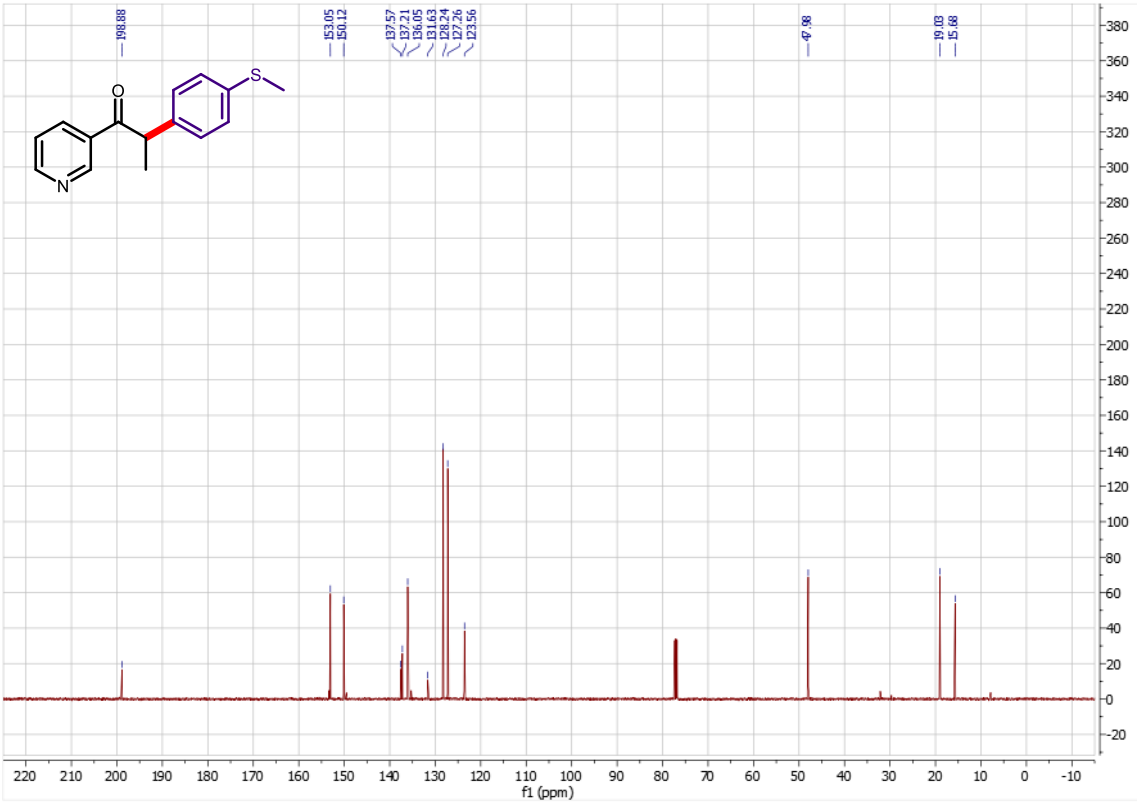
198.88
153.05
150.12
137.57
137.21
136.05
131.63
128.24
127.26
123.56
47.98
19.03
15.68
f1 (ppm)

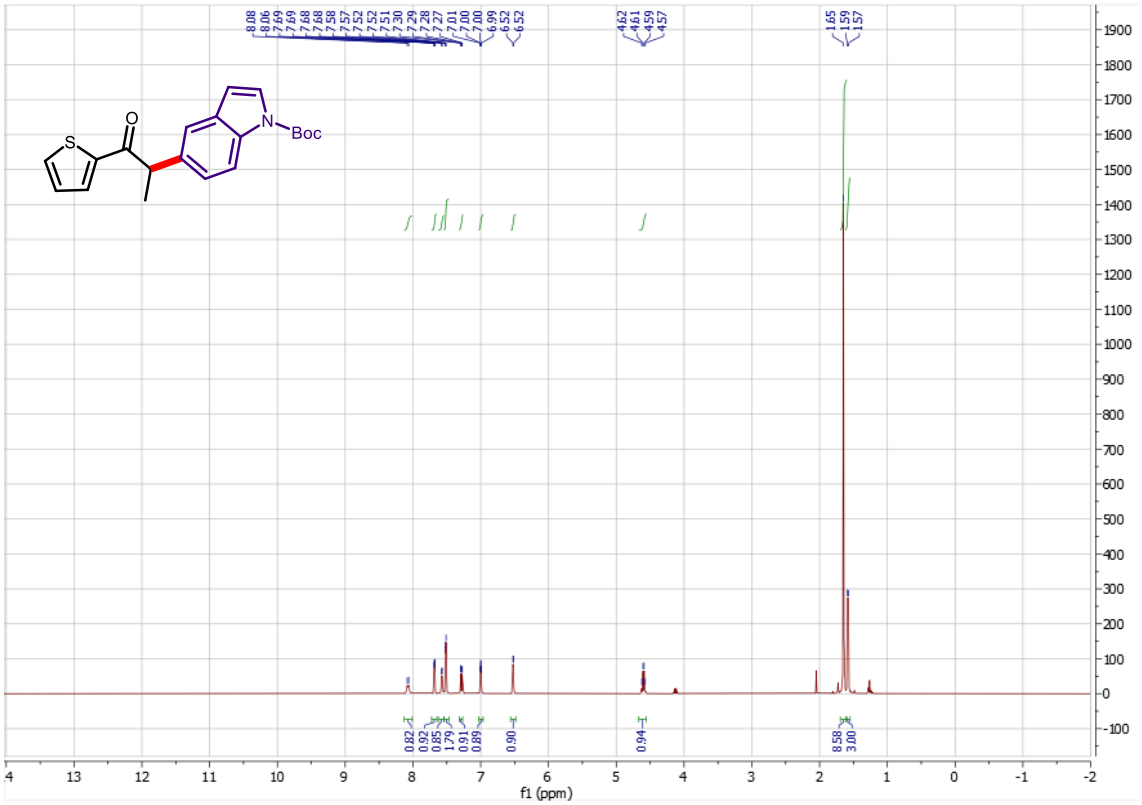
8.08
8.06
7.69
7.69
7.68
7.68
7.58
7.57
7.52
7.52
7.51
7.30
7.29
7.28
7.27
7.01
7.00
7.00
6.99
6.52
6.52
4.62
4.61
4.59
4.57
1.65
1.59
1.57
O
S
N
Boc
0.82
0.92
0.85
1.79
0.91
0.89
0.90
0.94
8.58
3.00
f1 (ppm)

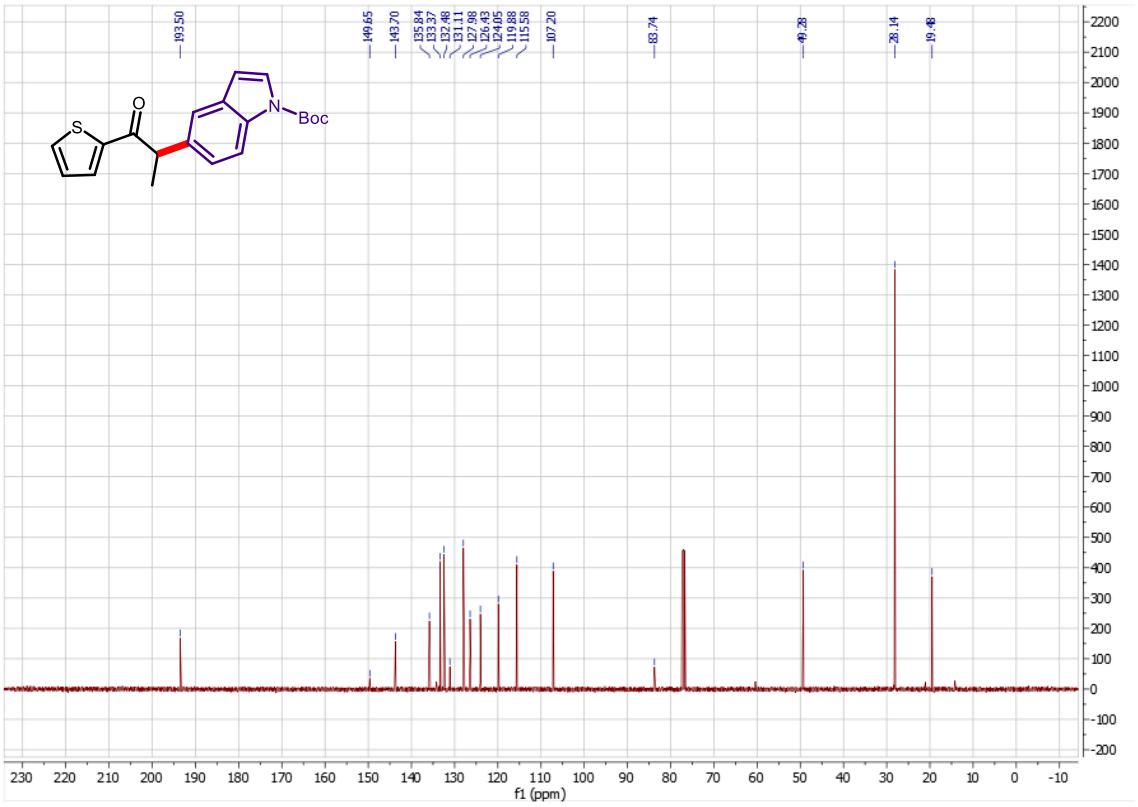
193.50
149.65
143.70
135.84
133.37
132.48
131.11
127.98
126.43
124.05
119.88
115.58
107.20
83.74
49.28
28.14
19.48
O
S
N
Boc
f1 (ppm)

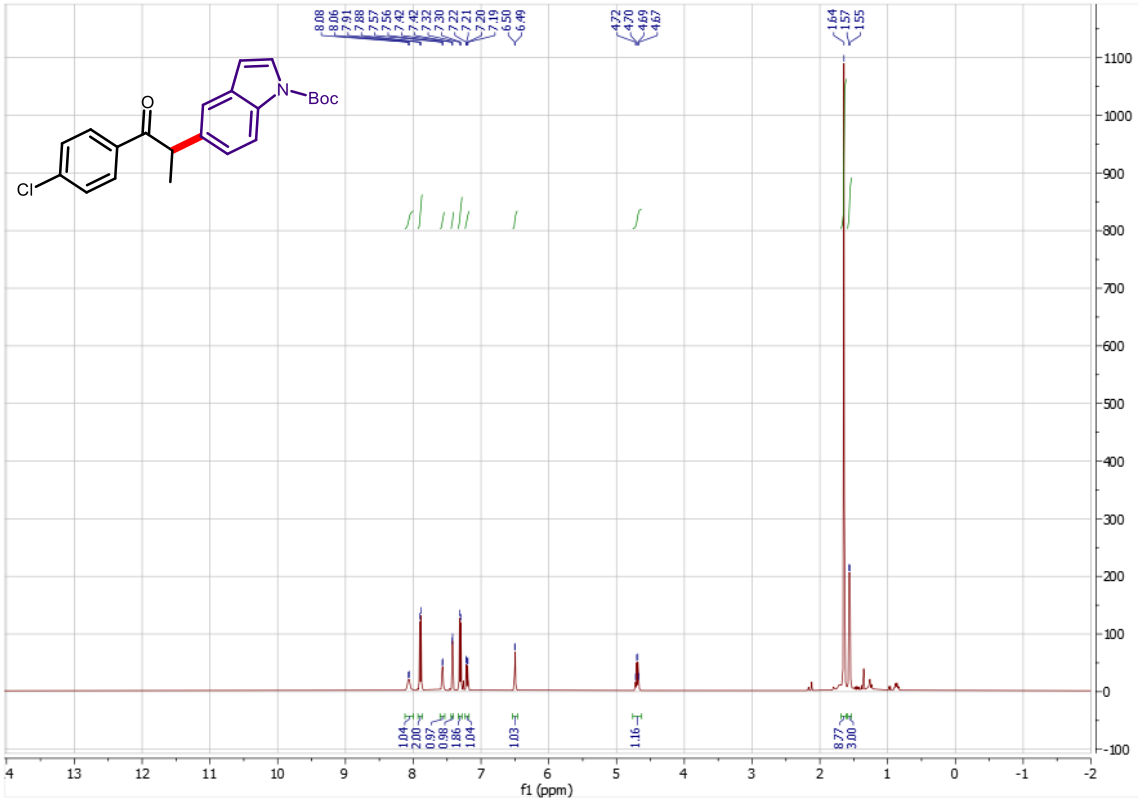
8.08
8.06
7.91
7.88
7.57
7.56
7.42
7.42
7.32
7.30
7.22
7.21
7.20
7.19
6.50
6.49
4.72
4.70
4.69
4.67
1.64
1.57
1.55
Boc
O
Cl
1.04
2.07
6.97
0.98
1.86
1.04
1.03
1.16
8.77
3.00
f1 (ppm)

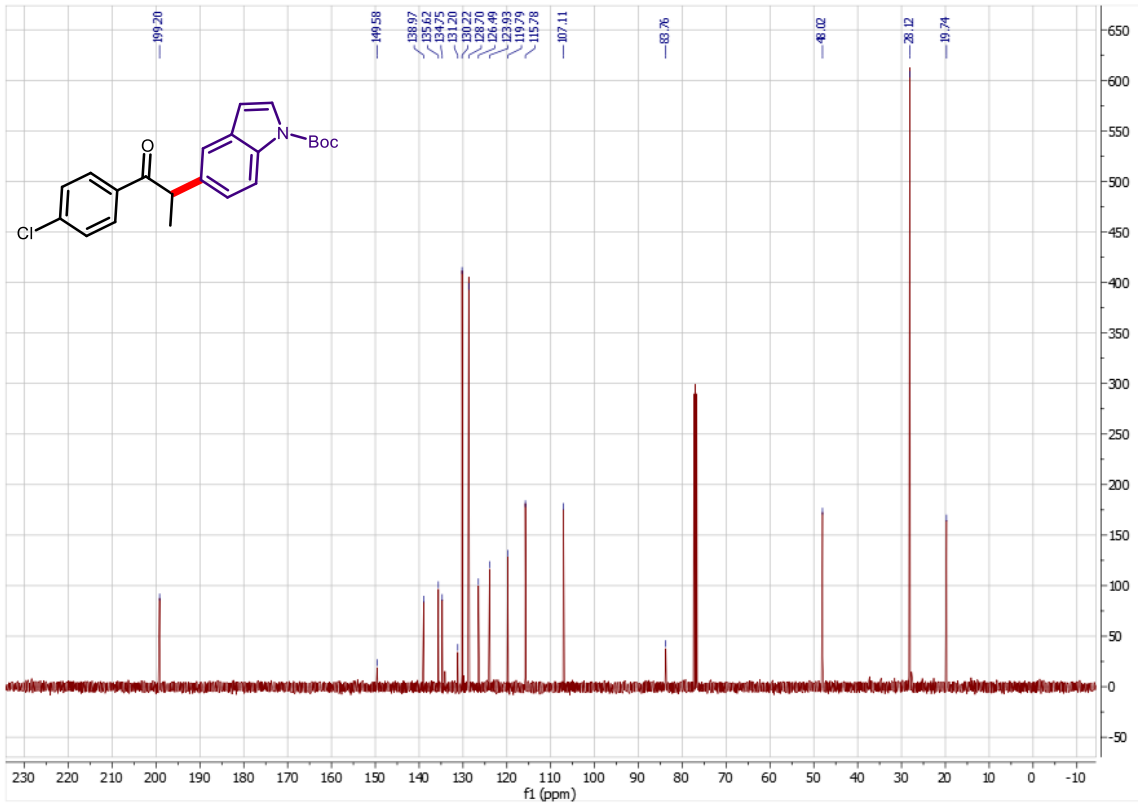
199.20
149.58
138.97
135.62
134.75
131.20
130.22
128.70
126.49
123.93
119.79
115.78
107.11
83.76
48.02
28.12
19.74
Boc
O
Cl
f1 (ppm)

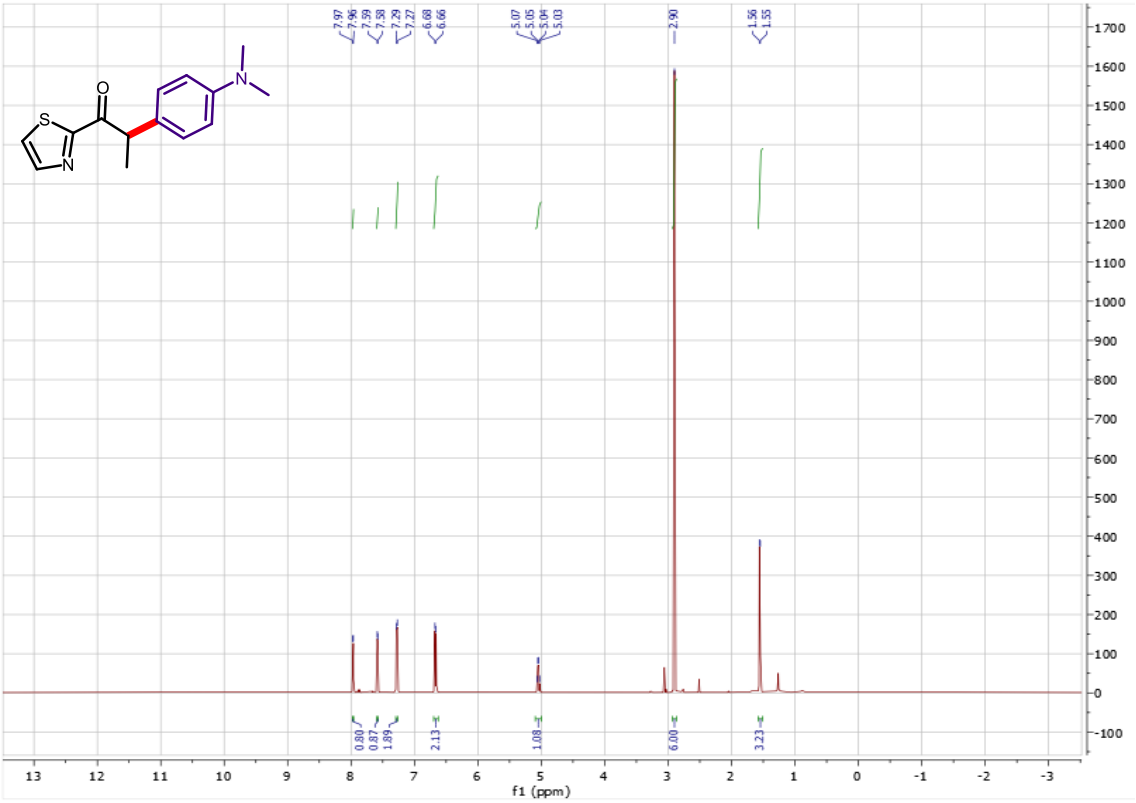
7.97
7.96
7.59
7.58
7.29
7.27
6.68
6.66
5.07
5.05
5.04
5.03
2.90
1.56
1.55
0.80
0.87
1.89
2.13
1.08
6.00
3.23
f1 (ppm)

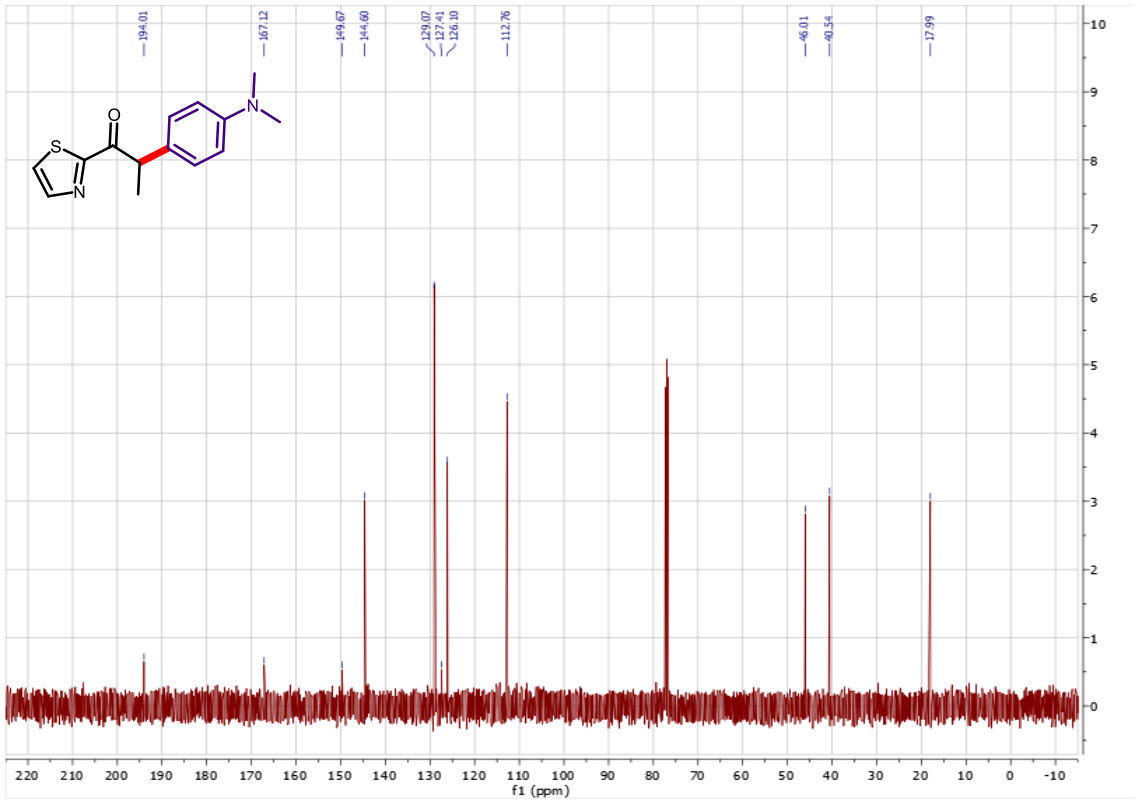
194.01
167.12
149.67
144.60
129.07
127.41
126.10
112.76
46.01
40.54
17.99
f1 (ppm)

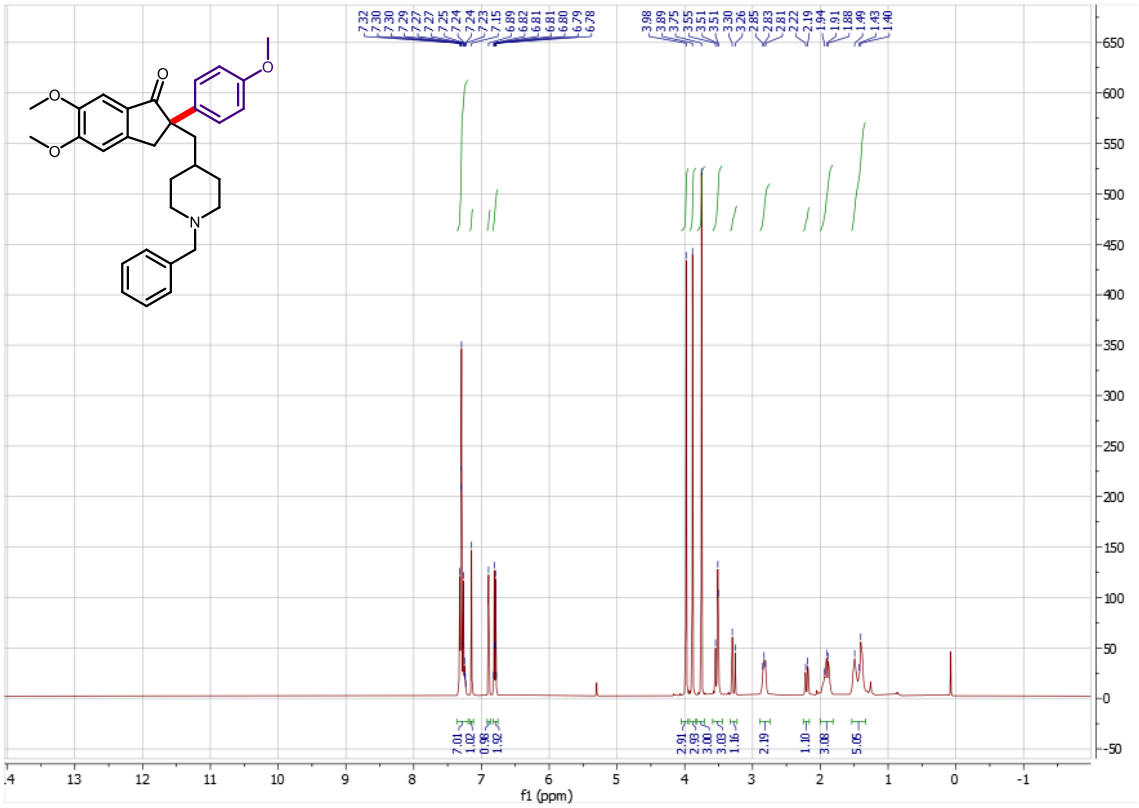
f1 (ppm)

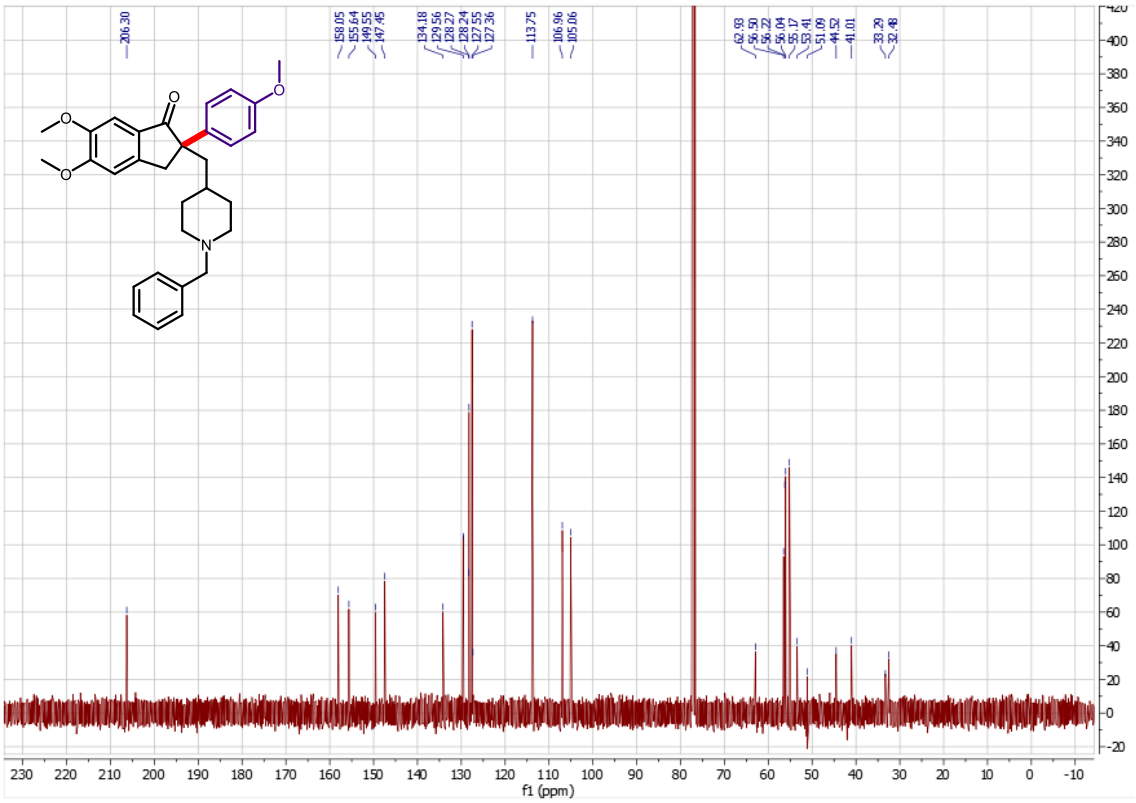
f1 (ppm)

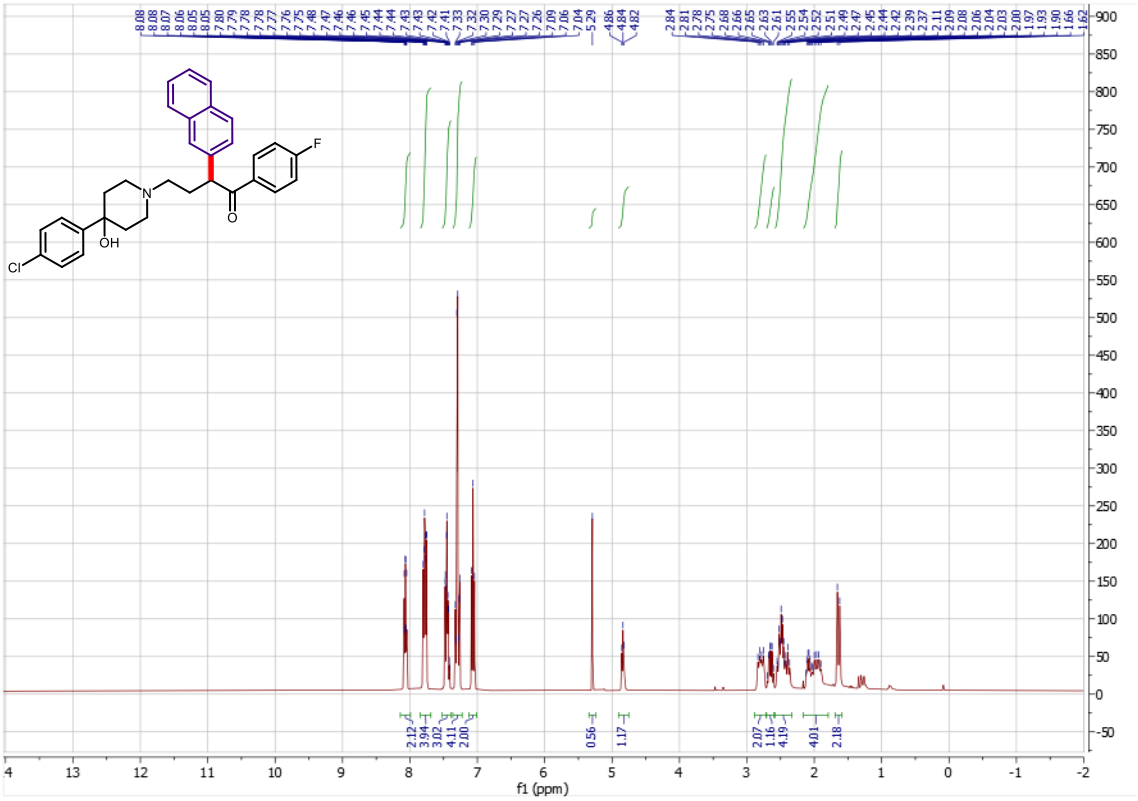
F
N
O
OH
Cl
f1 (ppm)

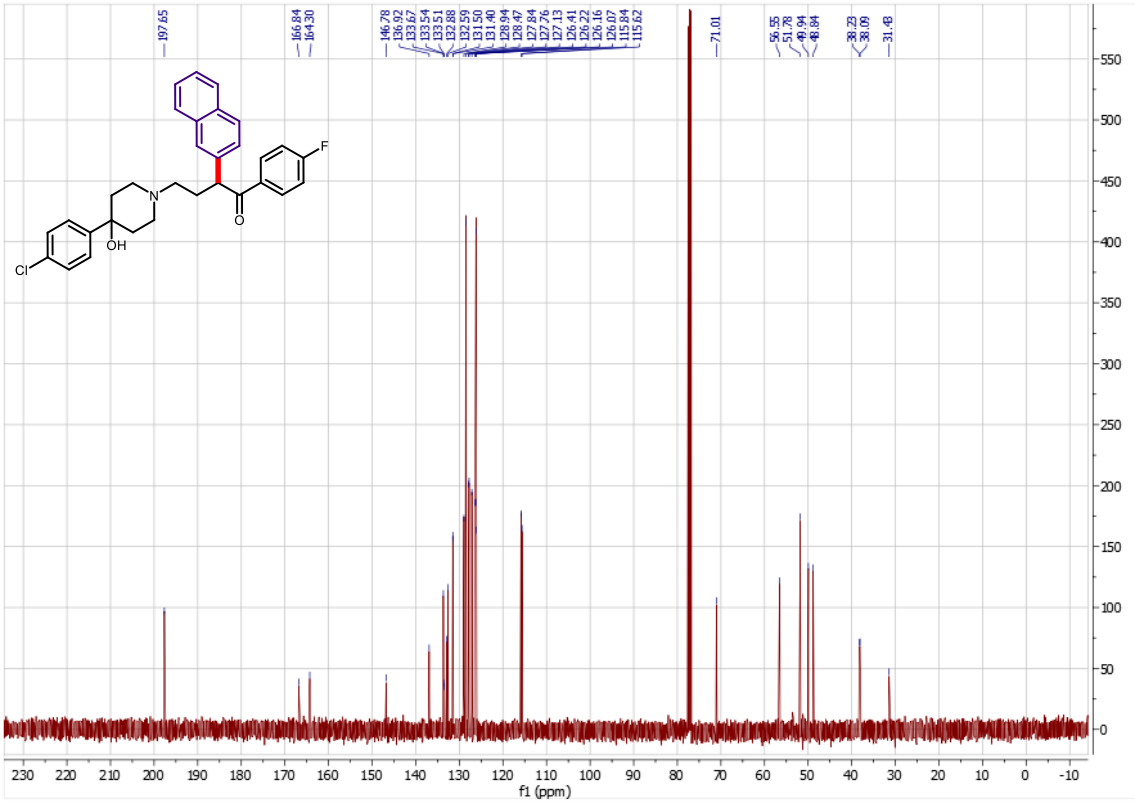
F
N
O
OH
Cl
f1 (ppm)

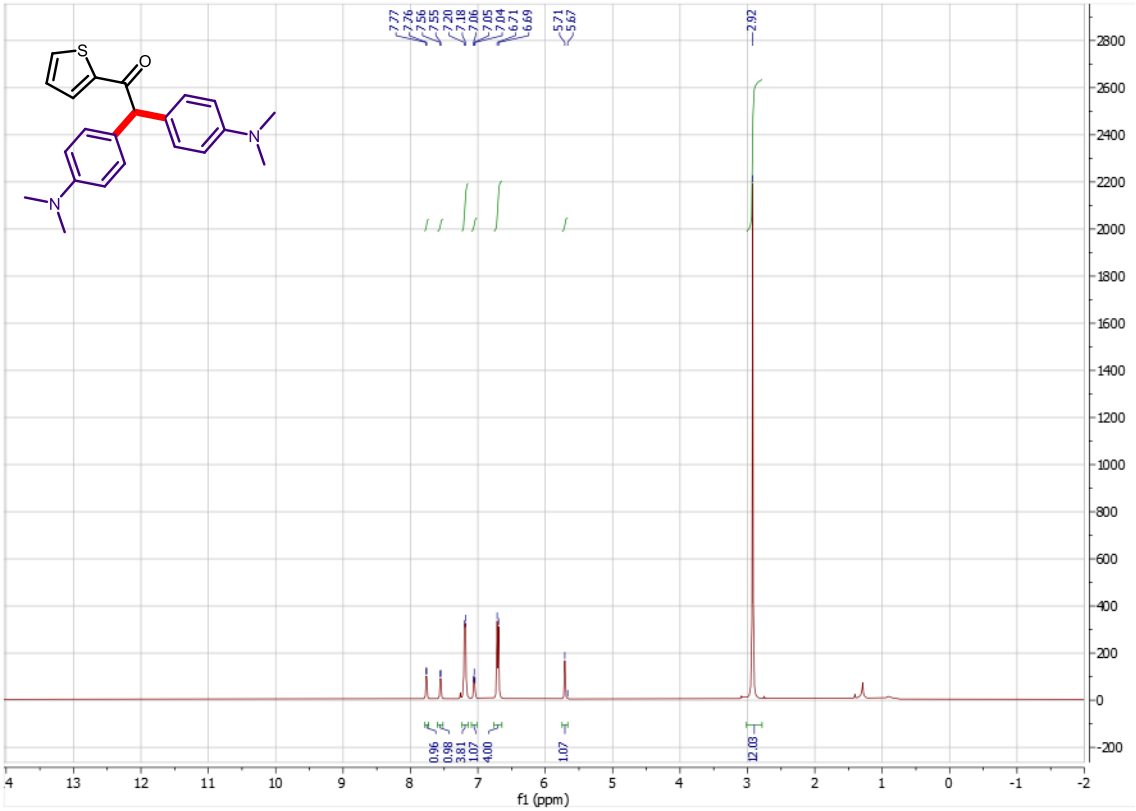
7.77
7.76
7.56
7.55
7.20
7.18
7.06
7.05
7.04
6.71
6.69
5.71
5.67
2.92
0.96
0.98
3.81
1.07
4.00
1.07
12.03
f1 (ppm)

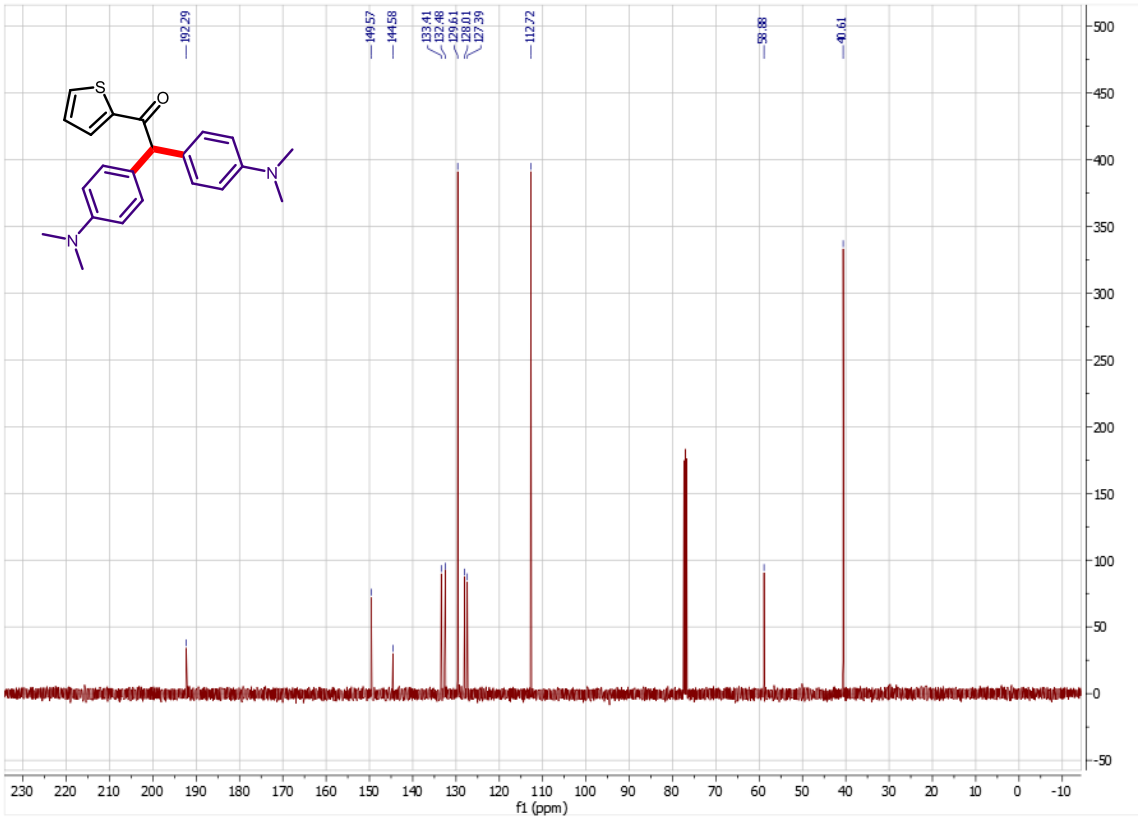
192.29
149.57
144.58
133.41
132.48
129.61
128.01
127.39
112.72
58.88
40.61
f1 (ppm)

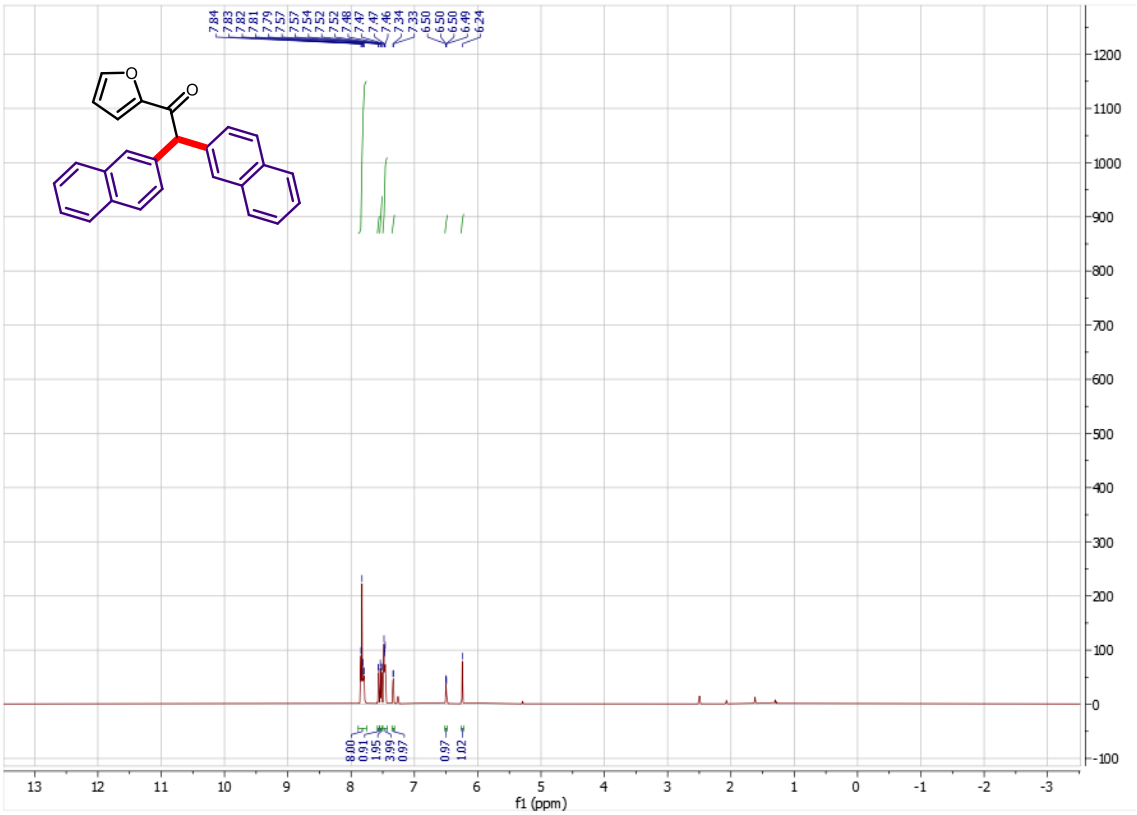
7.84
7.83
7.82
7.81
7.79
7.57
7.57
7.54
7.52
7.52
7.48
7.47
7.47
7.46
7.34
7.33
6.50
6.50
6.50
6.49
6.24
8.00
0.91
1.95
3.99
0.97
0.97
1.02
f1 (ppm)

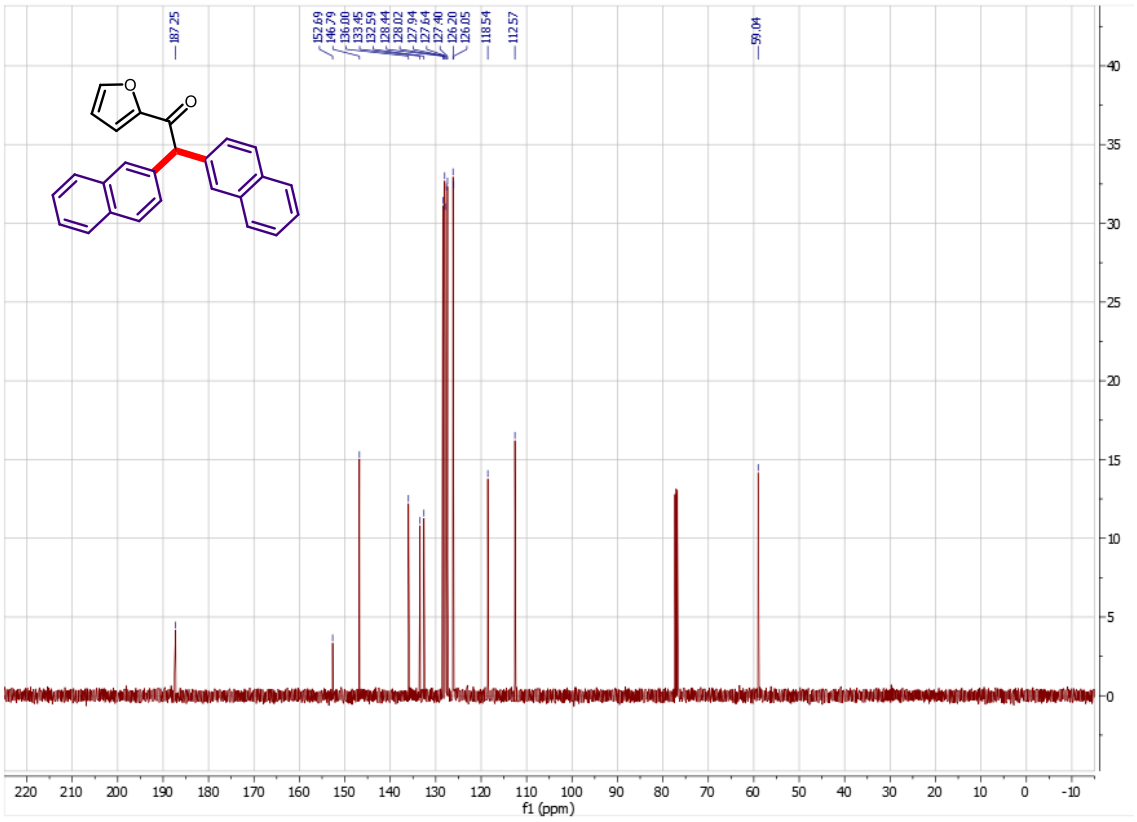
187.25
152.69
146.79
136.00
133.45
132.59
128.44
128.02
127.94
127.64
127.40
126.20
126.05
118.54
112.57
59.04
f1 (ppm)

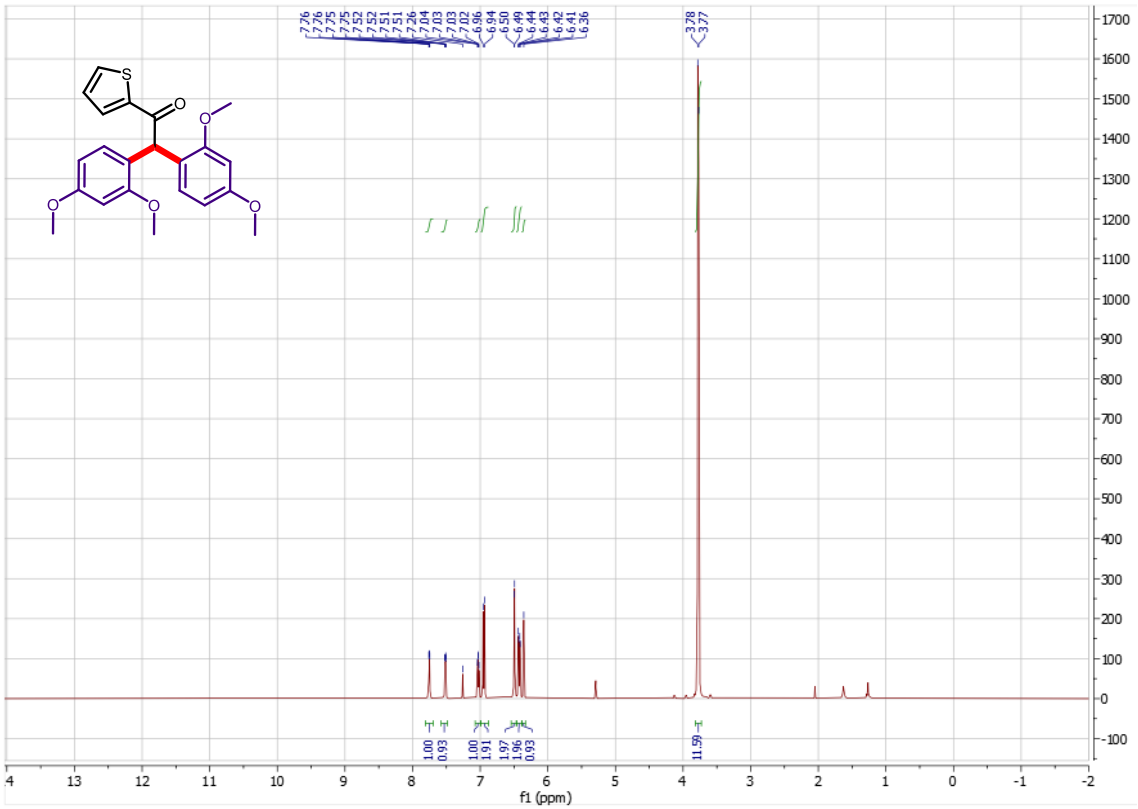
7.76
7.76
7.75
7.75
7.52
7.52
7.51
7.51
7.26
7.04
7.03
7.03
7.02
6.96
6.94
6.50
6.49
6.44
6.43
6.42
6.41
6.36
3.78
3.77
1.00
0.93
1.00
1.91
1.97
1.96
0.93
11.59
f1 (ppm)

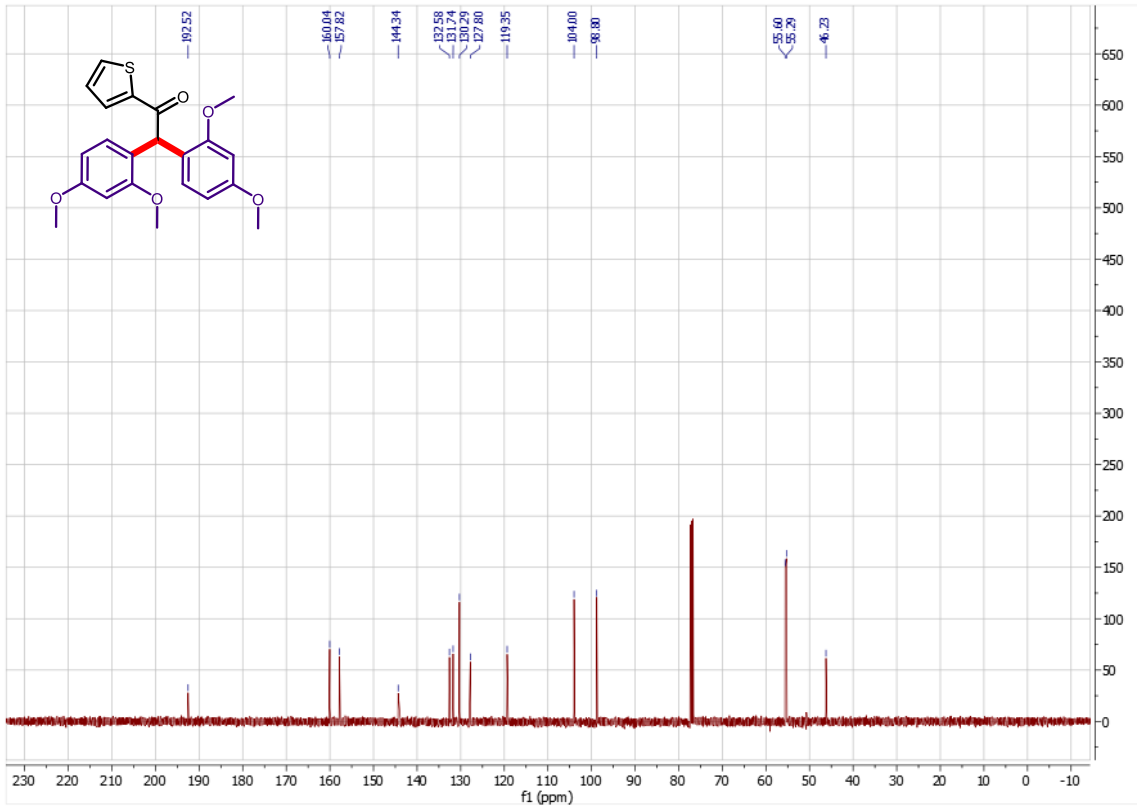
192.52
160.04
157.82
144.34
132.58
131.74
130.29
127.80
119.35
104.00
98.80
55.60
55.29
46.23
f1 (ppm)

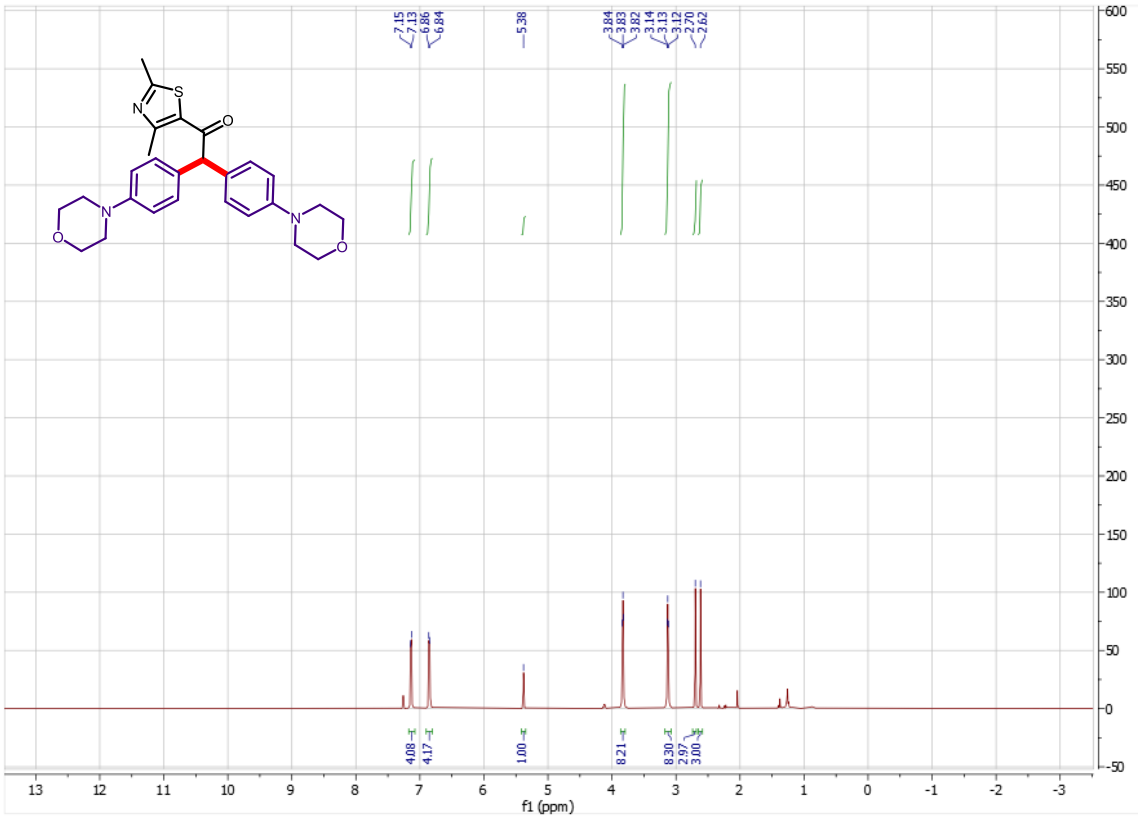
7.15
7.13
6.86
6.84
5.38
3.84
3.83
3.82
3.14
3.13
3.12
2.70
2.62
4.08
4.17
1.00
8.21
8.30
2.97
3.00
f1 (ppm)

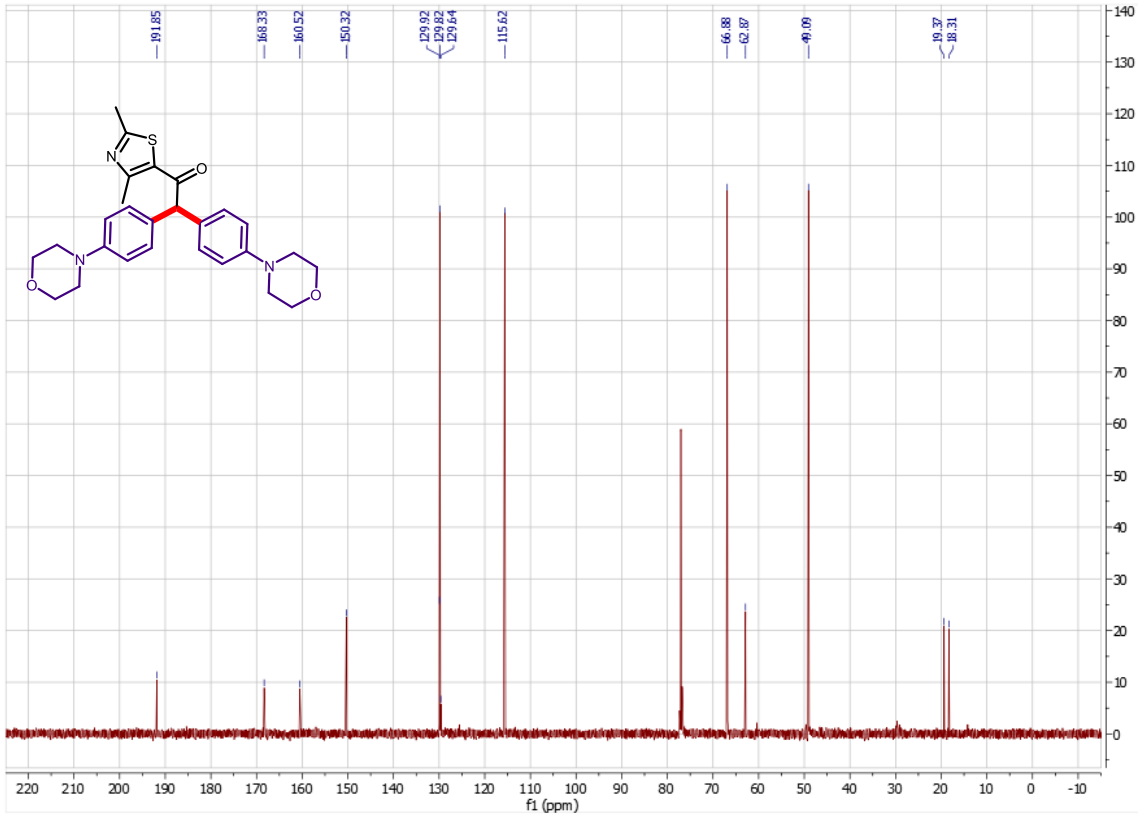
191.85
168.33
160.52
150.32
129.92
129.82
129.64
115.62
66.88
62.87
49.09
19.37
18.31
f1 (ppm)

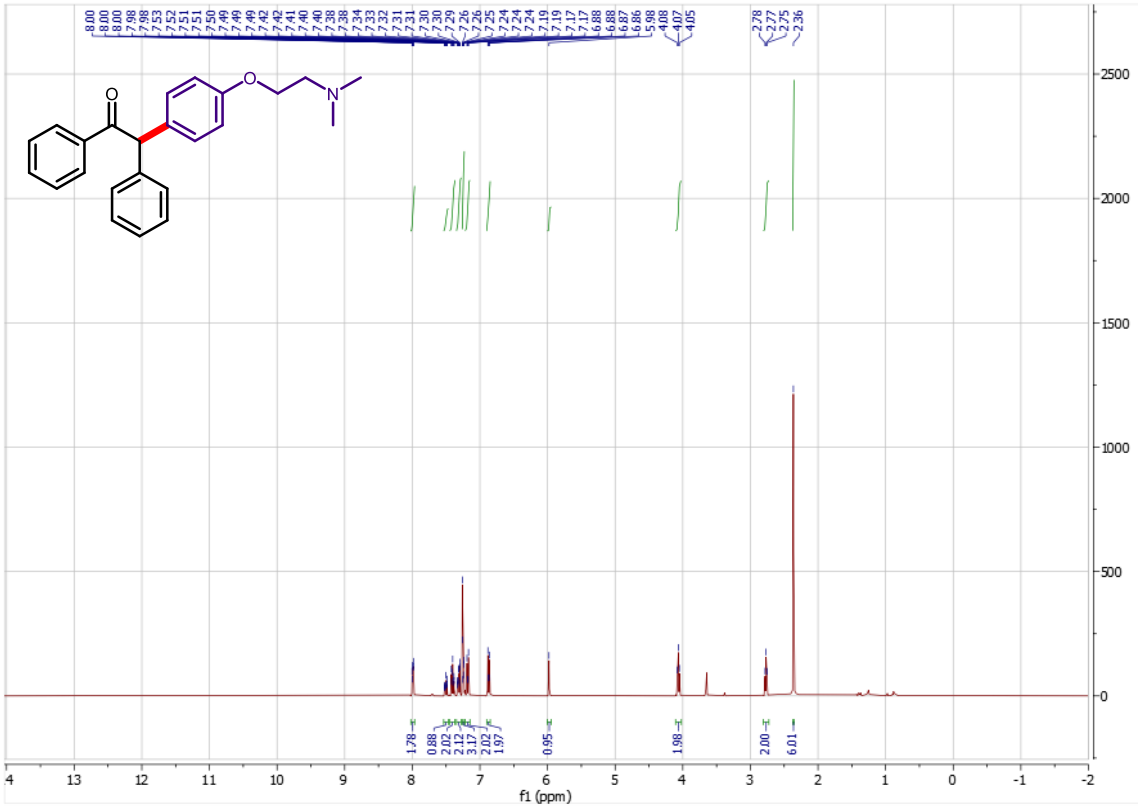
f1 (ppm)

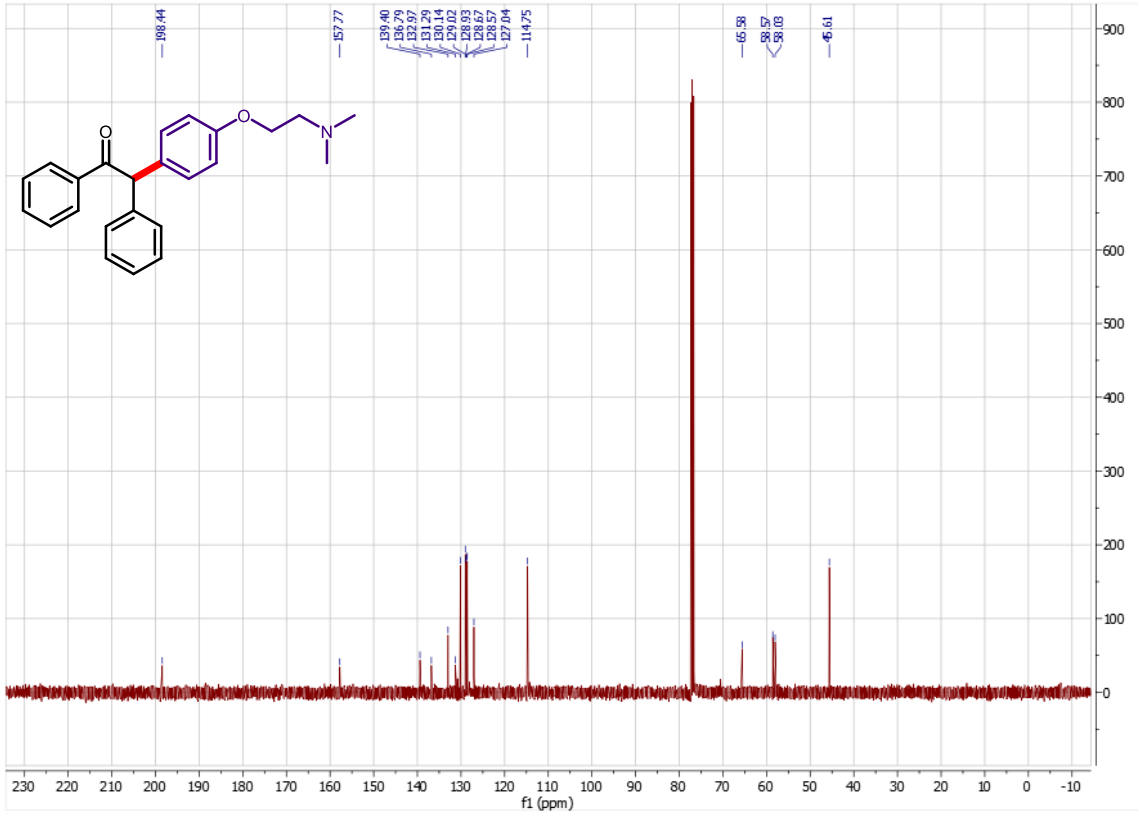
f1 (ppm)

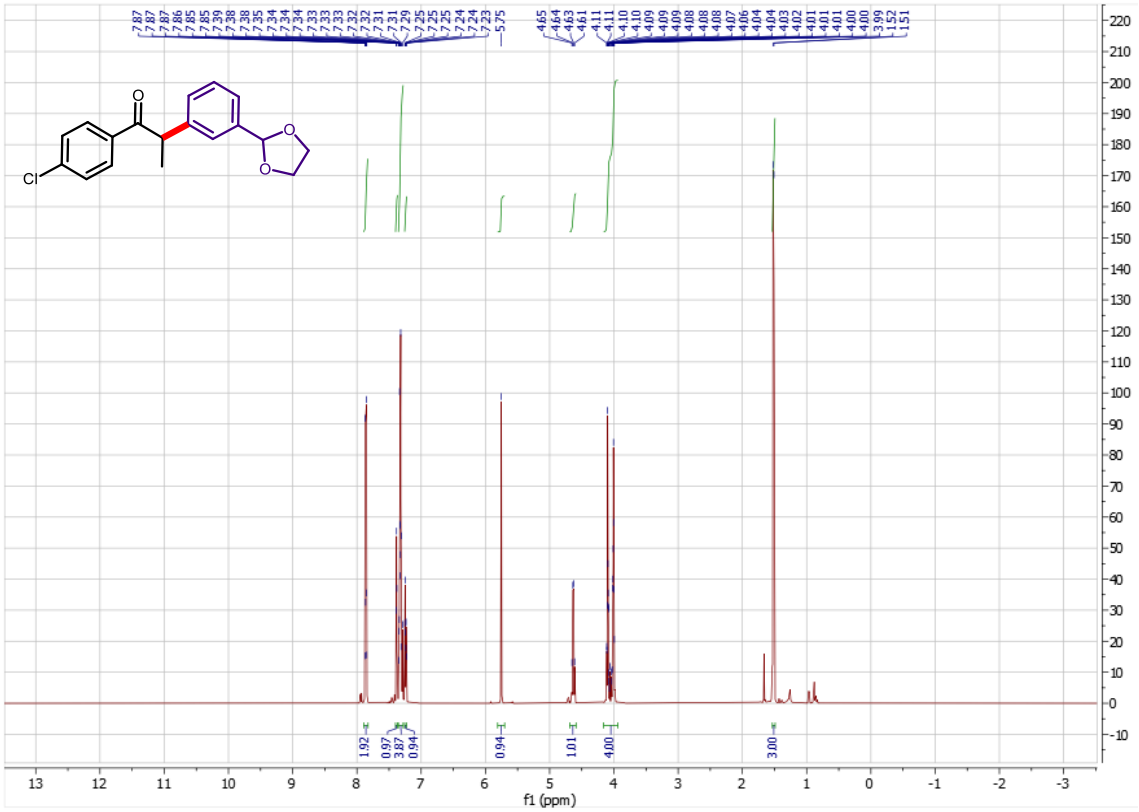
f1 (ppm)

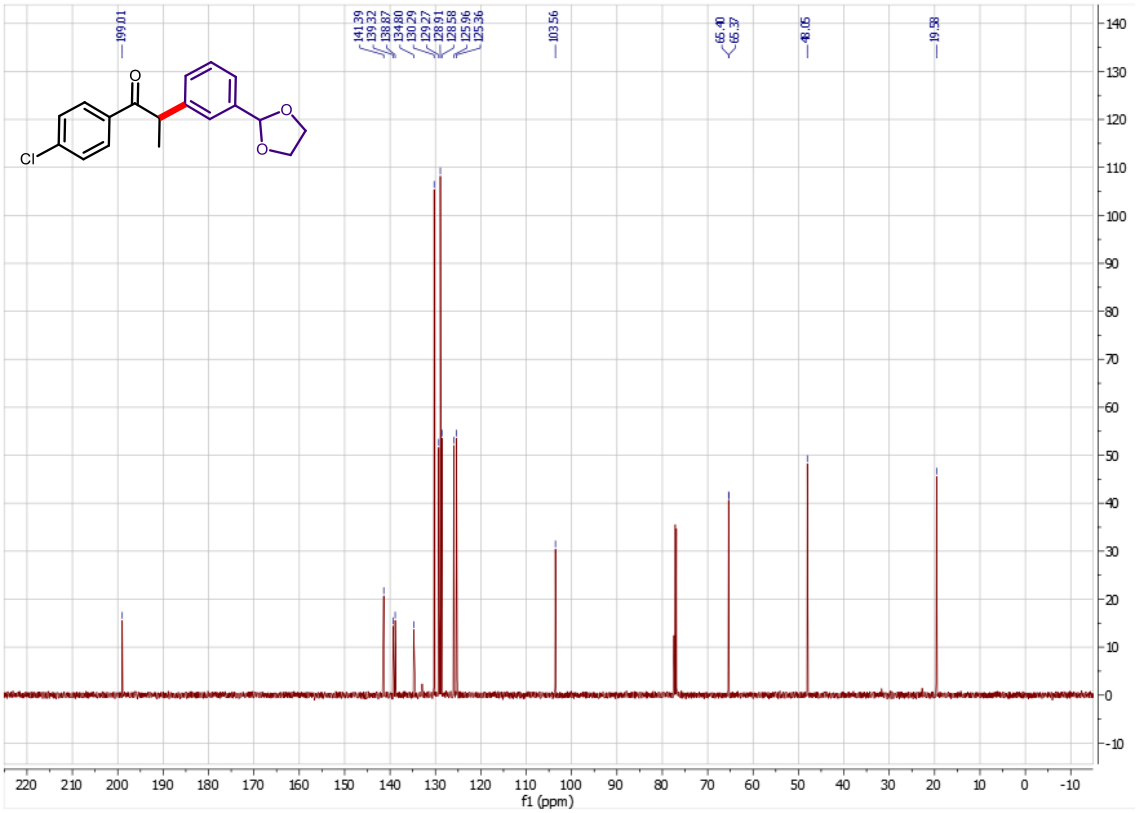
f1 (ppm)

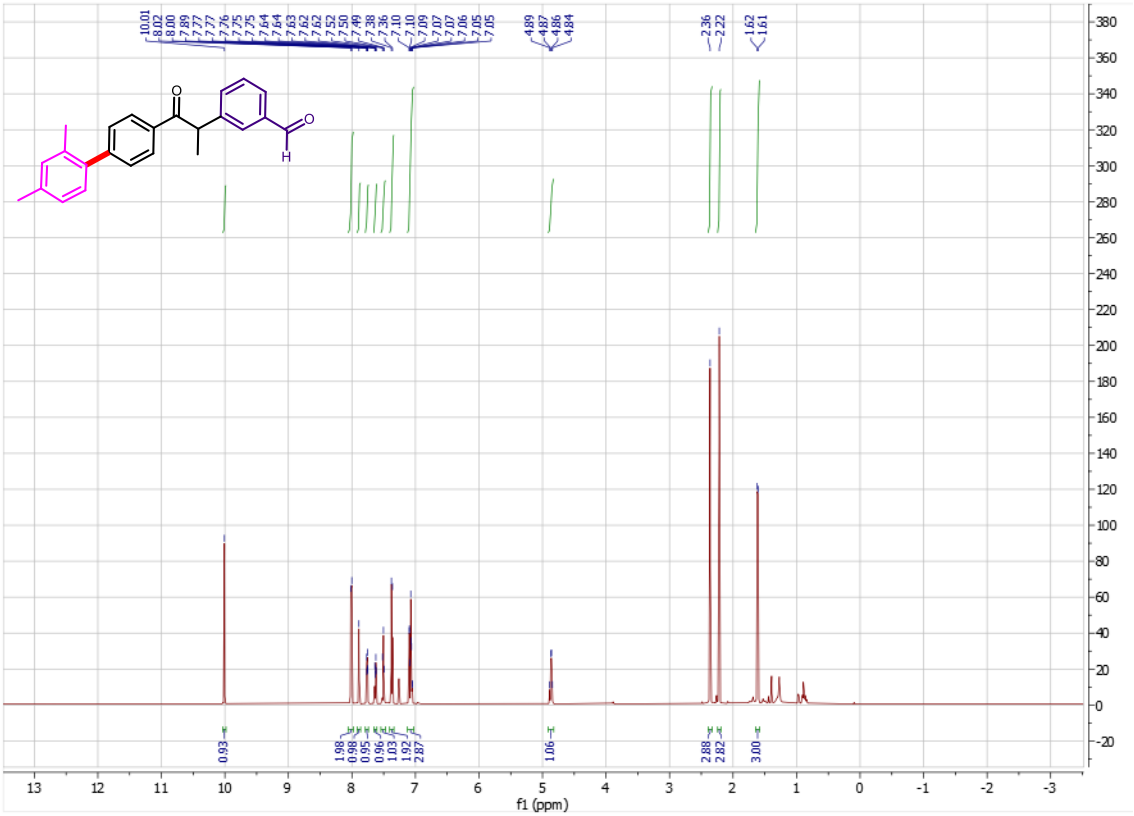
10.01
8.02
8.00
7.89
7.77
7.77
7.76
7.75
7.75
7.64
7.64
7.63
7.62
7.62
7.52
7.50
7.49
7.38
7.36
7.10
7.09
7.07
7.07
7.06
7.05
7.05
4.89
4.87
4.86
4.84
2.36
2.22
1.62
1.61
O
O
H
0.93
1.98
0.98
0.95
0.96
1.03
1.92
2.87
1.06
2.88
2.82
3.00
f1 (ppm)

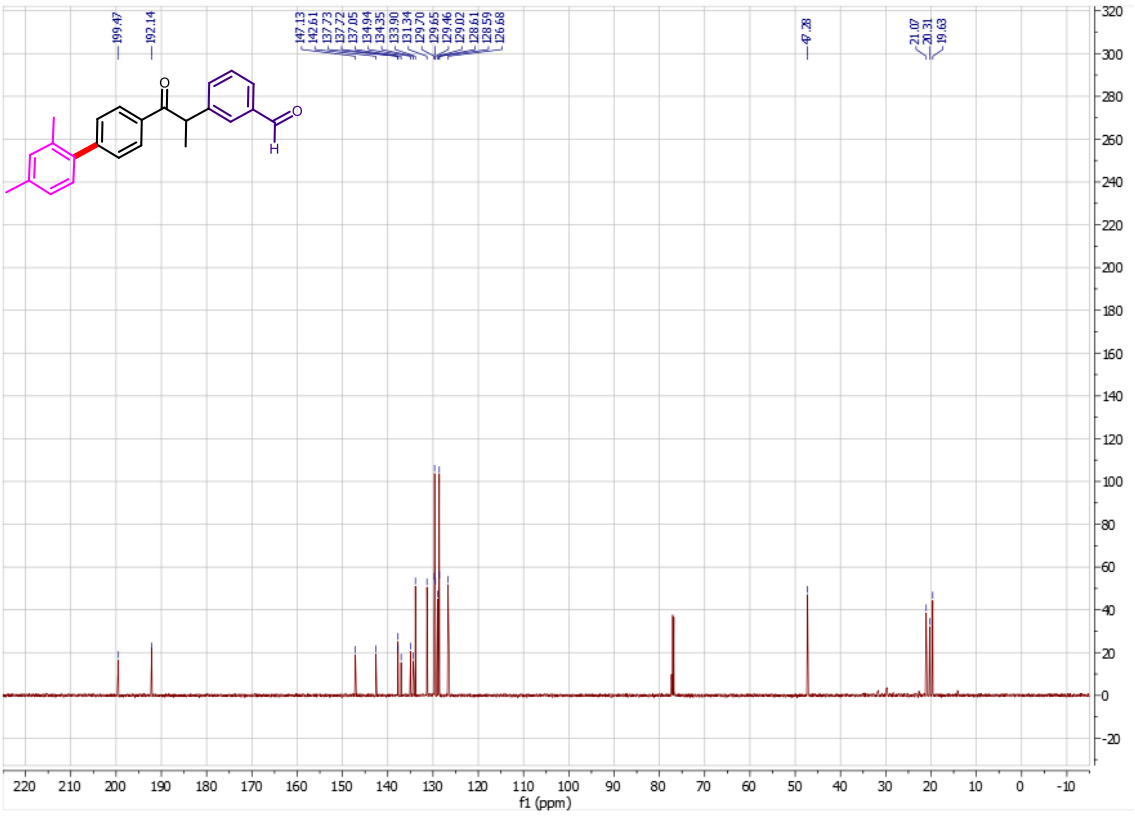
199.47
192.14
147.13
142.61
137.73
137.22
137.05
134.94
134.35
133.90
131.34
129.70
129.65
129.46
129.02
128.61
128.59
126.68
47.28
21.07
20.31
19.63
O
O
H
f1 (ppm)

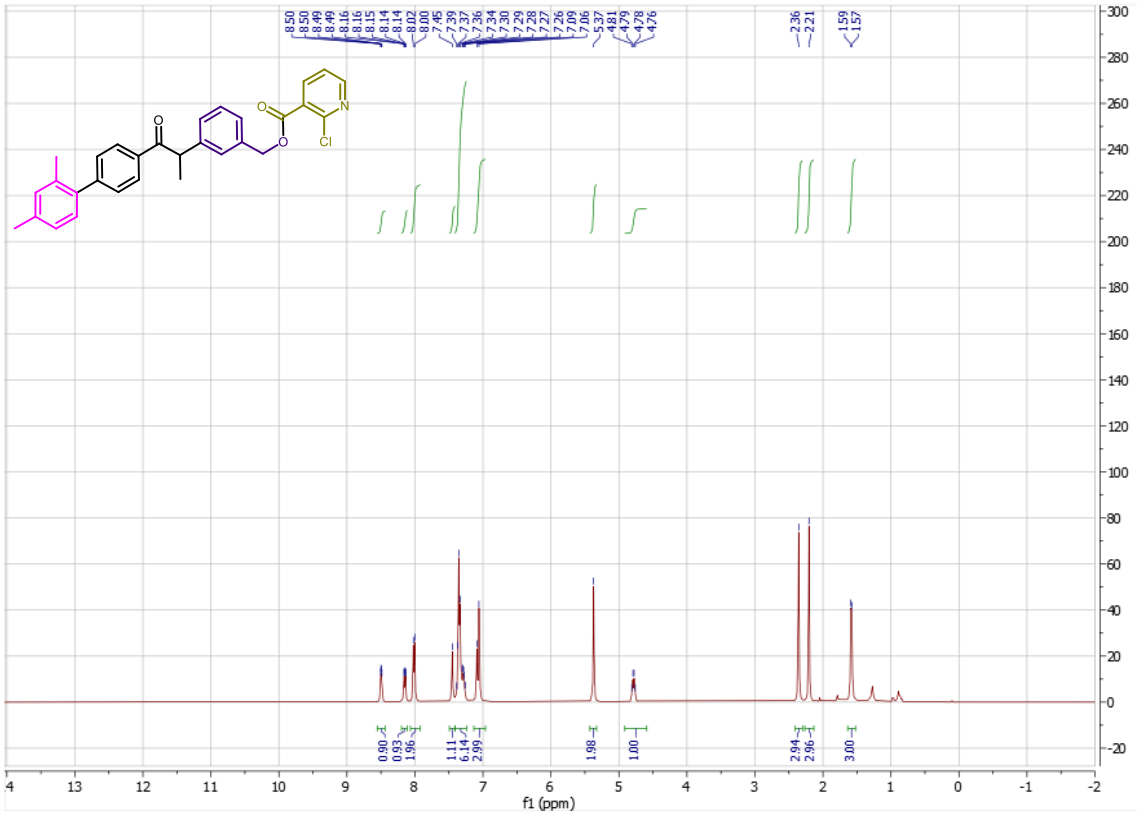
8.50
8.50
8.49
8.49
8.16
8.16
8.15
8.14
8.14
8.02
8.00
7.45
7.39
7.37
7.36
7.34
7.30
7.29
7.28
7.27
7.26
7.09
7.06
5.37
4.81
4.79
4.78
4.76
2.36
2.21
1.59
1.57
0.90
0.93
1.96
1.11
6.14
2.99
1.98
1.00
2.94
2.96
3.00
f1 (ppm)

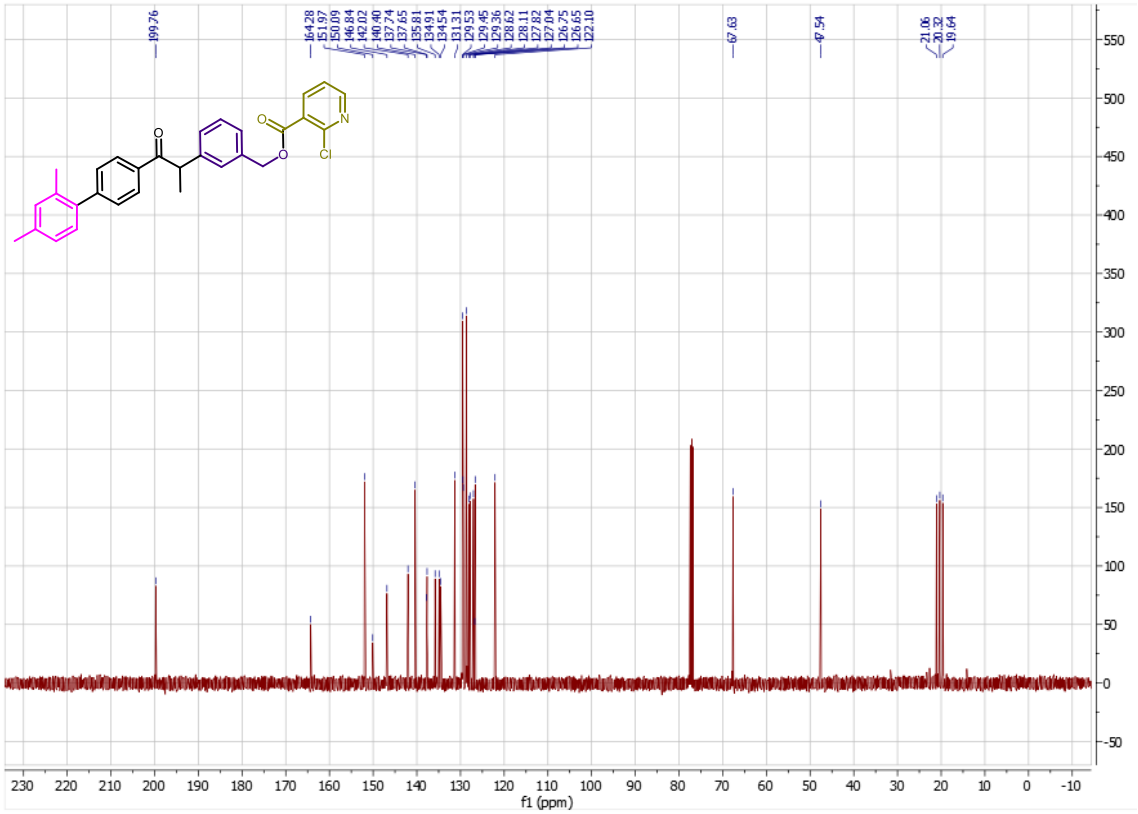
199.76
164.28
151.97
150.09
146.84
142.02
140.40
137.74
137.65
134.81
134.61
134.54
131.31
129.53
129.45
129.36
128.62
128.11
127.82
127.04
126.75
126.65
122.10
67.63
47.54
21.06
20.32
19.64
f1 (ppm)

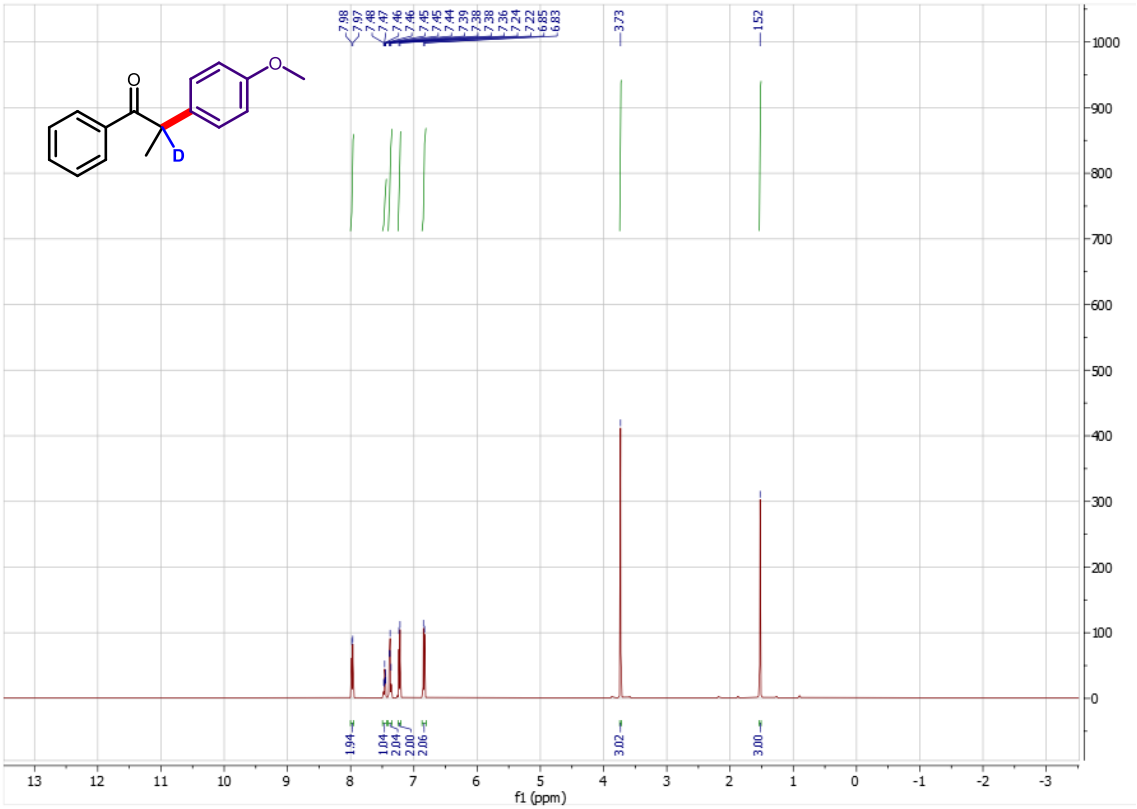
7.98
7.97
7.48
7.47
7.46
7.46
7.45
7.45
7.44
7.39
7.38
7.38
7.36
7.24
7.22
6.85
6.83
3.73
1.52
O
O
D
1.94
1.04
2.04
2.00
2.06
3.02
3.00
f1 (ppm)

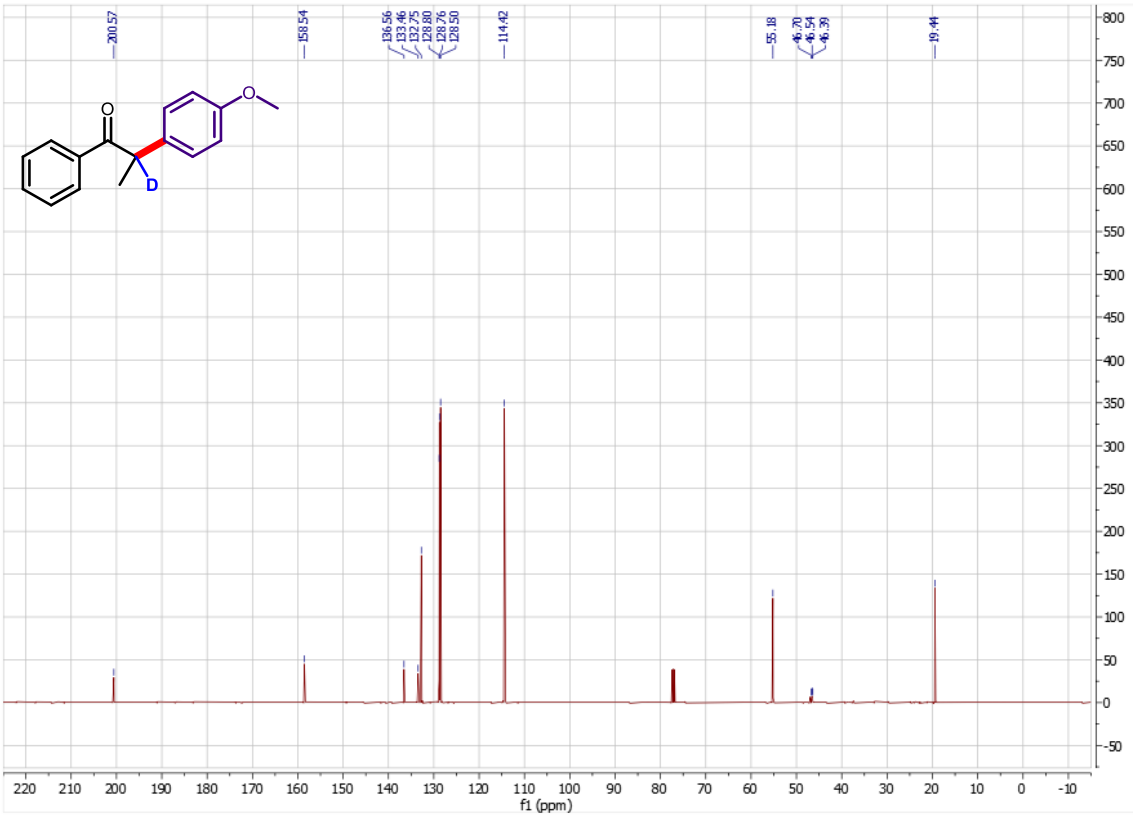
200.57
158.54
136.56
133.46
132.75
128.80
128.76
128.50
114.42
55.18
46.70
46.54
46.39
19.44
O
O
D
f1 (ppm)

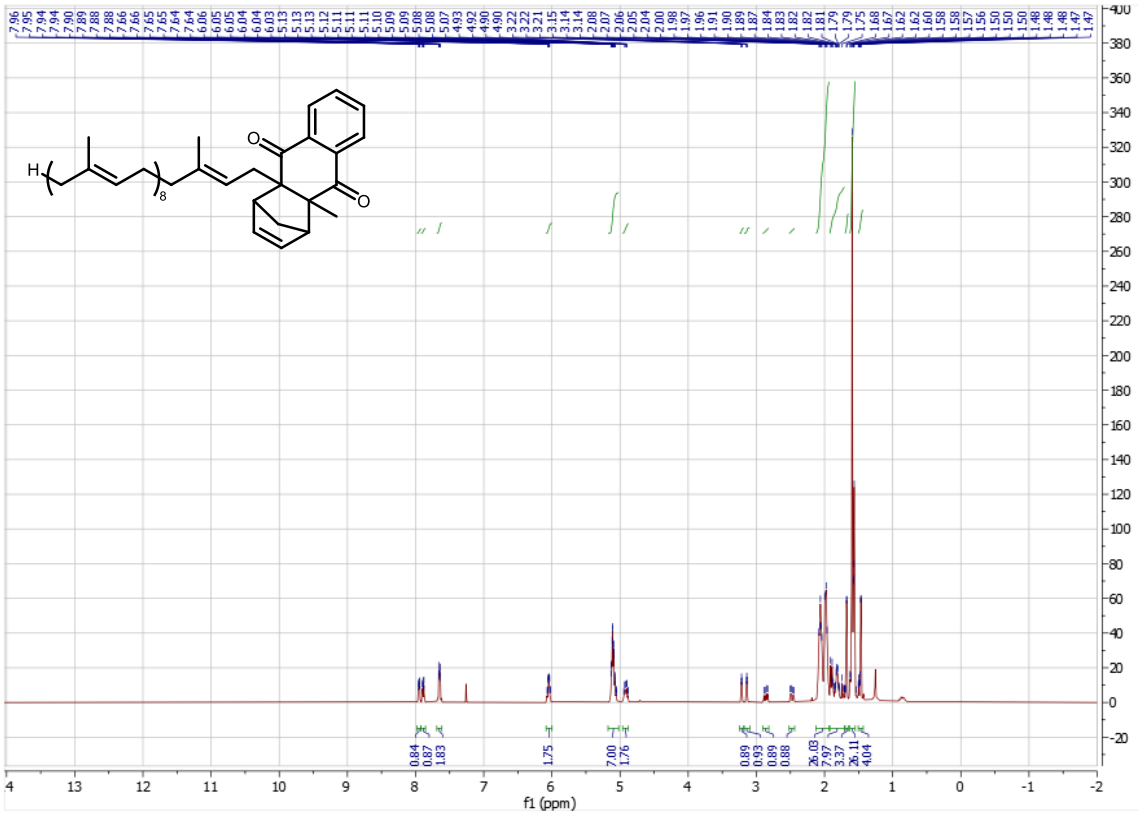
O
O
H
8
f1 (ppm)

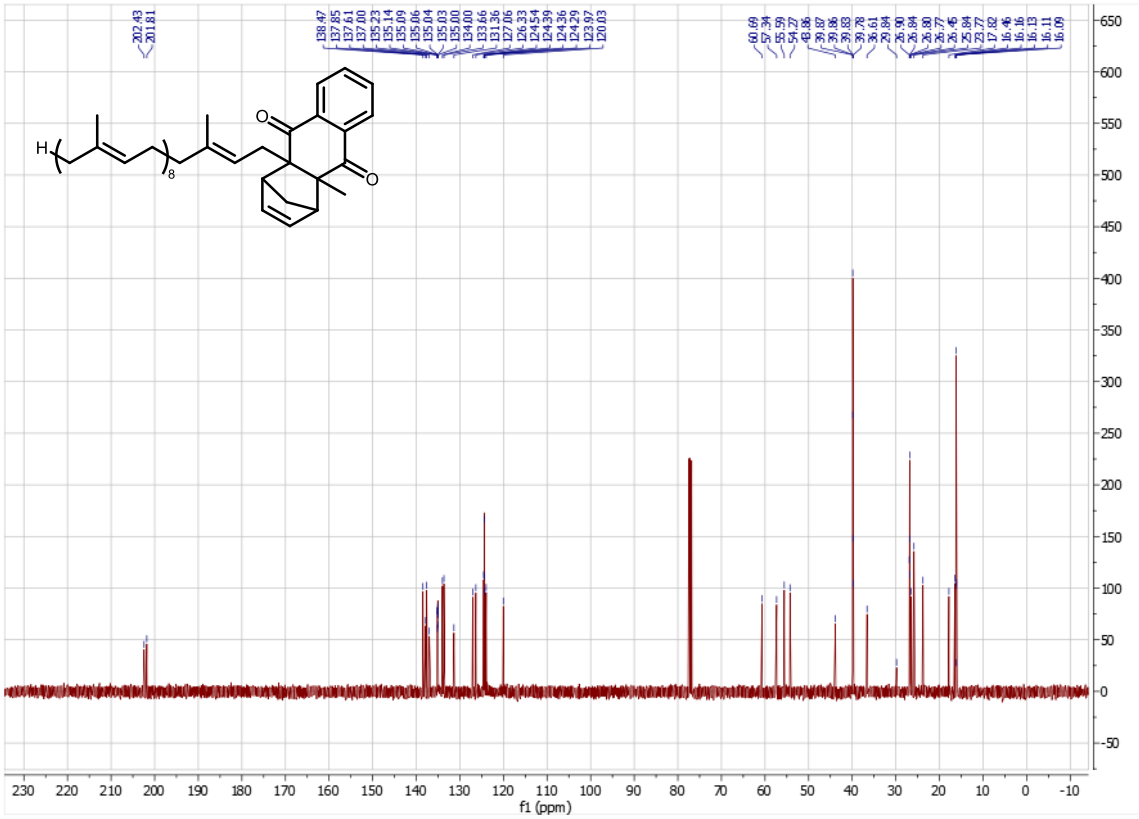
O
O
H
8
f1 (ppm)

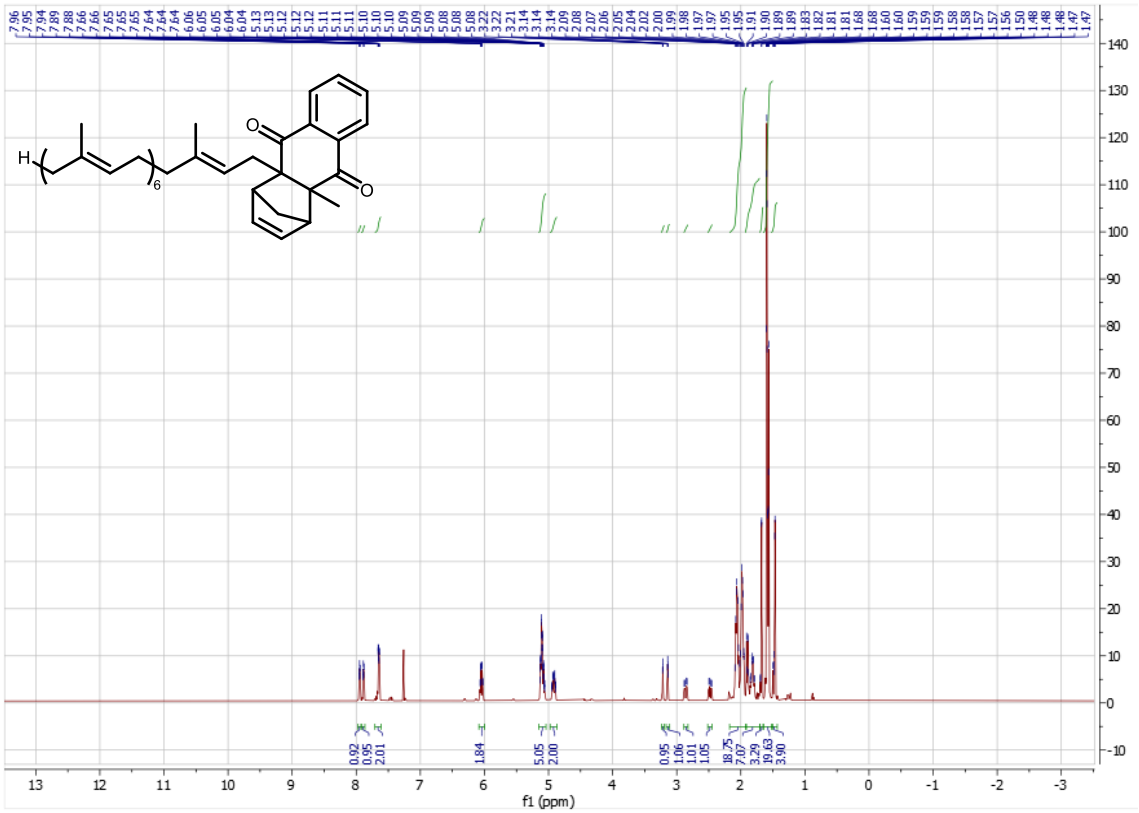
H
6
O
O
f1 (ppm)

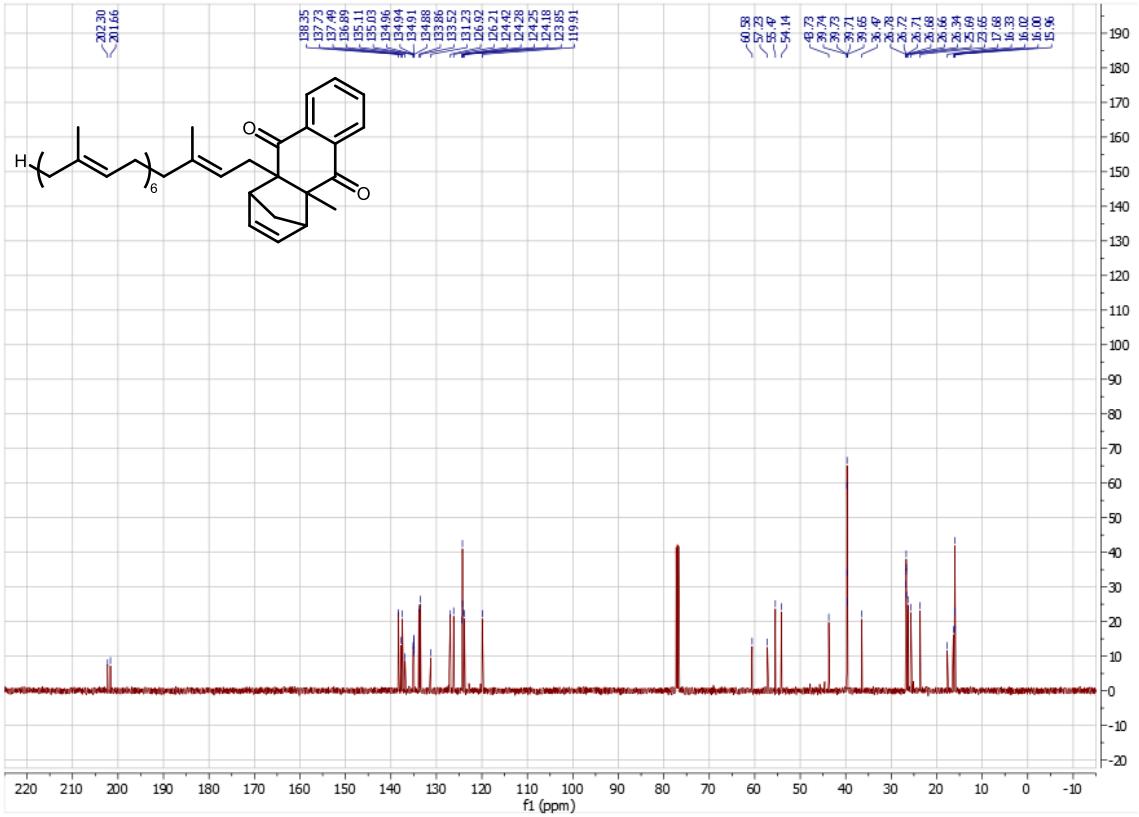
H
6
O
O
f1 (ppm)

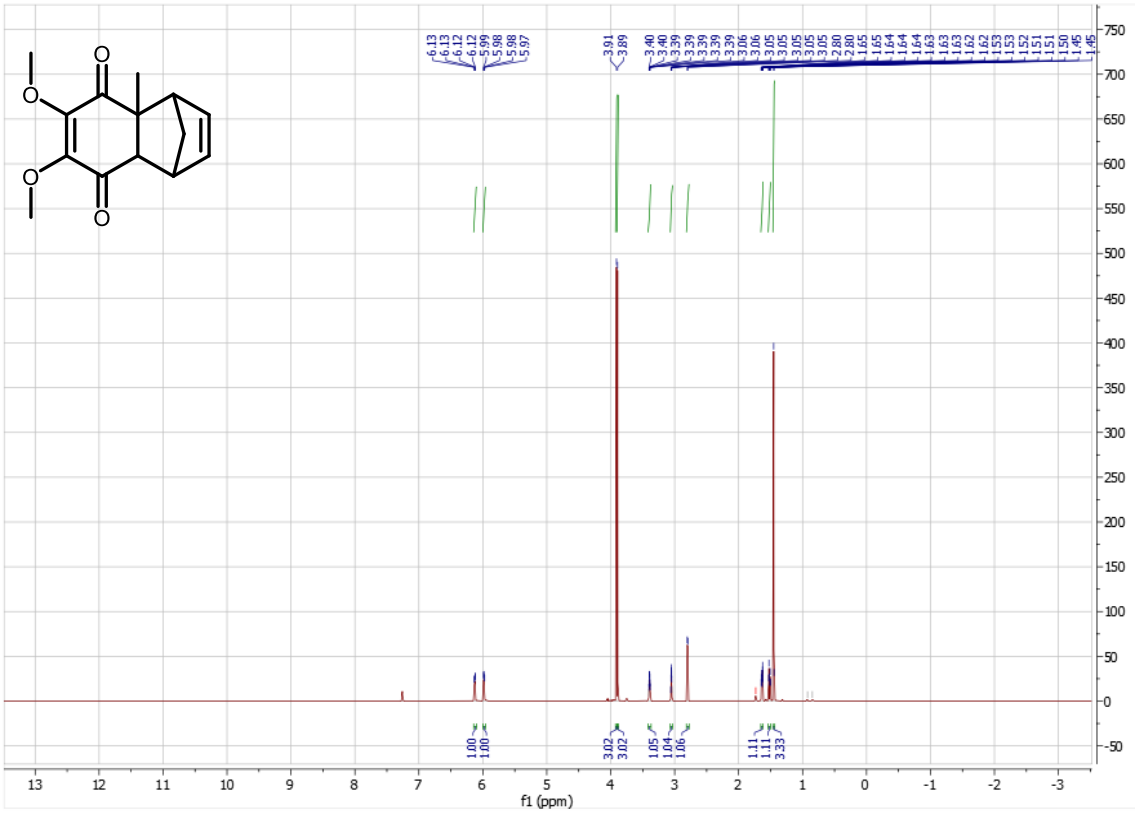
f1 (ppm)

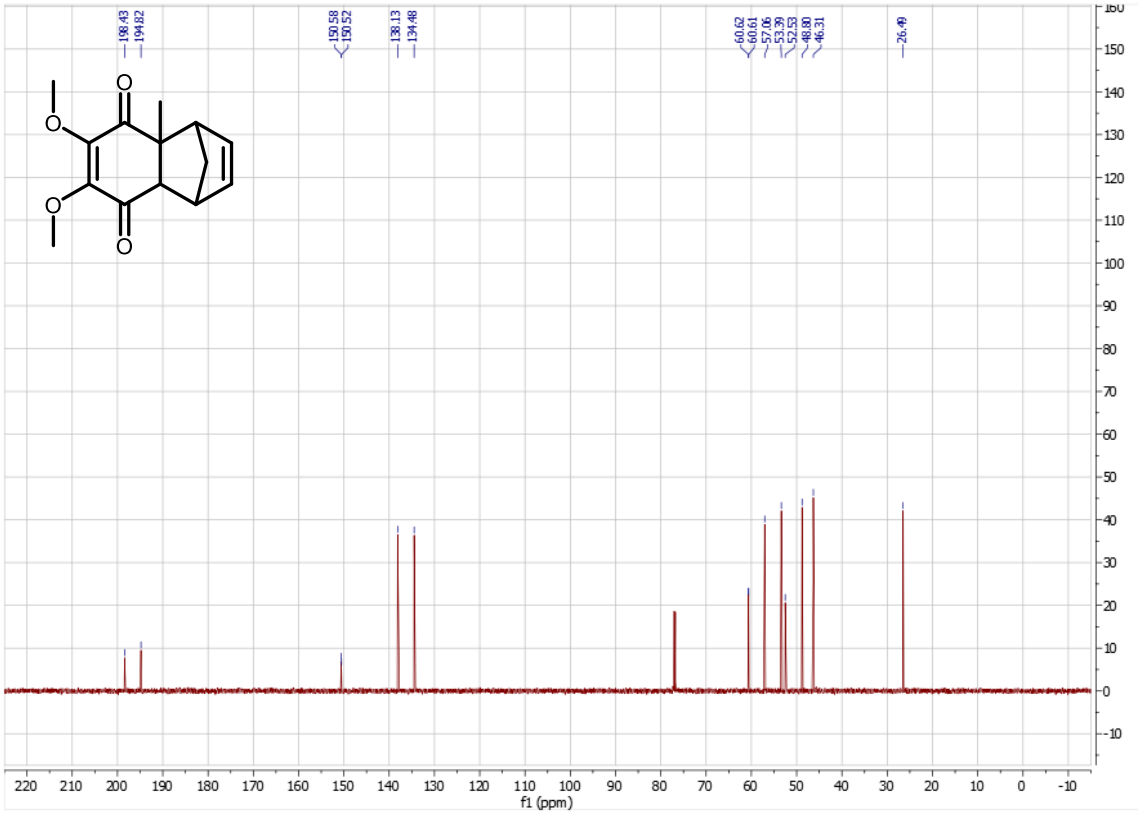
f1 (ppm)

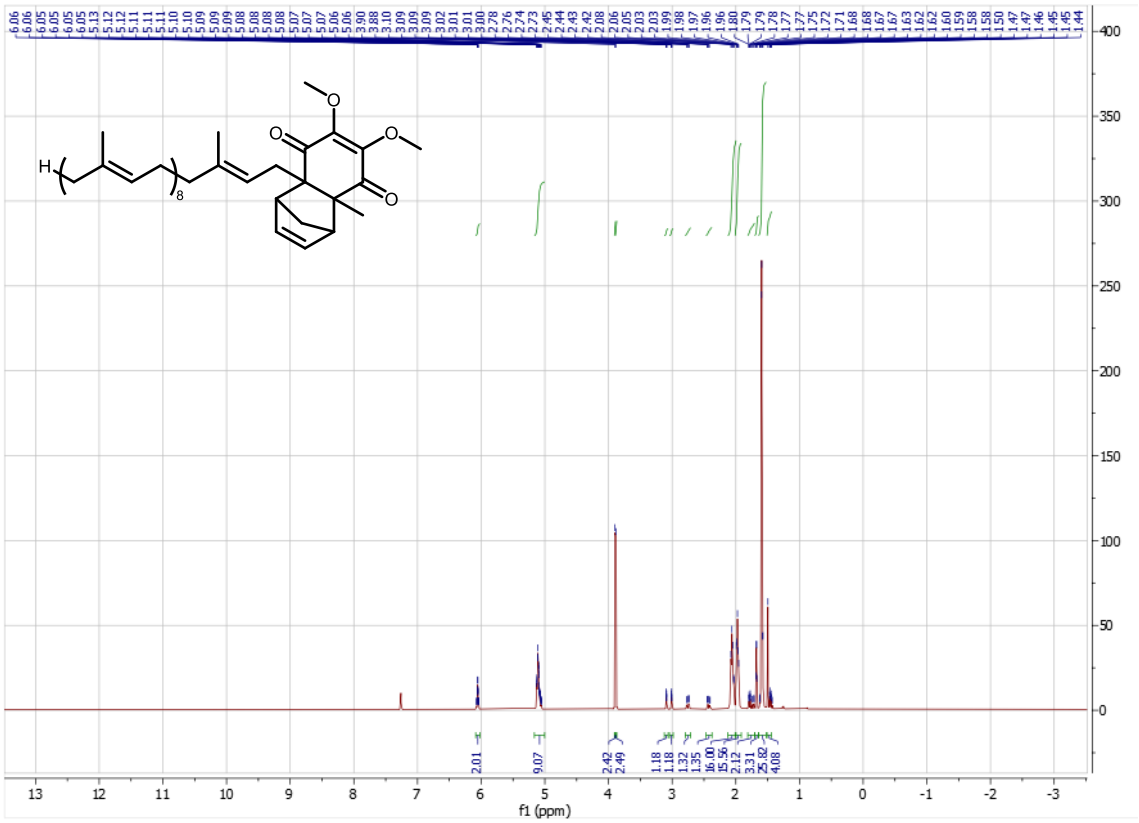
f1 (ppm)

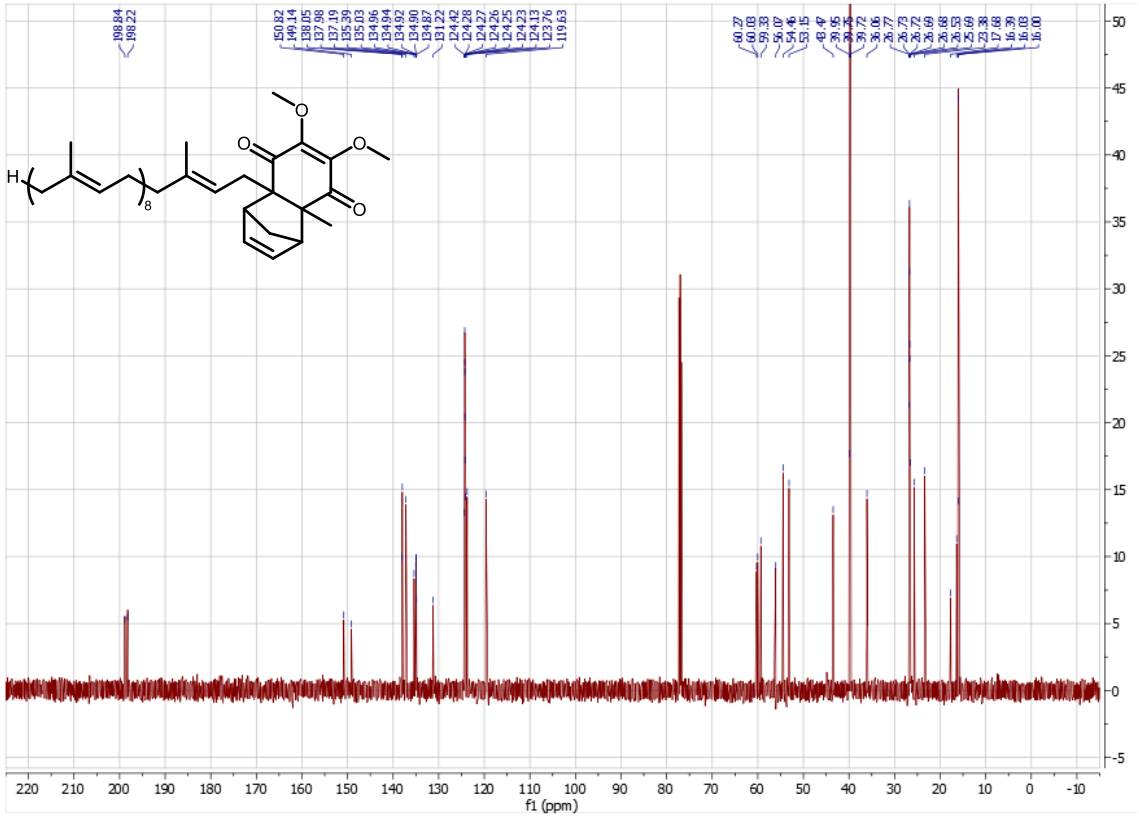
f1 (ppm)

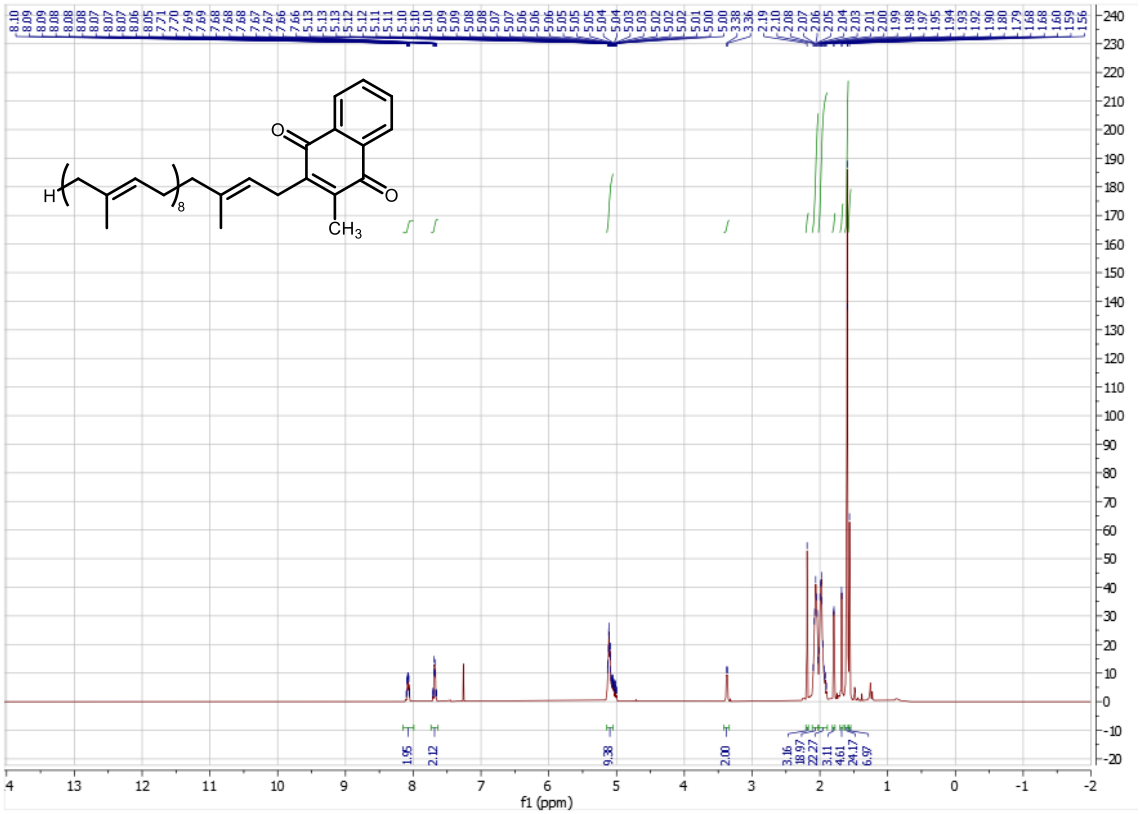
f1 (ppm)

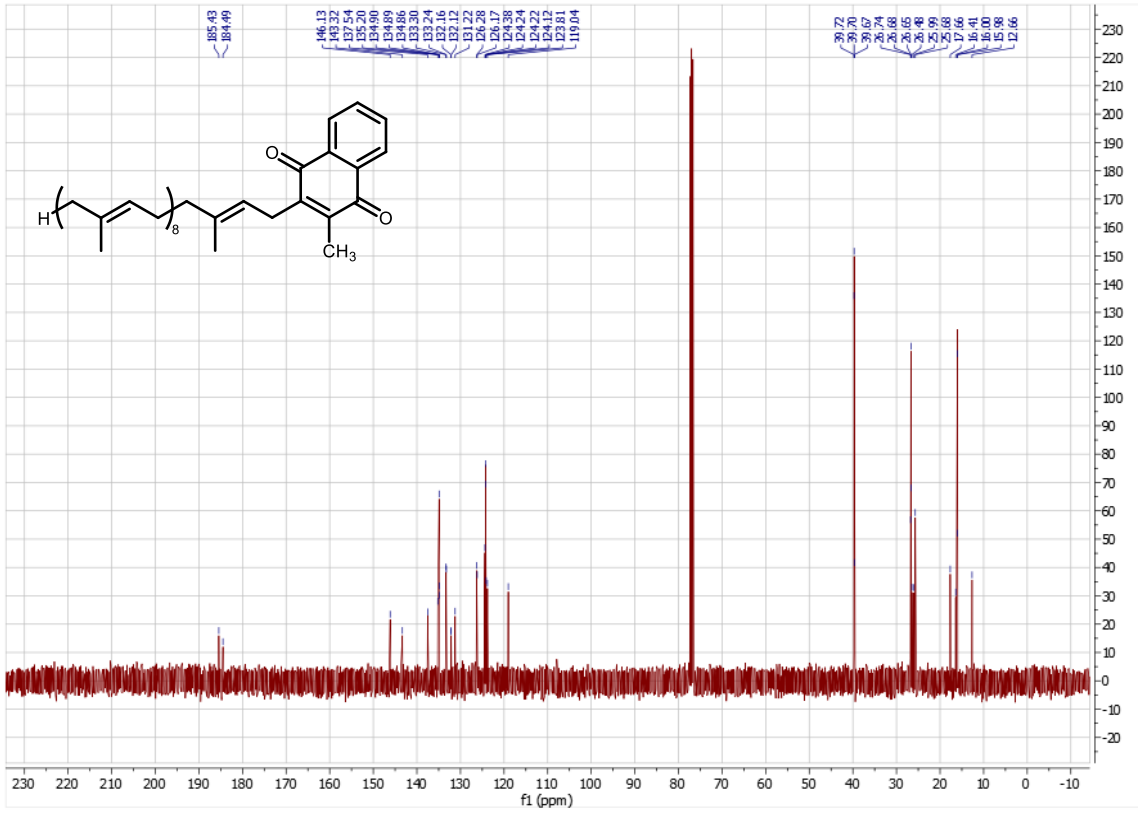
f1 (ppm)

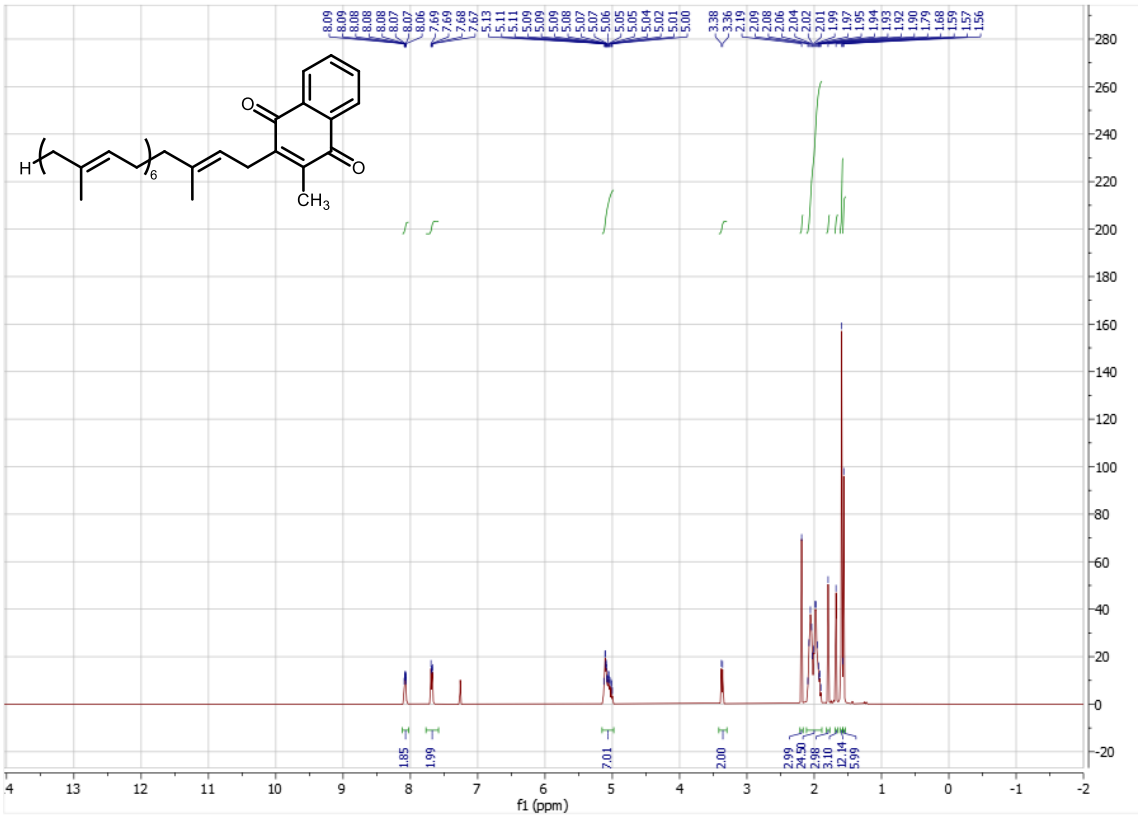
f1 (ppm)

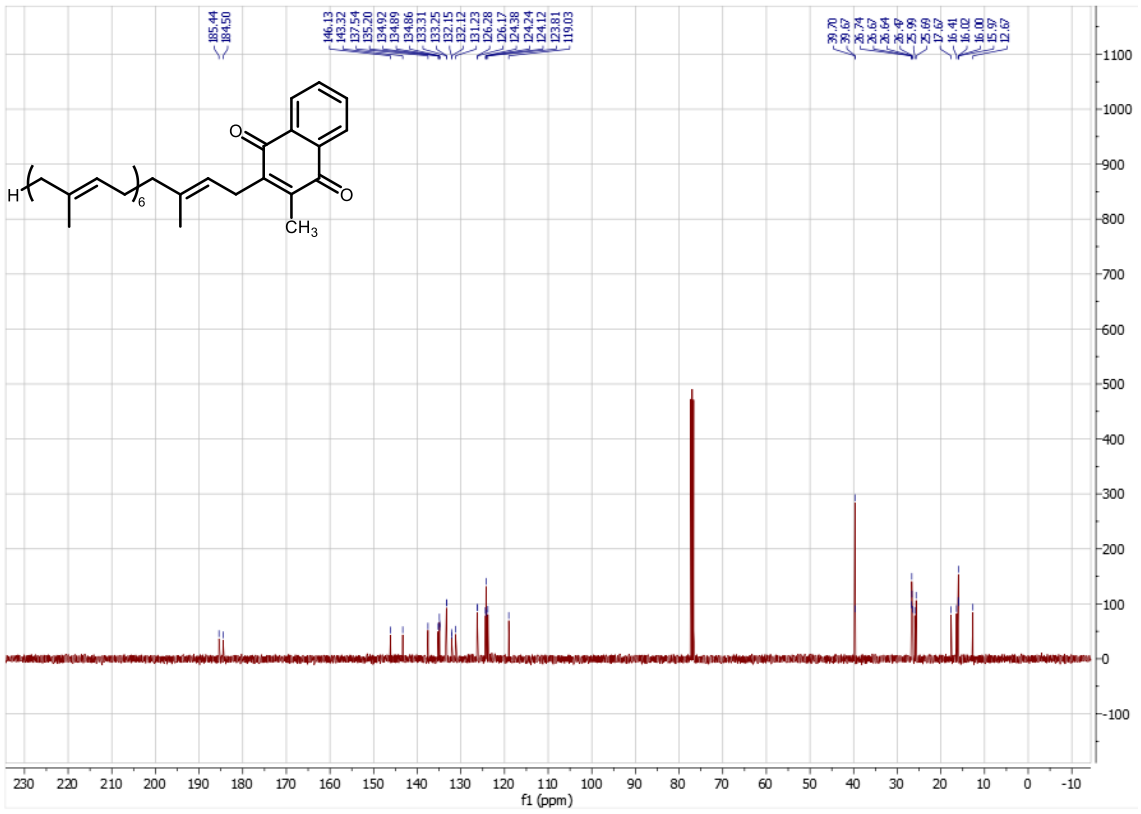
f1 (ppm)

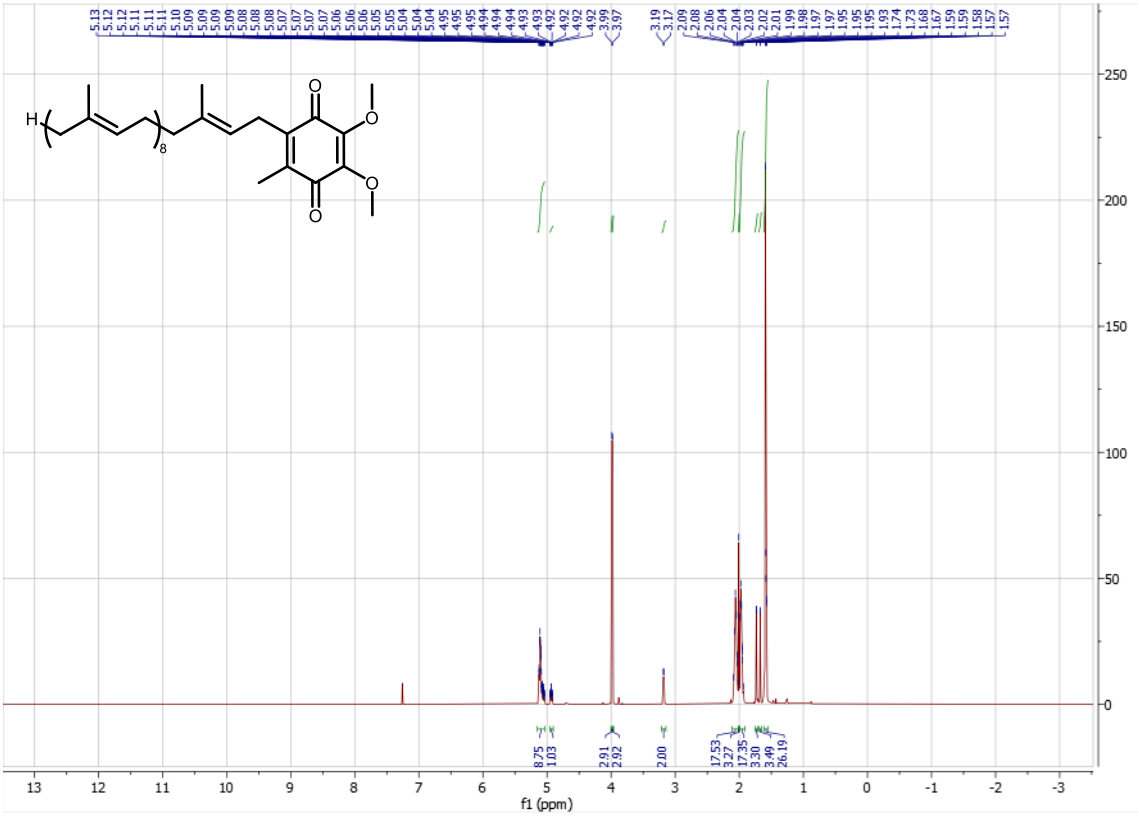
f1 (ppm)

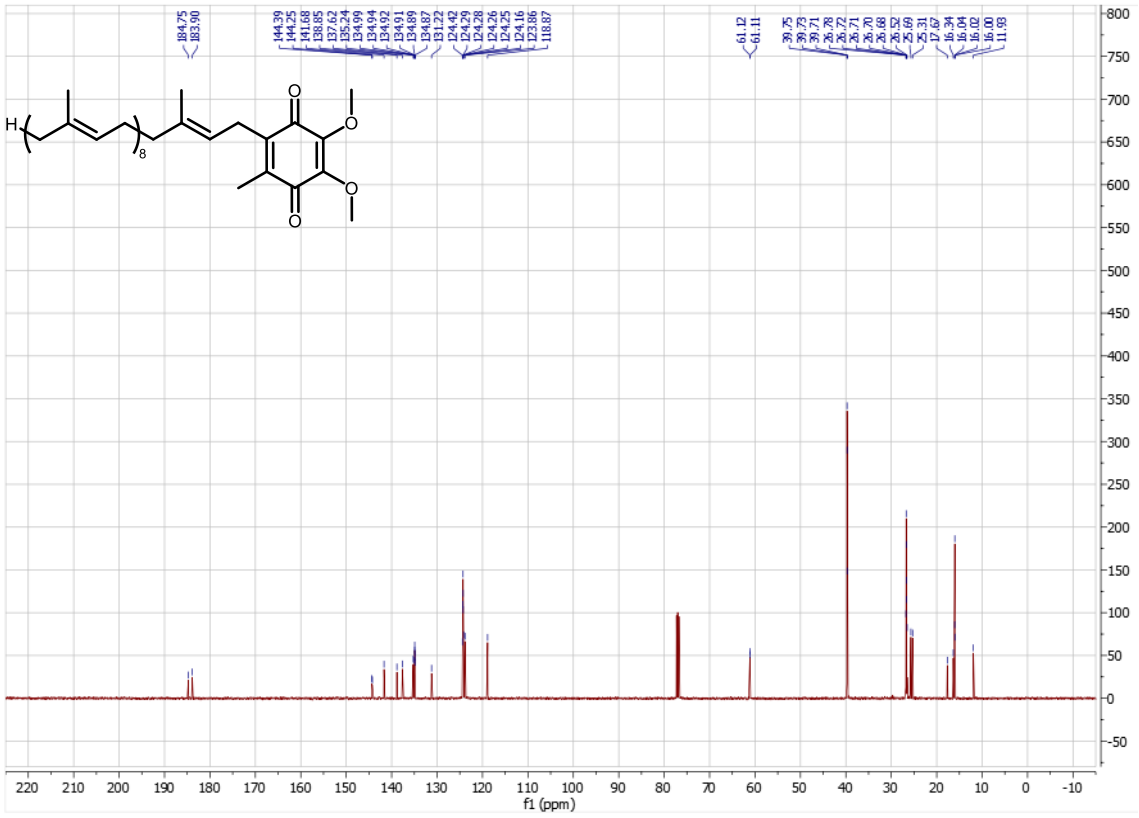
f1 (ppm)

III. Palladium Catalyzed Dehydration of Primary Amides to Nitriles in Water

Reproduced from

Wood, A. B.; Kincaid, J. R. A.; Lipshutz, B. H. *Green Chem.* **2022**, *24*, 2853–2858.

With permission from The Royal Society of Chemistry.

3.1 Personal Account

The α-arylation project was well underway, and the cyclopropane (Chapter 1) and CSTR (Chapter 4, part 2) papers had been written and submitted to their respective journals. I was sitting in my office lamenting to myself that I didn't have enough stuff to work on, other than writing, when serendipitously Bruce walked into my shared office to talk to Yuting about something. I let him know that I felt I could handle another project on my plate. His response to this was, of course, highly positive being a PI, and he exclaimed "That's the sort of stuff I want to hear!" (or, something to that affect).

Bruce had posed the amide dehydration problem as a thought exercise to me when I was discussing next steps earlier in my degree. I did not know that he had given it to other graduate students in the past, only to be turned down after minimal progress was made. The original thought was to take the Burgess reagent and add a ton of greasy appendages to it to try to get it into the micelle and essentially shield the reagent away from water. After a few attempts at this on my end, I found a lot of issues with the synthesis of the reagents, as well as no reactivity from either crude or "purified" material (isolation tended to destroy these reagents). Some of the proposed analogues were so bulky with alkyl groups that the volume of reagent required for the reaction was greater than that of the water used as the medium!

Discouraged, I went online to poke around and see what else I could find in the literature because I was determined to make this work. On Organic Chemistry Portal, I found that other groups had used palladium catalysis in mixtures of acetonitrile and water. It was immediately obvious to me that surfactant technology could further add value to this methodology, where the goal was to reduce the amount of organic solvent required to stoichiometric levels, while maintaining an aqueous medium. There was industrial demand from the company PHT for this

type of aqueous based dehydration chemistry. My success on this method initiated my relationship with a businessman/chemist David Gunn at PHT, which later facilitated my side project with him, funded directly by PHT, to develop a CSTR flow system for our lab at UCSB.

3.2 Introduction and Background

The nitrile moiety is a fundamental functional group in organic chemistry, with its importance spanning multiple subdisciplines from fine chemical synthesis to polymer and materials applications.[1] Beyond it's more technical industry specific uses, even a chemical layman can recall the "cyano-" or "nitrile" terminology from a variety of commonplace items. One major example is in the form of nitrile rubber-based commodities, where the inclusion of the carbon-nitrogen triple bond imparts improved chemical resistance against petroleum products (Figure 1).[2] Indeed, this material stability makes the synthetic rubber, which is generated from the co-polymerization of 1,3-butadiene and acrylonitrile, ideal for uses in seals, gaskets, and O-rings. Furthermore, nitrile rubber has been developed for personal protection equipment in the form of nitrile gloves, which are cheap to produce, chemical-resistant, and have superior strength compared to natural rubber,[3] making them ideal for use in laboratories and medical examinations.[4]

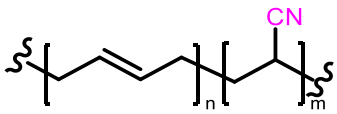

Figure 1: General chemical formula for nitrile rubber

With respect to fine chemicals, nitriles are familiar to organic chemists as either useful synthetic handles towards other functional groups *en route* to targets, or as a bioactive component of a molecule. On Earth, over 120 natural products have been observed to contain this group in both terrestrial and aquatic species,[5] not including a large variety of cyanogenic glycosides.[6] This ubiquity carries over into the pharmaceutical field, as this functionality can

be used to greatly alter the medicinal activity of an active pharmaceutical ingredient (API) based on its geometric and chemical properties. For example, the 180° bond angle of the triple bond results in minimal steric cost (*i.e.*, eight times less than a methyl group, a traditionally small moiety), making it ideal for examining crowded binding pockets.[7] The electronic properties of the nitrile also play a role, as the polarity of the carbon-nitrogen bond dipole results in greater interactions with bio-functional molecules through hydrogen bonding, and can increase aqueous solubility as determined by log P calculations.[8] Finally, the chemical strength of the triple bond may result in greater metabolic stability, and thus can be instrumental for maintaining the structural integrity of a drug by acting as a bioisostere for halogen, alcohol, and ketone functional groups which otherwise may be altered *in vivo*.[9] These crucial properties have resulted in the FDA approval of at least 1-5 nitrile-containing drugs every year over the past decade, including the most recent inclusion of the anti-viral remdesivir in 2020 for the treatment of COVID-19 (Figure 2).[10]

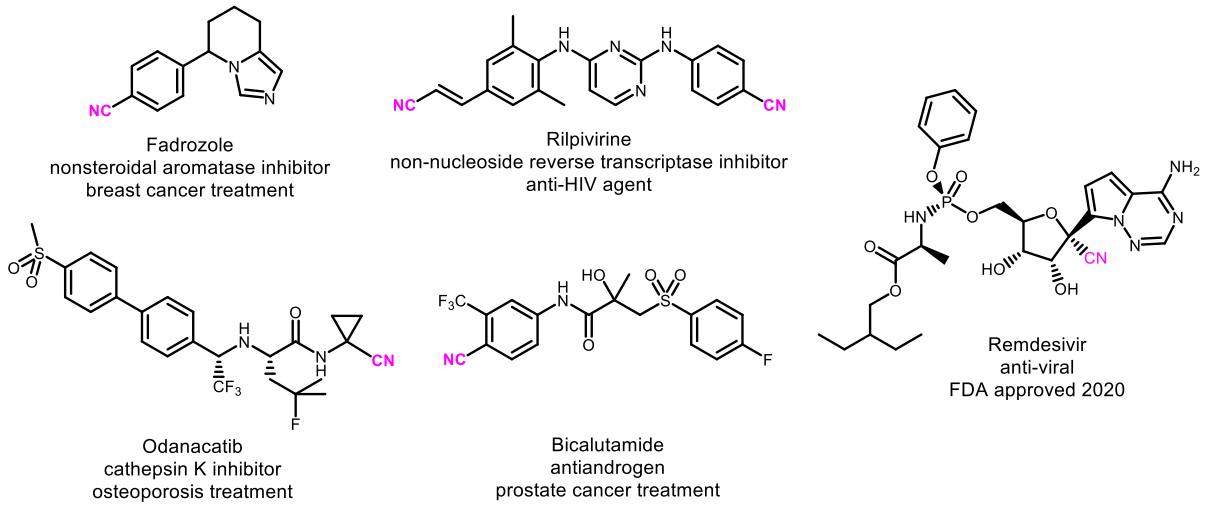

Figure 2: FDA-approved nitrile-containing pharmaceuticals

Given the fundamental nature of this functionality, a wide breadth of synthetic technologies exists for the installation of nitriles onto organic frameworks (Figure 3). In its simplest form, metal cyanides can be used to displace alkyl halides or pseudohalides to form alkyl nitriles, typically in dipolar aprotic solvents, such as DMF or DMSO.[11] Hydrogen cyanide can also be added to alkenes and alkynes to form the corresponding alkyl or alkenyl nitrile, respectively, or added to a carbonyl group to form the cyanohydrin.[12] In other cases, nitrogen can be pre-installed onto an alkane, and thus, dehydrogenative oxidation of an amine[13] or reduction of a nitro group[14] can also yield the alkyl nitrile. Finally, coupling between a metal cyanide and a diazoarene or haloarene using a transition metal results in the corresponding cyanoarene.[15] This latter technique was recently improved upon and given a more environmentally

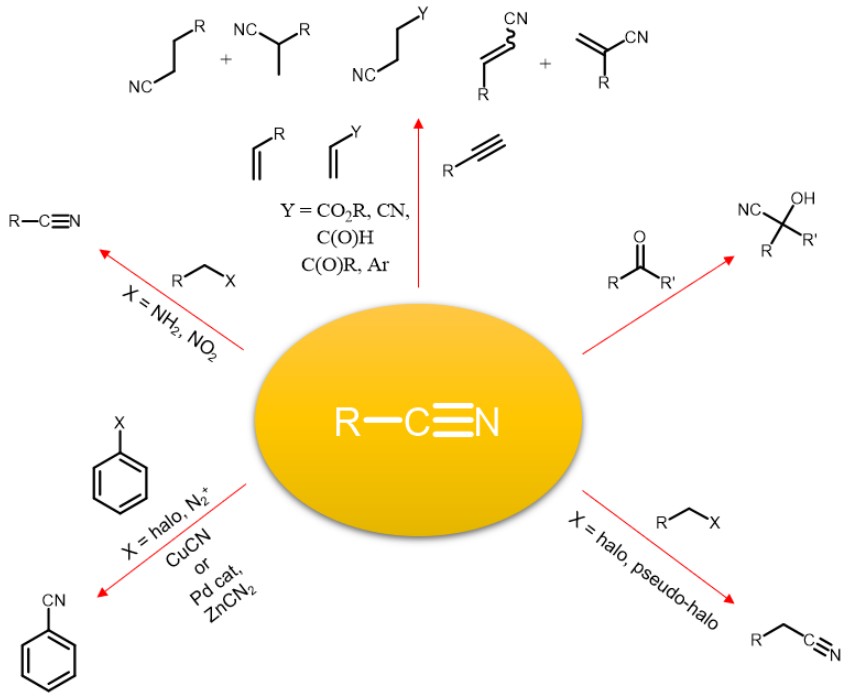

Figure 3: Traditional cyanation methods

responsible upgrade from the Lipshutz laboratory, requiring only 0.55 equivalents of $Zn(CN)_2$, one equivalent of PMHS, and 5000 ppm (0.5 mol %) Pd in the form of a Xantphos palladacycle to affect cyanation of late-stage functionalized aryl and heteroaryl halides in an aqueous micellar medium.[16]

While these methods are robust and result in formation of the organic nitrile, most of these enumerated techniques require use of highly toxic metal cyanides which pose significant safety hazards for scaling reactions and typically result in polluted aqueous workup streams.[17] An alternative route to nitriles eschews the use of these dangerous cyanide reagents by taking advantage of the dehydration of other functional groups. This is observed in the dehydration of primary amides to the corresponding nitriles. Methods were developed in the early 20th century using stoichiometric quantities of inorganic dehydrating reagents such as P_2O_5,[18] $POCl_3$,[19] and $SOCl_2$,[20] to name a few. This transformation can also be achieved using organic dehydration reagents, such as cyanuric chloride in DMF as both solvent and reagent.[21] However, despite the ubiquity and low cost of these dehydration reagents, one major drawback shared between these technologies is the requirement of not only using high temperatures to affect the transformation, but also rigorously dry organic solvent to avoid reagent sensitivity to moisture.

One major contribution to the stoichiometric dehydration of amides to nitriles was reported by Claremon and Phillips at Merck in 1988 using the Burgess reagent, methyl *N*-(triethylammoniumsulfonyl)carbamate.[22] This compound, originally developed for the *syn*-elimination of alcohols to form alkenes, was found to selectively dehydrate an amide under mild conditions, typically at room temperature, using only a slight excess of reagent (Figure 4). The appeal of this reagent is due to its ease of synthesis, and can be freshly prepared using

chlorosulfonyl isocyanate, methanol, and triethylamine in dry organic solvent.[23] Furthermore, the byproducts of the dehydration are easily removed via aqueous workup. Unfortunately, as it currently stands, the Burgess method is obligated to dry organic solvents to achieve high levels of conversion, as adventitious water will act as a competitive nucleophile to the amide resulting in decomposition of the reagent.

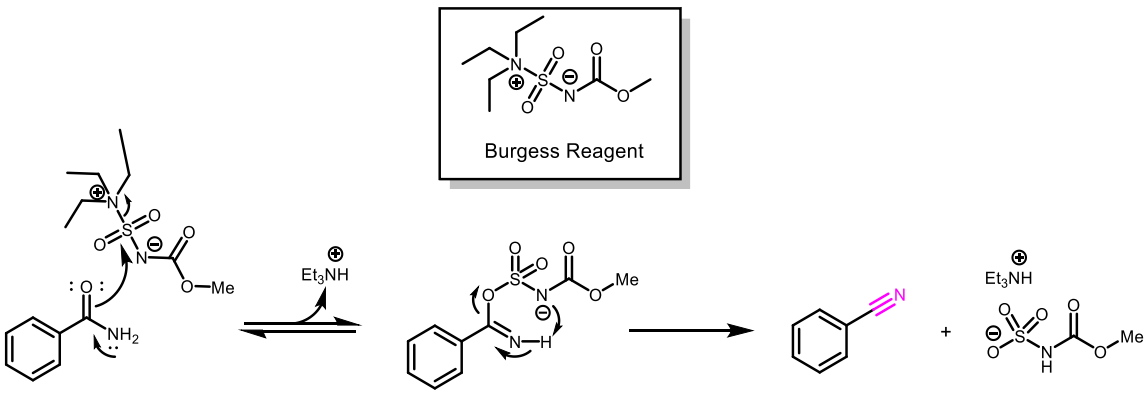

Figure 4: Burgess reagent and mechanism for primary amide dehydration

Despite the general success of these methodologies, the requirement of stoichiometric quantities of dehydrating agents to afford the targeted nitrile functionality is unattractive not only from a green chemistry perspective with respect to atom economy, but also from industrial applications, where process chemists must typically contend with either the large quantities of waste, or need for very dry reaction conditions, or both. Therefore, much emphasis has been placed on efforts aimed at developing catalytic methods in the form of d- and p-block metals. A myriad of metals has been utilized for this transformation, including rhenium, ruthenium, iron, tin, vanadium, zinc, and tungsten, among others.[24] A copper-catalyzed process has been put forth of late by Buchwald's group in 2018.[25] This technique can be run using only 2 mol

% of $Cu(OAc)_2$ at ambient conditions, but requires 2.2 mol % of expensive 1,2-bis(dicyclohexylphosphino)ethane as phosphine ligand.[26] Furthermore, this process still requires stoichiometric quantities of dimethoxymethylsilane (DMMS), which results in the disilylether as reaction byproduct, and must be run in organic solvents to be successful (Figure 5).

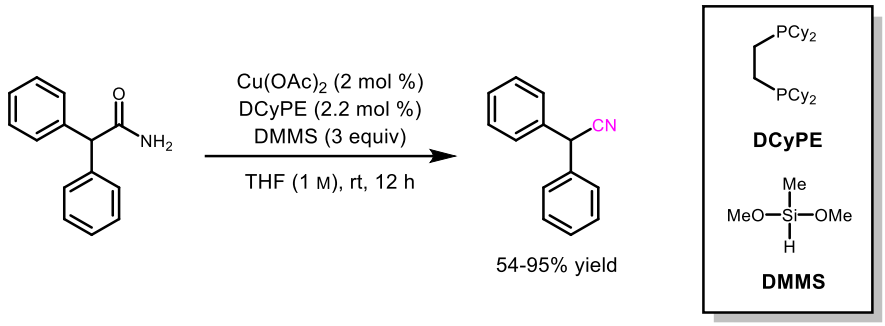

Figure 5: Cu-catalyzed method for amide dehydration in organic solvent

Given the need for more environmentally conscious methods in large scale chemical synthesis, a counter-intuitive, mostly water-based system has been developed for the dehydration of primary amides to nitriles. This chemistry utilizes palladium as transfer hydration agent, which allows for the chemistry to be amenable to aqueous media. This catalytic system was originally discovered by Maffioli *et al.* in 2005, utilizing a dilute mixture of 1:1 water (which was found to be critical for this transformation) and acetonitrile.[27] In their study, Pd facilitated the transfer of an equivalent of water from a primary amide to the vast excess of acetonitrile via a metal-stabilized iminic anhydride intermediate, resulting in the desired nitrile and acetamide as a cheap, easily removable byproduct (Figure 6).

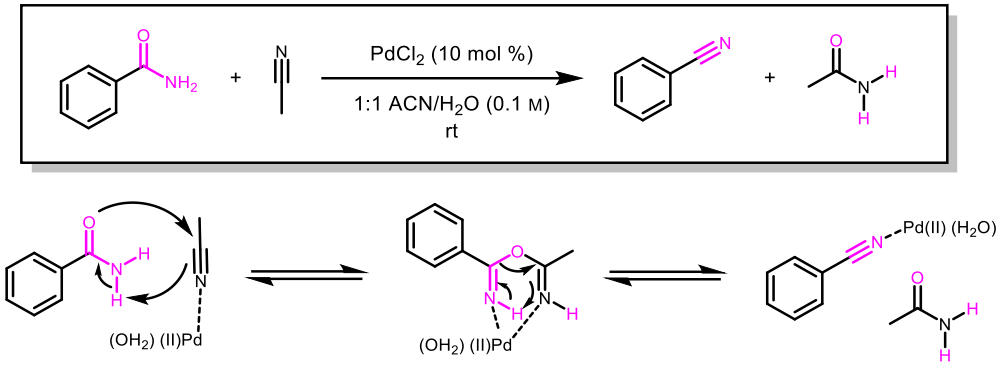

Figure 6: General scheme and mechanistic picture for Pd-catalyzed transfer hydration

While influential, the need for egregiously high loadings of a Pd catalyst (10 mol %) and the dilute nature of the reaction medium limits the improvement of the environmental impact for this transformation. Paradoxically, follow-up reports from Zhang[28] and Al-Huniti[29] focused away from the elegant simplicity of the aqueous-based aspect of this chemistry, and instead introduced additives such as silver or copper acetate (in the case of Zhang) or an oxidizing agent such as Selectfluor (in the case of Al-Huniti) to avoid the requirement of water for the chemistry to occur, all while maintaining the same large Pd loading. The major advancement in this technology came from Okabe *et al.*,[30] where they found that more electron-deficient "sacrificial nitriles" afforded improved water-accepting capabilities compared to acetonitrile. Thus, the use of 10 equivalents of dichloroacetonitrile vastly outperformed a system using only a 1:1 mixture of acetonitrile to water. It was theorized that the water-shuffling to dichloroacetonitrile was considerably more exergonic compared to that of acetonitrile, and thus the reverse reaction would be unfavored without the need to use more expensive dichloroacetonitrile than necessary (albeit at 10 equivalents) and maintaining acetonitrile/water as the main solvent system. Furthermore, the authors noted that transitioning

the catalyst away from traditional $Pd(OAc)_2$ to $Pd(O_2CCF_3)_2$ allowed for a decrease in catalyst loading from 10 mol % to 1 mol %, respectively (Figure 7).

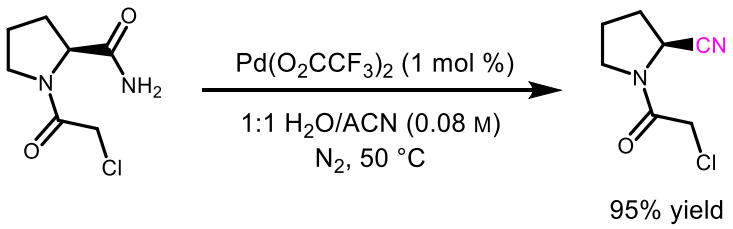

Figure 7: Okabe's Pd catalyzed amide dehydration conditions

Despite Okabe's success on this front, utilization of acetonitrile as organic solvent still poses an issue from a green chemistry standpoint. The system still requires a vast excess of acetonitrile as co-solvent, which will also act as a dehydrating agent alongside the more electron poor acetonitrile derivative. The use of a 1:1 mixture of acetonitrile *with* water, as opposed to *in* water, also imposes problems for downstream processing, as the recyclability of the acetonitrile is reduced. Furthermore, the substrate scope is limited to mostly a single type of primary amide in the form of amino acid derivatives. The functionality at the α-position directly influences the outcome of the reaction (*vide infra*), and thus the applicability towards other molecule types was ultimately under studied.

The requirement for water in this Pd catalyzed transformation immediately makes this reaction interesting from an aqueous surfactant angle. It is assumed that a major requirement for the inclusion of large volumes of acetonitrile is to not only act as a water-acceptor, but to also act as media for notoriously difficult to dissolve primary amides. This "solvation" issue has been shown to be overcome with the use of surfactants, such as TPGS-750-M, at very low concentrations (20 mg/mL, or 2 wt % in water).[31] It is also known that lipophilic molecules

tend to congregate in the interior of the micelles, including organic-soluble transition metal catalysts such as $Pd(OAc)_2$. Therefore, in this chapter we disclose a micellar medium enabled amide dehydration in a mostly aqueous-based system (*i.e.*, no included acetonitrile co-solvent). This technology utilizes lipophilic sacrificial nitriles in the form of methoxyaceotnitrile and fluoroacetonitrile, which should partition into the micelle to affect dehydration and then exit as the water-soluble acetamide preventing the reverse reaction. This technology can be applied to late-stage molecules with heightened functional complexity, and is amenable to 1-pot, multistep chemoenzymatic processes. Furthermore, the aqueous nature of the method allows for easy recycling of the water medium, allowing for multiple reactions to be run in series. This results in a very low E Factor, even including the use of stoichiometric amounts of the dehydrating nitrile in the calculation.

3.3 Results and Discussion

Inquiry into primary amide dehydrations in water stemmed from initial studies attempting to develop a Burgess reagent amenable to aqueous based systems, which could theoretically be applicable to a variety of related transformations. Typically, reactions involving the Burgess reagent are performed under strictly anhydrous conditions to avoid unintended hydrolysis. The eponymous reagent is developed from the reaction of chlorosulfonyl isocyanate first with methanol to form the carbamate, and then in 1-pot the chloride is displaced with two equivalents of triethylamine (the excess ammonium chloride is filtered off prior to isolation of the reagent). Therefore, it was theorized that the reagent could be modified by altering both the site of the alcohol as well as the trialkylammonium ion used. Increasing the lipophilic nature of both these handles should, in effect, improve the stability of the reagent and shield it inside of the micellar core and away from water. A small set of Burgess reagent analogues were prepared alongside the original reagent (**BR**) for the conversion of 4-methoxybenzamide (**1**) to 4-methoxybenzonitrile (**2**) in 2 wt % TPGS-750-M/H_2O (Figure 8).

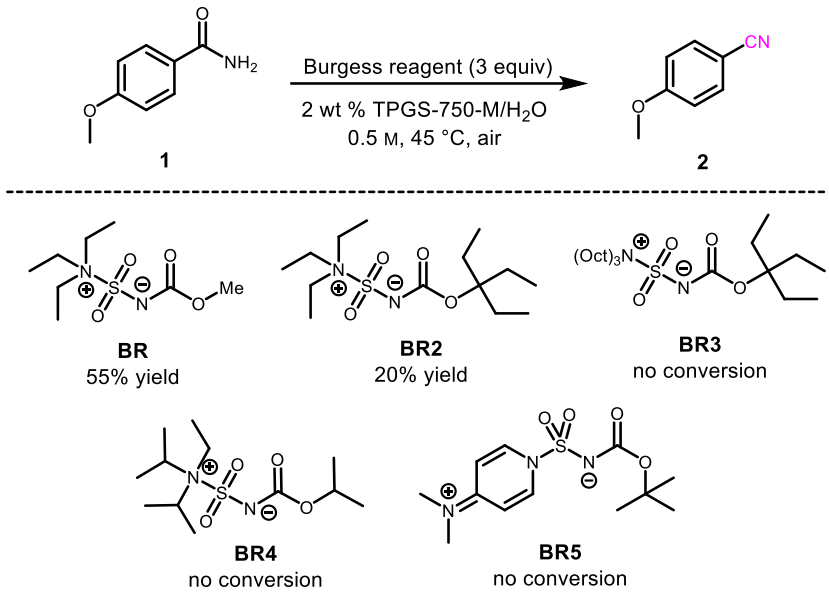

Figure 8: Burgess reagents prepared for amide dehydrations in water

The traditional Burgess reagent, when added in an excess (3 equiv), was able to partially convert **1** to **2** in 55% yield in an aqueous based system. Improvement of yield was not observed when adding another equivalent of the reagent; regardless, conservation of atom economy would dictate that the large amount of waste generated from the reagent would ultimately diminish the improvement in environmental impact with increased loading. Increase in concentration from 0.5 M to 1.0 M resulted in a drop in yield of **2** to 43% and use of 20 v/v % THF also resulted in a similar loss in yield to 34%. Considerably more lipophilic **BR2** resulted in lower conversion to **2** compared to that of the **BR** at 20% isolated yield. It was also noted that isolation of these more lipophilic reagents resulted in decomposition upon distillation of the aromatic solvent (benzene) via ^{1}H NMR. Furthermore, the trialkylammonium chloride byproduct would not precipitate out of solution when the alkyl chain length was increased making isolation difficult. Complete loss of conversion was observed for **BR3**; the inclusion of the trioctylammonium leaving group results in a very high molecular weight

material and attempts to run this chemistry with three equivalents resulted in greater volumes of the reagent added compared to the water used as medium. Analogue **BR4**, derived from Hünig's base and isopropyl alcohol, also gave zero yield in water. Interestingly, running this chemistry neat in **BR4** resulted in 40% yield of **2**, whereas a similar attempt of neat chemistry using **BR3** still gave zero conversion. **BR5** was a very interesting potential candidate, as the literature surrounding this species notes it's stability in the presence of water.[32] However, zero conversion was observed for this reagent, and the reaction mixture ultimately solidified completely using only three equivalents.

Given the failure of the modified Burgess reagent route, we decided to switch our focus towards palladium-catalyzed dehydrations in water utilizing acetonitrile as a water-acceptor in the "water-shuffling" mechanism. These initial studies were performed on the same model system of 4-methoxybenzamide (**1)** to 4-methoxybenzonitrile (**2)** using 2 wt % TPGS-750-M as surfactant and an oxidant, in most cases, as inspired by work from Al-Huniti *et al.* (Table 1).[29]

Table 1: Initial screening of Pd-catalyzed amide dehydrations in water

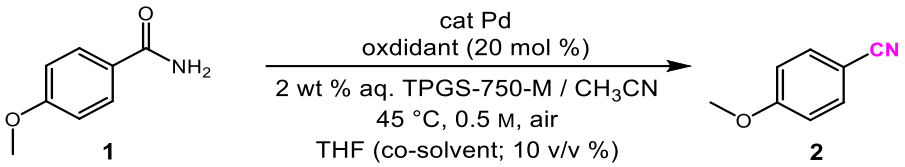

Entry	Pd (mol %)	Aq.:Org. volume ratio[a]	Nitrile (equiv)	[Oxidant]	**2** (%)[b]
1	$Pd(OAc)_2$ (10%)	1:1 (no THF)	ACN (19)	Selectfluor	40
2	$Pd(OAc)_2$ (1%)	1:1 (no THF)	ACN (19)	Selectfluor	53
3	$Pd(OAc)_2$ (10%)	9:1 (no THF)	ACN (4)	Selectfluor	39
4	5% Pd/C (10%)	1:1 (no THF)	ACN (19)	Selectfluor	47
5	$Pd(OAc)_2$ (1%)	9:1 (no THF)	ACN (4)	Selectfluor	49
6	5% Pd/C (0.2%)	9:1	ACN (4)	Selectfluor	trace
7	$Pd(OAc)_2$ (0.2%)	9:1	ACN (4)	Selectfluor	77
8	$Pd(OAc)_2$ (0.2%)	9 (3 M NaCl):1	ACN (4)	Selectfluor	trace
9	$Pd(OAc)_2$ (0.2%)	4:1 (1.0 M)	ACN (4)	Selectfluor	77
10	$Pd(OAc)_2$ (0.1%)	9:1	ACN (4)	Selectfluor	75
11	$Pd(OAc)_2$ (0.2%)	9:1	ACN (4)	air (none)	36
12	$Pd(OAc)_2$ (0.2%)	9:1	ACN (4)	benzoquinone	trace
13	$Pd(OAc)_2$ (0.4%)	9:1	ACN (4)	Selectfluor	72
14	$Pd(OAc)_2$ (0.2%)	9:1	ACN (4)	O_2 (1 atm)	trace
15	$Pd(OAc)_2$ (0.2%)	9:1	ACN (4)	Oxone	82
16	$Pd(OAc)_2$ (0.2%)	9:2	ACN (8)	Selectfluor	90
17	$Pd(OAc)_2$ (0.2%)	9:2	ACN (8)	Oxone	85
18	Pd[dtbpf]Cl_2 (0.2%)	9:2	ACN (8)	Oxone	85
19	[Xantphos]$PdCl_2$ (0.2%)	9:2	ACN (8)	Oxone	93
20	$Pd(OAc)_2$ (0.2%)	9:1.75	Isobutyronitrile (4)	Oxone	68
21	$Pd(OAc)_2$ (0.2%)	9:3.5	Isobutyronitrile (8)	Oxone	85
22	$Pd(OAc)_2$ (0.1%)	9:3.5	Isobutyronitrile (8)	Oxone	78
23[c]	$Pd(OAc)_2$ (0.1%)	9:3.5	Isobutyronitrile (8)	Oxone	43
24[d]	$Pd(OAc)_2$ (0.2%)	9:3.5	Isobutyronitrile (8)	Oxone	82
25[d]	$Pd(OAc)_2$ (0.1%)	9:3.5	Isobutyronitrile (8)	Oxone	76
26	$Pd(OAc)_2$ (0.1%)	1:1	ACN (19)	Oxone	97

[a] Run using 10 v/v% THF unless otherwise indicated. [b] Isolated yields. [c] Room temperature. [d] 70 °C.

When not using THF as co-solvent, there was some difference between 10 mol % $Pd(OAc)_2$ (entry 1) and 1 mol % $Pd(OAc)_2$ (entry 2), with an increase in 13% isolated yield of **2** with the ten-fold decrease in Pd loading and a 1:1 acetonitrile (ACN) to 2 wt % TPGS-750-M/H_2O mixture with 20 mol % Selectfluor as oxidizing agent. Interestingly, there was no difference at 10 mol % Pd when the aqueous to organic ratio was decreased from 1:1 to 1:9 (entry 3),

ultimately reducing the amount of ACN from nineteen to four equivalents. This was also observed for 1 mol % Pd, where four equivalents of ACN gave a comparable yield of 49% of **2** (entry 5) to the trial run with nineteen equivalents. 5 wt % Pd/C also gave comparable conversion with Pd loadings of 10 mol % compared to **1** (entry 4); however, reducing the global Pd loading to 0.2 mol % using the same Pd/C source gave only trace conversion (entry 6). Reducing the Pd loading to 0.2 mol % was also possible when 10 vol % THF was added as co-solvent (entry 7), giving an improved yield of 77% using only four equivalents of ACN. Inclusion of THF as co-solvent was found to be imperative for high conversion throughout this study, and was therefore used to make $Pd(OAc)_2$ stock solutions. Adding 3 M NaCl to the aqueous phase resulted in zero conversion (entry 8), and increasing the typical reaction concentration from 0.5 M to 1.0 M, maintaining the same four equivalents of ACN, produced the same yield of **2** at 77% (entry 9). Keeping the Pd loading at 0.2 mol %, altering the oxidizing agent to air (entry 11), benzoquinone (entry 12), and O_2 atmosphere (entry 14) gave little to no yield of product. However, a major breakthrough in the study came from the success of oxone, which is considerably cheaper than Selectfluor, which provided **2** in 82% yield with only four equivalents of ACN (entry 15). Varying between Selectfluor and oxone, increasing the ACN to eight equivalents saw improved conversion between 85-93% yield (entries 16-19). We theorized that increasing the lipophilicity of the sacrificial nitrile would improve its solubility in the micelle resulting in higher conversion of the intended primary amide. However, adding an alkyl moiety as in the case of isobutyronitrile gave no appreciable difference compared to ACN even at higher temperatures (entries 20-25). The lipophilicity and electron-donation capabilities of phosphine-ligated Pd(II) salts as $Pd[dtbpf]Cl_2$ (entry 18) and $[Xantphos]PdCl_2$ (entry 19) also acted in a similar capacity with respect to the cheaper and

more available $Pd(OAc)_2$. It was also later found that $Pd(O_2CCF_3)_2$, known to work well for Okabe *et al*.[30] in their studies allowing them to reduce their Pd loadings from 10 mol % to 1 mol %, gave similar conversion to the acetate salt. This study also found that exceptionally low loadings of $Pd(OAc)_2$ of 0.2 mol % using 1:1 ACN/H_2O, 10 vol % THF as co-solvent, and 20 mol % oxone as oxidant gave product in nearly quantitative yield at only 45 °C (entry 26).

It was hypothesized that a dinitrile "ligand" could be used to improve conversion by chelating to the metal and improving solubility. Therefore, 2,2'-(ethane-1,2-diylbis(oxy))dibenzonitrile (**DiCN**) was prepared, which is known to chelate to palladium, and tested as a potential additive for this reaction (Table 2).[33]

Table 2: Introduction of **DiCN** as additive for Pd-catalyzed amide dehydration

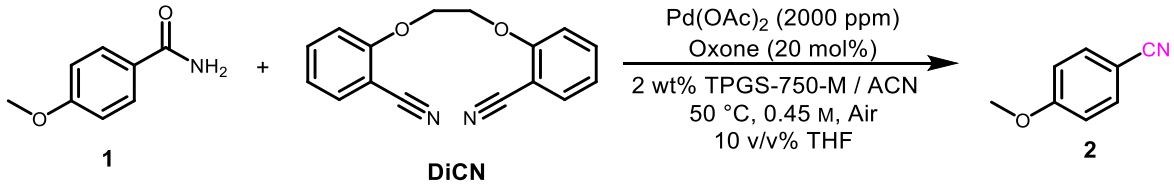

Entry	DiCN equiv	aq./org. ratio (ACN equiv)	**2** (%)[a]
1	0	9:2 (7.5 equiv)	85
2	4	aq. only	trace
3	2	aq. only	trace
4	0.2	9:2 (7.5 equiv)	93

[a] Isolated yields

Utilization of **DiCN** by itself at both two (entry 3) and four (entry 2) equivalents returned zero conversion of **1** to **2**. Furthermore, addition of a sub-stoichiometric amount of the additive alongside 7.5 equivalents of ACN gave only a slight increase in yield (entry 4). The difficulty in synthesis of **DiCN** (30% yield from the reaction of 2-hydroxybenzonitrile with dichloroethane) and the additional waste generated for this additive did not make it attractive for further studies.

Prior to further discussion on optimization of this reaction, it should be noted that there were considerable problems encountered when utilizing different sources of $Pd(OAc)_2$. Colacot noted in 2016 that not all $Pd(OAc)_2$ sources are equal, and the synthesis, workup, and purification protocols can vary the Pd activity not only from company-to-company, but also from batch-to-batch within the same company.[34] This has been known to cause major reproducibility issues, and thus, when we ran out of the batch used for the initial study in Table 1, we ran into similar problems. This was noted with a batch of $Pd(OAc)_2$ discovered in our laboratory, which acted as the new baseline (Table 3, entries 1 and 2). Initially, dehydration of **1** to **2** was easily reproducible at 0.2 mol % Pd loadings; however, attempting to use other batches, including high quality samples, resulted in only trace conversion at that same loading (Table 3). This study was run using methoxyacetonitrile (MeOACN) as the sacrificial nitrile, the importance of which will be discussed later.

Table 3: Pd source screening for dehydration chemistry

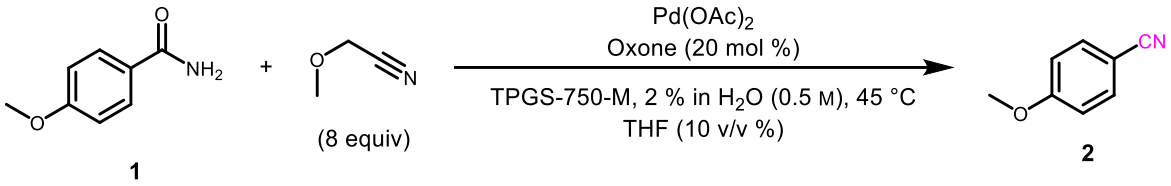

Entry	Pd Loading (ppm)	Alteration	Conversion (%)
1	2000	Old **1**	0
2	2000	New **1**	0
3	2000	Old **1** / RM 2237 Chemicals	0
4	2000	New **1** / RM 2237 Chemicals	0
5	2000	RM 2235 Chemicals and Pd	0
6	10000	RM 2235 Chemicals and Pd	100 (TLC)
7	4000	New **1**	>50 (TLC)
8	2000	RM 2235 Chemicals / Distilled THF	0
9	2000	RM 2235 Chemicals and Pd / Distilled THF	0
10	2000	RM 2235 Chemicals and Pd / Distilled THF / TPGS w/ air bubbled	0
11	2000	Different balance	0
12	2000	$Pd(OAc)_2$ from RM 2237	0
13	4000	$Pd(OAc)_2$ from RM 2237	>50 (TLC)
14	2000	Novartis $Pd(OAc)_2$	0
15	2000	Novartis $Pd(OAc)_2$, RM 2235 TPGS	0
16	4000	Novartis $Pd(OAc)_2$	<50 (TLC)
17	4000	Novartis $Pd(OAc)_2$, RM 2235 TPGS	<50 (TLC)
18	2000	Strem $Pd(OAc)_2$	0
19	4000	Strem $Pd(OAc)_2$	>50
20	2000	Added 5 mol % $NaNO_2$	0
21	2000	$Pd[dtbpf]Cl_2$	0
22	8000	1 mmol scale, plug + column and long hi-vac	72[a]
23	2000	1 mmol scale	0
24	8000	1 mmol scale, SM washed with hexane, column plus fast on hi-vac	97[a]
25	2000	Johnson-Matthey $Pd(OAc)_2$ – Regular	trace
26	2000	Johnson-Matthey $Pd(OAc)_2$ – High Purity	trace

[a] Isolated yields

The data from this set of trials indicates that the initial success using 0.2 mol % Pd was not reproduceable from batch-to-batch. This included attempts between old **1** (entry 1) and freshly synthesized **1** (entry 2). Increasing the Pd loading to 0.4 mol % (entry 4) also only achieved ~50% conversion based on TLC analysis. Changing sources of the chemicals (*i.e.*, methoxyacetonitrile, THF, etc.) also did not appear to affect conversion (entry 5) unless the Pd

loading was increased to 1 mol % (entry 6) which did result in complete conversion. Use of distilled THF, where the radical inhibitor is removed, was also found to not be the culprit, even in the case where air was bubbled through the aqueous phase ahead of the reaction (entries 8-10). Taking into consideration equipment error, trying to set up this reaction at 0.2 mol % Pd with a new balance also afforded the same lack of conversion (entry 11). Different sources of $Pd(OAc)_2$ from Novartis and Strem, which had been used by different group members, also did not produce **2** at 0.2 mol % Pd in previously observed yields (entries 13-19). To test Colacot's observation of nitrites as potential additives to industrial $Pd(OAc)_2$ sources, a trial was run using 5 mol % $NaNO_2$ yielding no difference in conversion (entry 20). Interestingly, previously successful Pd[dtbpf]Cl_2 also failed under these conditions (entry 21). Two samples from Johnson-Matthey were run, one at regular purity but kept under argon atmosphere (entry 25) and the other at very high purity (entry 26), also resulting in a similar lack of dehydration chemistry. The only way to reliably dehydrate the aromatic benzamide was to increase the $Pd(OAc)_2$ loading to 0.8 mol % (entries 22 and 24), where it was also found that the product would sublimate on high-vacuum and thus needed to be dried quickly to make accurate yield measurements.

With the new standard Pd loading of 0.8 mol %, we next set forth to develop a system that limits the need for excess acetonitrile for dehydration. Thus, our goal was to remove all acetonitrile used as organic co-solvent with water and, instead, utilize only a small excess of a more reactive nitrile as dehydrating agent which favors a cheap, easily removable acetamide derivative in the reaction equilibrium, yielding the desired nitrile in the process in a mostly aqueous medium. A variety of acetonitrile reagents derivatized at the α-position was tested with respect to the dehydration of **1** to **2** in 2 wt % TPGS-750-M in water (Table 4).

Table 4: Nitrile additive screening for benzamide dehydration chemistry in water

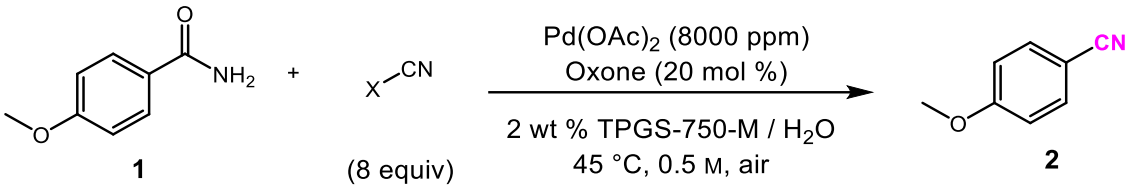

Entry	X	**2** (%)[a]
1	CH_2SMe	0
2	$CH_2N(Me)_2$	0
3	NH_2	<50 (TLC)
4	CH_2CN	0
5	CH_2SO_2Me	40
6	CH_2F	75
7	CH_2CF_3	90
8	$CHCl_2$	94
9	**CH_2OCH_3**	**97**

[a] Isolated yields

Both 2-(Methylthio)acetonitrile (entry 1) and 2-(dimethylamino)acetonitrile (entry 2) gave no conversion to benzonitrile **2**, most likely acting as competitive ligands for Pd in solution rather than as water-accepting agents. Interestingly, cyanamide (entry 3) gave some conversion to product via TLC analysis, and the hydration byproduct in this case should be urea. Malononitrile (entry 4) also gave no conversion, which is highly surprising given the electron-deficient nature of the nitrile and, ostensibly, "double" dehydrating power given the two available alkyl nitriles. (Methylsulfonyl)acetonitrile (entry 5) resulted in some isolable dehydration product; however, significant starting material was observed by TLC when this acetonitrile derivative was used, most likely because the nitrile reagent is a fairly polar solid at room temperature which may limit solubility inside of the micelle. Fluoroacetonitrile (entry 6) and trifluoromethylacetonitrile (entry 7) both gave good yields of 75% and 90%, respectively, under these conditions. Interestingly, fluoroacetonitrile was found to be a very powerful

dehydrating agent in some other cases with higher functional group complexity. Not surprisingly, dichloroacetonitrile (entry 8), which was found to be optimal in Okabe's case, gave nearly quantitative conversion at 94% yield. However, the cheaper, non-chlorinated alternative methoxyacetonitrile (entry 9, MeOACN) was found to perform the best at 97% isolated yield of **2**. We are not entirely sure why, in the case of aromatic nitriles, MeOACN outperforms dichloroacetonitrile under similar conditions. However, Okabe's substrate scope consisted solely of one type of primary amide source (amino acid derivatives) where, in our studies, we found that the functionality at the α-position is the major influence over the equilibrium towards the desired nitrile. Furthermore, their studies required the use of 1:1 acetonitrile/water mixtures, which is essentially running the chemistry in organic solvent *with* water rather than running the chemistry *in* water without organic co-solvent.

Given the superiority of MeOACN as a water-acceptor for the dehydration chemistry, the equivalents of the agent required was studied to determine the optimal amount with 0.8 mol % Pd loading and 20 mol % oxone in 2 wt % TPGS-750-M in water (Table 5). Running this transformation with eight equivalents of MeOACN, or roughly one third of the aqueous reaction volume, resulted in 97% isolated yield of **2** (entry 3). Decreasing the amount to seven (entry 2) and six (entry 1) equivalents resulted in loss in isolated yield to 86% and 72%, respectively. This data set indicates that the amount of nitrile additive directly influences the yield of the dehydrated product, most likely due to the reversable nature of the reaction even in the presence of micelles.

Table 5: Effect of methoxyacetonitrile additive quantity on yield of **2**

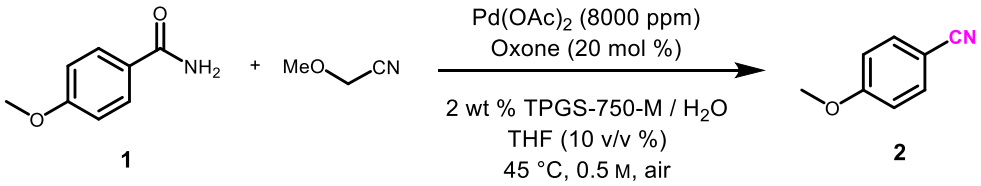

Entry	$MeOCH_2CN$ (equiv)	**2** (%)[a]
1	6	72
2	7	86
3	**8**	**97**

[a] Isolated yields

The amount of Oxone required for this reaction was also tested, in this case against not only the dehydration of **1** to **2**, but also orthogonally with the dehydration of a second system of 3,5-dichlorobenzamide to the corresponding 3,5-dichlorobenzonitrile **3** (Table 6). Standard conditions using 0.8 mol % Pd and 20 mol % oxone results in 97% yield of **2** and 93% yield of **3** (entry 4). Decreasing the additive (i.e., Oxone) by half to 10 mol % does not appear to diminish yield by too much, with 94% and 87% isolated yields of **2** and **3** respectively (entry 3). Furthermore, 5 mol % Oxone appears to give roughly the same yield of **3** as both 10 and 20 mol % at 90% isolated yield (entry 2). However, a marked decrease in yield can be observed for **2** when only 1 mol % of Oxone is used for this transformation, halting the reaction at 78% yield. Given the downward trend of Oxone loading *vs*. yield, as well as the minimal cost associated with the inorganic additive, we decided to maintain the Oxone amount at 20 mol % for future studies including analysis of the substrate scope.

Table 6: Effect of Oxone loading on yield of dehydration to **2** and **3**

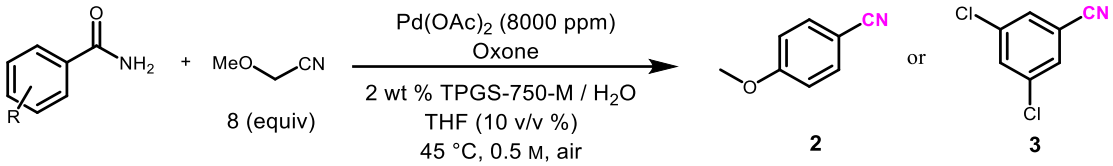

Entry	Oxone (mol %)	**2** (%)[a]	**3** (%)[a]
1	1	78	86
2	5	-	90
3	10	94	87
4	**20**	**97**	**93**

[a] Isolated yield

With additive loadings in hand, we decided to revisit the amount of $Pd(OAc)_2$ required to result in high yield of the dehydrated product **2** using MeOACN, as well as dichloroacetonitrile as a secondary measurement (Table 7). In the case of dichloroacetonitrile, decreasing the amount of Pd from 0.8 mol % to 0.4 mol % resulted in a drop in yield from 94% to 85% (entry 3). However, this same reduction in catalyst did not alter the amount of recovered **2** in the case of MeOACN, yielding 95% of the desired product. However, it was noted that the reliability of this reaction was still in question at this low loading of Pd, as side-by-side trials gave varying amounts of conversion by TLC analysis. Reduction of catalyst to 0.2 mol % (entry 4) ultimately resulted in only trace conversion. Given the variability between standard conditions and 0.6 mol % Pd (entry 2), it was decided that maintaining the Pd loading at 0.8 mol % would be best for delivering best yields of product. Furthermore, some more highly functionalized molecules (*vide infra*) would require higher loadings of Pd at 1 mol %.

Table 7: Effect of Pd catalyst loading on dehydration of **1** to **2**

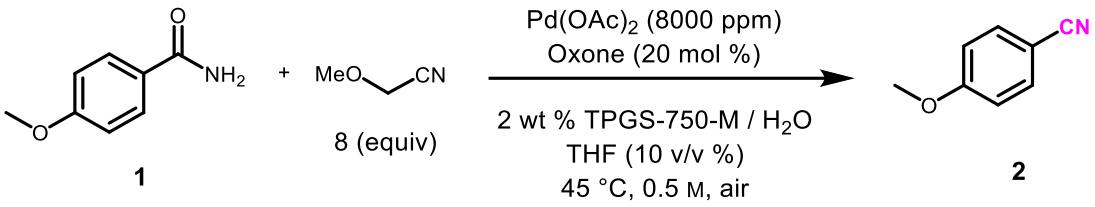

Entry	Pd loading (mol %)	X = OMe, **2** (%)[a]	X = Cl_2, **2** (%)[a]
1	**0.8**	**97**	**94**
2	0.6	89	-
3	0.4	95	85
4	0.2	trace	trace

[a] Isolated yields

The effect of the amphiphile on the dehydration to **2** was also observed (Table 8). 2 wt % TPGS-750-M in water was previously found to give optimal yields at 97% isolated yield (entry 1). Oddly, changing the surfactant to 5 wt % PTS-1000, which contains the identical α-tocopherol lipophilic interior, reduced the isolated yield to 90% (entry 2).[35] This could be due, in part, to the higher concentration of the amphiphile which would dilute the reactants and catalyst by virtue of the increased number of micelles present in solution. PEGylated alkylaromatic amphiphile Triton X-100 gave a similar conversion to that of PTS-1000 (entry 3) at 89% yield,[36] whereas PEGylated alkane Brij-30 gave a lower yield of 83% (entry 5),[37] most likely demonstrating the importance of aromatic functionality within the micellar core. Lipshutz group amphiphile Coolade, a low-foaming geminal surfactant,[38] gave the poorest yield at 80% (entry 4) even compared to an "on-water"[39] trial which gave 81% yield (entry 5).

Table 8: Effect of amphiphile on aqueous dehydration chemistry

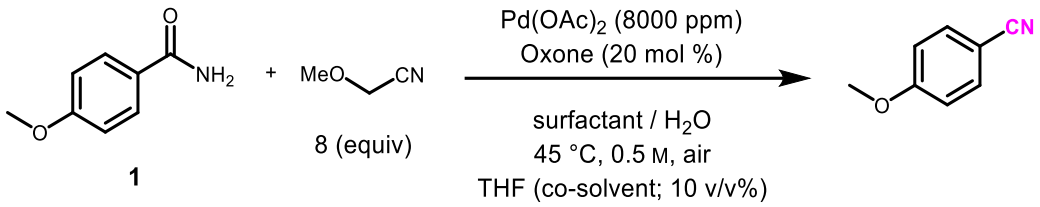

Entry	Amphiphile	**2** (%)[a]
1	**TPGS-750-M, 2 wt %**	**97**
2	PTS-1000, 5 wt %	90
3	Triton X-100, 2 wt %	89
4	Coolade, 2 wt %	80
5	Brij-30, 2 wt %	83
6	none (“on water”)	81

[a] Isolated yield

Despite the variability in results encountered for the dehydration of primary amides to nitriles in aqueous micellar media, especially when using parts-per-millions loadings of Pd, the general optimized conditions moving forward were running the chemistry at 45 °C in 2 wt % TPGS-750-M/H_2O at 0.5 M using eight equivalents of either methoxyacetonitrile (MeOACN) or fluoroacetonitrile (FACN) as the water-accepting agent. Most compounds were easily converted using MeOACN; however, in more difficult cases it was found that FACN was the superior sacrificial nitrile, typically in cases where nitrogen-containing heterocycles were involved. The amount of Pd used also varied between 0.8 mol % - 1.0 mol % with $Pd(OAc)_2$ as the source; as mentioned previously, use of other Pd(II) salts such as in the case of phosphine chelated Pd or use of another counter anion such as $Pd(O_2CCF_3)_2$ yielded no difference for converting benzamides to benzonitriles. With this data in hand, our first exploration into the versatility of this chemistry was based on simpler aromatic,

heteroaromatic, benzylic, and vinylic species, where the electronic nature of the substrate was the main variable tested (Figure 9).

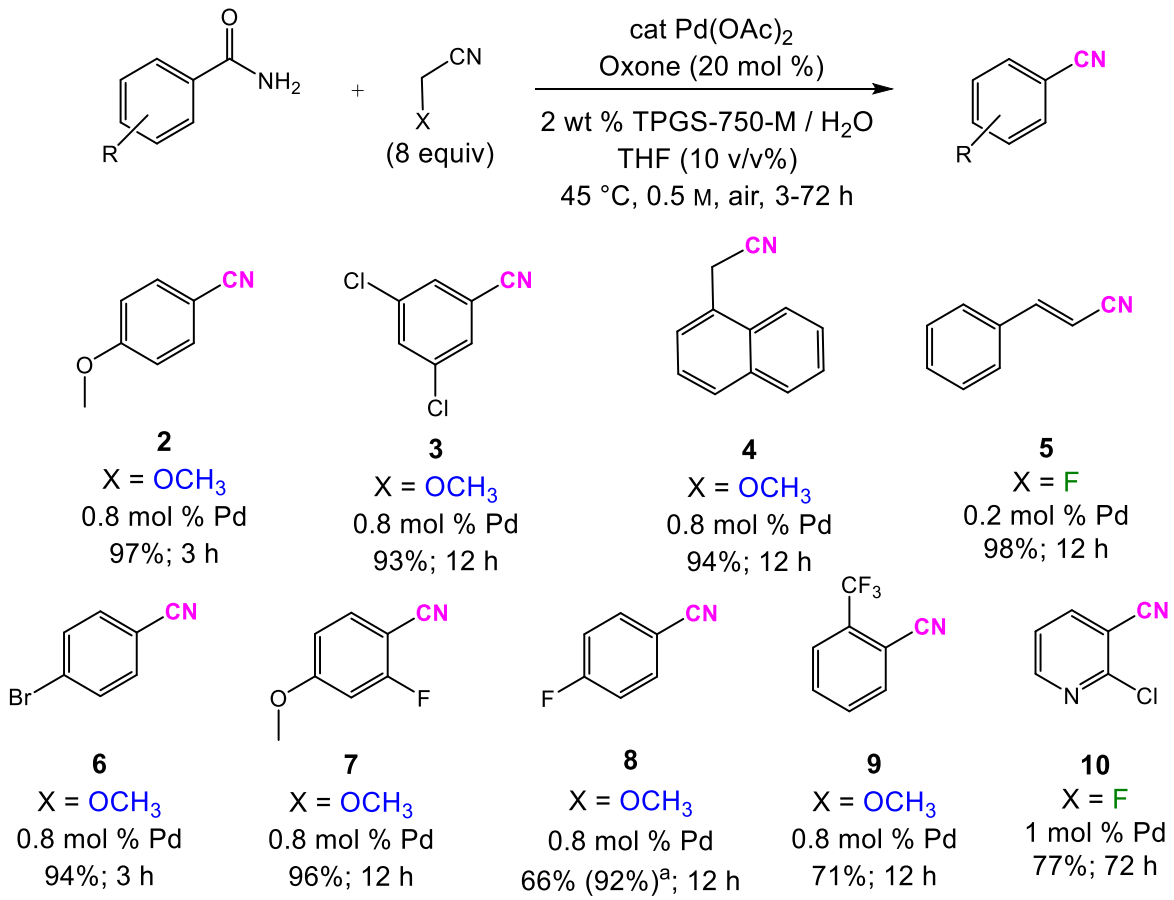

[a] NMR yield

Figure 9: Initial substrate scope varying the electronics of the amide

Electron-rich 4-methoxybenzonitrile (**2**) and electron-poor 3,5-dichlorobenzonitrile (**3**), used for the optimization studies of this transformation, gave product in high yields of 97% and 93%, respectively. Naphthylacetonitrile (**4**), a subsection of the antidepressant agomelatine, was also prepared in high yield at 94% using only 0.8 mol % Pd, exemplifying the versatility of this chemistry towards benzylic substrates. Cinnamyl nitrile (**5**) was obtained

in nearly quantitative yield, in this case using FACN which allowed for the Pd loading to be reduced to only 2000 ppm. 4-Bromobenzonitrile (**6**) was also obtained in high yield using ppm loadings of Pd, in this case only requiring three hours for full conversion. An aromatic nitrile with mixed electronics, such as in the case for compound **7**, also gave excellent isolated yields of 96%. Highly electron-poor 4-fluorobenzonitrile (**8**) and 2-trifluoromethylbenzonitrile (**9**), a fragment of bicalutamide,[40] were both prepared in modest yield when run on 2.5 mmol scale; however, NMR yield of **8** was significantly higher at 92% when using 1,2-dichloroethylene as internal standard, most likely due to the volatility of the product on high-vacuum post isolation. Chlorinated heteroaromatic **10**, derived from 2-chloronicatinamide, was also prepared in good yield at 77% using FACN; however, the reaction required nearly three days to reach this level of conversion. Interestingly, analogous heteroaromatic amides such as nicotinamide and quinoline-3-carboxamide gave little to no conversion (*vide infra*).

The next step for vetting this dehydration methodology in water was to examine its adaptability towards selectively transforming late-stage functionalized molecules (Figure 10). This includes molecules that are potentially unstable in water or are real-world intermediates encountered in pharmaceutical and agrochemical process development, the former of which are typically heteroaromatic species which can pose problems for Pd-catalyzed chemistry. Indeed, pyrimidine example **11** was formed in only a modest 53% yield, in this case requiring 10 v/v % DMSO as co-solvent additive (*vide infra*). Tosylated compound **12**, which could potentially undergo hydrolysis under aqueous conditions, was obtained in nearly quantitative yield using only 8000 ppm Pd. Non-steroidal anti-inflammatory drug (NSAID) derivatives obtained including **13**, from ibuprofen in 77% yield, and **14** from naproxen in quantitative yield, were both amenable to these conditions. In the case of **14**, no epimerization of the

stereocenter was observed by HPLC analysis at the α-position to the resulting nitrile. Highly derivatized quinoline **15**, a compound fragment towards the synthesis of the drug levatinib,[41] was also prepared in excellent yield (87%) with the inclusion of 20 v/v % DMSO as co-solvent.

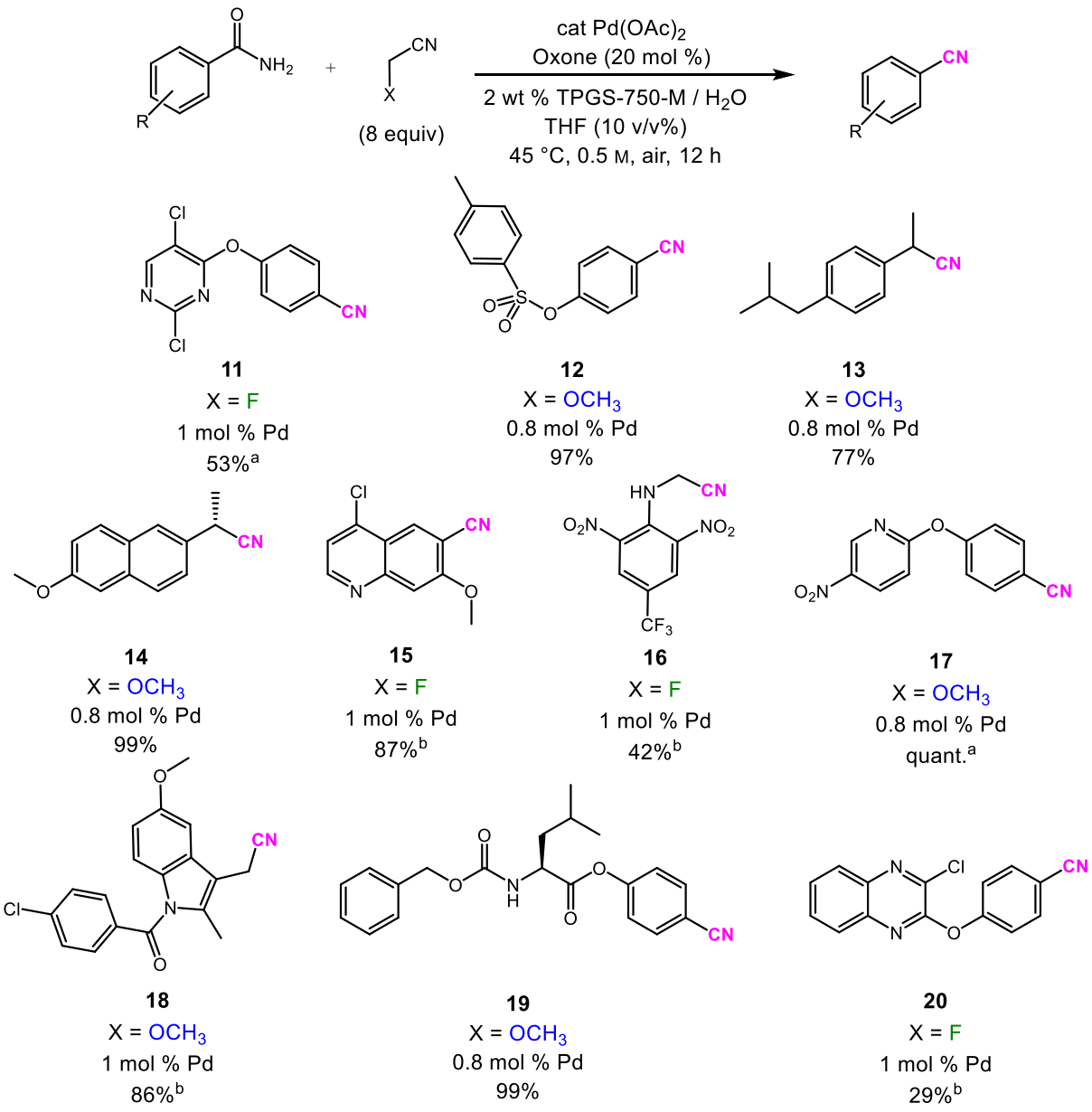

[a]10 v/v% DMSO added. [b]20 v/v% DMSO added

Figure 10: Nitriles formed via late-stage dehydration of amides

Surprisingly, compound **16** gave a modest 42% yield of the nitrile using 1 mol % Pd, despite the inclusion of an aniline nitrogen at the α-position of the corresponding *alkyl* amide. This compound exhibited very poor solubility in the micellar medium, even upon inclusion of 20 v/v % DMSO, which had no appreciable effect on the extent of conversion. Gratifyingly, nitropyridine **17** and Cbz-protected amino acid leucine derivative **19** were both formed in quantitative yield with only 0.8 mol % Pd. On the other hand, chloroquinoxaline derivative **20** was only obtained in 29% yield, even when using 1 mol % Pd and 20 v/v % DMSO.

The effect of DMSO on the amide dehydration in water was tested more in-depth leading to indomethacin derivative **18** (Table 9).

Table 9: Effect of co-solvent on yield of aqueous insoluble indomethacin derivative.

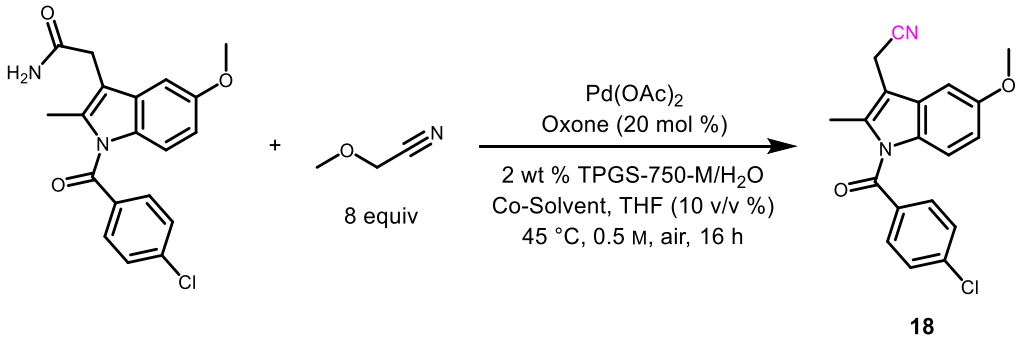

18

Entry	Pd Amount (ppm)	Co-Solvent (%)	**18** (%)[a]
1	2000	none	0
2	8000	*t*-BuOH (10%)	trace
3	8000	*t*-BuOH (50%)	44
4	8000	DMSO (10%)	65
5	8000	DMSO (20%)	73
6	10000	DMSO (10%)	79
7	**10000**	**DMSO (20%)**	**86**

[a]Isolated yields

No conversion of the starting material was observed when run with only 0.2 mol % Pd and no co-solvent (entry 1). Increasing the Pd loading to 0.8 mol % and using *t*-BuOH as co-solvent at 10 v/v % also gave only trace conversion (entry 2) but increasing the co-solvent ratio to 50 v/v % *t*-BuOH gave **18** in 44% isolated yield. Hot DMSO was found to be a very good solvent for the starting amide; therefore, a series of "pre-treatment" trials were attempted using 10-20 v/v % DMSO, where the organic solvent was added to the starting material and heated until a homogeneous solution formed prior to adding the aqueous medium and reagents. Running the reaction at 10 v/v % DMSO with 0.8 mol % (entry 4) and 1.0 mol % (entry 5) Pd gave product in 65% and 79% yield, respectively. However, increasing the DMSO co-solvent ratio to 20 v/v % with 0.8 mol % (entry 6) and 1.0 mol % (entry 7) gave the nitrile in 73% and 86% isolated yield, respectively, as the reaction was homogeneous with mechanical stirring at 45 °C.

Comparison of the optimized amide dehydration in water indicates the power and versatility of this methodology (Figure 11). Indeed, with respect to the synthesis of cinnamyl nitrile (**5**), the reported synthesis from Al-Huniti *et al.* requires 50 times more Pd, 20 mol % of expensive and non-environmentally friendly Selectfluor as oxidant, and dilute ACN (0.1 M) to afford the product in 91% yield. In comparison to this work, which requires only 0.2 mol % Pd, 20 mol % of cheap inorganic Oxone as oxidant, only eight equivalents of FACN are needed as the water-acceptor to give product in nearly quantitative yield. Further comparisons can be made with Buchwald's Cu-catalyzed chemistry, where the nitrile derivative of indomethacin was produced in only 54% yield using 2.2 mol % of DCyPE, an expensive ligand, and organic solvent with stoichiometric quantities of silyl ether being produced as byproduct. Our method utilizes only 1 mol % Pd and 8 equivalents of inexpensive MeOACN, with 20 v/v % DMSO as co-solvent to improve the conversion lead to an 86% isolated yield. This product can then

be easily recovered by dilution of the reaction medium with water and filtered to give the pure nitrile (*vide infra*).

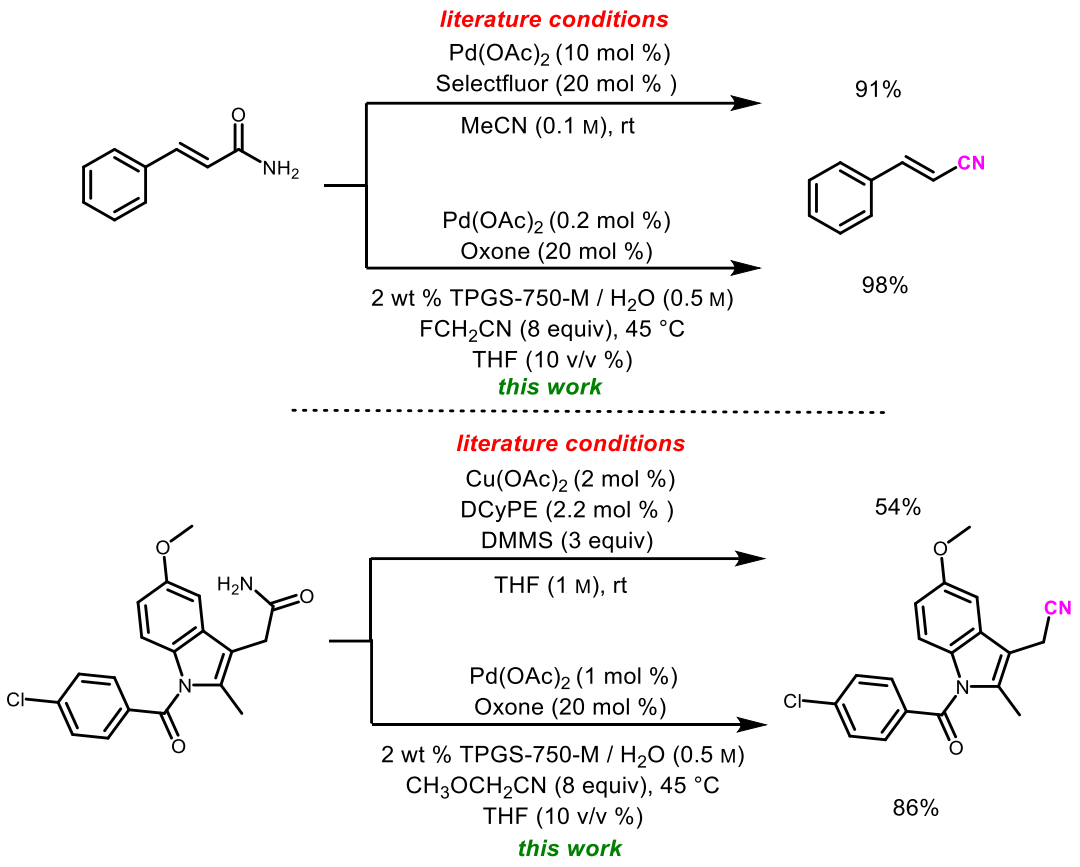

Figure 11: Comparison of this work with reported literature conditions

A variety of substrates did not perform well under the newly developed aqueous amide dehydration conditions (Figure 12). Simple aromatic compounds 4-nitobenzonitrile (**1a**) and 4-(dimethylamino)benzonitrile (**1b**) were not observed from the corresponding benzamide under optimized conditions. Compound **1c**, which exhibited very low solubility in the aqueous medium, was also not formed even when using 20 v/v % DMSO as co-solvent with heated pre-treatment. Modafinil fragments **1d** and **1e** formed in only trace amounts as presumably more

non-polar compounds by TLC analysis, whereas Buchwald's Cu-catalyzed organic solvent system produced **1d** in 74% yield. Boc-proline derivative **1f**, towards vildagliptin, and benzofuran derivative **1g** both gave less than 50% yield upon isolation. Synthesis of the nitrile derivative from ribavirin (**1h**) was unsuccessful, most likely due to the water solubility of the substrate; however, the protected derivative **1i**, where the silyl ether and acetonide should both increase the lipophilicity of the starting material, also gave no conversion, most likely pointing to the 1,2,4-triazole ring, where the primary amide is appended, as the culprit for the lack of conversion. Compound **1j**, derived from disopyramide, was not formed, most likely due to the tertiary amine. Labetalol derivative **1k** was also not formed under these conditions, and the reaction leading to tetracycline derivative **1l** gave a complex mixture of products by TLC analysis.

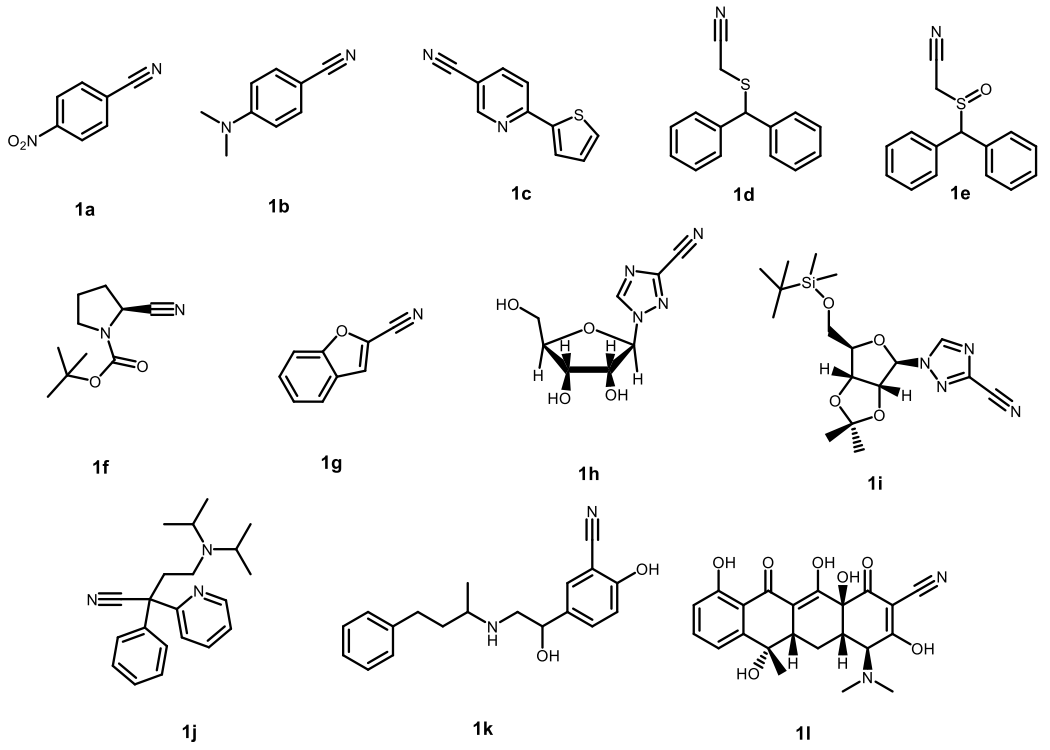

Figure 12: A selection of unreactive nitrile products under optimized conditions

Based on the success of the substrate scope for both simple and late-stage functionalized molecules, the E Factor of the process could then be determined. Unfortunately, the use of eight equivalents of MeOACN or FACN as water-acceptors inherently inflates the E Factor. We decided to study a system that not only uses MeOACN, but also the 20 v/v % DMSO as an organic co-solvent alongside the 10 v/v % THF. Therefore, dehydration to compound **18** was a prime candidate for these reasons, as well as the functionality within the molecule (Figure 13). The reaction is observed to go to completion by TLC analysis, and the product can easily be recovered by diluting the reaction mixture with four volumes of water and then filtering the precipitate. ^{1}H and ^{13}C analysis of this material following the workup protocol exhibits very high product purity, requiring no further chromatography or recrystallization. The E Factor can then be calculated by taking into consideration the quotient of the seven equivalents of leftover MeOACN (assuming full conversion), the one equivalent of the 2-methoxyacetamide produced as the reaction byproduct, and the mass of the DMSO and mass of the THF used as organic co-solvents over the amount of product recovered. Based on this analysis, an E Factor of 4.22 is reported for this procedure, with 83% yield of pure product.

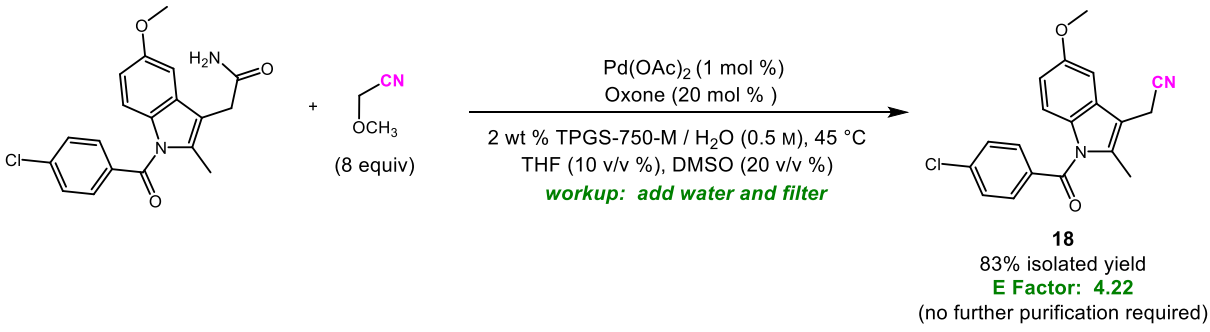

Figure 13: E Factor determination for product **18**

Recyclability of the aqueous medium post amide dehydration was also observed to be straightforward (Figure 14). The micellar medium, after an initial conversion of **1** to **2**, could simply be extracted using MTBE as solvent in air to afford the product in 97% yield. The resulting aqueous mixture lost some volume using this procedure, and thus concomitant reactions are slightly more concentrated than in the initial reaction. However, only the addition of fresh substrate **1**, MeOACN, THF co-solvent, $Pd(OAc)_2$, and Oxone is required to initiate a second and third reaction (first and second recycling, respectively) yielding product in 96% yield in both iterations. The last recycling results in a slurry of water with inorganic material, and thus subsequent trials would require the inclusion of fresh water and thus the recycling study was halted here. It should also be noted that the residual palladium analyzed in the silica gel purified product after the second recycling was less than 0.2 ppm, which is significantly lower than the FDA required 10 ppm/day/dose.[42]

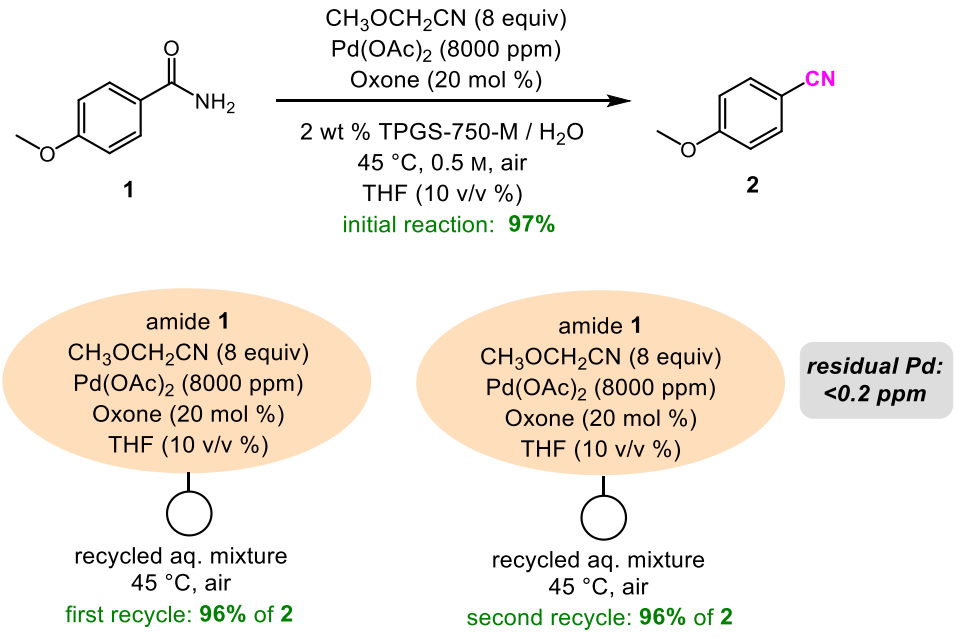

Figure 14: Recycling of aqueous media for amide dehydration chemistry

Finally, the commonality of a micellar media for use in many different reaction types lends itself towards multistep processes in one reaction vessel, which can reduce the industrial footprint as well as maximize efficiency with respect to time.[43a-b] Furthermore, the aqueous environment is primed for the use of enzymes, where water is the native medium for these biocatalysts. Our lab has developed a toolbox of enzymatic reactions that perform better in micellar media compared to just purely buffered water solutions, where the "reservoir effect" shields the inhibition of enzymes due to buildup of products.[44a-c] Therefore, an attractive combination of the enzymatic catalysis with the amide dehydration chemo-catalysis (*e.g.* chemoenzymatic catalysis) was explored in a 3-step, 1-pot sequence (Figure 15). Firstly, 4-bromobenzamide was dehydrated under optimized conditions and 0.8 mol % Pd to form the 4-bromobenzonitrile, which was not isolated. The aryl bromide was then coupled with 4-acetylphenylboronic acid under ambient conditions, requiring only an additional 0.23 mol % Pd[dtbpf]Cl_2 to afford the biaryl product. Interestingly, attempts to use group ligand N_2Phos failed under these 1-pot conditions, most likely due to the Oxone leftover from the previous reaction. Attempts to clean up the excess Oxone using PPh_3 resulted in not only no reaction for N_2Phos, but also inhibition of the Pd[dtbpf]Cl_2 catalyst that works without resorting to this scavenging technique. Finally, the acetyl group was reduced using the enzyme ADH-101 with NAD/NADPNa as co-factors and *i*PrOH as the hydride transfer source. This 3-step sequence resulted in the chiral biaryl benzyl alcohol in 93% isolated yield with >99% ee based on HPLC analysis. Of note, the nonracemic product alcohol contained <3.6 ppm residual Pd after passing through a silica gel column.

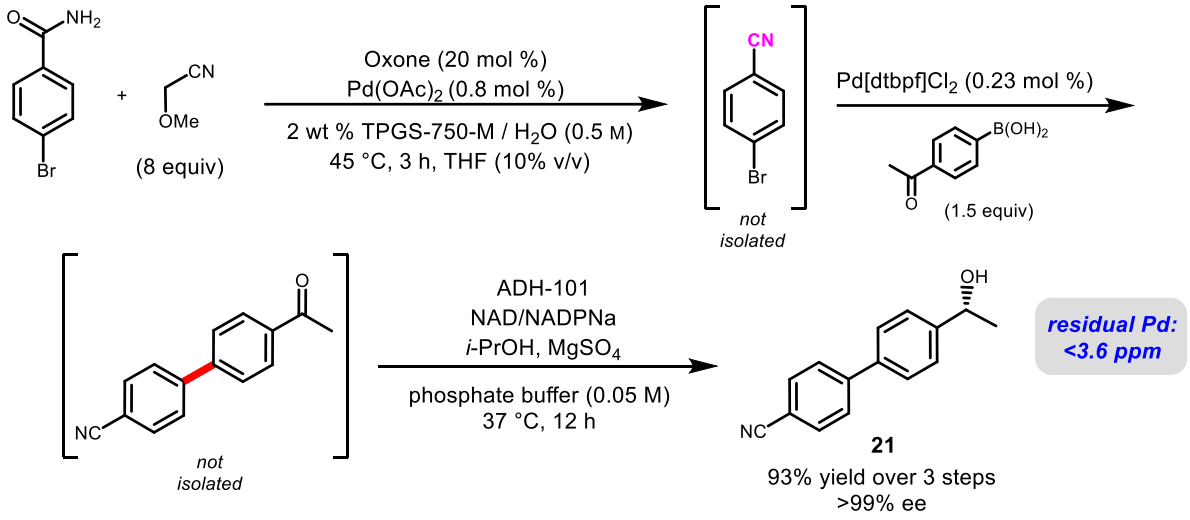

Figure 15: 3-step, 1-pot chemoenzymatic sequence utilizing amide dehydration

3.4 Conclusions

In conclusion, an environmentally attractive method for the dehydration of primary amides to nitriles has been developed. This technology outperforms current literature methods not only in terms of yield and applicability, but also with respect to reducing the amount of organic co-solvent required for the transformation in the form of acetonitrile. The chemistry can effect transformation of aromatic, benzylic, and vinylic amides to the corresponding nitriles using 0.2-1.0 mol % $Pd(OAc)_2$, together with eight equivalents of methoxyacetonitrile or fluoroacetonitrile as water-accepting agents. Furthermore, the dehydration chemistry works well to afford a wide array of electronically diverse aromatic nitriles, and can be utilized for late-stage functionalization. In some cases, DMSO as co-solvent was found to greatly enhance the reactivity of otherwise highly insoluble starting amides; however, the use of only 20 v/v % of the DMSO co-solvent does little to affect the overall strikingly low E Factor of 4.22 for a complex molecule. The aqueous phase was also found to be completely reusable post-extraction for at least two recycles. Finally, a 3-step, 1-pot chemoenzymatic process was amenable after the initial dehydration step, exemplifying the mild nature of the newly enhanced method.

3.5 References

1. Al-Huniti, M. H.; Croatt, M. P. *Asian J. Org. Chem.* **2019**, *8*, 1791–1799.
2. Threadingham, D.; Obrecht, W.; Wieder, W.; Wachholz, G.; Engehausen, R. Rubber, 3. Synthetic Rubbers, Introduction and Overview. In *Ullmann's Encyclopedia of Industrial Chemistry*; Wiley-VCH Verlag GmbH & Co. KGaA, Ed.; Wiley-VCH Verlag GmbH & Co. KGaA: Weinheim, Germany, **2011**.
3. Mackey, D.; Jorgensen, A. H. ''Nitrile Rubber'', Kirk Othmer Encyclopedia of Chemical Technology, 5th ed., John Wiley & Sons, Hoboken, NJ, **2000**, 1-15.
4. Critchley, E.; Pemberton, M. N. *Br. Dent. J.* **2021**, 1-5.
5. Fleming, F. F.; Fleming, F. F. *Nat. Prod. Rep*. **1999**, *16*, 597–606.
6. Hughes, M. A. Biosynthesis and Degradation of Cyanogenic Glycosides. In *Comprehensive Natural Products Chemistry*; Elsevier, **1999**; pp 881–895.
7. Wang, X.; Wang, Y.; Li, X.; Yu, Z.; Song, C.; Du, Y. *RSC Med. Chem*. **2021**, *12*, 1650-1671.
8. Fleming, F. F.; Yao, L.; Ravikumar, P. C.; Funk, L.; Shook, B. C. *J. Med. Chem.* **2010**, *53*, 7902–7917.
9. Wang, J.; Liu, H. *Chin. J. Org. Chem.* **2012**, *32*, 1643.
10. Beigel, J. H.; Tomashek, K. M.; Dodd, L. E.; Mehta, A. K.; Zingman, B. S.; Kalil, A. C.; Hohmann, E.; Chu, H. Y.; Luetkemeyer, A.; Kline, S.; Lopez de Castilla, D.; Finberg, R. W.; Dierberg, K.; Tapson, V.; Hsieh, L.; Patterson, T. F.; Paredes, R.; Sweeney, D. A.; Short, W. R.; Touloumi, G.; Lye, D. C.; Ohmagari, N.; Oh, M.; Ruiz-Palacios, G. M.; Benfield, T.; Fätkenheuer, G.; Kortepeter, M. G.; Atmar, R. L.; Creech, C. B.; Lundgren, J.; Babiker, A. G.; Pett, S.; Neaton, J. D.; Burgess, T. H.;

Bonnett, T.; Green, M.; Makowski, M.; Osinusi, A.; Nayak, S.; Lane, H. C. *N. Engl. J. Med*. **2020**, *383*, 1813–1826.

11. (a) Friedman, L.; Shechter, H. *J. Org. Chem*. **1960**, *25*, 877-879; (b) Kim, D. W.; Song, C. E.; Chi, D. Y. *J. Org. Chem*. **2003**, *68*, 4281–4285; (c) Zhou, W.; Xu, J.; Zhang, L.; Jiao, N. *Org. Lett.*, **2010**, *12*, 2888–2891.
12. (a) Rajanbabu, T. V. B. Hydrocyanation of Alkenes and Alkynes. In *Organic Reactions*; John Wiley & Sons, Inc., Ed.; John Wiley & Sons, Inc.: Hoboken, NJ, USA, **2011**; pp 1–74. (b) Saranya, S.; Neetha, M.; Aneeja, T.; Anilkumar, G. *Adv. Synth. Catal.* **2020**, *362*, 4543–4551.
13. Tseng, K.-N. T. *Synlett* **2014**, *25*, 2385-2389.
14. Czekelius, C.; Carreira, E. M. *Angew. Chem., Int. Ed.* **2005**, *117*, 618–621.
15. (a) Yu, H.; Richey, R. N.; Miller, W. D.; Xu, J.; May, S. A. *J. Org. Chem.* **2011**, *76*, 665–668; (b) Amal Joseph, P. J.; Priyadarshini, S. *Org. Process Res. Dev*. **2017**, *21*, 1889–1924; (c) Chahkamali, F. O.; Sobhani, S.; Sansano, J. M. *Catal. Lett.* **2021**. https://doi.org/10.1007/s10562-021-03824-0; (d) Zhao, D.; Xu, P.; Ritter, T. *Chem.* **2019**, *5*, 97–107; (e) Cohen, D. T.; Buchwald, S. L. *Org. Lett.* **2015**, *17*, 202–205.
16. Thakore, R. R.; Takale, B. S.; Singhania, V.; Gallou, F.; Lipshutz, B. H. *ChemCatChem* **2021**, *13*, 212–216.
17. Jaszczak, E.; Polkowska, Ż.; Narkowicz, S.; Namieśnik, J. *Environ. Sci. Pollut. Res*. **2017**, *24*, 15929–15948.
18. Kent, R. E.; McElvain, S.M. *Org. Synth.* **1945**, *25*, 61.
19. Reid, Wm. B.; Hunter, J. H. *J. Am. Chem. Soc.* **1948**, *70*, 3515–3515.
20. Rickborn, B.; Jensen, F. R. *J. Org. Chem*. **1962**, *27*, 4608–4610.

21. Maetz, P.; Rodriguez, M. *Tet. Lett.* **1997**, *38*, 4221-4222.

22. Caremon, D. A.; Phillips, B. T. *Tet. Lett.* **1988**, *29*, 2155-2158.

23. Atkins, G. M.; Burgess, E. M. *J. Am. Chem. Soc.* **1968**, *90*, 4744–4745.

24. Ganesan, M.; Nagaraaj, P. *Org. Chem. Front.* **2020**, *7*, 3792–3814.

25. Liu, R. Y.; Bae, M.; Buchwald, S. L. *J. Am. Chem. Soc.* **2018**, *140*, 1627–1631.

26. As of this writing, Millipore-Sigma lists this ligand's price as $122/g. See: https://www.sigmaaldrich.com/US/en/product/aldrich/479500. (Accessed February 20, 2022)

27. Maffioli, S. I.; Marzorati, E.; Marazzi, A. *Org. Lett.* **2005**, *7*, 5237–5239.

28. Zhang, W.; Haskins, C. W.; Yang, Y.; Dai, M. *Org. Biomol. Chem.* **2014**, *12*, 9109–9112.

29. Al-Huniti, M. H.; Rivera-Chávez, J.; Colón, K. L.; Stanley, J. L.; Burdette, J. E.; Pearce, C. J.; Oberlies, N. H.; Croatt, M. P. *Org. Lett.* **2018**, *20*, 6046–6050.

30. Okabe, H.; Naraoka, A.; Isogawa, T.; Oishi, S.; Naka, H. *Org. Lett.* **2019**, *21*, 4767–4770.

31. Lipshutz, B. H.; Ghorai, S.; Abela, A. R.; Moser, R.; Nishikata, T.; Duplais, C.; Krasovskiy, A.; Gaston, R. D.; Gadwood, R. C. *J. Org. Chem.* **2011**, *76*, 4379–4391.

32. Winum, J.-Y.; Toupet, L.; Barragan, V.; Dewynter, G.; Montero, J.-L. *Org. Lett.* **2001**, *3*, 2241–2243.

33. Angelici, R. J.; Quick, M. H.; Kraus, G. A. *Inorganica Chimica Acta* **1980**, *44*, L137–L138.

34. Carole, W. A.; Colacot, T. J. *Chem. Eur. J.* **2016**, *22*, 7686–7695.

35. Lipshutz, B. H.; Aguinaldo, G. T.; Ghorai, S.; Voigtritter, K. *Org. Lett.* **2008**, *10*, 1325–1328.

36. Koley, D.; Bard, A. J. *Proceedings of the National Academy of Sciences* **2010**, *107*, 16783–16787.

37. https://pubchem.ncbi.nlm.nih.gov/compound/Polyoxyethylene-_23_-lauryl-ether. (Accessed February 20, 2022).

38. Lee, N. R.; Cortes-Clerget, M.; Wood, A. B.; Lippincott, D. J.; Pang, H.; Moghadam, F. A.; Gallou, F.; Lipshutz, B. H. *ChemSusChem* **2019**, *12*, 3159–3165.

39. Rideout, D. C.; Breslow, R. *J. Am. Chem. Soc.* **1980**, *102*, 7816–7817.

40. Jones, L. H.; Summerhill, N. W.; Swain, N. A.; Mills, J. E. *Med. Chem. Commun.* **2010**, *1*, 309–318.

41. Sadineni, R. K.; Rapolu, R. K.; Raju, V. V. N. K. V. P.; Srinivasu, N.; Malladi, S.; Mulakayala, N. *Chem. Pap.* **2021**, *75*, 1475–1483.

42. Phillips, S.; Holdsworth, D.; Kauppinen, P.; Mac Namara, C. *Johnson Matthey Technol. Rev.* **2016**, *60*, 277–286.

43. (a) Hayashi, Y. *Chem. Sci.* **2016**, *7*, 866–880; (b) Hayashi, Y. *J. Org. Chem.* **2021**, *86*, 1–23.

44. (a) Cortes-Clerget, M.; Akporji, N.; Zhou, J.; Gao, F.; Guo, P.; Parmentier, M.; Gallou, F.; Berthon, J.-Y.; Lipshutz, B. H. *Nat. Commun.* **2019**, *10*, 2169; (b) Akporji, N.; Singhania, V.; Dussart-Gautheret, J.; Gallou, F.; Lipshutz, B. H. *Chem. Commun.* **2021**, *57*, 11847–11850; (c) (1) Singhania, V.; Cortes-Clerget, M.; Dussart-Gautheret, J.; Akkachairin, B.; Yu, J.; Akporji, N.; Gallou, F.; Lipshutz, B. H. *Chem. Sci.* **2022**, *13*, 1440–1445.

3.6 Experimental Data

1. General information

All commercial reagents were used without further purification unless otherwise noted. Organic solvents specified as dry and/or degassed such as THF or toluene were either taken from a solvent purification system (Pure-Solv 400, Innovative Technology, Inc. (now Inert, Inc.)), or degassed using a stream of bubbling argon for a minimum of 1 h and involved less than 25 mL of volume. All other solvents were used as received, such as MeOH, EtOAc, hexanes, and Et_2O, unless otherwise noted, and purchased from Fisher Scientific. Palladium acetate was purchased from Johnson Matthey and kept in its solid state within a glove box. Starting materials, such as carboxylic acids or primary amides, were purchased either from Millipore-Sigma or Combi-Blocks. The surfactant, TPGS-750-M, was prepared via a standard literature procedure,[1] or can be purchased from Millipore-Sigma (catalog #733857 for a 2 wt % solution of the wax dissolved in water). A standard 2 wt % aqueous solution of TPGS-750-M was typically prepared on a 100 g scale by dissolving 2 g of the wax into 98 g of thoroughly degassed (steady stream of argon, minimum of 1 h bubbling time with stirring) HPLC grade water in a 250 mL round bottomed flask equipped with a stir bar and allowed to dissolve overnight with vigorous stirring under argon pressure (**NOTE**: Do not attempt to degas the aqueous phase with surfactant wax submerged; vigorous foaming to the point of overflowing may occur). The 2 wt % TPGS-750-M/H_2O solution, once prepared, was kept under argon pressure at all times. Thin-layer chromatography (TLC) was performed using Silica Gel 60 F_{254} plates (Merck, 0.25 mm thick). Flash chromatography is either performed in glass columns or an automated Biotage system using Silica Gel 60 (Silicycle, 40-63 nm). ^{1}H and ^{13}C NMR were recorded at 25 °C on a Varian Unity Inova 400 MHz, a Varian Unity Inova 500 MHz, or

on a Varian Unity Inova 600 MHz spectrometer in $CDCl_3$ with residual $CHCl_3$ (^1H = 7.26 ppm, ^{13}C = 77.16 ppm) or in DMSO-d_6 with residual $(CH_3)_2SO$ (^1H = 2.50 ppm, ^{13}C = 39.52 ppm) as internal standards. Chemical shifts are reported in parts per million (ppm). NMR Data are reported as follows: chemical shift, multiplicity (s = singlet, d = doublet, dd = doublet of doublets, ddd = doublet of doublet of doublets, t = triplet, td = triplet of doublets, q = quartet, quin = quintet, m = multiplet), coupling constant (if applicable), and integration. High-resolution mass analyses (HRMS) were recorded on a Waters Micromass LCT TOF ES+ Premier mass spectrometer using ESI ionization.

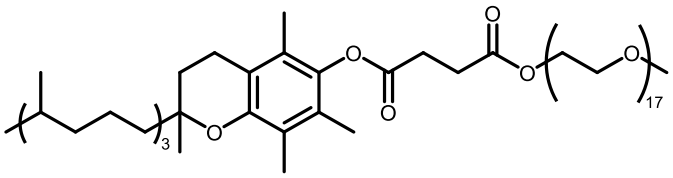

TPGS-750-M

2. General procedures for amide dehydrations in water

2a. General procedure A: Amide dehydration in water at 0.5 mmol scale with 0.8 mol % $Pd(OAc)_2$

A stock solution of catalyst was prepared by dissolving 4.5 mg of $Pd(OAc)_2$ into 500 μL of THF with gentle heating until an orange homogeneous solution had formed.

To a 1-dram vial containing a PTFE-coated magnetic stir bar was added Oxone (30 mg, 0.1 mmol, 0.2 equiv) and the primary amide (0.5 mmol, 1.0 equiv). 2 wt % TPGS-750-M in H_2O (0.9 mL, 0.56 M) was then added, followed by either methoxyacetonitrile (300 μL, 8 equiv) or fluoroacetonitrile (250 μL, 8 equiv). A sample of the catalyst stock solution (100 μL) in THF was then added and the vial was sealed using a threaded cap and PTFE tape. The

reaction was then allowed to stir vigorously (~1500 RPM) at 45 °C internal temperature (aluminum block reactor set to heat to 50 °C) until deemed complete by TLC. The aqueous phase was then extracted using EtOAc (3 x 1 mL) and dried directly onto SiO_2 to be purified via column chromatography.

Note: If DMSO is used as a co-solvent for the reaction, 10-20 v/v% of DMSO (compared to the total volume of water and THF) is added directly to the primary amide followed by heating with a heat gun until a change of the solid is noted, in many cases being liquefication. The TPGS-750-M solution, nitrile, and catalyst stock solution followed by Oxone are then added quickly. The vial is then sealed and allowed to stir as described above.

2b. General procedure B: Amide dehydration in water at 0.5 mmol scale with 1.0 mol % $Pd(OAc)_2$

A stock solution of catalyst was prepared by dissolving 5.6 mg of $Pd(OAc)_2$ into 500 μL of THF with gentle heating until an orange homogeneous solution had formed. The remainder of the experimental then follows General Procedure A.

3. Synthesis of unreported starting materials

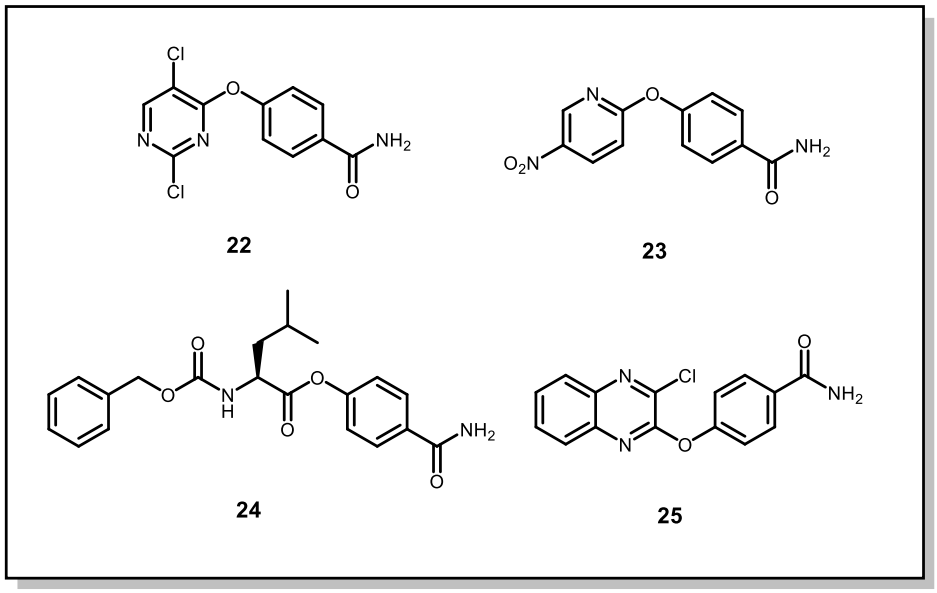

3.1 Synthesis of 4-((2,5-dichloropyrimidin-4-yl)oxy)benzonitrile (22)

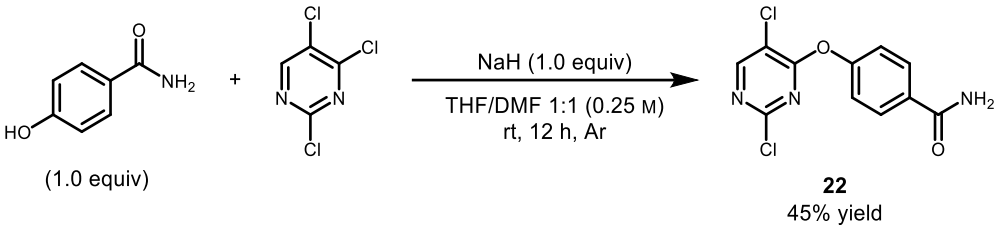

To an oven-dried 100 mL round-bottom flask equipped with a PTFE-coated magnetic stir bar was added NaH (60% in mineral oil, 200 mg, 5.0 mmol, 1 equiv) in an argon-filled glovebox. The flask was sealed with a rubber septum, removed from the glove box, and adapted to a stir plate. In a separate 50 mL oven-dried pear-shaped flask, 4-hydroxybenzamide (685.7 mg, 5.0 mmol, 1 equiv) was dissolved in a 50:50 mixture of anhydrous THF and DMF (20 mL), then this solution was transferred via syringe to the flask containing NaH, with stirring, under a positive flow of argon. The solution was allowed to stir until bubbling ceased, then 2,4,5-trichloropyrimidine (0.573 mL, 5.0 mmol, 1 equiv) was added via syringe and the reaction was allowed to stir at rt overnight. Upon completion, the resulting solids were filtered off and 150 mL of DI water was added to the filtrate to precipitate the product **22**, which was collected via filtration, washed twice with 50 mL of water, then dried on vacuum overnight resulting in a white solid (599 mg, 45% yield). R_f = 0.38 (7:3 EtOAc/hexanes).

3.2 Synthesis of 4-((5-nitropyridin-2-yl)oxy)benzamide (23)

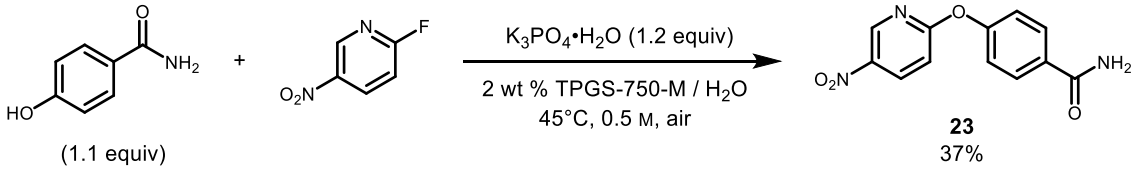

To a 25 mL round bottom flask equipped with a football-shaped stir bar was added 4-hydroxybenzamide (755 mg, 5.5 mmol, 1.1 equiv), 2-fluoro-5-nitropyridine (710 mg, 5.0 mmol, 1.0 equiv), and $K_3PO_4 \cdot H_2O$ (1400 mg, 6.0 mmol, 1.2 equiv). 2 wt % TPGS-750-M /

H_2O (10 mL, 0.5 M) was then added, and the flask was sealed using a rubber septum. The reaction mixture was then allowed to stir vigorously for 12 h in a 50 °C oil bath (45 °C internal temperature). The reaction mixture was then diluted in water (50 mL) and extracted with EtOAc (3 x 50 mL). The crude product mixture was then purified by column chromatography (eluent: 75% EtOAc/25% hexanes) and was ultimately recrystallized in hot EtOH to result in product as white crystals (480 mg, 37% yield). R_f = 0.35 (3:1 EtOAc/hexanes).

3.3 Synthesis of 4-carbamoylphenyl ((benzyloxy)carbonyl)-L-leucinate (24)

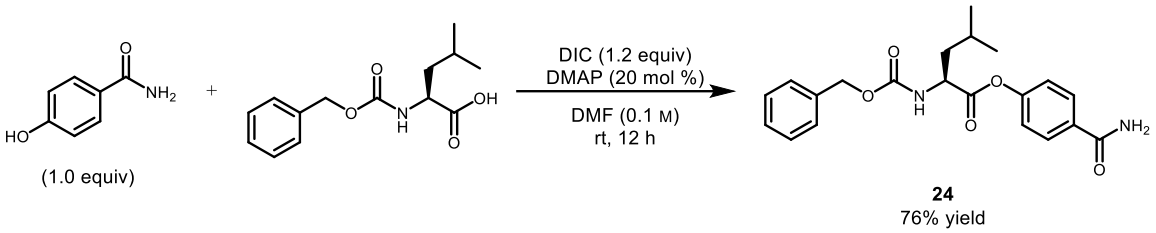

To a 1-dram vial equipped with a PTFE-coated magnetic stir bar was added Z-leu-OH (132.7 mg, 0.5 mmol, 1 equiv) and 4-hydroxybenzamide (68.6 mg, 0.5 mmol, 1 equiv) which were then dissolved in DMF (3 mL). Once dissolved, diisopropylcarbodiimide (94 μL, 0.6 mmol, 1.2 equiv) and DMAP (12.2 mg, 0.1 mmol, 0.2 equiv) were added and the reaction was allowed to stir at rt overnight. Upon completion, as determined by TLC, the reaction mixture was filtered through cotton and the product was precipitated with water (15 mL) and extracted with diethyl ether (3 x 5 mL). The combined organic extracts were washed with water (2 x 3 mL), brine (2 mL), and the solvent was removed *in vacuo*. The crude material was purified by column chromatography (eluent: 0-100% EtOAc/hexanes gradient) resulting in a white solid (146.1 mg, 76% yield). R_f = 0.34 (7:3 EtOAc/hexanes, CAM stain).

3.4 Synthesis of 4-((3-chloroquinoxalin-2-yl)oxy)benzamide (25)

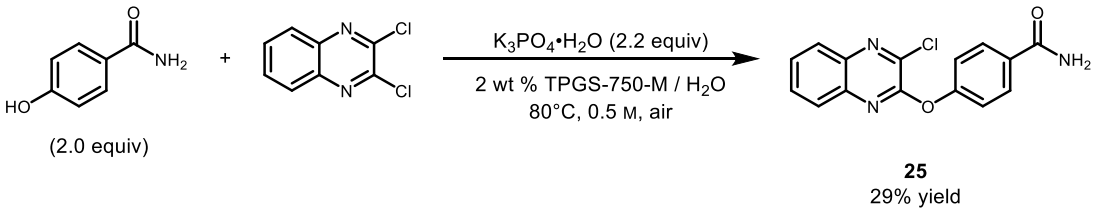

To a 25 mL round bottomed flask equipped with a football-shaped stir bar was added 4-hydroxybenzamide (1000 mg, 7.3 mmol, 2.0 equiv), 2,3-dichloroquinoxaline (730 mg, 3.67 mmol, 1.0 equiv), and $K_3PO_4 \cdot H_2O$ (1850 mg, 7.94 mmol, 2.2 equiv). 2 wt % TPGS-750-M / H_2O (7.5 mL, 0.5 M) was then added and the flask was sealed using a rubber septum. The reaction mixture was then allowed to stir vigorously for 48 h in a 90 °C oil bath (80 °C internal temperature). The crude product was then slurried with 2 M NaOH (50 mL), filtered, and washed with 1 M HCl. The filtrate was then slurried in EtOH, heated to reflux, and filtered hot to result in product as a white solid (314.5 mg, 29% yield). R_f = 0.31 (3:1 EtOAc/hexanes).

4. E Factor evaluation

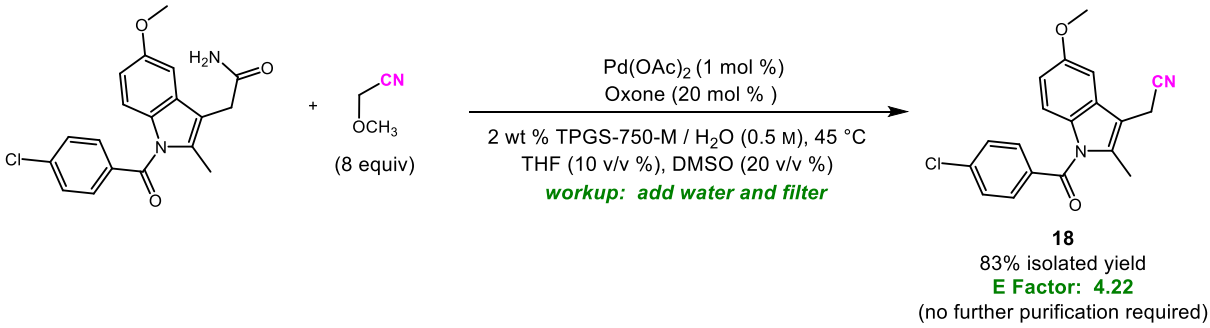

To a 1-dram vial was added 5.6 mg of $Pd(OAc)_2$ and THF (500 µL). The mixture was then gently heated using a heat gun until a homogeneous mixture had formed resulting in the catalyst stock solution.

To a separate 1-dram vial equipped with a Teflon coated stir bar was added the amide (89.0 mg, 0.25 mmol, 1 equiv) followed by DMSO (100 µL, 20 v/v %). The resulting slurry was

then heated with a heat gun until a homogeneous liquid formed. Very quickly after liquefication, methoxyacetonitrile (143.4 mg, 150 μL, 2.0 mmol, 8 equiv), 50 μL of the catalyst stock solution (1 mol % Pd), and 2 wt % TPGS-750-M / H_2O (450 μL) was added followed by Oxone (16 mg, 0.05 mmol, 20 mol %). This mixture was then stirred with a metal spatula until a mixture that could be stirred was achieved, and the vial was sealed using a screw cap followed by Teflon tape under air. The resulting slurry was then allowed to stir vigorously (~1500 RPM) in an aluminum block reactor at 45 °C internal temperature (aluminum block set to heat to 50 °C).

Figure 16: TLC of reaction for E Factor evaluation

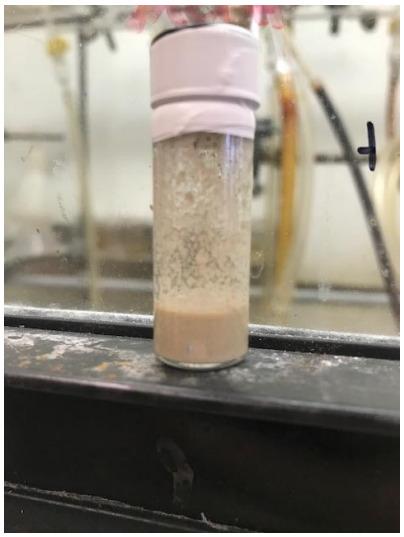

Figure 17: E Factor reaction prior to dilution and filtration

The resulting grey reaction mixture was then cooled to rt and water (4 mL) was then added and the product mixture stirred for 5 min. The suspension was then filtered, washed with water (10 mL), and allowed to dry under suction overnight resulting in product as a grey solid (70.1 mg, 83% yield).

E Factor = (mass waste organics) / (mass product)

$= (mass_{MeOACN} + mass_{2\text{-}MeOAcetamide} + mass_{DMSO} + mass_{THF}) / (mass_{product})$

= (138.4+22.3+90.9+44.4) / 70.1 = ***4.22***

5. Aqueous recycling study

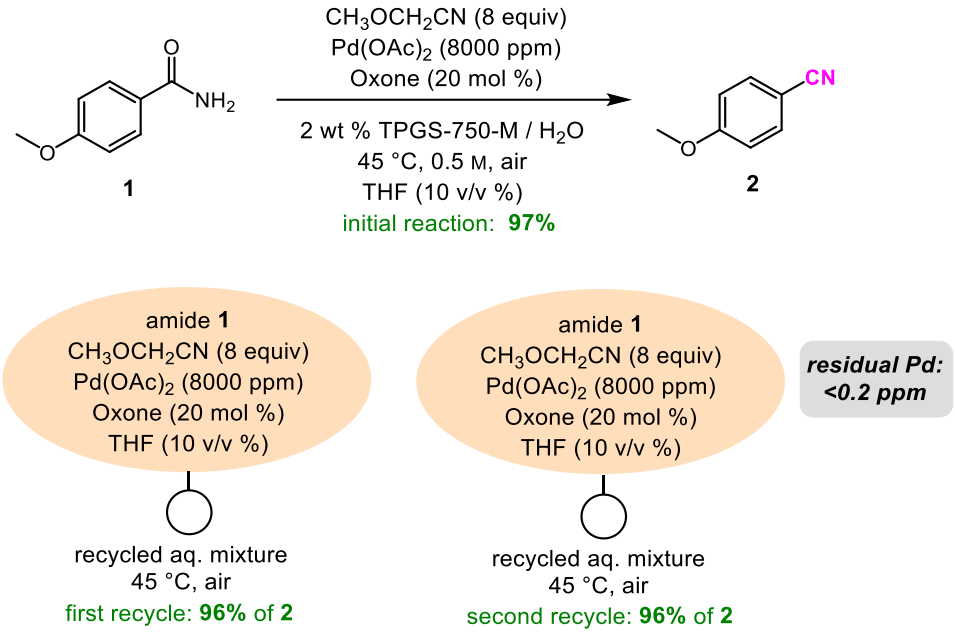

To a 1-dram vial was added 4.5 mg of $Pd(OAc)_2$ and THF (500 µL). The mixture was then gently heated using a heat gun until a homogeneous solution had formed resulting in the catalyst stock solution.

Initial reaction: To a 1-dram vial equipped with a Teflon coated stir bar was added benzamide **1** (75 mg, 0.5 mmol) and Oxone (30 mg, 0.1 mmol, 20 mol %). 2 wt % TPGS-750-M (900 µL), methoxyacetonitrile (300 µL, 4 mmol, 8 equiv), and 100 µL of the catalyst stock solution (0.8 mol % Pd) was then added and the vial was sealed under air using a threaded cap followed by Teflon tape. The resulting slurry was then allowed to stir vigorously (~1500 RPM) in an aluminum block reactor at 45 °C internal temperature (aluminum block set to heat to 50 °C) overnight. The contents of the vial were then extracted using methyl *t*-butyl ether (MTBE; 3 x 1.0 mL). The combined organics were then dried onto SiO_2 and purified via column chromatography (20% EtOAc/hexanes) and the product was dried under high vacuum to result in a white solid (64.3 mg, 97% yield).

First recycle: To the 1-dram vial containing the 2 wt % TPGS-750-M aqueous phase used for the previous reaction (and extracted with MTBE) was added fresh benzamide **1** (75 mg, 0.5 mmol) and Oxone (30 mg, 0.1 mmol, 20 mol %). Fresh methoxyacetonitrile (300 μL, 4 mmol, 8 equiv) and 100 μL of the catalyst stock solution (0.8 mol % Pd) was then added and the vial was sealed under air using a threaded cap followed by Teflon tape. The resulting slurry was then allowed to stir vigorously (~1500 RPM) in an aluminum block reactor at 45 °C internal temperature (aluminum block set to heat to 50 °C) overnight. The contents of the vial were then extracted using methyl *t*-butyl ether (MTBE; 1.0 mL x 3). The combined organics were then dried onto SiO_2 and purified via column chromatography (20% EtOAc/hexanes) and the product was dried under high vacuum to result in a white solid (63.4 mg, 96% yield).

Second recycle: To the 1-dram vial containing the 2 wt % TPGS-750-M aqueous phase used for the previous two reactions (and extracted with MTBE twice) was added fresh benzamide **1** (75 mg, 0.5 mmol) and Oxone (30 mg, 0.1 mmol, 20 mol %). Fresh methoxyacetonitrile (300 μL, 4 mmol, 8 equiv), and 100 μL of the catalyst stock solution (0.8 mol % Pd) was then added and the vial was sealed under air using a threaded cap followed by Teflon tape. The resulting slurry was then allowed to stir vigorously (~1500 RPM) in an aluminum block reactor at 45 °C internal temperature (aluminum block set to heat to 50 °C) overnight. The contents of the vial were then extracted using methyl *t*-butyl ether (MTBE; 1.0 mL x 3). The combined organics were then dried onto SiO_2 and purified via column chromatography (20% EtOAc/hexanes) and the product was dried under high vacuum to result in a white solid (63.5 mg, 96% yield).

At this point, the aqueous phase had become too saturated with salts (see picture) and much of the water had been lost due to small scale extraction.

Figure 18: Aqueous phase after two recycling steps

6. Multistep, 1-pot chemoenzymatic sequence

6a. Procedure for multi-step, 1-pot chemoenzymatic sequence in water: synthesis of 21

To a 1-dram vial was added 4.5 mg of $Pd(OAc)_2$ and THF (500 μL). The mixture was then gently heated using a heat gun until a homogeneous solution had formed resulting in the catalyst stock solution.

To a 1-dram vial equipped with a Teflon coated stir bar was added 4-bromobenzamide (107 mg, 0.535 mmol, 1 equiv) and Oxone (33 mg, 0.11 mmol, 20 mol %). 2 wt % TPGS-750-M / H_2O (900 μL), methoxyacetonitrile (300 μL, 4.5 mmol, 8 equiv), and 100 μL of the catalyst stock solution was then added and the vial was sealed under air using a threaded cap followed by Teflon tape. The resulting slurry was allowed to react for 3 h at 45 °C internal temperature where the reaction was deemed complete by TLC and the mixture had become homogeneous. This mixture was then carried through to the next step without isolation or workup.

To the vial containing the dehydration product mixture was added 4-acetylphenylboronic acid (123 mg, 0.75 mmol, 1.4 equiv) and $K_3PO_4 \cdot H_2O$ (233 mg, 1.0 mmol, 1.87 equiv). The

vial was sealed using a rubber septum and the headspace of the vial was then purged with argon for 10 min with constant stirring. In a separate vial was added 1.6 mg of Pd[dtbpf]Cl_2 which was taken up in 200 μL of dry, degassed toluene. To the argon purged reaction vial was then added 100 μL of this catalyst stock solution (0.8 mg Pd[dtbpf]Cl_2, 1.23 x 10^{-3} mmol, 2300 ppm Pd). The contents of the vial were allowed to stir vigorously (~1500 RPM) overnight at 45 °C internal temperature until deemed complete by TLC. This mixture was then carried through to the next step without isolation or workup.

To a 20 mL scintillation vial equipped with a Teflon coated stir bar was added NAD^+ (6.5 mg), $NADP^+$ (6.0 mg), $MgSO_4$ (2 mg), and ADH-101 (50 mg). The solids were then taken up in 2 wt % TPGS-750-M in 0.23 M phosphate buffer in H_2O (5.0 mL)[2] and allowed to stir for 5 min. The contents of the previous reaction vial containing the Suzuki-Miyaura product were then transferred to the 20 mL scintillation vial and the previous vial washed with 4.0 mL of the 2 wt % TPGS-750-M phosphate buffer solution in H_2O. The vial was then heated in a 20 mL scintillation vial aluminum block heater set to 37.5 °C, and the contents were stirred at ~750 RPM. This reaction was allowed to run overnight until deemed complete by TLC analysis. The contents of the vial were then extracted using EtOAc (3 x 5 mL), dried onto SiO_2, and purified via column chromatography (45% EtOAc/55% hexanes) resulting in product as a white solid (114.5 mg, 96% yield, >99% ee).

6b. Procedure: racemic 21

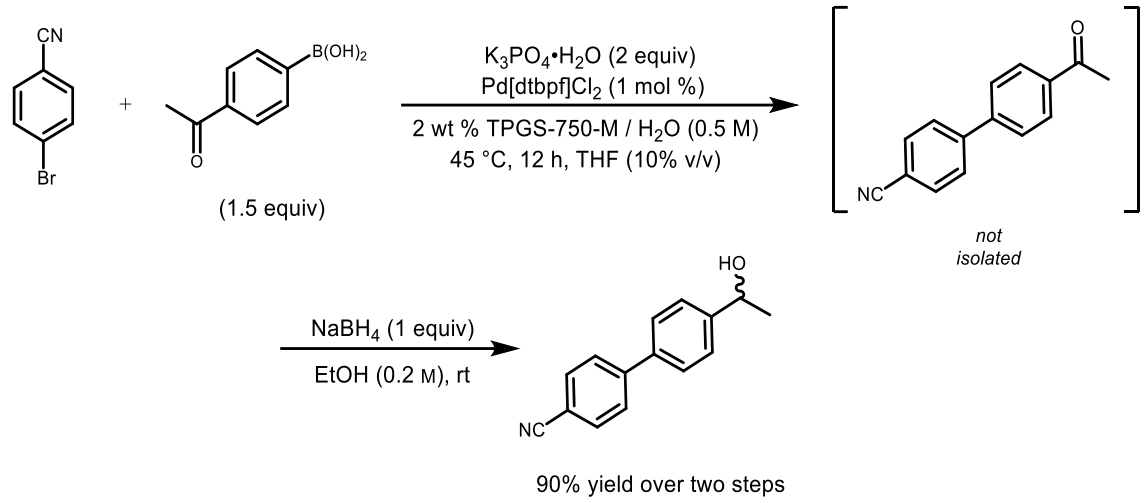

To a 1-dram vial equipped with a Teflon coated stir bar was added Pd[dtbpf]Cl_2 (3.2 mg, 0.005 mmol, 1 mol %), 4-bromobenzonitrile (91 mg, 0.5 mmol, 1.0 equiv), 4-acetylphenylboronic acid (123 mg, 0.75 mmol, 1.5 equiv), and $K_3PO_4 \cdot H_2O$ (233 mg, 1.0 mmol, 2.0 equiv). The headspace of the vial was then evacuated and backfilled with argon three times. 2 wt % TPGS-750-M / H_2O (900 μL) and degassed toluene (100 μL) were then added. The contents of the vial were then allowed to stir vigorously (~1500 RPM) in an aluminum block reactor at 45 °C internal temperature (aluminum block set to heat to 50 °C) overnight under argon pressure.

The aqueous phase was then extracted with EtOAc (3 x 1 mL). The combined organics were placed in a 10 mL round bottomed flask and evaporated. EtOH (2.5 mL) was then added followed by $NaBH_4$ (19 mg, 0.5 mmol, 1.0 equiv). This mixture was allowed to react at rt for 2 h until deemed complete by TLC analysis. The solvent was removed under vacuum and the crude organics were dried onto SiO_2 and purified via column chromatography (45% EtOAc/55% hexanes) to result in the racemic product as a white solid (99.7 mg, 90% yield).

6c. HPLC chromatographs for % ee determination of (*R*)-4'-(1-hydroxyethyl)-[1,1'-biphenyl]-4-carbonitrile (21)

HPLC: Chiracel AD-H, detected at 254 nm, eluent *n*-hexane/2-propanol = 90/10, flow rate = 1.0 mL/min, 25 °C.[3]

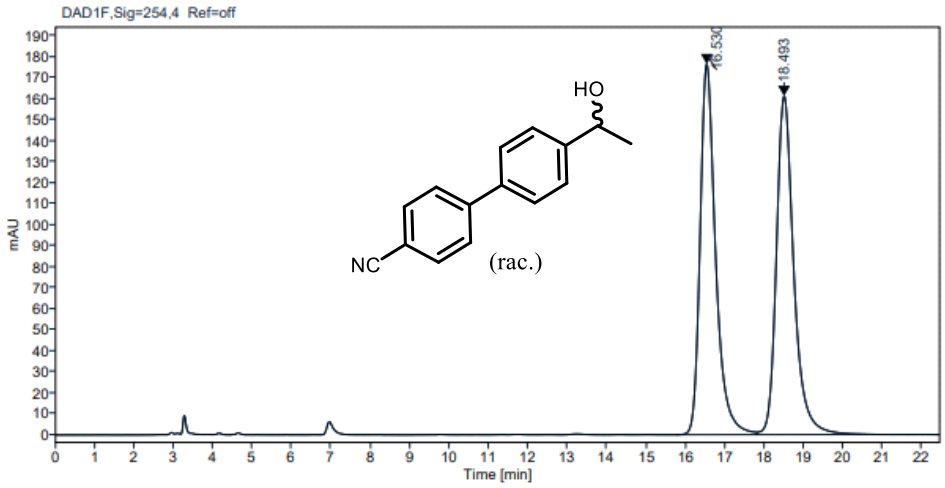

Signal:	DAD1F,Sig=254,4 Ref=off	
RT [min]	**Area**	**Area%**
16.530	4849.3089	49.6503
18.493	4917.6284	50.3497
Sum	9766.9374	

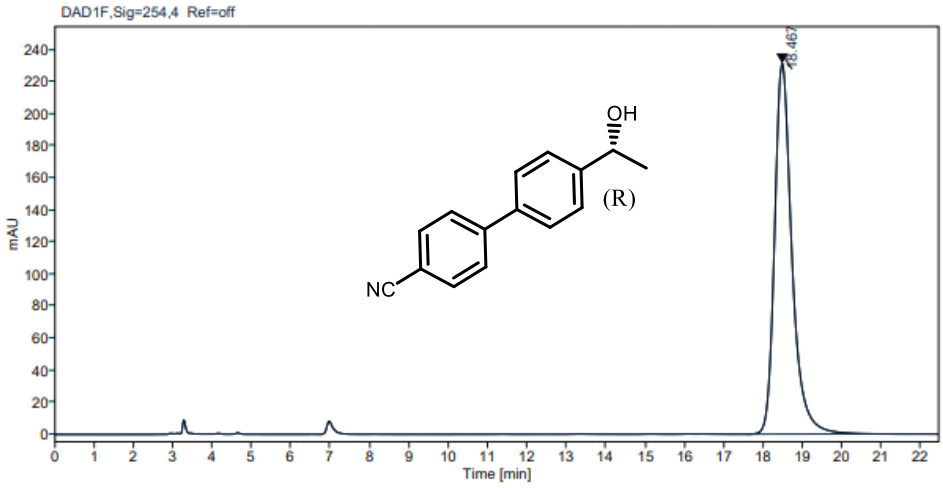

Signal:	DAD1F,Sig=254,4 Ref=off	
RT [min]	**Area**	**Area%**
18.467	7047.6374	100.0000
Sum	7047.6374	

7. ICP-MS data for residual palladium

ICP-MS data for residual Pd was obtained from University of California, Los Angeles ICP-MS Core Facility.

		Palladium		Source
		[µg/g]		
Sample #	Sample weight in analysis [mg]	Average*	stdev	
ABW.04.259	18.10	0.177	0.004	Second recycle product
ABW.04.263	14.50	3.592	0.030	Multi-step, final product

**Each sample was done in triplicated measurements with background correction.*
n/a represents below detection limit.

8. Analytical data

Synthesis of 4-methoxybenzonitrile (2)

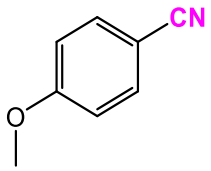

Compound **2** was obtained using the General Procedure A using methoxyacetonitrile on a 0.5 mmol scale. The crude product was purified by silica gel column chromatography (eluent: 20% EtOAc/80% hexanes) to provide the desired compound as a white solid (64.5 mg, 97% yield). R_f = 0.31 (1:4 EtOAc/hexanes).

^{1}H NMR (400 MHz, $CDCl_3$): δ 7.57 (d, *J* = 8.9 Hz, 2H), 6.94 (d, *J* = 8.9 Hz, 2H), 3.85 (s, 3H).

^{13}C NMR (101 MHz, $CDCl_3$): δ 162.8, 134.0, 119.2, 114.7, 103.9, 55.5.

Spectral data matched those previously reported.[4]

Synthesis of 3,5-dichlorobenzonitrile (3)

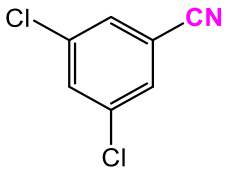

Compound **3** was obtained using the General Procedure A using methoxyacetonitrile on a 0.5 mmol scale. The crude product was purified by silica gel column chromatography (eluent: 10% EtOAc/90% hexanes) to provide the desired compound as a white solid (80.1 mg, 93% yield).

^{1}H NMR (400 MHz, $CDCl_3$): δ 7.58 (t, *J* = 1.8 Hz, 1H), 7.53 (d, *J* = 1.8 Hz, 2H).

^{13}C NMR (101 MHz, $CDCl_3$): δ 136.3, 133.5, 130.4, 116.3, 115.1.

Spectral data matched those previously reported.[5]

Synthesis of 2-(naphthalen-1-yl)acetonitrile (4)

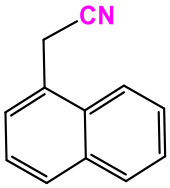

Compound **4** was obtained using the General Procedure A using methoxyacetonitrile on a 0.5 mmol scale. The crude product was purified by silica gel column chromatography (eluent: 20% EtOAc/80% hexanes) to provide the desired compound as a yellow oil (76.0 mg, 94% yield). R_f = 0.29 (1:4 EtOAc/hexanes).

^{1}H NMR (400 MHz, $CDCl_3$): δ 7.95 – 7.90 (m, 1H), 7.86 (d, *J* = 8.0 Hz, 2H), 7.65 – 7.53 (m, 3H), 7.51 – 7.44 (m, 1H), 4.11 (s, 2H).

^{13}C NMR (101 MHz, $CDCl_3$): δ 133.8, 130.8, 129.2, 129.1, 127.2, 126.5, 126.5, 125.8, 125.6, 122.5, 117.8, 21.8.

Spectral data matched those previously reported.[6]

Synthesis of cinnamonitrile (5)

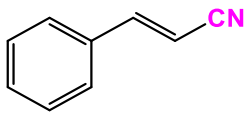

Compound **5** was obtained using the General Procedure A using fluoroacetonitrile on a 0.5 mmol scale, in this case only requiring 0.2 mol % (2000 ppm) $Pd(OAc)_2$. The crude product was purified by silica gel column chromatography (eluent: 20% EtOAc/80% hexanes) to provide the desired compound as a yellow oil (62.7 mg, 98% yield). R_f = 0.86 (2:3 EtOAc/hexanes).

^{1}H NMR (400 MHz, $CDCl_3$): δ 7.48 – 7.34 (m, 6H), 5.88 (d, *J* = 16.6 Hz, 1H).

^{13}C NMR (101 MHz, $CDCl_3$): δ 150.6, 133.5, 131.2, 129.1, 127.4, 118.2, 96.3.

Spectral data matched those previously reported.[7]

Synthesis of 4-bromobenzonitrile (6)

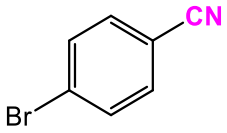

Compound **6** was obtained using the General Procedure A using methoxyacetonitrile on a 0.5 mmol scale. The crude product was purified by silica gel column chromatography (eluent: 20% EtOAc/80% hexanes) to provide the desired compound as a white solid (85.1 mg, 94% yield). R_f = 0.59 (1:4 EtOAc/hexanes).

^{1}H NMR (500 MHz, $CDCl_3$): δ 7.63 (d, *J* = 8.5 Hz, 2H), 7.52 (d, *J* = 8.5 Hz, 2H).

^{13}C NMR (126 MHz, $CDCl_3$): δ 133.5, 132.7, 128.1, 118.1, 111.4.

Spectral data matched those previously reported.[4]

Synthesis of 2-fluoro-4-methoxybenzonitrile (7)

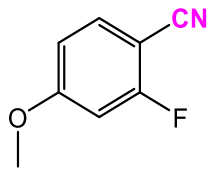

Compound **7** was obtained using the General Procedure A using methoxyacetonitrile on a 0.5 mmol scale. The crude product was purified by silica gel column chromatography (eluent: 50% EtOAc/50% hexanes) to provide the desired compound as a yellow solid (72.7 mg, 96% yield). R_f = 0.52 (1:1 EtOAc/hexanes).

^{1}H NMR (400 MHz, $CDCl_3$): δ 7.51 (dd, *J* = 8.7, 7.4 Hz, 1H), 6.76 (dd, *J* = 8.8, 2.5 Hz, 1H), 6.70 (dd, *J* = 11.0, 2.4 Hz, 1H), 3.86 (s, 3H).

^{13}C NMR (101 MHz, $CDCl_3$): δ 165.9, 164.8, 164.7, 163.3, 134.2 (d, *J* = 2.3 Hz), 114.4, 111.3 (d, *J* = 2.7 Hz), 102.3 (d, *J* = 22.9 Hz), 93.0 (d, *J* = 15.6 Hz), 56.0.

Spectral data matched those previously reported.[8]

Synthesis of 4-fluorobenzonitrile (8)

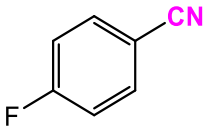

Compound **8** was obtained using the General Procedure A using methoxyacetonitrile on a 2.5 mmol scale. The crude product was purified by silica gel column chromatography (eluent: 15% Et_2O/85% hexanes) to provide the desired compound as white crystals (198 mg, 66% yield) which sublimate on high vacuum. R_f = 0.34 (1:9 EtOAc/hexanes).

^{1}H NMR (400 MHz, $CDCl_3$): δ 7.71 – 7.62 (m, 2H), 7.21 – 7.12 (m, 2H).

^{13}C NMR (101 MHz, $CDCl_3$): δ 165.1 (d, *J* = 256.7 Hz), 134.7 (d, *J* = 9.5 Hz), 118.1, 116.9 (d, *J* = 22.5 Hz), 108.6 (d, *J* = 3.4 Hz).

^{19}F NMR (376 MHz, $CDCl_3$): δ -102.5.

Spectral data matched those previously reported.[9]

Synthesis of 2-(trifluoromethyl)benzonitrile (9)

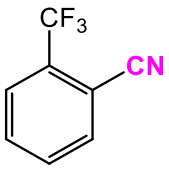

Compound **9** was obtained using the General Procedure A using methoxyacetonitrile on a 2.5 mmol scale. The crude product was purified by silica gel column chromatography (eluent: 25 Et_2O/75 hexanes) to provide the desired compound as a yellow oil (301.2 mg, 71% yield). R_f = 0.34 (1:4 EtOAc/hexanes).

^{1}H NMR (400 MHz, $CDCl_3$): δ 7.84 (d, *J* = 7.4 Hz, 1H), 7.82 – 7.73 (m, 2H), 7.70 (td, *J* = 7.4, 1.9 Hz, 1H).

^{13}C NMR (101 MHz, $CDCl_3$): δ 134.7, 133.0, 132.6 (q, *J* = 32.8 Hz), 132.4, 126.7 (q, *J* = 4.8 Hz), 126.5 – 118.1 (m), 115.5, 110.0 (q, *J* = 2.3 Hz).

^{19}F NMR (376 MHz, $CDCl_3$): δ -62.1.

Spectral data matched those previously reported.[10]

Synthesis of 2-chloronicotinonitrile (10)

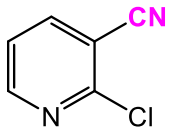

Compound **10** was obtained using the General Procedure B using fluoroacetonitrile on a 0.5 mmol scale. The crude product was purified by silica gel column chromatography (eluent: 50% Et_2O/50% pentanes) to provide the desired compound as a white solid (53.5 mg, 77% yield). R_f = 0.52 (1:1 EtOAc/hexanes).

^{1}H NMR (500 MHz, $CDCl_3$): δ 8.60 (dd, *J* = 4.9, 1.9 Hz, 1H), 8.01 (dd, *J* = 7.7, 2.0 Hz, 1H), 7.40 (dd, *J* = 7.7, 4.9 Hz, 1H).

^{13}C NMR (126 MHz, $CDCl_3$): δ 152.9, 152.8, 142.6, 122.2, 114.6, 110.9.

Spectral data matched those previously reported.[11]

Synthesis of 4-((2,5-dichloropyrimidin-4-yl)oxy)benzonitrile (11)

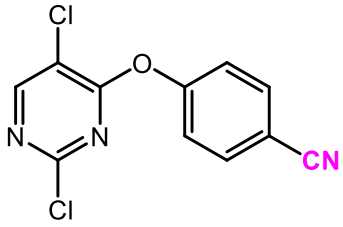

Compound **11** was obtained using the General Procedure B using fluoroacetonitrile on a 0.5 mmol scale with 10 v/v% DMSO. The crude product was purified by silica gel column chromatography (eluent: 20% EtOAc/80% hexanes) to provide the desired compound as a white solid (70.3 mg, 53% yield). R_f = 0.35 (1:4 EtOAc/hexanes).

^{1}H NMR (500 MHz, $CDCl_3$): δ 8.52 (s, 1H), 7.76 (d, *J* = 8.8 Hz, 2H), 7.34 (d, *J* = 8.7 Hz, 2H).

^{13}C NMR (126 MHz, $CDCl_3$): δ 164.3, 158.9, 157.4, 154.6, 134.1, 122.6, 118.0, 117.1, 110.5.

HRMS (CI): *m/z* calcd for $C_{11}H_5Cl_2N_3O^+$: 264.9810 $[M]^+$; found 264.9801.

Synthesis of 4-cyanophenyl 4-methylbenzenesulfonate (12)

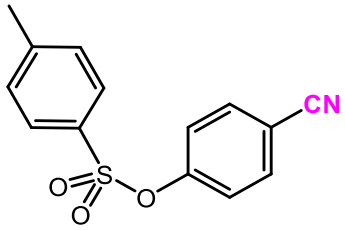

Compound **12** was obtained using the General Procedure A using methoxyacetonitrile on a 0.5 mmol scale. The crude product was purified by silica gel column chromatography (eluent: 20% EtOAc/80% hexanes) to provide the desired compound as a white solid (132.9 mg, 97% yield). R_f = 0.27 (1:4 EtOAc/hexanes).

^{1}H NMR (500 MHz, $CDCl_3$): δ 7.72 – 7.67 (m, 2H), 7.64 – 7.55 (m, 2H), 7.32 (d, *J* = 8.4 Hz, 2H), 7.14 – 7.08 (m, 2H), 2.44 (s, 3H).

^{13}C NMR (126 MHz, $CDCl_3$): δ 152.6, 146.2, 133.9, 131.8, 130.1, 128.4, 123.4, 117.8, 111.2, 21.8.

Spectral data matched those previously reported.[12]

Synthesis of 2-(4-isobutylphenyl)propanenitrile (13)

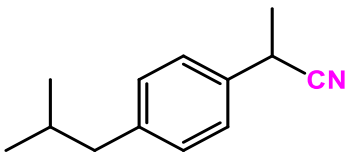

Compound **13** was obtained using the General Procedure A using methoxyacetonitrile on a 0.5 mmol scale. The crude product was purified by silica gel column chromatography (eluent: 5% EtOAc/95% hexanes) to provide the desired compound as a light-yellow oil (72.2 mg, 77% yield). R_f = 0.36 (5:95 EtOAc/hexanes).

^{1}H NMR (400 MHz, $CDCl_3$): δ 7.26 (d, J = 8.2 Hz, 2H), 7.16 (d, J = 8.2 Hz, 2H), 3.87 (q, J = 7.3 Hz, 1H), 2.47 (d, J = 7.2 Hz, 2H), 1.86 (m, 1H), 1.63 (d, J = 7.3 Hz, 3H), 0.90 (d, J = 6.6 Hz, 6H).

^{13}C NMR (101 MHz, $CDCl_3$): δ 141.8, 134.5, 130.0, 126.6, 122.0, 45.2, 31.1, 30.4, 22.5, 21.6.

Spectral data matched those previously reported.[13]

Synthesis of (S)-2-(6-methoxynaphthalen-2-yl)propanenitrile (14)

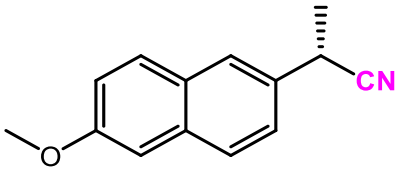

Compound **14** was obtained using the General Procedure A using methoxyacetonitrile on a 0.5 mmol scale. The crude product was purified by silica gel column chromatography (eluent: 20% EtOAc/80% hexanes) to provide the desired compound as a white solid (104.3 mg, 99% yield) with >99% ee. R_f = 0.66 (1:1 EtOAc/hexanes).

^{1}H NMR (400 MHz, $CDCl_3$): δ 7.81 – 7.67 (m, 3H), 7.39 (dd, *J* = 8.4, 2.1 Hz, 1H), 7.19 (dd, *J* = 8.9, 2.5 Hz, 1H), 7.14 (d, *J* = 2.6 Hz, 1H), 4.02 (q, *J* = 7.2 Hz, 1H), 3.92 (s, 3H), 1.71 (d, *J* = 7.3 Hz, 3H).

^{13}C NMR (101 MHz, $CDCl_3$): δ 158.1, 134.0, 132.0, 129.3, 128.8, 127.9, 125.4, 124.9, 121.8, 119.6, 105.6, 55.3, 31.2, 21.4.

Spectral data matched those previously reported.[14]

Enantiopure (>99% ee) starting material was used, and the enantiomeric excess of the product was obtained with respect to a racemic standard (Chiralcel OJ-H column, 4.6 x 250 mm, 5-micron, hexane/isopropanol 95:5, 1.0 mL/min flow rate, 230 nm detection).

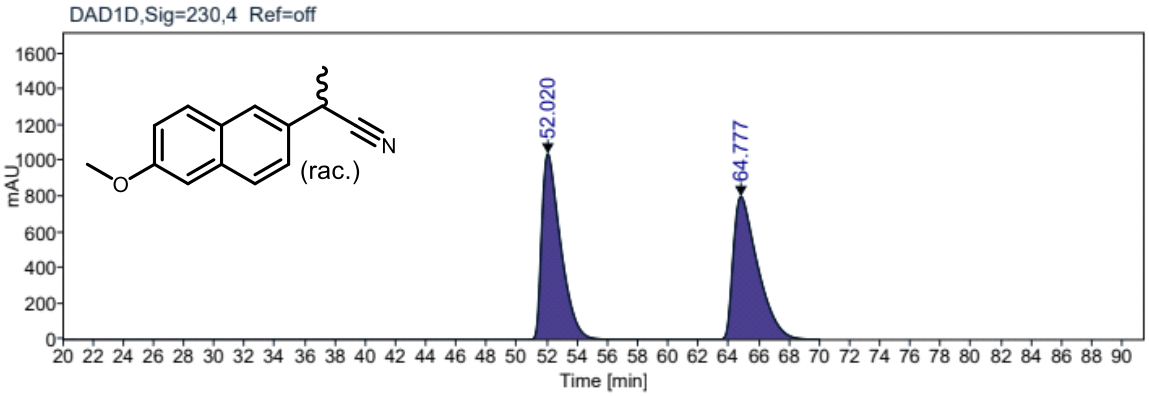

Signal: DAD1D,Sig=230,4 Ref=off

RT [min]	Area	Area%
3.174	57.6642	0.0
3.982	22.1529	0.0
7.624	245.2120	0.1
52.020	89651.9304	49.9
64.777	89785.6813	49.9
Sum	179762.6408	

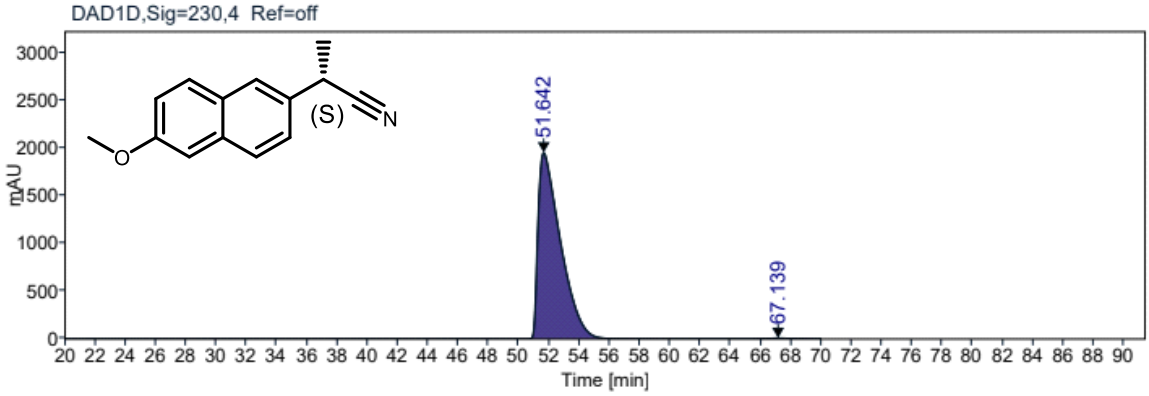

Signal: DAD1D,Sig=230,4 Ref=off

RT [min]	Area	Area%
3.172	82.8626	0.0
3.983	17.9895	0.0
7.638	233.5197	0.1
51.642	200958.9668	99.3
67.139	1076.1807	0.5
Sum	202369.5194	

Synthesis of 4-chloro-7-methoxyquinoline-6-carbonitrile (15)

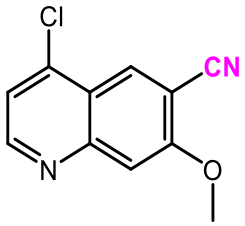

Compound **15** was obtained using the General Procedure B using fluoroacetonitrile on a 0.25 mmol scale with 20 v/v % DMSO. The crude product was purified by silica gel column chromatography (eluent: 70% EtOAc/30% hexanes) to provide the desired compound as a light-yellow solid (47.6 mg, 87% yield). R_f = 0.47 (7:3 EtOAc/hexanes).

^{1}H NMR (400 MHz, $CDCl_3$): δ 8.80 (d, *J* = 4.8 Hz, 1H), 8.53 (s, 1H), 7.51 (s, 1H), 7.44 (d, *J* = 4.8 Hz, 1H), 4.07 (s, 3H).

^{13}C NMR (101 MHz, $CDCl_3$): δ 160.1, 153.3, 151.9, 143.3, 132.5, 121.1, 120.8, 115.6, 108.9, 105.7, 56.8.

HRMS (CI): *m/z* calcd for $C_{11}H_7ClN_2O+H^+$: 219.0320 $[M+H]^+$: found 219.0325.

Synthesis of 2-((2,6-dinitro-4-(trifluoromethyl)phenyl)amino)acetonitrile (16)

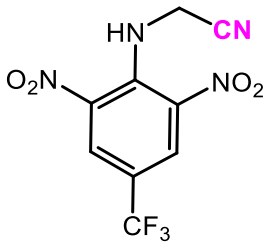

Compound **16** was obtained using the General Procedure B using fluoroacetonitrile on a 0.25 mmol scale with 20 v/v % DMSO. The crude product was purified by silica gel column

chromatography (eluent: 15% EtOAc/85% hexanes) to provide the desired compound as a yellow solid (30.6 mg, 42% yield). R_f = 0.28 (15:85 EtOAc/hexanes).

^{1}H NMR (400 MHz, $CDCl_3$): δ 8.86 (t, *J* = 5.9 Hz, 1H), 8.58 (s, 2H), 4.23 (d, *J* = 6.0 Hz, 2H).

^{13}C NMR (126 MHz, $CDCl_3$): δ 139.8, 138.7, 129.8 (q, *J* = 3.4 Hz), 122.2 (q, *J* = 272.7 Hz), 120.4 (q, *J* = 36.4 Hz), 113.8, 34.2.

^{19}F NMR (376 MHz, $CDCl_3$): δ -62.4.

HRMS (EI): *m/z* calcd for $C_9H_5F_3N_4O_4^+$: 290.0263 $[M]^+$; found 290.0251.

Synthesis of 4-((5-nitropyridin-2-yl)oxy)benzonitrile (17)

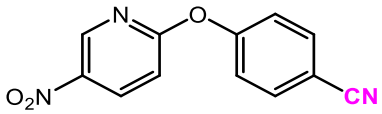

Compound **17** was obtained using the General Procedure A using methoxyacetonitrile on a 0.5 mmol scale with 10 v/v % DMSO. The crude product was purified by silica gel column chromatography (eluent: 20-70% EtOAc/hexanes gradient) to provide the desired compound as an off-white solid (120.0 mg, quant.). R_f = 0.29 (1:4 EtOAc/hexanes).

^{1}H NMR (500 MHz, $CDCl_3$): δ 9.02 (d, *J* = 2.9 Hz, 1H), 8.54 (dd, *J* = 9.0, 2.8 Hz, 1H), 7.79 – 7.72 (m, 2H), 7.34 – 7.27 (m, 2H), 7.15 (dd, *J* = 9.0, 0.6 Hz, 1H).

^{13}C NMR (126 MHz, $CDCl_3$): δ 165.6, 156.0, 144.7, 141.0, 135.4, 134.0, 122.6, 118.2, 112.1, 109.7.

HRMS (CI): *m/z* calcd for $C_{12}H_7N_3O_3^+$: 241.0487 $[M]^+$: found 241.0497.

Synthesis of 2-(1-(4-chlorobenzoyl)-5-methoxy-2-methyl-1H-indol-3-yl)acetonitrile (18)

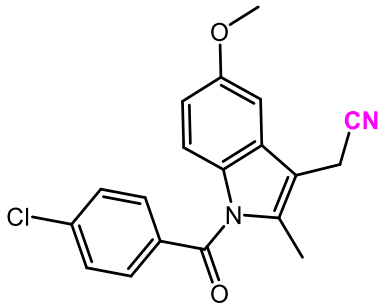

Compound **18** was obtained using the General Procedure A using methoxyacetonitrile on a 0.25 mmol scale with 20 v/v % DMSO. The crude product was purified by silica gel column chromatography (eluent: 40% EtOAc/60% hexanes with 0.5 % AcOH) to provide the desired compound as a white solid (72.8 mg, 86% yield). R_f = 0.59 (1:1 EtOAc/hexanes).

^{1}H NMR (400 MHz, $CDCl_3$): δ 7.66 (d, *J* = 8.2 Hz, 2H), 7.48 (d, *J* = 8.3 Hz, 2H), 6.98 (s, 1H), 6.83 (d, *J* = 9.1 Hz, 1H), 6.71 (d, *J* = 9.6 Hz, 1H), 3.85 (s, 3H), 3.73 (s, 2H), 2.42 (s, 3H).

^{13}C NMR (101 MHz, $CDCl_3$): δ 168.2, 156.3, 139.8, 136.0, 133.4, 131.4, 130.7, 129.3, 129.1, 117.1, 115.2, 112.5, 108.1, 100.5, 55.8, 13.2, 13.1.

Spectral data matched those previously reported.[14]

Synthesis of 4-cyanophenyl ((benzyloxy)carbonyl)-*L*-leucinate (19)

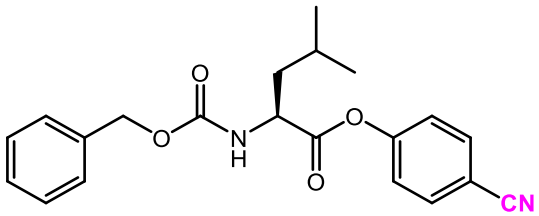

Compound **19** was obtained using the General Procedure A using methoxyacetonitrile on a 0.25 mmol scale. The crude product was purified by silica gel column chromatography

(eluent: 25% EtOAc/75% hexanes) to provide the desired compound as a white solid (91.4 mg, 99% yield). R_f = 0.21 (15:85 EtOAc/hexanes).

^{1}H NMR (400 MHz, $CDCl_3$): δ 7.69 (d, *J* = 8.6 Hz, 2H), 7.44 – 7.29 (m, 5H), 7.23 (d, *J* = 8.6 Hz, 2H), 5.15 (m, 3H), 4.60 (td, *J* = 8.9, 4.3 Hz, 1H), 1.81 (m, 2H), 1.70 (m, 1H), 1.01 (d, *J* = 6.2 Hz, 6H).

^{13}C NMR (101 MHz, $CDCl_3$): δ 171.3, 156.2, 153.9, 136.2, 133.9, 128.8, 128.5, 128.4, 122.8, 118.3, 110.3, 67.5, 53.0, 41.4, 25.1, 23.1, 22.0.

HRMS (ESI): *m/z* calcd for $C_{21}H_{22}N_2O_4$+Na^+: 389.1472 [*M*+Na]$^+$; found 389.1477.

Synthesis of 4-((3-chloroquinoxalin-2-yl)oxy)benzonitrile (20)

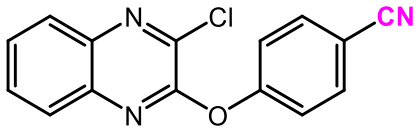

Compound **20** was obtained using General Procedure B using fluoroacetonitrile on a 0.25 mmol scale with 20 v/v % DMSO. The crude product was purified by silica gel column chromatography (eluent: 20% EtOAc/80% hexanes) to provide the desired compound as a white solid (20.7 mg, 29% yield). R_f = 0.45 (1:4 EtOAc/hexanes).

^{1}H NMR (500 MHz, $CDCl_3$): δ 8.04 – 7.98 (m, 1H), 7.82 – 7.77 (m, 2H), 7.77 – 7.73 (m, 1H), 7.73 – 7.66 (m, 2H), 7.48 – 7.42 (m, 2H).

^{13}C NMR (126 MHz, $CDCl_3$): δ 155.9, 151.8, 139.6, 138.9, 138.7, 133.9, 130.9, 129.0, 128.1, 127.3, 122.6, 118.3, 109.6.

HRMS (CI): *m/z* calcd for $C_{15}H_8ClN_3O^+$: 281.0356 [*M*]$^+$; found 281.0356.

Synthesis of (*R*)-4'-(1-hydroxyethyl)-[1,1'-biphenyl]-4-carbonitrile (21)

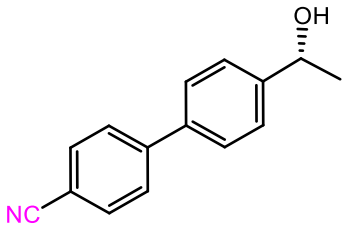

Compound **21** was prepared as outlined in the multi-step, 1-pot procedure outlined in **Section 4.4A.**

^{1}H NMR (500 MHz, $CDCl_3$): δ 7.71 (d, *J* = 8.6 Hz, 2H), 7.67 (d, *J* = 8.6 Hz, 2H), 7.58 (d, *J* = 8.4 Hz, 2H), 7.49 (d, *J* = 8.3 Hz, 2H), 4.97 (q, *J* = 6.5 Hz, 1H), 2.00 (s, 1H), 1.54 (d, *J* = 6.5 Hz, 3H).

^{13}C NMR (126 MHz, $CDCl_3$): δ 146.4, 145.3, 138.3, 132.6, 127.6, 127.4, 126.2, 118.9, 110.9, 70.0, 25.3.

Spectral data matched those previously reported.[15]

4-((2,5-dichloropyrimidin-4-yl)oxy)benzamide (22)

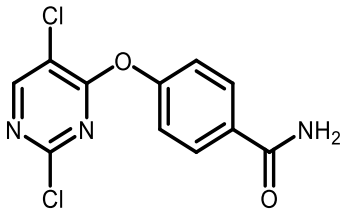

Compound **22** was prepared as in **Section 4.1**.

^{1}H NMR (600 MHz, DMSO-d_6): δ 8.83 (d, *J* = 3.3 Hz, 1H), 8.06 (s, 1H), 7.98 (d, *J* = 8.3 Hz, 2H), 7.44 (s, 1H), 7.39 (d, *J* = 8.5 Hz, 2H).

^{13}C NMR (101 MHz, DMSO-d_6): δ 167.0, 164.7, 159.3, 156.2, 153.6, 132.5, 129.4, 121.4, 116.8.

HRMS (ESI): *m/z* calcd for $C_{11}H_7Cl_2N_3O_2+H^+$: 283.9988 $[M+H]^+$: found 283.9994.

Synthesis of 4-((5-nitropyridin-2-yl)oxy)benzamide (23)

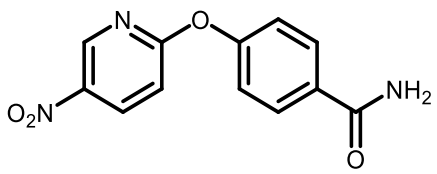

Compound **23** was prepared as in **Section 4.1**.

^{1}H NMR (500 MHz, DMSO-*d*$_6$): δ 9.02 (d, *J* = 2.9 Hz, 1H), 8.63 (dd, *J* = 9.1, 3.0 Hz, 1H), 8.00 (s, 1H), 7.95 (d, *J* = 8.7 Hz, 2H), 7.39 (s, 1H), 7.33 – 7.26 (m, 3H).

^{13}C NMR (126 MHz, DMSO-*d*$_6$): δ 167.6, 166.4, 155.4, 145.1, 141.2, 136.4, 132.2, 129.9, 121.8, 112.5.

HRMS (ESI): *m/z* calcd for $C_{12}H_9N_3O_4+H^+$: 260.0671 $[M+H]^+$: found 260.0676.

Synthesis of 4-carbamoylphenyl ((benzyloxy)carbonyl)-*L*-leucinate (24)

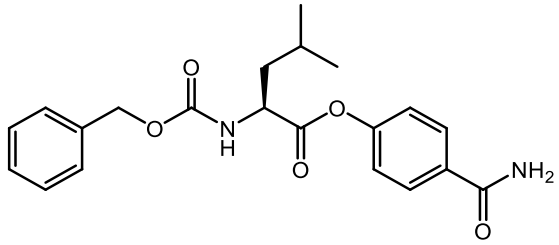

Compound **24** was prepared as in **Section 4.1**.

^{1}H NMR (400 MHz, CDCl$_3$): δ 7.84 (d, *J* = 8.7 Hz, 2H), 7.43 – 7.29 (m, 5H), 7.18 (d, *J* = 8.6 Hz, 2H), 6.02 (s, 1H), 5.88 (s, 1H), 5.22 (d, *J* = 8.7 Hz, 1H), 5.14 (s, 2H), 4.62 (td, *J* = 8.8, 4.6 Hz, 1H), 1.92 – 1.76 (m, 2H), 1.69 (m, 1H), 1.02 (m, 6H).

^{13}C NMR (101 MHz, CDCl$_3$): δ 171.8, 169.0, 156.3, 153.4, 136.3, 131.4, 129.2, 128.8, 128.5, 128.3, 121.8, 67.4, 53.0, 41.5, 25.1, 23.1, 22.0.

HRMS (ESI): *m/z* calcd for $C_{21}H_{24}N_2O_5$+Na^+: 407.1577 [*M*+Na]$^+$; found 407.1583.

Synthesis of 4-((3-chloroquinoxalin-2-yl)oxy)benzamide (25)

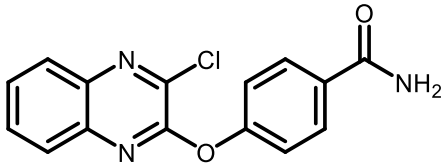

Compound **25** was prepared as in **Section 4.1**.

^{1}H NMR (500 MHz, DMSO-*d*6): δ 8.09 – 7.97 (m, 4H), 7.83 – 7.67 (m, 3H), 7.49 – 7.39 (m, 3H).

^{13}C NMR (126 MHz, DMSO-*d*6): δ 167.6, 155.2, 152.9, 139.3, 139.2, 139.0, 132.4, 131.5, 129.84, 129.2, 128.1, 127.4, 121.8.

HRMS (ESI): *m/z* calcd for $C_{15}H_{10}ClN_3O_2$+H^+: 300.0534 [*M*+H]$^+$; found 300.0540.

9. Experimental references

1. Lipshutz, B. H.; Ghorai, S.; Abela, A. R.; Moster, R.; Nishikata, T. Duplais, C.; Krasovskiy, A. *J. Org. Chem.*, **2011**, *76*, 4379–4391.
2. Akporji, N.; Singhania, V.; Dussart-Gautheret, J.; Gallou, F.; Lipshutz, B. H. *Chem. Commun.* **2021**, *57*, 11847–11850.
3. Shu, X.; Jin, R.; Zhao, Z.; Cheng, T.; Liu, G. *Chem. Commun.* **2018**, *54*, 13244–13247.
4. Nimnual, P.; Tummatorn, J.; Thongsornkleeb, C.; Ruchirawat, S. *J. Org. Chem.* **2015**, *80*, 8657–8667.
5. Liskey, C. W.; Liao, X.; Hartwig, J. F. *J. Am. Chem. Soc*. **2010**, *132*, 11389–11391.
6. Shang, R.; Ji, D.-S.; Chu, L.; Fu, Y.; Liu, L. *Angew. Chem., Int. Ed.* **2011**, *50*, 4470–4474.
7. Powell, K. J.; Han, L.-C.; Sharma, P.; Moses, J. E. *Org. Lett.* **2014**, *16*, 2158–2161.

8. Mills, L. R.; Edjoc, R. K.; Rousseaux, S. A. L. *J. Am. Chem. Soc.* **2021**, *143*, 10422–10428.

9. Xiao, J.; Guo, F.; Li, Y.; Li, F.; Li, Q.; Tang, Z.-L. *J. Org. Chem.* **2021**, *86*, 2028–2035.

10. Li, X.; Zhao, J.; Zhang, L.; Hu, M.; Wang, L.; Hu, J. *Org. Lett.* **2015**, *17*, 298–301.

11. Chen, Y.; Huang, J.; Hwang, T.-L.; Chen, M. J.; Tedrow, J. S.; Farrell, R. P.; Bio, M. M.; Cui, S. *Org. Lett.* **2015**, *17*, 2948–2951.

12. Kuroda, J.; Inamoto, K.; Hiroya, K.; Doi, T. *Eur. J. Org. Chem*. **2009**, *2009*, 2251–2261.

13. Frye, N. L.; Bhunia, A.; Studer, A. *Org. Lett*. **2020**, *22*, 4456-4460.

14. Liu, R. Y.; Bae, M.; Buchwald, S. L. *J. Am. Chem. Soc.* **2018**, *140*, 1627–1631.

15. Shu, X.; Jin, R.; Zhao, Z.; Cheng, T.; Liu, G. *Chem. Commun.* **2018**, *54*, 13244–13247.

3.7 Spectral data

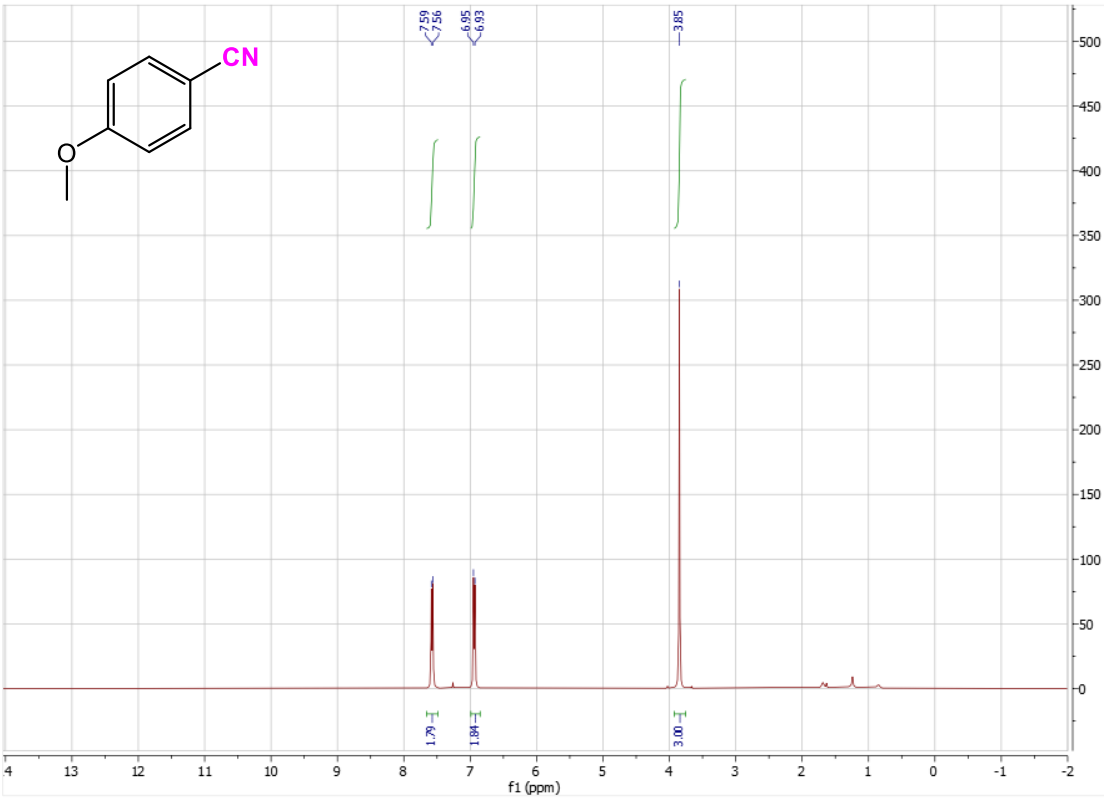

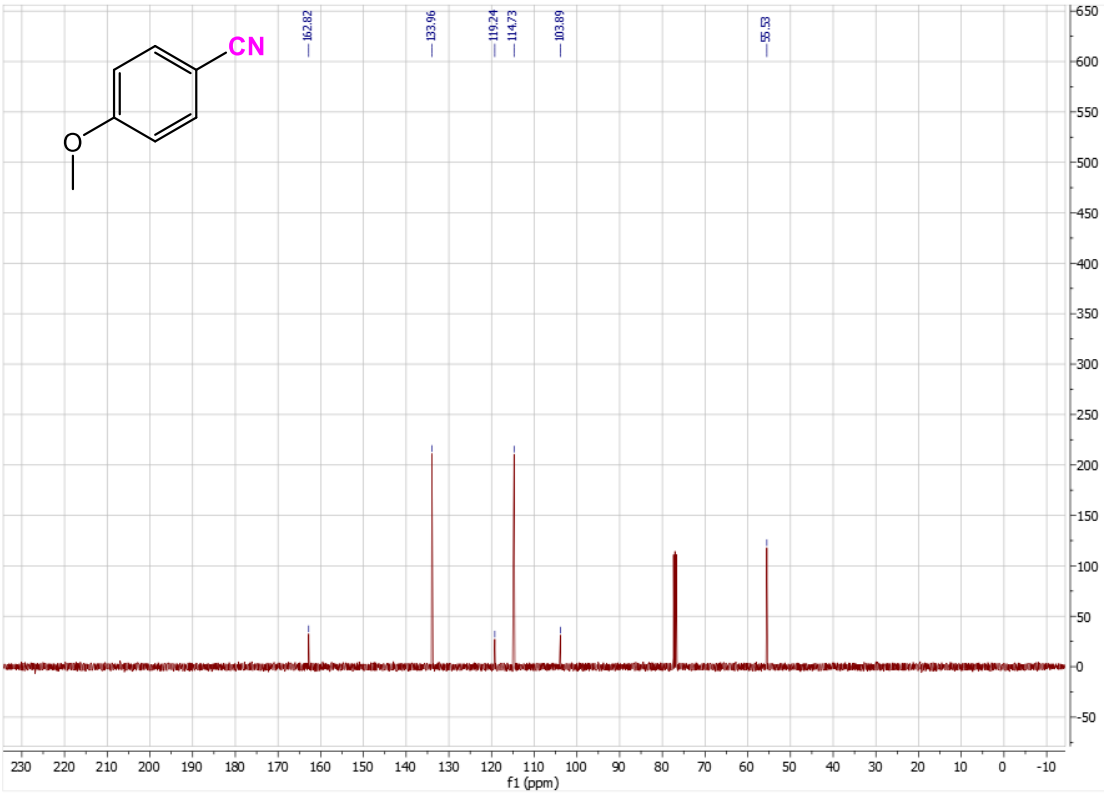

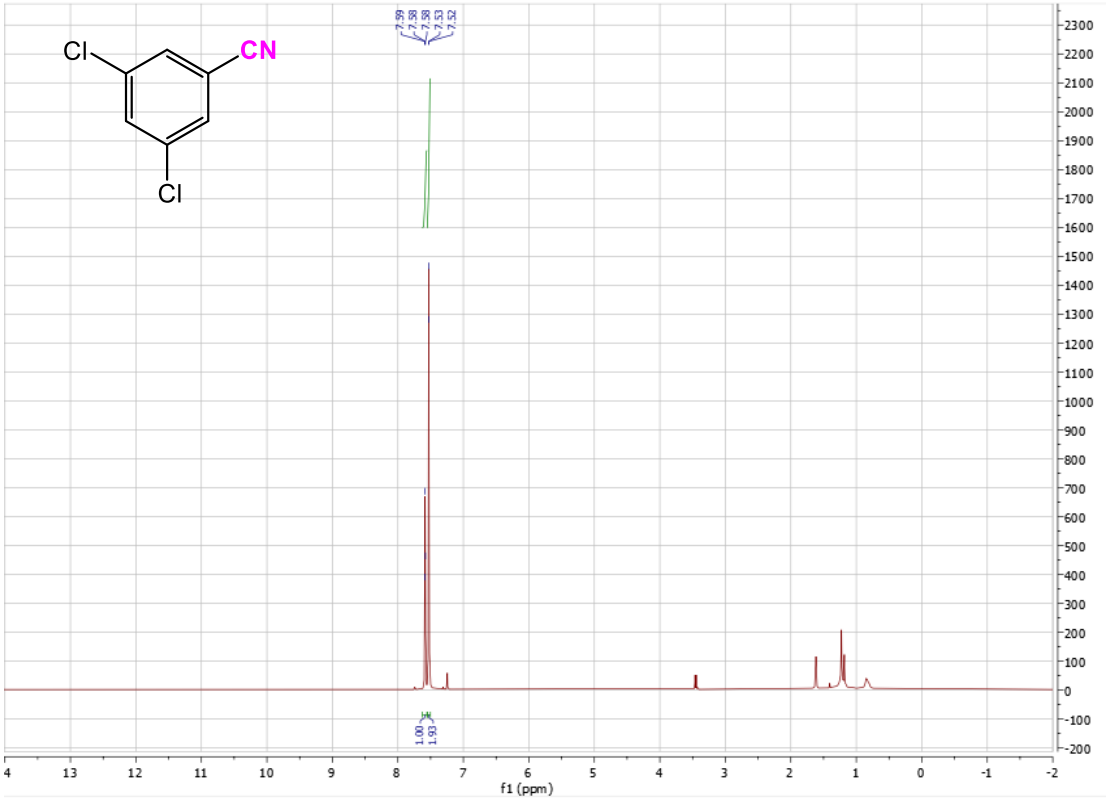
Cl
CN
Cl
7.59
7.58
7.58
7.53
7.52
1.00
1.93
f1 (ppm)

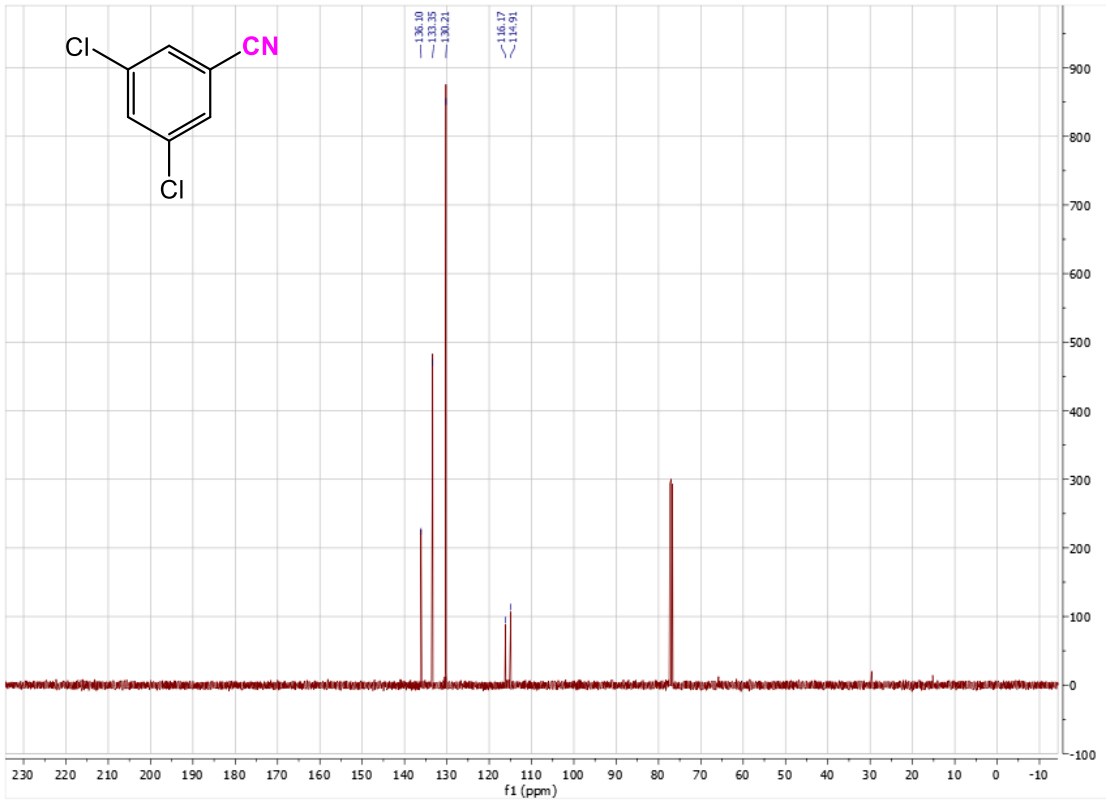
Cl
CN
Cl
136.10
133.35
130.21
116.17
114.91
f1 (ppm)

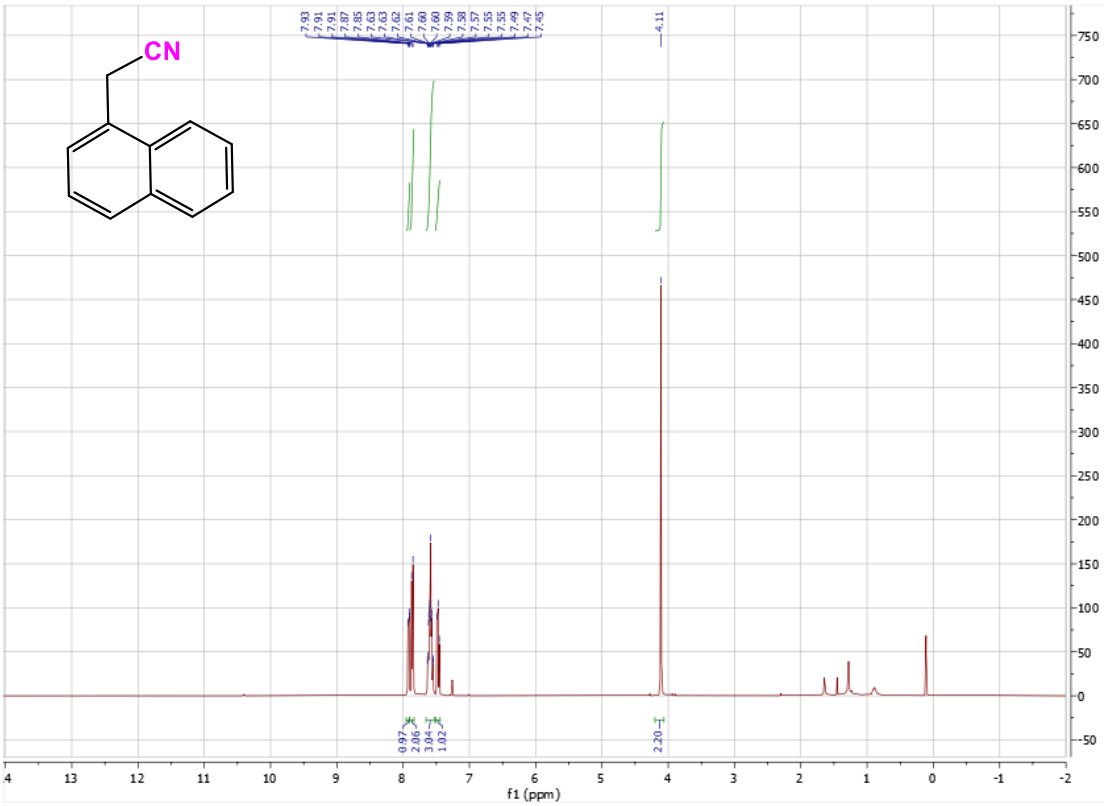
CN
7.93
7.91
7.91
7.87
7.85
7.63
7.63
7.62
7.61
7.60
7.60
7.59
7.58
7.57
7.55
7.55
7.49
7.47
7.45
4.11
0.97
2.06
3.04
1.02
2.20
f1 (ppm)

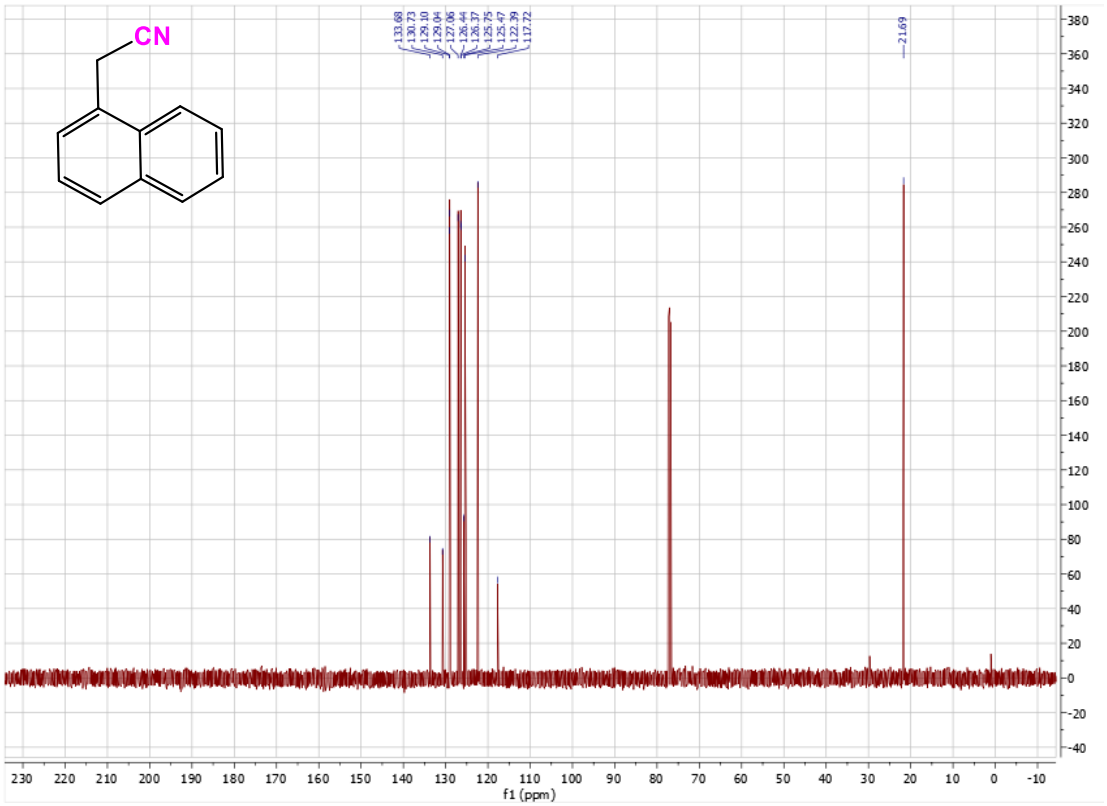
CN
133.68
130.23
129.10
129.04
127.06
126.44
126.37
125.75
125.47
122.39
117.72
21.69
f1 (ppm)

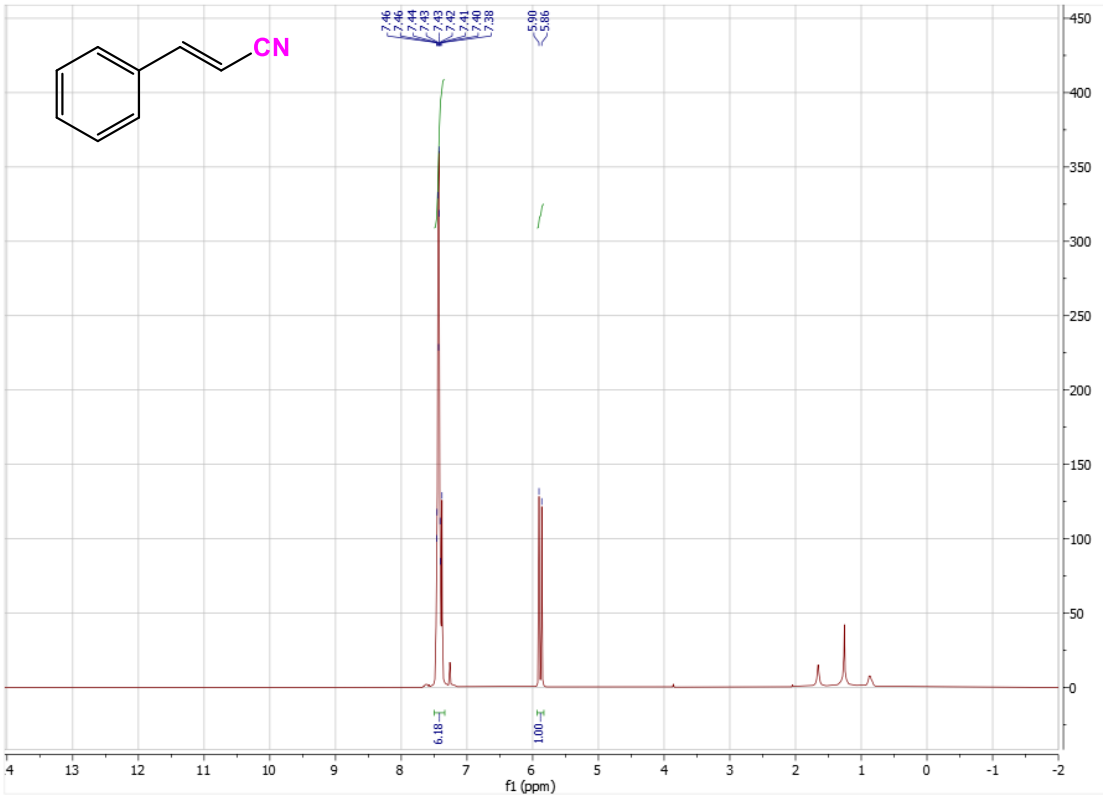
CN
7.46
7.46
7.44
7.43
7.43
7.42
7.41
7.40
7.38
5.90
5.86
6.18
1.00
f1 (ppm)

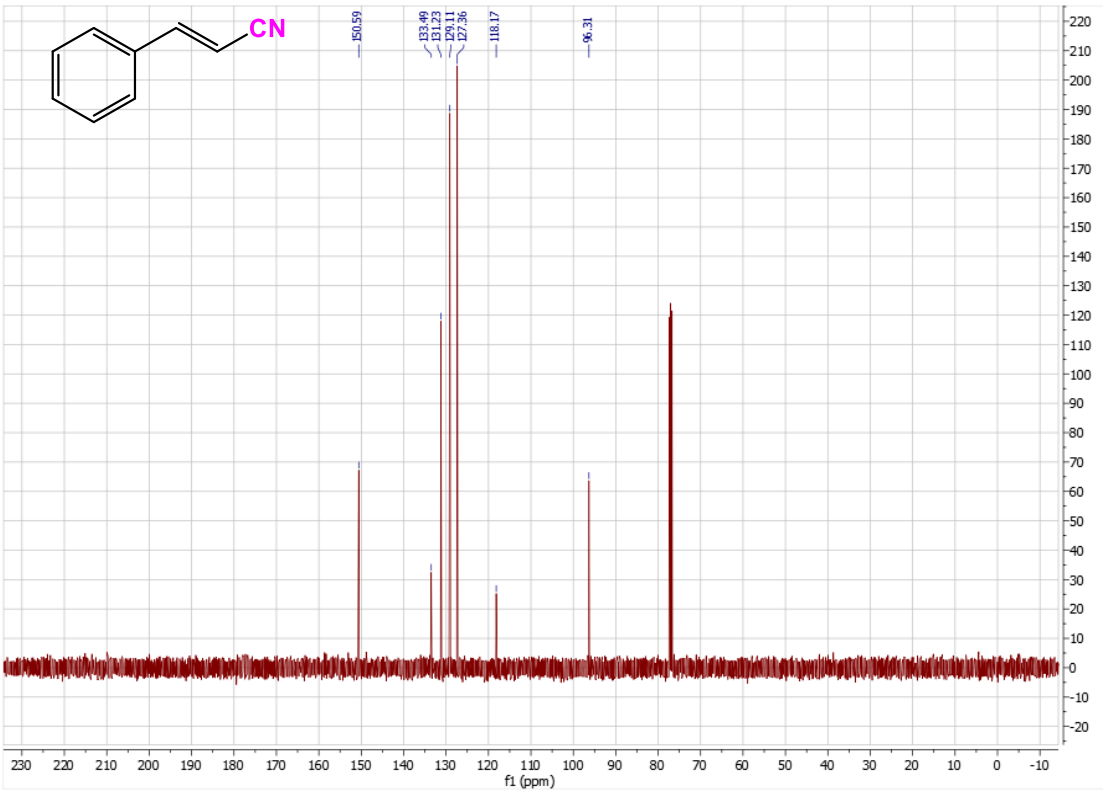
CN
150.59
133.49
131.23
129.11
127.36
118.17
96.31
f1 (ppm)

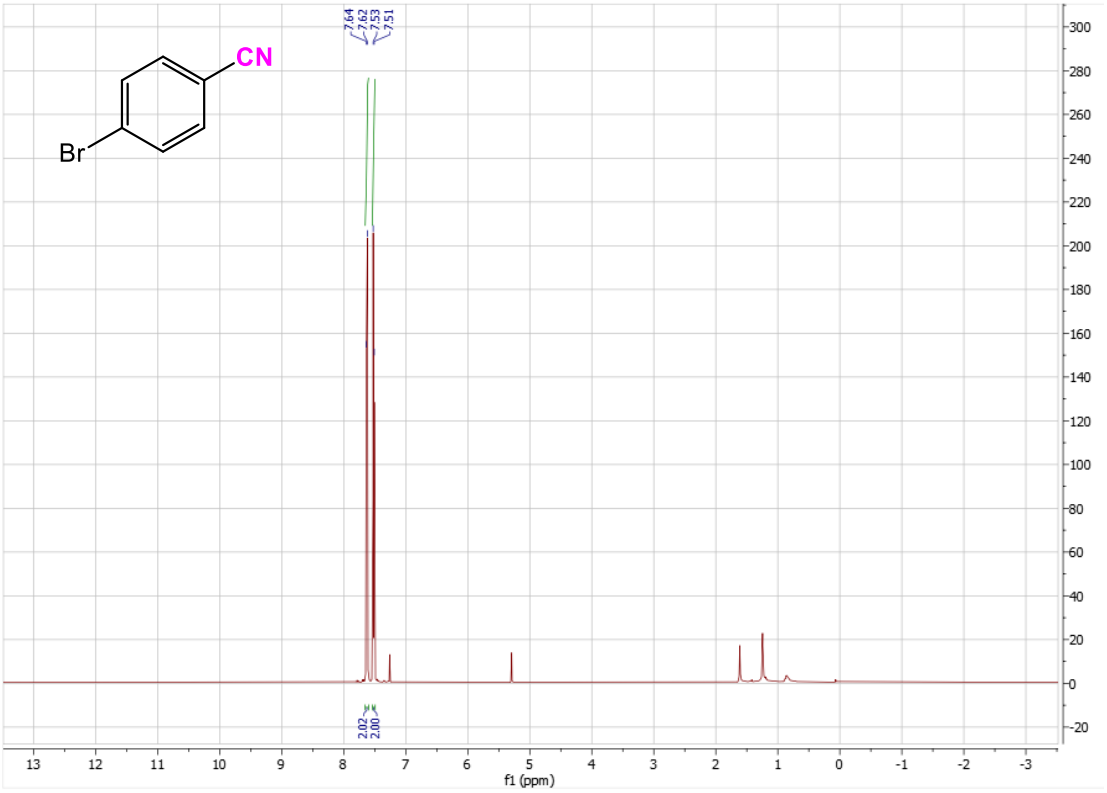
CN
Br
7.64
7.62
7.53
7.51
2.02
2.00
f1 (ppm)

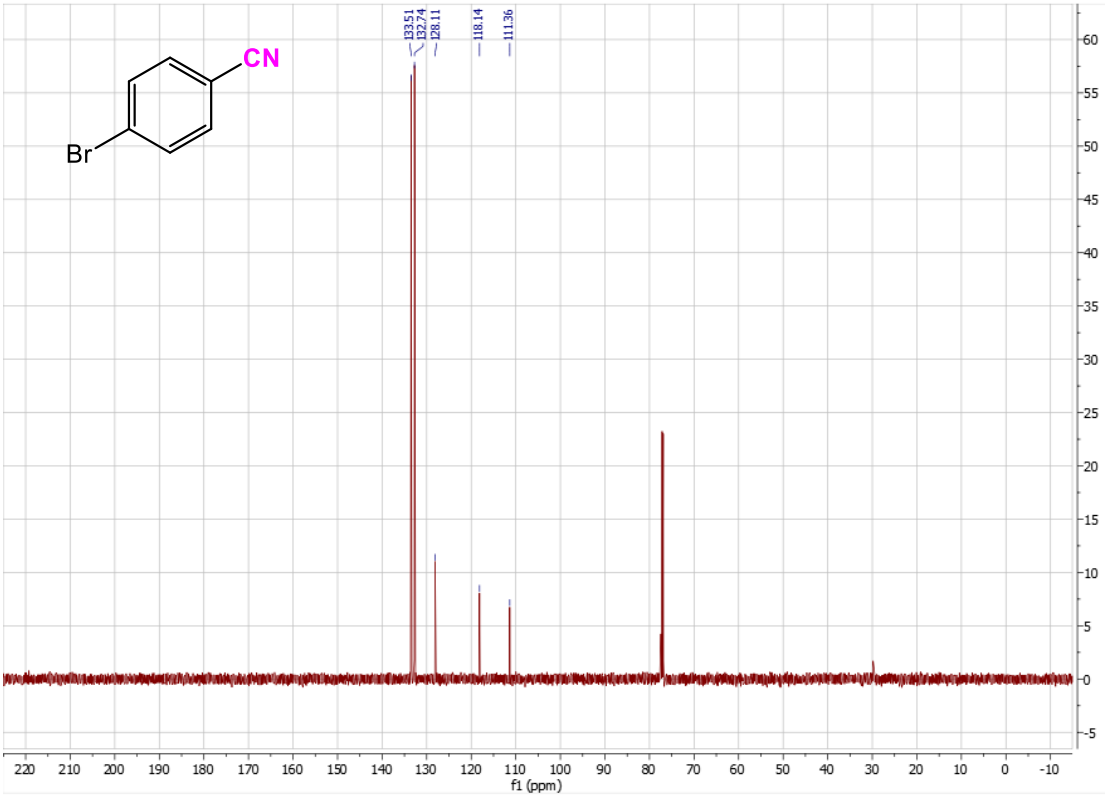
CN
Br
133.51
132.74
128.11
118.14
111.36
f1 (ppm)

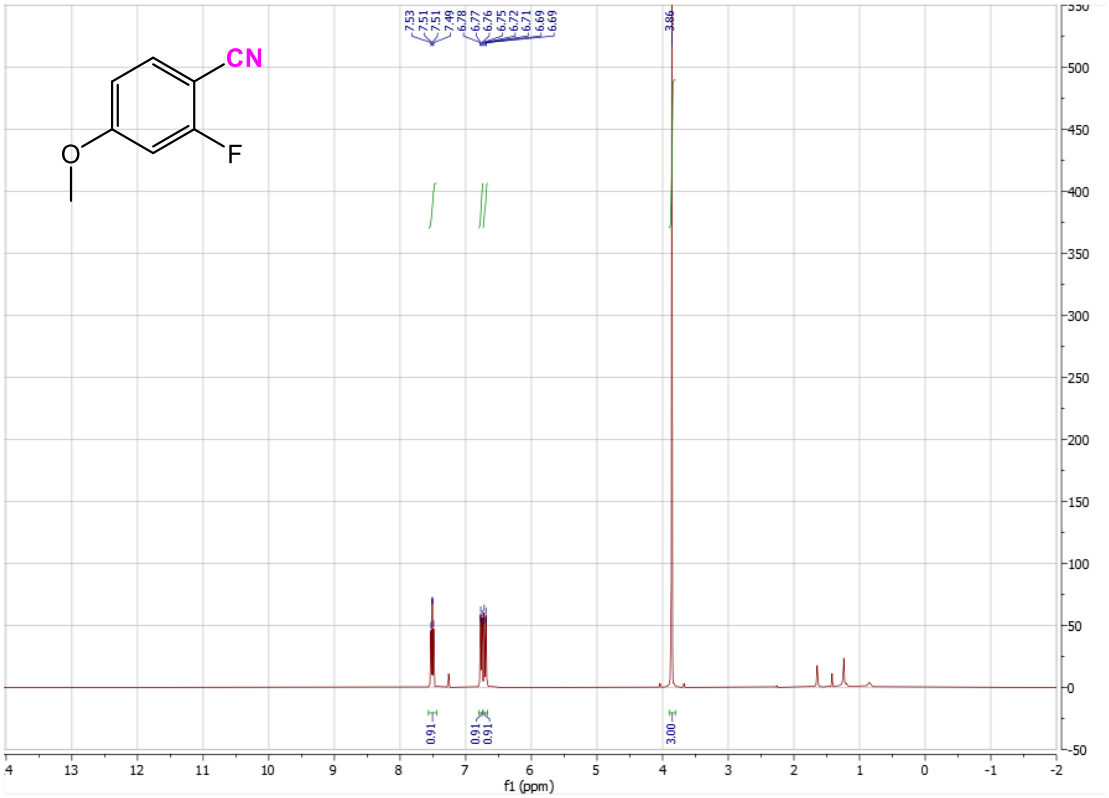
CN
O
F
7.53
7.51
7.51
7.49
6.78
6.77
6.76
6.75
6.72
6.71
6.69
6.69
3.86
0.91
0.91
0.91
3.00
f1 (ppm)

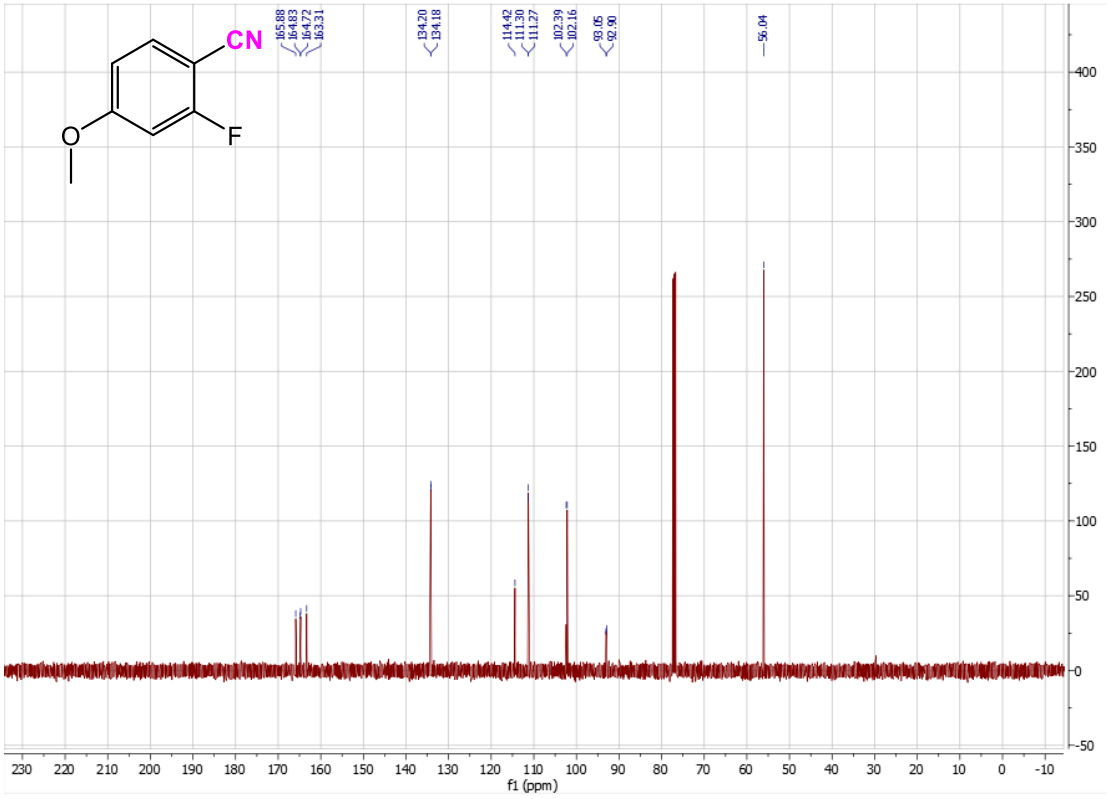
CN
O
F
165.88
164.83
164.72
163.31
134.20
134.18
114.42
111.30
111.27
102.39
102.16
93.05
92.90
56.04
f1 (ppm)

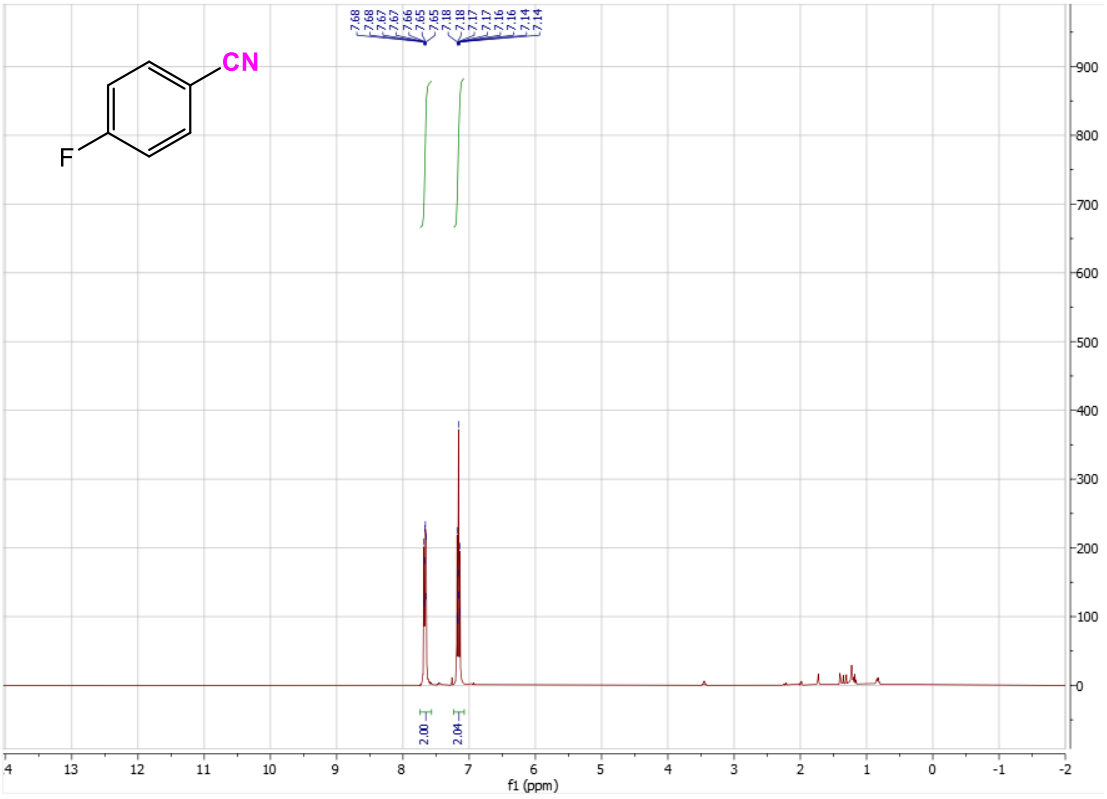
CN
F
7.68
7.68
7.67
7.67
7.66
7.65
7.65
7.18
7.18
7.17
7.17
7.16
7.16
7.14
7.14
2.00
2.04
f1 (ppm)

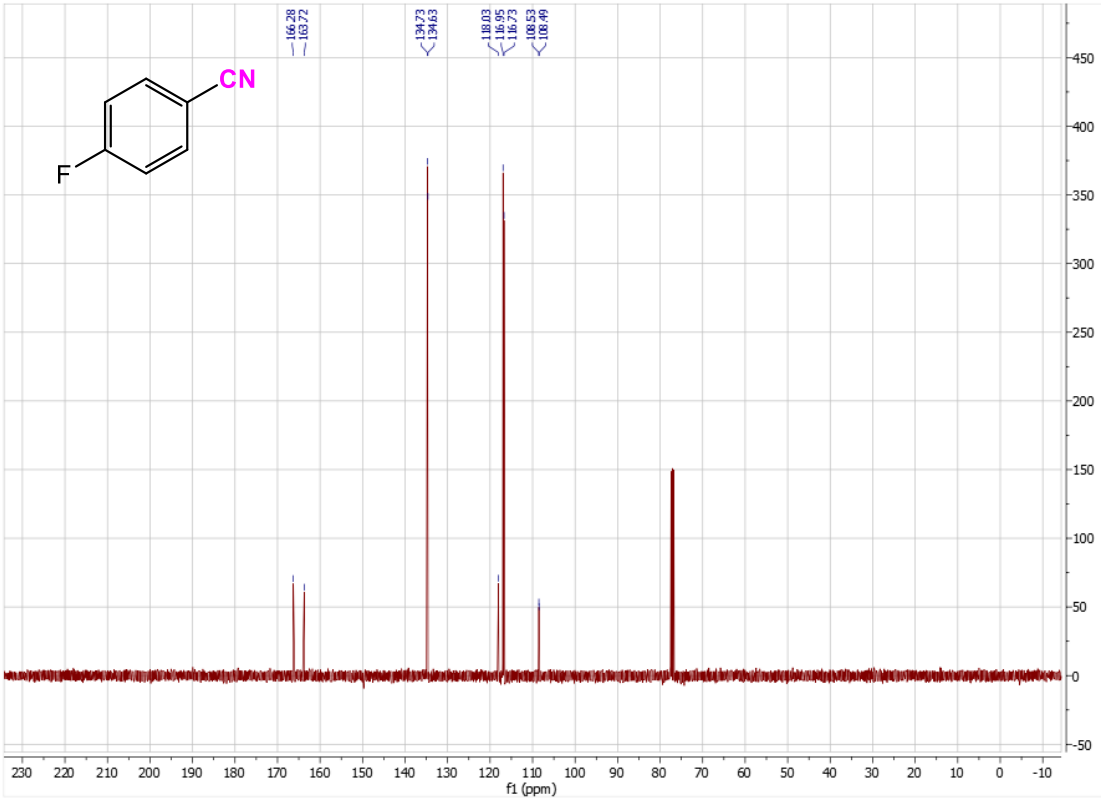
CN
F
166.28
163.72
134.73
134.63
118.03
116.95
116.73
108.53
108.49
f1 (ppm)

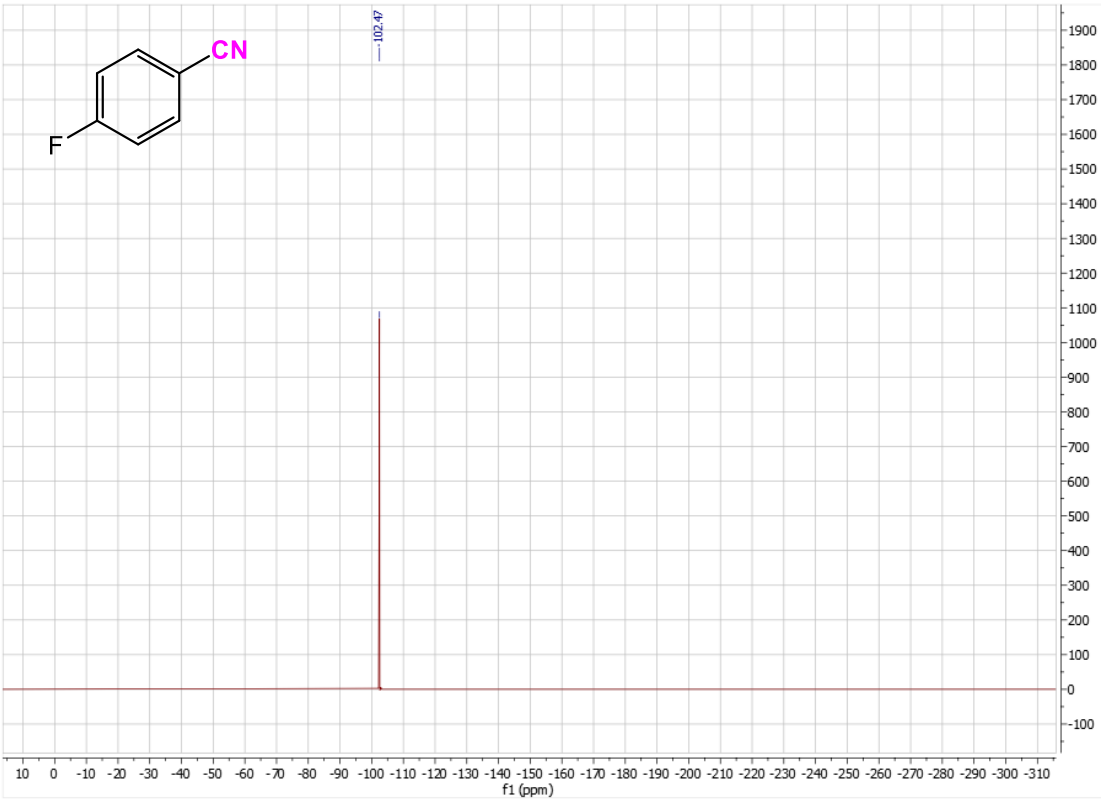
CN
F
102.47
1900
1800
1700
1600
1500
1400
1300
1200
1100
1000
900
800
700
600
500
400
300
200
100
0
-100
10 0 -10 -20 -30 -40 -50 -60 -70 -80 -90 -100 -110 -120 -130 -140 -150 -160 -170 -180 -190 -200 -210 -220 -230 -240 -250 -260 -270 -280 -290 -300 -310
f1 (ppm)

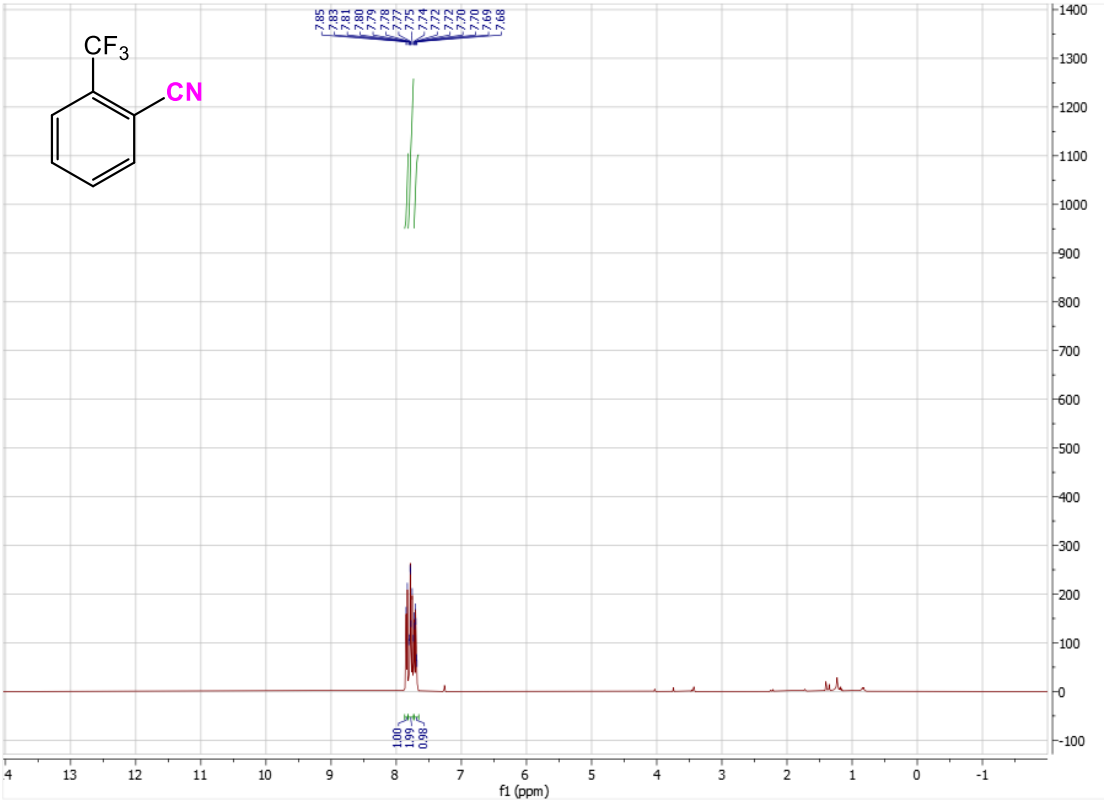
CF3
CN
7.85
7.83
7.81
7.80
7.79
7.79
7.77
7.75
7.74
7.72
7.72
7.70
7.70
7.69
7.68
1.00
1.99
0.98
f1 (ppm)

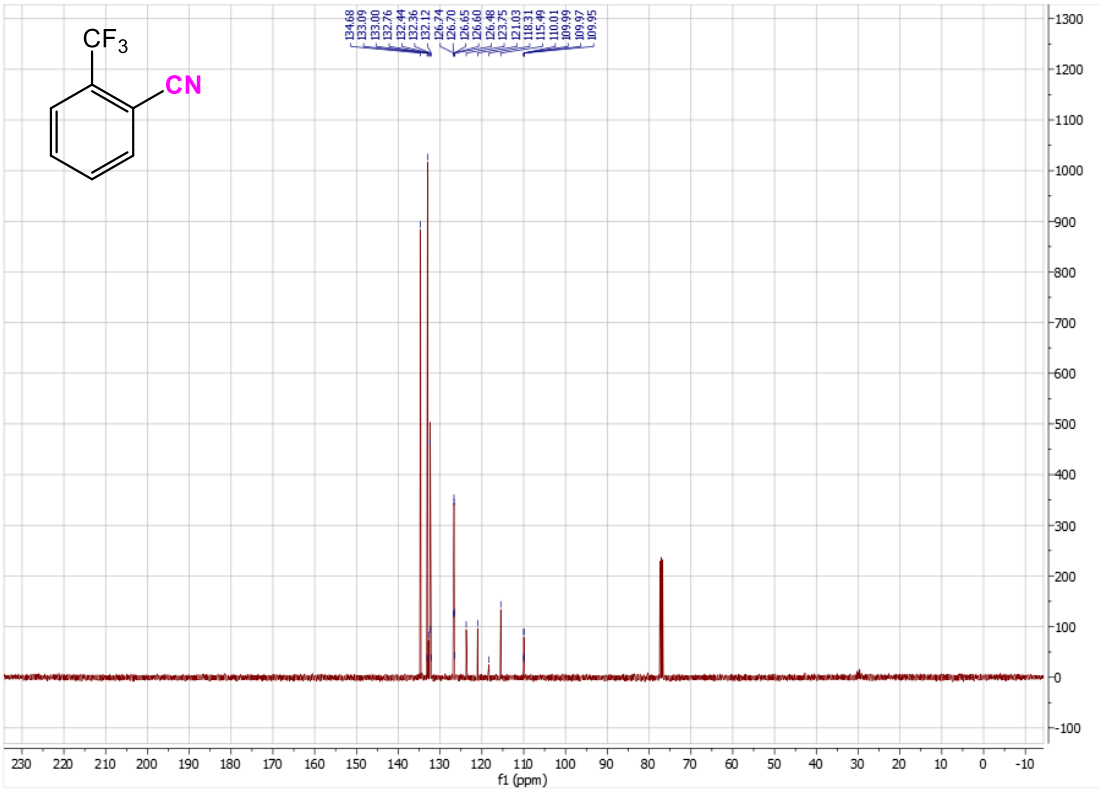
CF3
CN
134.68
133.09
133.00
132.76
132.44
132.36
132.12
126.74
126.70
126.65
126.60
126.48
123.75
121.03
118.31
115.49
110.01
109.99
109.97
109.95
f1 (ppm)

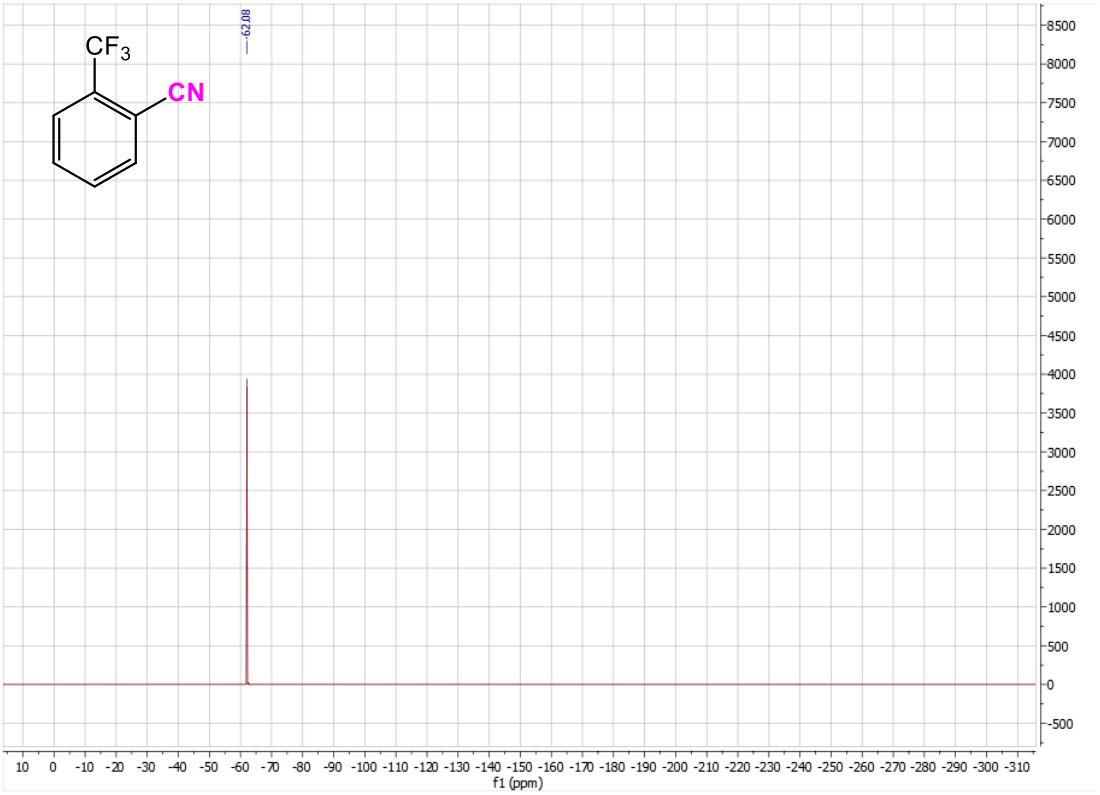
CF3
CN
-62.08
8500
8000
7500
7000
6500
6000
5500
5000
4500
4000
3500
3000
2500
2000
1500
1000
500
0
-500
10 0 -10 -20 -30 -40 -50 -60 -70 -80 -90 -100 -110 -120 -130 -140 -150 -160 -170 -180 -190 -200 -210 -220 -230 -240 -250 -260 -270 -280 -290 -300 -310
f1 (ppm)

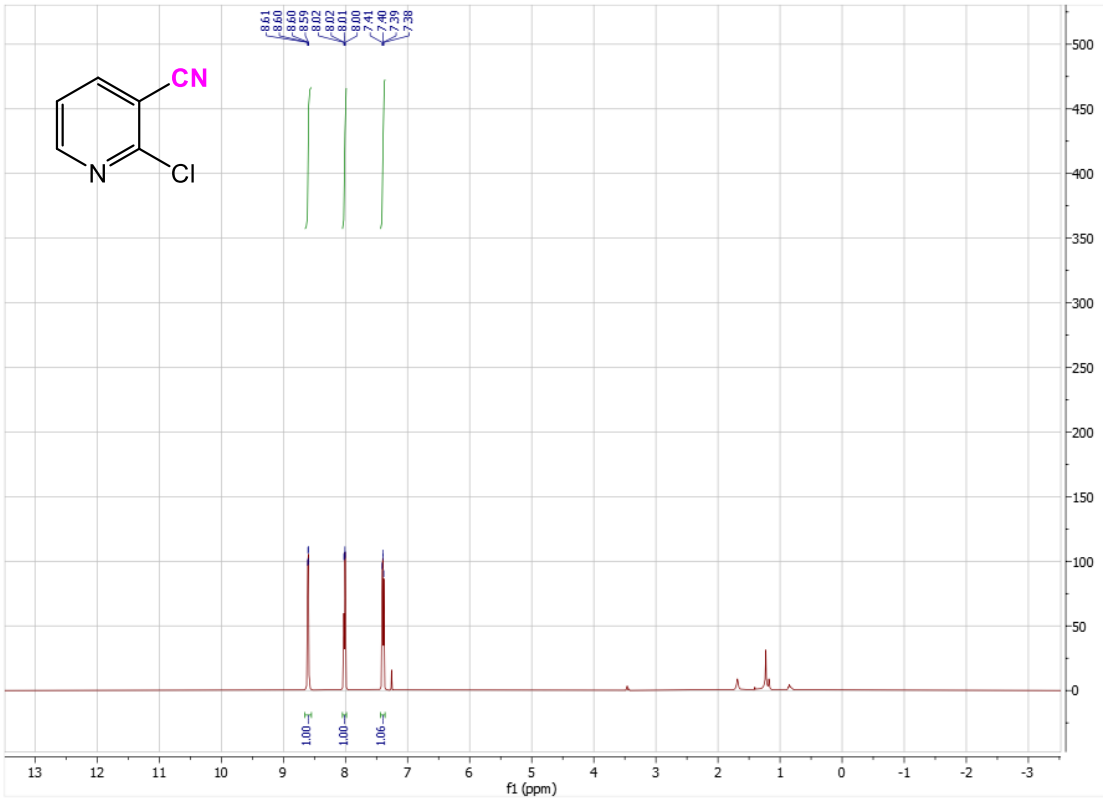
CN
N
Cl
8.61
8.60
8.60
8.59
8.02
8.02
8.01
8.01
7.41
7.40
7.39
7.38
1.00
1.00
1.06
f1 (ppm)

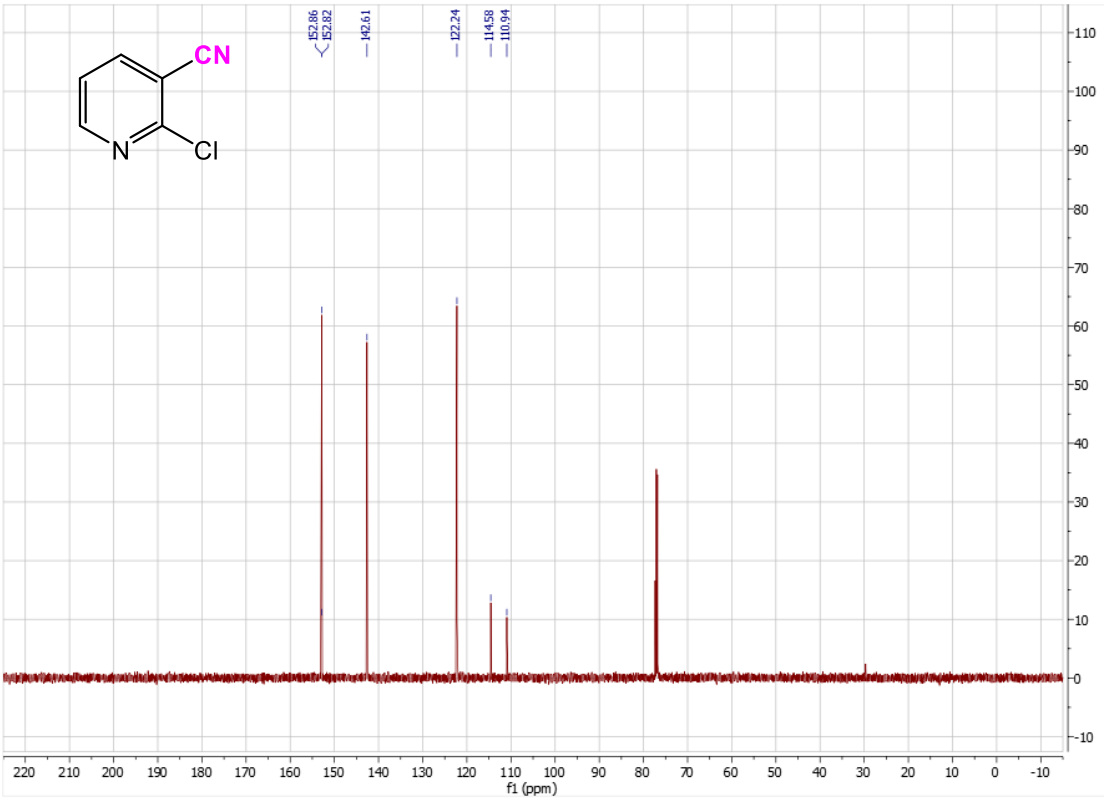
CN
N
Cl
152.86
152.82
142.61
122.24
114.58
110.94
f1 (ppm)

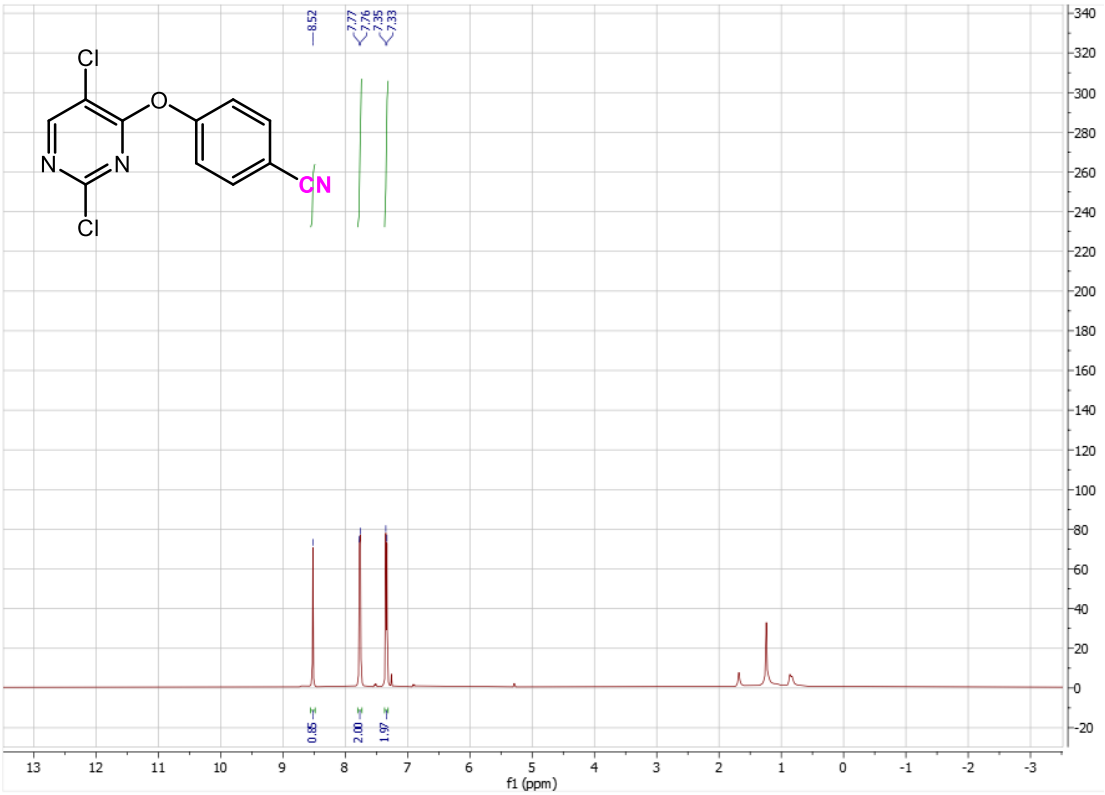
Cl
O
N
N
Cl
CN
8.52
7.77
7.76
7.35
7.33
0.85
2.00
1.97
f1 (ppm)

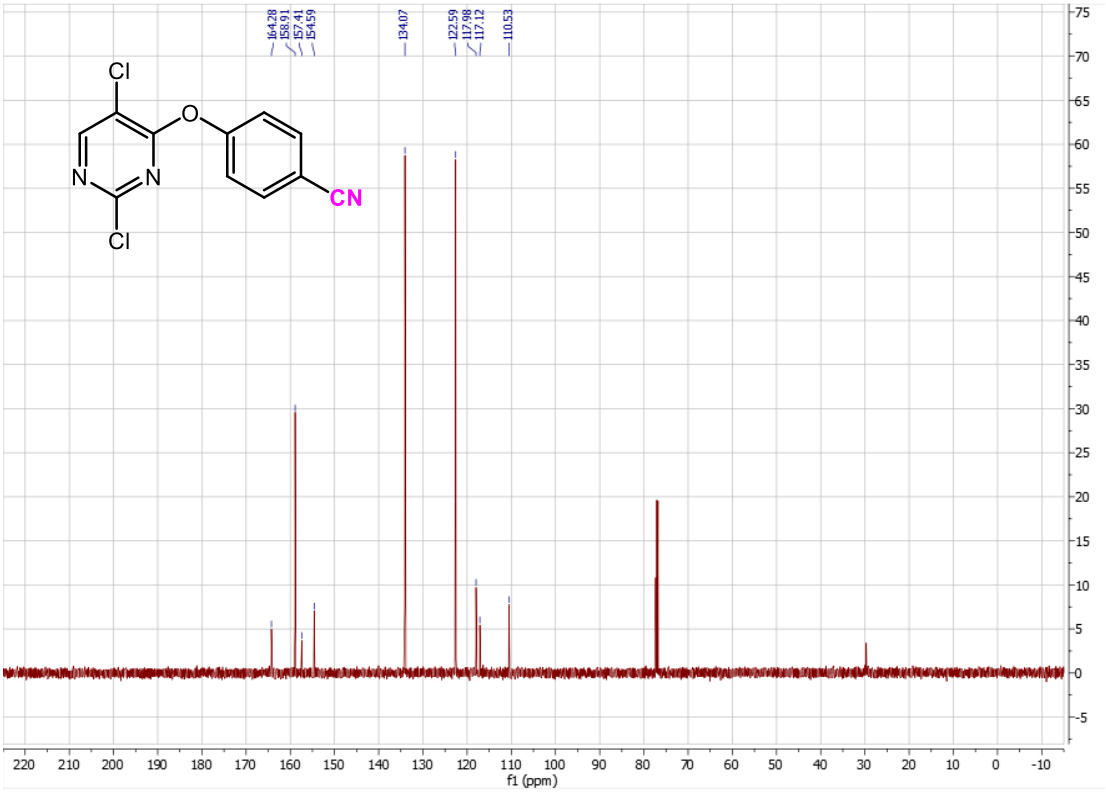
Cl
O
N
N
Cl
CN
164.28
158.91
157.41
154.59
134.07
122.59
117.98
117.12
110.53
f1 (ppm)

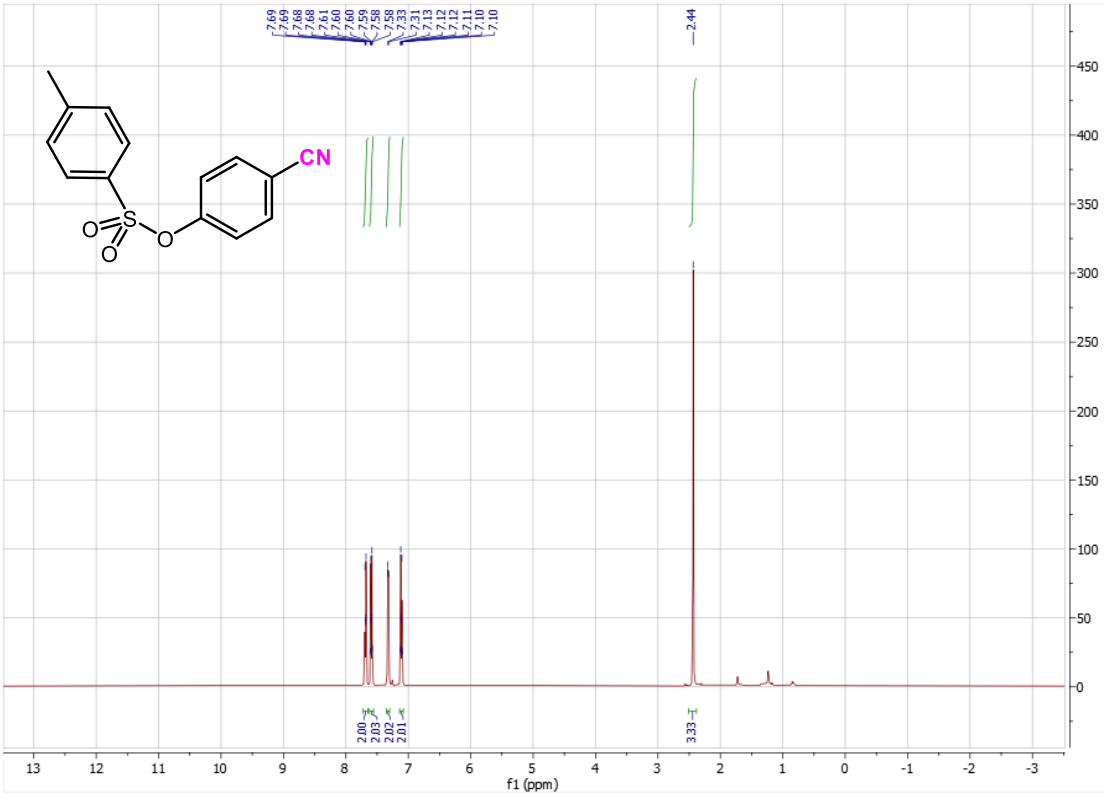
7.69
7.69
7.68
7.68
7.61
7.60
7.60
7.59
7.58
7.58
7.33
7.31
7.13
7.12
7.12
7.11
7.10
7.10
2.44
CN
O
S
O
O
2.00
2.03
2.02
2.01
3.33
f1 (ppm)

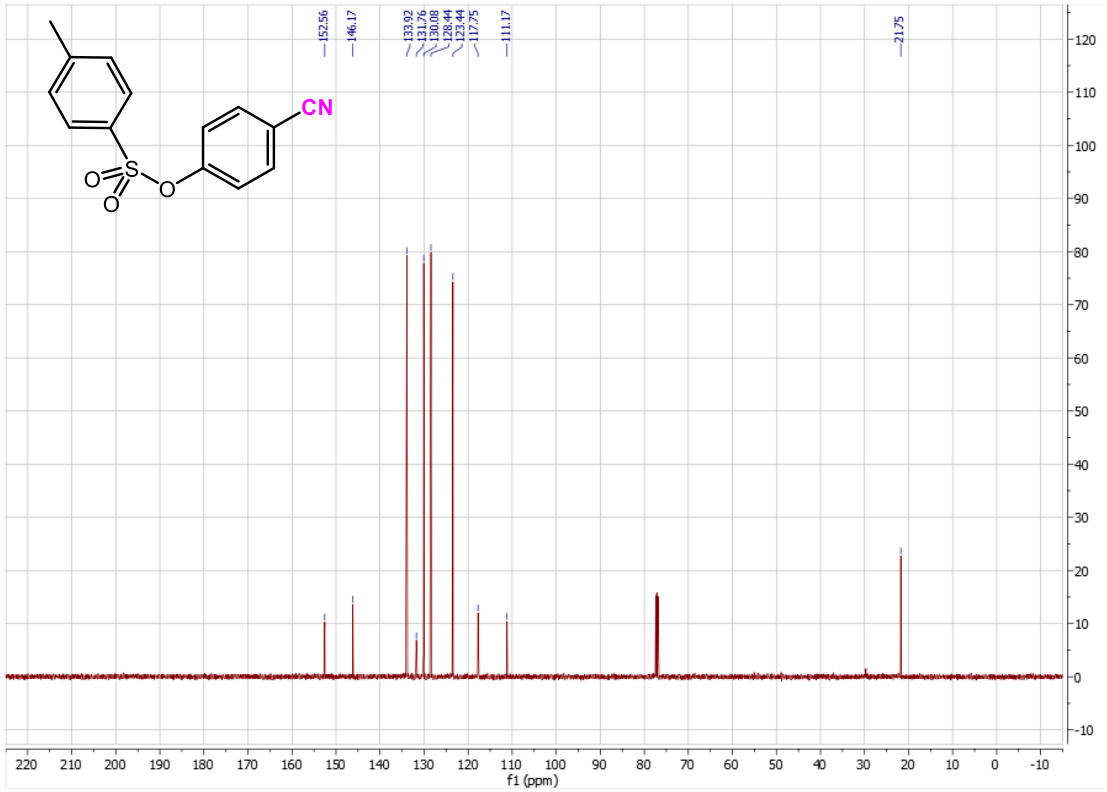
152.56
146.17
133.92
131.76
130.08
128.44
123.44
117.75
111.17
21.75
CN
O
S
O
O
f1 (ppm)

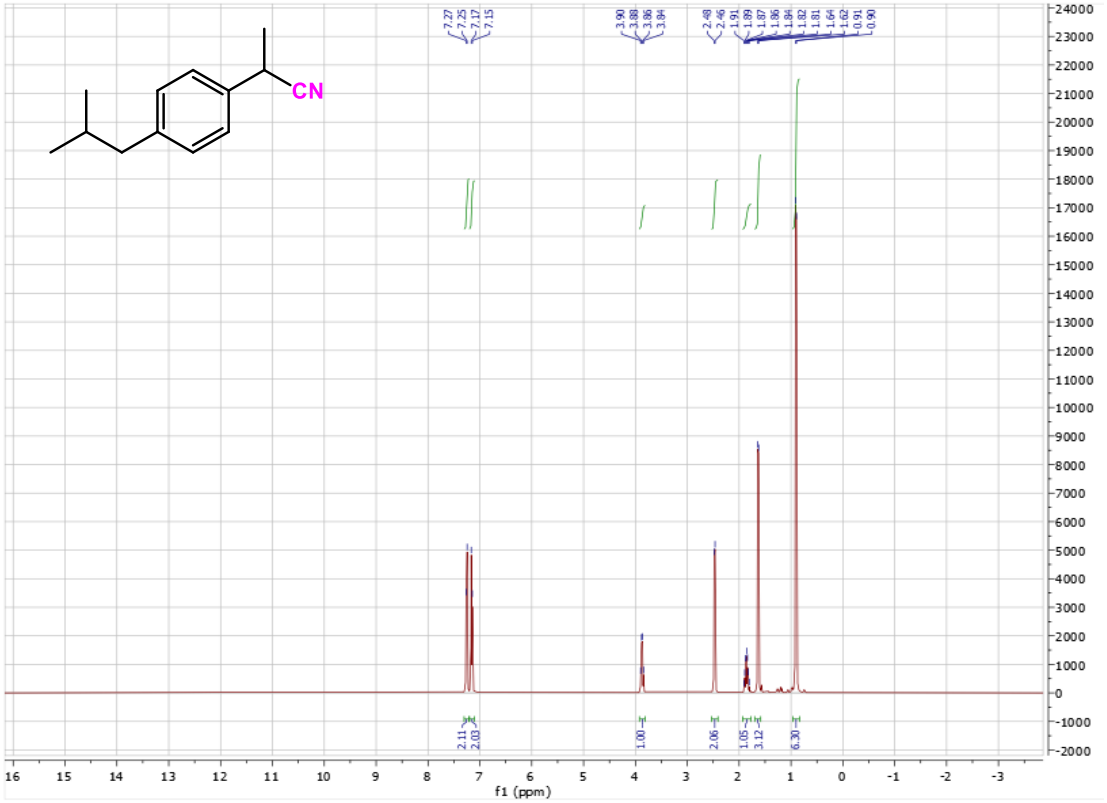
CN
f1 (ppm)

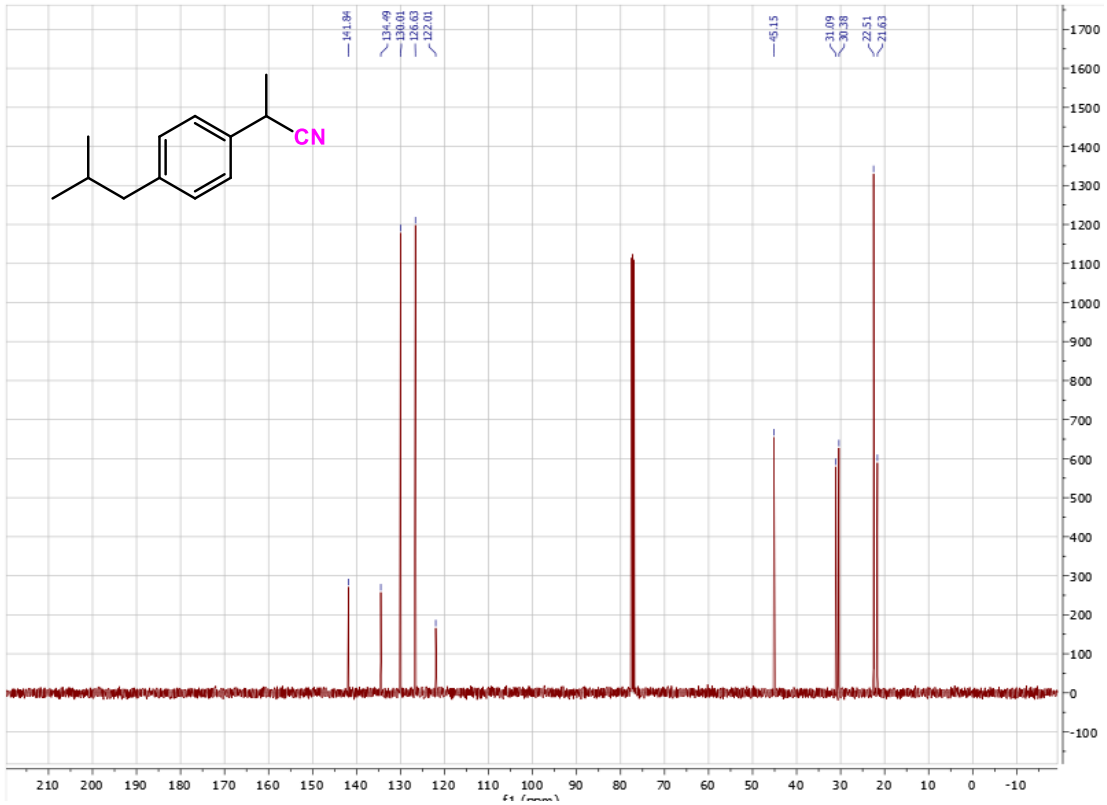
CN

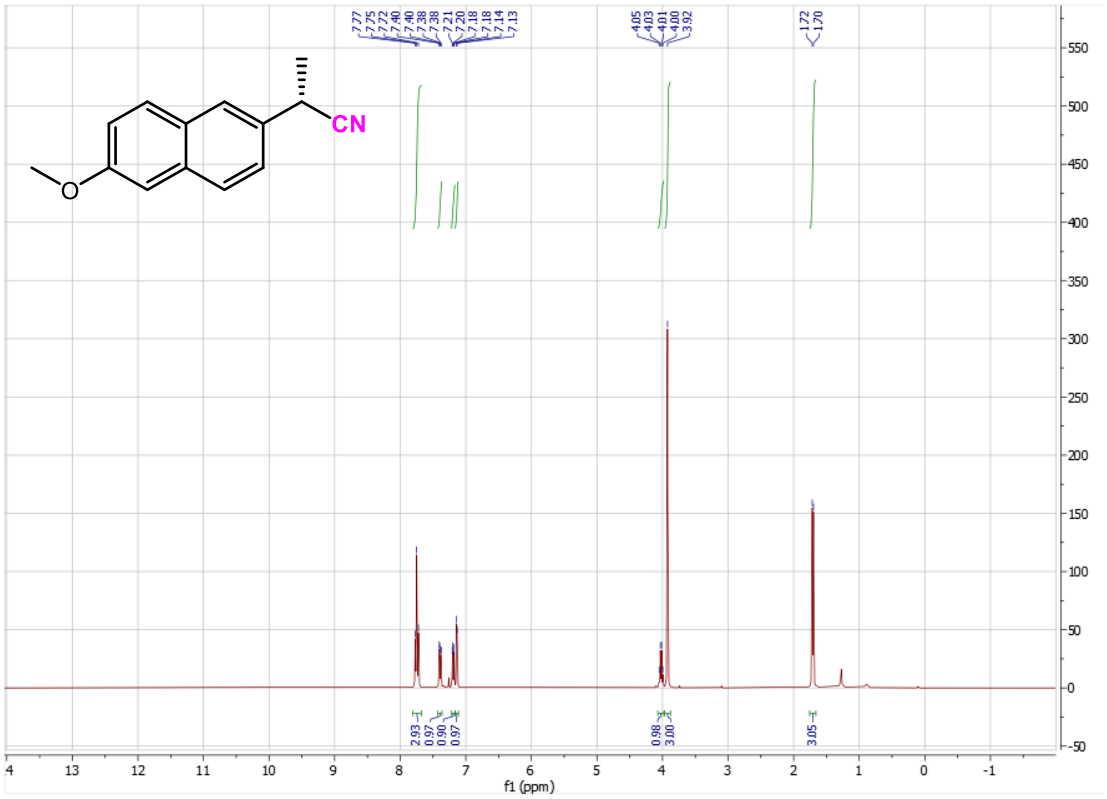
CN
O
7.77
7.75
7.72
7.40
7.40
7.38
7.38
7.21
7.20
7.18
7.18
7.14
7.13
4.05
4.03
4.01
4.00
3.92
1.72
1.70
2.93
0.97
0.90
0.97
0.98
3.00
3.05
f1 (ppm)

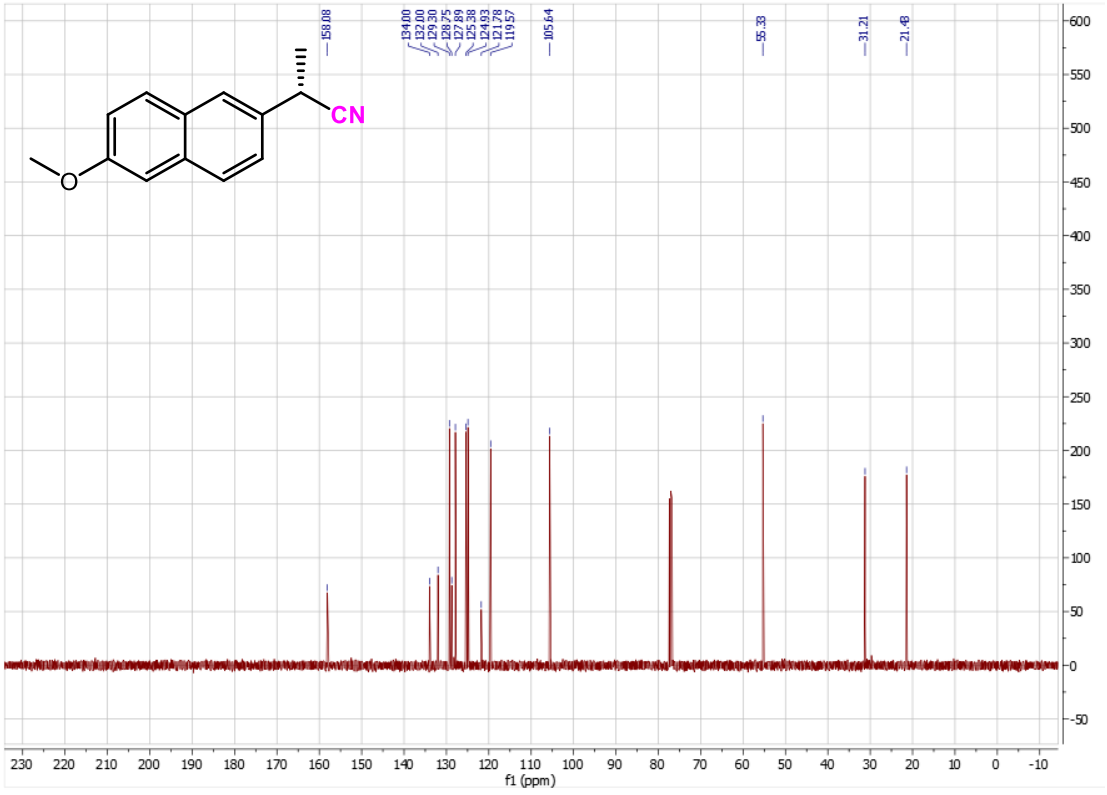
CN
O
159.08
134.00
132.00
129.30
128.75
127.89
125.38
124.93
121.78
119.57
105.64
55.33
31.21
21.48
f1 (ppm)

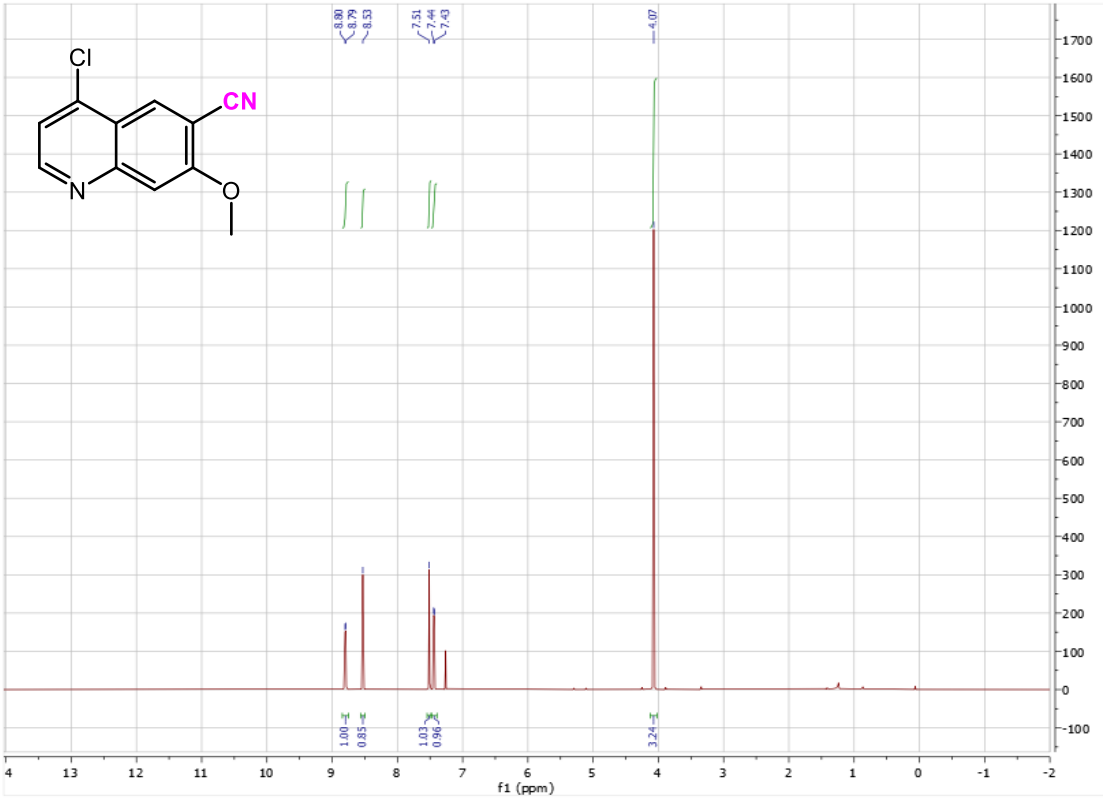
Cl
CN
N
O
8.80
8.79
8.53
7.51
7.44
7.43
4.07
1.00
0.85
1.03
0.96
3.24
f1 (ppm)

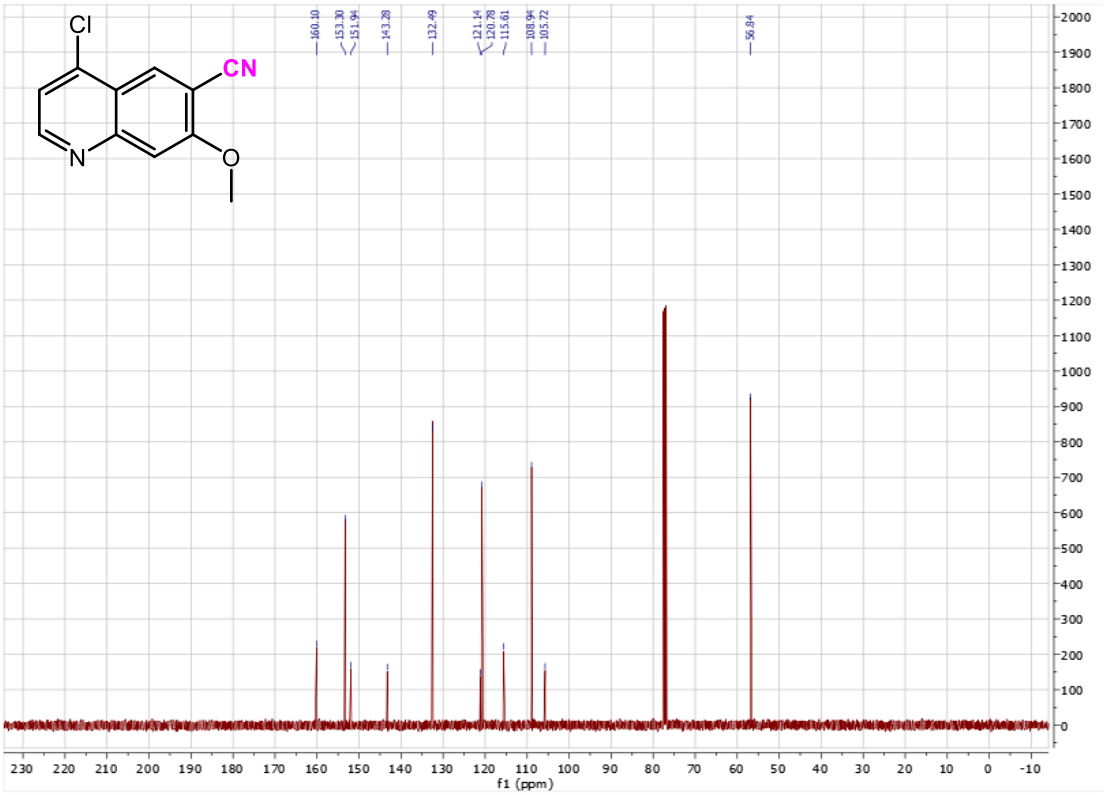
Cl
CN
N
O
160.10
153.30
151.94
143.28
132.49
121.14
120.78
115.61
108.94
105.72
56.84
f1 (ppm)

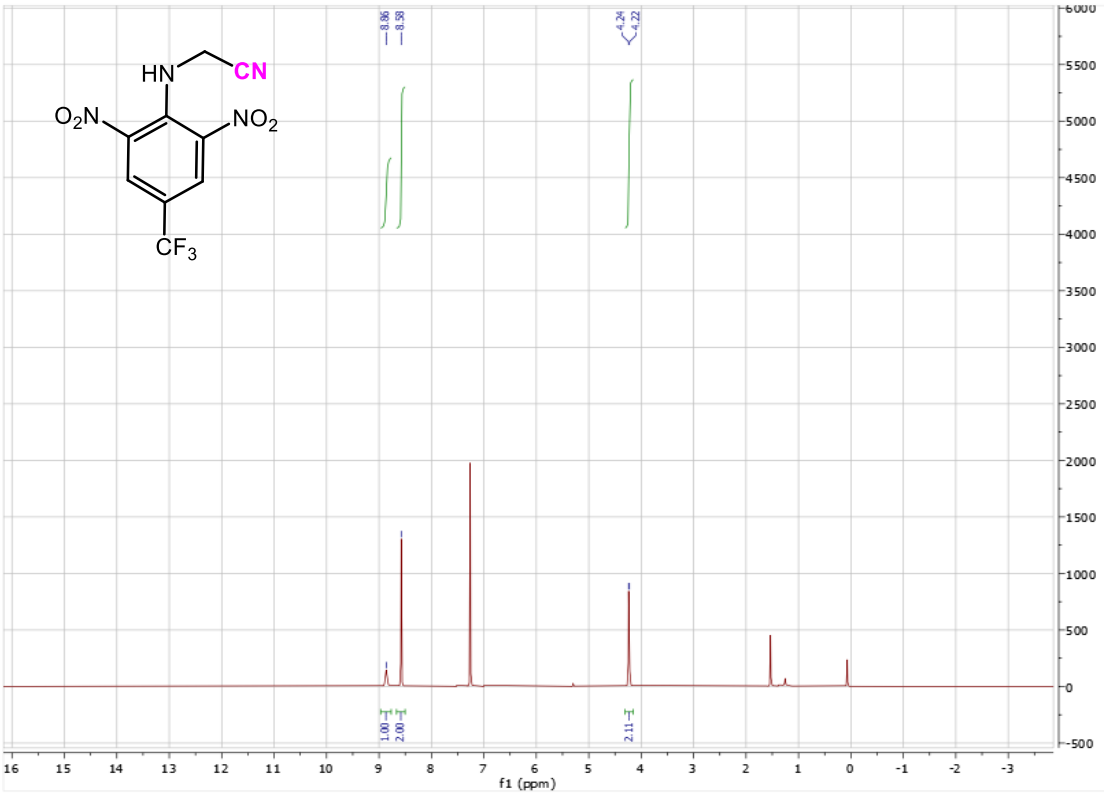
HN
CN
O2N
NO2
CF3
8.86
8.38
4.24
4.22
1.00
2.00
2.11
f1 (ppm)

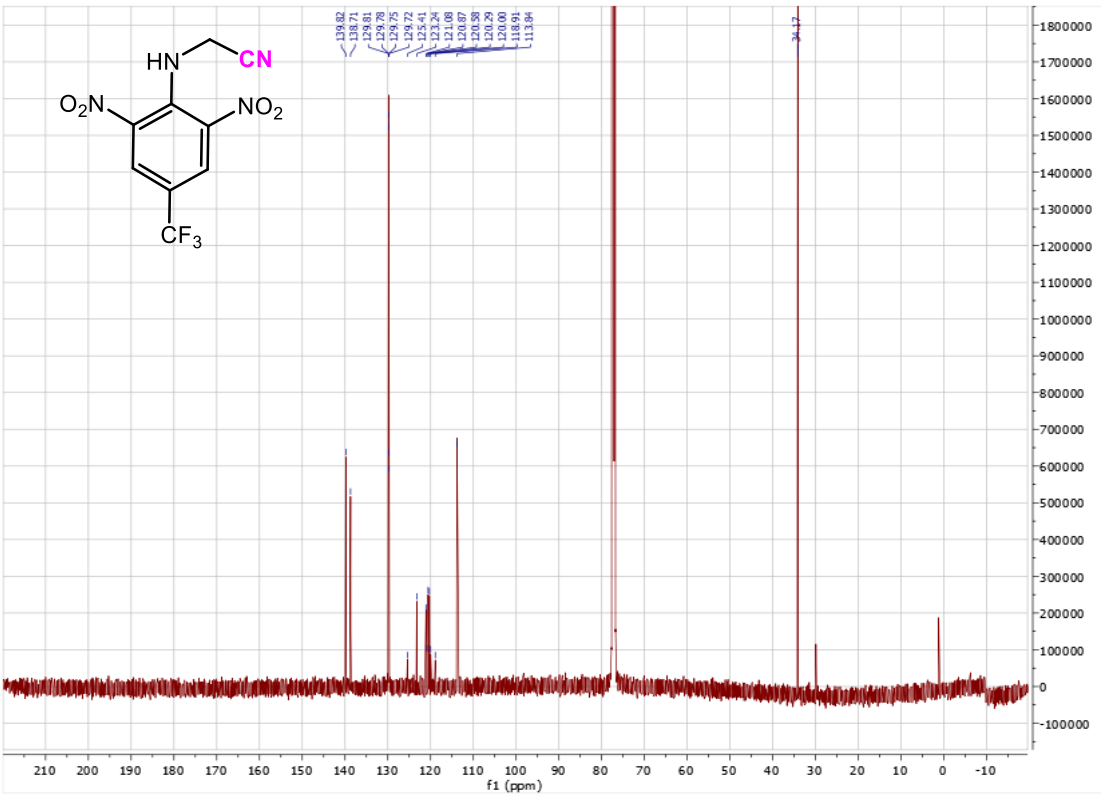
HN
CN
O2N
NO2
CF3
139.82
138.71
129.81
129.78
129.75
129.72
125.41
123.24
121.08
120.87
120.58
120.29
120.00
118.91
113.84
34.17
f1 (ppm)

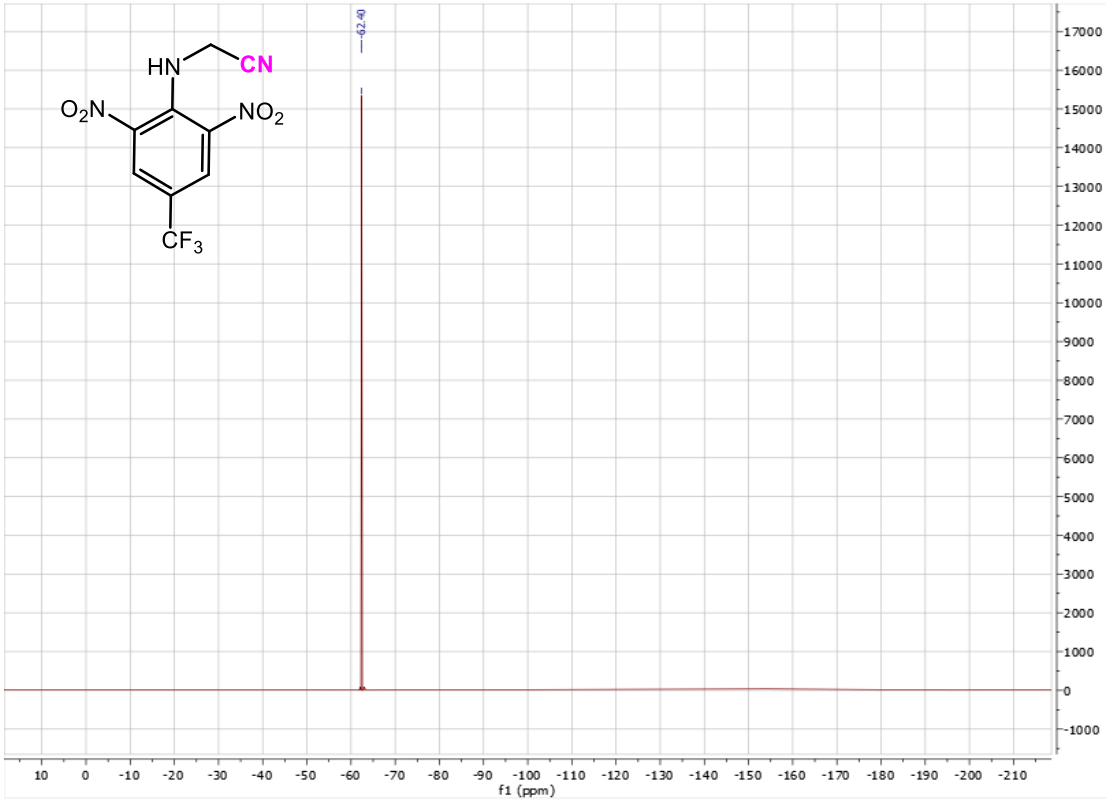
HN
CN
O2N
NO2
CF3
-62.40
17000
16000
15000
14000
13000
12000
11000
10000
9000
8000
7000
6000
5000
4000
3000
2000
1000
0
-1000
10 0 -10 -20 -30 -40 -50 -60 -70 -80 -90 -100 -110 -120 -130 -140 -150 -160 -170 -180 -190 -200 -210
f1 (ppm)

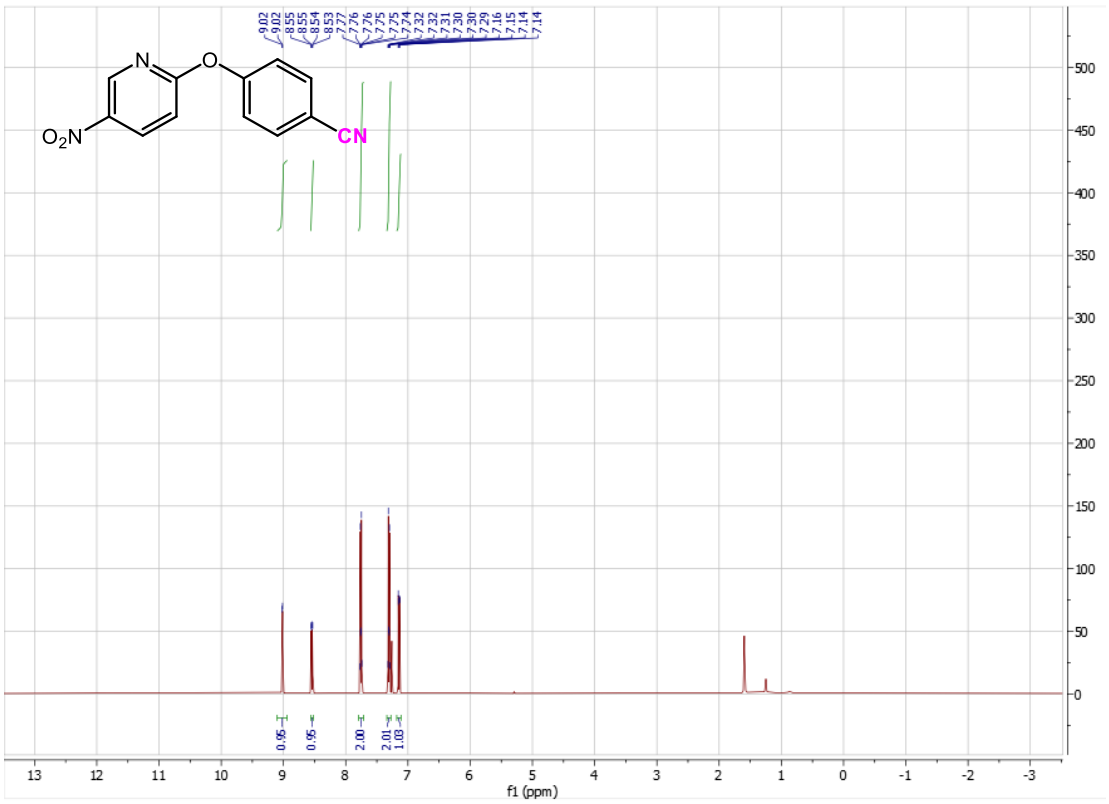
9.02
9.02
8.55
8.55
8.54
8.53
7.77
7.76
7.76
7.75
7.75
7.74
7.32
7.32
7.31
7.30
7.30
7.29
7.16
7.15
7.14
7.14
N
O
O_2N
CN
0.95
0.95
2.00
2.01
1.03
f1 (ppm)

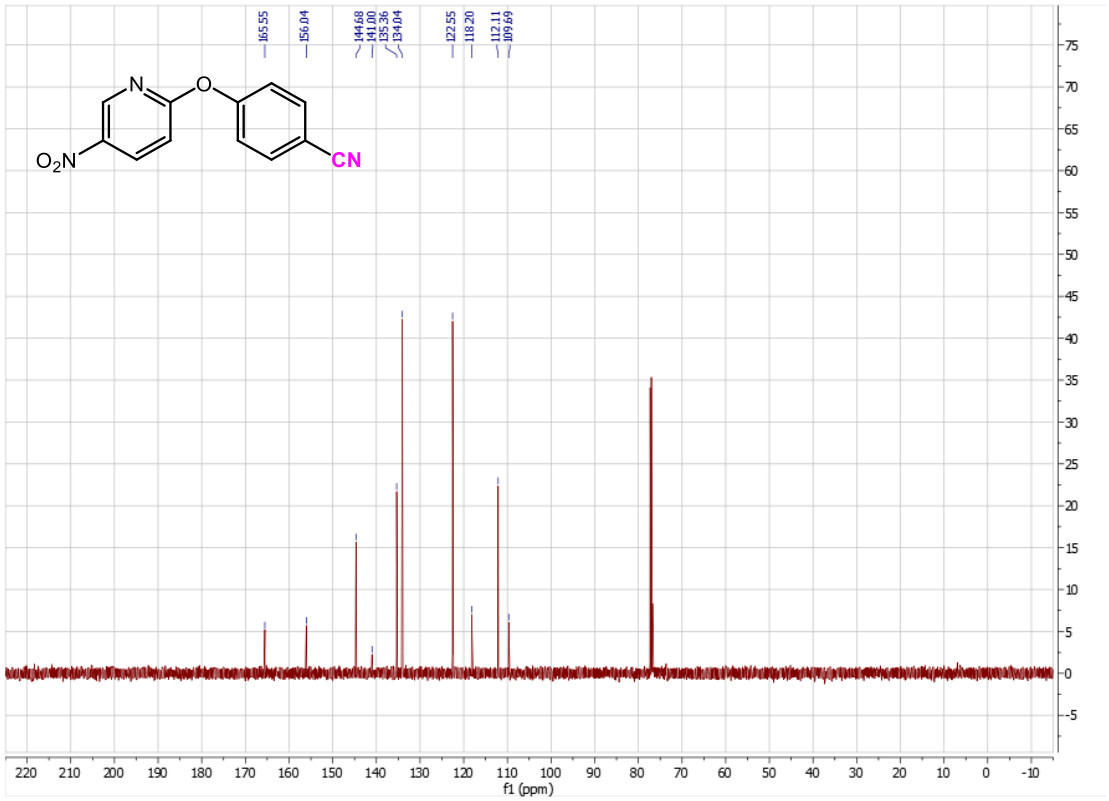
165.55
156.04
144.68
141.00
135.36
134.04
122.55
118.20
112.11
109.69
N
O
O_2N
CN
f1 (ppm)

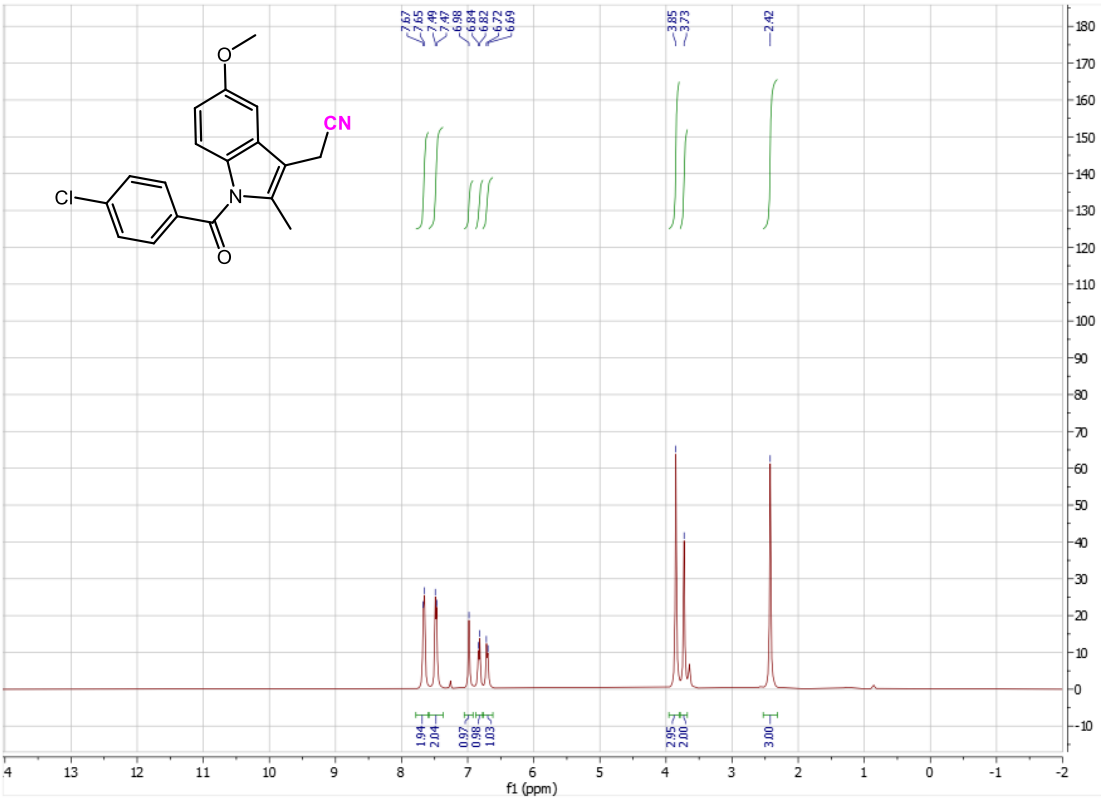
7.67
7.65
7.49
7.47
6.98
6.84
6.82
6.72
6.69
3.85
3.73
2.42
1.94
2.04
0.97
0.98
1.03
2.95
2.00
3.00
f1 (ppm)

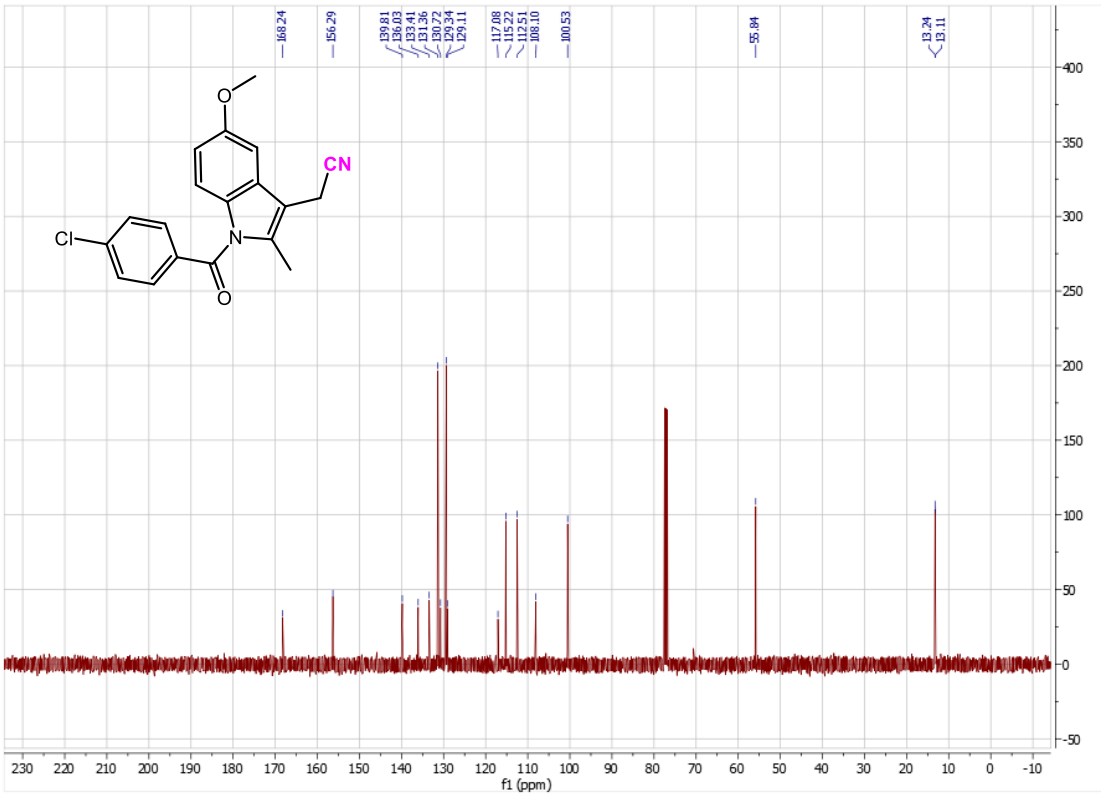
168.24
156.29
139.81
136.03
133.41
131.36
130.72
129.34
129.11
117.08
115.22
112.51
108.10
100.53
55.84
13.24
13.11
f1 (ppm)

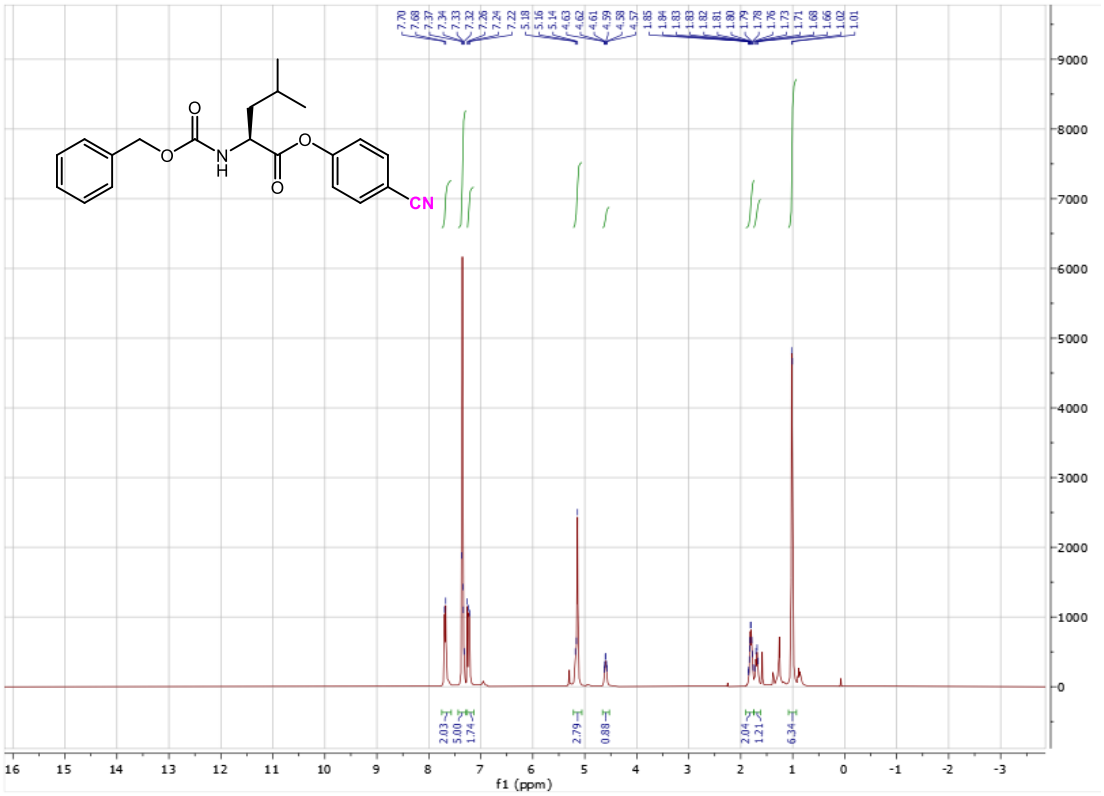
CN
f1 (ppm)

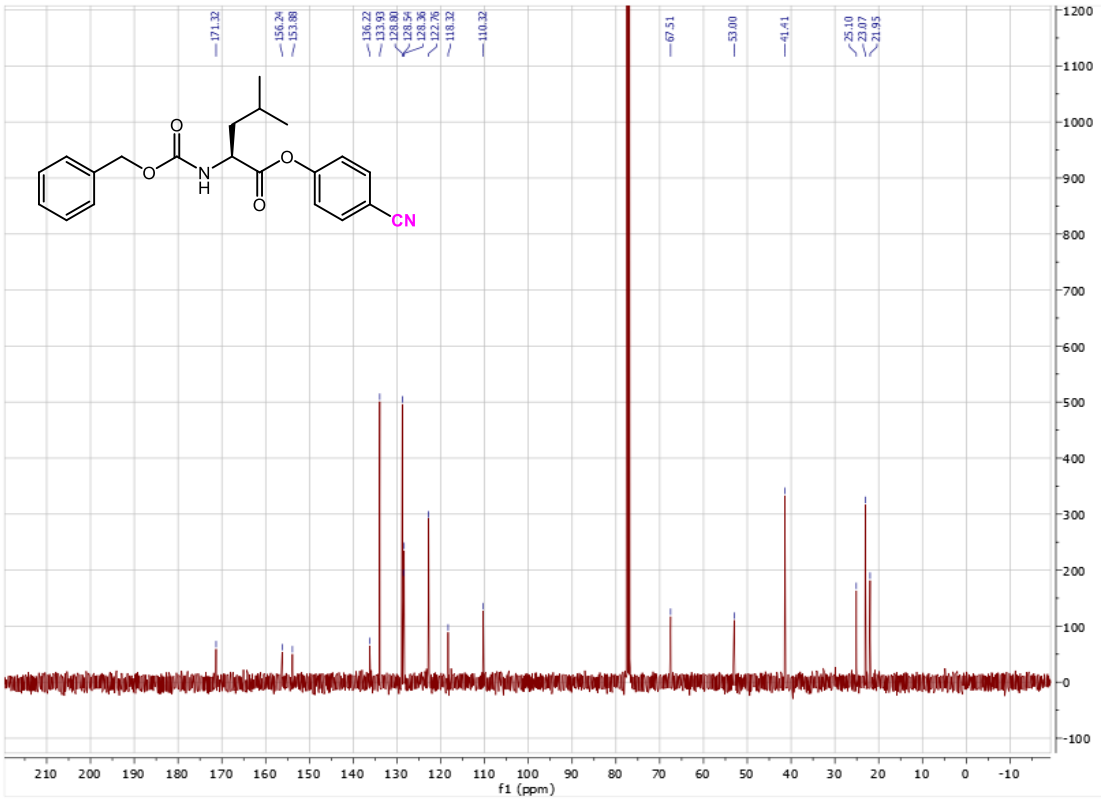
CN
f1 (ppm)

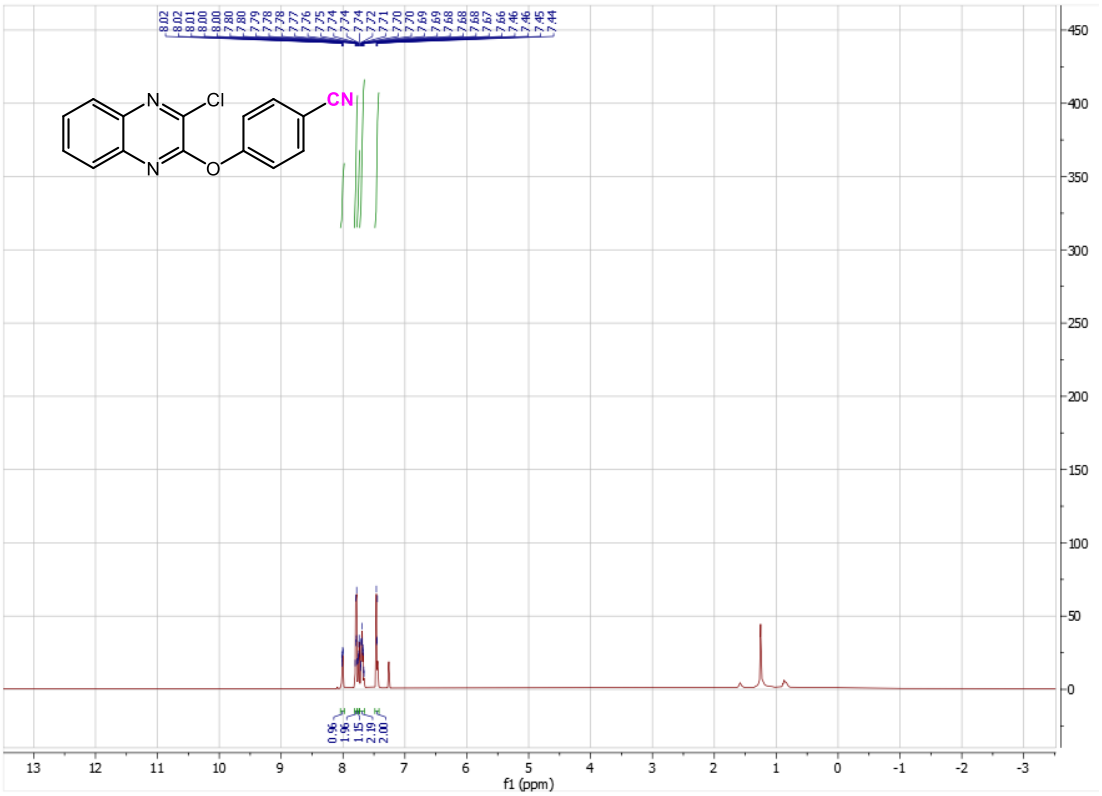
8.02
8.02
8.01
8.00
8.00
7.80
7.80
7.79
7.78
7.78
7.77
7.76
7.75
7.74
7.74
7.74
7.72
7.71
7.70
7.70
7.69
7.69
7.68
7.68
7.67
7.66
7.46
7.46
7.45
7.44
N
Cl
CN
N
O
0.96
1.96
1.15
2.19
2.00
f1 (ppm)

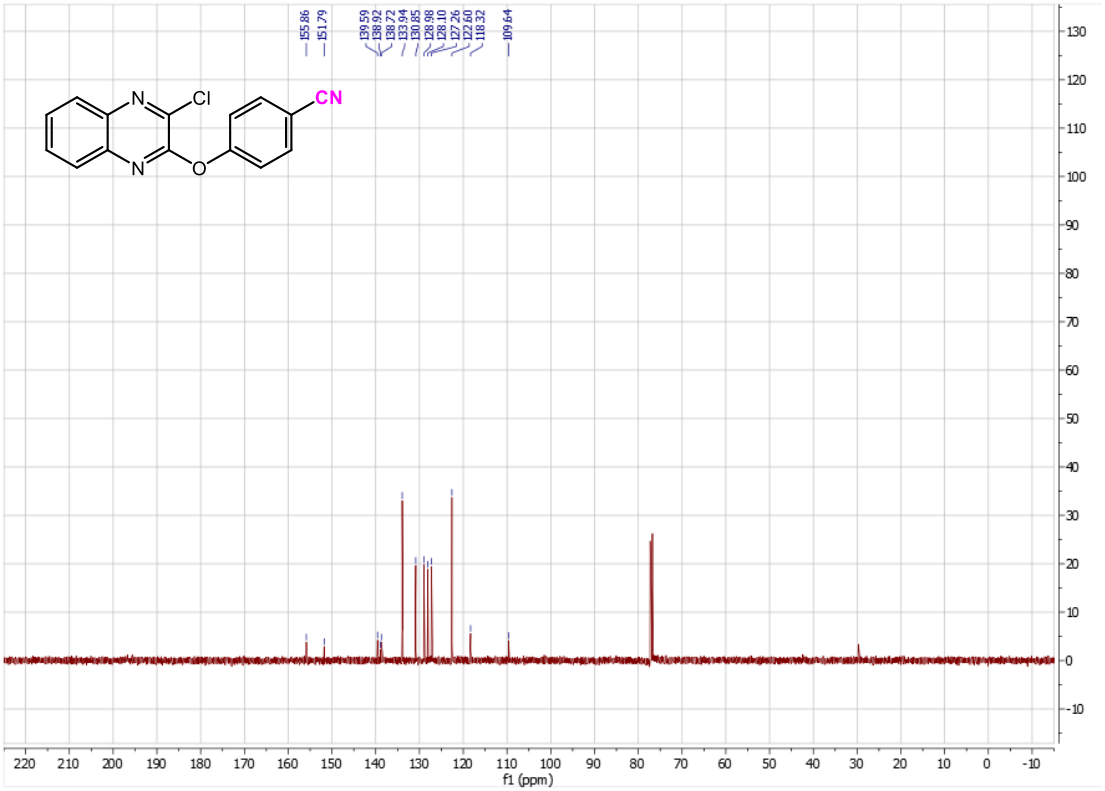
155.86
151.79
139.59
138.92
138.72
133.94
130.85
128.98
128.10
127.26
122.60
118.32
109.64
N
Cl
CN
N
O
f1 (ppm)

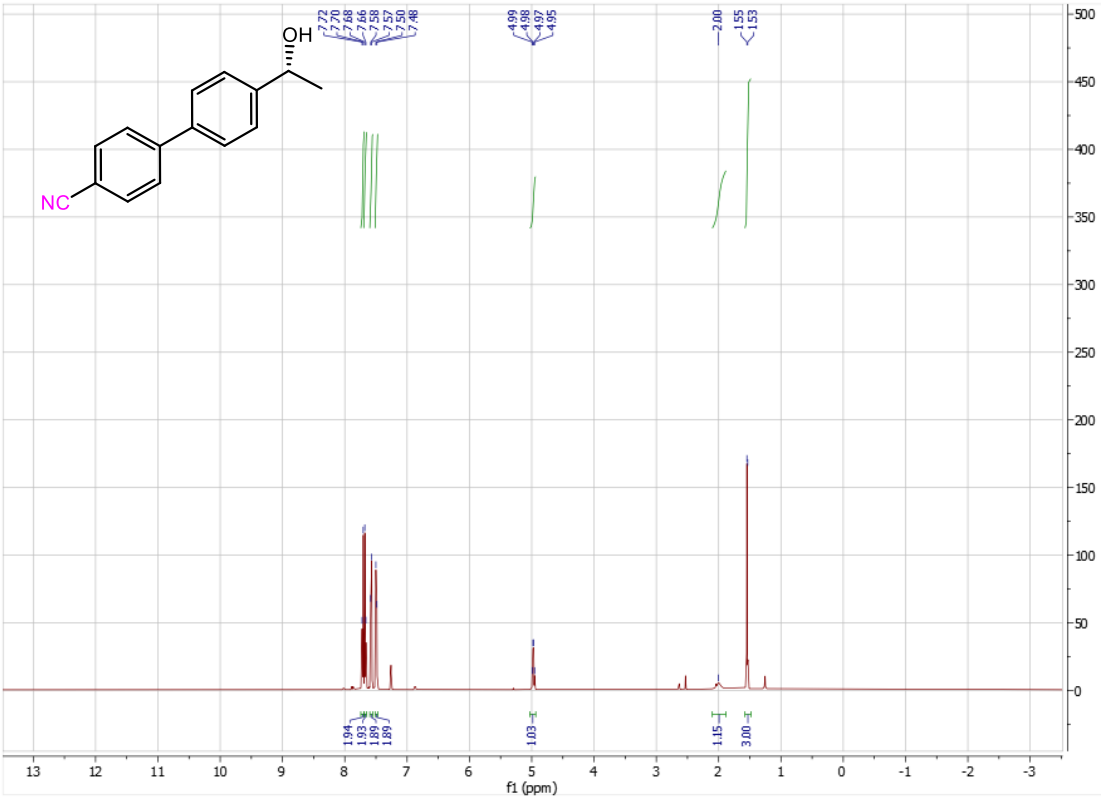
OH
NC
7.72
7.70
7.68
7.66
7.58
7.57
7.50
7.48
4.99
4.98
4.97
4.95
2.00
1.55
1.53
1.94
1.93
1.89
1.89
1.03
1.15
3.00
f1 (ppm)

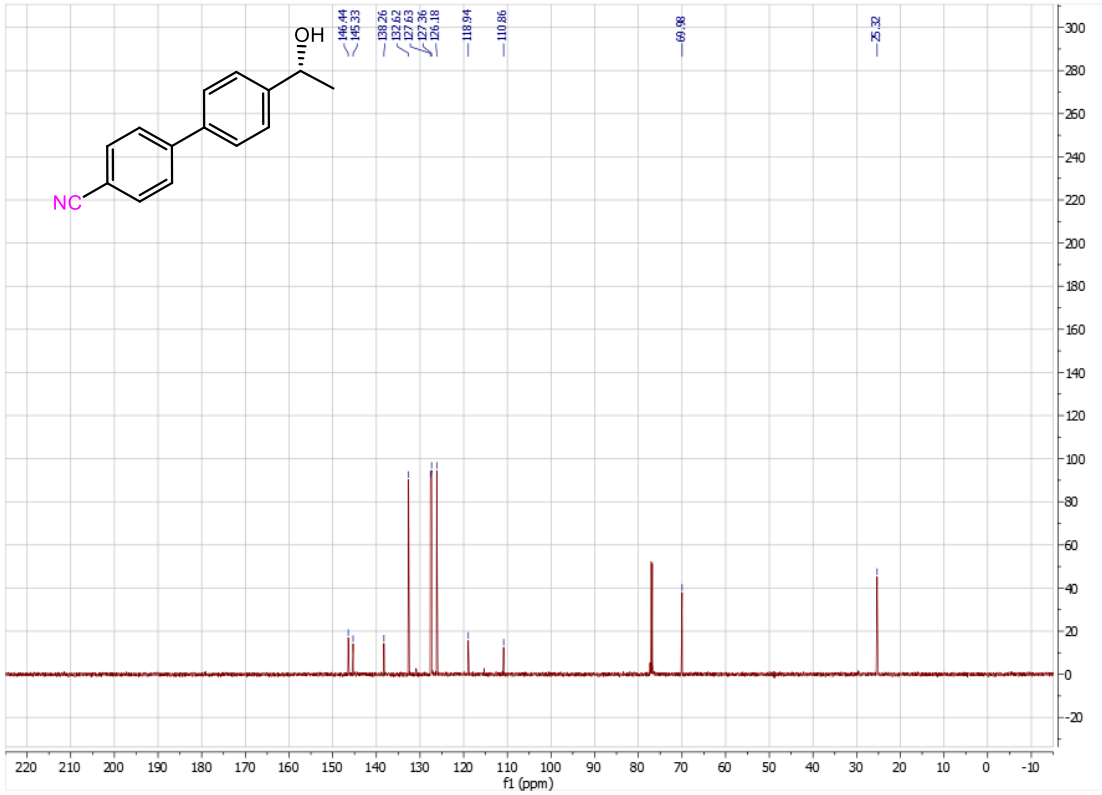
OH
NC
146.44
145.33
138.26
132.62
132.53
127.36
126.18
118.94
110.86
69.98
25.32
f1 (ppm)

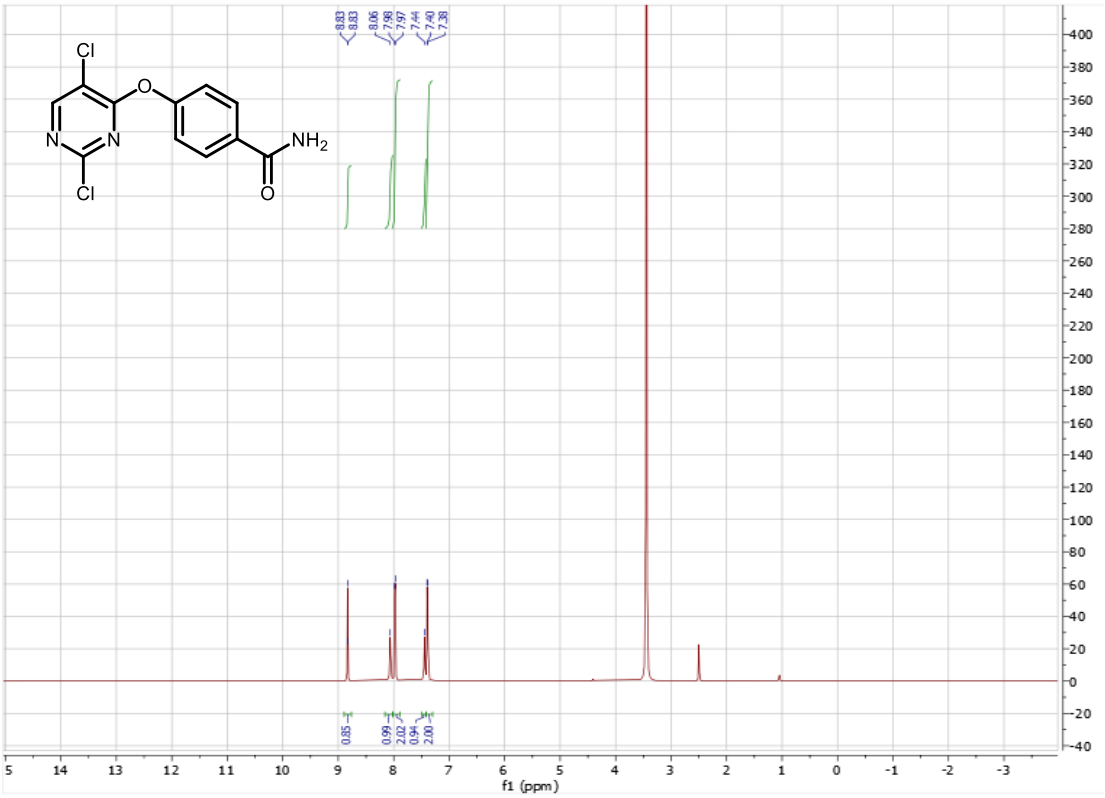
Cl
O
N
N
Cl
NH2
O
8.83
8.83
8.06
7.98
7.97
7.44
7.40
7.38
0.85
0.99
2.02
0.94
2.00
f1 (ppm)

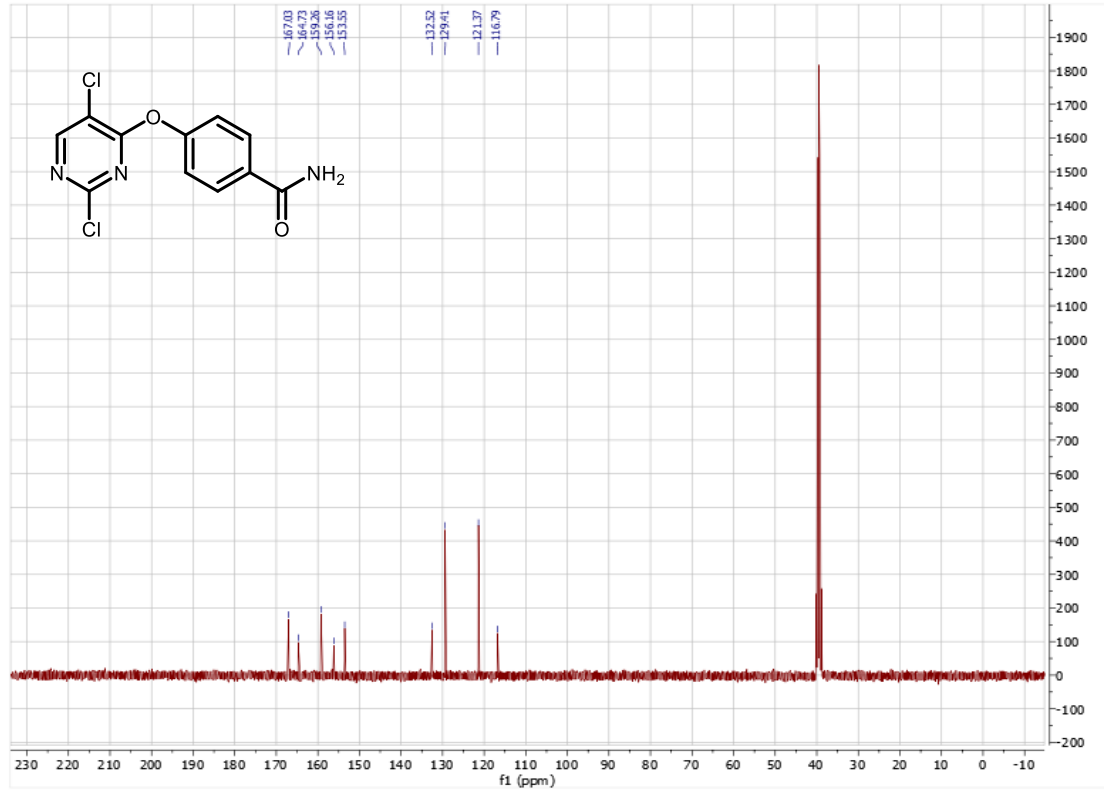
Cl
O
N
N
Cl
NH2
O
167.03
164.73
159.26
156.16
153.55
132.52
129.41
121.37
116.79
f1 (ppm)

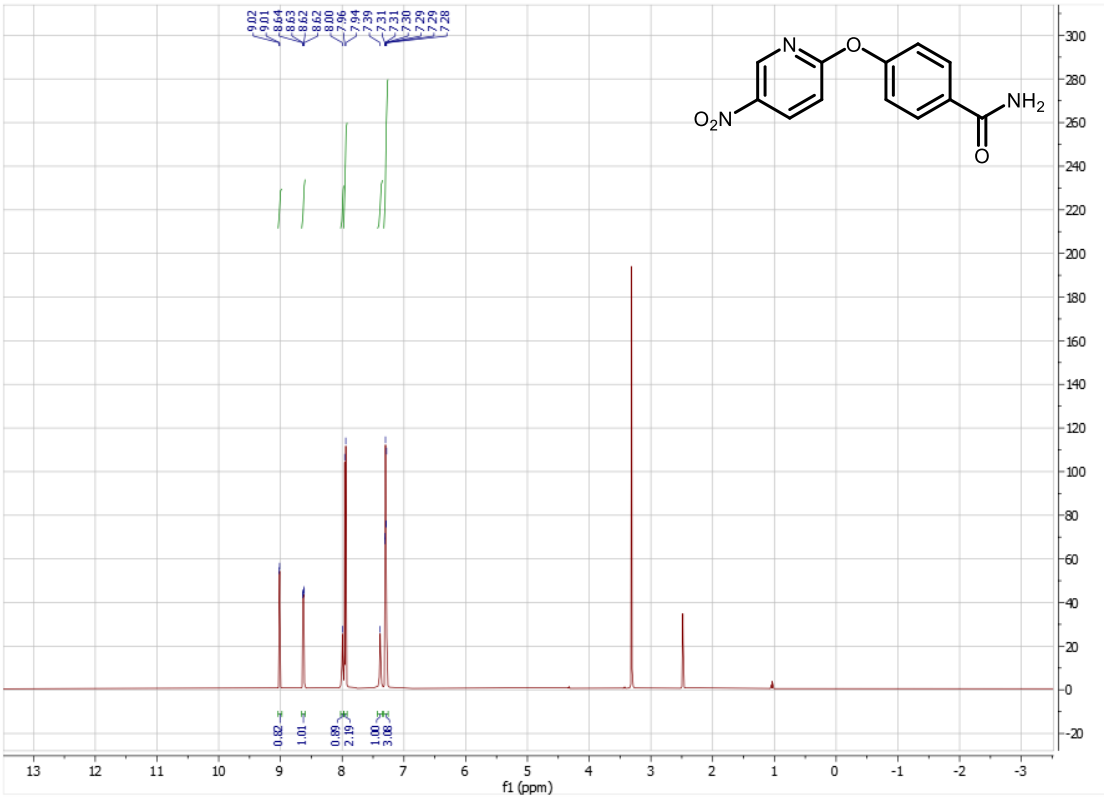
9.02
9.01
8.64
8.63
8.62
8.62
8.00
7.99
7.94
7.39
7.31
7.31
7.30
7.29
7.29
7.28
0.82
1.01
0.89
2.19
1.00
3.08
f1 (ppm)

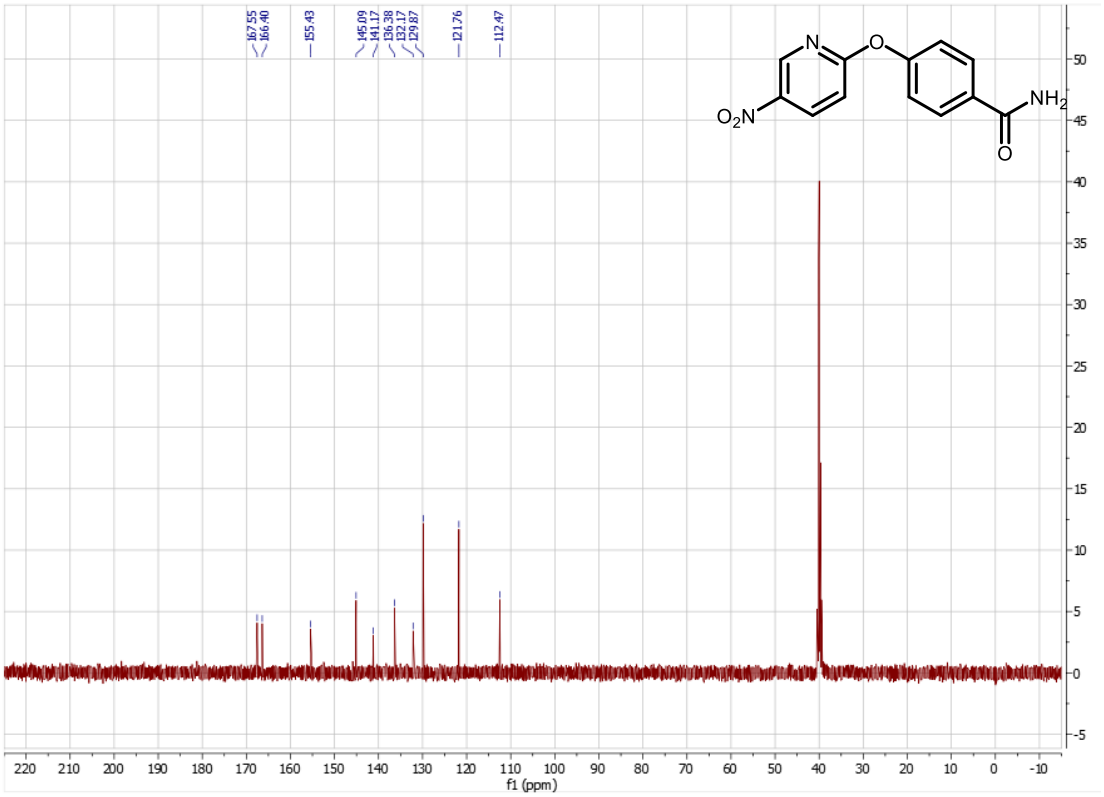
167.55
166.40
155.43
145.09
141.17
136.38
132.17
129.87
121.76
112.47
f1 (ppm)

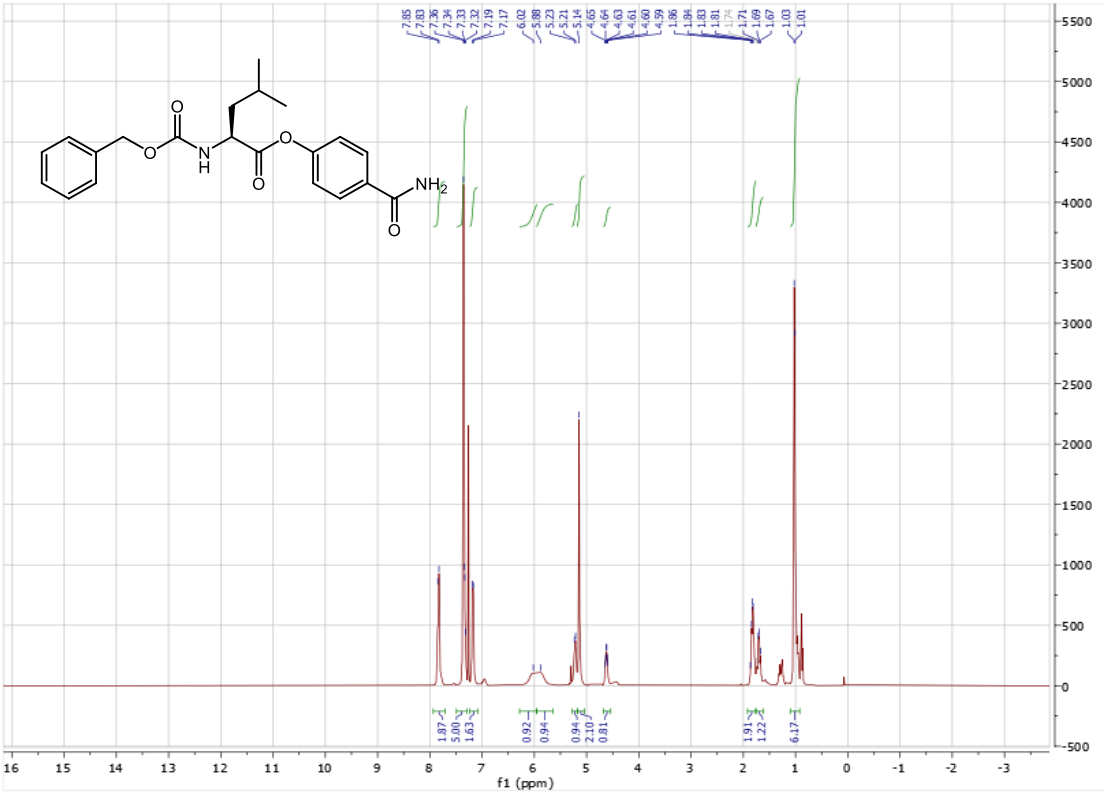
f1 (ppm)

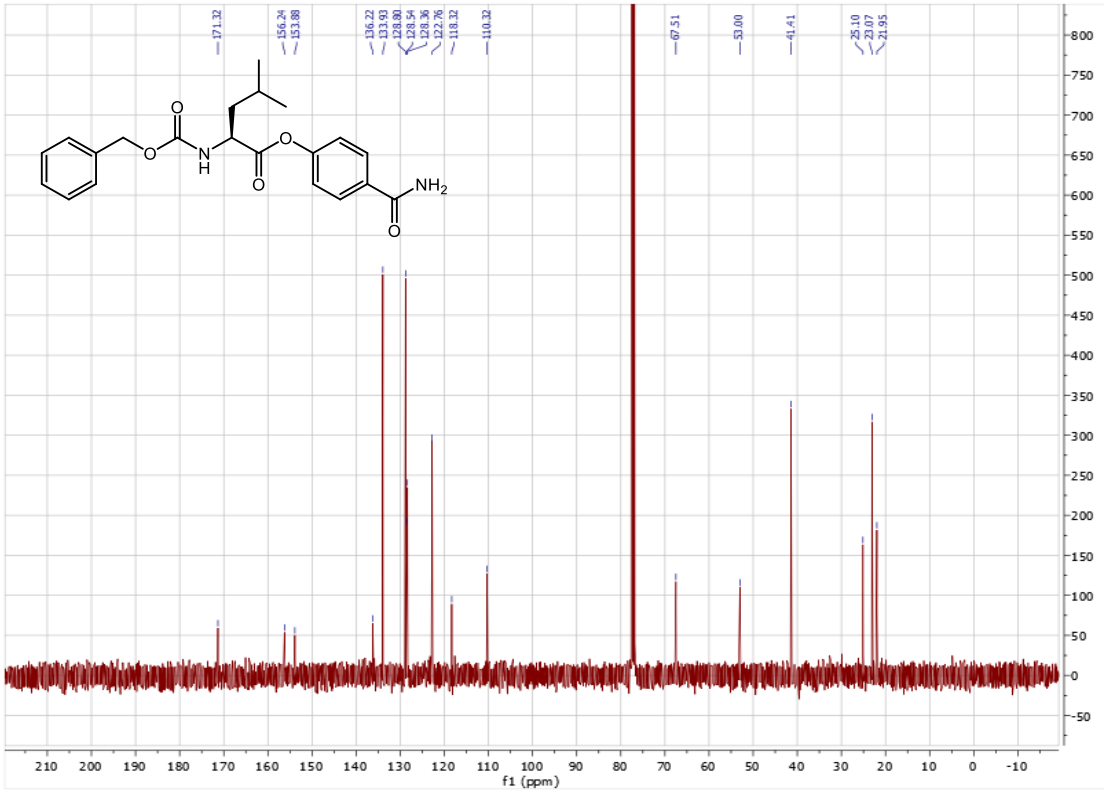
f1 (ppm)

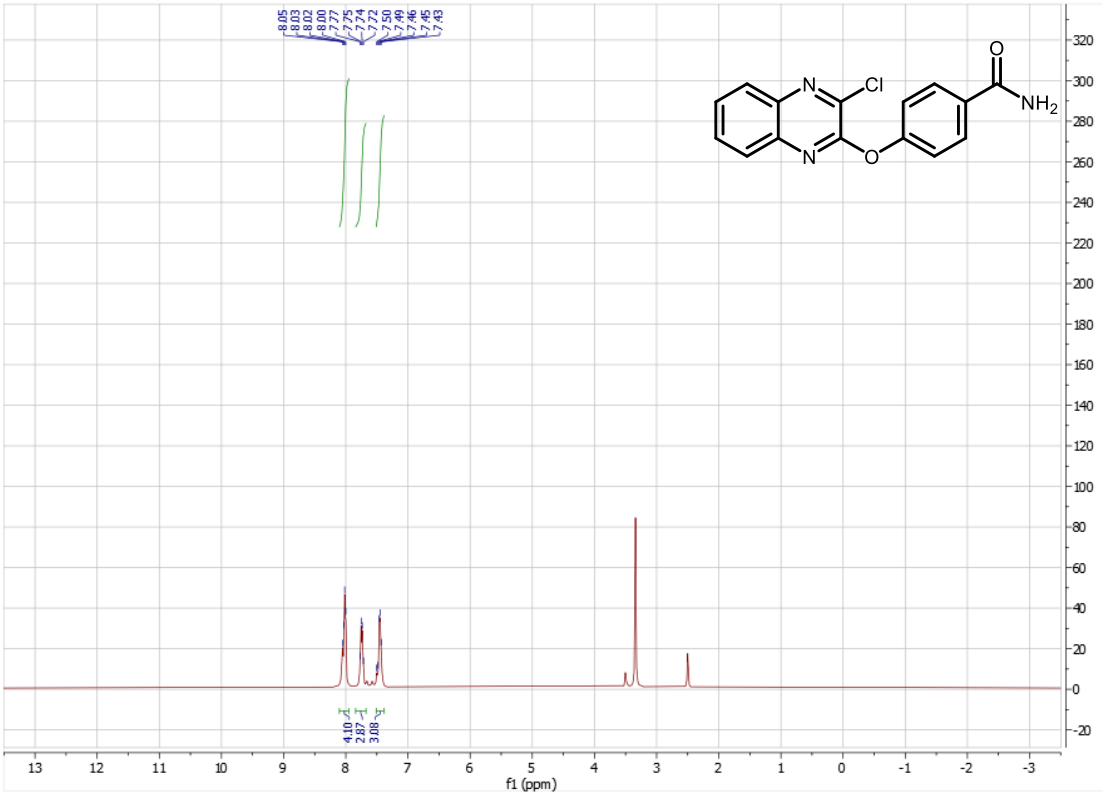
8.05
8.03
8.02
8.00
7.77
7.75
7.74
7.72
7.50
7.49
7.46
7.45
7.43
4.10
2.87
3.08
f1 (ppm)

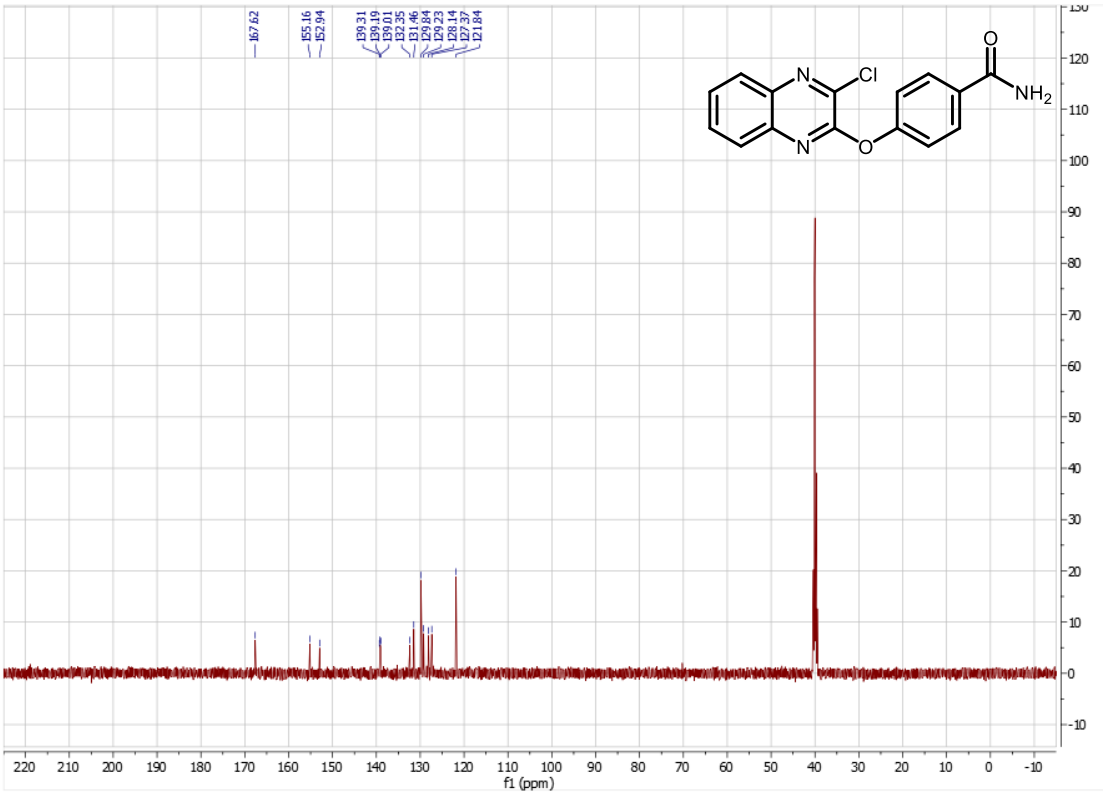
167.62
155.16
152.94
139.31
139.19
139.01
132.35
131.46
129.84
129.23
128.14
127.37
121.84
f1 (ppm)

IV. Solid Handling Equipment Advancements for Nanoparticle Catalyzed Flow Chemistry in Aqueous Micellar Media

Reproduced from

Wood, A. B.; Nandiwale, K. Y.; Mo, Y.; Jin, B.; Pomberger, A.; Schultz, V. L.; Gallou, F.; Jensen, K. F.; Lipshutz, B. H. *Green Chem.* **2020**, *22*, 3441–3444.

With permission from The Royal Society of Chemistry

And

Reproduced from

Wood, A. B.; Plummer, S.; Robinson, R. I.; Smith, M.; Chang, J.; Gallou, F.; Lipshutz, B. H. *Green Chem.* **2021**, *23*, 7724–7730.

With permission from The Royal Society of Chemistry

4.1 Personal Account

Prior to coming to graduate school, I worked as a process scientist at a startup company called Micromidas Inc., now known as Origin Materials. When I started there, I had a couple years of organic chemistry synthesis experience from my time in Mark Kurth's lab at UC Davis, so of course I thought I knew everything. I found out very quickly that I knew very, very little compared to what I was going to need to know to be successful at that company. I could spend a couple pages recounting five years of very intense growth as both a scientist as well as a person, but the takeaway is that I learned the value of skill hybridization as a scientist in the field. On the job, I learned both business/managerial skills, soft skills that changed who I was as a person on a fundamental level, as well as very important chemical engineering skills that, I believe, set me apart from others in my field. Proficiency in both of those disciplines, as well as improved organic chemistry skills, have served me well in my time in graduate school and, hopefully, more in my career moving forward and for that I am eternally grateful to my mentors at Origin.

I had always known that I wanted to go back to graduate school. Everyone in the field knows that staying at a B.Sc. level is a very fragile state, because if Origin went bankrupt (as it appeared that it was going to many times) I would not have a career path with which I would be happy. However, I had not been introduced to any graduate school groups that I thought were doing anything worthwhile, as I was a very practical chemist, and I didn't want to work on anything that wasn't directly applicable to industrial settings. That is, until I saw Bruce give a talk at the 2015 ACS conference in Denver, Colorado on his group's work doing synthetic organic chemistry in water. My boss at Origin, Mako, seemed very impressed with the presented work so I asked him if Bruce was for real. His response was "let me put it this way:

Lipshutz is the man", but not exactly in those words. I contacted Bruce a little while later once I had started to make up my mind on graduate school, and he got me caught up to speed on his chemistry by sending me three review articles on surfactant-based methodologies.

One factor that immediately stood out was the inherent heterogeneity of micellar catalysis. I had experience in the biomass conversion technology field with heterogeneous, four-phase chemistry run in a continuous way, and so I had a hunch that the next level move for surfactant chemistry was to apply it to flow. So, in November of 2016, I walked into Bruce's office and told him I had a golden idea; Bruce and I shared a knowing look that this was a high value project, one that I had no idea how I was going to pursue. However, Bruce jumped on the phone with Fabrice Gallou, who directed him to the chemists at the Cambridge, Massachusetts site who were doing some flow chemistry. Bruce stuck his head in Nick Lee and my lab and asked me if I was still interested in doing flow technology with surfactants. Of course, I responded in the affirmative, and he said that he might have a spot for me as an intern at the Novartis site in Cambridge to investigate this. There was some silence on this front for a little while, and I kind of forgot about it while focusing on my first-year duties. However, in March, Bruce asked again if I was ready to go and he said that we have the go-ahead to do the internship in Boston, if I was up to the challenge.

This was a dream come true, and in September of 2017 I embarked on probably the greatest adventure of my life. I had the opportunity to live in Harvard Square, right next to the Harvard campus, completely on Novartis's dime. I also had the opportunity to have facetime with very accomplished chemists at the Global Discovery Chemistry (GDC) group at Novartis and work on a plug flow (PF) project using surfactant and nanoparticles. Furthermore, our success in plug flow opened up a collaboration with Klavs Jensen's lab at MIT Chemical Engineering to

begin looking into a second-generation flow device in the form of a miniaturized cascading continuously-stirred tank reactor (CSTR), where I had the opportunity to work in their lab as well. These ultimately culminated into two publications, both in Green Chemistry, as well as a collaboration in the future with David Gunn at PHT to develop a flow instrument of our own use here at UCSB.

4.2 Introduction and Background

All chemists, from the undergraduate student to the seasoned industrial or academic scientist, are inherently aware of batch processing for synthesizing organic compounds. This is not surprising, as the barrier to entry for running reactions in batch is very low and typically requires only very cheap and easily sourced equipment in the form of vials or flasks on a small-to-medium laboratory scale. Indeed, a quick search for images of the alchemist, the closest pre-modern relative of the chemist, readily yields picturesque images of a bearded man hunched over some glowing or bubbling glass round-bottomed flask. In the vast majority of cases, chemical transformations are performed on both lab and industrial scale simply by adding substrates, reagents, catalysts, and solvent into a batch reactor container (glass, stainless steel, hastelloy, etc.) with some method of internal mixing, either by magnetic stir bar or motor-driven impeller, to promote agitation such that the kinetics of chemical reactions are not limited to diffusion. Therefore, a batch process can be thought of as a single, ever-evolving solution (*e.g.*, not at "steady-state") that is governed mostly by three main parameters: mixing, temperature, and time (Figure 1).[1] Being at unsteady-state implies that the variable parameters across time and space are not constant, and thus concentrations of starting materials, intermediates, and products are in flux, as well as potential temperature gradients throughout the reaction time.[2] This can be illustrated by the addition of a highly reactive organometallic reagent such as an alkyllithium dropwise to a stirred reactor containing substrate at cryogenic temperature, followed by warming to room temperature prior to a batch workup.[3]

While batch processes have been the gold standard in the pharmaceutical and agrochemical fields over the past *ca.* 100 years, the use of a large reaction vessel for scale-up purposes does come with various drawbacks.[4] The direct increase in reaction size can mean difficulty in

stirring heterogeneous reaction mixtures based on clumping not encountered on small scale, as well as settling of solid material in the reactor. Temperature gradients inside of the reactor can also pose issues on large scale, where uneven heat transfer from the outer walls of the reactor can result in difficulty in forming a homogeneously heated mixture. Large volumes of organic liquid material with inconsistent temperature (and dispersion of solids or undissolved reactants and catalysts, in some cases) can also result in reaction thermal runaways that can be highly destructive and have precipitated very dangerous situations.[5] Furthermore, industrial chemists have noted a general increase in total processing time from the lab scale to the production scale, in some cases due to heat transfer limitations, as well as other traditionally perfunctory steps such as drying which, on a lab scale may only take one hour, can require overnight processing to affect the same outcome on greater than kilogram quantities.[4] While not limited to these downsides, the overall outcome of an improperly scaled batch reaction can ultimately result in poor quality product which cannot be marketed.

A burgeoning alternative approach to running reactions in batch is to perform the chemistry under continuous manufacturing conditions, colloquially known as "flow" chemistry.[6] Continuous production is not new to massive chemical manufacturing, as the petroleum industry heavily relies upon related techniques to refine crude oil and gas into valorized material or commodities such as syngas, gasolines and fuels, asphalt materials, and naphtha.[7a-c] The scale of the raw material, and the demand of the resulting product,[8] necessitates the use of constant and mostly uninterrupted processing.

The basic "plug flow" (PF) process can be envisioned simply as a tube reactor, where on one end starting materials and reagents are added using pumps and on the other end the downstream product effluent is collected (Figure 1). The construction of this tube reactor is

highly flexible, allowing for facile assembly of various modules such as mixing ports, where reagents can be flowed together in microchannels to maximize interaction, heated or cooled areas, and maintenance of reactor pressure with the use of a variety of commercially available back pressure regulators which allow for superheating of the solvent and, thus, higher possible temperatures compared to their batch counterparts run at atmospheric conditions. The flow regime, therefore, is governed by three main parameters: flow rate (residence time of the material inside of the reactor), temperature, and pressure.[6]

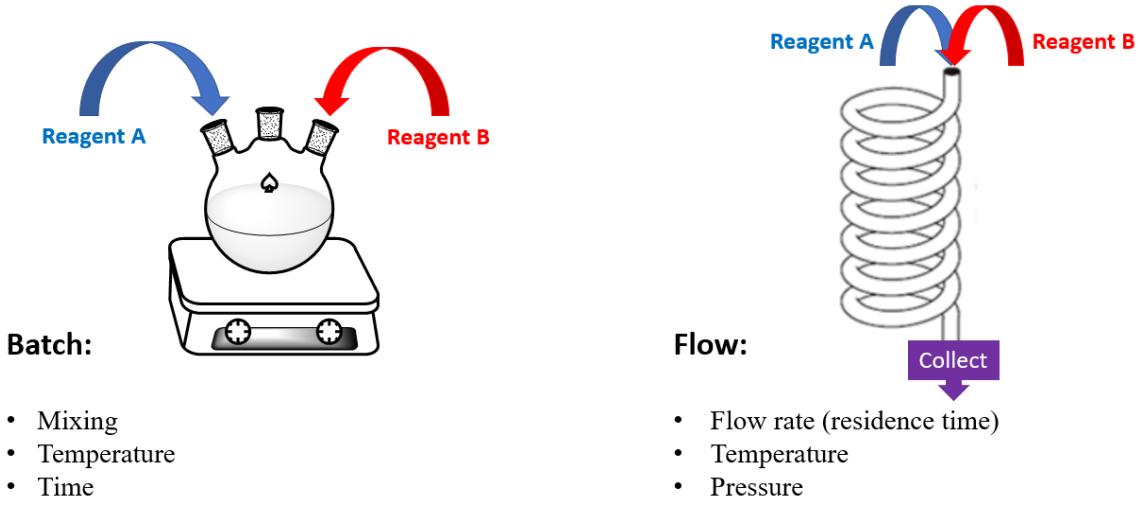

Figure 1: Batch vs. flow technology parameters (flow diagram image credit to © 2022 Silicycle)

Running under flow conditions allows for considerably improved reaction control, as only a small portion of the material is being operated upon at any given time. Many PF reactions are run in microchannels[9] (*i.e.*, tubes with internal diameters on the sub-millimeter scale), which provide many benefits to the chemical process of interest. These include improved heat transfer and control, where small amounts of solvent are heated and cooled nearly

instantaneously akin to microwave irradiation chemistry, enhanced mass transfer *via* fast, diffusion limited radial mixing in microchannels, safer containment of hazardous reagents *via* handling through pumps and automation, reduced reactor footprint (flow reactor with a small continuous working volume *vs.* a single large batch reactor), and less chemical waste produced not only from the reaction itself, but also from avoidance of cleaning and chemical transfer steps from a batch reactor.[10] Furthermore, achieving the steady-state functionality of a flow reactor, which is by definition impossible in a working batch system (*vide supra*), means that every unit volume inside the length of the reactor is equal to the last unit volume at that same space, and thus, each molecule reacts under the same conditions thereby providing better product quality control. These benefits ultimately place continuous manufacturing squarely within the purview of green chemistry technologies.[11]

It isn't until more recently (the last *ca.* twenty years) that there has been considerable interest from the fine chemical process[12] and medicinal chemistry[13] disciplines to embrace continuous manufacturing protocols at both the lab and production scale. Since adoption, however, use of flow chemistry has emerged as a disruptive technology in the field, and has enacted a sea change by which practitioners at any scale can target intermediates and active pharmaceutical ingredients (APIs). While the barrier to entry for a PF chemistry instrument is greater than that of a simple vial or flask batch reactor in a laboratory setting, a rudimentary setup only requires the procurement of pumps (in many cases, syringe pumps are sufficient), tubing of varying materials of construction (fluorocarbon tubing such as PFA, stainless steel, etc.), inexpensive nuts/ferrules and mixing channels such as tees or cross-mixers, and perhaps a back pressure regulator (BPR) depending upon need to pressurize the reactor.[14] The temperature of the tubular reactor can then easily be modified using a heated or cooled bath.

The short pathlength of the microchannels also lends itself well to photochemical applications, and thus the reaction coil can be constructed near or around an irradiation lamp of the desired light wavelength.[15] Microchannel reactor systems of smaller size exist, such as chip reactors (also known as "Lab-on-a-Chip"), as well as more involved reactors of greater scale from vendors such as Vapourtec[16] that boast all-in-one pump, reactor, and BPR containing systems that can also be purchased (Figure 2).

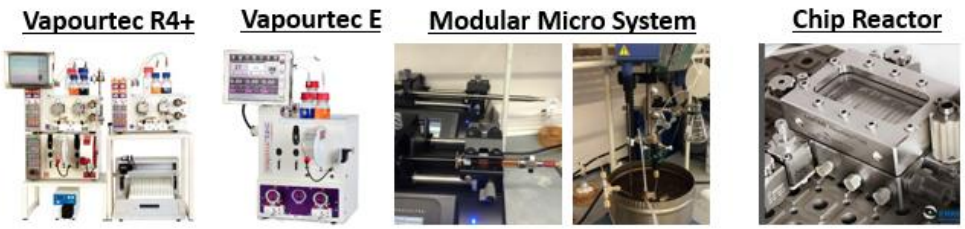

	Vapourtec R4+	Vapourtec E	Modular Micro System	Chip Reactor
Reactor Size	2-10 mL	2-10 mL	20 µL - 2 mL	100 µL
Productivity	200 mg – 10 g/h	200 mg – 10 g/h	2 mg – 2 g/h	1 mg – 200 mg/L
Application	Scale up	Photochemistry and Scale up	Reaction condition study, novel chemistry development	Reaction condition study, novel chemistry development
Features	Automation	Automation/ organometallics	Flexible	Mercury lamp for photochemistry

Figure 2: Large to microscale commercially available tubular flow systems (Vapourtec R4+[16a] and Vapourtec E[16b] image credit to © 2022 Vapourtec; chip reactor Lonza FlowPlate®, Ehrfeld Mikrotechnik[17])

Despite the powerful advancements made in the PF chemistry field over the past two decades, major problems still plague the technology which makes widespread adoption over the entirety of the chemical methodology space difficult. One issue is the inclusion or genesis of solids in tubular reactors that can induce clogging of the lines, which greatly limits the

amount of available chemistry using heterogeneous materials.[18] Given the narrow nature of microchannels, solid formation poses problems of clogging anywhere inside of the reactor, but generally with a greater chance at squeeze points or 90° turns where bridging of solids can result in a filtration mechanism and over pressurization.[19] The outcome of channel clogging may result in reduction in quality of product due to inconsistency of steady-state operation and conversion of starting materials, as well as safety issues due to complete reactor failure and difficulty in dislodging the solid mass from the reactor which can cause degradation or totaling of equipment.[20]

A variety of techniques have been developed in the field as a response to these clogging issues. With respect to basic tubular reactors, these strategies have been developed to reduce the overall investment into new and potentially expensive equipment, or modalities that would not directly correlate to the intended scaleup application of the system (*i.e.*, not in a PF regime). One such application is the use of sonicator systems, which serve to break up solid aggregates and maintain suspension in solution to avoid clogging.[21] Indeed, sonicators have worked well with aqueous nanoparticle systems (*vide infra*) to maintain well dispersed catalyst in solution prior to introduction into a tubular reactor using a syringe pump. However, an elegant solution to this issue is through the use of gas-liquid segmented flow.[22] This methodology utilizes the Taylor flow biphasic mechanism of segmented fluids in a tube of varying viscosities, where a flow is induced in the discontinuous phase such that a "churning effect" allows for the dispersion of solid particulates (Figure 3).[23] One particularly interesting account of this is from Seeberger, *et al.*[24] utilizing a nitrogen gas-liquid segmented flow for the photochemical decarboxylative fluorination of phenoxyacetic acid derivatives, where the formation of

churning serial micro-batch reactors (SMBRs) in flow allowed for the dispersion of a solid catalyst in an organic "slug" (Figure 3).

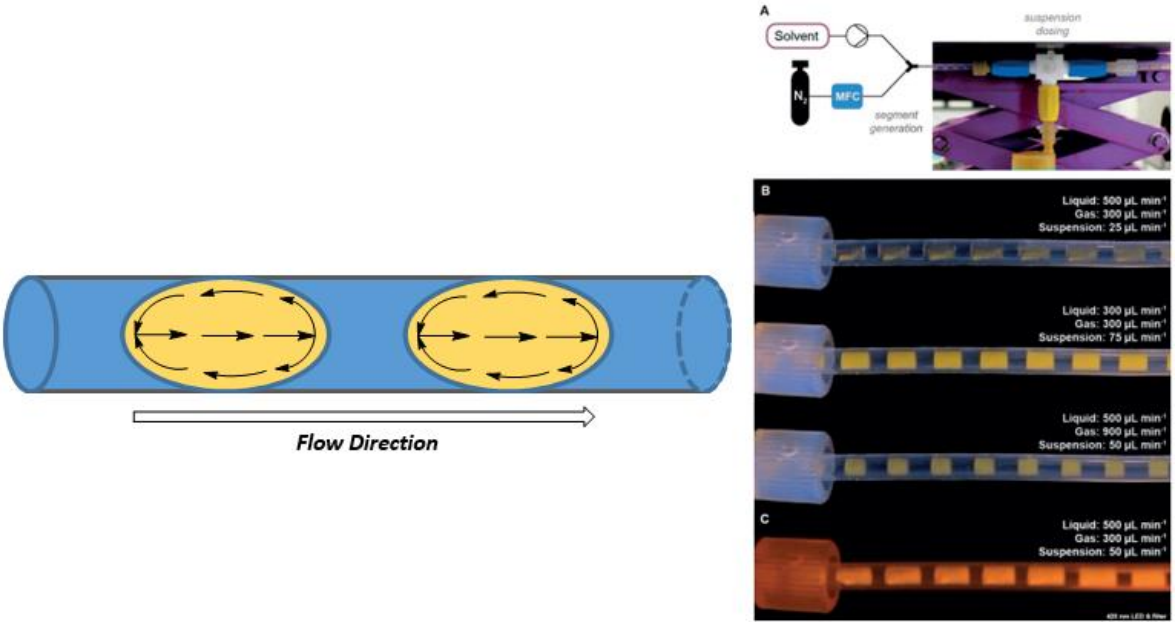

Figure 3: Taylor flow in a biphasic flow tubular reactor (left) and gas-liquid segmented churning flow for heterogeneous-catalyzed photochemical reaction (right)[24]

New equipment has also been developed both academically as well as industrially to solve the issues associated with the use of solids in flow. These reactors generally take advantage of some form of mechanical mixing to increase the cavity size of the reactor, while maintaining the continuity of the process. One such example is the Coflore system developed by AM Technology, which can be purchased on laboratory scale (30 mL working volume) or on production scale. This system utilizes a dynamic rotating/shaking block reactor with internal mechanical agitators in the form of stationary cylinders, where flow is directed through the block using pumps.[25] The materials of construction and the type of agitator can also be altered depending on the solvent required for reaction (Figure 4).

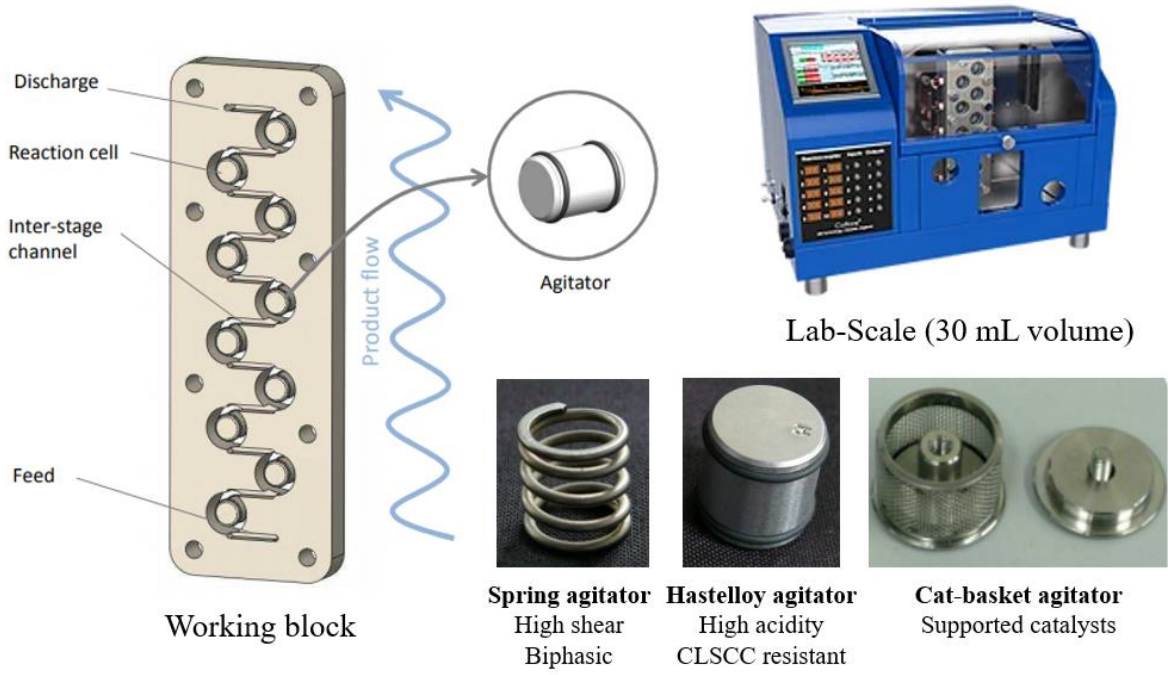

Figure 4: Laboratory scale Coflore system[26]

Another entry into this category is the use of a continuous-oscillatory baffled reactor (COBR) system.[27] This uses a tubular reactor that is baffled throughout with a piston that pumps in parallel to the net flow of the reaction stream. This induces churning eddy currents within the open chambers formed from the baffles and allows for significantly larger tubing to be used without loss of mixing capabilities (Figure 5). This system has been used not only for reactions, but also for continuous crystallization processes where the crystal size can be controlled based on its location in the steady-state tube reactor.[28]

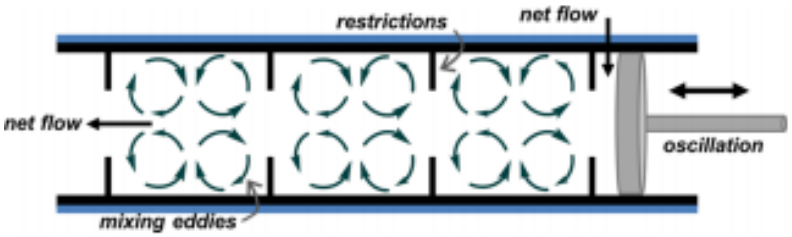

Figure 5: Section of COBR tube including baffles and oscillating pump[27]

The continuous-stirred tank reactor (CSTR) is a fundamental reactor type in the field of chemical engineering, and has had applications to pharmaceuticals, agrochemicals, and polymers.[29] While a single CSTR can be sufficient, the efficacy of a CSTR system can be enhanced by placing multiple reactors in series (cascading), the resulting kinetics of which begin to resemble that of a PF reactor, and multiple reactors mitigate the possibility of non-ideal hydraulic behavior of short-circuiting and dead space phenomena.[30] Until recently, CSTR systems have been relegated to large scale processing; however, Jensen *et al.* in 2016 and 2018 developed cascading reactors for solid-forming[31] and biphasic[32] reactions, respectively, that operate on the laboratory scale (Figure 6). These miniaturized systems have revolutionized the amount and quality of data that can be developed on lab scale that is used directly to influence the behavior of a cascading CSTR reactor at scale, including reactions that contain or generate solids *in situ*.

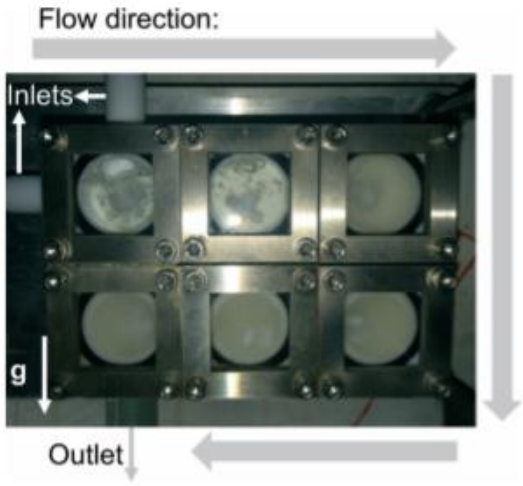

Figure 6: Miniature cascading CSTR reactor block that can handle solids in flow[31]

Given the vast advancements in aqueous micellar catalyzed chemistry within the past decade,[33] the next logical step from a technology standpoint is exploration into the capacity for surfactant-based flow chemistry. However, a dearth of information in the literature exists for such an applied science. This is due to the issues of solids handling in flow, where the inherent insolubility of organic reagents, products, and, in some cases, heterogeneous catalysts pose an issue from a clogging standpoint. Therefore, a major engineering feat for micellar catalysis is the study and development of new solids handling equipment that can enable this chemistry in continuous manufacturing platforms. Herein are described two systems that accomplish this goal: firstly, a PF system was achieved utilizing aqueous chemistry with a heterogeneous metal catalyst using both a commercially available reactor as well as a specially fabricated back pressure regulator (BPR); secondly, a (previously reported[34]) next generation miniature cascading CSTR module was developed to handle the same chemistry for the synthesis of advanced pharmaceutical intermediates in some cases *utilizing no working organic solvents for the flow chemistry process*.

4.3 Results and Discussion

In order to completely test the equipment advancements for solids handling required for aqueous micellar catalysis in flow, a reaction needed to be chosen to best reflect insolubility of starting materials, products, as well as catalyst. Reactions involving gas formation were avoided for these initial studies, as in the case of Fe/ppm Pd + Ni nanoparticle (NP) catalyzed aryl nitro group reductions in water,[35] where pockets of gas in PF and CSTR instruments would cause issues with back pressure regulation as well as inconsistency of residence time. However, initial trials on the formation of active NPs in flow, where the pre-formed Fe/ppm Pd + Ni NPs are mixed with a stream of dissolved sodium borohydride, appeared to form the black active catalyst well in line, and thus remains an option to be explored in later developments. Instead, NP-catalyzed Suzuki-Miyaura couplings[36] to form biaryl compounds was chosen for the embarkation point for surfactant chemistry in flow, as the reagents and especially the products and catalysts would inherently be insoluble in the aqueous media. Furthermore, the increase in temperature control afforded by steady-state flow chemistry would also allow for previously unreported studies of hot aqueous surfactant catalysis, where TPGS-750-M is empirically known to alter its morphology at 70 °C from micelles to an array of vesicles and sheets.

Given the chosen chemical transformation, the kinetics of such a hot aqueous micellar NP system needed to be determined in batch prior to running in flow. Microwave chemistry is known to best approximate flow conditions based on its ability to quickly heat and cool, as well as maintain internal pressure. Thus, a batch reaction of 4-bromoanisole and 1-naphthaleneboronic acid was chosen using 800 ppm Fe/ppm Pd-SPhos NPs at 0.5 M global concentration to form biaryl compound **2**. The thermal profile of the reaction needs to be elevated to a high temperature because the nature of flow chemistry requires fast reaction times

to maintain good productivity, and published reactions in batch require 24-72 hours at 45 °C. Thus, this reaction was performed at 95 °C, which was found to be the upper temperature limit for TPGS-750-M; greater than or equal to 100 °C results in precipitation of a gummy material assumed to be undispersed surfactant. Microwave irradiation of this reaction mixture for 15 min at 95 °C resulted in complete conversion by UPLC-UV/Vis analysis, and simple extraction with ethyl acetate and passing the crude organics through a plug of silica gel afforded the desired biaryl compound **2** in 89% isolated yield (Figure 7), compared to the 91% isolated reported yield in 24 hours reported in the original publication.[36]

With sufficient kinetics and comparable yield in hand, a rudimentary PF system was developed to test parameters required to flow the aqueous/NP Suzuki-Miyaura reaction. Initial analysis of the NP slurry found that the particles could easily be suspended for greater than two hours in the micellar medium (without substrate present) after sonication for *ca.* 20 minutes; the NP suspension time could then be increased indefinitely with mechanical stirring. Thus, running short trials with a syringe-driven PF reactor could be possible on small scale. However, scaling such a reaction would require the use of a much larger system with equipment that could handle slurries and small aggregates of inorganic or organic material over an extended reaction period. Thus, the Vapourtec E-Series[16b] was explored to act not only as a delivery system, as the peristaltic pumps have large bore tubing (1/8" OD, 1/6" ID) that are marketed to handle solids in flow, but also as the heating element for the flow reactor, the thermal well temperature of which can be programmed and monitored by an automated computer system. Furthermore, and quite serendipitously, the Vapourtec E-Series had recently been upgraded with a software patch that allowed for the peristaltic pumps, when run in

reverse, to act as a large bore BPR for up to 10 bar, which could handle solids in downstream processing.

To test "flowability", a 2 mL batch-to-flow aqueous NP Suzuki-Miyaura reaction was set up initially in a 2-dram vial with mechanical stirring. It was found quickly that the starting reagents to form **2** would quickly coagulate in a purely 2 wt % TPGS-750-M/H_2O system, and thus 20 v/v % THF was found to nicely disperse the reaction with light stirring. This reaction was then pumped into a 10 mL, 0.03" ID reaction coil set to heat to 95 °C with a flow rate of 0.667 mL/min, resulting in a 15 min residence time in comparison to the batch reaction. The reaction "slug" was bracketed on both the front and back ends using an 80% TPGS-750-M/20% THF mobile phase to ensure that the reagents remain suspended in the reaction mixture. After a 15 minute residence time, the entire coil was then quickly extracted using ethyl acetate flowing at 2 mL/min for 10 minutes to recover all organic material. Upon purification, the resulting isolated yield of the coupling product was found to be 72% in flow, which is comparable to the batch reaction given the possibility of dilution on the front and back ends of the reaction slug (Figure 7).

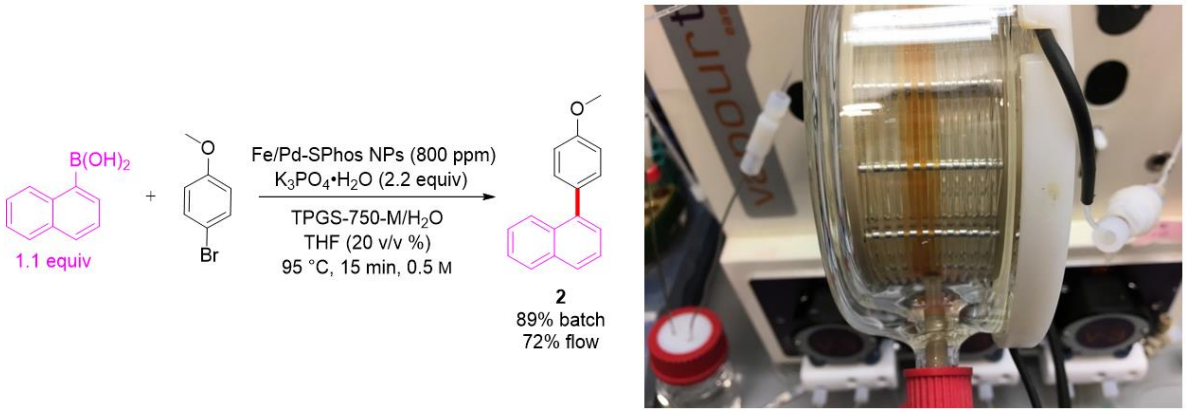

Figure 7: Reaction scheme for batch-to-flow reaction (left) and aqueous NP slurry in flow (right)

While this initial aqueous micellar flow reaction was successful, some problems were encountered during initial trials. Firstly, there is no apparent benefit for studying a flow reaction where the catalyst and reagents are mixed and then are flowed into the reactor, especially when the reaction works well in batch as is and some product is formed in the interim period. It should also be noted that the introduction of base to the catalyst results in aggregation of the NPs, an observation not made on laboratory batch scale due to mechanical stirring. Therefore, a system was developed (*vide infra*) that segregated the components into homogeneous solutions such that there was constant and even introduction of material in the tubular reaction without any prior reaction. This included separating the NPs dispersed in surfactant solution, the base dissolved in water or as a neat material, and the organic reagents dissolved in a green, water-soluble organic co-solvent. The arrived upon co-solvent was tetrahydrofurfuryl alcohol (THFA), which is a product of the reduction of furfural from woody biomass and is, as such, a renewable solvent. THFA has a high boiling point which does not increase the back pressure requirements from the system, dissolves the starting reagents well (even at high concentrations of >1 M), and can easily be separated from the crude organics by dissolution in excess water. Ethanol was also found to be a competent organic co-solvent for many of the same reasons; however, the low boiling point greatly increases the pressure of the reaction and thus decreases the available back pressure window provided by the peristaltic pump BPR. Secondly, insoluble nanoparticles, as expected, were found to be filtered out at switching valves and 90° turns (Figure 8), and thus these needed to be avoided, and the reverse peristaltic pump BPR was found to be crucial to avoid clogging. Thirdly, studies using larger reaction slugs without hot organic extraction of the reaction coil resulted in phasing out of the biaryl organic product from the surfactant and, at room temperature, crystallization in the lines

resulting in complete reactor failure (Figure 8). Thus, a heated in-line extraction tee was constructed in the thermal well using a green organic solvent, in this case 2-methyltetrahydrofuran (2-MeTHF) to continuously perform hot extraction prior to cooling of the line entering the BPR.

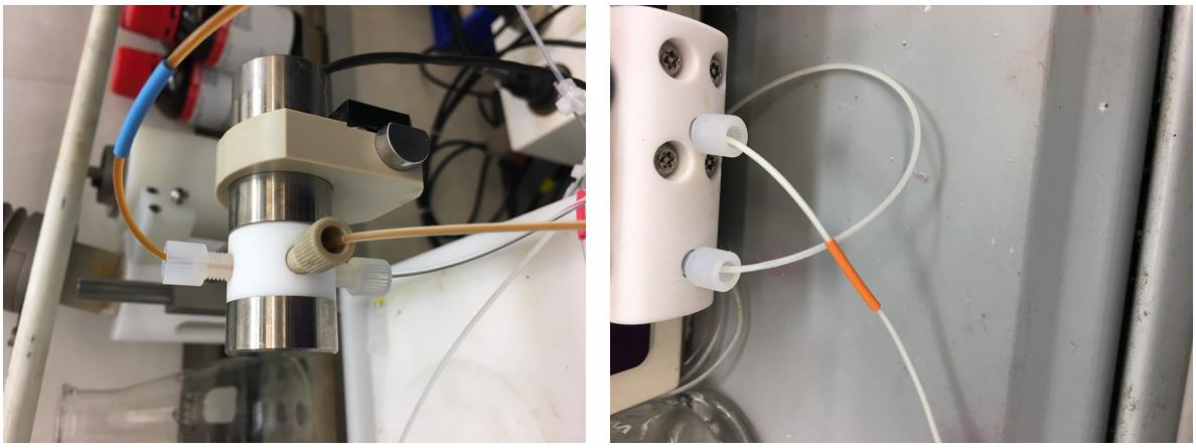

Figure 8: Filtering of NPs in line at switching valves and 90° turns (left) and crystallization of organic product in line at BPR (right)

Given these key observations, a small scale 2 mL reaction coil (PFA, 0.03" ID) was constructed using the Vapourtec E-Series equipment to evaluate aqueous micellar NP-catalyzed chemistry in flow using aqueous soluble base, in this case being K_3PO_4•H_2O (Figure 9). An initial trial was run on the coupling of 4-bromoanisole with phenylboronic acid to form product **1** in flow. This product was chosen as the first candidate due to the relatively low melting point (*ca.* 90 °C) which is below the reaction temperature and thus eliminates precipitation of solid product inside of the reactor as a potential failure point. In this case, NPs were suspended in 4 wt % TPGS-750-M/H_2O using sonication at a concentration of 50 mg/mL. This stream would be diluted with a 1.78 M solution of K_3PO_4•H_2O in water at an equal flow rate, resulting in 25 mg/mL catalyst in a global 2 wt % TPGS-750-M/H_2O solution.

Concentrated organics pre-dissolved in THFA at a precisely known volume are then introduced into the reactor such that the total volume of THFA is considerably below 20 v/v % of the total reactor effluent (considering the volume taken by the reagents during the dilution process). Each of these streams was introduced into the reactor coil using stainless steel syringes and Harvard Apparatus syringe pumps, the material of construction of which and the brand of pumps were both found to be crucial for high pressure applications (Figure 10).[37] The reagents are then allowed to react at 95 °C in the reactor coil and are subsequently extracted in-line using 2-MeTHF at an equal flow rate at a 90° angle and allowed to extract in a 50 cm extraction coil prior to the peristaltic pump BPR.

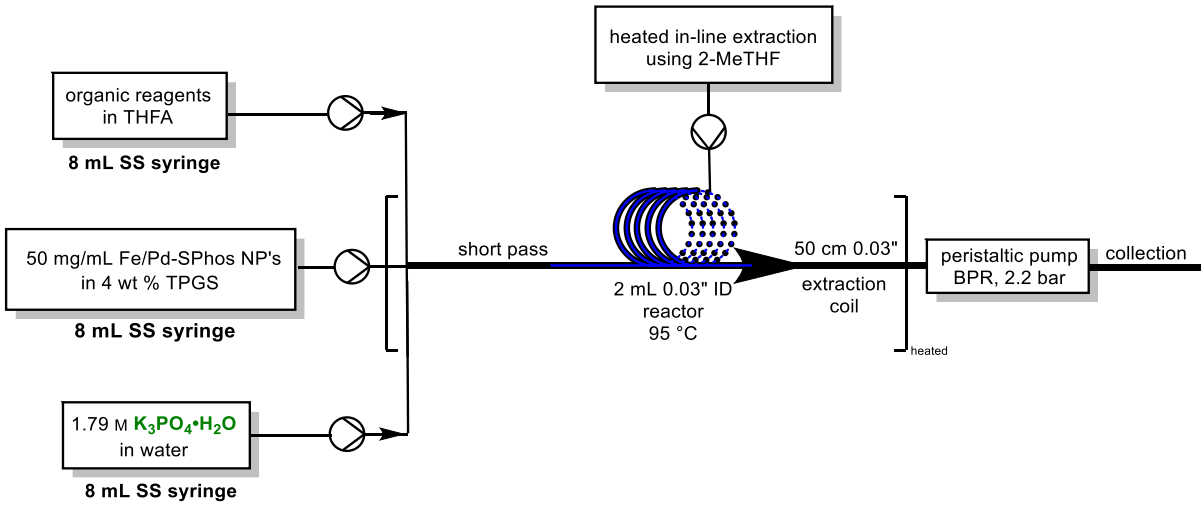

Figure 9: Water-soluble base PF instrument

Workup of the flow reaction was found to be facile, as the extracted organics can be separated followed by evaporation and recollection of the 2-MeTHF resulting in a crude organic oil, followed by removal of the THFA by dissolving the mixture in water followed by filtration. Passing the organics through a silica gel plug resulted in product in very high purity.

In the case of **1**, the yield of the reaction was found to be 97% with a 10 min residence time, resulting in a productivity of 517 mg/h on a 2 mL scale. The use of this apparatus was applied to the synthesis of **2** which provided the product in 88% yield in flow in only 2 minute residence time, despite the product's high melting point, compared to the 89% yield in batch, as well as compound **3**, which is an oil of low viscosity at room temperature, with no collection problems encountered within the 10 minute residence time (Figure 10).

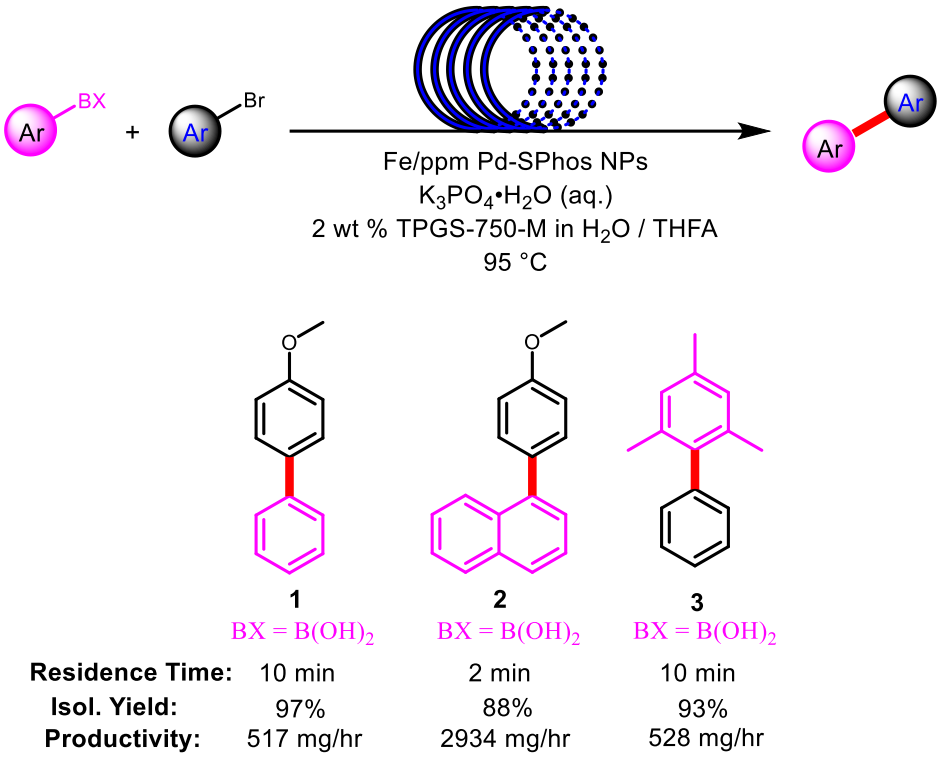

Figure 10: Substrate scope for aqueous micellar NP catalyzed couplings using aqueous-soluble base

Despite the success of this initial flow instrument for NP/micellar catalyzed couplings, the system did have some problems associated with the selection of base. The inclusion of $K_3PO_4•H_2O$ results not only in poor solubility of the reagents and products, resulting in some

crystallization problems in-line, but also the solubility of the surfactant itself which is not encountered on a batch scale. Indeed, introduction of the phosphate base results in a gummy precipitate similar to overheating the aqueous mixture to 100 °C, which reduces the solubilizing properties of the micellar medium. Ultimately, the combination of these issues results in reactor clogging, especially when compounds of higher melting points or crystallinity were attempted, as in the case with biaryl product **4**. Therefore, an improved system was developed using liquid organic base triethylamine (TEA), which serves to act not only as base, but also potentially as a competent organic co-solvent to maintain solution at high temperatures. Separation of the base and NPs was maintained, as even the introduction of TEA to the NP mixture resulted in aggregation of the catalyst. Based on this, the NP concentration could be reduced from 50 mg/mL to 28.5 mg/mL, and the resulting surfactant concentration could be reduced to 2 wt % TPGS-750-M/H_2O. Based on the volume and flow rate required for the surfactant phase, the Vapourtec E-Series peristaltic pumps were used to deliver the NP/surfactant slurry maintained in suspension with stirring. Organic reagents in THFA and neat TEA could then easily be delivered using syringes into the same 2 mL reactor coil as well as the same 2-MeTHF extraction line (Figure 11).

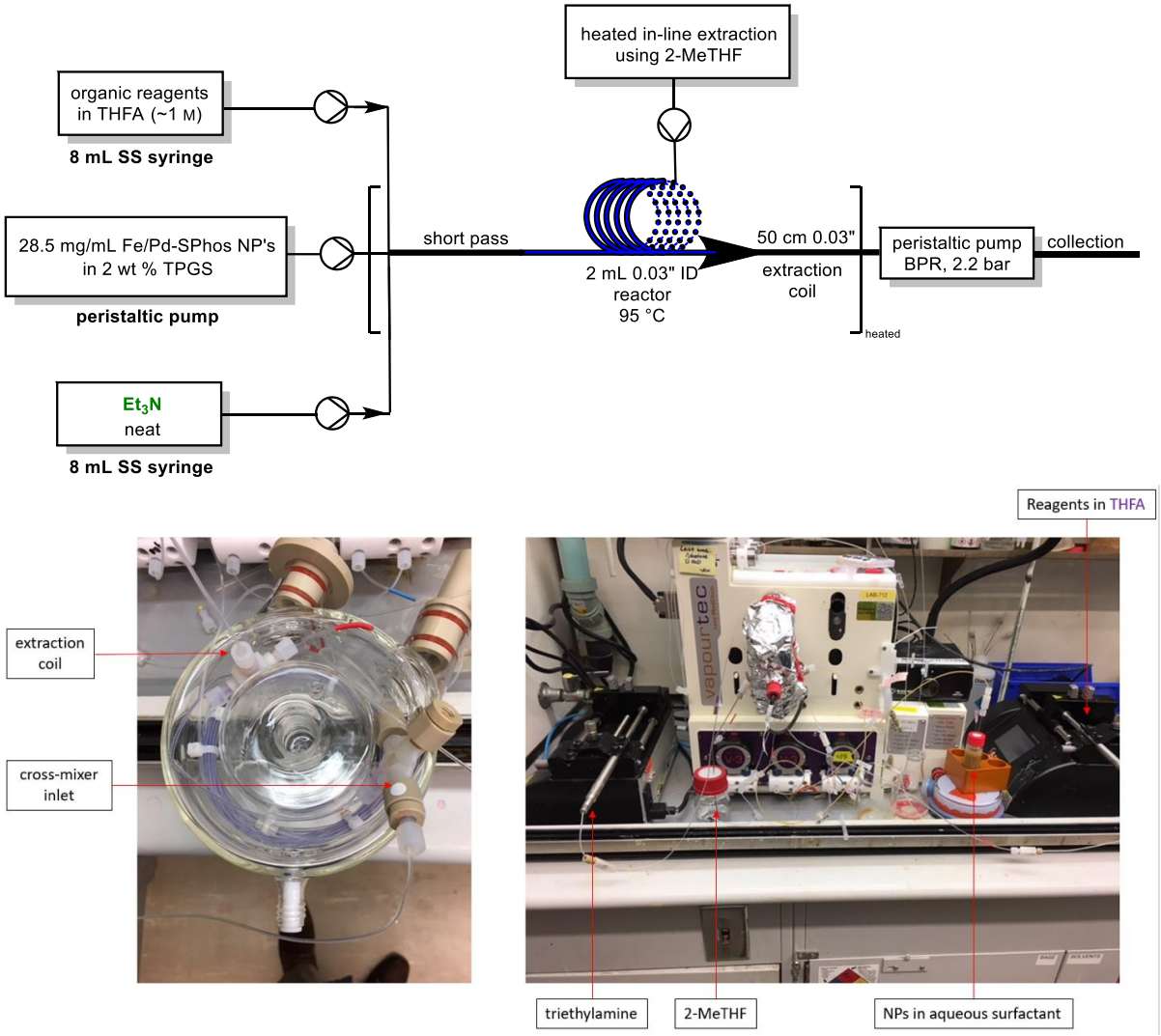

Figure 11: Diagram of organic base PF system (top), packed heating cavity containing cross-mixer inlet, reactor, and extraction coil (bottom left), and constructed flow system (bottom right)

With this new setup, three more products were prepared in aqueous micellar flow using the NP catalyst (Figure 12). Product **4**, a crystalline biaryl carbamate that clogged the phosphate base system, was prepared in nearly quantitative yield at 95 °C in an 8 minute residence time with no observed deprotection of the Boc protecting group. Product **5**, prepared from the coupling of the vinylboronic acid pinacol ester with bromobenzene, was prepared in 80% yield

within a 10 minute residence time as a yellow solid despite the high temperature of reaction. Biaryl compound **6**, a precursor to a NEP inhibitor API, was also synthesized in a very high yield of 91% with no observed byproduct of coupling with the aryl chloride. Interestingly, under reaction conditions a small amount of the THFA acetal of **6** was formed which had to be removed using an acidic batch workup. While not included in this work, it is theorized that an acidic aqueous workup stream prior to extraction at reaction temperature would result in an in-line purification system that would yield the aldehyde directly.

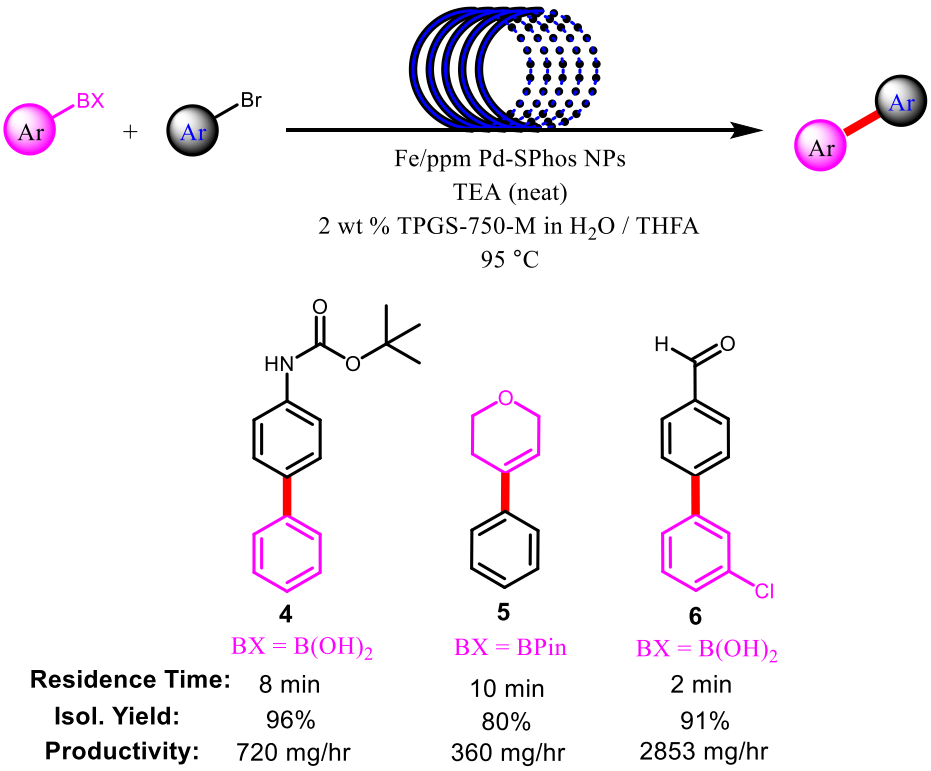

A major hurdle for the development of a fully automated flow system is the ability to scale not only to size, but also to production capacity over an extended period. Therefore, the final stage of research focused on the five times scale up of the reactor from a 2 mL coil to a 10 mL reactor coil. In this situation, a pre-woven PF reactor of the same ID (0.03”) as the smaller

scale reactor was used. The goal was to replicate the synthesis of the NEP inhibitor precursor **6** over the course of a 90 minute total production time, resulting in a theoretical >20 g of product (Figure 13). Due to the volumes and flow rates required for such a scale, all three peristaltic pumps from the Vapourtec E-Series were used to deliver reagents into the reactor system. The inlet cross mixer as well as the extraction inlet were adhered to the reactor coil inside of the heated reactor cavity, and thus aluminum foil was required to maintain reaction temperature.

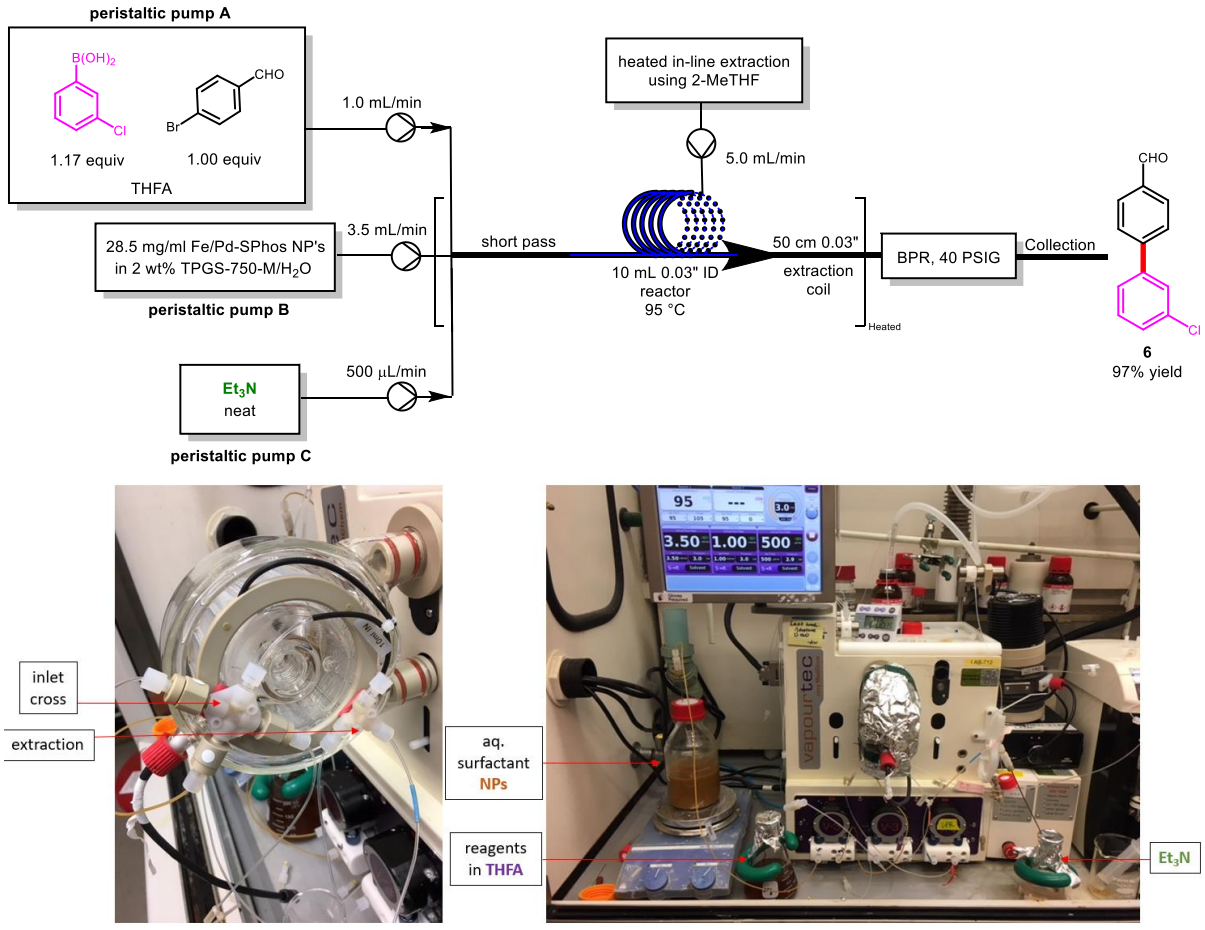

Figure 13: Diagram of large-scale PF reaction of **6** (top), inlet cross and inline extraction tee on reactor coil (bottom left), constructed reactor (bottom right)

The 2-MeTHF was constantly introduced into the reactor using a dual-infusion pump at high velocity (5 mL/min). The large-scale reactor pressure was retained by utilizing a new clog resistant BPR system developed by a mechanical engineering group from the Genomics Institute of the Novartis Research Foundation (GNF). This system was comprised of a nitrogen gas pressurized (40 PSIG in this case, the instrument can handle up to 100 PSIG) stainless-steel bomb container (185 x 145 x 145 mm) fitted internally with a 150 mL glass beaker, and the gas pressure was used to maintain back pressure throughout the entire reactor. Reactor effluent fed from the extraction coil was pumped into the 150 mL glass beaker inside of the stainless-steel shell utilizing a 1/16" ID tube. The volume of the liquid inside of the beaker is monitored using a sonic liquid level detector. When the liquid level passes the volume of the suspended sensor inside of the beaker, a valve actuates which uses the gas pressure to push the collected reactor effluent out of the beaker through a separate 1/16" ID tube into a larger collection vessel at a rate of 20-40 mL/sec (Figure 14).

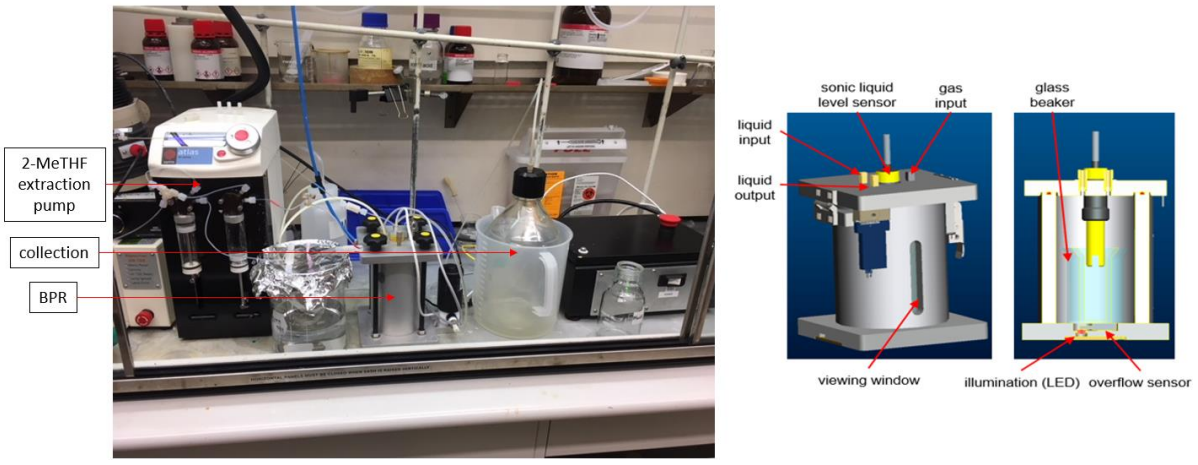

Figure 14: Downstream system consisting of 2-MeTHF pump, BPR, and collection unit (left), drawings of BPR system (right)

This scaled up reactor system was able to perform well over the course of a 90 minute total production time for a reaction that requires only a 2 minute residence time. The total yield, after acidic workup and column purification, resulted in **6** in 97% overall isolated yield, or 22.8 g of product. The 2-MeTHF used as extraction solvent was mostly recovered via distillation. The NP slurry in water could easily be separated as well; however, attempts to reuse the aqueous NPs yielded no reaction to form **6** on both flow and microwave batch systems. However, in a separate study, it was found that the introduction of new phosphine ligand to the now inactive NPs can result in rejuvenation of the catalyst, and thus this could be a viable pathway in the future for a fully recyclable Suzuki-Miyaura flow system.[38]

While this PFR system was able to continuously produce NP-catalyzed biaryl couplings in flow in an aqueous environment, it was determined that a second-generation reactor would need to be developed to overcome certain otherwise unsolvable issues encountered in PF. These issues mostly centered on the consistency and reliability of the system to avoid problems, *e.g.*, reactor pressure-spikes stemming from partial or complete clogging of the system. Unfortunately, the size limitations of the reactor itself (0.03" ID PFA tubing), as well as the junction pieces including the cross-mixer and the in-line extraction tee, would become blocked at random times during the reaction, most likely due to agglomeration of NPs or due to the precipitation of reagents or products, especially in the case for more crystalline biaryl products such as **4**. The size of the inner diameter of the tubing could also not be increased because this would result in NPs losing suspension in solution, especially when in the presence of base, which would cause them to form aggregates (*vide supra*). Therefore, it was essential to design a cascading CSTR system with agitated reaction wells to handle partial insolubility

of reagents and catalyst, and hence, would serve as a next generation continuous flow system for aqueous-based chemistry.

The CSTR cascade was designed by the Jensen lab at MIT Chemical Engineering to be able to handle slurries with considerably large aggregates of solids, especially in the case of organic materials that exhibit poor emulsification with the aqueous surfactant bulk stream. These features, along with mechanical stirring within the wells using small stir bars, would obviate the need for small inner diameter tubing required in PF for adequate mass transfer and would greatly reduce the potential for blockage in the reactor. We also surmised that the low surface tension of polytetrafluoroethylene (PTFE) would serve well as a material of construction for the working reactor piece where the reaction takes place, as there would be less chance of agglomeration of organics or, in this case, heterogeneous NP catalyst while still withstanding the high temperature of the reaction. The newly engineered cascading CSTR[34] consists of a PFTR reactor block, an aluminum chassis which houses the reactor block, a window that can either be fabricated out of aluminum or, in the case where photoredox chemistry is required, polycarbonate protected with a transparent FEP adhesive for chemical resistance,[39] and two covers which serve to seal the reactor with M4 bolts using a Viton O-ring gasket which fits into a groove constructed into the PTFE reactor (Figure 15). The aluminum and PTFE pieces were designed in SolidWorks and CNC milled by ProtoLabs, and ports are threaded to standard ¼-28 IDEX fittings, like that for an HPLC. The combination of an aluminum frame and PTFE inlay allows for optimal heat transfer and stability for harsh chemical environments.

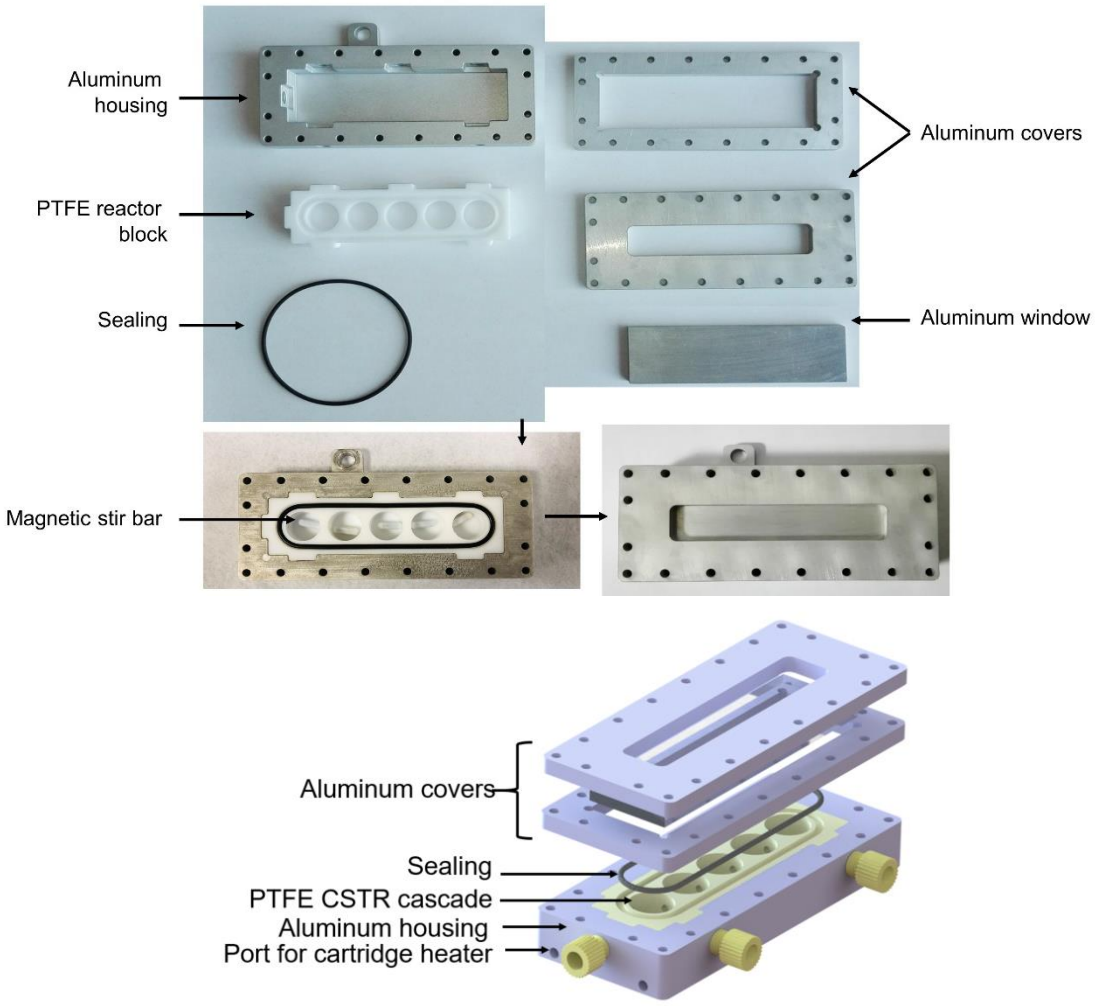

Figure 15: Separated CSTR pieces and constructed apparatus with aluminum window (top), exploded diagram of the CSTR (bottom)

Reactions performed in the CSTR were small enough scale that reagents could be pumped into the reactor using stainless steel syringes (20 mL). Catalyst slurry in aqueous micelles could be kept as homogeneous simply by adding a stir bar to the syringe body and suspending a stir plate upside down and above the syringe in the syringe pump, using mechanical stirring to maintain suspension of the particles. Prior to the CSTR, a small oscillator was also installed to maintain the homogeneity of the slurry mixture. Starting material streams are combined in the

first well of the CSTR reactor, rather than by use of tees or cross-mixers, to avoid potential clogging issues with catalyst agglomeration or partial insolubility of the reagents. Prior to running the reaction, the entirety of the reactor is filled with argon purged water and heated to temperature, and the reagent pumps were then allowed to displace this water and the reactor was run for three residence times prior to collection to achieve steady-state operation. As in the PF system, downstream material exiting the fifth CSTR chamber was insulated to maintain high temperature (90-95 °C) prior to being extracted with an equal flow rate of 2-MeTHF prior to reaching the BPR. The BPR in this case was the BP-10 obtained from Zaiput Flow Technologies and maintained a reactor pressure of 30 PSIG using inert case monitored by a pressure controller.[40] Temperature was monitored using a K-type thermocouple[41] drilled into the aluminum chassis and kept in place using thermal epoxy, and heating filaments[42] drilled into four corners of the apparatus were controlled using a PID controller from J-KEM (Figure 16).[43]

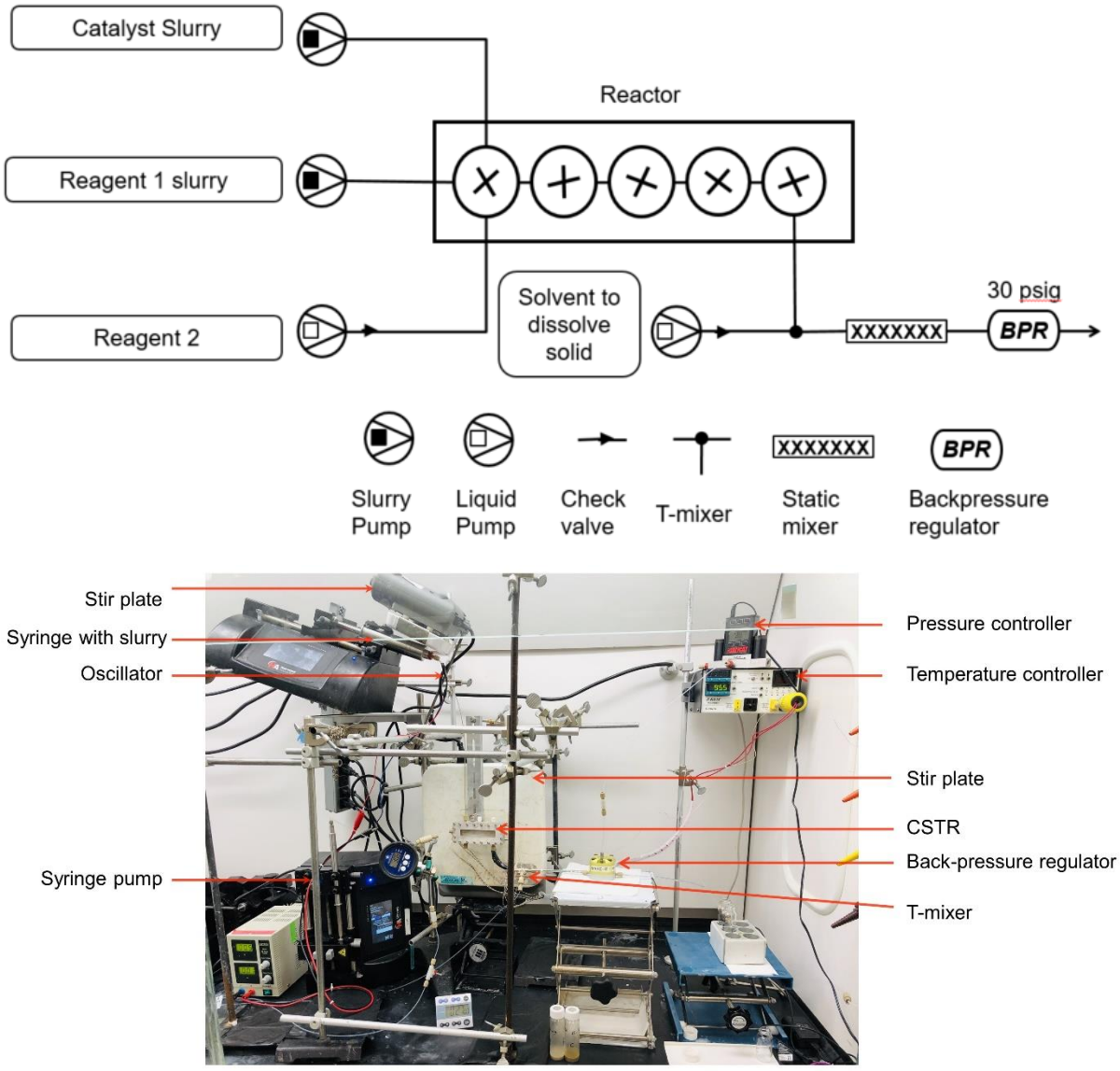

Figure 16: Flow diagram of CSTR system (top), constructed system during a run (bottom)

To first test this system, the same model biaryl **1** was synthesized using slightly modified conditions. The temperature of the reaction was reduced from 95 °C to 90 °C and the residence time was increased to 20 minutes to account not only for that temperature change, but also the wider array of retention times inherent to a CSTR system (Figure 17). Product **1** could be prepared in 81% yield upon isolation after 2.5 total residence times were collected which, while

not entirely consistent with the 97% yield afforded via plug flow, was a very encouraging starting point for this new technology. Most importantly, the issues encountered using phosphate base were rendered moot using this system due to the increased reaction cavity size as well as mechanical stirring. To introduce 4-bromoanisole and phenylboronic acid into the reactor, in this case, THFA was used as a carrier organic co-solvent, much in the same way as used in the PF reactor system.

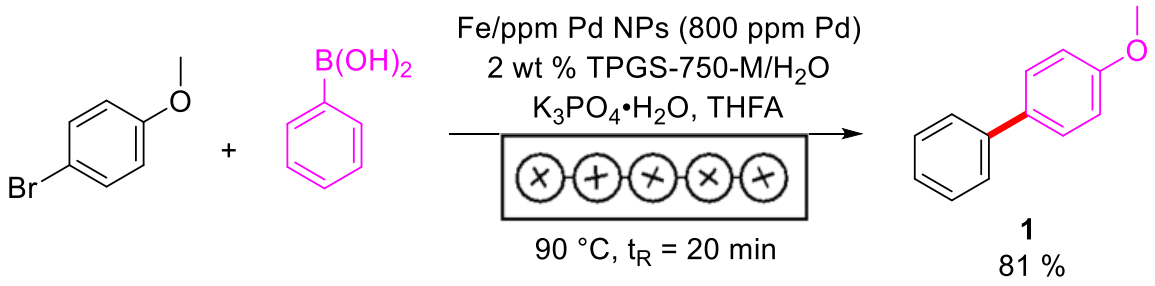

Figure 17: Synthesis of **1** in cascading CSTR using aqueous soluble base

Emboldened by these advancements in aqueous micellar NP catalyzed chemistry in flow, the next goal was to synthesize pharmaceutically relevant molecules, *i.e.*, intermediates *en route* to target APIs. The first entry into this research was the synthesis of the biaryl building blocks used to prepare sartans used to treat hypertension. Indeed, losartan (**7**), valsartan (**8**), and olmesartan (**9**), amongst others, are all placed in the top 200 selling drug products of 2018, and thus, are high value targets.[44] Therefore, the common biaryl motif between these compounds of **10**, prepared by Suzuki-Miyaura coupling between 2-bromobenzonitrile and *p*-tolylboronic acid, was explored as another simple example. In this situation, no carrier solvent was required for the introduction of these starting materials into the reactor, as the reagents could be nicely suspended in a stirred "slurry pump." The reaction was run under the same

conditions as used in the synthesis of **1**, arriving at compound **10** in 95% isolated yield utilizing no organic solvent, exemplifying the power of the CSTR platform for aqueous micellar chemistry (Figure 18).

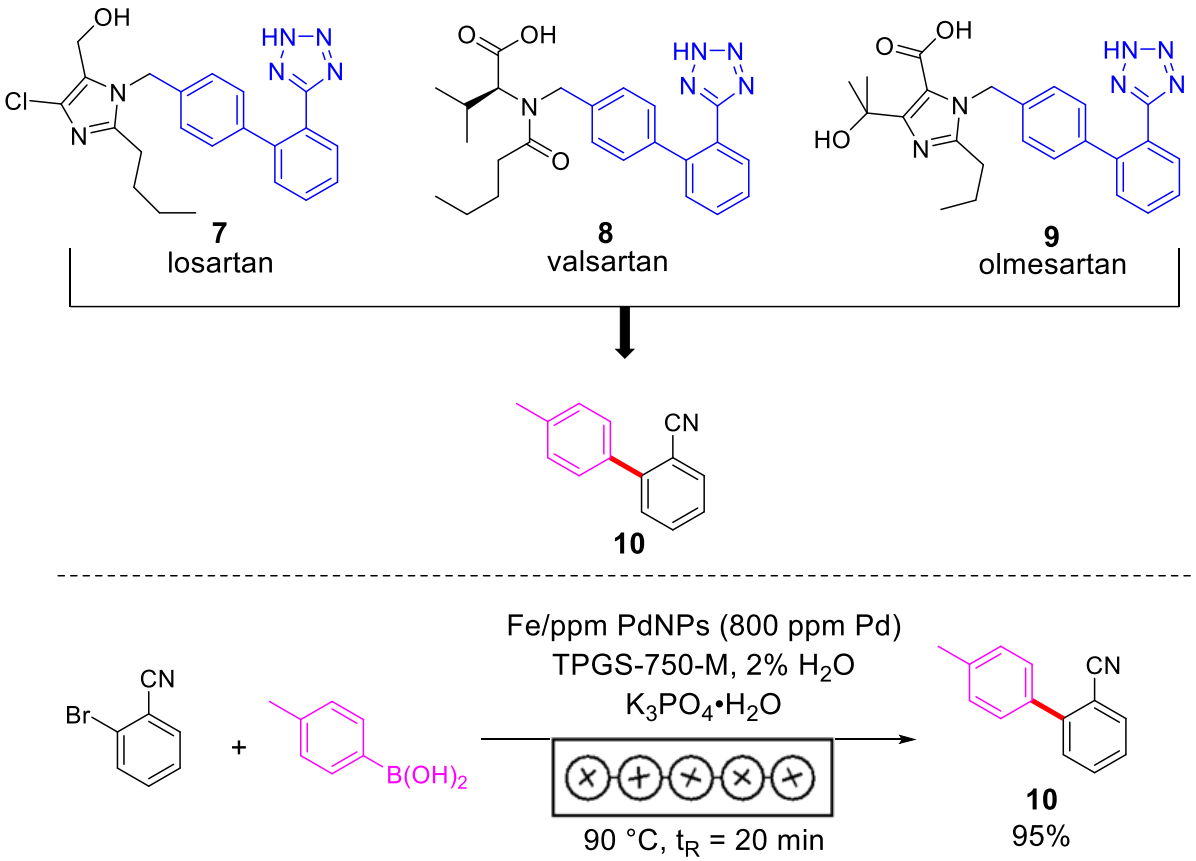

Figure 18: Sartan drugs bearing substructure precursor **10** (top), synthesis of **10** using CSTR platform (bottom)

Another drug subset of interest included JAK inhibitors, which are quickly dominating the tyrosine kinase inhibitor pharmaceutical market. Indeed, ruxolitinib (**11**) is ranked within the top 150 pharmaceuticals by sales in 2018,[44] and this class also includes baricitib (**12**) and itacitinib (**13**). A common motif exists between these drugs in the form of compound **16**, the

synthesis of which can be realized by the Suzuki-Miyaura coupling between benzyl protected chloride **14** and boronic ester **15**. This chemistry was subjected to CSTR flow conditions, and it was found that TEA was the optimal base for this transformation at 95 °C. The starting materials were suspended in aqueous micelles in the presence of the NPs at room temperature prior to being introduced into the hot reactor. The amount of Fe/ppm Pd-SPhos NPs was held at 800 ppm Pd, which yielded biaryl product **16** in 82% isolated yield with a 20 minute residence time (Figure 19).

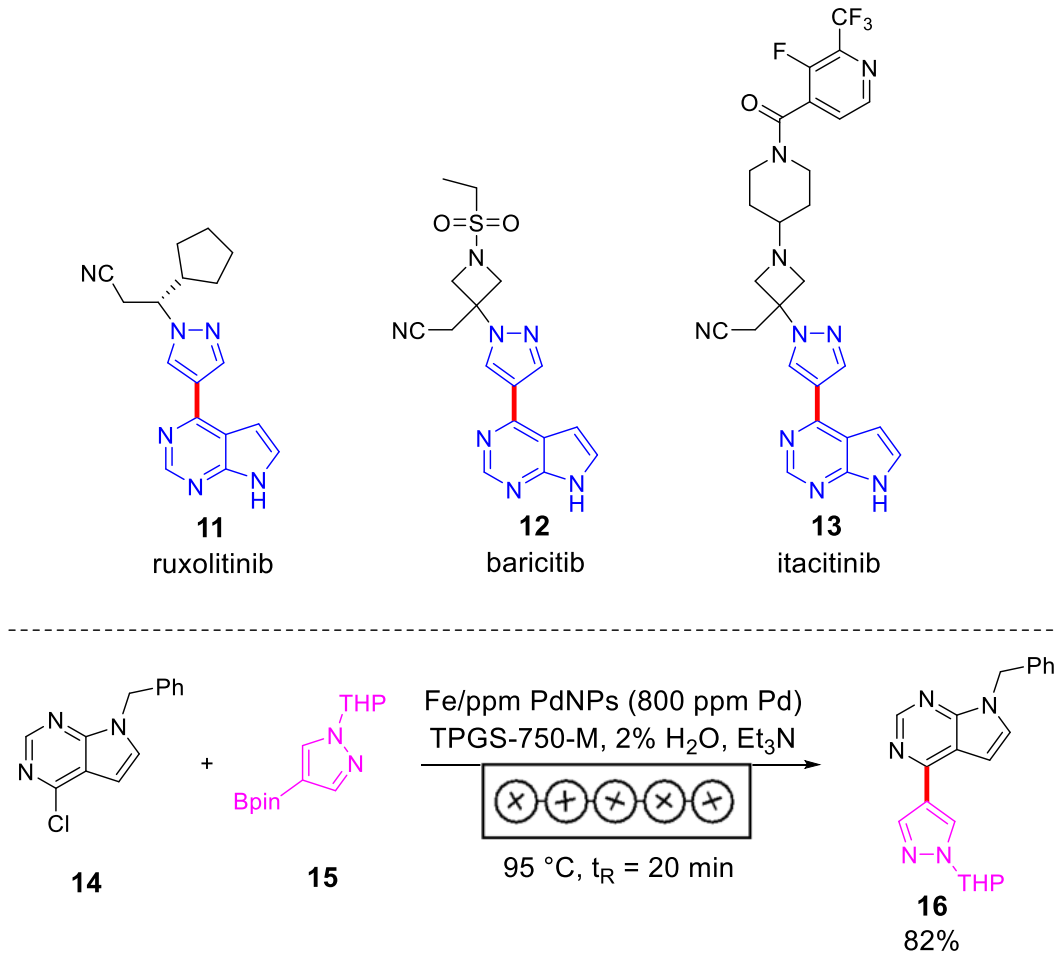

Figure 19: JAK inhibitor examples (top), synthesis of key structural motif of JAK inhibitors in CSTR flow (bottom)

Finally, BRAF enzyme inhibitors are important for treatment of melanoma (**17-19**). The core of one such inhibitor, vemurafenib (**18**), can be synthesized via the coupling of a 5-bromo-7-azaindole (**20**) with 4-chlorophenylboronic acid (**21**) to form biaryl product **22**. This reaction in flow can be facilitated by flowing NPs in aqueous surfactant, compounds **20** and **21** suspended in just pure water with no surfactant, both syringes of which were kept in a constant mixing state using an internal stir bar and external stir plate, and neat triethylamine. Following continuous reaction for a residence time of 20 minutes at 95 °C, the product **22** could be isolated after collection for 15 minutes in an excellent 94% yield with no clogging (Figure 20).

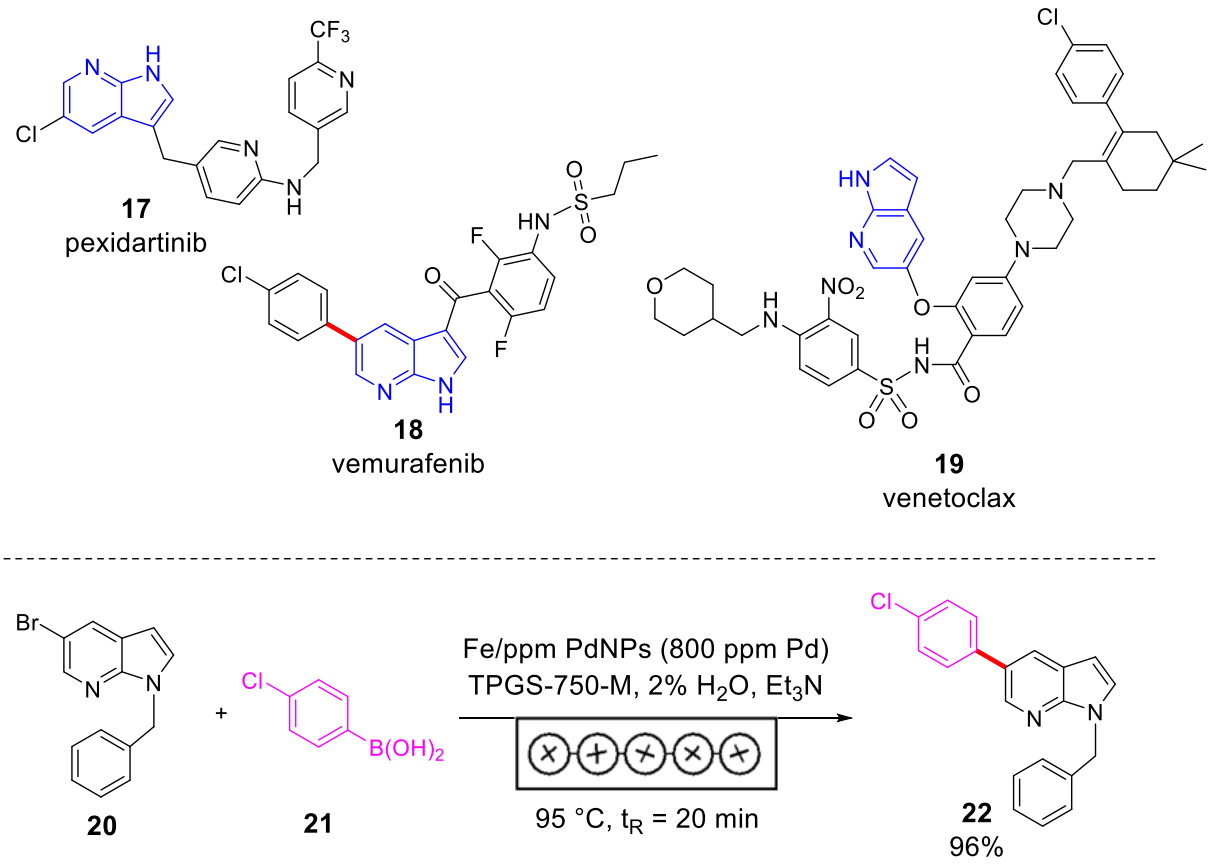

Figure 20: BRAF enzyme inhibitors including compound of interest vemurafenib **18** (top), aqueous micellar CSTR flow synthesis of **18** precursor **22** using NPs

4.4 Conclusions

In conclusion, two flow systems were constructed to satisfy the solids handling requirements encountered for running aqueous micellar catalysis in flow. Both reactors were able to handle a nanoparticle catalyzed Suzuki-Miyaura coupling reaction where the starting materials, products, and catalyst inherently pose problems due to poor, or no, solubility in the aqueous media. In one instance, a plug flow system was developed to run this chemistry in microchannels, where the greatest non-mechanical mixing mass transfer is observed. This utilized new equipment developments from suppliers, in the form of a peristaltic pump back pressure regulator system developed by Vapourtec for their E-Series model, as well as internally *via* research performed by Novartis engineers for a continuously collect-and-drain back pressure regulation system. This plug flow system was amenable to both aqueous soluble inorganic base as well as neat organic base for six diverse substrates. The formation of an API intermediate could also be scaled to 13 g/h production over the course of a 90 min total run time. Furthermore, collaboration with the Jensen lab at MIT Chemical Engineering led to development of a cascading CSTR reactor that could handle solids in the form of an aqueous micellar nanoparticle slurry. This technology was applied to a variety of pharmaceutically interesting API intermediates, yielding products in high yield with very fast (*ca.* 20 min) residence times. In the future, the hope for this CSTR system is to apply it to a variety of other aqueous micellar systems to demonstrate a greater breadth of the water chemistry in flow.

4.5 References

1. Camps, L.; Moens, L.; Groth, U.; Braeken, L.; Kuhn, S.; Thomassen, L. C. J. *Chem. Eng. Res. Des.* **2020**, *156*, 300–310.
2. Peil, K. *J. Catal.* **1991**, *132*, 556–559.
3. Hafner, A.; Filipponi, P.; Piccioni, L.; Meisenbach, M.; Schenkel, B.; Venturoni, F.; Sedelmeier, J. *Org. Process Res. Dev.* **2016**, *20*, 1833–1837.
4. Atherton, J. H.; Hall, A. *Chimica Oggi*. **2011**, *29*, 4.
5. Barton, J. A.; Nolan, P. F. Incidents in the Chemical Industry Due to Thermal-Runaway Chemical Reactions. No. 115, 15.
6. Plutschack, M. B.; Pieber, B.; Gilmore, K.; Seeberger, P. H. *Chem. Rev.* **2017**, *117*, 11796–11893.
7. (a) Gary, J.H.; Handwerk, G.E. *Petroleum Refining Technology and Economics*. Marcel Dekker, Inc. **1984**; (b) Leffler, W. L. *Petroleum Refining for the Nontechnical Person*. PennWell Books, **1985**; (c) Speight, J. G. *The Chemistry and Technology of Petroleum*. CRC Press, **2006**.
8. As of 2021, the US alone has an oil refining capacity of over 18 million barrels of oil/day https://www.statista.com/statistics/273579/countries-with-the-largest-oil-refinery-capacity/ (Accessed February 18, 2022).
9. (a) Jähnisch, K.; Hessel, V.; Löwe, H.; Baerns, M. *Angew. Chem., Int. Ed.* **2004**, *43*, 406–446; (b) Hessel, V.; Kralisch, D.; Kockmann, N.; Noël, T.; Wang, Q. *ChemSusChem* **2013**, *6*, 746–789; (c) Jensen, K. F. *AIChE J.* **2017**, *63*, 858–869; (d) Dong, Z.; Wen, Z.; Zhao, F.; Kuhn, S.; Noël, T. *Chem. Eng. Sci.* **2021**, *10*, 100097.

10. (a) Akwi, F. M.; Watts, P. *Chem. Commun.* **2018**, *54*, 13894–13928; (b) Coley, C. W.; Thomas, D. A.; Lummiss, J. A. M.; Jaworski, J. N.; Breen, C. P.; Schultz, V.; Hart, T.; Fishman, J. S.; Rogers, L.; Gao, H.; Hicklin, R. W.; Plehiers, P. P.; Byington, J.; Piotti, J. S.; Green, W. H.; Hart, A. J.; Jamison, T. F.; Jensen, K. F. *Science* **2019**, *365*, eaax1566; (c) Hone, C. A.; Boyd, A.; O'Kearney-McMullan, A.; Bourne, R. A.; Muller, F. L. *React. Chem. Eng.* **2019**, *4*, 1565–1570; (d) Sagmeister, P.; Williams, J. D.; Hone, C. A.; Kappe, C. O. *React. Chem. Eng.* **2019**, *4*, 1571–1578.
11. (a) Newman, S. G.; Jensen, K. F. *Green Chem.* **2013**, *15*, 1456-1472; (b) Rogers, L.; Jensen, K. F. *Green Chem.* **2019**, *21*, 3481–3498; (c) Kerr, M. S.; Cole, K. P. *CRGSC* **2022**, *5*, 100279.
12. Kobayashi, S. *Chem. Asian J.* **2016**, *11*, 425–436.
13. Bogdan, A. R.; Dombrowski, A. W. *J. Med. Chem.* **2019**, *62*, 6422–6468.
14. Britton, J.; Jamison, T. F. *Nat. Protoc.* **2017**, *12*, 2423–2446.
15. Noël, T. *J. Flow Chem*. **2017**, *7*, 87–93.
16. (a) For the Vapourtec R-Series model, see: https://www.vapourtec.com/products/r-series-flow-chemistry-system-overview/ (Accessed February 19, 2022); (b) For the Vapourtec E-Series model, see: https://www.vapourtec.com/products/e-series-flow-chemistry-system-overview/ (Accessed February 19, 2022).
17. Reproduced from Mielke, E.; Plouffe, P.; Koushik, N.; Eyholzer, M.; Gottsponer, M.; Kockmann, N.; Macchi, A.; Roberge, D. M. *React. Chem. Eng*. **2017**, 2, 763–775. With permission from the Royal Society of Chemistry.

18. (a) Gutmann, B.; Cantillo, D.; Kappe, C. O. *Angew. Chem., Int. Ed.* **2015**, *54*, 6688–6728; (b) Ingham, R. J.; Battilocchio, C.; Fitzpatrick, D. E.; Sliwinski, E.; Hawkins, J. M.; Ley, S. V. *Angew. Chem., Int. Ed.* **2015**, *54*, 144–148.
19. Hartman, R. L.; Naber, J. R.; Zaborenko, N.; Buchwald, S. L.; Jensen, K. F. *Org. Process Res. Dev.* **2010**, *14*, 1347–1357.
20. Hartman, R. L. *Org. Process Res. Dev.* **2012**, *16*, 870–887.
21. (a) Noël, T.; Naber, J. R.; Hartman, R. L.; McMullen, J. P.; Jensen, K. F.; Buchwald, S. L. *Chem. Sci.* **2011**, *2*, 287–290; (b) Mascia, S.; Heider, P. L.; Zhang, H.; Lakerveld, R.; Benyahia, B.; Barton, P. I.; Braatz, R. D.; Cooney, C. L.; Evans, J. M. B.; Jamison, T. F.; Jensen, K. F.; Myerson, A. S.; Trout, B. L. *Angew. Chem., Int. Ed.* **2013**, *52*, 12359–12363; (c) Kuhn, S.; Noël, T.; Gu, L.; Heider, P. L.; Jensen, K. F. *Lab Chip* **2011**, *11*, 2488.
22. Liedtke, A.-K.; Scheiff, F.; Bornette, F.; Philippe, R.; Agar, D. W.; de Bellefon, C. *Ind. Eng. Chem. Res*. **2015**, *54*, 4699–4708.
23. Taylor, G. I. *Philos. Trans. Royal Soc.* **1923**, *223*, 289-343.
24. Pieber, B.; Shalom, M.; Antonietti, M.; Seeberger, P. H.; Gilmore, K. Continuous Heterogeneous Photocatalysis in Serial Micro-Batch Reactors, *Angew. Chem., Int. Ed.* **2018**, *57*, 9976–9979. Copyright Wiley-VCH GmbH. Reproduced with permission.
25. Filipponi, P.; Gioiello, A.; Baxendale, I. R. *Org. Process Res. Dev.* **2016**, *20*, 371–375.
26. © 2022 AM Technology https://www.amt.uk/coflore-flow-reactors (Accessed February 19, 2022).

27. Reprinted (adapted) with permission from McGlone, T.; Briggs, N. E. B.; Clark, C. A.; Brown, C. J.; Sefcik, J.; Florence, A. J. *Org. Process Res. Dev.* **2015**, *19*, 1186–1202. Copyright 2015 American Chemical Society.
28. Jiang, M.; Ni, X.-W. *Org. Process Res. Dev.* **2019**, *23*, 882–890.
29. Hu, C. *J. Flow Chem.* **2021**, *11*, 243–263.
30. Davis, M. E.; Davis, R. J. *Fundamentals of chemical reaction engineering*. Boston: McGraw-Hill, **2003**.
31. Reproduced from Mo, Y.; Jensen, K. F. *React. Chem. Eng.* **2016**, *1*, 501–507. With permission from the Royal Society of Chemistry.
32. Mo, Y.; Lin, H.; Jensen, K. F. *Chem. Eng. J.* **2018**, *335*, 936–944.
33. Lipshutz, B. H. *Curr. Opin. Green Sustain. Chem.* **2018**, *11*, 1–8.
34. Pomberger, A.; Mo, Y.; Nandiwale, K. Y.; Schultz, V. L.; Duvadie, R.; Robinson, R. I.; Altinoglu, E. I.; Jensen, K. F. *Org. Process Res. Dev.* **2019**, *23*, 2699–2706.
35. Pang, H.; Gallou, F.; Sohn, H.; Camacho-Bunquin, J.; Delferro, M.; Lipshutz, B. H. *Green Chem.* **2018**, *20*, 130–135.
36. Handa, S.; Wang, Y.; Gallou, F.; Lipshutz, B. H. *Science* **2015**, *349*, 1087–1091.
37. Harvard Apparatus https://www.harvardapparatus.com/catalog/product/view/id/8355/s/standard-infusion-only-phd-ultra-syringe-pumps/category/500/ (Accessed February 21, 2022).
38. Pang, H.; Hu, Y.; Yu, J.; Gallou, F.; Lipshutz, B. H. *J. Am. Chem. Soc.* **2021**, *143*, 3373–3382.

39. Duvadie, R.; Pomberger, A.; Mo, Y.; Altinoglu, E. I.; Hsieh, H.-W.; Nandiwale, K. Y.; Schultz, V. L.; Jensen, K. F.; Robinson, R. I. *Org. Process Res. Dev.* **2021**, *25*, 2323–2330.
40. Zaiput Flow Technologies https://www.zaiput.com/product/back-pressure-regulators/ (Accessed February 21, 2022).
41. https://www.omega.com/en-us/temperature-measurement/temperature-wire-sensors/5lsc-5srtc/p/5SRTC-KK-K-24-36 (Accessed February 21, 2022).
42. https://www.mcmaster.com/3618K514/ (Accessed February 21, 2022).
43. J-Kem Scientific https://www.jkem.com/product-category/temperature/precision-controllers/single-channel-temperature-controllers/ (Accessed February 21, 2022).
44. Njardarson Group, *Top 200 Pharmaceutical Products by Retail Sales in 2018*. https://njardarson.lab.arizona.edu/sites/njardarson.lab.arizona.edu/files/2018Top200PharmaceuticalRetailSalesPosterLowResFinalV2.pdf. **2019** (Accessed February 21, 2022).

4.6 Experimental Data

1. General information

All commercial reagents were used without further purification. Organic solvents such as THF, tetrahydrofurfural alcohol (THFA), EtOAc, heptanes, and DCM were used as is from commercial sources and were not dried or degassed. Fe/ppm Pd (SPhos) NP catalyst was prepared as noted previously in the literature and stored at rt under a N_2 atmosphere for short periods of time.[1] The surfactant, TPGS-750-M, was prepared via a standard literature procedure,[2] or can be purchased from Millipore-Sigma (catalog #733857 for a 2 wt % solution of the wax dissolved in water). A standard aqueous solution of TPGS-750-M was prepared by dissolving the wax into thoroughly degassed (steady stream of argon, minimum of 1 h bubbling time with stirring) HPLC grade water over the course of 12 h under N_2 gas pressure (**NOTE:** Do not attempt to degas the water with surfactant wax submerged; vigorous foaming to the point of overflow will occur). ^{1}H and ^{13}C NMR were recorded at 25 °C on a Varian Unity Inova 400 MHz, a Varian Unity Inova 500 MHz, or on a Varian Unity Inova 600 MHz spectrometer in $CDCl_3$ with residual $CHCl_3$ (^{1}H = 7.26 ppm, ^{13}C = 77.16 ppm) as internal standard. Chemical shifts are reported in parts per million (ppm). NMR data are reported as follows: chemical shift, multiplicity (s = singlet, d = doublet, dd = doublet of doublets, ddd = doublet of doublet of doublets, t = triplet, td = triplet of doublets, q = quartet, quin = quintet, m = multiplet), coupling constant (if applicable), and integration.

Plug Flow Reactions:

2. Synthesis of 2 in batch mode

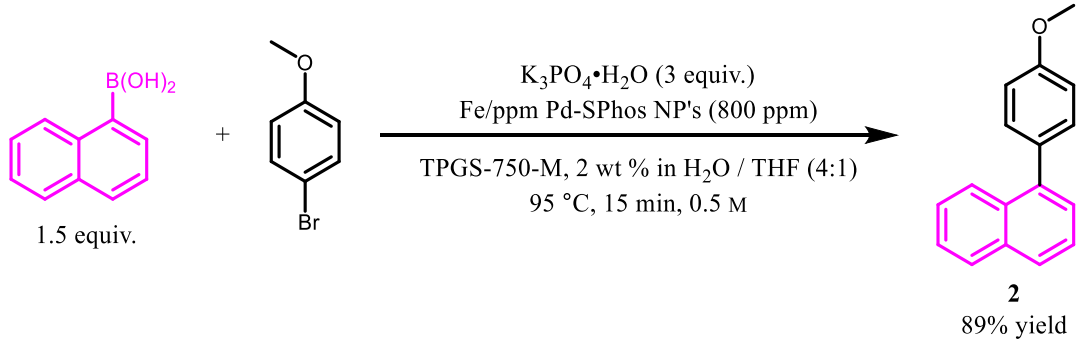

To a 2.0-5.0 mL conical microwave vial equipped with a magnetic stir vane was added 4-bromoanisole (95.1 mg, 0.508 mmol, 1.00 equiv), naphthalene-1-ylboronic acid (133 mg, 0.773 mmol, 1.52 equiv), potassium phosphate tribasic monohydrate (351 mg, 1.525 mmol, 3.00 equiv), and Fe/ppm Pd (SPhos) nanoparticles (20 mg). TPGS-750-M, 2 wt % in water (0.8 mL) and tetrahydrofuran (0.2 mL) were then added and the vial was sealed using an aluminum crimp-cap fitted with a septum. The contents of the vial were then allowed to stir at rt until a homogeneous mixture had formed. The vial was then placed in a microwave reactor and allowed to react for 15 min at 95 °C. The resulting reaction mixture was then extracted with EtOAc (3 x 0.5 mL) and passed through a plug of silica gel resulting in **2** as an off-white solid (106 mg, 89% yield).

Note: Screening of subsequent examples of NP-catalyzed coupling reactions in plug flow were tested using microwave conditions in a similar manner as a guide towards optimization. For example, this reaction was found to undergo 100% conversion via UPLC UV/Vis analysis within 2 min of reaction time. All other reactions were tested within a 2-10 min reaction window at 95 °C using either $K_3PO_4•H_2O$ or triethylamine as base, and reagent flow rates were adjusted accordingly.

3. Batch-to-flow synthesis of 2

A flow reactor was prepared by pumping a 4:1 ratio solution of TPGS-750-M, 2 wt % in water and tetrahydrofuran using a VapourTec E-Series peristaltic pump into a 10 mL reactor coil (PFA tubing, 0.3" ID) pre-heated to 95 °C. A VapourTec E-Series pump configured to act as a back-pressure regulator set to 3 bar was used on the downstream end of the reactor prior to collection.

To a 2-dram vial equipped with a stir bar was added 4-bromoanisole (179.0 mg, 0.948 mmol, 1 equiv), naphthalene-1-ylboronic acid (283.0 mg, 1.645 mmol, 1.74 equiv), potassium phosphate tribasic monohydrate (685 mg, 2.97 mmol, 3.14 equiv), and Fe/ppm Pd (SPhos) NPs (41 mg). TPGS-750-M, 2 wt % in water (1.6 mL) and tetrahydrofuran (0.4 mL) were then added to the vial and the contents were then allowed to stir at rt until a homogeneous mixture had formed. The resulting suspension was then stirred continuously at rt and pumped using the TPGS/THF pre-conditioned peristaltic pump into the 10 mL reactor coil at a 0.667 mL/min flow rate. After the entirety of the suspension was injected into the reactor coil, a timer was started for 15 min (the residence time of the reaction) and the reaction slug was chased with a mixture of aqueous TPGS-750-M/THF immediately afterwards.

After 15 min, the peristaltic pump and reaction coil were washed with EtOAc at a flow rate of 2 mL/min for 10 min, and the aqueous inside of the reaction coil along with the organics were collected and pooled together. The resulting bi-phase was then separated and the aqueous phase was extracted with EtOAc (2 x 10 mL). The crude organics were then passed through a plug of silica gel, evaporated under reduced vacuum, and dried until constant mass using a vacuum oven resulting in **2** as an off-white solid (154 mg, 69% yield).

4. Synthesis of 1 in flow

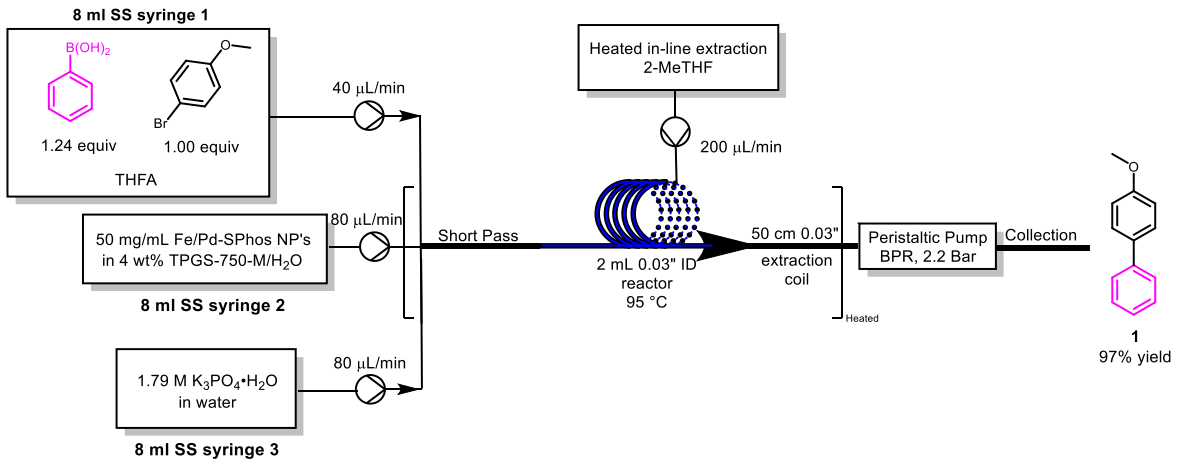

Syringe 1: To a 5 mL volumetric flask was added 4-bromoanisole (1,150 mg, 6.14 mmol, 1.00 equiv) and phenylboronic acid (930 mg, 7.62 mmol, 1.24 equiv). The flask was then mostly filled with tetrahydrofurfuryl alcohol (THFA) and the starting reagents were dissolved using gentle heating. Upon dissolution, the flask was cooled to rt and filled to the volumetric line using THFA. The resulting solution was then transferred to an 8 mL stainless steel syringe prior to the reaction and set to deliver 40 µL/min.

Syringe 2: A 50 mg/mL catalyst stock solution was prepared by suspending 1 g of freshly prepared Fe/ppm Pd (SPhos) NP catalyst in 20 mL of TPGS-750-M, 4 wt % in water. After the addition of the aqueous surfactant solution to the NPs the mixture was sonicated for 20 min in a rt water bath and stirred continuously prior to use. The catalyst suspension was transferred to an 8 mL stainless steel syringe immediately prior to a coupling reaction in flow and set to deliver at 80 µL/min.

Syringe 3: A 1.78 M stock solution of $K_3PO_4•H_2O$ was transferred into an 8 mL stainless steel syringe prior to the reaction. The syringe was then set to deliver at 80 µL/min.

Reactor Design: The three prepared syringes were plumbed into a cross mixer (Tefzel, 0.03" ID) such that **Syringe 2**, containing the NPs, was delivered at 180° through the mixer and that **Syringes 1 and 3** were delivered perpendicular and through check-valves. The cross mixer was then plumbed directly into a 2 mL reactor coil (PFA, 0.03" ID). The reactor coil was then plumbed into a T-mixer (Tefzel, 0.03" ID) wherein 2-methyltetrahydrofuran is delivered perpendicularly through a check valve into that stream as an in-line extractor. The cross mixer, reaction coil, and in-line extraction units are all heated to 95 °C and held at this temperature during the run. The extraction mixture prior to the run is then delivered through a VapourTec E-Series peristaltic pump configured to act as a back-pressure regulator holding at 2.2 bar.

The 2 mL reactor / back-pressure system described above was then pre-filled with TPGS-750-M, 2 wt % in water prior to fitting the syringes containing the starting reagents to the cross mixer. All three syringes were then simultaneously turned on, and the reaction was allowed to run for a combined flow rate of 200 µL/min for four residence times (40 min) prior to steady state. The reaction was then collected for a total of five residence times (50 min) with simultaneous in-line extraction using 2-MeTHF at 200 µL/min. The combined aqueous and organics were then separated, and the solvent was evaporated under reduced pressure. The residual organics were then treated with 200 mL of water resulting in the precipitation of a solid. This solid was then recovered via filtration, dissolved in DCM, and passed through a plug of silica gel resulting in the product as an off-white solid (431 mg, 97% yield).

5. Synthesis of 2 in flow

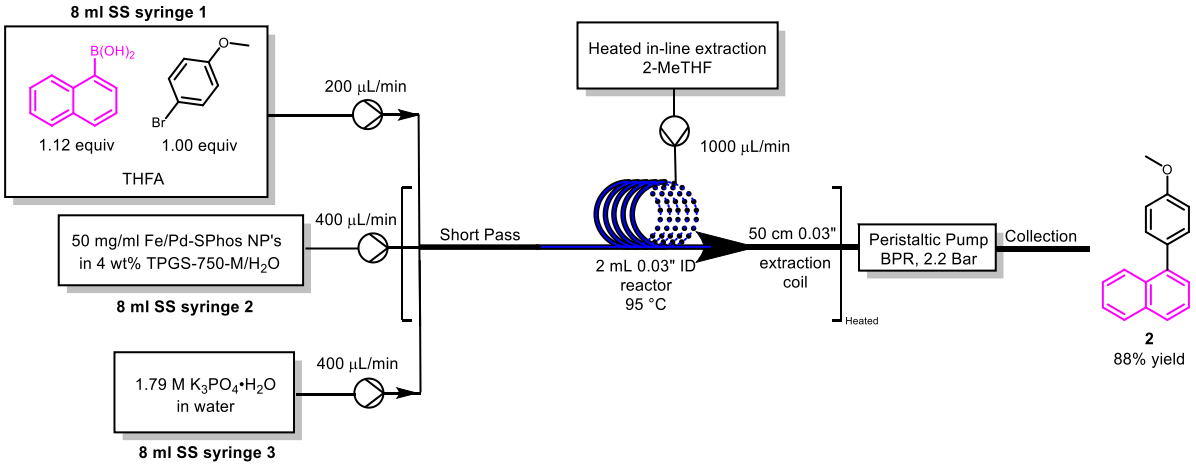

Syringe 1: To a 5 mL volumetric flask was added 4-bromoanisole (1,150 mg, 6.14 mmol, 1.00 equiv) and naphthalene-1-ylboronic acid (1,185 mg, 6.89 mmol, 1.12 equiv). The flask was then mostly filled with tetrahydrofurfuryl alcohol (THFA) and the starting reagents were dissolved using gentle heating. Upon dissolution, the flask was cooled to rt and filled to the volumetric line using THFA. The resulting solution was then transferred to an 8 mL stainless steel syringe prior to the reaction and set to deliver 200 µL/min.

Syringe 2: A 50 mg/mL catalyst stock solution was prepared in a similar manner as the synthesis of **1**. The catalyst suspension was transferred to an 8 mL stainless steel syringe immediately prior to a coupling reaction in flow and set to deliver 400 µL/min.

Syringe 3: A 1.78 M stock solution of $K_3PO_4•H_2O$ was transferred into an 8 mL stainless steel syringe prior to the reaction. The syringe was then set to deliver at 400 µL/min.

Reactor Design: This synthesis was performed using the same apparatus prepared for the flow synthesis of **1** and run in a similar fashion using the flow rates listed above. The combined flow rate of 1 mL/min was allowed to run for two residence times on the 2 mL reactor to reach

steady state. Seven residence times were then collected using a 1 mL/min heated in-line extraction using 2-MeTHF.

The crude product stream was then worked up as in example **1**, resulting in the product as an off-white solid (685 mg, 88% yield).

6. Synthesis of 3 in flow

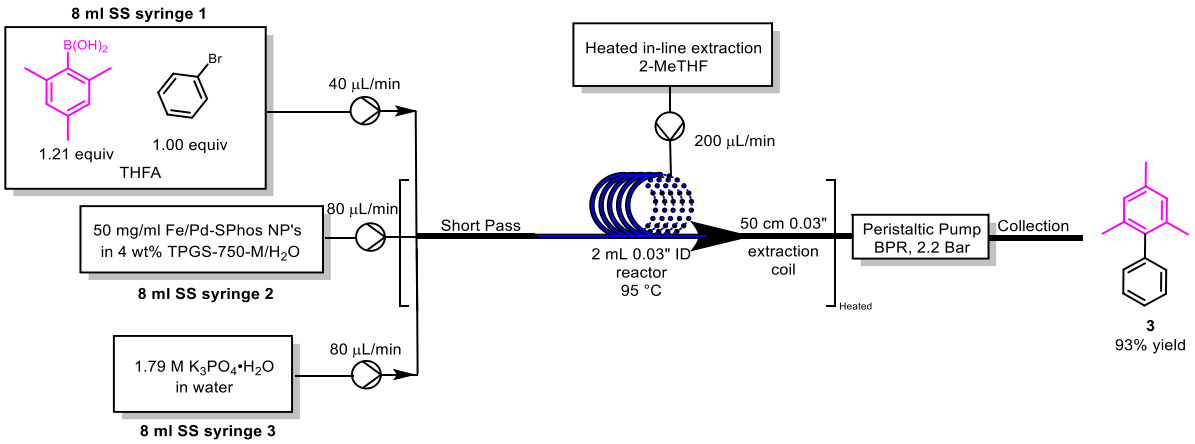

Syringe 1: To a 5 mL volumetric flask was added phenyl bromide (925 mg, 5.89 mmol, 1.00 equiv) and mesitylboronic acid (1,175 mg, 7.16 mmol, 1.21 equiv). The flask was then mostly filled with tetrahydrofurfuryl alcohol (THFA) and the starting reagents were dissolved using gentle heating. Upon dissolution, the flask was cooled to rt and filled to the volumetric line using THFA. The resulting solution was then transferred to an 8 mL stainless steel syringe prior to the reaction and set to deliver 40 µL/min.

Syringe 2: A 50 mg/mL catalyst stock solution was prepared in a similar manner as the synthesis of **1**. The catalyst suspension was transferred to an 8 mL stainless steel syringe immediately prior to a coupling reaction in flow and set to deliver 80 µL/min.

Syringe 3: A 1.78 M stock solution of $K_3PO_4•H_2O$ was transferred into an 8 mL stainless steel syringe prior to the reaction. The syringe was then set to deliver at 80 µL/min.

Reactor Design: This synthesis was performed using the same apparatus prepared for the flow synthesis of **1** and run in a similar fashion using the flow rates listed above. The combined flow rate of 200 µL/min was allowed to run for two residence times on the 2 mL reactor to reach steady state. A product mixture sample of 4.9 residence times was then collected using a 200 µL/min heated in-line extraction using 2-MeTHF.

The resulting bi-phase was then separated and the organics were concentrated down to an oil under reduced pressure. The residual organics were then treated with water (200 mL) and extracted with heptane (3 x 50 mL). The organics were then dried over sodium sulfate, filtered, evaporated under reduced pressure, and passed through a plug of silica gel using EtOAc. The organics were then dried under high vacuum until constant mass resulting in product as a tan oil (431 mg, 93% yield).

7. Synthesis of 4 in flow

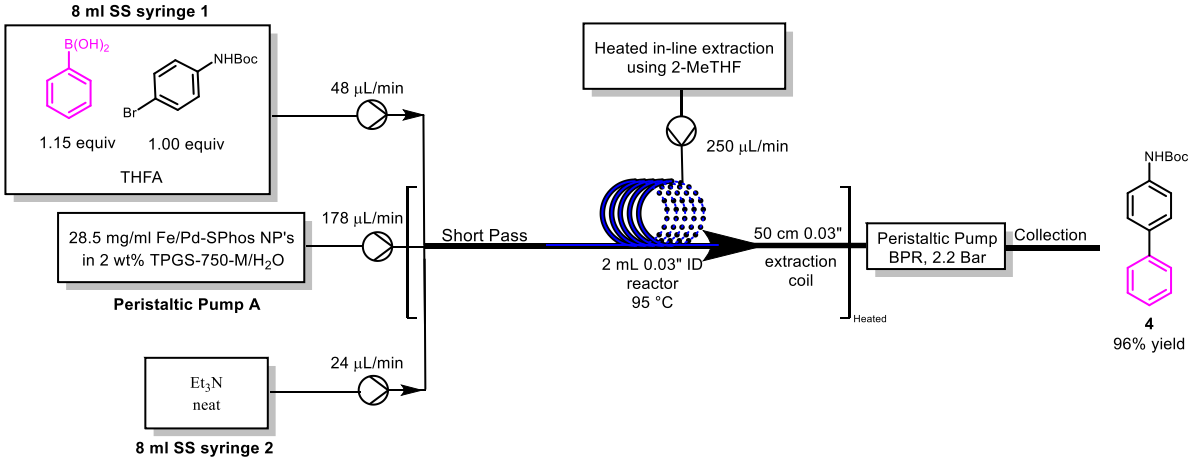

Syringe 1: To a 5 mL volumetric flask was added *tert*-butyl (4-bromophenyl)carbamate (1,650 mg, 6.06 mmol, 1.00 equiv) and phenylboronic acid (850 mg, 6.97 mmol, 1.15 equiv). The flask was then mostly filled with tetrahydrofurfuryl alcohol (THFA) and the starting reagents were dissolved using gentle heating. Upon dissolution, the flask was cooled to rt and

filled to the volumetric line using THFA. The resulting solution was then transferred to an 8 mL stainless steel syringe prior to the reaction and set to deliver 48 µL/min.

Peristaltic Pump A: A 28.5 mg/mL catalyst stock solution was prepared by suspending 570 mg of freshly prepared Fe/ppm Pd (SPhos) NP catalyst in 20 mL of TPGS-750-M, 2 wt % in water. Upon addition of the aqueous surfactant solution to the NPs, the mixture was sonicated for 20 min in a rt water bath and stirred continuously prior to use. The catalyst suspension was then stirred continuously on a stir plate and was used to prime a VapourTec E-Series peristaltic pump immediately prior to a flow coupling reaction. The peristaltic pump was then set to deliver 178 µL/min.

Syringe 2: An 8 mL stainless steel syringe was charged with neat trimethylamine and set to deliver 24 µL/min.

Reactor Design: The two syringes and peristaltic pump were plumbed into a cross mixer (Tefzel, 0.03" ID) such that **Peristaltic Pump A**, containing the nanoparticles, was delivered at 180° through the mixer and that **Syringes 1 and 2** were delivered perpendicular and through check-valves. The cross mixer was then plumbed directly into a 2 mL reactor coil (PFA, 0.03" ID). The reactor coil was then plumbed into a T-mixer (Tefzel, 0.03" ID) wherein which 2-methyltetrahydrofuran is delivered perpendicularly through a check valve into that stream as an in-line extractor. The cross mixer, reaction coil, and in-line extraction units are all heated to 95 °C and held at temperature during the run. The extraction mixture prior to the run is then delivered through a VapourTec E-Series peristaltic pump configured to act as a back-pressure regulator holding at 2.2 bar.

The 2 mL reactor / back-pressure system described above was then pre-filled with TPGS-750-M, 2 wt % in water prior to fitting the syringes and peristaltic pump to the cross mixer.

The two syringes and pump were then started simultaneously, and the flow system was allowed to reach steady state for four residence times of a combined flow rate of 250 µL/min (8 min retention time). The reaction was then collected for a total of five residence times with simultaneous heated in-line extraction using 250 µL/min 2-MeTHF after the 2 mL reactor coil.

The collected bi-phase was then separated and the organics were evaporated under reduced pressure. The residual oil was then treated with cold water (200 mL) and allowed to rest in an ice bath. The resulting precipitate was then filtered, collected, and dissolved in EtOAc. The organics were then passed through a plug of sodium sulfate followed by silica gel, evaporated under reduced pressure, and dried under hi-vacuum until constant mass was achieved resulting in a yellow crystalline solid (480 mg, 96% yield).

8. Synthesis of 5 in flow

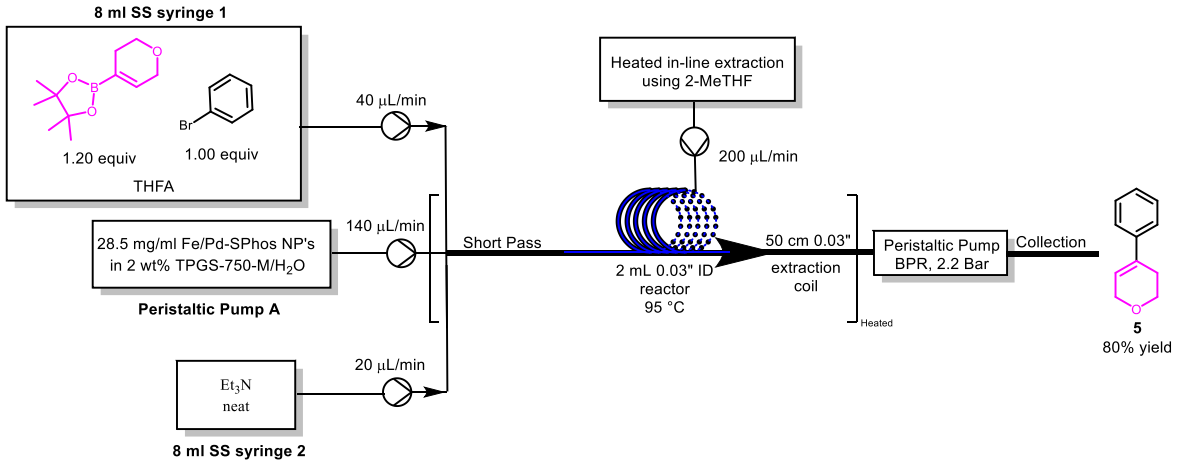

Syringe 1: To a 5 mL volumetric flask was added bromobenzene (927.5 mg, 5.91 mmol, 1.00 equiv) and 2-(3,6-dihydro-2*H*-pyran-4-yl)-4,4,5,5-tetramethyl-1,3,2-dioxaborolane (1,484 mg, 7.07 mmol, 1.20 equiv). The flask was then mostly filled with tetrahydrofurfuryl alcohol (THFA) and the starting reagents were dissolved using gentle heating. Upon dissolution, the flask was cooled to rt and filled to the volumetric line using THFA. The

resulting solution was then transferred to an 8 mL stainless steel syringe prior to the reaction and set to deliver 40 µL/min.

Peristaltic Pump A: A 28.5 mg/mL catalyst stock solution was prepared in a similar manner as the synthesis of **4**. The catalyst suspension was stirred continuously on a stir plate and used to prime a VapourTec E-Series peristaltic pump prior to a flow coupling reaction. The peristaltic pump was then set to deliver 140 µL/min.

Syringe 2: An 8 mL stainless steel syringe was charged with neat trimethylamine and set to deliver 20 µL/min.

Reactor Design: This synthesis was performed using the same apparatus prepared for the flow synthesis of **4** and run in a similar fashion using the flow rates listed above. The combined flow rate of 200 µl/min was allowed to run for four residence times (40 min) to reach steady state. The steady state product mixture was then collected for five residence times (50 min) with a simultaneous heated in-line extraction using 200 µL/min 2-MeTHF.

The collected bi-phase was then separated and the organic solvent was evaporated under reduced pressure. The residual oil was then treated with 200 mL of cold water and allowed to sit an ice bath. The resulting solid was then filtered and washed with cold water. The retained material was then dissolved in EtOAc and passed through a plug of sodium sulfate followed by silica gel. The solvent was then removed, and the product was dried under high vacuum until constant mass was achieved resulting in product as a yellow solid (300 mg, 80% yield).

9. Synthesis of 6 in flow

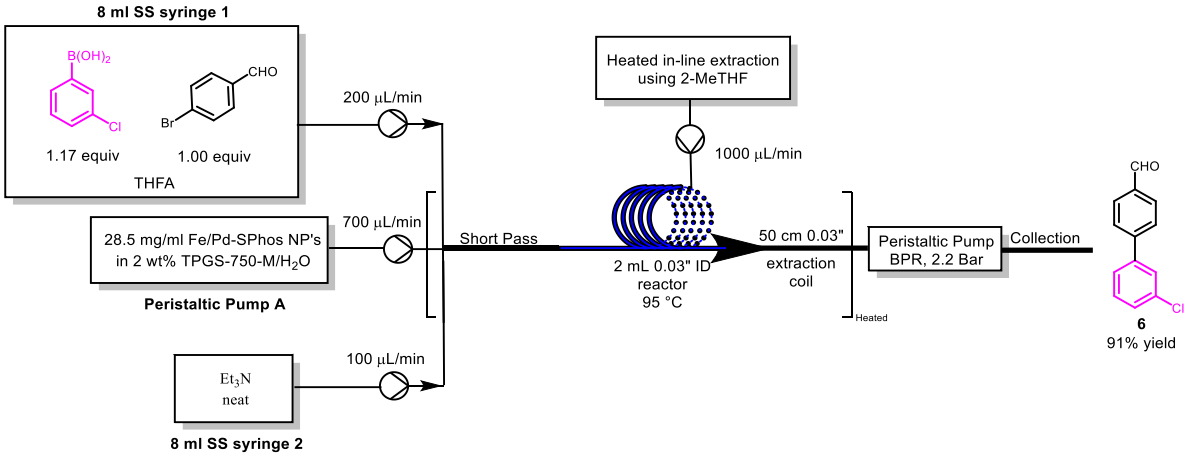

Syringe 1: To a 5 mL volumetric flask was added 4-bromobenzaldehyde (1,14.7 mg, 6.02 mmol, 1.00 equiv) and (3-chlorophenyl)boronic acid (1098.9 mg, 7.03 mmol, 1.17 equiv). The flask was then mostly filled with tetrahydrofurfuryl alcohol (THFA) and allowed to dissolve at rt.

NOTE: This mixture should not be heated; heating will result in acetal formation between THFA and 4-bromobenzaldehyde which will not couple under the reaction conditions.

Once homogeneous, the flask was then filled to the volumetric line using THFA. The resulting solution was then transferred to an 8 mL stainless steel syringe prior to the reaction and set to deliver 200 µL/min.

Peristaltic Pump A: A 28.5 mg/mL catalyst stock solution was prepared in a similar manner as the synthesis of **4**. The catalyst suspension was stirred continuously on a stir plate and used to prime a VapourTec E-Series peristaltic pump prior to a flow coupling reaction. The peristaltic pump was then set to deliver 700 µL/min.

Syringe 2: An 8 mL stainless steel syringe was charged with neat trimethylamine and set to deliver 100 µL/min.

Reactor Design: This synthesis was performed using the same apparatus prepared for the flow synthesis of **4** and run in a similar fashion using the flow rates listed above. The combined flow rate of 1000 µL/min was allowed to run for four residence times (8 min) to reach steady state. The steady state product mixture was then collected for five residence times (10 min) with a simultaneous heated in-line extraction using 1000 µL/min 2-MeTHF.

The collected bi-phase was then separated and the organic solvent was evaporated under reduced pressure. The residual oil was then dissolved in 3 mL of DCM and stirred vigorously with 3 mL of 1 N HCl to remove any acetal formation from the product. The organics were then removed and the aqueous was then extracted with DCM (2 x 1 mL). The product solution was then dried over anhydrous sodium sulfate and purified via SiO_2 column (3:7 EtOAc/heptanes). The collected fractions were then combined and the solvent evaporated until constant mass was achieved resulting in product as a yellow solid (475.5 mg, 91% yield).

10. Scale-Up synthesis of 6 in flow

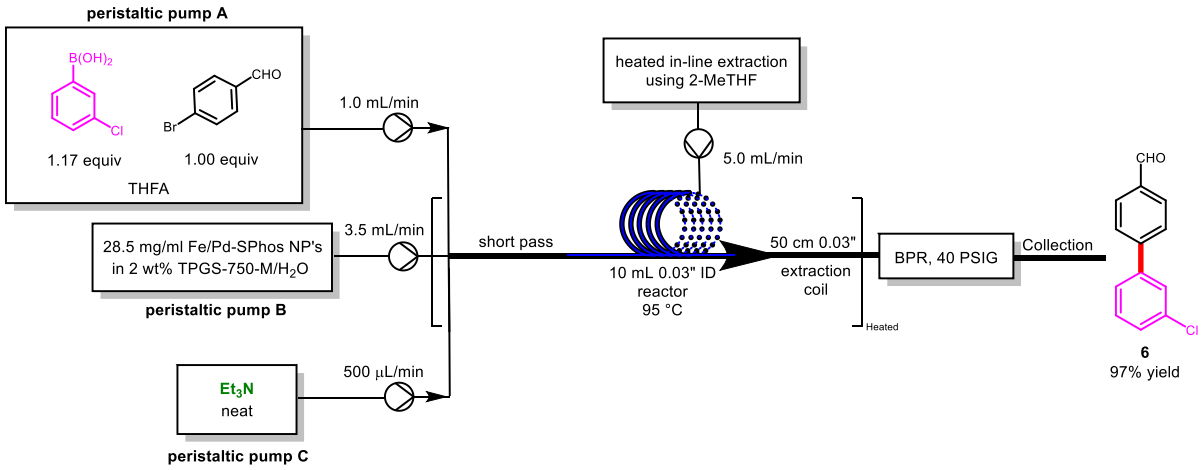

Peristaltic Pump A: To a 250 mL volumetric flask was added 4-bromobenzaldehyde (55.75 g, 301.32 mmol, 1.00 equiv) and (3-chlorophenylboronic acid (54.95 g, 351.37 mmol,

1.17 equiv). The flask was then mostly filled with tetrahydrofurfuryl alcohol (THFA) and allowed to dissolve at rt.

NOTE: This mixture should not be heated; heating will result in acetal formation between THFA and 4-bromobenzaldehyde which will not couple under the reaction conditions.

Once homogeneous, the flask was then filled to the volumetric line using THFA. This solution was then used to prime a VapourTec E-Series pump prior to a flow coupling run. The peristaltic pump was then set to deliver 1 mL/min.

Peristaltic Pump B: A 28.5 mg/mL catalyst stock solution was prepared by suspending 28.5 g of freshly prepared Fe/ppm Pd (SPhos) NPs in 1 L of TPGS-750-M, 2 wt % in water. Upon addition of the aqueous surfactant solution to the NPs, the mixture was sonicated for 1 h in a rt water bath and stirred continuously prior to use. The catalyst suspension was then stirred continuously on a stir plate and was used to prime a VapourTec E-Series peristaltic pump immediately prior to a flow coupling reaction. The peristaltic pump was then set to deliver 3.5 mL/min.

Peristaltic Pump C: A VapourTec E-Series pump was primed using neat triethylamine and set to deliver 0.5 mL/min.

Reactor Design: The three peristaltic pumps were plumbed into a cross mixer (Tefzel, 0.03" ID) such that **Peristaltic Pump B**, containing the NPs, was delivered at 180 °C through the mixer and that **Peristaltic Pumps A and C** were delivered perpendicular and through check-valves (DATA). The cross mixer was then plumbed directly into a 10 mL reactor coil (PFA, 0.03" ID). The reactor coil was then plumbed into a T-mixer (Tefzel, 0.03" ID) wherein which 2-methyltetrahydrofuran is delivered perpendicularly through a check valve into that stream as an in-line extractor. The cross mixer, reaction coil, and in-line extraction units are

all heated to 95 °C and held at that temperature during the run. The extraction mixture prior to the run is then delivered into a self-draining pressurized back-pressure regulator held at 40 PSIG.

The 10 mL reactor / back-pressure system described above was then pre-filled with TPGS-750-M, 2 wt % in water prior to fitting peristaltic pumps to the cross mixer. The three peristaltic pumps were then turned on simultaneously and the system was allowed to reach steady state at a combined flow rate of 5 mL/min over three residence times (6 min). The product mixture was then collected, along with a 5 mL/min heated in-line extraction using 2-MeTHF, over the course of 90 min.

After the flow reaction was complete, the collected bi-phase was then separated and the organics were evaporated under reduced pressure. The resulting residual oil was then treated with water (500 mL) in a separatory funnel and the crude oil was collected from the bottom. The aqueous layer was then extracted with DCM (2 x 100 mL), which was then combined with the collected oil. The DCM layer was then treated with 1 N HCl (100 mL) to remove any acetal formation from the product. The DCM layer was then removed, and the aqueous layer was extracted with DCM (1 x 50 mL). The combined organics were then dried over anhydrous sodium sulfate, filtered, and the solvent was evaporated under reduced pressure. The crude organics were then purified via SiO_2 column (3:7 EtOAc/heptanes). The recovered fractions were then evaporated under reduced pressure and dried under high vacuum until constant mass was achieved resulting in a yellow solid (22.8 g, 97% yield).

CSTR Reactions:

11. Synthesis of 1 in CSTR flow

Under flow conditions: 4-Bromoanisole (1.25 mL, 10.0 mmol), phenylboronic acid (1460 mg, 12.0 mmol, 1.2 equiv.), Fe/ppm Pd NPs (718 mg, 800 ppm Pd), TPGS-750-M (800 mg, 2 wt %), and K_3PO_4•H_2O (3450 mg, 15.0 mmol, 1.5 equiv) with total volume of ~40 mL (34.8 mL H_2O + 3.95 mL THFA) were distributed among three streams, as discussed below.

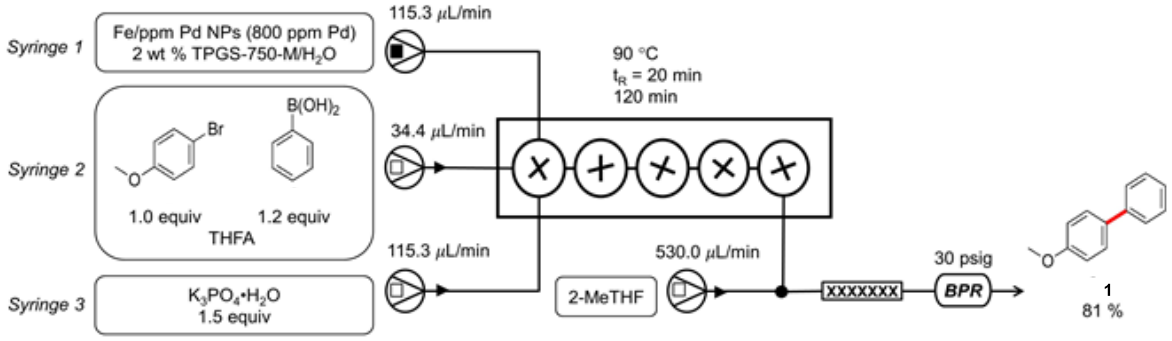

Syringe 1. In glass vial containing a PTFE coated magnetic stir bar, TPGS-750-M (800 mg, 2 wt %) was added and sealed with a rubber septum. The vial was then placed under argon and degassed H_2O (17.4 mL) was added under argon flow *via* syringe and stirred at rt for 2 h. In a separate second vial containing a PTFE coated magnetic stir bar, Fe/ppm Pd NPs (718 mg, 800 ppm Pd) were added, sealed with a rubber septum, and placed under argon. A solution of TPGS-750-M/H_2O (17.4 mL) from the first vial was then added to the second vial *via* inerted syringe under an argon flow. The mixture was then stirred at rt for 1 h. This catalyst slurry was then transferred to an inerted stainless steel syringe containing a PTFE coated magnetic stir bar and attached to syringe pump 1.

Syringe 2. In a glass vial containing a PTFE coated magnetic stir bar, 4-bromoanisole (1.25 mL, 10.0 mmol, 1 equiv), and phenylboronic acid (1460 mg, 12.0 mmol, 1.2 equiv) were added, sealed with a rubber septum, and placed under argon. Degassed THFA (3.95 mL) was

added to the vial under argon flow *via* inerted syringe and stirred at rt for 1 h. This solution of substrates was then transferred to inerted stainless steel syringe and attached to syringe pump 2.

Syringe 3. In a glass vial containing a PTFE coated magnetic stir bar, $K_3PO_4•H_2O$ (3450 mg, 15.0 mmol, 1.5 equiv) was added and sealed with a rubber septum. The vial was evacuated and backfilled with argon three times. Degassed H_2O (17.4 mL) was added to the vial under argon flow *via* inerted syringe and stirred at rt for 1 h. This solution was then transferred to an inerted stainless-steel syringe and attached to syringe pump 3.

After achieving steady state (~3 residence times, 60 min), the sample was collected for 50 min and used to calculate the isolated yield of product. In 50 min, 3.3 mmol of substrate had been introduced into the reactor. The organic layer was concentrated *in vacuo* and then purified by flash column chromatography (Et_2O/hexane = 10/90) to afford 493 mg (2.67 mmol, ~81%) of product **1**.

12. Synthesis of 10 in CSTR flow

Under flow conditions. 2-Bromobenzonitrile (1370 mg, 7.5 mmol, 1 equiv), *p*-tolylboronic acid (1220 mg, 9.0 mmol, 1.2 equiv), Fe/ppm Pd NPs (538 mg, 800 ppm Pd), TPGS-750-M (600 mg, 2 wt %), and $K_3PO_4•H_2O$ (2.590 g, 11.3 mmol, 1.5 equiv.) with the total volume of 30 mL (H_2O) was distributed among two streams, as discussed below. The flow rates of two streams were adjusted to achieve the desired concentration of reagents, catalyst, and the surfactant in the CSTR.

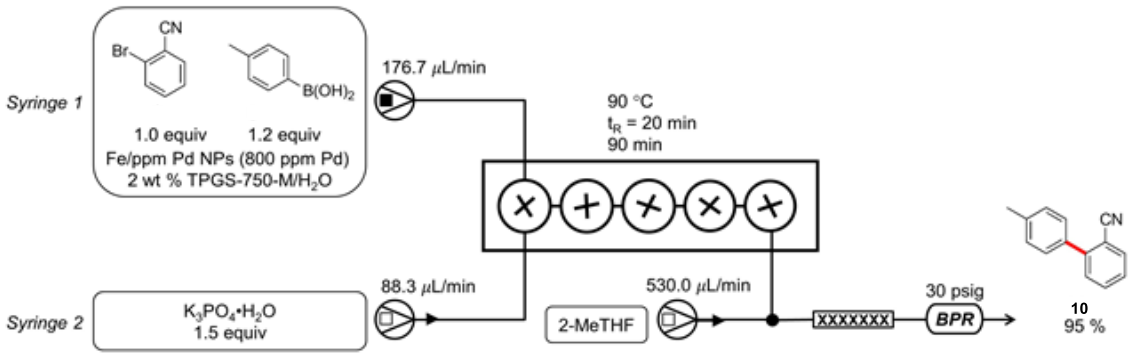

Syringe 1: In a glass vial containing a PTFE coated magnetic stir bar, TPGS-750-M (600 mg, 2 wt %) was added and sealed with a rubber septum. The vial was evacuated and backfilled with argon three times. Degassed H_2O (20 mL) was added to the vial under argon flow *via* inerted syringe and stirred at rt for 2 h. In a separate second vial containing a PTFE coated magnetic stir bar, Fe/ppm Pd NPs (538 mg, 800 ppm Pd), 2-bromobenzonitrile (1370 mg, 7.5 mmol, 1 equiv), and *p*-tolylboronic acid (1.220 g, 9.0 mmol, 1.2 equiv) were added, sealed with a rubber septum, and inerted with argon. A solution of TPGS-750-M/H_2O (20 mL) from the first vial was then added to second vail *via* inerted syringe under argon flow. The mixture was then stirred at rt for 1 h. This reaction slurry was then transferred to inerted stainless steel syringe containing a PTFE coated magnetic stir bar and attached to syringe pump 1.

Syringe 2: In a glass vial containing a PTFE coated magnetic stir bar, K_3PO_4•H_2O (2.590 g, 11.3 mmol, 1.5 equiv) was added, sealed with a rubber septum, and inerted with argon. Degassed H_2O (10 mL) was added to the vial under argon flow *via* inerted syringe and stirred at rt for 1 h. This solution was then transferred to an inerted stainless-steel syringe and attached to syringe pump 2.

After achieving steady state (~3 residence times, 60 min), the sample was collected for 20 min and used to calculate isolated yield of product. In 20 min, 1.32 mmol of substrate is introduced in the reactor. The organic layer of sample was concentrated *in vacuo* and then

purified by flash column chromatography (Et_2O/hexane = 10/90) to afford 243 mg (1.26 mmol, 95%) of product **10**.

13. Synthesis of 16 in CSTR flow

Under flow conditions. Heteroaromatic **14** (1830 mg, 7.5 mmol, 1 equiv), and pinacol ester **15** (2.500 g, 9.0 mmol, 1.2 equiv), Fe/ppm Pd NPs (538 mg, 800 ppm Pd), TPGS-750-M (600 mg, 2 wt %), Et_3N (1.57 mL, 11.3 mmol, 1.5 equiv.) with the total volume of 30 mL (28.43 mL H_2O + 1.57 mL Et_3N) were distributed among two streams as discussed below.

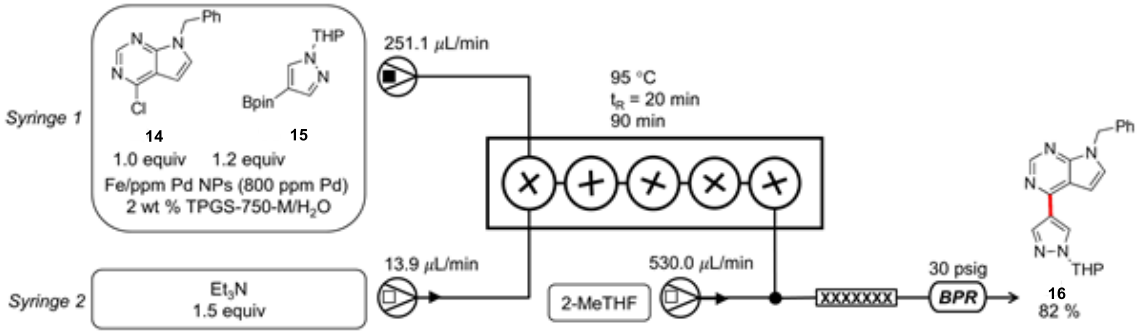

Syringe 1: In a glass vial containing a PTFE coated magnetic stir bar, TPGS-750-M (600 mg, 2 wt.%) was added and sealed with a rubber septum. The vial was evacuated and backfilled with argon three times. Degassed H_2O (28.43 mL) was added to the vial under argon flow *via* syringe and stirred at rt for 2 h. In a separate second vial containing a PTFE coated magnetic stir bar, Fe/ppm Pd NPs (538 mg, 800 ppm Pd), **14** (1.830 g, 7.5 mmol, 1 equiv), and **15** (2500 mg, 9.0 mmol, 1.2 equiv) were added and sealed with a rubber septum. The vial was evacuated and backfilled with argon three times. A solution of TPGS-750-M/H_2O (28.43 mL) from the first vial was then added to second vail *via* syringe under argon flow. The reaction mixture was then stirred at rt for 1 h. This reaction slurry was then transferred to 50 mL stainless steel syringe containing a PTFE coated magnetic stir bar and attached to syringe pump 1.

Syringe 2: Second stainless-steel syringe was filled with degassed Et_3N (1.57 mL, 11.3 mmol, 1.5 equiv) and attached to syringe pump 2.

After achieving steady state (~3 residence times, 60 min), the sample was collected for 15 min and used to calculate the isolated yield of product. In 15 min, 0.99 mmol of substrate is introduced in the reactor. The organic layer was concentrated *in vacuo* and then purified by flash column chromatography (EtOAc/hexane = 50/50) to afford 291 mg (0.81 mmol, 82%) of product **16**.

14. Synthesis of 22 in CSTR flow

Under flow conditions. **20 (**1080 mg, 3.75 mmol, 1.0 equiv) and **21** (704 mg, 4.5 mmol, 1.2 equiv), Fe/ppm Pd NPs (538 mg, 800 ppm Pd), TPGS-750-M (600 mg, 2 wt %), and Et_3N (1.57 mL, 11.3 mmol, 3.0 equiv) with total volume of ~30 mL (28.44 mL H_2O + 1.57 mL Et_3N) were distributed among three streams as discussed below. The flowrates of three streams were adjusted to achieve desired concentration of reagents, nanoparticles, and the surfactant in the CSTR.

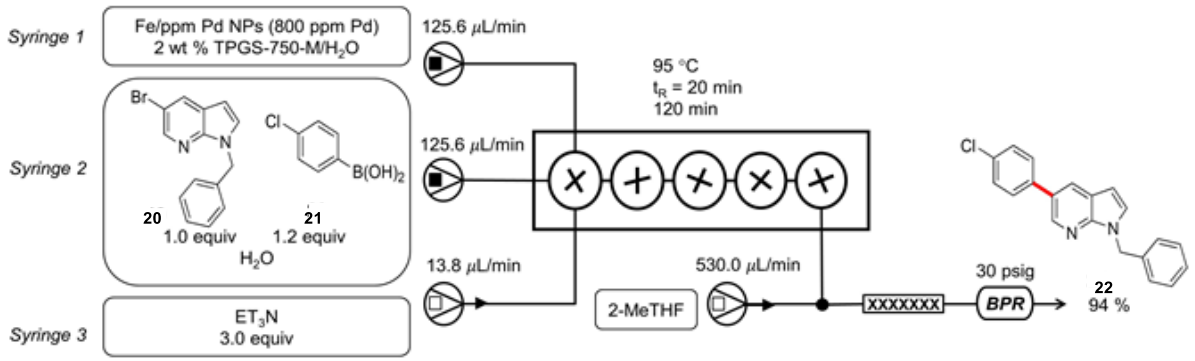

Syringe 1: In a glass vial containing a PTFE coated magnetic stir bar, TPGS-750-M (600 mg, 2 wt.%) was added and sealed with a rubber septum. The vial was evacuated and backfilled with argon three times. Degassed H_2O (14.22 mL) was added to the vial under argon flow *via* syringe and stirred at rt for 2 h. In a separate second vial containing a PTFE coated magnetic

stir bar, Fe/ppm Pd NPs (538 mg, 800 ppm Pd) was added and sealed with a rubber septum. The vial was evacuated and backfilled with argon three times. A solution of TPGS-750-M/H_2O (14.22 mL) from the first vial was then added to second vial *via* syringe under argon flow. The mixture was then stirred at rt for 1 h. This mixture slurry of catalyst was then transferred to stainless steel syringe containing a PTFE coated magnetic stir bar and attached to syringe pump 1.

Syringe 2: In a glass vial containing a PTFE coated magnetic stir bar, 1-benzyl-5-bromo-1H-pyrrolo[2,3-b] pyridine **20 (**1080 mg, 3.75 mmol, 1.0 equiv) and (4-chlorophenyl) boronic acid **21** (704 mg, 4.5 mmol, 1.2 equiv) and sealed with a rubber septum. The vial was evacuated and backfilled with argon three times. Degassed H_2O (14.22 mL) was added to the vial under argon flow *via* syringe and stirred at rt for 2 h. This slurry of substrates was then transferred to a stainless-steel syringe containing a PTFE coated magnetic stir bar and attached to syringe pump 2.

Syringe 3: Third stainless-steel syringe was filled with degassed Et_3N (1.57 mL, 11.3 mmol, 3.0 equiv) and attached to syringe pump 3.

After achieving steady state (~3 residence times, 60 min), the sample was collected for 15 min and used to calculate the isolated yield of product. In 15 min, 0.49 mmol of substrate had been introduced in the reactor. The organic layer was concentrated *in vacuo* and then purified by flash column chromatography (DCM/hexane = 10/90) to afford 147 mg (0.46 mmol, ~94%) of product **22**.

15. Batch reaction procedures

15.1 Reaction 1. Batch synthesis of PFR model reaction **1**

To a 5 mL microwave vial equipped with a PTFE coated magnetic spin vein was added 20 mg of Fe/ppm Pd NPs (800 ppm Pd), 4-bromoanisole (93.52 mg, 0.5 mmol, 1.0 equiv), phenylboronic acid (76.2 mg, 0.625 mmol, 1.25 equiv), and potassium phosphate tribasic monohydrate (351 mg, 1.525 mmol, 3 equiv). A 2 wt % solution of TPGS-750-M (0.8 mL) was added to the vial followed by tetrahydrofurfuryl alcohol (0.2 mL) and the vial was sealed using an aluminum crimp cap fitted with a PTFE septum. The contents of the vial were then allowed to stir at rt until a semi-homogeneous mixture had formed and was then transferred to a microwave reactor. The contents of the vial were heated to 95 °C and stirred vigorously for 10 min. The resulting homogeneous mixture was then extracted with EtOAc (0.5 mL x 3). The organics were then evaporated under reduced pressure resulting in a crude oil, which was then taken up into 200 mL of cold water and allowed to sit cold for 30 min. The precipitate was then filtered, washed with water, and taken up in EtOAc. The crude organic mixture was then passed through a plug of silica gel to afford 89.1 mg (97%) of 4-methoxy-1,1'-biphenyl **1** as an off-white solid.

15.2 Reaction 2. Batch synthesis of the biaryl precursor to the sartans **10**.

To a 4 mL reaction vial containing a PTFE coated magnetic stir bar, 19.8 mg of Fe/ppm Pd NPs (800 ppm Pd) was added in a glove box. The reaction vial was sealed with a rubber septum. 2-Bromobenzonitrile (91 mg, 0.5 mmol, 1.0 equiv), *p*-tolylboronic acid (81.6 mg, 0.6 mmol, 1.2 equiv) and potassium phosphate tribasic monohydrate (173 mg, 0.75 mmol, 1.5 equiv) were added to the reaction vial under argon flow. The reaction vial was then evacuated and backfilled with dry argon three times. A solution of 2 wt % TPGS-750-M (1.0 mL) was added via syringe. The reaction vial was sealed with PTFE tape over rubber septum and then stirred vigorously at 90 ^{o}C for 20 minutes. The reaction vial was then allowed to cool to rt and

the reaction mixture was extracted with EtOAc (1.0 mL x 5). The combined organic layer was dried over anhydrous Na_2SO_4 and solvent was removed *in vacuo*. Crude product was purified by flash chromatography over silica gel to afford 95.9 mg (99 %) of 2-cyano-4'-methylbiphenyl **10** as a white solid (Et_2O/hexane = 6/94).

15.3 Reaction 3. Batch synthesis of the biaryl **16**.

To a 4 mL reaction vial containing a PTFE coated magnetic stir bar, 19.8 mg of Fe/ppm Pd NPs (800 ppm Pd) was added in a glove box. The reaction vial was sealed with a rubber septum. 7-Benzyl-4-chloro-7H-pyrrolo[2,3-d]pyrimidine **14** (121.5 mg, 0.5 mmol, 1.0 equiv) and 1-(2-tetrahydropyranyl)-1H-pyrazole-4-boronic acid, pinacol ester **15** (167 mg, 0.6 mmol, 1.2 equiv) were added to the reaction vial under argon flow. The reaction vial was then evacuated and backfilled with dry argon three times. A solution of 2 wt % TPGS-750-M (1.0 mL) and Et_3N (105 µL, 0.75 mmol, 1.5 equiv) were added via syringe. The reaction vial was sealed with PTFE tape over rubber septum and then stirred vigorously at 95 ^oC for 20 min. The reaction vial was then allowed to cool to rt and the reaction mixture was extracted with EtOAc (1.0 mL x 5). The combined organic layer was dried over anhydrous Na_2SO_4 and solvent was removed *in vacuo*. Crude product was purified by flash chromatography over silica gel to afford 160.2 mg (89 %) of 7-benzyl-4-(1-(tetrahydro-2H-pyran-2-yl)-1H-pyrazol-4-yl)-7H-pyrrolo[2,3-d]pyrimidine **16** as a white solid (EtOAc/hexane = 1/1).

15.4 Reaction 4. Batch synthesis of the biaryl **22**.

To a 4 mL reaction vial containing a PTFE coated magnetic stir bar, 19.8 mg of Fe/ppm Pd NPs (800 ppm Pd) was added in a glove box. The reaction vial was sealed with a rubber septum. 1-Benzyl-5-bromo-1H-pyrrolo[2,3-b]pyridine **20** (143.5 mg, 0.5 mmol, 1.0 equiv) and 4-chlorophenylboronic acid **21** (93.6 mg, 0.6 mmol, 1.2 equiv) were added to the reaction vial

under argon flow. The reaction vial was then evacuated and backfilled with dry argon three times. A solution of 2 wt % TPGS-750-M (1.0 mL) and Et_3N (105 µL, 0.75 mmol, 1.5 equiv) were added via syringe. The reaction vial was sealed with PTFE tape over rubber septum and then stirred vigorously at 95 ^oC for 20 min. The reaction vial was then allowed to cool to rt and the reaction mixture was extracted with EtOAc (1.0 mL x 5). The combined organic layer was dried over anhydrous Na_2SO_4 and solvent was removed *in vacuo*. Crude product was purified by flash chromatography over silica gel to afford 153.4 mg (96 %) of 1-benzyl-5-(4-chlorophenyl)-1H-pyrrolo[2,3-b]pyridine **22** as a white solid (DCM/hexane = 1/9).

16. Analytical data

4-Methoxy-1,1'-biphenyl (1)

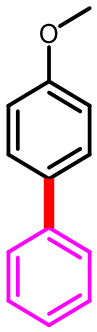

1

^{1}H NMR (500 MHz, $CDCl_3$): δ 7.59 – 7.52 (m, 4H), 7.43 (t, *J* = 7.8 Hz, 2H), 7.34 – 7.30 (m, 1H), 7.04 – 6.95 (m, 2H), 3.87 (s, 3H).

^{13}C NMR (126 MHz, $CDCl_3$): δ 159.3, 141.0, 133.9, 128.9, 128.3, 126.9, 127.0, 114.3, 55.5.[3]

1-(4-Methoxyphenyl)naphthalene (2)

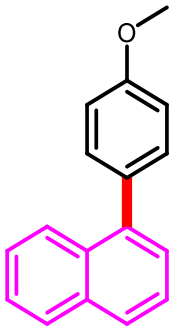

2

^{1}H NMR (500 MHz, $CDCl_3$): δ 7.98 (d, *J* = 8.4 Hz, 1H), 7.94 (d, *J* = 8.0 Hz, 1H), 7.88 (d, *J* = 8.2 Hz, 1H), 7.58 – 7.50 (m, 2H), 7.50 – 7.42 (m, 4H), 7.11 – 7.04 (m, 2H), 3.92 (s, 3H).

^{13}C NMR (126 MHz, $CDCl_3$): δ 159.1, 140.0, 134.0, 133.2, 132.0, 131.2, 128.4, 127.5, 127.0, 126.2, 126.0, 125.8, 125.5, 113.8, 55.5.[4]

2,4,6-Trimethyl-1,1'-biphenyl (3)

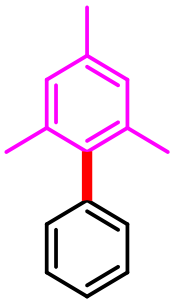

3

^{1}H NMR (500 MHz, $CDCl_3$): δ 7.46 (tt, *J* = 8.0, 1.5 Hz, 2H), 7.40 – 7.34 (m, 1H), 7.22 – 7.16 (m, 2H), 7.00 (s, 2H), 2.39 (s, 3H), 2.07 (s, 6H).

^{13}C NMR (126 MHz, $CDCl_3$): δ 141.2, 139.2, 136.8, 136.1, 129.4, 128.5, 128.2, 126.6, 21.2, 20.9.[5]

_t_-Butyl [1,1'-biphenyl]-4-ylcarbamate (4)

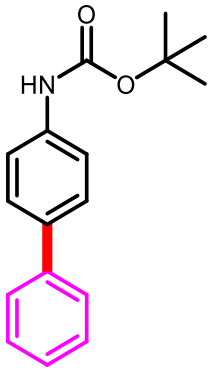

4

^{1}H NMR (500 MHz, $CDCl_3$): δ 7.56 (ddd, *J* = 15.6, 7.5, 1.8 Hz, 4H), 7.50 – 7.38 (m, 4H), 7.37 – 7.28 (m, 1H), 6.61 (s, 1H), 1.55 (s, 9H).

^{13}C NMR (126 MHz, $CDCl_3$): δ 152.9, 140.8, 137.8, 136.0, 128.9, 127.7, 127.0, 126.9, 119.0, 80.8, 28.5.[6]

4-Phenyl-3,6-dihydro-2H-pyran (5)

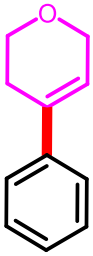

5

^{1}H NMR (500 MHz, $CDCl_3$): δ 7.46 – 7.40 (m, 2H), 7.37 (td, *J* = 6.9, 1.9 Hz, 2H), 7.32 – 7.26 (m, 1H), 6.15 (dp, *J* = 3.0, 1.6 Hz, 1H), 4.36 (q, *J* = 2.8 Hz, 2H), 3.97 (t, *J* = 5.4 Hz, 2H), 2.56 (dddq, *J* = 5.6, 3.9, 2.9, 1.4 Hz, 2H).

^{13}C NMR (126 MHz, $CDCl_3$): δ 140.4, 134.2, 128.5, 127.4, 124.8, 122.5, 66.0, 64.6, 27.3.[7]

3'-Chloro-[1,1'-biphenyl]-4-carbaldehyde (6)

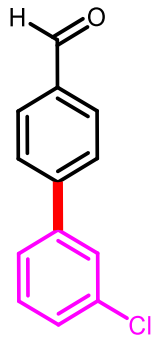

6

^{1}H NMR (500 MHz, $CDCl_3$): δ 10.06 (s, 1H), 7.95 (d, *J* = 8.4 Hz, 2H), 7.71 (d, *J* = 8.3 Hz, 2H), 7.60 (t, *J* = 2.0 Hz, 1H), 7.50 (dt, *J* = 7.1, 1.8 Hz, 1H), 7.43 – 7.36 (m, 2H).

^{13}C NMR (126 MHz, $CDCl_3$): δ 191.9, 145.7, 141.6, 135.7, 135.1, 130.4, 130.4, 128.6, 127.8, 127.6, 125.6.[8]

4'-Methyl-[1,1'-biphenyl]-2-carbonitrile (10)

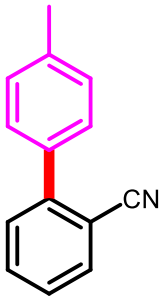

10

^{1}H NMR (500 MHz, $CDCl_3$) δ 7.75 (dd, *J* = 7.7, 1.4 Hz, 1H), 7.63 (td, *J* = 7.7, 1.4 Hz, 1H), 7.51 (dd, *J* = 8.0, 1.3 Hz, 1H), 7.49 – 7.45 (m, 2H), 7.42 (td, *J* = 7.6, 1.2 Hz, 1H), 7.34 – 7.28 (m, 2H), 2.43 (s, 3H).[2]

^{13}C NMR (126 MHz, $CDCl_3$) δ 145.7, 138.8, 135.4, 133.8, 132.9, 130.1, 129.6, 128.7, 127.4, 119.0, 111.3, 21.4.[9]

7-Benzyl-4-(1-(tetrahydro-2H-pyran-2-yl)-1H-pyrazol-4-yl)-7H-pyrrolo[2,3-d]pyrimidine (16)

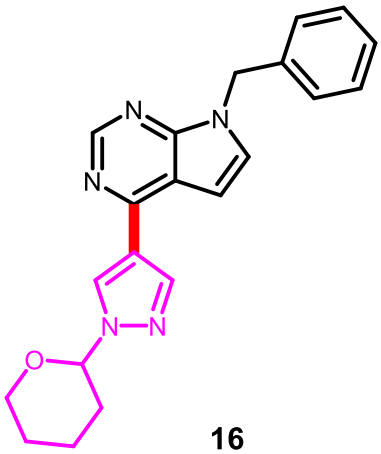

16

^{1}H NMR (500 MHz, $CDCl_3$) δ 8.86 (s, 1H), 8.42 (s, 1H), 8.29 (s, 1H), 7.31 (tt, *J* = 7.0, 6.1 Hz, 3H), 7.25 – 7.21 (m, 2H), 7.20 (d, *J* = 3.6 Hz, 1H), 6.76 (d, *J* = 3.6 Hz, 1H), 5.48 (s, 3H), 4.13 – 4.06 (m, 1H), 3.80 – 3.71 (m, 1H), 2.17 (dt, *J* = 6.2, 1.8 Hz, 2H), 2.10 – 2.01 (m, 1H), 1.78 – 1.57 (m, 4H).

^{13}C NMR (126 MHz, $CDCl_3$) δ 151.9, 151.7, 151.2, 139.6, 137.0, 129.0, 128.6, 128.5, 128.1, 127.7, 122.1, 114.3, 100.3, 88.0, 67.9, 48.0, 30.7, 25.1, 22.3.

HRMS: (ESI, [$C_{21}H_{21}N_5O$ + H]) calcd, 360.1824; found *m/z*: 360.1825.

1-Benzyl-5-(4-chlorophenyl)-1H-pyrrolo[2,3-b]pyridine (22)

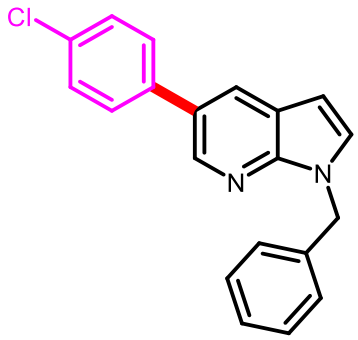

22

^{1}H NMR (500 MHz, $CDCl_3$) δ 8.55 (d, *J* = 2.1 Hz, 1H), 8.07 (d, *J* = 2.2 Hz, 1H), 7.55 (d, *J* = 8.5 Hz, 2H), 7.44 (d, *J* = 8.5 Hz, 2H), 7.35 – 7.27 (m, 3H), 7.24 (dd, *J* = 7.5, 2.4 Hz, 3H), 6.54 (d, *J* = 3.5 Hz, 1H), 5.53 (s, 2H).

^{13}C NMR (126 MHz, $CDCl_3$) δ 147.5, 142.3, 138.3, 137.8, 133.2, 129.17, 129.0, 128.9, 128.7, 128.6, 127.8, 127.6, 127.2, 120.6, 100.5, 48.1.

HRMS: (ESI, [$C_{20}H_{15}ClN_2$ + H]) calcd, 319.1002; found *m/z*: 319.1003.

17. Experimental references

1. Handa, S.; Wang, Y.; Gallou, F.; Lipshutz, B. H. *Science* **2015**, *349*, 1087–1091.
2. Lipshutz, B. H.; Ghorai, S.; Abela, A. R.; Moser, R.; Nishikata, T.; Duplais, C.; Krasovskiy, A.; Gaston, R. D.; Gadwood, R. C. *J. Org. Chem.* **2011**, *76*, 4379–4391.
3. Guo, W. J.; Want, Z. X. *J. Org. Chem.* **2013**, *78*, 1054-1061.
4. Bangar, P. G.; Nahide, P. D.; Meroliya, H. K.; Waghmode, S. A.; Iyer, S. *Synth. Comm.* **2021**, *51*, 308–316.
5. Gauchot, V.; Lee, A.-L. *Chem. Commun.* **2016**, *52*, 10163–10166.
6. Simpson, Q.; Sinclair, M. J. G.; Lupton, D. W.; Chaplin, A. B.; Hooper, J. F. *Org. Lett.* **2018**, *20*, 5537–5540.
7. Murakami, K.; Sasano, Y.; Tomizawa, M.; Shibuya, M.; Kwon, E.; Iwabuchi, Y. *J. Am. Chem. Soc.* **2014**, *136*, 17591–17600.
8. Wijtmans, M.; Scholten, D. J.; Roumne, L.; Canals, M.; Custers, H.; Glas, M.; Vrekker, M. C. A.; de Kanter, F. J. J.; de Graaf, C.l Smit, M. J.; de Esch, I. J. P.; Leurs R. *J. Med. Chem.* **2012**, *55*, 10572–10583.
9. Liang, Q.; Xing, P.; Huang, Z.; Dong, J.; Sharpless, K. B.; Li, X.; Jiang, B. *Org. Lett.* **2015,** *17*, 1942-1945.

4.7 Spectral Data

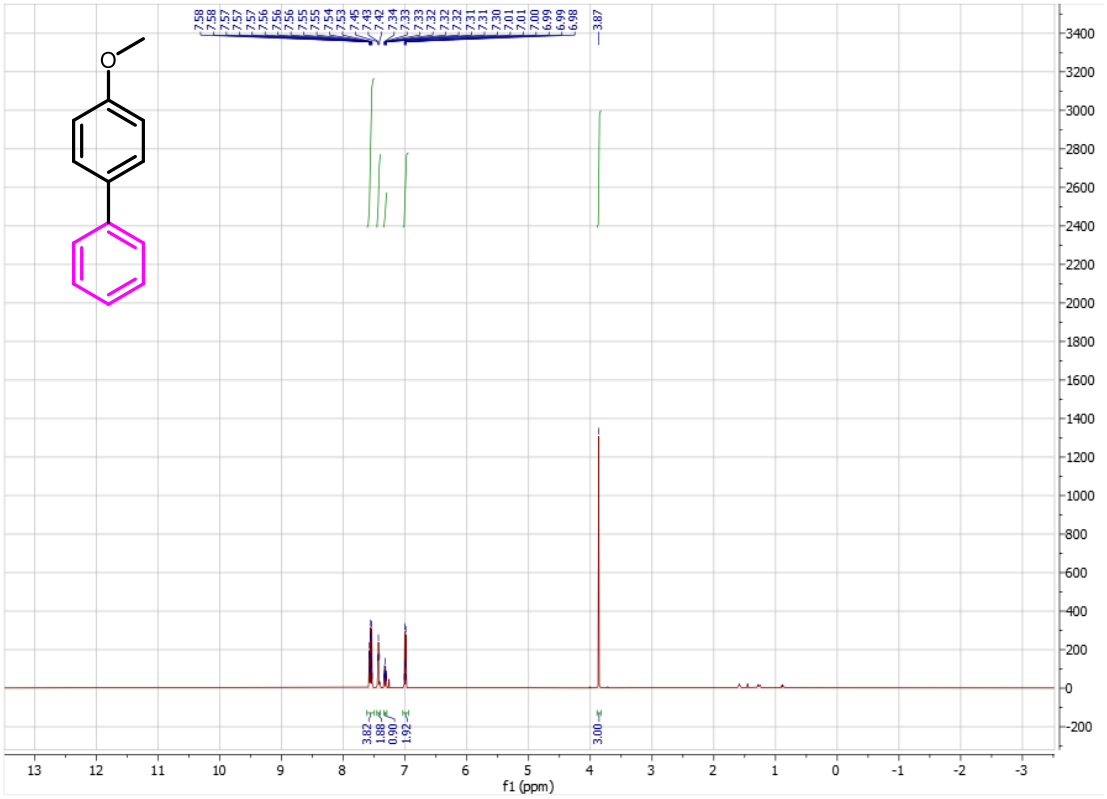

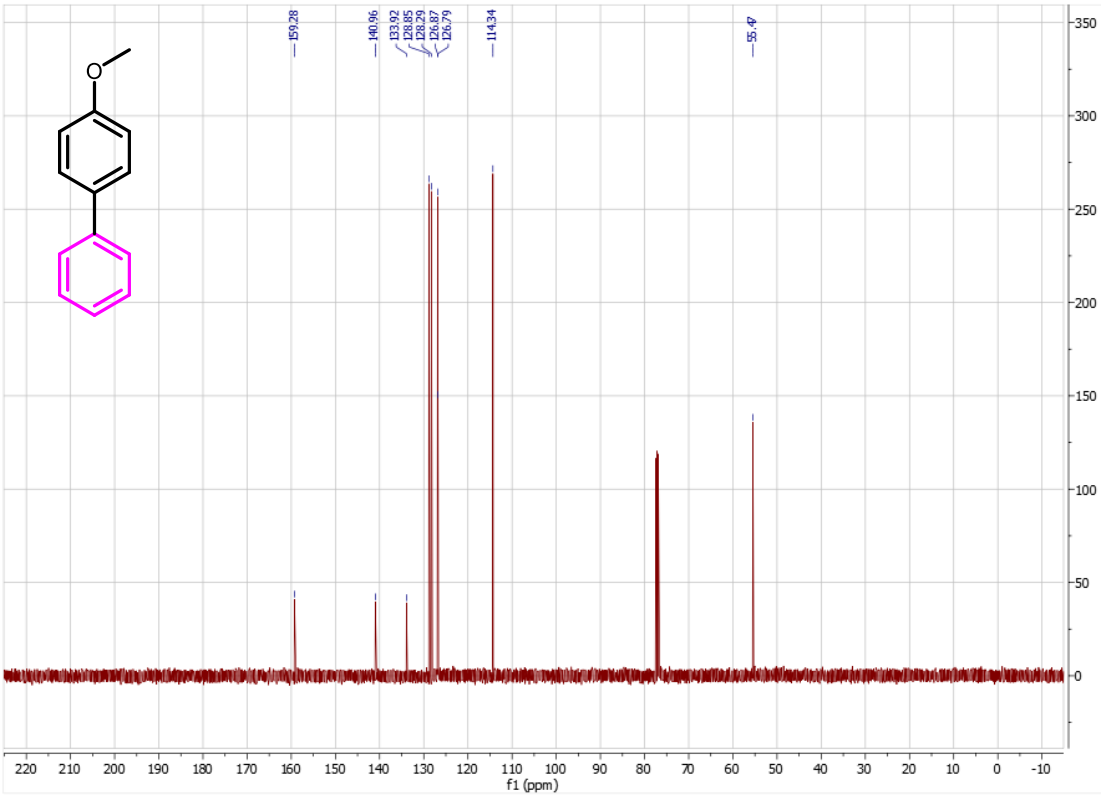

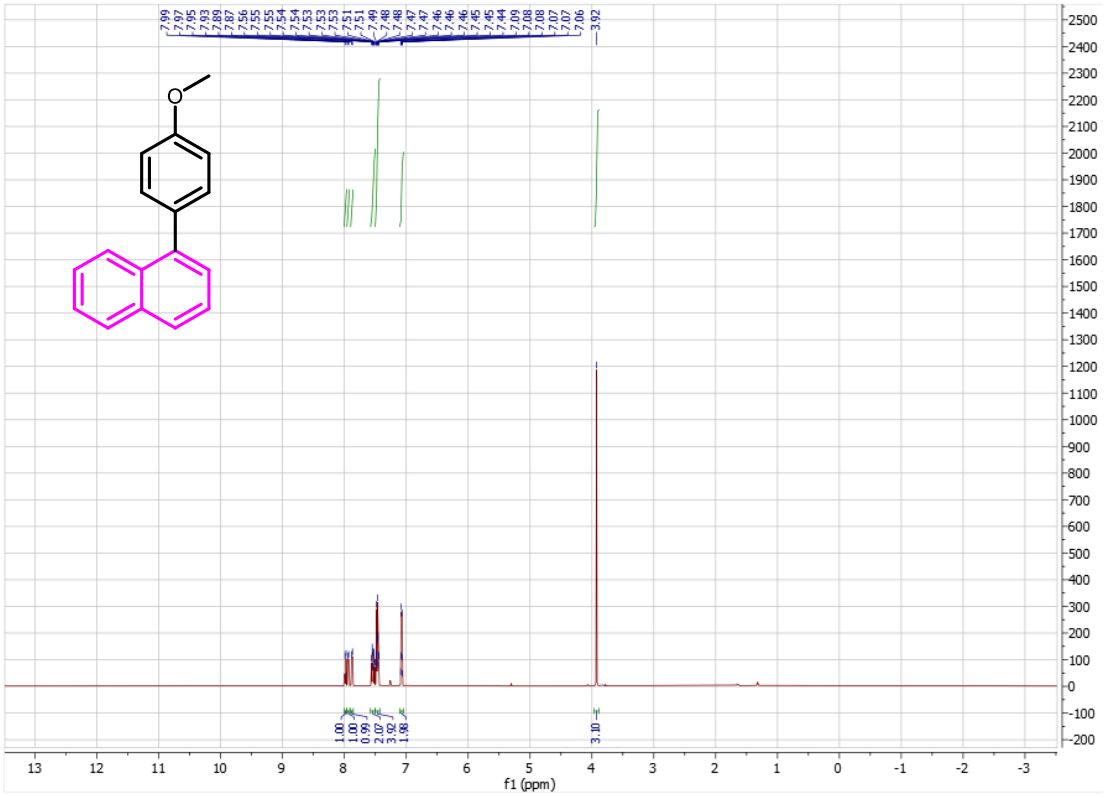
7.99
7.97
7.95
7.93
7.89
7.87
7.56
7.55
7.55
7.54
7.54
7.53
7.53
7.51
7.51
7.49
7.48
7.48
7.47
7.47
7.46
7.46
7.46
7.46
7.45
7.45
7.44
7.09
7.08
7.08
7.07
7.07
7.06
3.92
1.00
1.00
0.99
2.07
3.92
1.98
3.10
f1 (ppm)

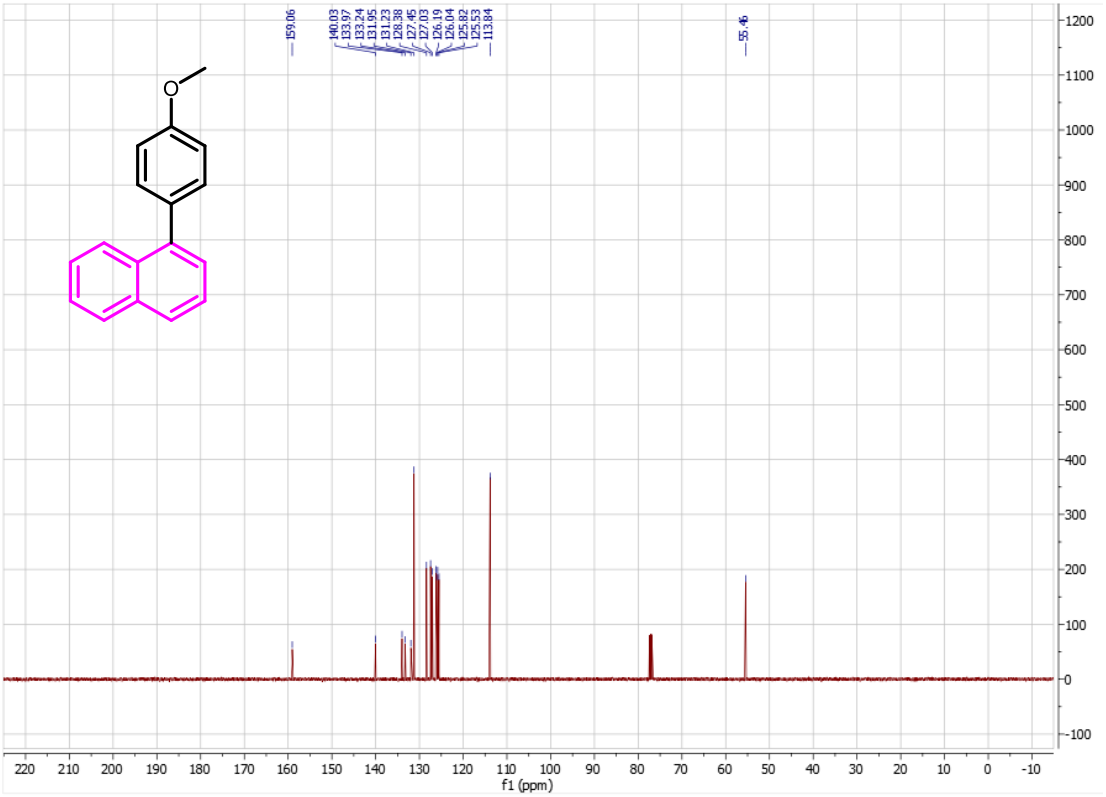
159.06
140.03
133.97
133.24
131.95
131.23
129.38
127.45
127.03
126.19
126.04
125.82
125.53
113.84
55.46
f1 (ppm)

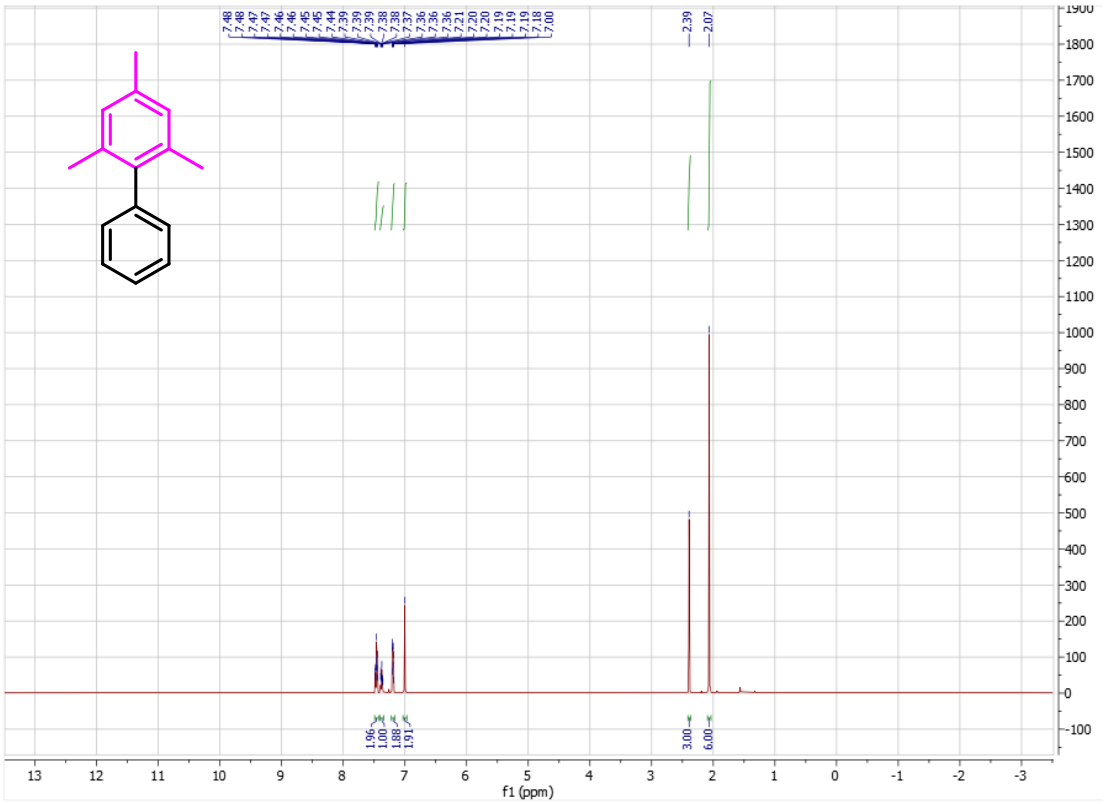
7.48
7.48
7.47
7.47
7.46
7.46
7.45
7.45
7.44
7.39
7.39
7.39
7.38
7.38
7.37
7.36
7.36
7.36
7.21
7.20
7.20
7.19
7.19
7.19
7.18
7.00
2.39
2.07
1.96
1.00
1.88
1.91
3.00
6.00
f1 (ppm)

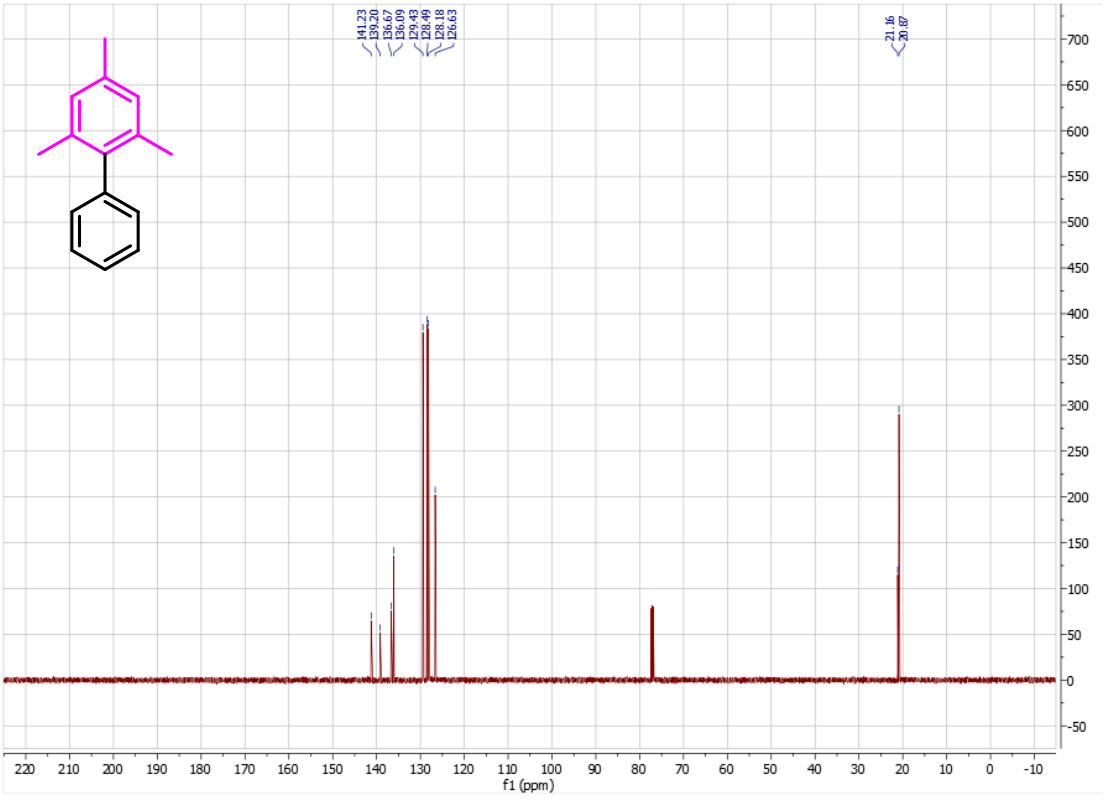
141.23
139.20
136.67
136.09
129.43
128.49
128.18
126.63
21.46
20.87
f1 (ppm)

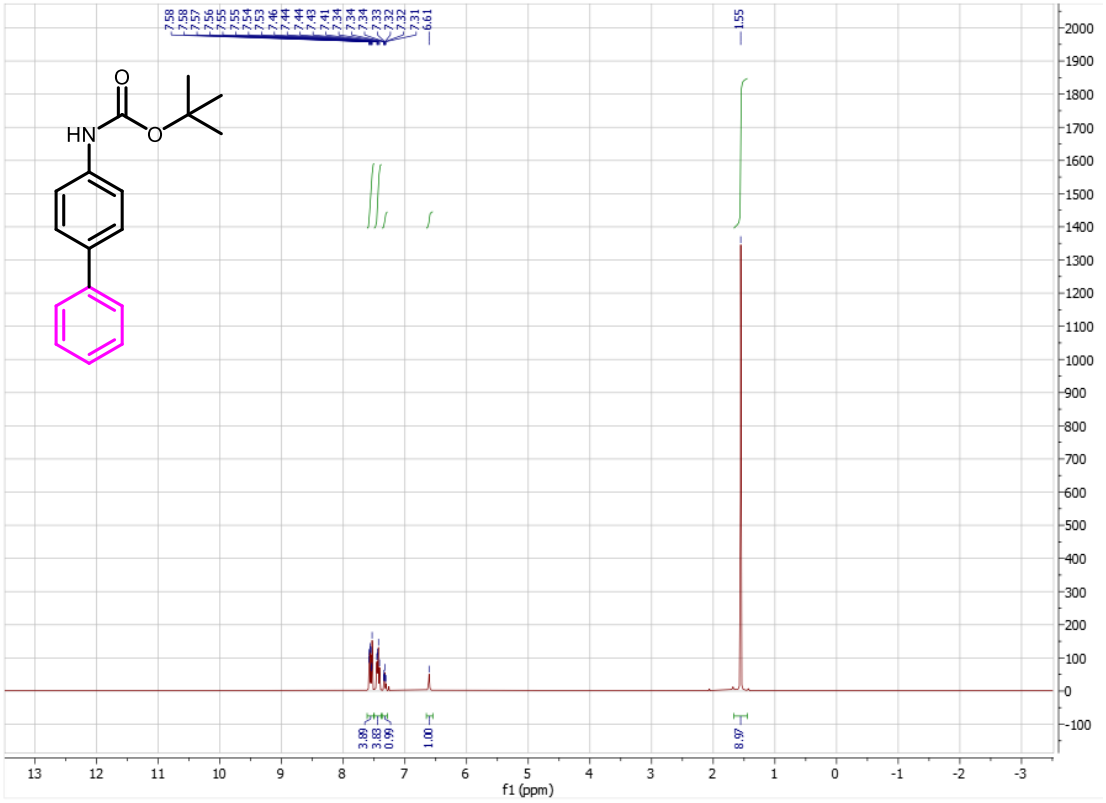
HN
O
O
f1 (ppm)

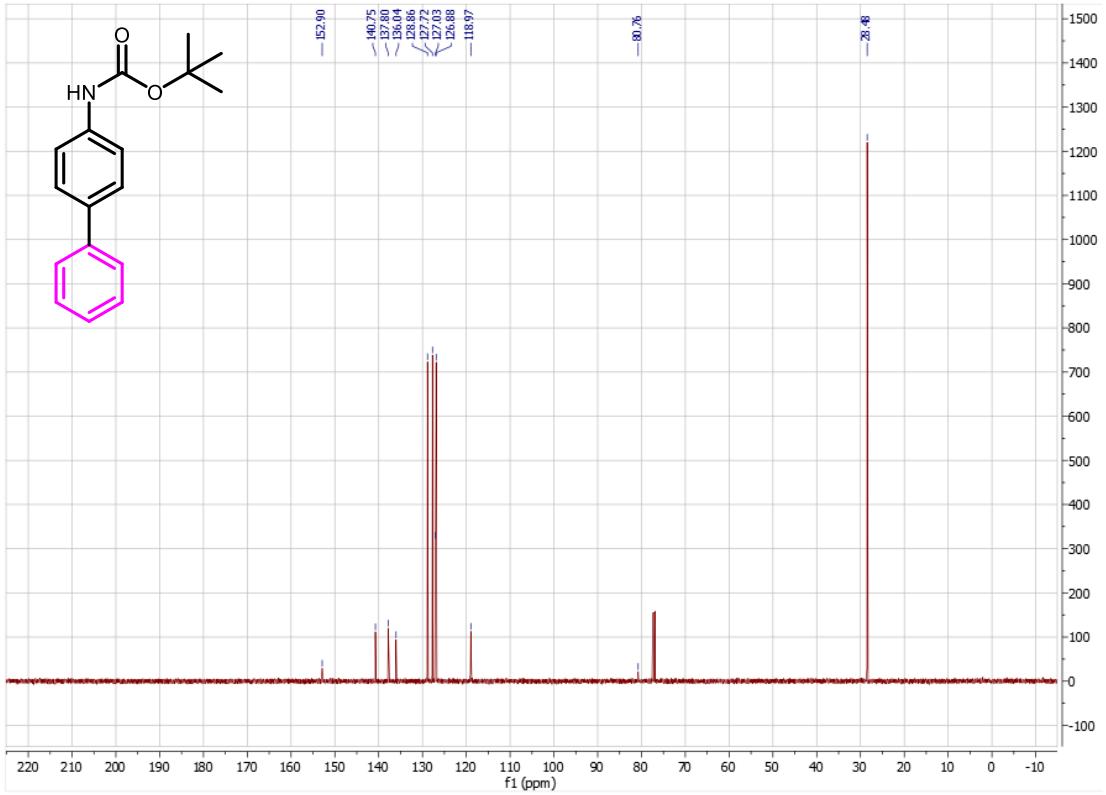
HN
O
O
f1 (ppm)

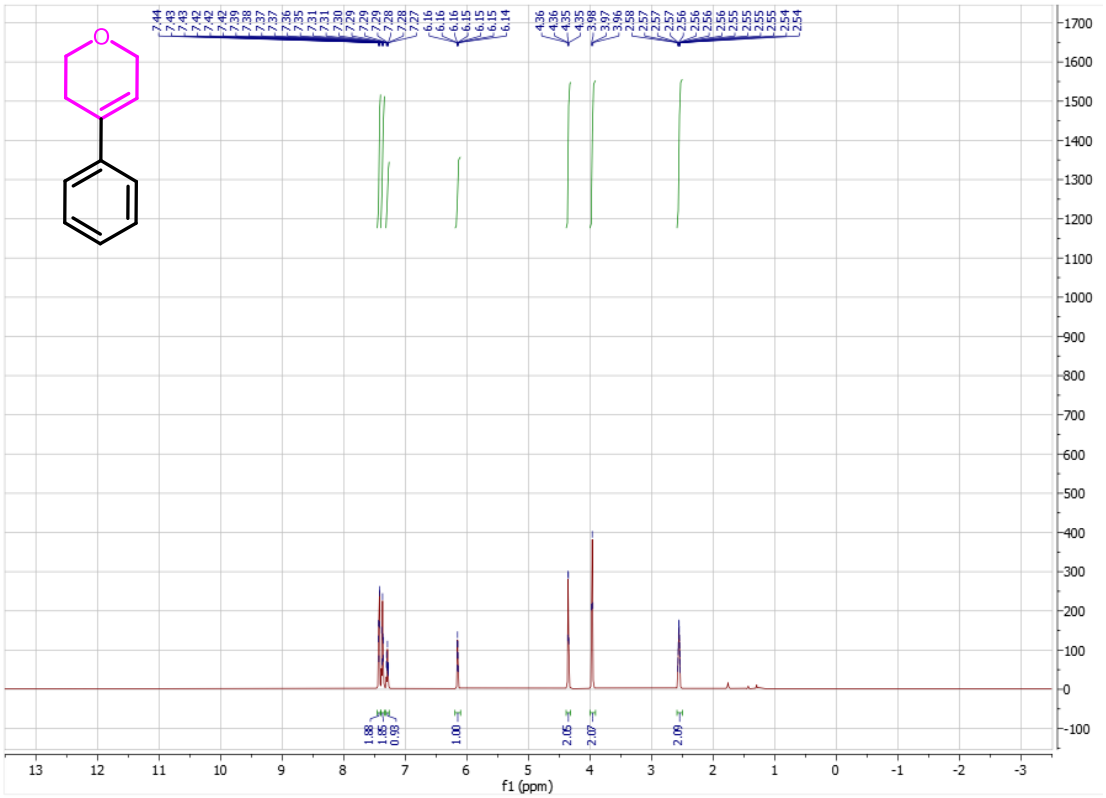
7.44
7.43
7.43
7.42
7.42
7.42
7.39
7.38
7.37
7.37
7.36
7.35
7.31
7.31
7.30
7.29
7.29
7.29
7.28
7.28
7.27
6.16
6.16
6.16
6.16
6.15
6.15
6.15
6.14
4.36
4.36
4.36
4.35
4.35
3.98
3.97
3.96
2.58
2.57
2.57
2.57
2.56
2.56
2.56
2.56
2.56
2.55
2.55
2.55
2.55
2.54
2.54
1.88
1.85
0.93
1.00
2.05
2.07
2.09
f1 (ppm)

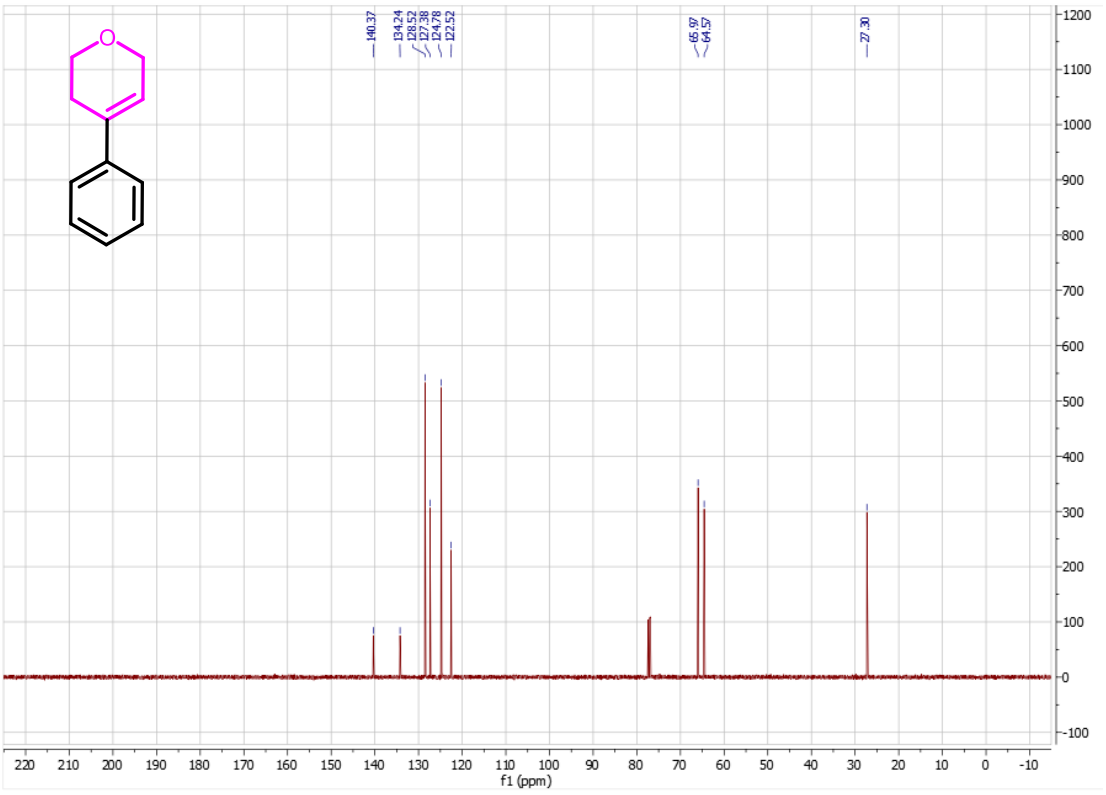
140.37
134.24
129.52
127.38
124.78
122.52
65.97
64.57
27.30
f1 (ppm)

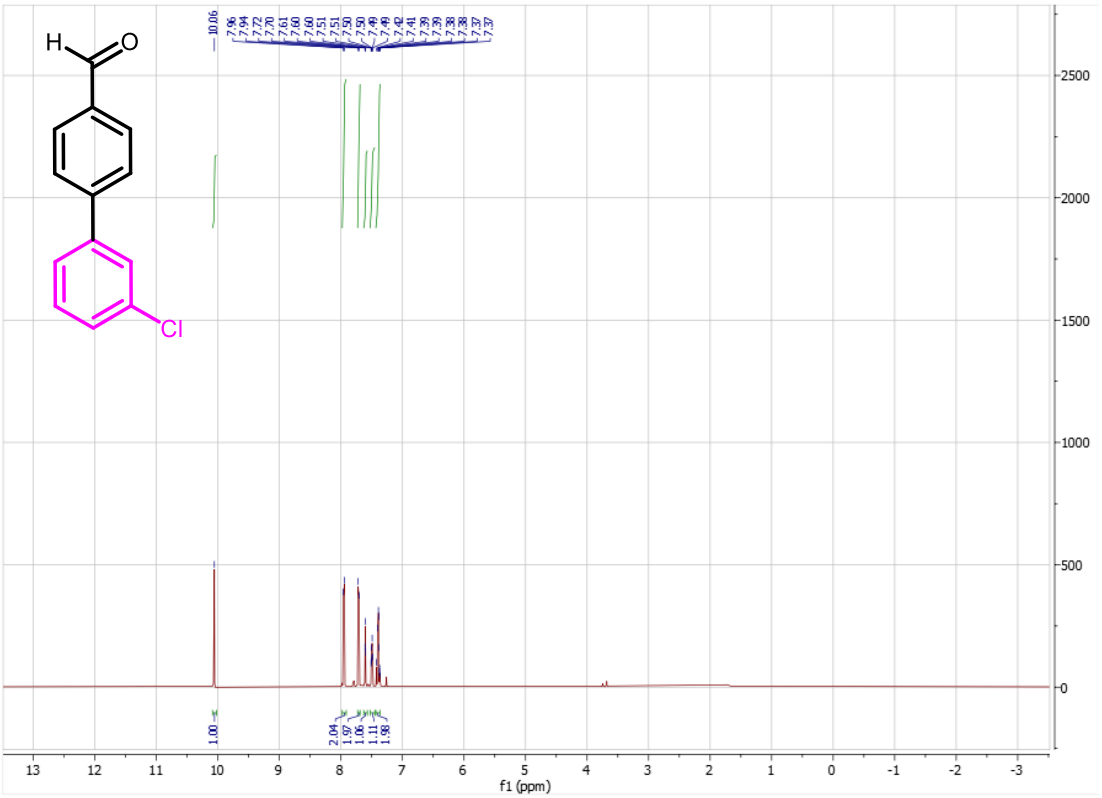
H
O
Cl
10.06
7.96
7.94
7.72
7.70
7.61
7.60
7.51
7.50
7.49
7.42
7.41
7.39
7.38
7.37
1.00
2.04
1.97
1.06
1.11
1.98
f1 (ppm)

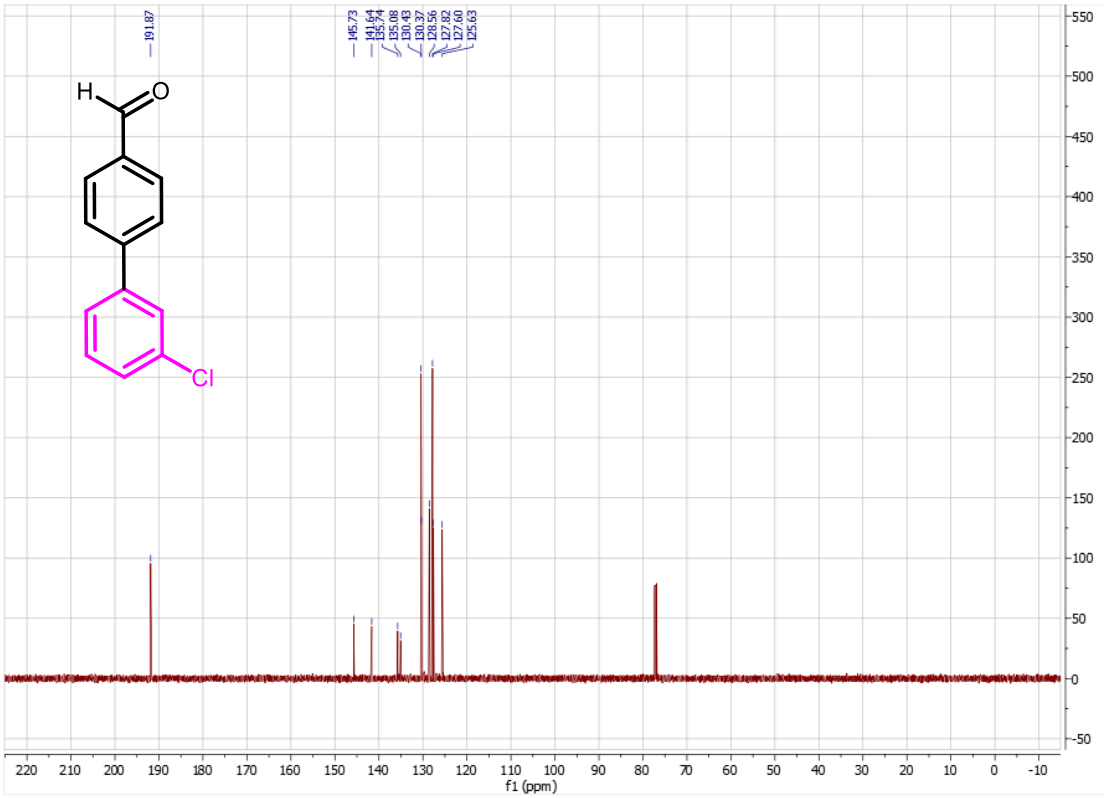
H
O
Cl
191.87
145.73
141.64
135.74
135.08
130.43
130.37
128.56
127.82
127.60
125.63
f1 (ppm)

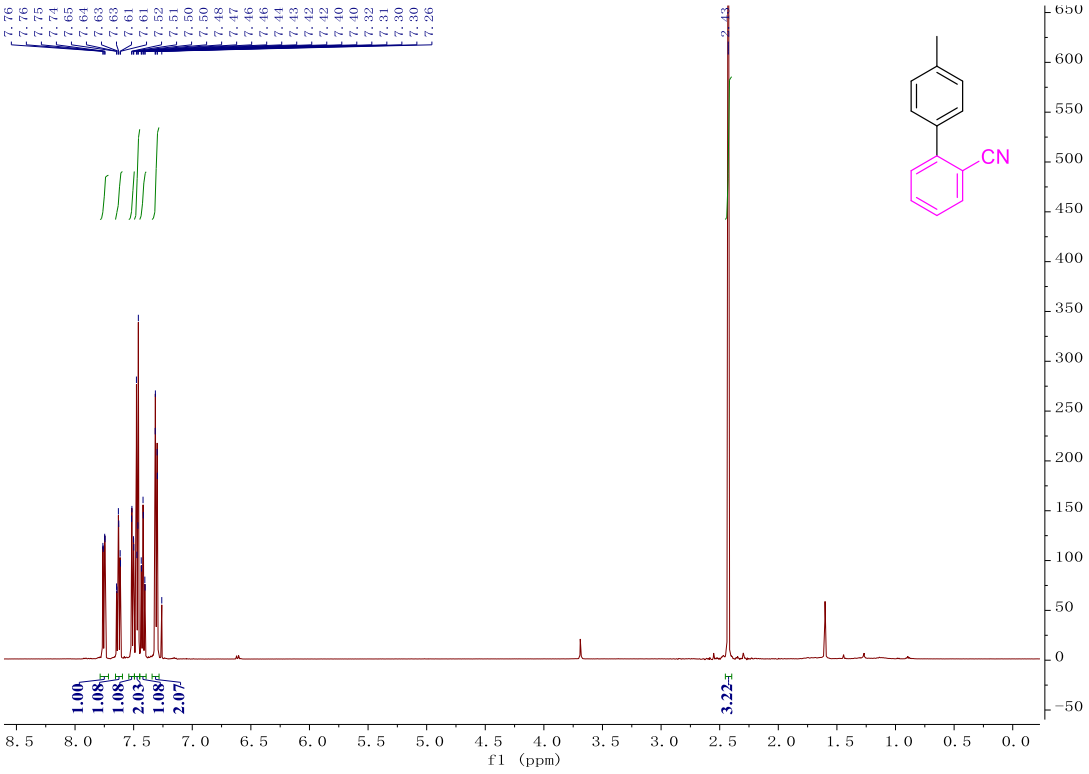
7.76
7.76
7.75
7.74
7.65
7.64
7.63
7.63
7.61
7.61
7.52
7.51
7.50
7.50
7.48
7.47
7.46
7.46
7.44
7.43
7.42
7.42
7.40
7.40
7.32
7.31
7.30
7.30
7.26
2.43
CN
1.00
1.08
1.08
2.03
1.08
2.07
3.22
f1 (ppm)

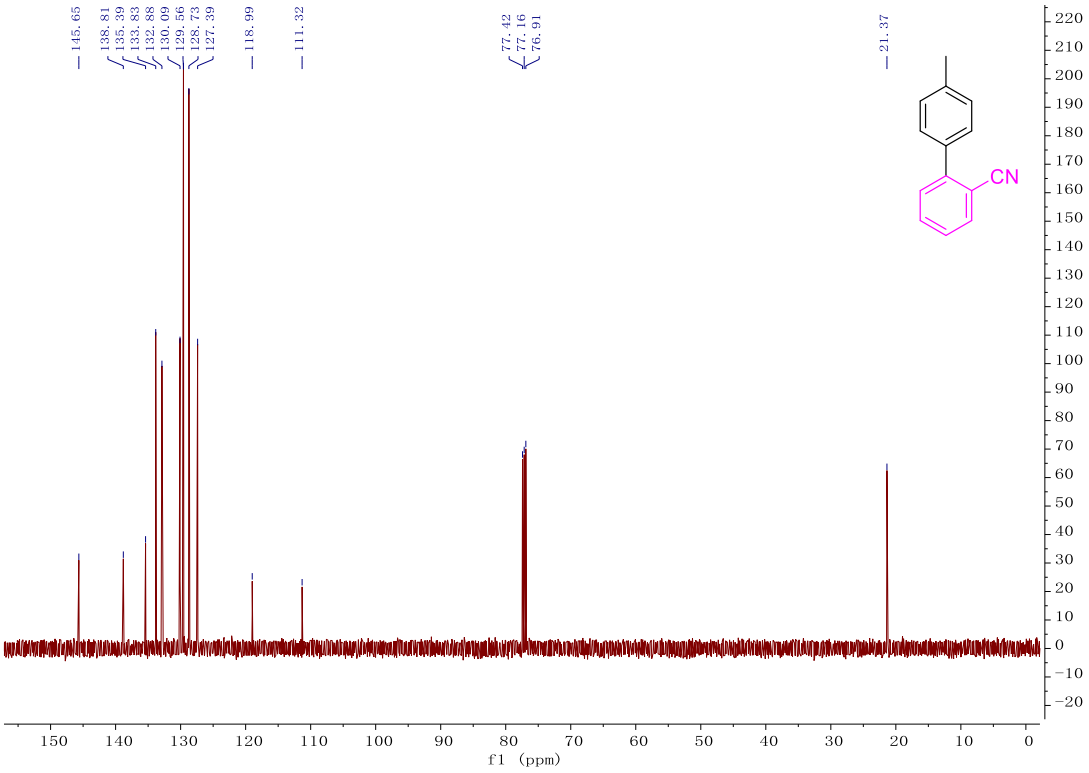
145.65
138.81
135.39
133.83
132.88
130.09
129.56
128.73
127.39
118.99
111.32
77.42
77.16
76.91
21.37
CN
f1 (ppm)

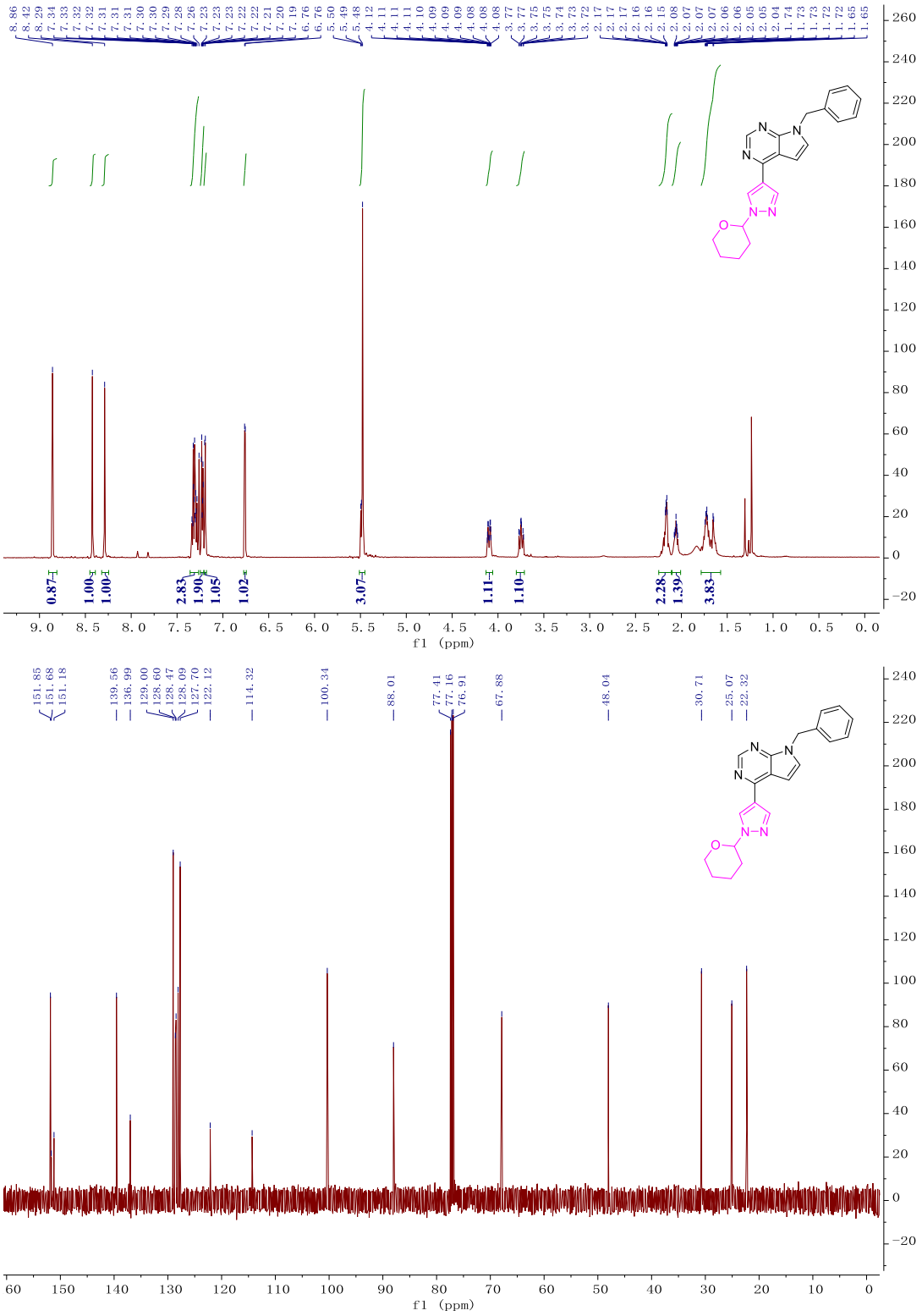
8.86 8.42 8.29 7.34 7.33 7.32 7.32 7.31 7.31 7.31 7.30 7.30 7.29 7.28 7.26 7.23 7.23 7.23 7.22 7.22 7.21 7.20 7.19 6.76 6.76 5.50 5.49 5.48 4.12 4.11 4.11 4.10 4.09 4.09 4.09 4.08 4.08 4.08 3.77 3.77 3.75 3.75 3.74 3.73 3.72 2.17 2.17 2.17 2.16 2.16 2.15 2.08 2.07 2.07 2.06 2.06 2.05 2.05 2.04 1.74 1.73 1.73 1.72 1.72 1.65 1.65
0.87 1.00 1.00 2.83 1.90 1.05 1.02 3.07 1.11 1.10 2.28 1.39 3.83
f1 (ppm)
151.85 151.68 151.18 139.56 136.99 129.00 128.60 128.47 128.09 127.70 122.12 114.32 100.34 88.01 77.41 77.16 76.91 67.88 48.04 30.71 25.07 22.32
f1 (ppm)

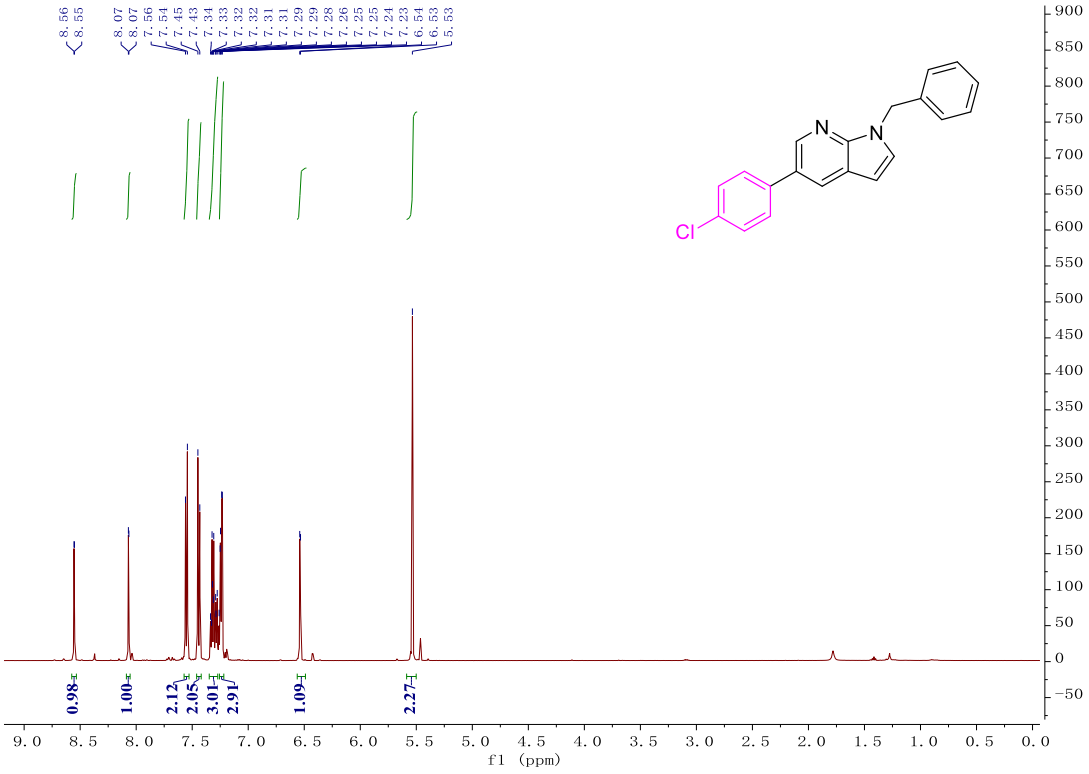
8.56
8.55
8.07
8.07
7.56
7.54
7.45
7.43
7.34
7.33
7.32
7.32
7.31
7.31
7.29
7.29
7.28
7.26
7.25
7.25
7.24
7.23
6.54
6.53
5.53
N
N
Cl
0.98
1.00
2.12
2.05
3.01
2.91
1.09
2.27
f1 (ppm)

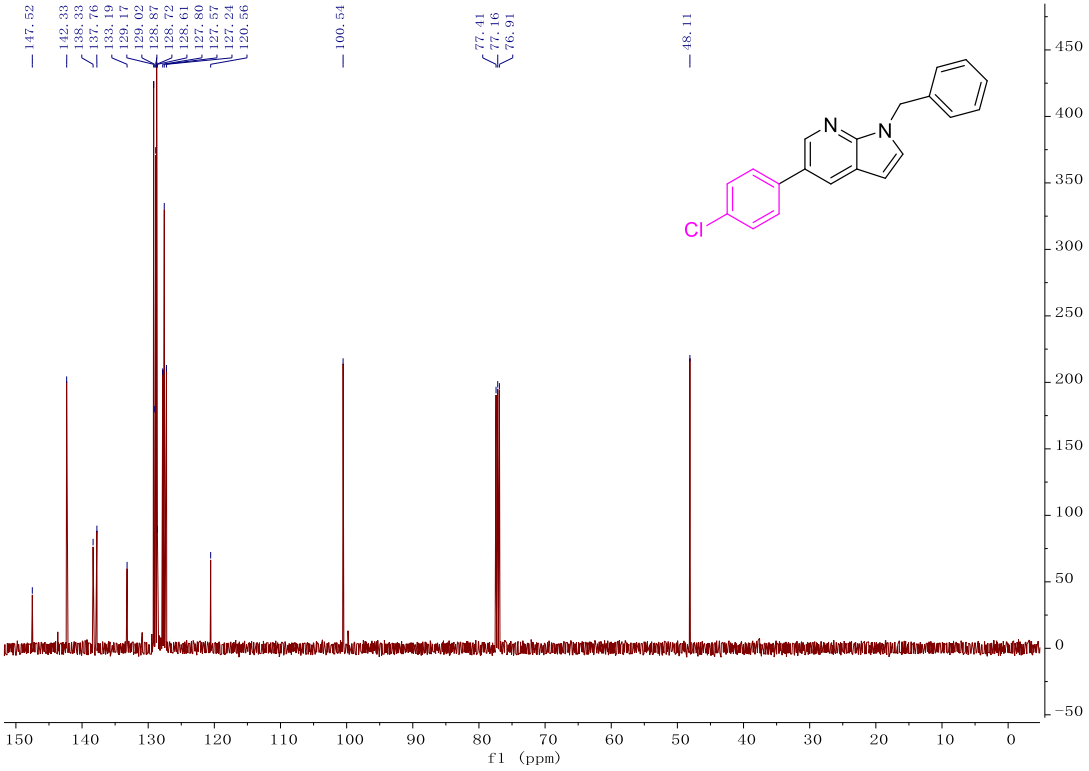
147.52
142.33
138.33
137.76
133.19
129.17
129.02
128.87
128.72
128.61
127.80
127.57
127.24
120.56
100.54
77.41
77.16
76.91
48.11
N
N
Cl
f1 (ppm)